

**Synthesis of sulfonate esters containing heterocyclic
scaffolds *via* sp^3 C-H activation and their biological
evaluation**

Thesis

Submitted in partial fulfilment of the requirement

For the Degree of

DOCTOR OF PHILOSOPHY

(In Chemistry)

To

NATIONAL INSTITUTE OF TECHNOLOGY

WARANGAL

By

Neeli Satyanarayana

(Roll No. 714167)

Under the supervision of

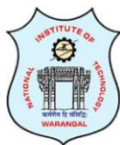
Dr. Dhurke Kashinath

Associate Professor



**Department of Chemistry
National Institute of Technology, Warangal-506004
India
June 2022**

Dr. Dhurke Kashinath
Associate Professor
Department Chemistry
National Institute of Technology, Warangal
Warangal - 506 004, Telangana, India.



Tel: +91-870-246-2677; +91-833-296-9502
Fax: +91-870-2459547
Email: kashinath@nitw.ac.in
kashinath.dhurke@gmail.com

CERTIFICATE

I certify that **Mr. Neeli Satyanarayana**, a bonafide student of Ph. D degree in National Institute of Technology, Warangal, has carried out research work under my direct supervision. The investigations, observations and the conclusions reported by him in this thesis entitled ***“Synthesis of sulfonate esters containing heterocyclic scaffolds via sp^3 C-H activation and their biological evaluation.”*** being submitted for the award of Ph. D degree in Chemistry are his original contributions to the Chemical Sciences. It is also certified that he has not submitted the same in part or in full to this or any other University for the award of a degree or diploma.

Date: 23-06-2022
Place: **Warangal**

(Dr. D. Kashinath)

Residence address: H. No. 31-3-744, Parimala Colony, Hanamkonda, Warangal-506 009

ACKNOWLEDGEMENT

It has been a long and a wonderful journey since I started my research career in Organic Research Lab-I, Department of Chemistry, National Institute of Technology, Warangal. Although, the first year of my Ph. D. was a bit challenging due to new working atmosphere but I was fortunate to join the Department that helped me to overcome and improve my curiosity towards research. Completion of this thesis was impossible without the support and guidance of the people mentioned here.

It gives me immense pleasure to express my sincere gratitude and respect for my supervisor Dr. D. Kashinath, Associate Professor, Department of Chemistry, National Institute of Technology, Warangal for his guidance and unconditional support throughout different stages of my doctoral studies.

I express my sincere thanks to the Directors, National Institute of Technology, Warangal, for giving me the opportunity to carry out my research work. I am grateful to MHRD for providing the fellowship during my Ph. D. tenure.

I express my heartfelt gratitude to Heads, Department of Chemistry (Dr. Vishnu Shanker and Prof. V. Rajeswer Rao, Prof. K. V. Gobi and Prof. P. V. Srilakshmi) for their timely help to get fellowship and provided facilities in time to my research.

I express my sincere thanks to my DSC members Prof. K. Laxma Reddy, Prof. P. V. Srilakshmi, Department of Chemistry, National Institute of Technology and Prof. Prof. Sonawane Shirish Hari, Department of Chemical Engineering, National Institute of Technology, Warangal for their suggestions and assessing my work progress throughout the tenure of my Ph. D. period for institute academic proceedings during my tenure.

I take this opportunity to express thanks to the faculty members of the Department of Chemistry, Prof. Appa Rao, Prof. I Ajith Kumar Reddy, Prof. A. Ramachandraiah, Prof. K. Laxma Reddy, Prof. P. Nageswar Rao, Prof. V. Rajeswar Rao, Prof. K. V. Gobi, Prof. P. V. Srilakshmi, Dr. Vishnu Shankar, Dr. Venkatathri Narayanan, Dr. B. Srinivas and Dr. K. Hari Prasad, Dr. Raghu Chitta, Dr. S. Nagarajan, Dr. M. Raghasudha, Dr. C. Jugun Prakash, Dr. Ravinder Pawar, Dr. Mukul Pradhan, Dr. Rajeshkhanna Gaddam, Dr. V. Rajeshkumar for their valuable advice, encouragement and moral support in my Ph. D tenure.

I could like express my thanks to Dr. Ravinder Pawar, (Assistant Professor) Department of Chemistry, National Institute of Technology Warangal, for his help in computational studies. I could like express my thanks to Dr. K. Divakar (Inspire faculty), B. Ramya Sri Biotechnology Dept, Department of Chemistry, National Institute of Technology Warangal, for his help in anti-diabetes activity

The thesis would not have come to a successful completion, without the help of my lab mates (group members) Dr. S. Nagaraju, Dr. B. Paplal, Dr. K. Sathish, T. Shirisha and M. Subir. Also thankful to co-Scholars Dr. Mallikarjun, Dr. G. Ramesh, Dr. K. Vimal Kumar, Dr. M. Venkanna, Ashitosh Yadav, R. Hithavani, P. Soumya, G. Shivaparwathi, Akanksha ashok sangolkar, J. Swathi, R. Vara prasad, R. Arun, K. Madhu A. Naveen, Dr. K. Sujatha, Dr.T. Sanjeeva, Dr. J. Parameshwara Chary, Dr. A. Varun, Dr. N. V. Bharath, Dr. P. Vinay, Ch. Raju, Dr. M. Srikanth, Dr. K. Ramaiah, Dr. M. Sai kumar, Dr. S. Suresh, Dr. G. Ambedkar, K. Vijender Reddy, Dr. P. Babji, Dr. B. Prasanth, Ramesh, and all of non-teaching staff, other Research Scholars in the Department of Chemistry, other scholars from maths, physics, ECE departments of NITW, Scholars from (IICT, Hyderabad) and friends (K Mahalaxmi, Aruna, Swapna, Ashok bade and other childhood friends).

I also gratefully acknowledge to Venkana (NMR technician, NITW), Narasimha (NMR technician, BITS Hyderabad) for analyses help during my Ph. D. tenure.

I would like to express my gratitude to our parents N. Nookaraju, N. Satyavathi, brothers N. Chidambaram, N. Ramu, our cousins brothers N. Ramu, N. Chidambaram, N. Srinu, N. Nagababu, T. Shiva (and T. Shanthi), well-wishers for giving advice, taking care and financial help during my PhD. days.

(Neeli Satyanarayana)

DECLARATION

I hereby declare that the research work presented in this thesis entitled “**Synthesis of sulfonate esters containing heterocyclic scaffolds *via* sp^3 C-H activation and their biological evaluation.**” has been carried out by me under the supervision of **Dr. D. Kashinath**, Associate Professor, Department of Chemistry, National Institute of Technology Warangal. I declare that this work is original and has not been submitted in part or full, for any degree or diploma to this or any other Institute/University.

Warangal

(Neeli Satyanarayana)

23th June 2022

List of Abbreviations

AcOH	Acetic acid
ACN	Acetonitrile
AIDS	Acquired immune deficiency syndrome
AMPA	α -Amino-3-hydroxy-5-methyl-4-isoxazolepropionic acid receptor
Bn	Benzyl
CAN	Ceric ammonium nitrate
CuSO ₄	Copper sulphate
CsF	Cesium fluoride
CNS	Central nerves system
CDCl ₃	Deuterated chloroform
¹³ C NMR	Carbon nuclear magnetic resonance
DHP	Dihydro pyridine
DBU	1,8-Diazabicyclo(5.4.0)undec-7-ene
DABCO	1,4-Diazabicyclo[2.2.2]octane
DEA	Diethylamine
TEA	Triethylamine
DNA	Deoxyribo Nucleic Acid
DMSO	Dimethyl sulfoxide
d	Doublets
dd	Doubly doublet
DMSO	Dimethyl sulfoxide
Py	Pyridine
DMF	Dimethylformamide
DCM	Dichloromethane
DCE	1,2-Dichloroethane
DMAP	4-Dimethylaminopyridine

MCF-7	Michigan Cancer Foundation-7
PTP1B	Protein-tyrosine Phosphatase 1B
NEt ₂ H	Diethylamine
EAA	Ethylacetoacetate
ESI	Electronic supplementary information
FeCl ₃	Iron (III) chloride
FeCl ₂	Iron (II) chloride
SnCl ₂	Stannous (II) chloride
DCM	Dichloromethane
EtOAc	Ethyl acetate
GABA	γ -Amino butyric acid
PIDA	Phenyliodine (III)-diacetate
Hz	Hertz
h	Hours
I ₂	Iodine
<i>J</i>	Coupling constant
H ₂ O ₂	Hydrogen peroxide
HCOOH	Formic acid
H ₂ O	Water
HIV	Human immunodeficiency virus
HCV	Hepatitis-C virus
IR	Infrared spectroscopy
IC ₅₀	Half maximal inhibitory concentration
V _{MAX}	Maximal value of reaction rate of an enzyme catalysed reaction
K _m	Michaelis constant of the enzyme
AUROC	Area Under the Receiver Operating Characteristics
MCC	Matthew's correlation coefficient
1,3-DMU	1,3-Dimethylurea
LTA	L-Tartaric acid
DESs	Deep Eutectic Solvents

Ts	Tosyl
Ms	Mesyl
<i>m</i> CPBA	meta-Chloroperoxybenzoic acid
m	Multiplet
MP	Melting point
Mwt	Molecular weight
μM	Micromolar
mL	Millilitre
mmol	Millimoles
min	Minutes
mg	milligram
MW	Micro wave
MCRs	Multicomponent reactions
NMDA	<i>N</i> -Nethyl-d-aspartate
NPs	Nanoparticles
NCs	Nanocomposites
nm	Nanometer
NMR	Nuclear magnetic resonance
NH ₄ OAc	Ammonium acetate
NaOAc	Sodium acetate
OPDA	<i>o</i> -Phenylenediamine
PTSA	<i>p</i> -Toluenesulfonic acid
Ph ₃ P	Triphenyl Phosphine
PEG-400	Poly ethylene glycol
Ph	Phenyl
q	Quartet
RT	Room temperature
RNA	Ribo Nucleic Acid
s	Singlet
TBHP	<i>tert</i> -Butyl hydroperoxide

TEA	Triethylamine
t	Triplet
a.u.	arbitrary units
TS	Transitional states
TLC	Thin layer chromatography
HRMS	High-resolution mass spectrometry
THF	Tetrahydrofuran
TEMPO	(2,2,6,6-Tetramethylpiperidin-1-yl)oxyl
ZnO	Zinc oxide nanoparticles
TLC	Thin layer chromatography
LCMS	Liquid Chromatography mass spectrometry
LC-HRMS	Liquid Chromatography-High Resolution Mass Spectrometry
ICT	Intramolecular Charge Transfer affect
λ_{em}	Emission/fluorescence wavelength
λ_{abs}	Absorption wavelength
(Φ)	Quantum yield
$\Delta\lambda$	Stokes shift
(Φ_f)	Fluorescence Quantum yield
UV-Visible	Ultra Violate-Visible

CONTENTS

Chapter No.	List of abbreviations	Page No.
I	Chapter- I: Introduction of biologically active heterocyclic compounds	1
	1.1 Natural and biologically active compounds with quinoline moiety	2
	1.2 Natural and biologically active compounds with substituted 2,4-thiozolidinones, 4 <i>H</i> -Chromenes and tetrahydrothiophenes.	3

	1.3 Natural and biologically active compounds with quinoxalines-2-one and quinazoline moieties.	5
	1.4 Natural and biologically active compounds with dibenzo-[1,4]-diazepin- 1-one moieties.	5
	1.5 Biologically active compounds of the quinazoline-ones	7
	1.6 Biologically active compounds of isoxazole moiety	8
	1.7 Biologically active compounds of 1,3,4-oxadiazoles	9
	1.8 Biologically active compounds with benzene sulfonate esters.	10
	1.9 Catalyst-free, water mediated reactions in organic synthesis	10
	1.10 Deep Eutectic Solvents in organic synthesis	11
	1.11 Multicomponent (one-pot) reactions.	11
	1.12 Objectives of the thesis	12
II	Chapter- II: Deep Eutectic Solvents (DES) mediated synthesis of styrylquinolines and styrylquinoline-sulfonates via Friedländer synthesis and sp³ C-H activation, their biological evaluation as α-Glucosidase inhibitors and photophysical studies	19
	2.1 Introduction	20
	2.1.1 Reported methods for the synthesis of substituted 2-styrylquinolines	20
	2.2 Present study	21
	2.3 Results and discussion	22
	2.4 DFT Calculation	29
	2.4.1 Detailed computational methodology	29
	2.7 Photophysical properties	34
	2.7.1 UV-Visible and PL spectroscopy experimental studies of styrylquinolines	34
	2.7.2 UV-Visible and PL spectroscopy experimental studies of styrylquinoline sulfonate esters (11a-11m) and (12a-12m).	37
	2.8 Biological activity	40
	2. 8.1 α -D-glucosidase assay	40
	2.9 Conclusion	48
	2.10 Experimental supporting information	48
	2.10.1 General	48
	2.10.2 General procedure for the one-pot synthesis of styrylquinoline derivatives:	48

	2.10.3 General procedure for the formation of Friedlander annulation intermediate (substituted 2-methyl quinolines) products (3b, 3c, 3f)	49
	2.11. Spectral data of the synthesized compounds:	49
	2.12. References	69
	2.13. Selected Spectral data	71
III	Chapter- III: Facile synthesis of quinoxaline, quinoxaline-2-one, quinazoline-based styryls, sulfonate-styryls <i>via</i> sp³ C-H activation and their evaluation as α-glucosidase inhibitors	82
	3.1 Introduction	83
	3.1.1 Reported methods for the synthesis of 3-styrylquinoxalin-2-ones, 2-styrylquinazolines, (E)-2-methyl-3-styrylquinoxaline and 2,3-distyrylquinoxalines	83
	3.2 Present study	87
	3.3 Results and Discussion	89
	3.4 Photo physical properties	99
	3.4.1 Fluorescent properties of simple 3-styrylquinoxaline-2-ol and 2-styrylquinazoline hybrids	99
	3.5 Biological activity	104
	3.5.1 Biological activity of 2,3-di((E)-styryl) quinoxalines (14a-14ae) and their sulfonate derivatives (18a-18k)	104
	3.5.1.1 α -D-glucosidase assay, materials and methods	104
	3.5.1.2 Determination of IC ₅₀ values of the 2,3-di((E)-styryl) quinoxaline and their sulfonate derivatives (14a-ae) and (18a-18k)	104
	3.5.2 Biological activity of 2-styryl-quinazoline (20a-20r) and 3-styryl-quinoxaline based sulfonate ester derivatives (21a-21p)	121
	3.5.2.1 α -Glucosidase assay, materials and methods	121
	3.6 Experimental Section	121
	3.6.1 General Procedure	121
	3.6.2 General procedure for the one-pot synthesis of 2-methyl-styrylquinoxaline	123
	3.6.3 General Procedure	150
	3.7 References	154
	3.8 Selected spectral data:	

IV	Chapter- IV; Synthesis of spiro and bicyclic thiolane derivatives via 1,4-Michael addition followed by intra molecular aldol reactions 4.1 Introduction 4.1.1 Synthetic methods for the tetrahydrothiophenes 4.2 Present study 4.3 Results and discussions 4.3.1 One-pot synthesis of spiro-tetrahydrothiophene (thiolanes) hybrids 4.4 Plausible reaction mechanism: 4.5 Conclusion 4.6 Experimental Section 4.6.1 General 4.6.2 General procedures 4.6.3 Spectral data of the synthesized compounds: 4.7 References 4.8 Selected Spectral data	163 163 163 166 168 168 172 173 173 173 174 182 183
V	Chapter- V: SnCl₂-catalyzed synthesis of dibenzo-[1,4]-diazepin-1-one, phenyl quinazoline and 2,5-substituted 1,3,4-oxadiazoles based sulfonate esters and their evaluation as α-glucosidase inhibitors 5.1 Introduction 5.1.1 Reported methods for the synthesis of dibenzo- [1,4]-diazepin-1-ones 5.1.2 Reported methods for the synthesis of substituted- 2,4-diphenyl quinazolines. 5.1.4 Synthetic methods for the 2,5-substituted 1, 3, 4-oxadiazole scaffolds. 5.2 Present study	193 194 194 194 196 198

	5.3	Results and Discussion	198
	5.5	Photophysical properties	206
	5.5	Biological activity	208
	5.5.1	α -Glucosidase activity	208
	5.5	Conclusion	216
	5.6	Experimental section	216
	5.6.1	General	216
	5.6.2	Experimental procedures and data	216
	5.7	References	226
	5.8	Selected Spectral data:	228
VI		Chapter-VI: Synthesis of quinazolinone Schiff base, isoxazole-styrene and isoxazole-thiolane sulfonate ester conjugates	238
	6.1	Introduction	239
	6.1.1	Synthetic methods for the preparation 2-phenyl quinazolinones and isoxazole-styryl conjugates	239
	6.2	Present study	241
	6.3	Results and Discussion	241
	6.3.1	Synthesis of efficient sulfonate ester based substituted quinazolinones scaffolds	244
	6.3.2	Synthesis of isoxazole-tetrahydrothiophene sulfonate esters	247
	6.3.3	Photophysical properties of isoxazole-styryl sulfonate esters.	248
	6.4	Conclusions	248
	6.5	Supporting information	248
	6.5.1	General	249
	6.5.2	Spectral data of the synthesized compounds	256
	6.6	References	259
	6.7	Selected spectra	259
		Summary of the thesis	
		List of Publications	

CHAPTER-1

Introduction of biologically active heterocyclic compounds

Abstract:

*The heterocyclic compounds play a vital role in medicinal, synthetic organic, and materials chemistry. The majority of the marketed drugs contain heterocyclic units either as core structure (pharmacophore) or as subunit (auxophore). It is well known that the introduction of heteroatom (O, S and N) helps in improving the biological activity (pharmacokinetics and pharmacodynamics) of the molecule. Considering, the potential biological activity of the molecules like, quinolones, quinoxalines, quinoxalines, tetrahydrothiophenes, barbiturates, rhodamines, dibenzo-[1,4]-diazepin-1-ones, isoxazole, 2,5-substituted 1,3,4-oxadiazole, sulfonate esters, the present thesis is aimed to the synthesis of the functionalized derivatives based on these molecules and their evaluation for the α -glucosidase inhibition. Some of the scaffolds discussed here are useful for the development of fluorescent materials. The synthesis of some of these molecules is based on sp^3 C-H activation as a concept. Thus, a brief introduction to the synthetic methods and biology of these molecules along with outlines of the present work is discussed in this **chapter-1**.*

1. Introduction

Heterocyclic compounds are an important class of organic chemistry. Two third of the existing molecules in the literature contain one or more hetero atoms (O, N and S) in different rings (5, 6-membered, bicyclic, tricyclic spiro cycles). The heterocyclics are common in agrochemicals,¹ pharmaceutical industry,² and the materials industry.³ Due to their remarkable importance researchers pay interest in the design and development of a new class of heterocyclic molecules, which is one of the attractive research fields in organic synthesis.

1.1 Natural and biologically active compounds with quinoline moiety

Quinoline and its derivatives are found in a wide range of natural products and are considered a privileged molecule in medicinal chemistry. The quinoline moiety is present in many pharmacologically active compounds with antiparasitic, antimalarial (**1**), antiviral (**2**), antimicrobial (**3**), anti-inflammatory (**4a**), antiprotozoal, anti-neoplastic, anti-platelet, anti-asthmatic, anti-tubercular, anti-plasmodia (**4b**) immunosuppressive and anti-HIV-1 activity, anticancer agents (**5a-c**) and cancer chemotherapy drugs (**5b/c**), P13K inhibitor (**6**) cytotoxic (**7**) activity (**Figure-1**).^{4a,b}

The alkenylazaarenes,^{5a} 2-styrylquinolines derivatives show high anti-HIV activity (**8**), and HIV-integrase enzyme (**9**), additionally, these scaffolds act such as chloroquine, pamaquine (**10**), mefloquine and amodiaquine (**11**) as antimalarial and anti-inflammatory agents. The quinoline derivatives are known as inhibitors of efflux pump,^{5b} PDGFR kinase (**12**), ALK5 (**13**), antileishmanial (**14**), EKB1 (EGFR) (**15**). Alkenyl azaarenes activate the estrogen receptor-b (ER b) (**16**) and which is involved in the functioning, maintenance, and development of the reproductive system of the mammals. The derivatives of quinolone are also employed in photo luminescent^{5c} and optoelectronics as organic functional devices, OLEDs, and light-emitting diodes (**17**).

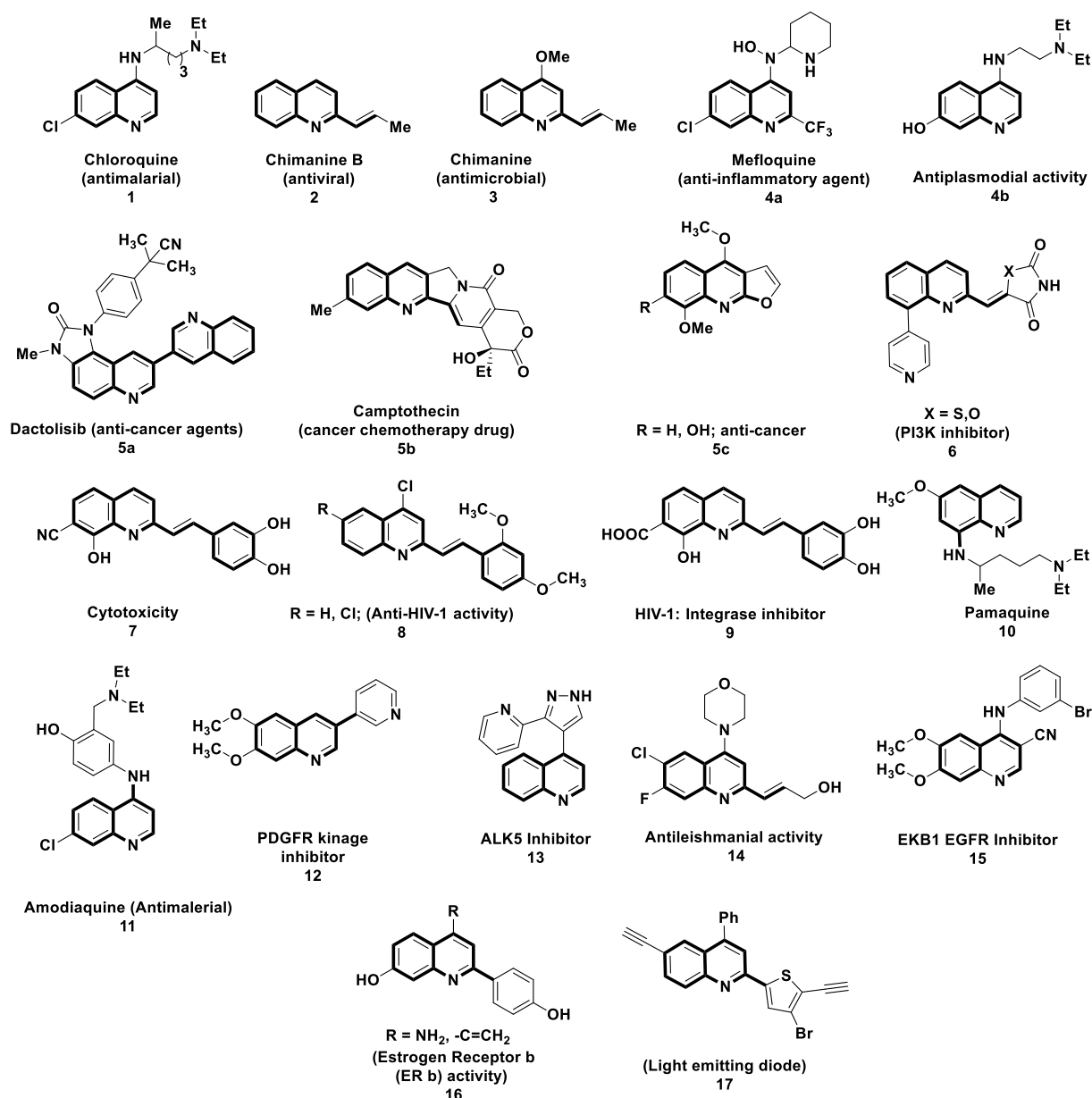


Figure-1: Natural and biologically active molecules of substituted quinolines.

1.1.2 Natural and biologically active compounds with substituted 2,4-thiazolidinones, 4H-Chromenes, and tetrahydrothiophene.

2,4-thiazolidinedione analogs are an important class of heterocyclic compounds and play a significant role in medicinal and pharmaceutical chemistry.^{6a-f} The derivatives of 2,4-thiazolidinediones show biological properties such as anti-bacterial (18), anti-cancer (19), amoebicidal, anti-tubercular (20), and inflammatory activity (21) as shown in **Figure-2a** and can be found in the naturally occurring penicillin and pioglitazone molecule (22). These derivatives control the inflammation diseases and work as TFA- α cytokine, muscarinic receptor-1 agonist,^{7a} KRP297 antagonist (23), TNF- α antagonistic activity, and chikungunya viral action^{7b} (ChikV

activity) (**24**). Tetrahydrothiophenes (THT) are limited in natural, biologically active compounds like salacinol (**25**, glucosidase inhibitor),^{8a} biotin (**26**, coenzymes), penicillin analogs,^{8b} breynolide (spiroketal, a glycoside inhibitor), phosphodiesterase inhibitor^{8c} and tetronothiodin (cholecystokinin type-B receptor antagonist). Tetrahydrothiophene bases compounds are known for pulmonary hypertension activity, hepatitis-B, HIV-inhibition (**27**), anti-arrhythmic activity,^{8d} anti-diabetic activity^{8e}, and functioning as FSH-receptor. In addition, this moiety served as a 4-thioadenosine receptor (**28**),^{9a} A3-adenosine receptor antagonist, and developed antiviral activity in the 4-thionucleosides (**29**) (see in **Figure-2a**) for enhancing the bacterial activity of sulopenem,^{9b} penicillin (**30**), GABA analogs^{9c} (**31**) which proved to be better a molecule than vigabatrin.

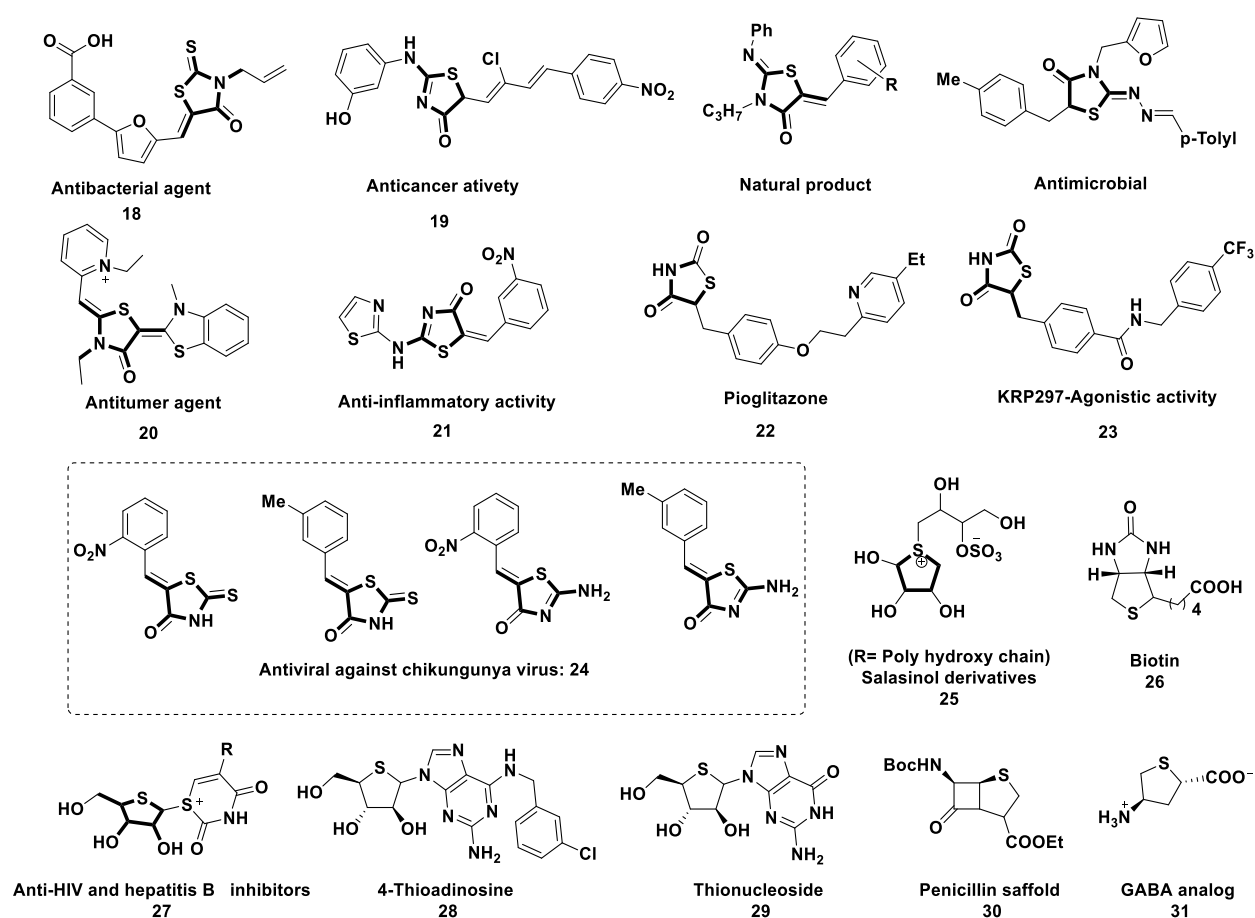


Figure-2a: Natural and biologically active molecules of 2,4-thiazolidinediones, and tetrahydrothiophene.

[4*H*]-chromene/[2*H*]-chromenes are part of naturally occurring compounds having a wide range of biological properties.^{10a-c} Especially 2*H*-chromene derivatives^{10d-e} known for anticoagulant, anti-fungal (**32**), antimicrobial, antimalarial, anti-inflammatory (**33**), anti-hyperglycemic, antiviral, antioxidant, and diuretic properties. Specifically, 3-nitro-[4*H*]-chromene derivatives show antifungal, anticancer (**34**) (breast and lung cancer) activity,¹¹ effectively

involved in urinary incontinence positive modulation of the AMPA receptor, and cyclooxygenase-2 inhibition (**35**) as shown in **Figure-2b**.

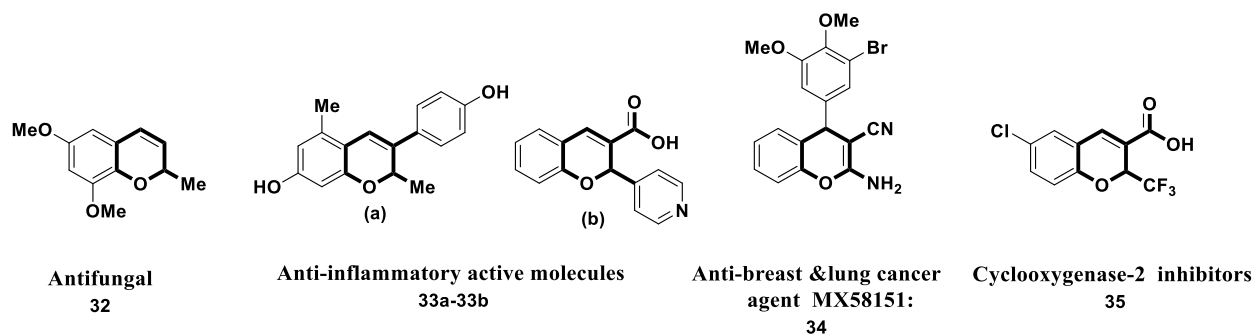


Figure-2b: Natural and biologically active molecules related to *[2H]* and *[4H]*-chromenes.

1.3 Natural and biologically active compounds with quinoxalines-2-one and quinazoline moieties.

Quinoxalines-2-one scaffolds are attractive bicyclic-fused nitrogen-containing heterocyclic compounds.^{12a-e} These compounds show antimicrobial, antiviral (**36**), anti-inflammatory, antithrombotic, anti-depressant, anti-epilepsy,¹³ anticancer (**37**),¹⁴ anti-HIV (**38**), antibiotics,^{15a} glucagon receptor antagonist (**39**), animal growth promoters^{15b} properties. Quinoxalinone scaffolds work as DNA cleaving agents,^{15c} different transplantable tumors.¹⁶ Additionally these compounds show photophysical properties (**40**),^{17a} OLEDs,^{17b} organic semiconductors, and chemically controllable switches (see **Figure-3**).

Quinazoline units are known for anti-influenza (**41a**), anti-inflammatory (**41b**),^{17c} antibacterial (**42**), CNS-depressant and T-type calcium channel blocking activity,^{17d} inhibition of tyrosine kinase receptors, EGFR tyrosine kinase^{18a} (gefitinib (**43**), neratinib (CI 1033) medicines) (**44**), hyperlipidemic inhibition^{18b} (**45**) and potent anticonvulsant inhibition. Besides, the quinazoline core used in cancer^{18c} as anticancer drugs like circumdatin F (**46**), and terazosin^{19a-b} which are selectively used for adrenoceptor blocking agents (**47**), actions like 5-HT_{5A} disease type receptors,²⁰ vasopressin V3 receptor and sedative-hypnotic drugs (piriqualone) (**48**).

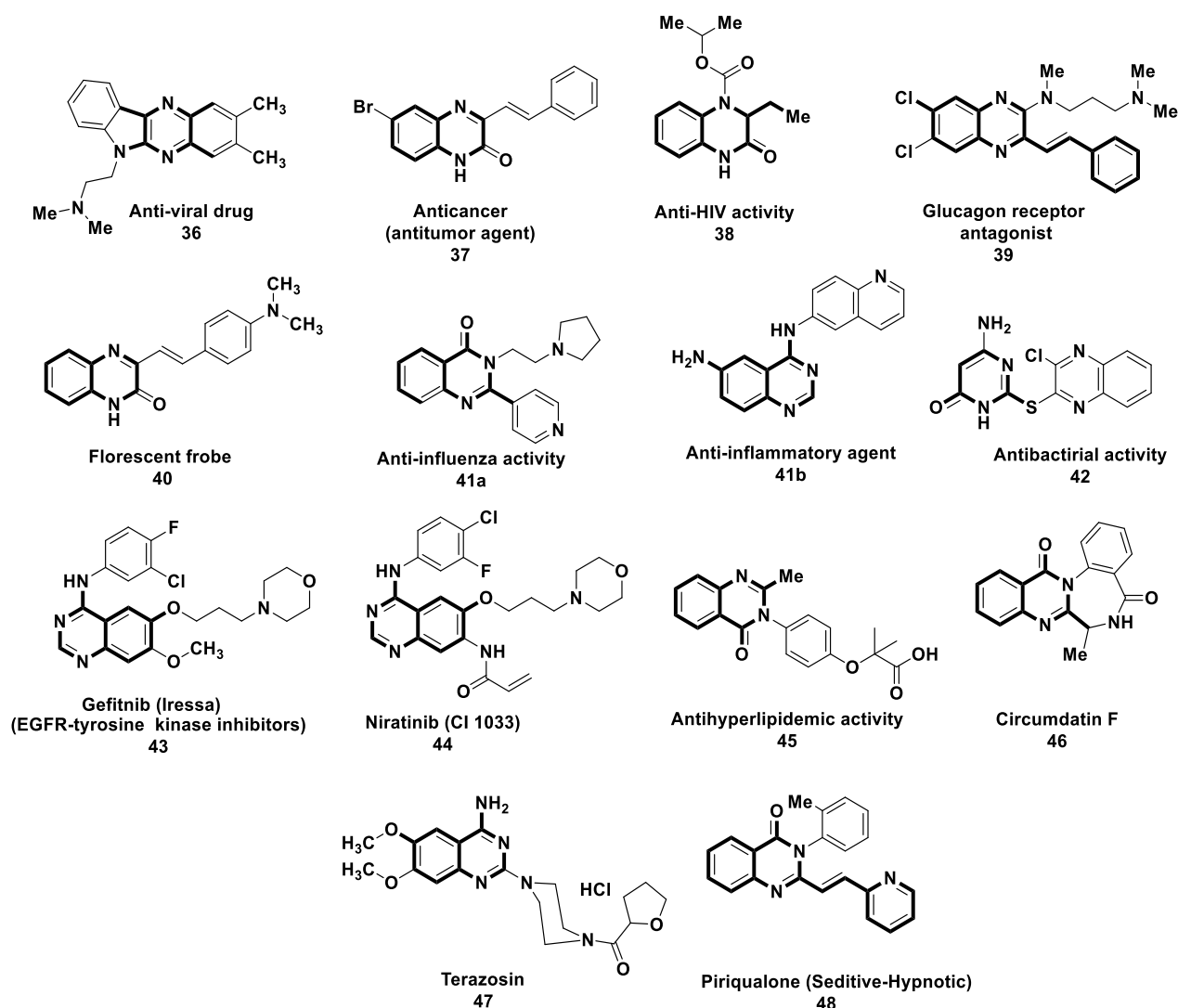


Figure-3: Natural and biologically active molecules related to bioactive compounds with quinoxalines-2-one and quinazoline moieties.

1.4 Natural and biologically active compounds with dibenzo-[1,4]-diazepin-1-one moieties.

Isomeric structures 1,4- and 1,5-benzodiazepine derivatives are another privileged class of heterocyclic compounds,^{21a-c} poses many biological, particularly in the central nervous system (CNS) (as shown in **Figure-4**). Along with this, they show antimicrobial (**49**), anti-inflammatory, hepatitis-C-virus (HCV) NS5B polymerize inhibition^{22a} (**50**) and anticoagulant,^{22b} psychotropic (chlordiazepoxide; anti-anxiety)^{22c} (**51**) and clozapine (**52**) (schizophrenia). Some benzodiazepine derivatives^{22d-e} work as platelet-activating factor inhibitors, muscarinic receptor-M1 antagonist (pirenzepine) phosphodiesterase inhibitors, and non-competitive metabotropic receptor-2 antagonist^{22f} and histamine H4 receptor antagonists.^{23a} In addition, dibenzo-[1,4]-diazepin-1-one

effectively demonstrated for α -glucosidase inhibitors activity^{23b} for non-insulin-dependent type-2 diabetes mellitus and cystathionine β -synthase inhibitors (**53**), selective antagonist GABA,^{23c} neuromedin B receptor antagonists with IC₅₀ 5.5 μ M (R= Cl) (**54**) and IC₅₀ 580 μ M (R = H) (**55**) respectively. Similarly, compound (**56**) demonstrated as HIV protease inhibitor^{24(a-c)} and screened for hepatitis-C virus NS5B polymerase inhibitor with IC₅₀ = 0.9 μ M, EC₅₀ = 2.3 μ M as shown in **Figure-4**.

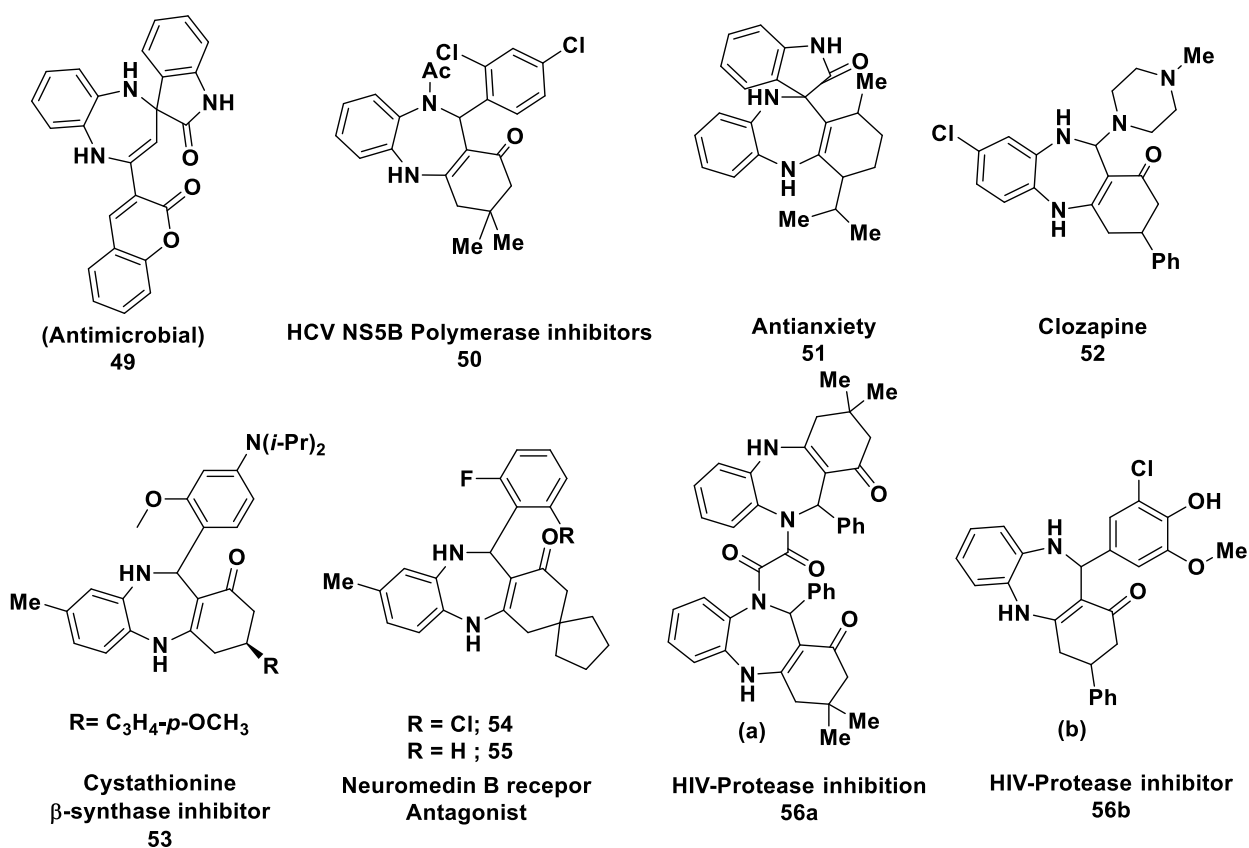


Figure-4: Selected biologically active molecules of dibenzodiazepin-1-ones.

1.5 Biologically active compounds of the quinazoline-ones

Quinazolinones potent class of fused heterocyclic compounds exhibits characteristic features in biology.^{25a-c} They show anticonvulsant, anti-TB, anti-influenza (**57**), anti-HIV, analgesic/anti-inflammatory properties and are used in chemotherapy [ispinesib (**58**) and asperilicin (**59**),^{26a} (**60**),**61**]^{26(b,c)} 6,8-Dibromo-4(3H)quinazolinone,^{27a} quinazolinone ZD1839 were tested for breast cancer (**62**) and inhibition action against EGFR tyrosine kinase activity (as shown in **Figure-5**).^{27b} Recently, Zahedifard et al.^{27c} screened quinazolinone Schiff bases for apoptotic activity against MCF-7 cancer cell lines(**63a-63b**).

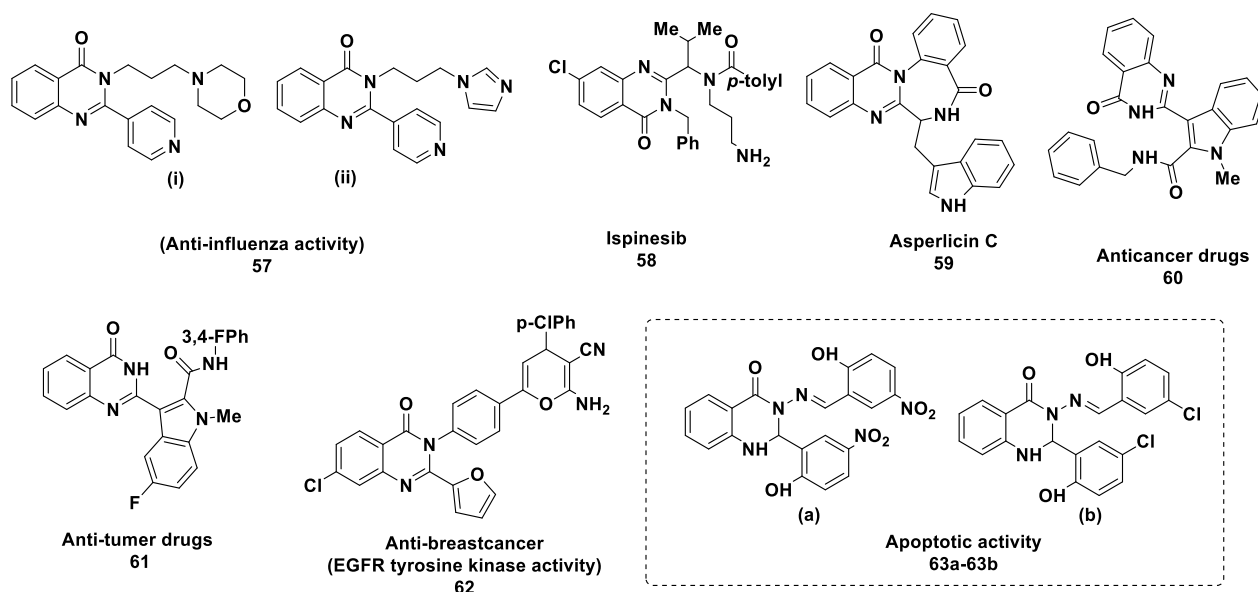


Figure-5: Selected biological active molecules with quinazoline-one as a core moiety.

1.6 Biologically active compounds of isoxazole moiety

Isoxazoles are five-membered heterocyclic molecules with adjacent nitrogen and oxygen and are a privileged class of compounds. This scaffold is a part of biological molecules^{28a,b} with ulcerogenic, antiviral (**64**), analgesic, and anticancer activity. Some of the isoxazoles work as modulators of nicotinic receptors (**65**), anti-inflammatory (Valdecoxib; **66**),^{29a} anti-rheumatic (Leflunomide; **67**), antibiotic (sulfamethoxazole; **68**),^{29b} herbicide (isoxaflutole; **69**).^{29c} Isoxazole skeleton also can be seen in natural molecules like muscimol (**70**), GABA receptor, anti-depressant and psychoactive compounds (Ibotenic acid; **71**),^{30a} penicillin, AMPA, and inotropic glutamate receptor antagonist (**72**), central nervous system (CNS) receptors^{30b} and anticancer activity against human cancer cell lines (cervical breast, MCF-7, HeLa, prostate)^{30c} and can be used as bioisosteres for the carbocycles and SAR studies in drug development methods.

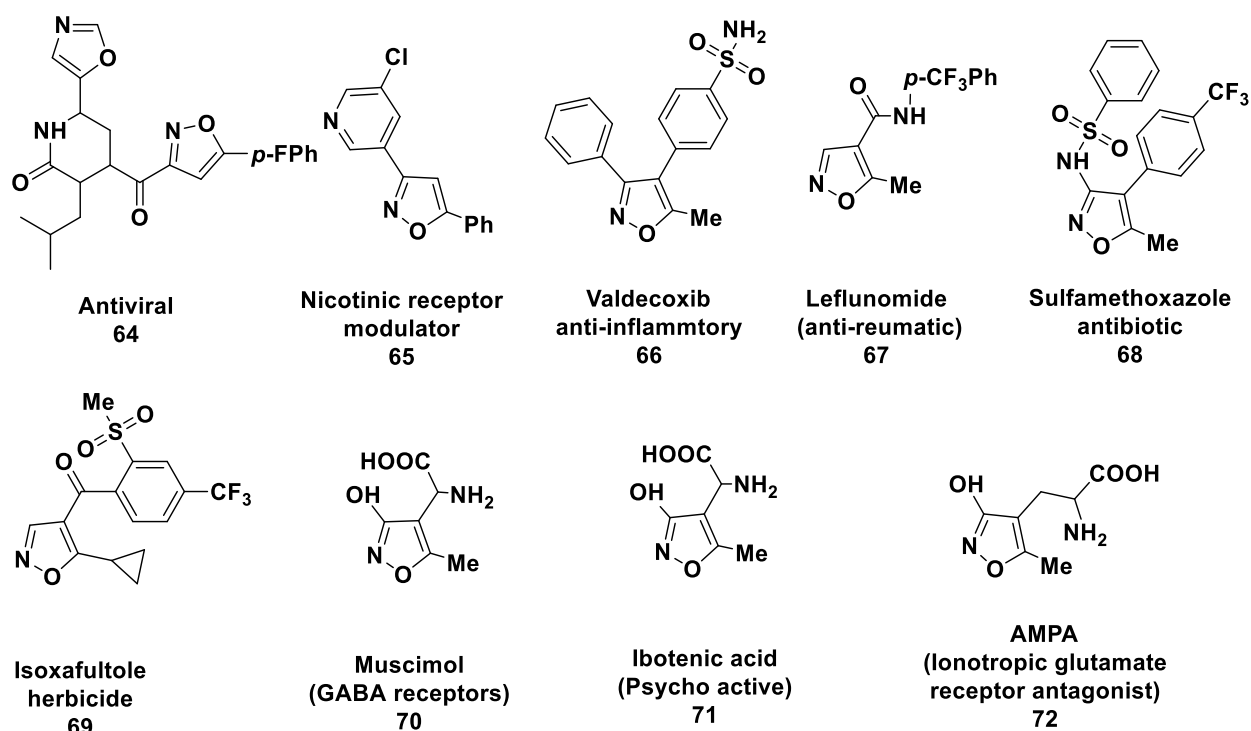


Figure-6: Selected biological active molecules of isoxazole moieties.

1.7 Biologically active compounds of 1,3,4-oxadiazoles

1,3,4-Oxadiazoles are five-membered heterocyclic compounds present in natural and biological compounds^{31a} as anti-proliferative (73), insecticidal (74),^{31b} anti-TB (75),^{31c} cytotoxicity (76), anti-mycobacterial (77),^{31d} anti-malarial (78),^{31e} anti trypanosomal^{32a} (79), anthelmintic^{32b} (80) antitumor activity (81),^{32c} α -glucosidase inhibitor (82),^{32d} monoamine oxidase inhibitor, stimulation of central nervous system (CNS), benzodiazepine receptor agonist^{33a} and pseudomonas quorum-sensing receptor antagonist. Substituted 1,3,4-oxadiazole are excellent compounds for luminescent properties and are widely utilized in the electron transporters (83), development of OLEDs, and chemosensors.^{33b}

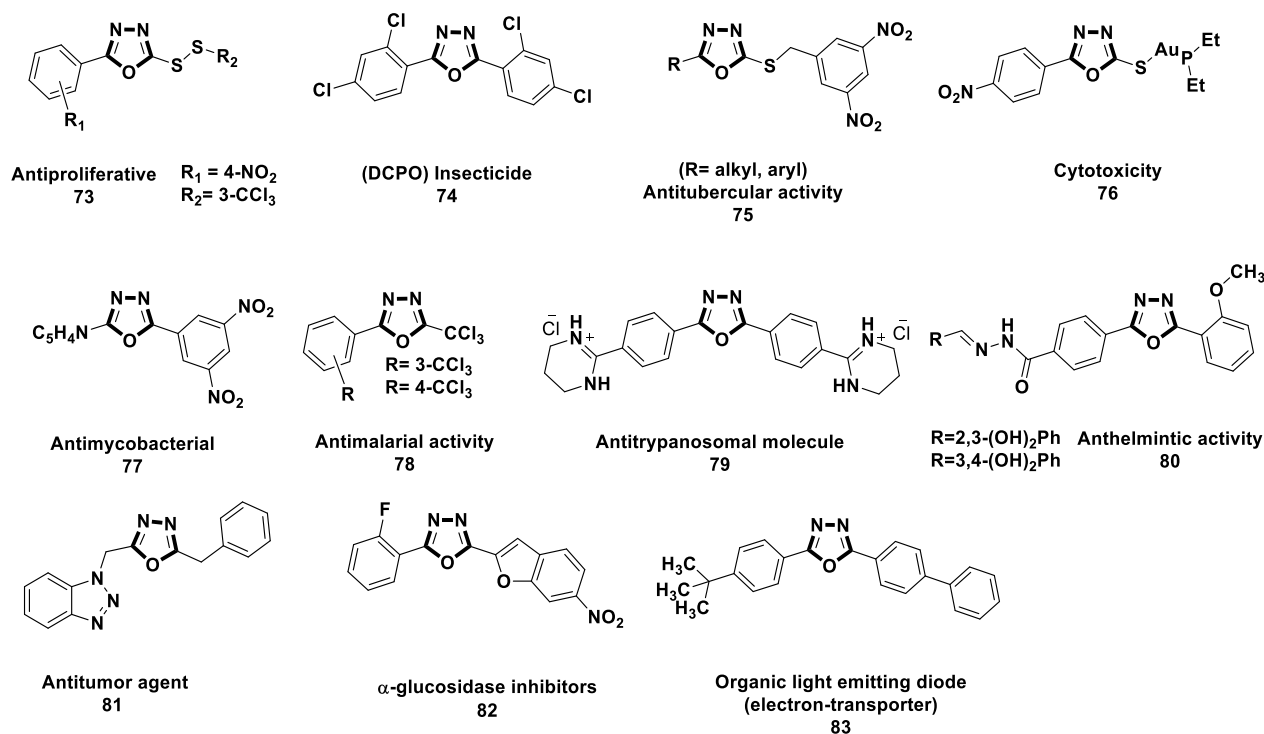


Figure-7: Selected biologically active molecules of 1,3,4-oxadiazoles.

1.8 Biologically active compounds with benzene sulfonate esters

The benzene sulfonate ester is an attractive functional group seen in medicinal and biologically active molecules.^{33c-d} Thiozolidinone sulfonate ester scaffolds are known to show monoamine oxidase,^{34a} aldose reductase^{34b} (**84**), and MAO-Is (**85**) inhibition. In addition, 2,4-thiazolidinone sulfonate ester conjugates exhibit anti-hyperglycemic activities and PTP1B inhibitor (A and B) (**86**)^{34c} properties as shown in **Figure-8a**.

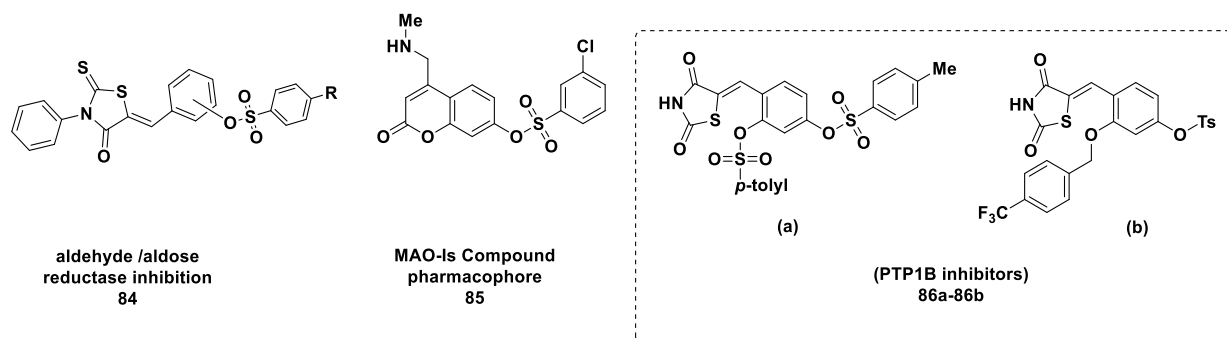


Figure-8a: Selected biologically active molecules of benzene sulfonate esters.

1.9 Catalyst-free, water-mediated reactions in organic synthesis

Green chemical reactions are the current focus of academic and industrial research. Many green solvents like the use of water and ionic liquids under catalyst-free conditions have been a main focus in the past few decades. The use of water as a solvent minimizes time, labor, cost,

production of waste, and emission of hazardous and toxic chemicals.^{35a} The inter and intramolecular H-bonding of water are responsible for inducing the hydrophobic interactions with organic molecules. As a result, the aggregations of organic molecules make the inter-atomic interaction and success of the reaction (**Figure-8b (B)**). The replacing of volatile solvents with water in organic reactions is an important aim of green chemistry.^{35b} This has been triggered by the inventions of the “on water concept” by Breslow and Sharpless groups.^{35(c-f)}

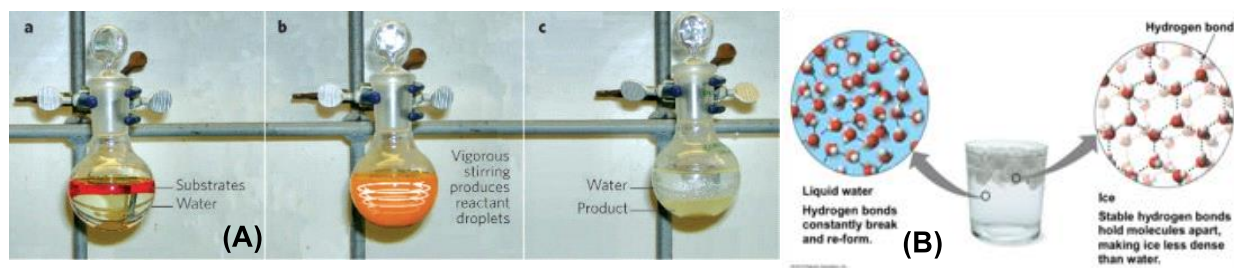


Figure 8b: (A) Organic reaction carried in three stages in ‘on water’ protocol. (B) Formation of hydrogen bonding in water and Ice.

1.10 Deep Eutectic Solvents in organic synthesis:

Deep eutectic solvents (DESs) are also termed as deep eutectic ionic liquids (DEILs) which are formed by mixing two components,^{36a} with hydrogen bond donor (HBD) and hydrogen bond acceptor (HBAs) with the capability to have a self-association with intermolecular hydrogen bonding. These two components collectively form a transparent liquid at or below 100 °C whose melting points are lower than that of two independent components. The DES mixture enhances the reactivity of the reaction mixture with the formation of strong hydrogen bonding with the starting materials. Interestingly, DESs is an advanced version of ionic liquids and work as a green catalyst as well as a reaction medium. DESs are unique in their physicochemical properties such as freezing point, ionic conductivity, density, and viscosity compared to ionic liquids and thus has many advantages in synthetic organic chemistry. They can be easily made from commercially available, cheap components including biological molecules like α -amino acids and monosaccharides, etc.^{36(b-f)} Thus, they can be used as alternative solvents for the enzyme-catalyzed reactions, CO₂ absorption, electrochemistry, material preparation, biodiesel synthesis, nanotechnology, and organic chemistry.

1.11 Multicomponent (one-pot) reactions.

Multicomponent reaction in which three or more components are combined to form a new product in a single pot. The characteristic feature of MCRs is final adducts having nearly all parts

of precursors without forming any by-products. The Strecker synthesis^{37a} of α -amino nitriles is one of the first examples of multi-component approaches reported in the 1950s. Ivar Ugi discovered a ugi four-component reaction^{37b} with isocyanides is a pioneering contribution in this area. MCRs are ideal for atom economy, eco-friendly reaction conditions, avoiding multiple steps, decreasing chemical wastage, and isolation of the products that are suitable for library generation in drug discovery.

1.12 Objectives of the thesis

Based on the above discussion and considering the biological importance of the heterocyclic scaffolds the present thesis is divided into the chapters with the titles given below

Chapter-2: *Deep Eutectic Solvents (DES) mediated synthesis of styrylquinolines and styrylquinoline-sulfonates via Friedländer synthesis and sp^3 C-H activation, their biological evaluation as α -Glucosidase inhibitors and photophysical studies*

Chapter-3: *Facile synthesis of quinoxaline, quinoxaline-2-one, quinazoline-based styryls, sulfonate-styryls via sp^3 C-H activation and their evaluation as α -glucosidase inhibitors*

Chapter-4: *Synthesis of spiro and bicyclic thiolane derivatives via 1,4-Michael addition followed by intramolecular aldol reactions*

Chapter-5: *$SnCl_2$ -catalyzed synthesis of dibenzo-[1,4]-diazepin-1-one, phenyl quinazoline, and 2,5-substituted 1,3,4-oxadiazoles based sulfonate esters and their evaluation as α -glucosidase inhibitors*

Chapter-6: *Synthesis of quinazolinone Schiff base, isoxazole-styrene, and isoxazole-thiolane sulfonate ester conjugates*

Based on these titles, a brief introduction to specific examples of the title compounds, and literature methods for their synthesis are discussed along with the importance of current findings (biological evaluation, photophysical properties, computational studies) and spectral analysis.

References:

- 1 Harikishan, S.; Kapoor, V. K. *A textbook of medicinal & pharmaceutical chemistry*. 2nd edition, **2008**, 264.
- 2 Gupta, M. *Int. J. Physical, Chem. Mat. Sci.* **2015**, 4(1), 21.
- 3 Saini, M. S.; Kumar, A.; Dwivedi, J.; Singh, R. *Int. J. Pharm. Sci. Res.* **2013**, 4(3), 66.

- 4 (a) Ebenso, E. E.; Kabanda, M. M.; Arslan, T.; Saracoglu, M.; Kandemirli, F.; Murulana, L. C.; Singh, A. K.; Shukla, S. K.; Hammouti B. and Khaled, K. *Int. J. Electrochem. Sci.* **2012**, 7, 5643. (b) Musiol, R. *Curr. Pharm. Des.* **2013**, 19, 1835.
- 5 (a) Chang, F. -S.; Chen, W.; Wang, C.; Tzeng, C.-C.; Chen, Y.-L. *Bioorg. Med. Chem.* **2010**, 18, 124. (b) Mahamoud, A.; Chevalier, J.; Davin-Regli, A.; Barbe J. and Pagès, J. M. *Curr. Drug Targets* **2006**, 7, 843. (c) Basabe - Desmonts, L.; Reinhoudt, D. N. and Crego-Calama, M. *Chem. Soc. Rev.* **2007**, 36, 993.
- 6 (a) Sayed, M.; Mokle, S.; Bokhare, M.; Mankar, A.; Surwase, S.; Bhusare, S.; Vibhute, Y. *ARKIVOC.* **2006**, II, 187. (b) Liesen, A. P.; Aquino T. M.; Carvalho, C. S.; Lima, V. T.; Araujo, J. M.; Lima, J. G.; Faria, A. R.; Melo, E. J. T.; Alves, A. J.; Alves, E. W.; Alves, A. Q.; Goes, A. S. *Eur. J. Med. Chem.* **2010**, 45, 3685. (c) Rawal, R. K.; Srivastava, T.; Haq, W and Katti, S. B. *J. Chem. Res.* **2004**, 5, 368. (d) Chandrappa, S.; Kavitha, C. V.; Shahabuddin, M. S.; Vinaya, K.; Anandakumar, C. S.; Ranganatha, S. R.; Raghavan, S. C.; Rangappa, K. S. *Bioorg. Med. Chem.* **2009**, 17, 2576. (e) Dave, T. K.; Purohit, D. H.; Akbari, J. D.; Joshi, H. S. *Ind. J. Chem.* **2007**, 46B, 352. (f) Rawal, R. K.; Tripathi, R. K.; Katti, S. B.; Pannecouque, C.; Clercq, D. E. *Med. Chem.* **2007**, 3, 355.
- 7 (a) Rawal, R. K.; Prabhakar, Y. S.; Katti, S. B.; Clercq, De. E. *Bioorg. Med. Chem.* **2005**, 13(24), 6771–6776. (b) Surender, S. J.; Nayan, S. B.; Hilgenfeld, R.; Pastorino, B.; Xavier de. L.; Jayaprakash, V. *Eur. J. Med. Chem.* **2015**, 89, 172.
- 8 (a) Yuasa, H.; Takada, J and Hashimoto, H. *Bioorg. Med. Chem. Lett.* **2001**, 11, 1137. (b) Johnson, J. W.; Evanoff, D. P.; Savard, M. E.; Lange, G.; Ramadhar, T. R.; Assoud, A.; Taylor, N. J.; Dmitrienko, G. I. *J. Org. Chem.* **2008**, 73, 6970. (c) Ibrahim, P. N.; Cho, H.; England, B.; Gillette, S.; Artis, D. R.; Zuckerman, R. and Zhang, C. *US Pat.* **2013**, 8, 470, 821, B2. (d) Maclean, D.; Holden, F.; Davis, A. M.; Scheuerman, R. A.; Yanofsky, S.; Holmes, C. P.; Fitch W L, Tsutsui K, Barrett R W, Gallop M. A. *J. Comb. Chem.* **2004**, 6, 196. (e) Ottana, A.; Maccari, R.; Giglio, M.; Corso, A. D.; Cappiello, M.; Mura, U.; Cosconati, S.; Marinelli, M.; Novellino, E.; Sartini, S.; La-Motta, C.; Settimo, F. D. *Eur. J. Med. Chem.* **2011**, 46, 2797.
- 9 (a) Reynolds, R. C.; Campbell, S. R.; Fairchild, R. G.; Kisliuk, R. L.; Micca, P. L.; Queener, S. F.; Riordan, J. M.; Sedwick, W. D.; Waud, W. R.; Leung, A. K.; Dixon, R. W.; Suling, W. J.; Borhani, D. W. *J. Med. Chem.* **2007**, 50, 3283. (b) Volkmann, R. A.; Kelbaugh, P. R.; Nason, D. M.; Jasys, V. J. *J. Org. Chem.* **1992**, 57, 4352. (c) Le, H. V.; Hawker, D. D.; Wu, R.; Doud, E. H.; Widom, J. R.; Sanishvili, R.; Liu, D.; Kelleher, N. L.; Silverman. R. B. *J. Am. Chem. Soc.* **2015**, 137, 4525.

- 10 (a) Foye, W. O. *Principi di Chemico Farmaceutica*; Piccin: Padora, Italy, **1991**, 416. (b) Feuer, G.; *Progress in Medicinal Chemistry*; Ellis, G. P., West, G. P., Eds.; *North-Holland Publishing Company: New York*, **1974**, 10, 85. (c) Livingstone, R. *Nature* **1963**, 200, 509. (d) Morgan, L. R.; Jursic, B. S.; Hooper, C. L.; Neumann, D. M.; Thangaraj, K.; Leblance, B. *Bioorg. Med. Chem. Lett.* **2002**, 12, 3407. (e) De Andrade-Neto, V. F.; Goulart, M. O.; 17 Da Silva Filho, J. F.; Da Silva, M. J.; Pinto, M. D. C.; Pinto, A. V.; Zalis, M. G.; Carvalho, L. H.; Krettli, A. U. *Bioorg. Med. Chem. Lett.* **2004**, 14, 1145.
- 11 Solary, E.; Dubrez, L.; Eymin, B. *Eur. Respir. J.* **1996**, 9, 1293-1305.
- 12 (a) Arthur, G.; Elor, K. B.; Robert, G. S.; Guo, Z. Z.; Richard, J. P.; Stanley, D.; John, R. K.; Sean, T. *J. Med. Chem.* **2005**, 48, 744. (b) Ajani, O. O.; Obafemi, C. A.; Nwinyi, O. C.; Akinpelu, D. A. *Bioorg. Med. Chem.* **2010**, 18, 214. (c) Xu, B.; Sun, Y.; Guo, Y.; Cao, Y.; Yu, T. *Bioorg. Med. Chem.* **2009**, 17, 2767. (d) Wagle, S.; Adhikari, A. V.; Kumari, N. S. *Indian J. Chem.* **2008**, 47B, 439. (e) Ries, U. J.; Priepke, H. W. M.; Hael, N. H.; Handschuh, S.; Mihm, G.; Stassen, J. M.; Wienen, W.; Nar, H. *Bioorg. Med. Chem. Lett.* **2003**, 13, 2297.
- 13 Wang, L.; Liu, J.; Tian, H.; Qian, C. *Synth. Commun.* **2004**, 34, 1349.
- 14 Esther, V.; Pablo, R.; Duchowicz, B.; Eduardo, A.; Castro, A.; Antonio, M. *J. Mol. Graph. Model.* **2009**, 28, 28.
- 15 (a) Hegedus, L. S.; Greenberg, M. M.; Wendling, J. J.; Bullock, J. P. *J. Org. Chem.* **2003**, 68, 4179. (b) Monge, A.; Palop, J. A.; Urbasos, I.; Fernández-Alvarez, E. *J. Heterocyclic Chem.* **1989**, 26 (6), 1623. (c) Kim, Y. B.; Kim, Y. H.; Park, J. Y.; Kim, S. K. *Bioorg. Med. Chem. Lett.* **2004**, 14, 541.
- 16 Bhosale, R. S.; Sarda, S. R.; Andhapure, S. S.; Jadhav, W. N.; Bhusare, S.R.; Pawar, R. P. *Tetrahedron Lett.* **2005**, 46, 7183.
- 17 (a) Tsami, A.; Bunnagel, T.W.; Farrell, T.; Scharber, M.; Choulis, S. A.; Brabec, C. J.; Scherf, U. *J. Mater. Chem.* **2007**, 17, 1353. (b) Thomas, K R. J.; Velusamy, M.; Lin, J. T.; Chuen, C. H.; Tao, Y. T. *Chem. Mater.* **1860**, 2005, 17. (c) Yadav, M. R.; Shirude, S. T.; Parmar, A.; Balaraman, R. and Giridhar, R. *Chem. heterocycl. comp.* **2006**, 42, 1038. (d) Seo, H. N.; Choi, J. Y.; Choe, Y. J.; Kim, Y.; Rhim, H.; Lee, S. H.; Kim, J.; Joo, D. J.; Lee, J. Y. *Bioorg. Med. Chem. Lett.* **2007**, 17, 5740.
- 18 (a) Slichenmeyer, W. J.; Elliott, W. L.; Fry, D. W. *Semin. Oncol.* **2001**, 28, 67. (b) Santosh N. M.; Akash, D. P.; Pritam, N. D.; Nikhil, S. S.; Pankaj, B. M., *Bioorg. Med. Chem. Lett.* **2016**, 26, 272. (c) Xia, Y.; Yang, S.Y.; Hou, M. J.; Kuo, S. C.; Xia, P.; Bastow, K. F., Nakanishi,

- Y.; Nampoothiri, P.; Hackl, T.; Hamel, E. and Lee, K. H. *Bioorg. Med. Chem. Lett.* **2001**, *11*, 1193.
- 19 (a) Abdel, G. N. M.; Georgey, H. H.; Youssef, R. M.; El-Sayed, N. A. *Eur. J. Med. Chem.* **2010**, *45*, 6058. (b) Yuasa, H.; Takada, J. and Hashimoto, H. *Bioorg. Med. Chem. Lett.* **2001**, *11*, 1137.
- 20 Alanine, A.; Gobbi, L. C.; Kolczewski, S.; Luebbbers, T.; Peters, J.-U.; Steward, L. *U.S. Pat.*, US2006293350 A1, **2006**, *146*, 100721.
- 21 (a) Cortés, E.C.; Ana, L.V.C.; Olivia, G.M. *J. Heterocycl. Chem.* **2007**, *44*, 183. (b) Micale, N.; Kozikowski, A. P.; Ettari, R.; Grasso, S.; Zappala, M.; Jeong, J. J.; Kumar, A.; Hanspal, M. and Chishti, A. H.; *J. Med. Chem.* **2006**, *49*, 3064. (c) Klaubert, D. H.; Flemington, N. J.; Stanley, C. B.; Pattison, T.W and Rees, R. W., *US Pat.*, 4 495101, **1985**.
- 22 (a) Vandyck, K.; Cummings, M. D.; Nyanguile, O.; Boutton, C.W.; Vendeville, S.; McGowan, D.; Devogelaere, B.; Amssoms, K.; Last S., Rombauts K., Tahri A., Lory P., Hu L.; Beauchamp, D. A.; Simmen, K.; Raboisson, P. *J. Med. Chem.* **2009**, *52*, 4099. (b) Yi, W.B.; Cai, C. *J. Fluorine Chem.* **2009**, *130*, 1054. (c) Cortés, E.C.; Ana, L.V.C.; Olivia, G.M. *J. Heterocycl. Chem.* **2007**, *44*, 183. (d) Naeimi, H.; Foroughi, H. *New J. Chem.* **2015**, *39*, 1228. (e) Collado, M. C.; Beleta, J.; Martinez, E.; Miralpeix, M.; Dome`nech, T.; Palacios, J. M.; Herna´ndez J. *Br. J. Pharmacol.* **1998**, *123*, 1047. (f) Wang, Y.; Konkoy, C.S.; Ilyin, V. I.; Vanover, K. E.; Carter, R. B.; Weber, E.; Keana, J. F. W.; Woodward, R. M.; Cai S. X. *J. Med. Chem.* **1998**, *41*, 2621.
- 23 (a) Smits, R. A.; Lim, H. D.; Stegink, B.; Bakker, R. A.; de Esch, I. J. P.; Leurs, R. *J. Med. Chem.* **2006**, *49*, 4512. (b) Yakeya, D.; Kitou, N.; Kinugawa, S.; Moriguchi, T.; Tsuge, A. *Tetrahedron* **2017**, *73*, 3973. (c) Ramajayam, R.; Girdhar, R.; Yadav, M. R. *Mini-Rev. Med. Chem.* **2007**, *7*, 793.
- 24 (a) Fu, J.-S.; Shuttleworth, S. J.; Connors, R. V.; Chai, A.; Coward, P.; *Bioorg. Med. Chem. Lett.* **2009**, *19*, 4264. (b) Schimer, J.; Cigler, P.; Vesely, J.; Grantz-Saskova, K.; Lepsik, M.; Brynda, J.; Rezacova, P.; Kozisek, M.; Cisarova, I.; Oberwinkler, H.; Kraeusslich, H.-G.; Konvalinka, J. *J. Med. Chem.* **2012**, *55*, 10130.
- 25 (a) Patel, N. B.; Patel, V. N.; Hemant, R. P; Faiyaz, M. S.; Jaymin, C. P. *Acta Polo Pharm Drug Res.* **2010**, *67*, 267. (b) Fadhil, L.F.; Maryam, Z.; Mohammadjavad P.; Chung, Y. L.; Nazia, A. M.; Hapipah, M. A.; Noraini, A.; Nura, S. G. and Mahmood, A. A. *Sci. World J.* **2014**, *15*, 212096. (c) Abid, O.H. & Ahmed, A.H. *Inter J. Appl. Nat. Sci.* **2013**, *2*, 11.

- 26 (a) Demeunynck, M.; Baussanne, I. *Curr. Med. Chem.* **2013**, *20*, 794. (b) Manasa, A.K.; Sidhaye, R.V.; Radhika, G.; Nalini, C.N. *Current Pharma Research.* **2011**, *1*, 101. (c) Danilov, A.V. *Clin. Ther.* **2013**, *35*, 1258.
- 27 (a) Ahmed, M. F.; Youns, M. *Archiv der Pharmazie.* **2013**, *346*, 610. (b) Stacy, L. M.; Michael, Y. F.; Senthil K. M.; Roberto, B.; Jean, F. S.; Carlos L. A. *Cancer research.* **2001**, *61*, 8887. (c) Maryam, Z.; Fadhil, L. F.; Mohammadjavad, P.; Chung, Y. L.; Maryam, H.; Mohadeseh, H.; Behnam, K.; Nazia, A. M.; Hapipah, M. A.; Mahmood, A. A. *Sci. Rep.*, **2015**, *5*, 11544.
- 28 (a) Katritzky, A. R.; Ramsden, C. A.; Scriven, E. F. V.; Taylor, R. J. K. *Comprehensive Heterocyclic Chemistry III, Pergamon, Oxford, UK*, **2008**. (b) Daidone, G.; Raffa, D.; Maggio, B.; Plescia, F.; Cutuli, V. M. C.; Mangano, N. G.; Caruso, A. *Arch. Pharm. Pharm. Med. Chem.* **1999**, *332*, 50.
- 29 (a) Kankala, S.; Kankala, R. K.; Gundepaka, P.; Thota, N.; Nerella, S.; Gangula, M. R.; Guguloth, H.; Kagga, M.; Vadde, R.; Vasam, C. S. *Bioorg. Med. Chem. Lett.* **2013**, *23*, 1306. (b) Kakarla, R.; Liu, J.; Naduthambi, D.; Chang, W.; Mosley, R. T.; Bao, D.; Steuer, H. M. M.; Keilman, M.; Bansal, S.; Lam, A. M.; Seibel, W. *J. Med. Chem.* **2014**, *57*, 2136. (c) Monge, D.; Jiang, H.; Alvarez-Casao, Y. *Chem. Eur. J.* **2015**, *12*, 4494.
- 30 (a) Barmade, M. A.; Murumkar, P. R.; Sharma, M. K.; Yadav, M. R. *Curr Top Med Chem.* **2016**, *16*, 2863. (b) George, N. P.; Fereniki, P.; Petros, G. T. and George, V. *Chem. Med. Chem.* **2017**, *12*, 1. (c) Kumar, G. B.; Bukhari, S. N. A.; Qin, H.-L. *Chem. Biol. Drug Des.* **2017**, *89*, 634.
- 31 (a) Wen, C.-R.; Wang, Y.-J.; Wang, H.-C.; Sheu, H.-S.; Lee, G.-H.; Lai, C. K. *Chem.Mater.* **2005**, *17*, 1646. (b) Zheng, X.; Li, Z.; Wang, Y.; Chen, W.; Huang, Q.; Liu, C.; Song, G. J. *Fluorine Chem.* **2003**, *123*, 163. (c) Sonia, G.; Ravi, T. K. *Med. Chem. Res.* **2013**, *22*, 3428. (d) Dhumal, S. T.; Deshmukh, A. R.; Bhosle, M. R.; Khedkar, V. M.; Nawale, L. U.; Sarkar, D.; Mane, R. A. *Bioorg. Med. Chem.Lett.* **2016**, *26*, 3646. (e) Hutt, M. P.; Elslager, E. F.; Werbel, L. M. *J. Heterocycl. Chem.* **1970**, *7*, 511.
- 32 (a) Das, B. P.; Boykin, D. W. *J. Med. Chem.* **1977**, *20*, 531. (b) Patel, K.; Chandran, J. E.; Shah, R.; Vijaya, J.; Sreenivasa, G. M. *Int. J. Pharma Bio Sci.* **2010**, *1*, 1. (c) Luo, Y.; Liu, Z. J.; Chen, G.; Shi, J.; Li, J. R.; Zhu, H.-L. *Med. Chem. Commun.* **2016**, *7*, 263. (d) Taha, M.; Ismail, N. H.; Imran, S.; Wadood, A.; Rahim, F.; Saad, S. M.; Khan, K. M.; Nasir, A. *Bioorg. Chem.* **2016**, *66*, 117.
- 33 (a) Carroll, F. I.; Gray, J. L.; Abrahm, P.; Kuzemko, M. A.; Lewin, A. H.; Boja, J. W.; Kuhar, M. J. *J. Med. Chem.* **1993**, *36*, 2886. (b) Ogata, M.; Atobe, H.; Kushida, H.; Yamamoto, K. *J. Antibiot.* **1971**, *24*, 443. (c) Pisani, L.; Bareletta, M.; Soto-Otero, R.; Nicolotti, O.; Mendez-

- Alvarez, E.; Catto, M.; Introcaso, A.; Stefanachi, A.; Cellamare, S.; Altomare, C. and Carotti A. *J. Med. Chem.* **2013**, 56, 2651. (d) Wang, P.; Min, J.; Nwachukwu, J. C.; Cavett, V.; Carlson, K. E.; Guo, P.; Zhu, M.; Zheng, Y.; Dong, C.; Katzenellenbogen, J. A.; Nettles, K. W.; Zhou, H. *J. Med. Chem.* **2012**, 55, 2324.
- 34 (a) Wang, P.; Min, J.; Nwachukwu, J. C.; Cavett, V.; Carlson, K. E.; Guo, P.; Zhu, M.; Zheng, Y.; Dong, C.; Katzenellenbogen, J. A.; Nettles, K. W.; Zhou, H. *J. Med. Chem.*, **2012**, 55, 2324. (b) Hina, A.; Yildiz, T.; Farrukh, J.; Imtiaz, K.; Jamshed, I.; Shahid, H. *Bio.Org. Chem.* **2017**, 75, 1. (c) Manoj, K. M.; Rajnish, K.; Manoj, K. *Med. Chem. Res.* **2018**, 27, 476.
- 35 (a) Sachdeva, H.; Khaturia, S. *Biorg. Org. Chem.* **2017**, 1 (7), 239. (b) Mikami, K. *Blackwell Publishing Ltd*, 9600 Garsington Road, Oxford OX4 2DQ, UK. **2005**, 26. (c) Breslow, R. *Acc. Chem. Res.* **2004**, 37, 471. (d) Duan, J.; Jiang, B.; Chen, L.; Lu, Z.; Barbosa, J.; Pitts, W. J. *US Pat. Appl.* **2003**, 0229084. (e) Zarei, M.; Jarrahpour, A. *Iran. J. Sci. Technol. Trans. A: Sci.* **2011**, A3, 235. (f) Pravin, V. S.; Jitendra, B. G.; Bapurao, B. S.; Murlidhar, S. S. *Bull Kor. Chem. Soc.* **2012**, 33 (4), 1345.
- 36 (a) Peng, L.; Jian W. H.; Li-Ping, M.; Zhan, H. Z. *RSC Adv.* **2015**, 5, 48675. (b) Smith, E. L.; Abbott, A. P.; Ryder, K. S. *Chem. Rev.* **2014**, 114, 11060. (c) Durand, E.; Lecomte, J.; Villeneuve, P. *Eur. J. Lipid Sci. Technol.* **2013**, 115, 379. (d) Rodriguez, N. R.; Gonzalez, A. S. B.; Tijssen, P. M. A.; Kroon, M. C. *Fluid Phase Equilib.* **2015**, 385, 72. (e) Hillman, A. R.; Ryder, K. S.; Zaleski, C. J.; Ferreira, V.; Beasley, C. A.; Vieil, E. *Electrochim. Acta*, **2014**, 135, 42. (f) Wagle, D. V.; Zhao, H.; Baker, G. A. *Acc. Chem. Res.* **2014**, 47, 2299.
- 37 (a) Strecker, A.; Justus, L. *Ann. Chem.* **1850**, 75, 27. (b) Ugi, I. *Pure Appl. Chem.* **2001**, 73 (1), 187.

CHAPTER-2

Deep Eutectic Solvents (DES) mediated synthesis of styrylquinolines and styrylquinoline-sulfonates via Friedländer synthesis and sp^3 C-H activation, their biological evaluation as α -Glucosidase inhibitors, and photophysical studies

Abstract

Functionalized quinoline derivatives have emerged as one of the key scaffolds in medicinal chemistry. Similarly, 2-styrylquinolines are gaining attention in synthetic organic and materials chemistry for the functionalization (via sp^3 C-H activation) and photophysical properties. In this backdrop, we intended to develop a simple strategy for the synthesis of styrylquinolines. Thus, a green and catalyst-free protocol for the synthesis of 2-styrylquinolines using dimethyl urea and L-tartaric acid as deep eutectic solvent is described in this chapter. The photophysical properties of the synthesized 2-styrylquinolines are studied along with DFT calculations. Also, the resulting molecules were evaluated for the α -Glucosidase inhibition activity. The detailed methodology and description of photophysical, and computational studies and the results of α -Glucosidase inhibition activity are discussed in this chapter.

2.1 Introduction

2.1.1 Reported methods for the synthesis of substituted 2-styrylquinolines

Quinoline moiety is one of the important and privileged scaffolds in medicinal chemistry and some of the examples are discussed in Chapter-1 in this regard. Along with these, 2-styrylquinolines are also found in many natural,^{1a-c} and biological compounds.^{1d-e,2a-b} As a result, quinoline scaffold has emerged as one of the important structures for the development of antimalarial,^{3a} anti-cancer,^{3b} and anti-inflammatory drugs.^{3c} Usually, 2-/4-styrylquinolines are synthesized using a two-step protocol i.e., the Friedländer or Pfitzinger reaction^{4a-c} aldol/Perkin,^{5a-d} Wittig-type^{6a} reactions. The synthesis of quinolone-based molecules is also reported using Sonogashira coupling of propargyl alcohols with 2-haloanilines followed by isomerization^{6b} and multicomponent reactions.⁷

Recently, this trend shifted towards the sp^3 C–H activation of the methyl group of azaarenes (α -picoline and 2-methyl quinoline) as nucleophiles because of their possible enamine tautomeric form. Some of these methods include the dehydrogenative direct olefination of alcohols in the presence of $NiBr_2$ ^{8a,b} or $Mn(CO)_5Br$,^{8c} using aldehydes as partners in the presence of $Fe(OAc)_2$,^{8d} $InCl_3$,^{8e} $CoCl_2$,^{8f} or $Ca(OTf)_2$,^{8g} an iron-based metal-organic framework $[Fe_3O(BPDC)_3]$ ^{8h} and Al_2O_3 -supported Pt ⁸ⁱ as heterogeneous and homogeneous catalysts, $Fe(OAc)_2$ -catalyzed alkenylation of N-sulfonyl imines,^{8j} metal-free oxidative olefination of primary amines,^{8k} and the catalyst-free activation of 2-methyl azaarenes using 1,4-dioxane^{9a} or water^{9b} as reaction medium. Along with these, 2-styrylquinolines were synthesized using a one-pot approach *via* Friedländer annulation and Knoevenagel condensation reactions in the presence of 1-methylimidazolium trifluoroacetate ($[Hmim]TFA$),^{10a} (Scheme-1) Brønsted acidic imidazolium ionic liquids as the reaction medium,^{10b} and $In(OTf)_3$ as the Lewis acid under solvent-free conditions¹¹ (**Figure-1**). During the preparation of the revised document, we found that Nawaz Khan's group used ruthenium and iridium-based catalysts for the synthesis of 2-styrylquinolines via the sequential dehydrogenative Friedlander reaction and sp^3 C–H activation.^{12(a-b)} Also, the use of benzophenones or isatins as starting materials is a known method for 2-styrylquinolines.¹³

Deep eutectic solvents (DESs) are prepared from natural materials and show unique physicochemical and non-toxic/biodegradable properties.^{14,15} Considering this, DESs have been extensively used in organic synthesis^{16,17} and biocatalysis.¹⁸

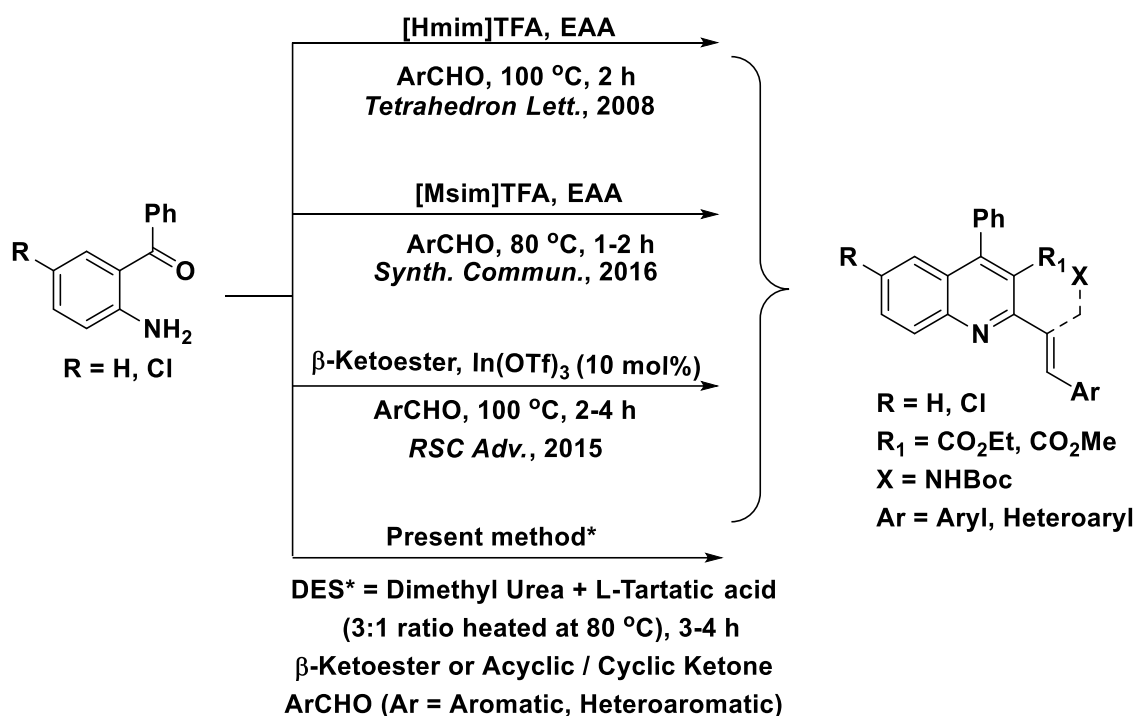


Figure-1: Literature methods for the one-pot synthesis of 2-styrylquinolines *via* sp³ C–H activation and the present method.

2.2 Present study

Considering the biological and materials importance of the 2-styrylquinolines and based on the literature reports for the sp³ C–H activation of azaarenes, we envisaged the synthesis of functionalized quinolines and tetrahydroacridine/1,2,3,4-tetrahydrobenzo[*b*][1,6]-naphthyridines *via* a multicomponent sp³ C–H functionalization starting from aminobenzophenones, carbonyl compounds and aldehydes under green conditions (using deep eutectic solvents as shown below (**Figure-2**)).

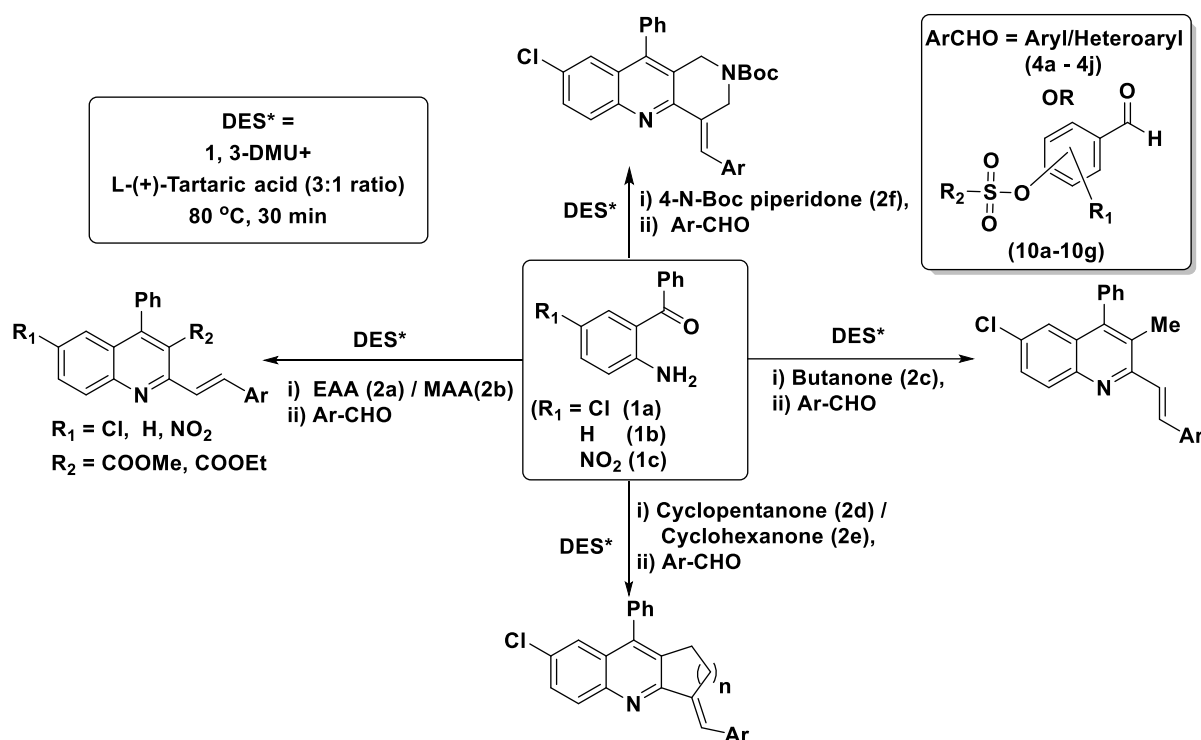
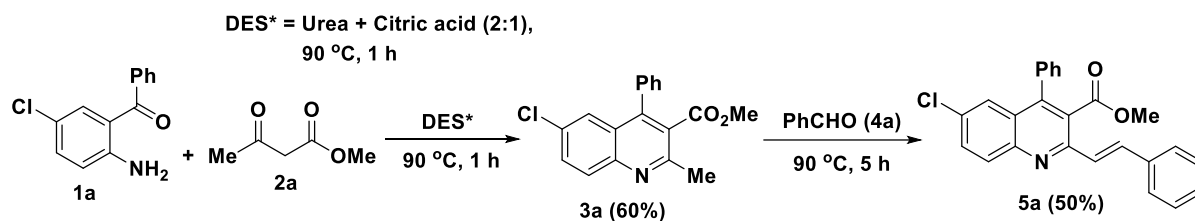


Figure-2: Present study of the synthesis of substituted 2-styrylquinolines.

2.3 Results and discussion

Towards achieving the goal, an initial study was started with the preparation of DES (1.5 g) by heating urea and citric acid (2:1; as hydrogen bond donor-acceptor) mixture for 1 h at 90 °C as shown in **Scheme-1**. After that, 2-amino-5-chlorobenzophenone (**1a**) (1.0 mmol) and methyl acetoacetate (**2a**) (1.0 mmol) were added and heated at 90 °C for 1 h to get 2-methyl quinoline (**3a**) in 60% yield. To this, benzaldehyde (**4a**) (1 mmol) was added and heating continued at 90 °C for 5 h to give the activation product (**5a**) in 50% yield (**Scheme-1**). The same reaction was also attempted by trapping the 2-methylquinoline (**3a**) in situ and treating it with an aldehyde to give the activation product **5a** with the same yield. Encouraged by these results and to improve the yield, experiments were performed using different combinations of hydrogen bond donor (urea/dimethyl urea/thiourea) and acceptor (citric acid/tartaric acid/oxalic acid) as shown in **Table-1**. Among the screened conditions, a combination of 1,3-DMU+LTA (3:1) at 80 °C for 3 h was found to be a suitable condition for the success of the reaction with the desired product up to **95% yield (Entry-6; Table-1)**.



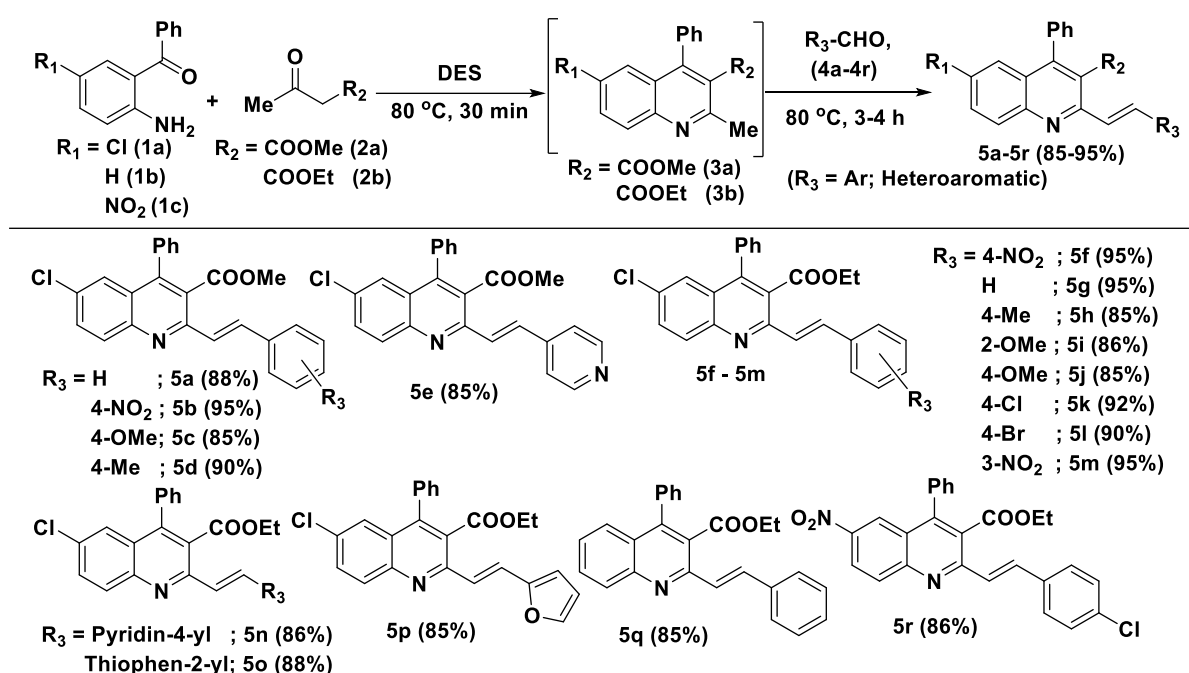
Scheme-1. Initial attempt for the synthesis of styrylquinoline (**5a**) using DES.

Table-1: Optimization conditions

Entry	Catalyst composition (Mole ratio)	1 st step		2 nd step		Yield (%) ^[c]
		Temp (°C) ^[a]	Time (min) ^[b]	Temp (°C) ^[a]	Time (min) ^[b]	
1	Urea + Citric acid (2:1)	90	30	90	10	50
2	Urea + Citric acid (3:1)	80	60	80	8	55
3	Urea + LTA (3:1)	80	60	80	10	60
4	1,3-DMU + Citric acid (2:1)	80	60	80	6	60
5	1,3-DMU + Citric acid (3:1)	80	30	80	6	65
6	1,3-DMU + LTA (3:1)	80	30	80	3	95
7	1,3-DMU + LTA (2:1)	80	30	80	4	75
8	1,3-DMU + LTA (1:1)	80	30	80	6	70
9	1,3-DMU + Citric acid (2:1)	80	60	80	6	75
10	1,3-DMU + Citric acid (1:1)	80	60	80	6	65
11	1,3-DMU+Oxalic acid (3:1)	80	30	80	6	65
12	1,3-DMU + Citric acid (3:1)	80	30	80	6	50
13	1,3-DMU+Oxalic acid (2:1)	80	30	80	8	30
14	1,3-DMU+Oxalic acid (1:1)	80	30	80	8	trace
15	1,3-DMU + LTA (4:1)	80	30	80	6	60
16	1,3-DMU + LTA (5:1)	80	30	80	6	50
17	Thiourea + Citric acid (3:1)	80	30	80	6	40
18	Thiourea + Citric acid (2:1)	80	60	80	6	30
19	Thiourea + LTA (3:1)	90	30	90	6	trace
20	Thiourea + LTA (2:1)	90	60	90	6	trace

Reaction conditions: All the reactions were carried out at a 1.0 mmol scale using **1a**, **2a**, **4a**, and DES (0.5 M molar concentration); ^[a]Temperature and time required for the first step; ^[b] Temperature and time required for the first step; ^[c] Isolated yield.

After optimizing reaction conditions, our focus was shifted toward testing these conditions for substrate scope. Thus, substituted 2-amino-benzophenones **1a/1b/1c** were reacted with MAA (**2a**) /EAA (**2b**) in presence of DES (1,3-DMU + LTA; 3:1) for 30 min to give 2-methylquinolines which on reaction with different aldehydes (**4a-4r**) gave styrylquinolines (**5a-5r**) [one-pot approach] in good to excellent yields (85-95%) in 3-4h (**Scheme-2**). Interestingly aldehydes with electron-withdrawing groups (-NO₂) exhibit better reactivity (yields up to **95%**) in shorter reaction time (3 h) in comparison to the substrates with an electron-donating group (yields up to **85%**) (**Scheme-3**).

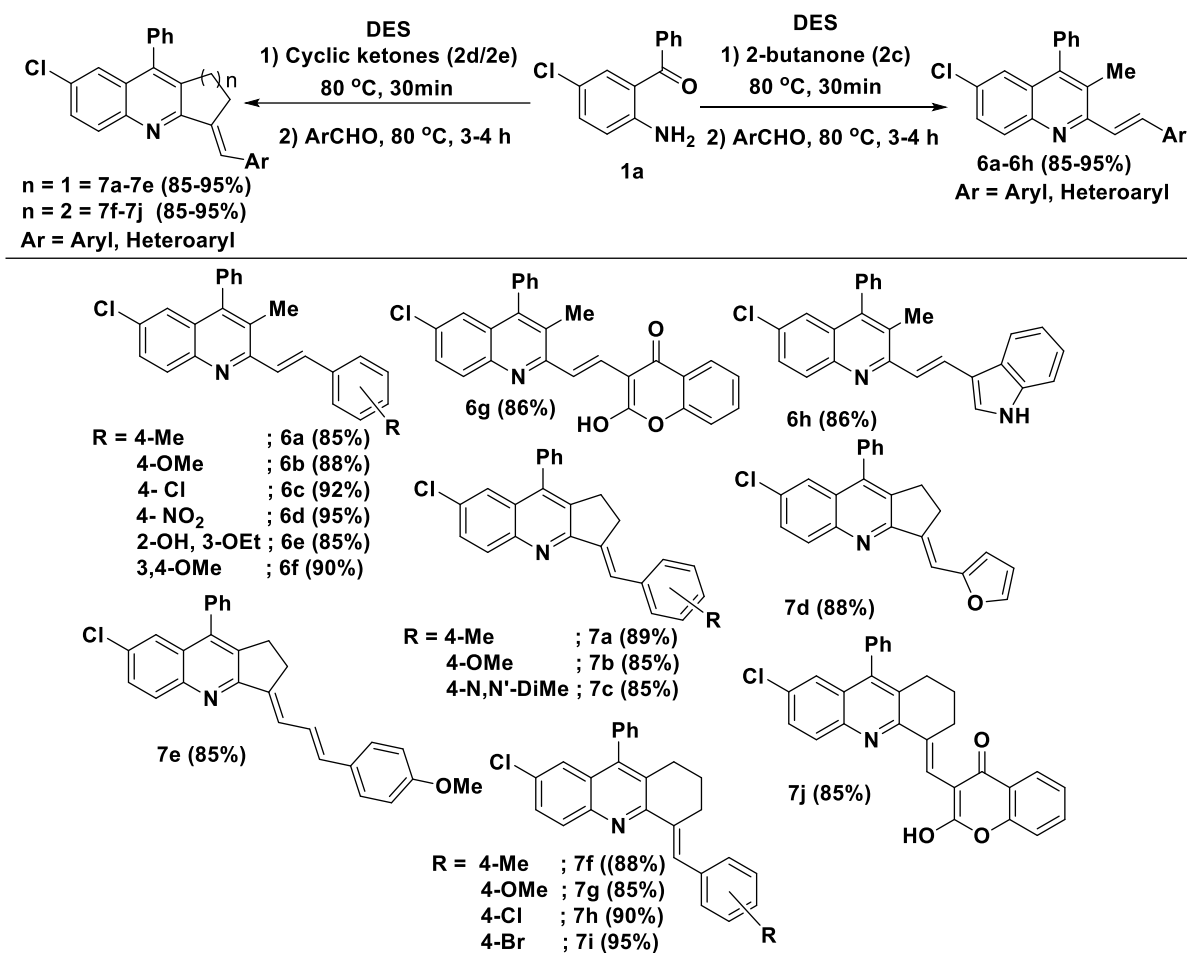


Reaction condition: **1a/1b/1c** (1mmol), **2a/2b** (1.0 mmol), (**4a-4r**) (1.0 mmol), DES: **0.5M** of DMU + L-tartaric acid (3:1) heated at 80 °C, for 30 min, then 3-4 h. (total reaction time 3.5 - 4.5 h).

Scheme 2: One-pot synthesis of 2-styrylquinoline derivatives **5a-5r**.

Having successfully demonstrated the one-pot synthesis of styrylquinolines containing –COOR groups at the 2nd position from the methyl group (sp³ C-H activation), we decided to check the hierarchical reactivity of methyl with another sp³ carbon at the 2nd position and 4th position (benzylic carbon from top). Thus, 5-chloro-2-amino benzophenone (**1a**) was reacted with acyclic and cyclic ketones (2-butanone (**2c**), cyclopentanone (**2d**), cyclohexanone (**2e**)) under optimized conditions to give corresponding quinoline derivatives (**3c-3e**; *in situ*) which were further treated with aldehydes (aromatic and hetero aromatic) to give functionalized styrylquinoline derivatives (**6a-6h** and **7a-7j**) in 85-95% yields (**Scheme-3**). It is noteworthy to mention that only sp³ carbon adjacent to nitrogen is

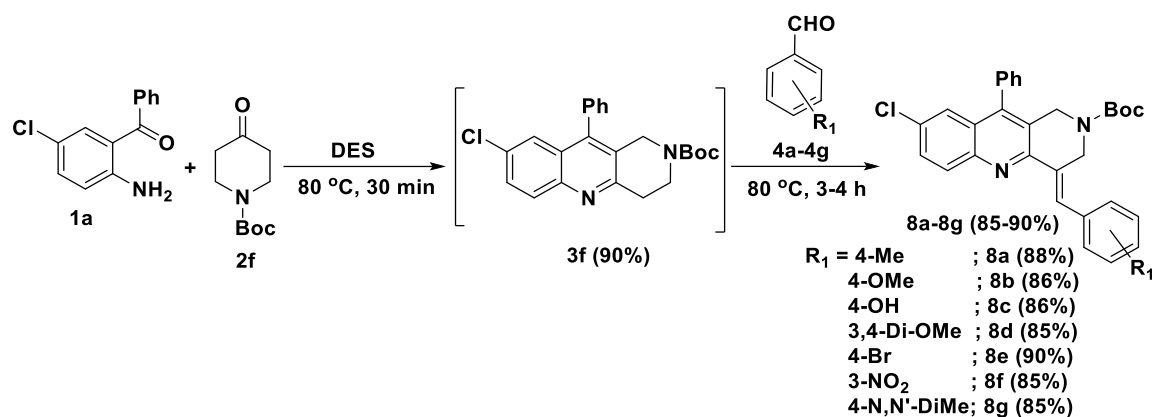
getting activated selectively with a similar trend of reactivity with both acyclic and cyclic ketones in the first step, and simple and conjugated aromatic aldehydes (cinnamaldehyde) and hetero aromatic aldehydes in the second step.



Reaction condition: 1a (1.0 mmol), 2c-2e (1.0 mmol), 4 (1.0 mmol), DES; 0.5 M of 1,3-DMU+L-tartaric acid (3:1) at 80 °C for 3-4h.

Scheme 3: Synthesis of functionalized 2-styrylquinoline derivatives (**6a-6h** and **7a-7j**).

In addition to the above and towards testing the electronic factors of the starting material, a more complex intermediate (**3f**) was prepared *in situ* using *N*-Boc protected piperidinone (**2f**) as electrophile and treated with 5-chloro-2-amino benzophenone (**1**) and aromatic aldehydes (**4a-4g**) under the optimized condition to give corresponding styrylquinoline hybrids (**8a-8g**) with good yields (85-90%) as shown in (**Scheme-4**).



Reaction condition: **1a** (1.0 mmol), **2f** (1.0 mmol), and (**4a-4g**) (1.0 mmol), DES: 0.5 M of DMU+L-tartaric acid (3:1) stirred at 80 °C, 3-4 h.

Scheme 4: Synthesis of functionalized styrylquinoline derivatives (**8a-8g**).

Based on the experimental results and observations in the present study, a plausible reaction mechanism is proposed for the formation of 2-styrylquinolines as shown in (**Figure-2**). Initially, the DES is formed by the heating of dimethyl urea and L-tartaric acid which are associated through intermolecular hydrogen bonding. The resulting DES induces the keto-enol tautomerism in carbonyl compound (**A**). Simultaneously the carbonyl carbon of benzophenone is activated by DES (**B**) which is reacting with an enolic form of ketone *via* a Michael-type attack to give intermediate (**D**). This will undergo cyclization followed by elimination of NH₃ and H₂O to give a thermodynamically stable intermediate (**E**). The tautomeric structure of (**E**) will react with aldehyde *via* Aldol-type condensation with aldehyde which intern will undergo dehydration (Knoevenagel condensation) to give the final product (**7**) (**Figure-2**).

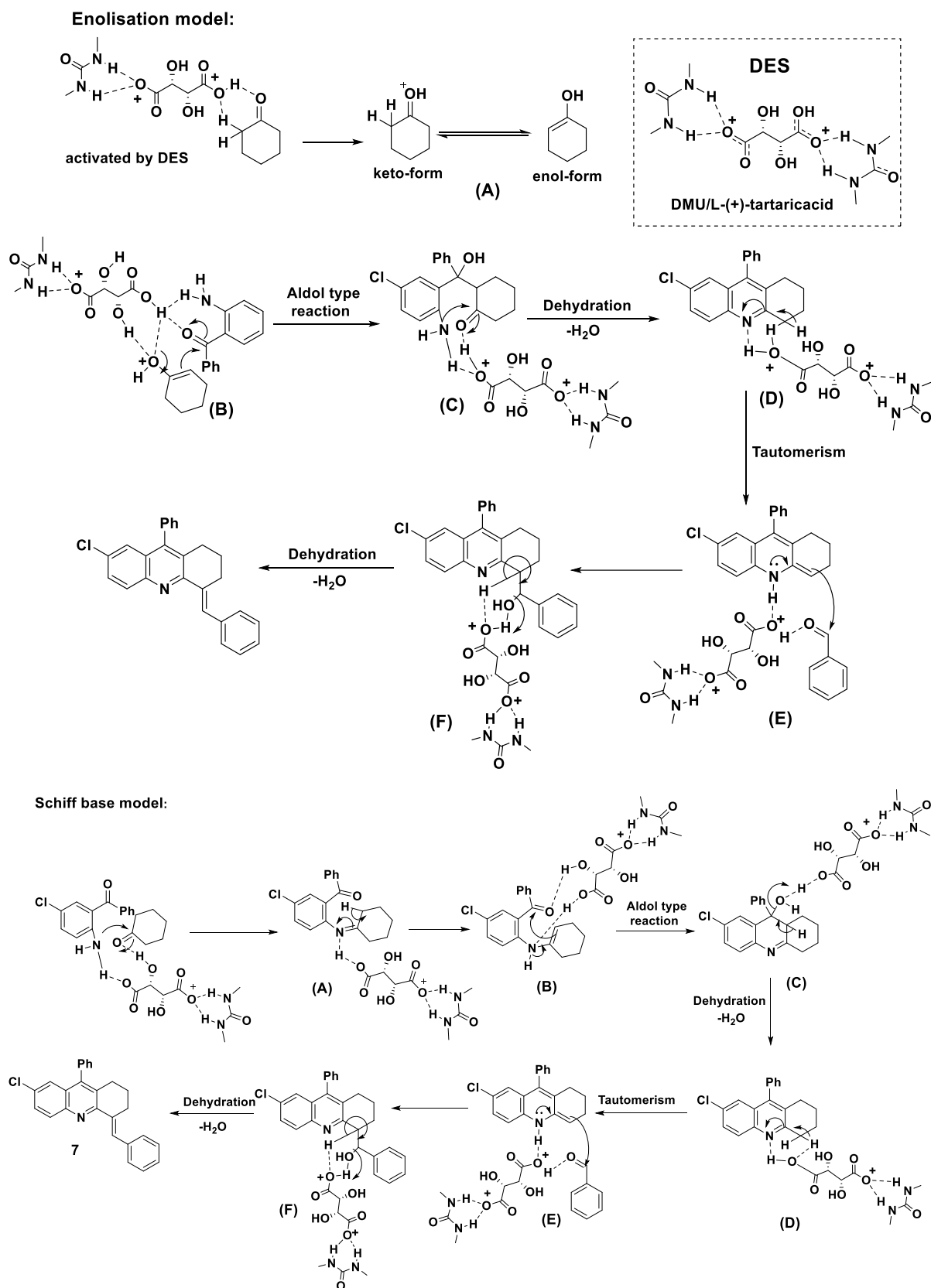
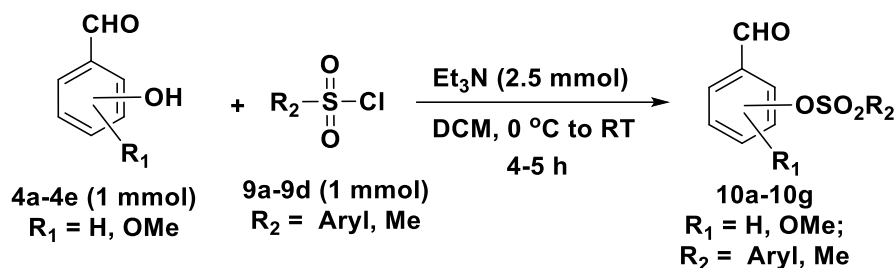
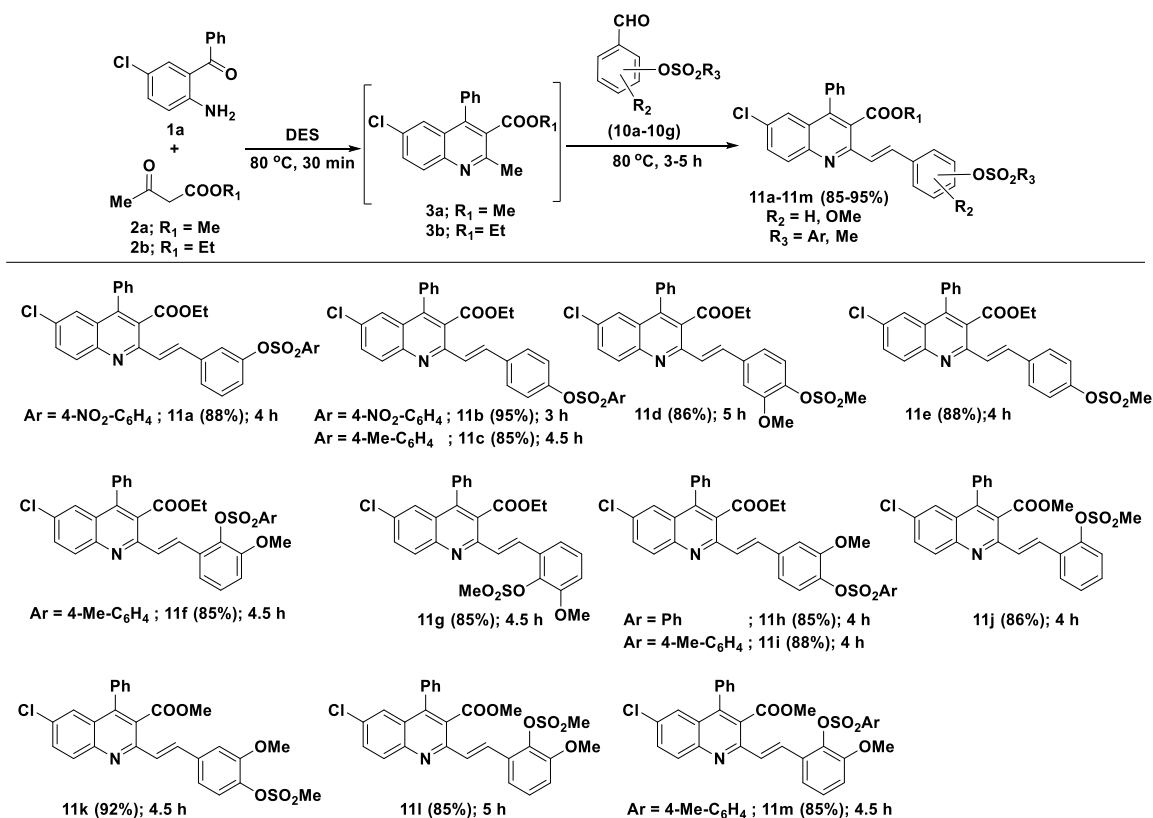


Figure-2: Plausible reaction mechanism based on the experimental observation.

After the successful synthesis of 2-styrylquinoline using DES as a reaction medium, the synthesis of sulfonate ester based 2-styrylquinolines was planned. Thus, sulfonate ester-based aldehydes (**10a-10g**) were prepared by sulfonation/tosylation/methylation of salicylaldehyde or meta/para hydroxy benzaldehydes under the basic conditions as shown in **Scheme-5**. These generated aldehydes were further reacted with methylacetoacetate (**3a**)/ethylacetoacetate (**3b**) under optimized conditions (1,3-DMU/LT, 3:1 ratio, 80°C) to afford styrylquinoline sulfonates (**11a-11m**) with good to excellent (85-95%) yields (**Scheme-6**).



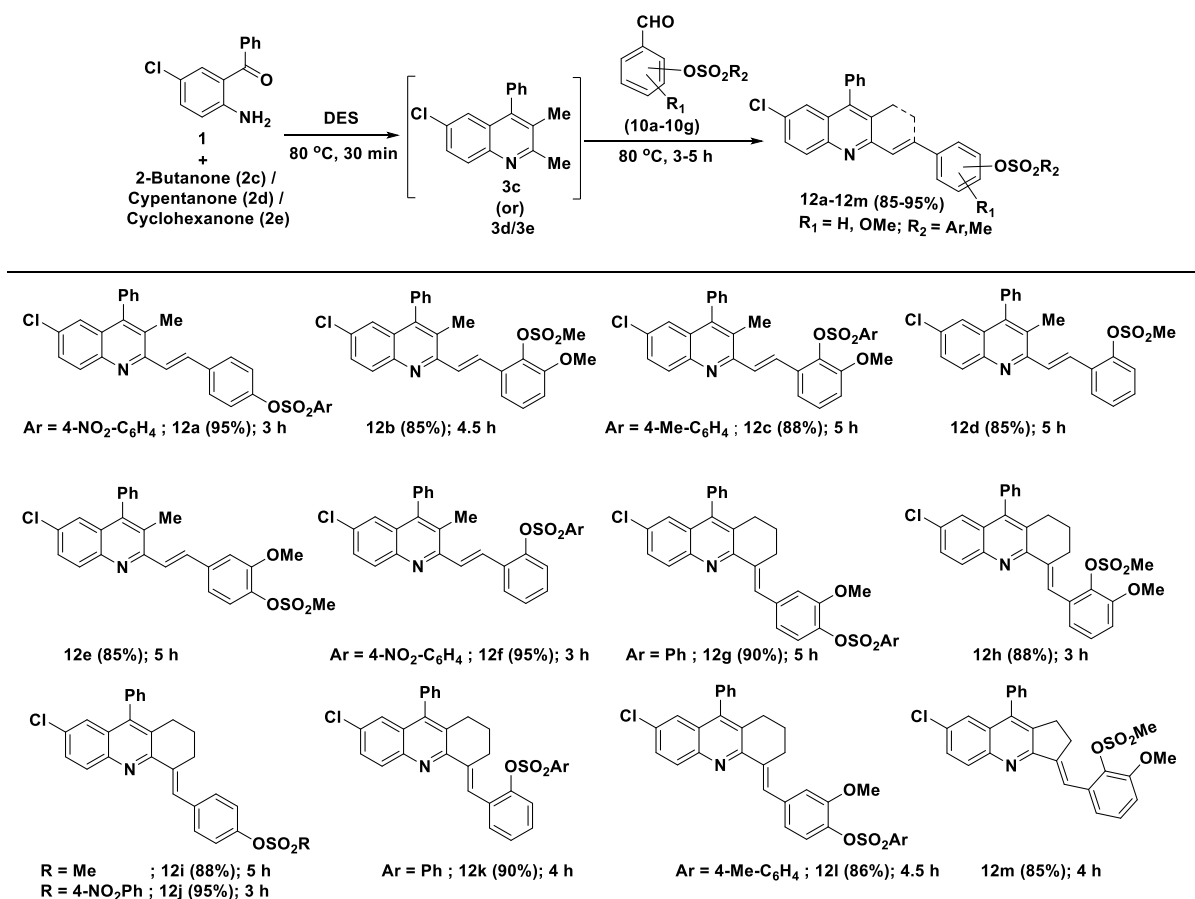
Scheme-5: Preparation of sulfonate ester aldehydes (**10a-10g**).



Reagent and condition: **1a** (1.0 mmol), **10a-10g** (1.0 mmol), **2a/2b** (1.0 mmol), DES: 1,3-DMU+L-tartaric acid (**3:1**) heated at 80 °C for 3-5 h.

Scheme-6: Synthesis of sulfonate ester-based styrylquinoline scaffolds (**11a-11m**).

In addition, to the above examples, the same procedure was extended to butanone (**2c**), cyclopentanone (**2d**), cyclohexanone (**2e**) in combination with 2-amino-5-chloro benzophenones (**1a**), and benzene sulfonate ester aldehydes (**10a-10g**) under optimized conditions to give corresponding activated products (**12a-12m**) as shown in **Scheme-7** in 3-5 h with good to excellent yields (85-95%).



Reagent and condition: **1a** (1.0 mmol), **10a-10g** (1.0 mmol), **2c/2d/2e** (1.0 mmol), DES; 1,3-DMU+L-tartaric acid (3:1) heated at 80 °C for 3-5 h.

Scheme-7: Substrate scope of styrylquinoline sulfonate esters using aliphatic/cyclic electrophiles (**12a-12m**).

2.4 DFT Calculation

2.4.1. Detailed computational methodology

In this investigation, an attempt has been made to understand the reaction mechanism with the aid of density functional theory (DFT) calculations. Geometries of all the reactants, TSs, intermediates, and products were fully optimized without any geometrical/symmetrical constraints using DFT-based B3 exchange and Lee, Yong, and Paar (LYP) correlation functional with inclusion empirical dispersion correction (D3) as suggested by Grimme's utilizing 6-31G* basis

set.^{19(a-c)} The energetics of various reactions were calculated at 298.15 K temperature and 1 atm pressure in the gaseous phase.

Catalyst Investigation

Both the forms of catalyst were investigated to understand the stability of the catalyst. The geometries of both complexes were optimized using B3LYP-D3 employing the 6-31+G* level of theory. The H-bond interaction energies (IEs) of various complexes were calculated using the following equation.

$$IE = E_{\text{complex}} - \sum E_{\text{monomer}}$$

where, E_{complex} and E_{monomer} are the energy of complex and the energy of monomeric units, respectively. The energies of the monomers were calculated from the respective monomer geometries in the complexes (as shown in **Figure-3**) in other words, the energy that results from complexation was taken into account. The calculated IEs were corrected for basis set superposition error using the counterpoise method suggested by Boys and Bernardi.^{19d}

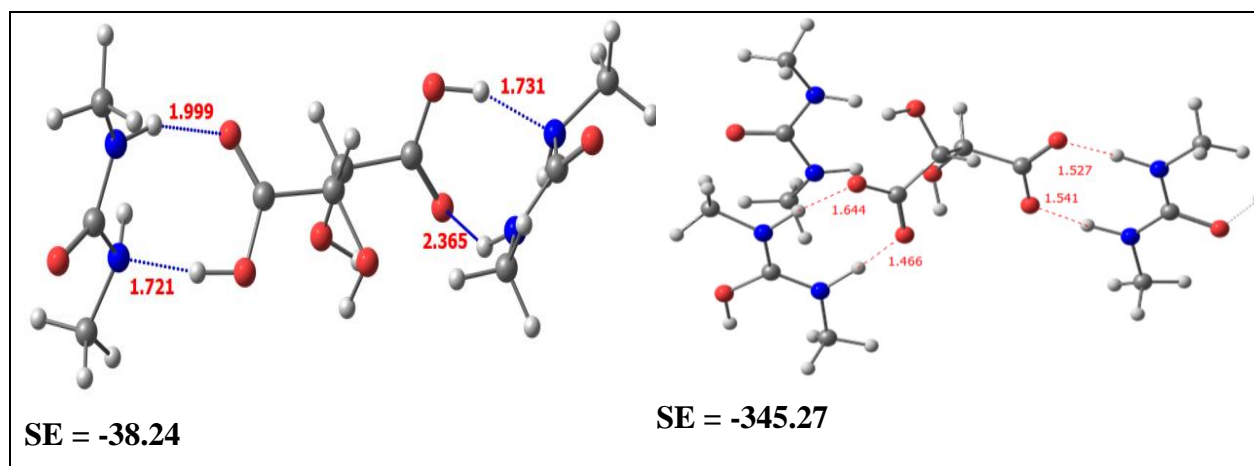


Figure- 3. Optimized geometries of both complexes.

It can be noted that the H-bonded complex involved proton from LT to DMU is more stable when compared to the non-proton transferred complex. Therefore, in the present investigation proton transferred form of the catalyst is considered.

Reaction mechanism

To support the results of the present investigation and proposed mechanism, theoretical calculations were performed using density functional theory (DFT) based

B3LYP-D3 method employing a 6-31+G* basis set. For ease in the calculation, the reaction is considered in three stages, which are

- a) Keto-enol tautomerism of the carbonyl compound in the presence of the DES
- b) Reaction of the enolic form of the ketone with the activated benzophenone compound to give a thermodynamically stable intermediate E
- c) Reaction of the activated tautomer of stable intermediate with the activated aldehydic compound *via* aldol condensation to give final products.

a) Reaction mechanism of Enolization

A close analysis of the geometries of various transitions states that the enolization of cyclohexanone undergoes a concerted reaction mechanism in the presence of DES as a catalyst *via* proton transfer between the DES mixture to the cyclohexanone. It can be observed from the optimized geometries, where the DES catalyst also provides the stabilizing environment for various transition states. It is important to note that the gas-phase conversion of cyclohexanone to cyclohexanol, requires 67.7 kcal/mol of energy. The same conversion in the presence of DES occurs at 25.65 kcal/mol. The difference in energy indicates the part played by the catalyst in the reaction. Therefore, the presence of the catalyst decreases the energy barrier considerably, as predicted in **Figure-4**.

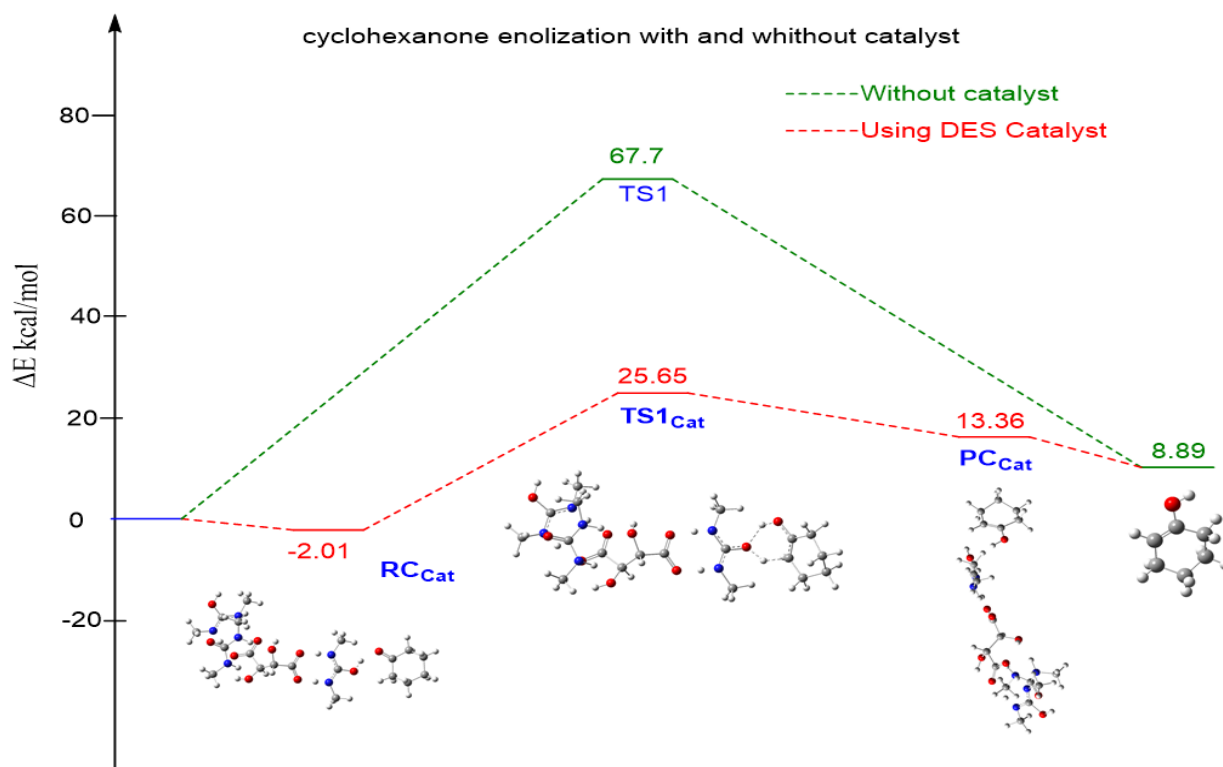


Figure-4. Optimized geometries and energetics of enolization of cyclohexanone (**2e**) obtained using B3LYP-D3/6-31+G** level of calculations.

b) Mechanism for the reaction of activated Benzophenone with Enolic form

The carbonyl carbon of benzophenone gets activated by proton transfer from DES, which reacts with an enolic form of the ketone to give the intermediate D *via* TS₁. D readily loses water molecules to give D1. From the profile, it can be observed that the activation energy for this step is 11.97 kcal/mol. Further, D1 is activated by DES and undergoes cyclization *via* proton transfer to give D2, which dehydrates to give the thermodynamically stable intermediate E. The relative free energy for E is -30.67 kcal/mol, which highlights its stability.

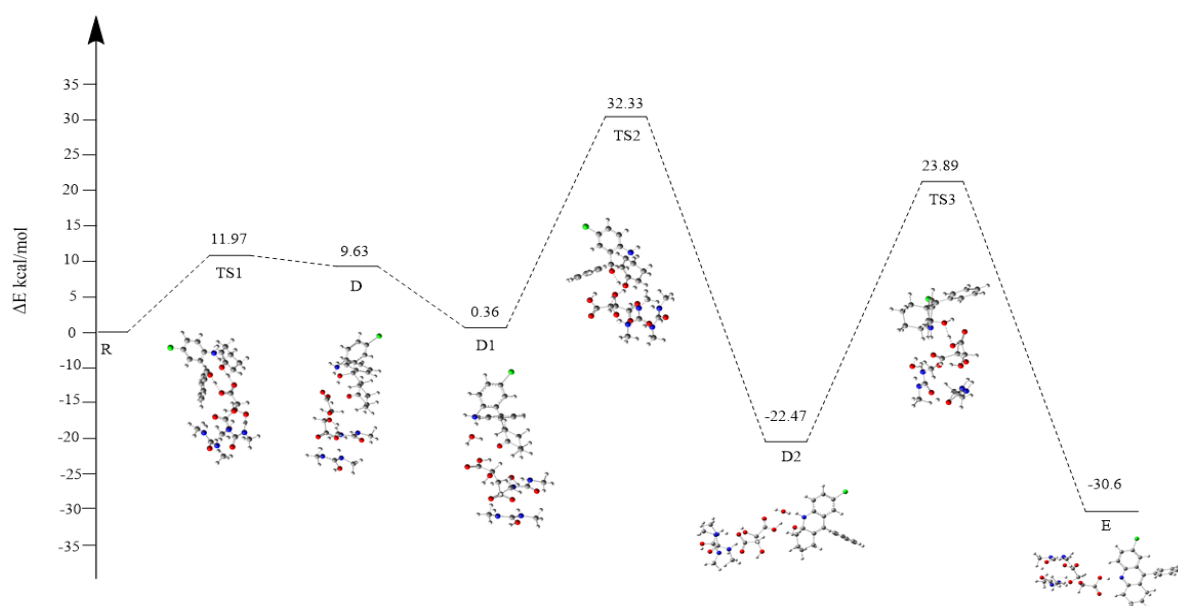


Figure-5. Optimized geometries and energetics of reaction between activated benzophenone with enolic form obtained using B3LYP-D3/6-31+G** level of calculations.

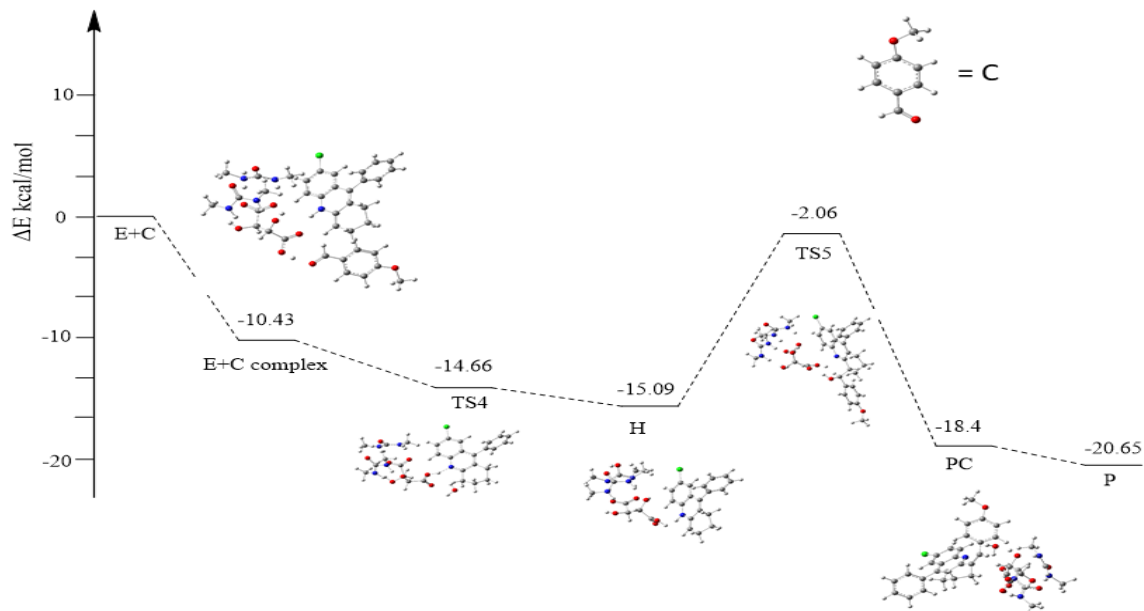


Figure-6. Optimized geometries and energetics of reaction between stable intermediate with activated aldehyde obtained using B3LYP-D3/6-31+G** level of calculations.

c) Reaction mechanism of the stable intermediate with activated Aldehyde.

The tautomeric form of the stable intermediate E obtained from the previous step reacts with the activated aldehydic compound, which gives intermediate H *via* TS₄. From the profile, it can be seen that the relative energy of TS₄ was -14.66 kcal/mol, which shows that it is a low barrier reaction. Finally, H undergoes dehydration to give the product complex PC *via* TS₅, as represented in **Figure-6**. The energy required for this step is 13.03 kcal/mol. From the profile, it can be seen that this reaction is energetically feasible.

It is also worth noting that the IMs are found to be very stable throughout the reaction. This is because of the hydrogen bonding by the catalytic mixture with the IMs. Hence, the theoretical calculations complement the proposed mechanism and show that the use of DES effectively reduces the activation energy and efficiently catalyzes the reaction.

2.7 Photophysical properties

2.7.1 UV-Visible and PL spectroscopy experimental studies of styrylquinolines

Following the successful synthesis of the title compounds, and due to the importance of styrylquinolines for the development of fluorescent probes, dye-sensitized solar cells,^{20a} organic light-emitting diodes (OLEDs)^{20b}, and functional devices^{20c} our next task was to study the photophysical properties of these compounds. Thus, the fluorescence and emission spectra of compounds (**5n–6h**) and (**7b–8d**) were recorded in CHCl₃ (100 mM) at room temperature. The absorption maxima of compounds **5n**, **5o**, **5p**, **6b**, **6f**, and **6h** were observed in the range of 375–458 nm (**Figure-7A**). The emission maxima were found in the range of 484–557 nm with **5o** and **6f** showing the maximum emission wavelength (**Figure-7B**) (**Table-2**).

Among the acyclic compounds (**5n–6h**), compound **5o** exhibits the maximum emission peak at 557 nm with the larger Stokes shift at 182 nm (due to the presence of the electron-donating group). Generally, fluorophores with larger Stokes shifts have enhanced applications in the biological regime due to lower autofluorescence. Compounds **5n**, **5p**, **6b**, **6f**, and **6h** also displayed strong Stokes shifts at 113, 100, 108, 90, and 84 nm, respectively, and all the data are represented in **Table-2**. Compound **5o** has the highest emission peak at 557 nm and the largest Stokes shift at 182 nm among the acyclic compounds (**5n–6h**) (due to the presence of the electron-donating group). Due to decreased autofluorescence, fluorophores with bigger Stokes shifts have more applicability in the biological regime. Compounds **5n**, **5o**, **5p**, **6b**, **6f**, and **6h** have

substantial Stokes shifts at 113, 182, 100, 108, 90, and 84 nm, respectively, and all of the data is shown in **Table-2**.

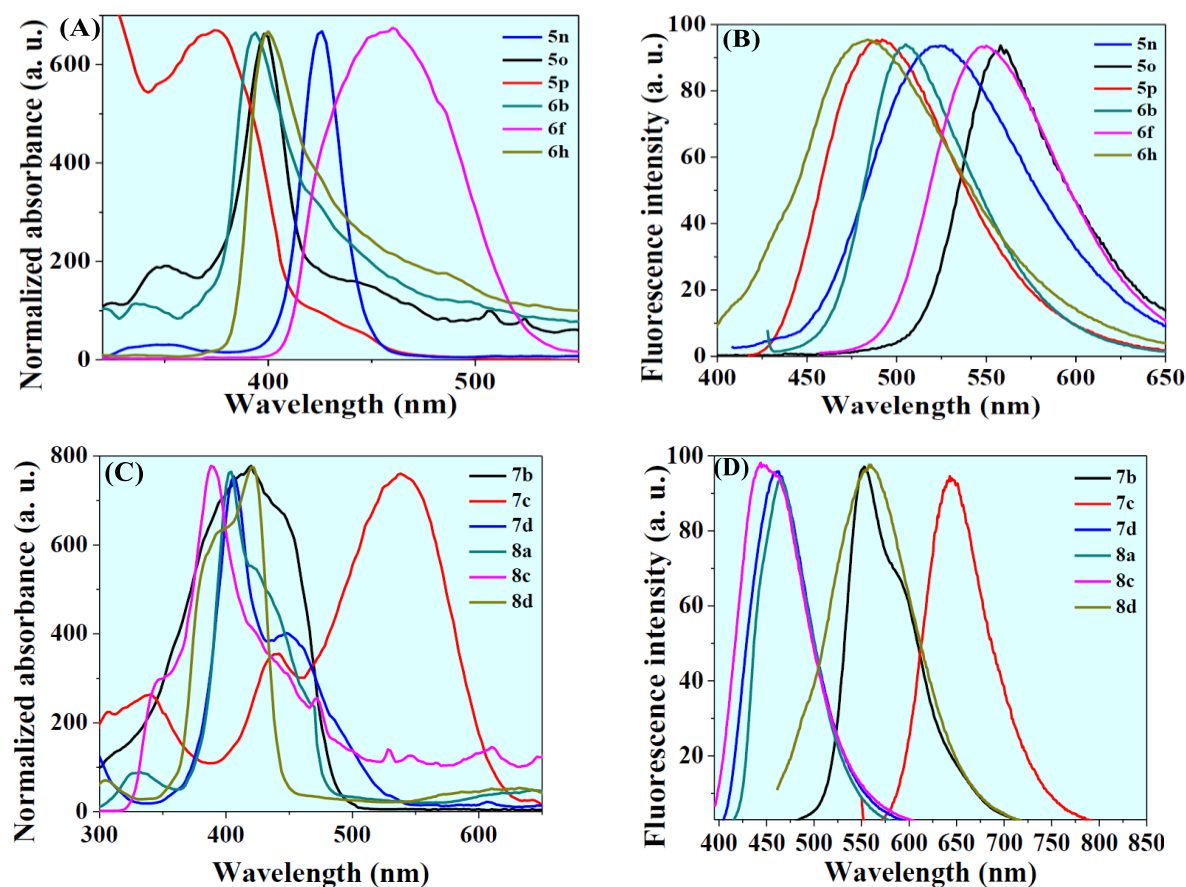


Figure-7 (A) Absorption and (B) emission spectra of compounds **5n–6h**; (C) absorption and (D) emission spectra of compounds **7b–8d**.

Further, the absorption and photoluminescence properties of the cyclic molecules (**7b–8d**) studied and observed that the absorption maxima of the compounds **7b**, **7c**, **7d**, **8a**, **8c**, and **8d** at **420, 536, 411, 400, 390 and 420 nm** as shown in **Figure-7c** (all the data are tabulated in **Table-3**). Correspondingly, their emission bands were observed at **551, 644, 464, 464, 449, and 558 nm**. Interestingly, the emission bands of **7b**, **7c**, and **8d** show a bathochromic shift with impressive Stokes shifts at **131, 108, and 138 nm** with a change in the solvent polarity as a consequence of the intramolecular charge-transfer effect. The highest Stokes shift was observed in the acyclic series, *i.e.*, compound (**5o**) ($\Delta\lambda$ **182 nm**), but compound (**7c**) of the cyclic series exhibited the highest emission band maximum at **644 nm**, as shown in **Table-3**. Further, the solvatochromic effects of compound (**7e**) were also investigated and the absorption and

emission band maxima were measured in different solvents. The UV-vis absorption maximum (λ_{max}) and emission maximum (λ_{max}) data of (**7e**) are listed in **Table-4**. The variable absorption band of compound (**7e**) was observed when the solvent polarity was increased from *n*-hexane to DMSO (**Figure-8; (A) and (B)**) with different colors under irradiation with UV radiation (**Figure-8; (C)**). This stronger solvatochromism in (**7e**) is partly due to the presence of extended conjugation and donor-acceptor groups and the strong emission wavelength bands are attributed to the ICT effect. In addition, with an increase in solvent polarity, the emission bands also showed bathochromic shifts and strong Stokes shifts.

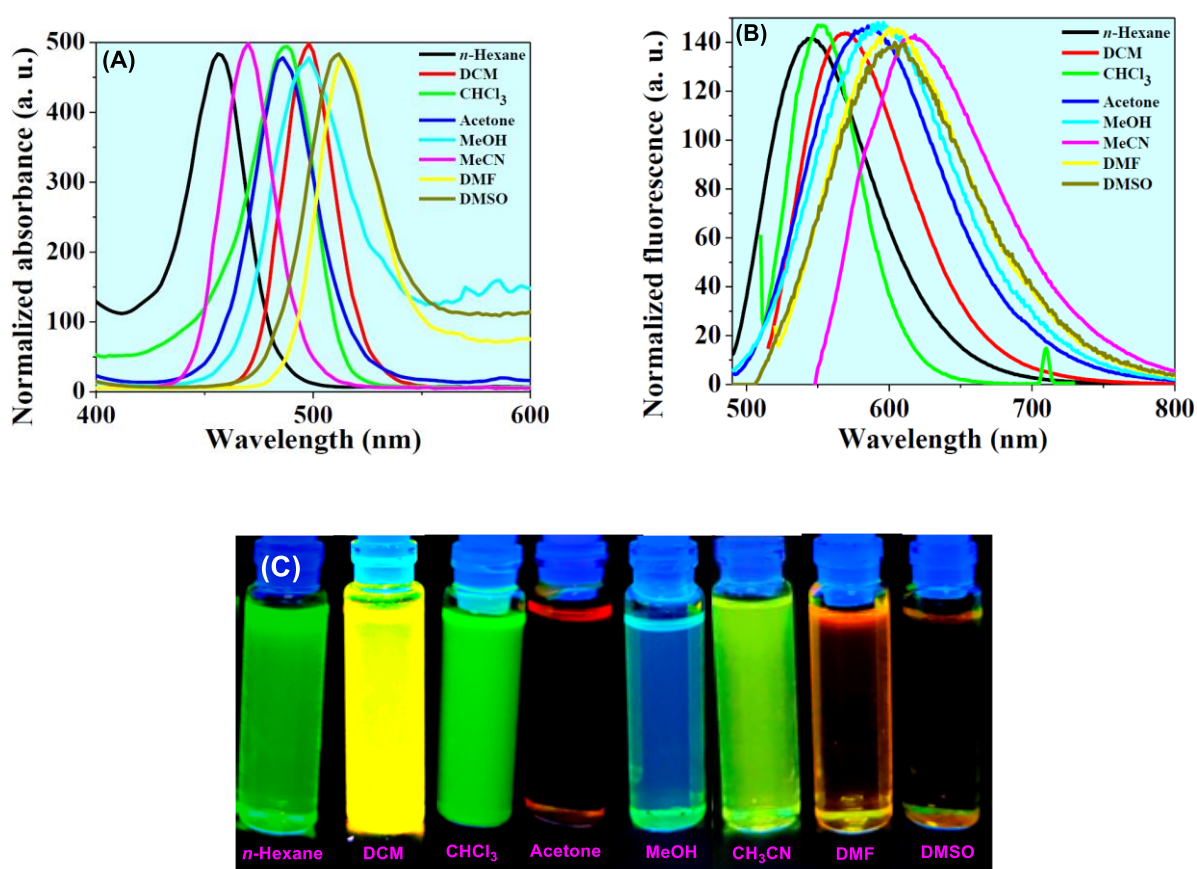


Figure-8: (A) Absorption (B) Emission spectra of the compound (**7e**) in different solvents (C) UV (long-range) irradiation images of compound (**7e**) in different solvents at 100 μM concentration.

Table-2: Photo physical properties data of the resulting acyclic/aliphatic compounds (**5n-6h**):

Compounds	λ_{Abs} (nm)	λ_{em} (nm)	Stokes shift ($\Delta\lambda$ nm)
5n	410	525	123
5o	375	557	182
5p	425	525	100
6b	394	502	108

6f	458	548	90
6h	400	484	84

Table-3: Photo physical properties data of the resulting cyclic compounds (**7b-8d**):

Compounds	λ_{Abs} (nm)	λ_{em} (nm)	Stokes shift ($\Delta\lambda$ nm)
7b	420	551	131
7c	536	644	108
7d	411	464	53
8a	400	464	64
8c	390	449	59
8d	420	558	138

Table-4: Data of the solvatochromic effect of compound **7e** in various solvents.

solvent	λ_{Abs} (nm)	λ_{em} (nm)	Stokes shift ($\Delta\lambda$ nm)
<i>n</i> -Hexane	456	543	87
DCM	498	568	70
CHCl ₃	488	553	65
Acetone	485	585	100
MeOH	496	597	101
MeCN	470	618	148
DMF	514	601	87
DMSO	511	605	94

2.7.2 UV-Visible and PL spectroscopy studies of styrylquinoline sulfonate esters (**11a-11m**) and (**12a-12m**).

Similar to the above discussion, the photophysical properties of the synthesized styrylquinoline sulfonates (**11a-11m**) and (**12a-12m**) were studied in DMSO (100 μM) at room temperature. Absorption maxima of acyclic compounds (**11a-11m**) were observed in the range of **391-404** nm as shown in **Figure-9; (A)** and their corresponding emission spectra in the range of **443-511** nm (**Table-5**). Due to the Intramolecular charge transfer (ICT) effect, the compound **11f** with the aromatic ring has two electron-donating groups (i.e., 3-methoxy, and 4-methyl groups,) emission band **511** nm (bathochromic shift) with stokes shift at **111** nm. This $n-\pi^*$ transitions. Similarly, the compounds **12a-12m** displayed absorption at **392-431** nm and emission intensity at **426-537** nm. The **12i**, **12d**, and **12l** compounds are exhibiting maximum emission (bathochromic

shift) at **537, 515, and 516 nm** as shown in **Figure-6 (Table-5)**. The **11b-11m** series (cyclic derivatives) show higher absorption, emission intensities, and Stoke shifts compared to the acyclic series **12a-12m**.

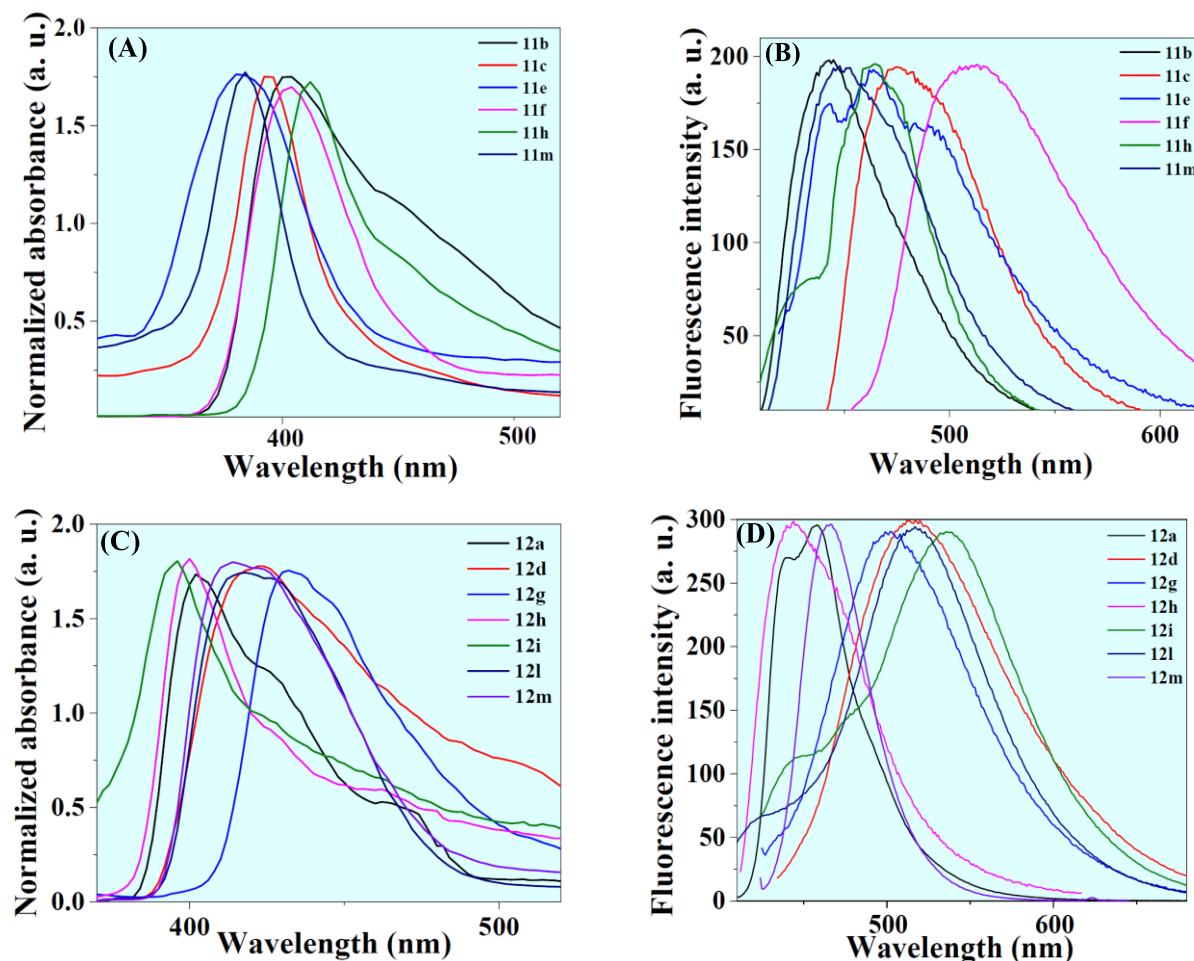


Figure-9: (A) Absorption (B) Emission spectra of the compounds (**11a-11m**) (C) Absorption (D) Emission spectra of the compounds (**12a-12m**).

The solvatochromic effect of the compound **12g** was studied at room temperature in a 100 μM concentration. in various solvents [non-polar (*n*-hexane) to polar (DMSO)] solvents were seen in the range of **396-431nm** and emission spectra at **426, 451, 445, 471, 472, 460, 480, 484** and **503 nm** respectively (*n*-Hexane, DCM, CHCl_3 , EtOAc, Acetone, MeOH, MeCN, DMF and DMSO) as shown in **Figure-10 (Table-7)**. It is observed that the polarity of the solvent (the emission bands in DMF and DMSO at **484** and **503**) play role in the bathochromic shift of the peaks due to the intramolecular charge transfer (ITC).^{24f} These may be helpful for the development of fluorescent probes and solar cells based on these compounds.

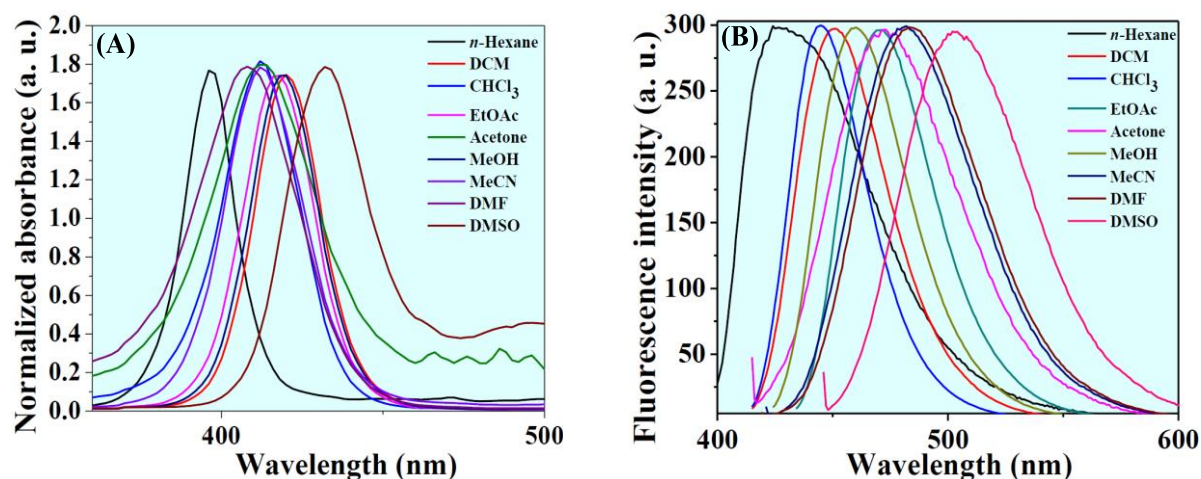


Figure 10: (A) Absorption (B) Emission spectra of the compound **12g** in non-polar to polar solvents (n-Hexane to DMSO) at 100 μ M.

Table-5: Photo physical properties data of the compounds (**11b-11m**).

Solvent	λ_{Abs} (nm)	λ_{em} (nm)	Stokes shift ($\Delta\lambda$ nm)
11b	400	443	43
11c	397	479	82
11e	392	450	60
11f	400	511	111
11h	404	463	59
11m	391	450	60

Table-6: Photo physical properties data of the compounds (**12a-12m**).

Solvent	λ_{Abs} (nm)	λ_{em} (nm)	Stokes shift ($\Delta\lambda$ nm)
12a	401	472	71
12d	415	515	100
12g	431	503	72
12h	400	444	44
12i	392	537	145
12l	414	516	102
12m	415	464	49

Table-7: Solvatochromic effect data of compound (**12g**).

Solvent	λ_{Abs} (nm)	λ_{em} (nm)	Stokes shift ($\Delta\lambda$ nm)
<i>n</i> -Hexane	396	426	30
DCM	419	451	32
CHCl ₃	411	445	44
EtOAc	418	471	53
Acetone	412	472	60
MeOH	419	460	41
MeCN	411	480	69
DMF	408	484	76
DMSO	431	503	72

2.8 Biological activity

2.8.1 α -D-glucosidase assay

The α -glucosidase activity was determined calorimetrically with 4-nitrophenyl D-glucopyranoside (4-NPG) as the substrate. The enzymatic reaction was performed by adding 40 μ l of 4-NPG (substrate stock of 2mg/ml made in 0.1M Tris- HCl pH 7.5) and 10 μ l of α -glucosidase (1mg/ml made in 0.1M Tris- HCl pH 7.5) to 150 μ l 0.1M Tris-HCl pH 7.5 and the reaction mixture was incubated at 37 °C for 5 min. The activity was estimated by reading the absorbance of 4-nitrophenol formed at 410 nm against an enzyme-free blank. For studying inhibition kinetics, the enzyme was incubated with the inhibitors, [(**11a-11m**) and (**12a-12m**)] (1mg/ml in DMSO) for 15 min at room temperature before the addition of substrate. 1 unit of glycolytic activity is defined as the quantity of enzyme required to liberate 1 μ g of 4-nitrophenol per minute under standard assay conditions.

Determination of IC₅₀ values

IC₅₀ values of inhibitors were calculated based on the concentration of inhibitor required to inhibit 50% of α -glucosidase activity under the standard assay conditions. For quantification of IC₅₀ values, the enzyme inhibition assays were carried out at different concentrations (20 to 100 μ g) of inhibitors, without varying concentrations of enzyme. The enzyme reaction was performed by pre-incubating the enzyme within the inhibitor at room temperature for 15 min and inhibitory activity was determined under standard assay conditions. For those molecules which showed significant inhibition, the mode of inhibition exhibited by the inhibitor was examined by carrying out Michaelis-Menten enzyme kinetics by varying substrate (4-NPG) concentration (8, 16, 32, 40, and 80 μ g) in the absence and presence of the inhibitor molecules at three different concentrations (20, 40 and 100 μ g). Mode of inhibition was determined by Lineweaver-Burk plot analysis of the data obtained. All IC₅₀ values are represented as Mean \pm Standard Deviation.

Insilico - Ligand Preparation

The 2D structures of all 26 synthetic inhibitor molecules were sketched using VLife MDS software v.4.6 and saved in mol format. The 3D coordinate files were generated and saved in mol2 format. The geometry of the ligand molecules was optimized using MMFF forcefield until a gradient of 0.001 kcal/mol/Å was achieved.

Homology Modelling

As the structure of *Saccharomyces cerevisiae* α -glucosidase MAL12 (UniProtID P53341) is not available in the public domain, its theoretical model was built by homology modeling. It was accomplished by retrieving the sequence of the MAL12 protein from the UniProt database (Sequence ID P53341). A potential template with PDB ID 3AJ7 was identified by BLAST analysis using the BLOSUM62 matrix in the PDB database, based on the sequence identity. The template had 72% identical residues, 85% positive residues, and negligible gaps. Its coordinates were further modified to make it suitable for automated homology modeling and a model was generated by the Biopredicta module of the VLife® program. Superimposing the template and the generated protein model yielded an RMSD value of 0.251094.

Docking method Validation and GRIP Docking

Molecular docking simulations were carried out using the GRIP docking method in the VLife® Biopredicta module. The largest cavity with greater volume was chosen for docking the compounds. Scoring of the docked poses was done by the PLP method and dock score. The docking interactions were critically analyzed and the analysis revealed the key amino acid residues within the binding pocket contributing to α -glucosidase inhibition.

Results and Discussions

The inhibition of α -glucosidase activity by a series of styrylquinoline sulfonate ester derivatives showed a wide range of inhibition with IC₅₀ values ranging from **38.82 μ M** to **280.22 μ M** (**Table-8**). Acarbose was selected as a control inhibitor, the IC₅₀ value of which was found to be **32.15 μ M** under the same assay conditions. Among the tested compounds compound **12a**, showed the lowest IC₅₀ value of **38.82 μ M** and compound **11k** showed a maximum IC₅₀ value of 280.22 μ M. Among the tested compounds, compounds **11b**, **12a**, and **12l** showed minimal IC₅₀ values for α -glucosidase enzyme activity and were selected for further studies to find out the mode of binding of inhibitor against α -glucosidase enzyme experimentally by comparing the Michaelis-Menten kinetic constants. Results of K_m and V_{max} of α -glucosidase in the presence of tested

compounds were shown in **Table-11**. By studying the kinetics of α -glucosidase it was observed that the presence of **compound-11b** greatly affected the K_m and V_{max} values. From Lineweaver–Burk double reciprocal plot for the inhibition of α -glucosidase by **compound-11b**, it was observed that the mode of inhibition is mixed uncompetitive type. For **compound-12a and 12l** increase in the inhibitor concentration showed a significant decrease in V_{max} , but there is no significant change in K_m , this shows that **compound-12a and 12l** bind to the enzyme non-competitively. Different modes of inhibition were studied by varying the inhibitors and reported for α -glucosidase activity by Jaikai et al., Deng et al. recently reported a similar type of mixed inhibition of α -glucosidase by Pu-erh tea polysaccharide. Berna et al.^{21a} reported that α -glucosidase was competitively inhibited by Anti desmabunius L plant extract. In contrast to our findings, Farhad et al.^{21b} reported that their pyrimidine-fused derivatives inhibited the activity of glucosidase in a mixed-competitive mode. Zhenhua et al.^{21c} reported inhibition profiles of various medicinal plant extracts having different modes of inhibition like competitive, uncompetitive and mixed competitive. Insilico docking analysis of all three **compound-11b, 12a, and 12l** showed at least hydrophobic interactions, **compound-11b, and 12a** formed hydrophobic interactions with HIS239 and H-bond with HIS279. Two amino acid residues HIS239 and HIS279 were involved in major interactions found between ligand and MAL12 protein.

Table-8: In-vitro α -D-glucosidase inhibition (IC_{50}) values of quinoline sulfonate esters (**11** and **12** series).

Entry	Compound	Ligand	IC ₅₀ (μM)
1	11a	1	92.11.14
2	11b	2	41.57 ± 1.01
3	11c	3	85.02 ± 1.58
4	11d	4	88.06 ± 2.14
5	11e	5	82.69 ± 1.09
6	11f	6	71.22 ± 2.01
7	11g	7	92.66 ± 3.94
8	11h	8	55.24 ± 2.36
9	11i	9	74.48 ± 2.06
10	11j	10	103.41 ± 2.07
11	11k	11	280.22 ± 6.84
12	11l	12	58.91 ± 1.17
13	11m	13	61.36 ± 2.11
14	12a	14	38.82 ± 1.17
15	12b	15	112.39 ± 3.27
16	12c	16	184.84 ± 5.31
17	12d	17	87.66 ± 3.47
18	12e	18	48.22 ± 2.01
19	12f	19	104.37 ± 4.05
20	12g	20	49.28 ± 3.21
21	12h	21	60.59 ± 2.35
22	12i	22	84.45 ± 3.54
23	12j	23	56.53 ± 1.27
24	12k	24	48.37 ± 1.10
25	12l	25	47.37 ± 1.10
26	12m	26	148.33 ± 5.08
27	-	Acarbose	32.15 ± 2.04

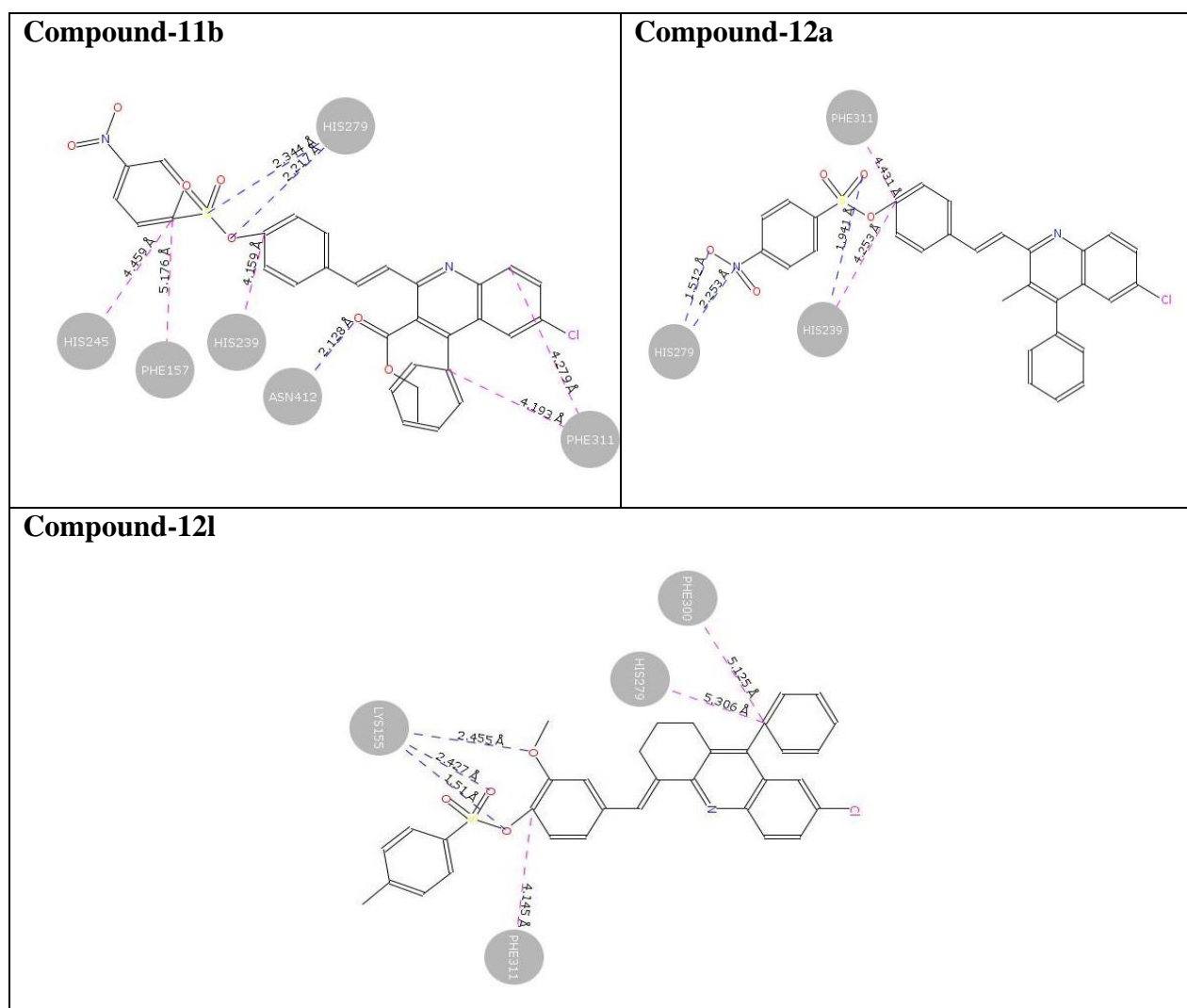


Figure-8: 2D docking interactions of compounds **11b**, **12a**, and **12l** with MAL12 protein model using rigid docking, PLP scoring function (GRIP docking algorithm).

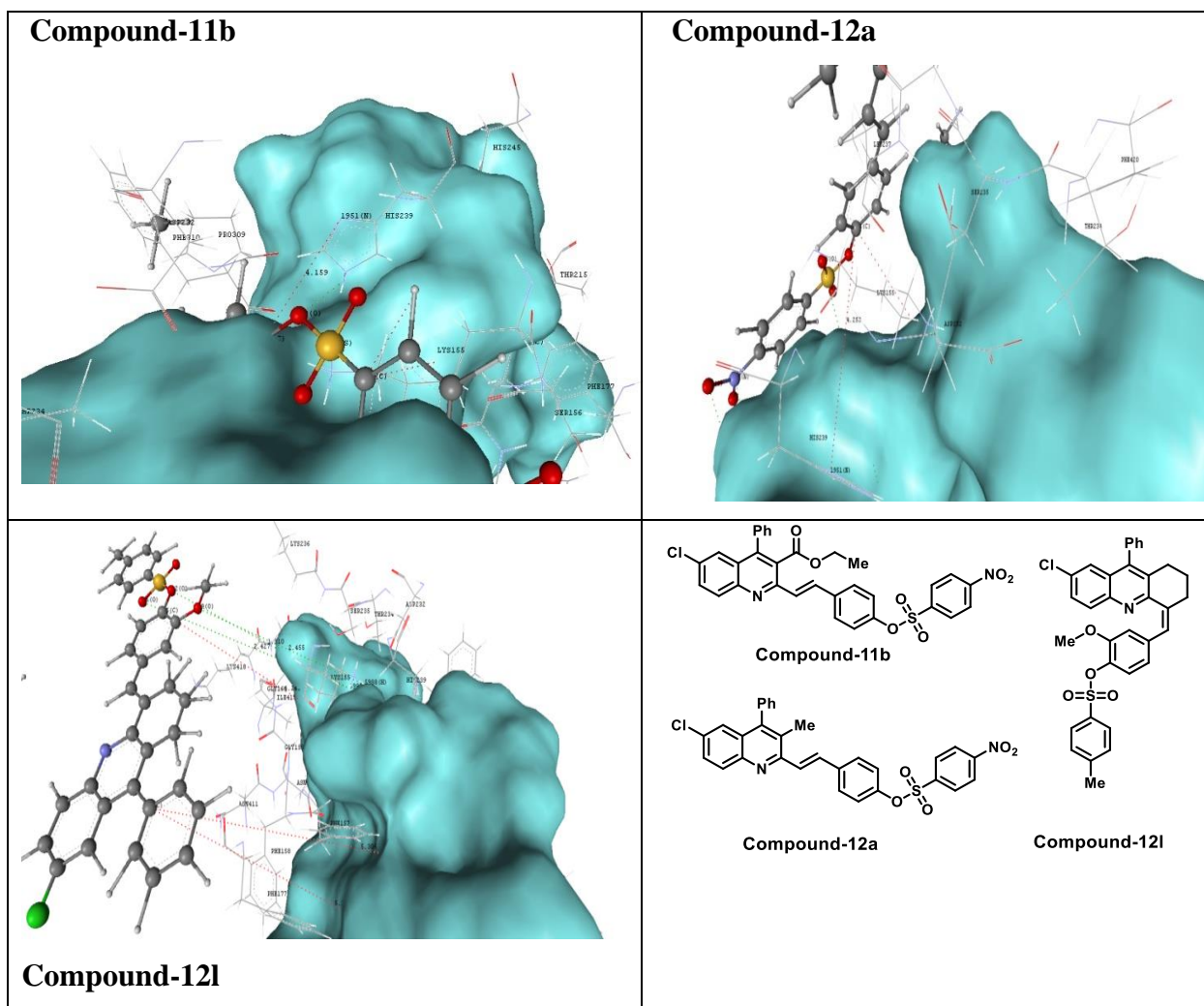


Figure-9: 3D docking interactions of compounds **11a**, **12b**, and **12l** with MAL12 protein model using rigid docking, PLP scoring function (GRIP docking algorithm)

Table -10: Molecular docking interactions between the MAL12 protein model and the most potent ligand molecules **11b**, **12a**, and **12l**.

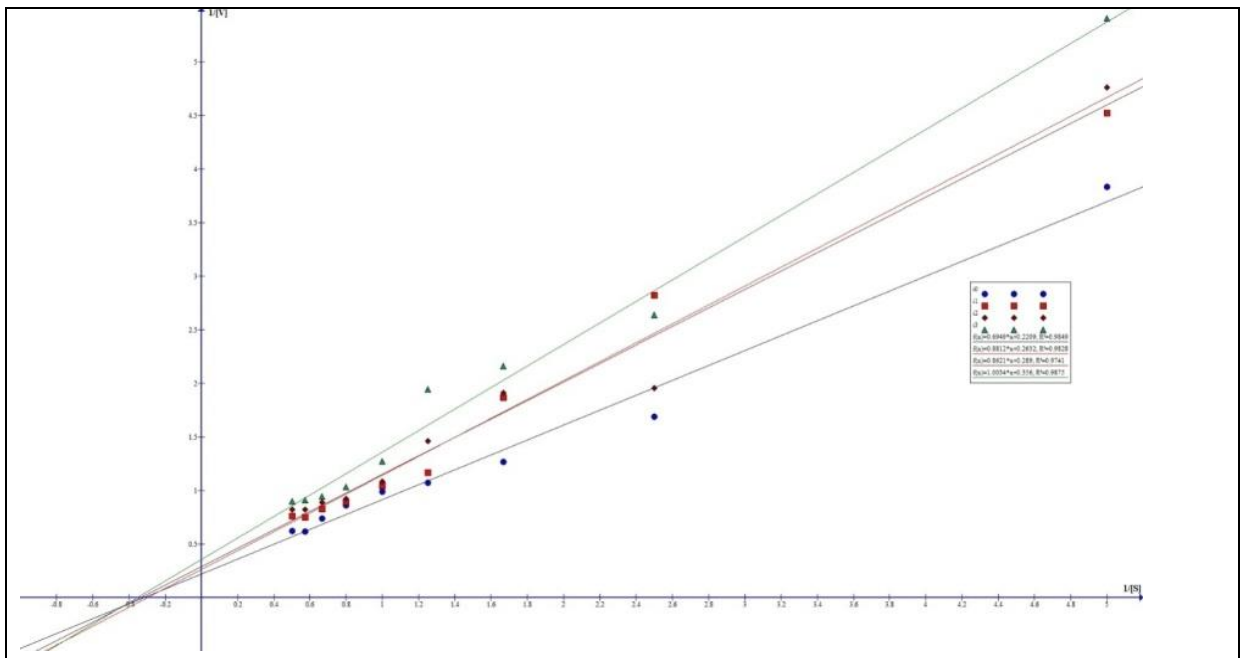
Compound	Residue Atom		Ligand Atom	Distance Å	Interaction
11b	PHE157	1281C	23C	5.176	π -STACKING
	HIS239	1951N	15C	4.159	π -STACKING
	HIS245	2000N	23C	4.459	π -STACKING
	PHE311	2535C	1C	4.279	π -STACKING
	PHE311	2535C	8C	4.193	π -STACKING
	HIS279	6938H	22O	2.217	H-BOND
	HIS279	6938H	24S	2.344	H-BOND

	ASN412	7977H	38O	2.128	H-BOND
12a	HIS239	1951N	14C	4.253	π -STACKING
	PHE311	2535C	14C	4.431	π -STACKING
	HIS239	6622H	25O	1.941	H-BOND
	HIS279	6938H	37N	2.253	H-BOND
	HIS279	6938H	39O	1.512	H-BOND
12l	HIS279	2286N	8C	5.306	π -STACKING
	PHE300	2449C	8C	5.125	π -STACKING
	PHE311	2535C	15C	4.145	π -STACKING
	LYS155	5988H	39O	2.455	H-BOND
	LYS155	5989H	22O	1.510	H-BOND
	LYS155	5989H	26O	2.427	H-BOND

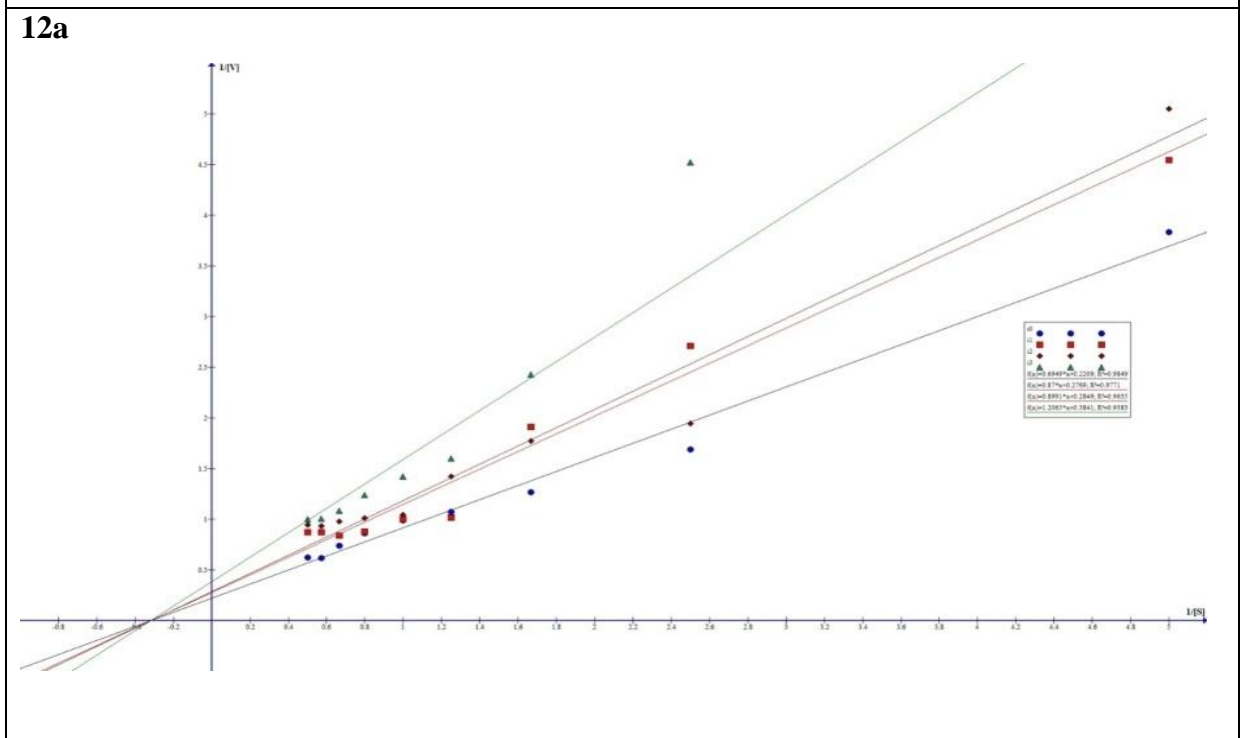
Table-11: IC₅₀, K_{im}, V_{max} and modes of inhibition of selected synthetic ligands. K_m and V_{max} values of α -D-glycosidase for 4-NPG without inhibitor were 3.14 μ M and 4.52 μ M/min respectively.

Compound	IC ₅₀ (μM)	K _{im} (μM)	V _{max} (μM/min)	Mode of inhibition
		Inhibitor concentration of 25 μg		
11b	41.57 ± 1.01	3.34	3.79	Mixed- Uncompetitive
12a	38.82 ± 1.17	3.14	3.61	Non-competitive
12l	47.37 ± 1.10	3.15	3.80	Non-competitive

11b



12a



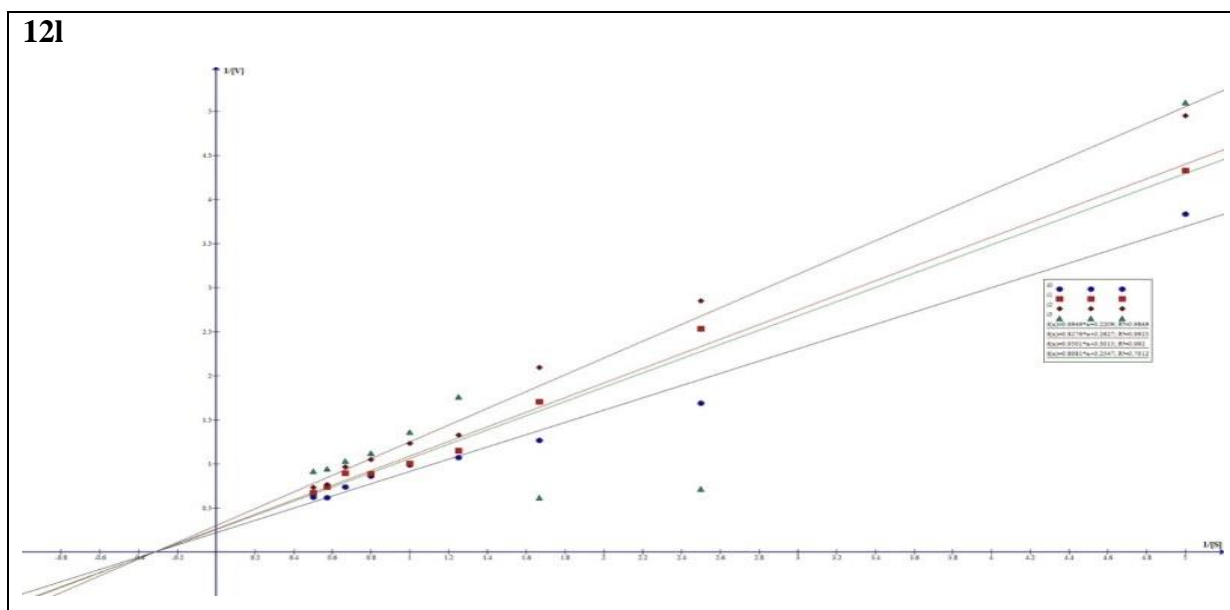


Figure-10: Lineweaver-Burk plot for understanding the mode of Inhibition of α -D-glucosidase by (a) **11b** (b) **12a** and (c) **12l**.

2.9 Conclusion

In conclusion, a simple method for the synthesis of 2-styrylquinolines was developed via sp^3 C-H activation under catalyst-free (metal-free) condition DES [DMU + L-tartaric acid (3:1)] as a catalyst as well as solvent. The developed method was extended for the sulfonate ester-based aldehydes to give sulfonate ester-based styrylquinolines in good yields. The photophysical activities of the resulting styrylquinolines were studied. Similarly, the sulfonate based styrylquinolines were evaluated for the α -Glucosidase activity inhibition (*in-vitro*) against Acarbose as a standard drug (IC_{50} **32.15 \pm 2.04**), and observed that compound **12a** is showing good IC_{50} values (best IC_{50} 38.82 \pm 1.17).

2.10 Experimental section

2.10.1 General: The starting materials were purchased from Sigma-Aldrich, SRL, Spectrochem, and SD-Fine and used as received. 1H and ^{13}C -NMR spectra are recorded on Bruker 400 MHz spectrometer using $CDCl_3$ or $DMSO-d_6$ as solvents and reported in δ ppm. The mass spectra were recorded on Shimadzu LCMS-2020 and Agilent QTOF machine. Melting points were recorded on the Stuart melting point apparatus. UV-visible spectra were taken using Agilent-Cary 100 UV-Visible spectrometer. Emission spectra were recorded by Horiba FluoroLog spectrophotometer.

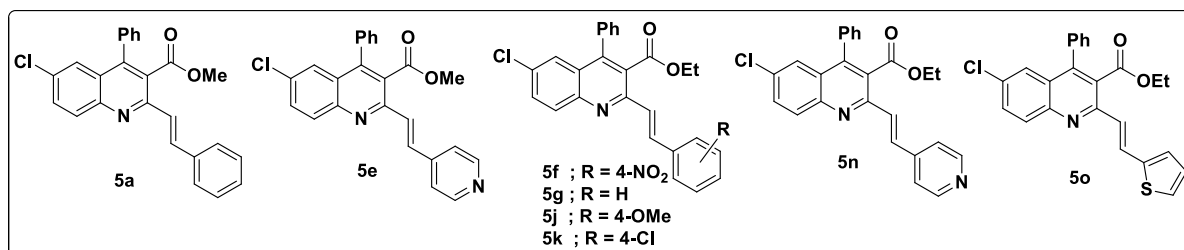
2.10.2 General procedure for the one-pot synthesis of styrylquinoline derivatives:

Deep eutectic solvent was prepared by heating 1,3-dimethyl urea (0.525g) + L-tartaric acid (0.250g) (3:1 ratio) at 80°C for 30 min. To this, 5-chloro 2-amino benzophenone 0.231g (1 mmol) and β -diketone/ketone/piperidone (1 mmol) were added and heating continued for another 30 minutes at 80°C to give the Friedländer annulation product (*in situ*). To the same pot aldehydes (1.1 mmol) were added and heating continued till the styrylquinoline derivatives formed (Knoevenagel condensation product *via* sp^3 C-H activation). The crude products obtained were purified by column chromatography on silica gel using petroleum ether-ethyl acetate (7:3 v/v) as eluent to give the desired products.

2.10.3 General procedure for the formation of Friedländer annulation intermediate (substituted 2-methyl quinolines 3b, 3c, 3f):

Deep eutectic solvent was prepared by heating of 1,3-dimethyl urea (0.525g) + L-tartaric acid (0.250g) (with 3:1 ratio) at 80°C for 30 min. To this, 5-chloro 2-amino benzophenone 0.231g (1 mmol) and EAA/2-butanone/N-Boc-piperidone (1 mmol) were added and heated continuously for another 30 minutes at 80°C to provide a sticky solid. After completion of the reaction (monitoring by TLC), the mixture was cooled to room temperature and washed with water. The crude product obtained was purified by crystallization.

Confirmation of the reported molecules by reported melting points:^{22(a-b)}



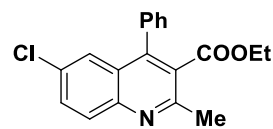
S. No.	Compound No.	M.P °C (Found)	M.P °C (Reported) ²²
1	5a	206-207	207-208
2	5e	200-201	199-200
3	5f	204-205	205-206
4	5g	142-143	143-145
5	5j	146-147	147-148
6	5k	171-172	170-171
7	5n	164-165	163-164
8	5o	161-162	160-161

2.11. Spectral data of the synthesized compounds:

Ethyl 6-chloro-2-methyl-4-phenylquinoline-3-carboxylate (3b): White

solid, mp 175–176°C, 90% yield. ¹H NMR (400 MHz, CDCl₃) δ 7.94 (d, *J* = 7.2 Hz, 1H), 7.57 (d, *J* = 6.0 Hz, 1H), 7.45–7.42 (m, 4H), 7.27–7.19

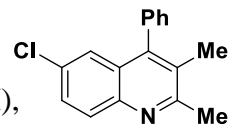
(m, 2H), 3.98 (s, 2H), 2.70 (s, 3H), 0.88 (s, 3H); IR (KBr, thin film, cm⁻¹): ν_{max} 3085, 2976, 1730, 1580, 1487, 1232, 842.



6-Chloro-2,3-dimethyl-4-phenylquinoline (3c): White solid, mp 210–

211°C, 90% yield. ¹H NMR (400 MHz, CDCl₃) δ 7.97 (d, *J* = 8.4 Hz, 1H),

7.53–7.48 (m, 4H), 7.26–7.20 (m, 3H), 2.74 (s, 3H), 2.17 (s, 3H); HRMS (ESI, *m/z*): Calcd. For C₁₇H₁₄ClNH⁺ 268.0888, found 268.0879.

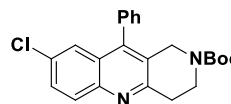


Tert-butyl-8-chloro-10-phenyl-3,4-dihydrobenzo[b][1,6]naphthyridine-2(1H)-carboxylate (3f):

White solid, mp 178–179°C, 90% yield. ¹H NMR (500 MHz, CDCl₃) δ 7.98

(d, *J* = 8.9 Hz, 1H), 7.66–7.45 (m, 4H), 7.35 (s, 1H), 7.26–7.23 (m, 2H), 4.43

(s, 2H), 3.82 (t, *J* = 5.5 Hz, 2H), 3.25 (s, 2H), 1.44 (s, 9H); HRMS (ESI, *m/z*): Calcd. For C₂₃H₂₃ClN₂O₂H⁺ 395.1531, found 395.1520.



Methyl 6-chloro-2-(3-nitrostyryl)-4-phenylquinoline-3-carboxylate (5b): White solid, mp 210–

211°C, 95% yield. ¹H NMR (400 MHz, CDCl₃) δ 8.25 (d, *J* = 8.8 Hz, 2H),

8.16–8.103 (m, 2H), 7.75 (d, *J* = 8.8 Hz, 2H), 7.72–7.69 (m, 1H), 7.57 (d,

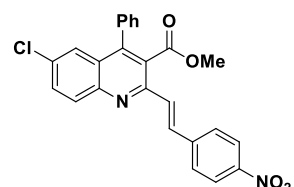
J = 2.4 Hz, 1H), 7.54–7.50 (m, 3H), 7.43 (d, *J* = 15.6 Hz, 1H), 7.37–7.35

(m, 2H), 3.60 (s, 3H); ¹³C NMR (100 MHz, CDCl₃) δ 168.4, 150.2, 147.6,

146.6, 146.5, 142.8, 134.9, 134.2, 133.3, 131.9, 131.3, 130.5, 129.1, 129.0, 128.9, 128.6, 128.5,

128.1, 127.6, 126.7, 125.4, 125.3, 124.1, 52.6; HRMS (ESI, *m/z*): Calcd. For C₂₅H₁₇ClN₂O₄H⁺

445.0950, found 445.0928; IR (KBr, thin film, cm⁻¹): ν_{max} 3042, 2958, 1718, 1564, 1527, 1227, 835.



Methyl 6-chloro-2-(4-methoxystyryl)-4-phenylquinoline-3-carboxylate (5c): White solid, mp

169–170 °C, 85% yield. ¹H NMR (500 MHz, CDCl₃) δ 8.08–8.03 (m,

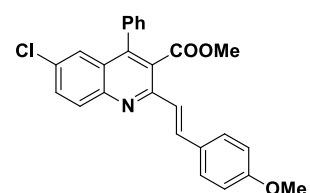
2H), 7.65 (dd, *J* = 7.2, 2.0 Hz, 1H), 7.57 (d, *J* = 7.2 Hz, 2H), 7.52–7.50

(m, 4H), 7.36 (dd, *J* = 6.0, 1.6 Hz, 2H), 7.13 (d, *J* = 14.5 Hz, 1H), 6.92

(d, *J* = 6.8 Hz, 2H), 3.84 (s, 3H), 3.60 (s, 3H); ¹³C NMR (125 MHz,

CDCl₃) δ 168.6, 160.4, 151.6, 146.6, 145.9, 136.6, 135.1, 132.3, 131.4, 131.1, 131.0, 129.2, 129.1,

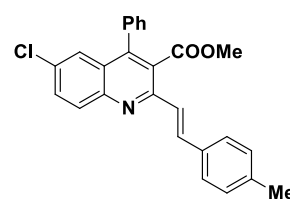
128.8, 128.5, 127.4, 126.2, 125.2, 121.6, 114.2, 55.3, 52.4; HRMS (ESI, *m/z*): Calcd. For



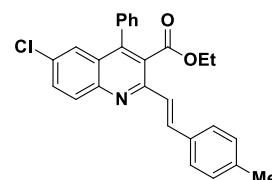
C₂₆H₂₀ClNO₃H⁺ 430.1132, found 430.1177; IR (KBr, thin film, cm⁻¹): ν_{max} 3065, 2974, 1736, 1603, 1256, 1207, 1028, 829.

Methyl-6-chloro-2-(4-methylstyryl)-4-phenylquinoline-3-carboxylate

(5d): White solid, mp 162–163 °C, 90% yield. ¹H NMR (500 MHz, CDCl₃) δ 8.02 (s, 1H), 8.00 (s, 1H), 7.66 (d, *J* = 2.0 Hz, 1H), 7.66 (d, *J* = 2.0 Hz, 1H), 7.55–7.53 (m, 2H), 7.52–7.49 (m, 5H), 7.34–7.32 (m, 3H), 3.59 (s, 3H), 2.77 (s, 3H); ¹³C NMR (125 MHz, CDCl₃) δ 168.6, 154.9, 146.1, 145.6, 135.6, 134.9, 134.2, 132.4, 131.6, 131.2, 131.1, 130.5, 129.1, 128.9, 128.8, 128.5, 128.0, 125.9, 125.2, 124.4, 52.3, 23.7; HRMS (ESI, *m/z*): Calcd. For C₂₆H₂₀ClNO₂H⁺ 414.1255, found 414.0342; IR (KBr, thin film, cm⁻¹): ν_{max} 3080, 2986, 1729, 1633, 1215, 1177, 820.

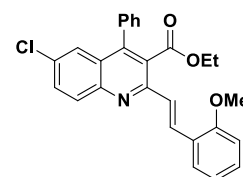


Ethyl-6-chloro-2-(4-methylstyryl)-4-phenylquinoline-3-carboxylate (5h): White solid, mp 162–163 °C, 85% yield. ¹H NMR (400 MHz, CDCl₃) δ 8.09 (d, *J* = 3.2 Hz, 1H), 8.06 (d, *J* = 9.6 Hz, 1H), 7.66 (dd, *J* = 6.4, 2.4 Hz, 1H), 7.52–7.50 (m, 6H), 7.38–7.36 (m, 2H), 7.25 (d, *J* = 3.2 Hz, 1H), 7.19 (d, *J* = 7.6 Hz, 2H), 4.10 (q, *J* = 14.0, 6.8 Hz, 2H), 2.38 (s, 3H), 0.96 (t, *J* = 7.2 Hz, 3H); ¹³C NMR (100 MHz, CDCl₃) δ 168.0, 151.5, 146.5, 145.8, 139.1, 136.97, 135.1, 133.7, 132.4, 131.4, 131.1, 129.5, 129.4, 128.8, 128.6, 128.4, 127.6, 126.3, 125.2, 122.9, 61.6, 21.4, 13.7; HRMS (ESI, *m/z*): Calcd. For C₂₇H₂₂ClNO₂H⁺ 428.1412, found 428.1407; IR (KBr, thin film, cm⁻¹): ν_{max} 3050, 2952, 1724, 1621, 1214, 1156, 832.



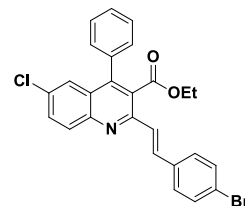
Ethyl-6-chloro-2-(2-methoxystyryl)-4-phenylquinoline-3-carboxylate (5i):

Pale yellow solid, mp 164–165 °C, 86% yield. ¹H NMR (400 MHz, CDCl₃) δ 8.08–8.07 (m, 2H), 7.65 (d, *J* = 8.8 Hz, 1H), 7.56 (d, *J* = 8.4 Hz, 2H), 7.50 (s, 4H), 7.38–7.36 (m, 2H), 7.18 (d, *J* = 15.6 Hz, 1H), 6.92 (d, *J* = 8.4 Hz, 2H), 4.10 (q, *J* = 13.8, 6.8 Hz, 2H), 3.84 (s, 3H), 0.96 (t, *J* = 7.2 Hz, 3H); ¹³C NMR (100 MHz, CDCl₃): δ 168.1, 160.3, 151.6, 146.5, 145.8, 136.5, 135.1, 132.2, 131.3, 131.0, 129.4, 129.3, 129.1, 128.7, 128.4, 127.6, 126.2, 125.2, 121.6, 114.2, 61.6, 55.3, 13.7; HRMS (ESI, thin film, *m/z*): Calcd. For C₂₇H₂₂ClNO₃H⁺ 444.1361, found 444.1371.



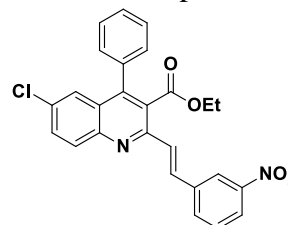
Ethyl-2-(4-bromostyryl)-6-chloro-4-phenylquinoline-3-carboxylate(5l):

White solid, mp 189–190°C, 90% yield. ¹H NMR (400 MHz, CDCl₃) δ 8.45 (s, 1H), 8.19–8.10 (m, 3H), 7.92 (d, *J* = 7.6 Hz, 1H), 7.70 (d, *J* = 9.2 Hz, 1H), 7.59–7.57 (m, 5H), 7.44 (d, *J* = 15.6 Hz, 1H), 7.38 (d, *J* = 3.2 Hz, 2H), 4.12 (q, *J* = 13.8, 6.8 Hz, 2H), 0.95 (t, *J* = 7.2 Hz, 3H); ¹³C NMR (100 MHz, CDCl₃+DMSO-d₆) δ 169.4, 156.3, 147.4, 141.2, 139.1, 135.8, 134.3, 133.8, 133.0, 132.8, 132.2, 131.7, 130.7, 130.0, 128.6, 127.1, 125.7, 124.3, 121.3, 117.4, 60.3, 15.1; HRMS (ESI, *m/z*): Calcd. For C₂₆H₁₉BrClNO₂H₂⁺ 493.0433, found 493.9371; IR (KBr, thin film, cm⁻¹): ν_{max} 3025, 2980, 1717, 1564, 1073, 835, 678.



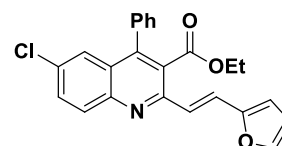
Ethyl-6-chloro-2-(3-nitrostyryl)-4-phenylquinoline-3-carboxylate (5m): White solid, mp 176–

177°C, 95% yield. ¹H NMR (400 MHz, CDCl₃) δ 8.47 (s, 1H), 8.20–8.12 (m, 3H), 7.94 (d, *J* = 7.6 Hz, 1H), 7.72 (m, 1H), 7.60–7.54 (m, 5H), 7.48–7.39 (m, 3H), 7.28 (s, 1H), 4.14 (q, *J* = 6.8 Hz, 2H), 0.98 (t, *J* = 6.8 Hz, 3H). ¹³C NMR (125 MHz, CDCl₃) δ 167.8, 150.3, 148.7, 146.4, 146.3, 138.2, 135.0, 134.2, 133.2, 133.1, 131.7, 131.2, 129.7, 129.3, 128.9, 128.5, 127.7, 126.9, 126.7, 125.3, 123.2, 122.0, 61.9, 13.6; HRMS (ESI, *m/z*): Calcd. For C₂₆H₁₉ClN₂O₄H⁺ 459.1106, found 459.0182; IR (KBr, thin film, cm⁻¹): ν_{max} 2990, 1737, 1604, 1540, 1350, 1256, 829.



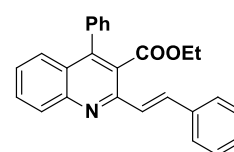
Ethyl-6-chloro-2-(2-(furan-2-yl)vinyl)-4-phenylquinoline-3-carboxylate (5p): White solid, mp

160–161°C, 85% yield. ¹H NMR (500 MHz, CDCl₃) δ 8.04 (d, *J* = 9.0 Hz, 1H), 7.90 (d, *J* = 15.5 Hz, 1H), 7.65 (dd, *J* = 9.0, 2.0 Hz, 1H), 7.53–7.49 (m, 4H), 7.46 (d, *J* = 1.5 Hz, 1H), 7.38–7.37 (m, 1H), 7.36 (d, *J* = 2.0 Hz, 1H), 7.20 (d, *J* = 15.3 Hz, 1H), 6.58 (d, *J* = 3.0 Hz, 1H), 6.47 (dd, *J* = 3.0, 1.5 Hz, 1H), 4.12 (q, *J* = 18.0, 7.5 Hz, 2H), 0.97 (t, *J* = 7.0 Hz, 3H); ¹³C NMR (125 MHz, CDCl₃) δ 168.6, 154.9, 146.1, 145.6, 135.6, 134.9, 133.0, 132.4, 131.6, 131.2, 131.1, 130.5, 129.0, 128.9, 128.8, 128.5, 128.0, 125.9, 125.28, 124.44, 52.31, 13.67; HRMS (ESI, *m/z*): Calcd. For C₂₄H₁₈ClNO₃H⁺ 404.1048, found 404.1056. IR (KBr, thin film, cm⁻¹): ν_{max} 3012, 2982, 1732, 1610, 1542, 1217, 829.



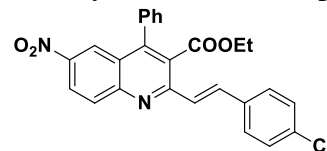
(E)-Ethyl 4-phenyl-2-styrylquinoline-3-carboxylate (5q): White solid, mp

186–187°C, 85% yield. ¹H NMR (400 MHz, CDCl₃) δ 8.09 (d, *J* = 8.4 Hz, 1H), 8.02 (d, *J* = 15.6 Hz, 1H), 7.66–7.62 (m, 1H), 7.55 (d, *J* = 7.6 Hz, 2H),

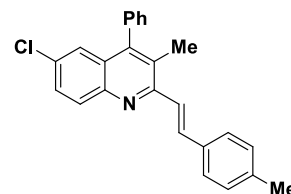


7.48 (d, $J = 8.4$ Hz, 1H), 7.41–7.39 (m, 3H), 7.35–7.23 (m, 7H), 4.02 (q, $J = 7.2$ Hz, 2H), 0.88 (t, $J = 7.2$ Hz, 3H); IR (KBr, thin film, cm^{-1}): ν_{max} 3075, 2976, 1740, 1615, 1520, 1460, 1055.

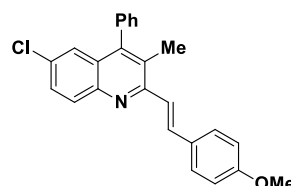
(E)-Ethyl-2-(4-chlorostyryl)-6-nitro-4-phenylquinoline-3-carboxylate (5r): yellow solid, mp 170–171°C, 86% yield. ^1H NMR (400 MHz, CDCl_3) δ 8.01–7.92 (m, 2H), 7.58 (d, $J = 8.0$ Hz, 1H), 7.42 (s, 8H), 7.29–7.17 (m, 3H), 4.01 (d, $J = 6.4$ Hz, 2H), 0.86 (s, 3H); ^{13}C NMR (100 MHz, CDCl_3) δ 168.94, 152.02, 147.51, 147.11, 136.61, 136.42, 136.10, 133.75, 132.94, 132.54, 132.15, 130.36, 130.06, 129.85, 129.51, 128.64, 127.52, 126.27, 125.63, 123.89, 62.73, 14.66; IR (KBr, thin film, cm^{-1}): ν_{max} 3083, 2986, 1736, 1620, 1545, 1452, 1063, 862.



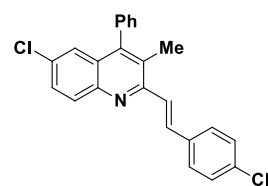
6-Chloro-3-methyl-2-(4-methylstyryl)-4-phenylquinoline (6a): White solid, mp 191–192°C, 85% yield. ^1H NMR (500 MHz, CDCl_3) δ 8.04 (d, $J = 9.0$ Hz, 1H), 8.00 (d, $J = 15.5$ Hz, 1H), 7.57–7.52 (m, 5H), 7.50–7.47 (m, 2H), 7.26–7.24 (m, 3H), 2.38 (s, 3H), 2.31 (s, 3H); ^{13}C NMR (125 MHz, CDCl_3) δ 155.4, 146.2, 144.9, 138.7, 137.0, 136.3, 134.2, 131.4, 130.8, 129.5, 129.3, 129.1, 128.8, 128.0, 127.9, 127.8, 127.4, 124.9, 123.6, 21.4, 16.8; HRMS (ESI, m/z): Calcd. For $\text{C}_{25}\text{H}_{20}\text{ClNH}^+$ 370.1357, found 370.1372; IR (KBr, thin film, cm^{-1}): ν_{max} 3014, 2985, 2919, 1631, 1572, 1163, 805.



6-Chloro-2-(4-methoxystyryl)-3-methyl-4-phenylquinoline (6b): Yellow solid, mp 174–175 °C, 88% yield. ^1H NMR (400 MHz, CDCl_3) δ 8.03–7.96 (m, 2H), 7.62–7.49 (m, 6H), 7.43 (d, $J = 15.6$ Hz, 1H), 7.24 (d, $J = 7.6$ Hz, 3H), 6.93 (d, $J = 8.0$ Hz, 2H), 3.85 (s, 3H), 2.31 (s, 3H); ^{13}C NMR (100 MHz, CDCl_3) δ 160.1, 155.5, 146.2, 144.9, 137.1, 135.9, 131.3, 130.7, 129.7, 129.3, 129.3, 128.9, 128.7, 128.1, 127.8, 127.7, 127.7, 124.9, 122.3, 114.2, 55.3, 16.8; HRMS (ESI, m/z): Calcd. For $\text{C}_{25}\text{H}_{20}\text{ClNOH}^+$ 386.1306, found 386.1321; IR (KBr, thin film, cm^{-1}): ν_{max} 2924, 3010, 1627, 1603, 1443, 1171, 831.



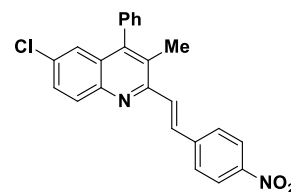
6-Chloro-2-(4-chlorostyryl)-3-methyl-4-phenylquinoline (6c): Pale yellow solid, mp 165–166 °C, 92% yield. ^1H NMR (500 MHz, CDCl_3) δ 8.04 (d, $J = 9.0$ Hz, 1H), 7.97 (d, $J = 15.5$ Hz, 1H), 7.85 (s, 1H), 7.60–7.48 (m, 5H), 7.37–7.32 (m, 3H), 7.27 (s, 1H), 7.24 (d, $J = 7.0$ Hz, 1H), 7.06 (d, $J = 2.0$ Hz, 1H), 2.32 (s, 3H); ^{13}C NMR (125 MHz, CDCl_3) δ 160.0, 154.7, 146.3, 145.2, 144.8, 143.6, 136.8, 135.3, 134.8, 134.1, 130.8, 130.3, 129.2, 128.9, 128.7, 128.4, 127.8, 125.1, 124.8,



16.7; HRMS (ESI, m/z): Calcd. For $C_{24}H_{17}Cl_2NH^+$ 390.0811, found 389.9901; IR (KBr, thin film, cm^{-1}): ν_{max} 3064, 2910, 1571, 1420, 721, 702.

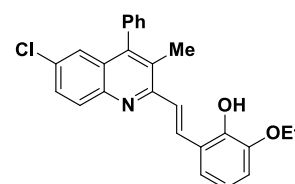
6-Chloro-3-methyl-2-(4-nitrostyryl)-4-phenylquinoline (6d): Yellow

solid, mp 219–220°C, 95% yield. 1H NMR (500 MHz, $CDCl_3$) δ 8.38 (d, $J = 15.0$ Hz, 1H), 8.05 (d, $J = 9.0$ Hz, 1H), 8.01 (d, $J = 8.0$ Hz, 1H), 7.83 (d, $J = 8.0$ Hz, 1H), 7.64 (t, $J = 7.5$ Hz, 1H), 7.51–7.45 (m, 6H), 7.27–7.23 (m, 3H), 2.32 (s, 3H); ^{13}C NMR (125 MHz, $CDCl_3 + DMSO-d_6$) δ 154.2, 148.6, 146.6, 144.9, 136.8, 133.1, 132.8, 132.1, 131.4, 131.2, 129.8, 129.6, 129.3, 128.9, 128.8, 128.2, 127.9, 124.8, 124.8, 16.8; HRMS (ESI, m/z): Calcd. For $C_{24}H_{17}ClN_2O_2H^+$ 401.1051, found 401.1065; IR (KBr, thin film, cm^{-1}): ν_{max} 3010, 298, 1567, 1511, 1337, 1166, 824.



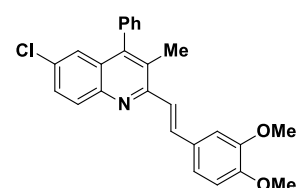
5-(2-(6-Chloro-3-methyl-4-phenylquinolin-2-yl) vinyl)-2-ethoxyphenol (6e): White solid, mp

152–153 °C, 85% yield. 1H NMR (500 MHz, $CDCl_3$) δ 8.03 (d, $J = 9.0$ Hz, 1H), 7.95 (d, $J = 16.5$ Hz, 1H), 7.54–7.49 (m, 5H), 7.40–7.36 (m, 2H), 7.25–7.21 (m, 3H), 7.14 (s, 1H), 4.19 (q, $J = 14.0, 7.0$ Hz, 2H), 2.31 (s, 3H), 1.47 (t, $J = 7.0$ Hz, 3H); ^{13}C NMR (125 MHz, $CDCl_3 + DMSO-d_6$) δ 167.6, 149.8, 147.9, 144.1, 141.7, 140.4, 139.8, 139.7, 138.7, 137.7, 136.6, 136.2, 136.0, 135.8, 134.8, 134.0, 130.9, 129.4, 127.9, 127.1, 115.6, 61.0, 17.8, 13.5; HRMS (ESI, m/z): Calcd. For $C_{26}H_{22}ClNO_2H^+$ 416.1412, found 416.1404.



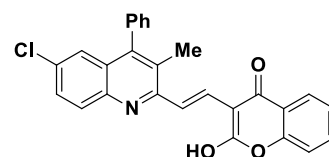
6-Chloro-2-(3,4-dimethoxystyryl)-3-methyl-4-phenylquinoline (6f): White solid, mp 175–176°C,

90% yield. 1H NMR (400 MHz, $CDCl_3$) δ 8.15 – 8.05 (m, 2H), 7.59 – 7.53 (m, 4H), 7.43 (d, $J = 15.6$ Hz, 1H), 7.30 – 7.28 (m, 4H), 7.23 (s, 1H), 6.93 (d, $J = 8.4$ Hz, 1H), 3.99 (s, 3H), 3.95 (s, 3H), 2.36 (s, 3H); ^{13}C NMR (125 MHz, $CDCl_3$) δ 160.5, 155.4, 149.8, 149.1, 146.2, 144.9, 137.0, 136.5, 136.3, 131.3, 130.7, 129.3, 128.8, 128.8, 128.1, 127.8, 127.7, 127.3, 124.9, 122.6, 121.0, 119.4, 111.2, 110.0, 56.0, 16.8; HRMS (ESI, m/z): Calcd. For $C_{26}H_{22}ClNO_2H^+$ 416.1412, found 416.1404; IR (KBr, thin film, cm^{-1}): ν_{max} 3029, 2954, 1568, 1261, 1245, 1027, 828.



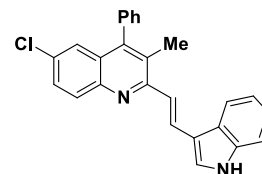
3-(2-(6-Chloro-3-methyl-4-phenylquinolin-2-yl) vinyl)-2-hydroxy-4H-chromen-4-one (6g):

Dark red solid, 86% yield. 1H NMR (400 MHz, $CDCl_3$) δ 8.00 (d, $J = 9.2$ Hz, 1H), 7.93 (d, $J = 15.6$ Hz, 1H), 7.58–7.42 (m, 5H), 7.40–7.24 (m, 3H), 7.2–7.13 (m, 3H), 7.03 (d, $J = 6.0$ Hz, 1H), 2.26 (s, 3H); ^{13}C



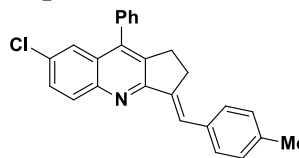
NMR (100 MHz, CDCl₃+DMSOd₆) δ 198.5, 172.0, 160.0, 152.7, 148.5, 141.4, 141.2, 133.6, 133.5, 132.5, 131.9, 131.7, 130.3, 129.7, 129.6, 129.4, 129.1, 129.0, 128.3, 127.7, 127.4, 124.7, 118.4, 85.6, 16.4; HRMS (ESI, m/z): Calcd. For C₂₇H₁₈ClNO₃NH₄⁺ 457.1313, found 457.0365; IR (KBr, thin film, cm⁻¹): ν_{\max} 3395, 3052, 2963, 1720, 1642, 1266, 1088, 748.

2-(2-(1H-Indol-3-yl)vinyl)-6-chloro-3-methyl-4-phenylquinoline (6h):



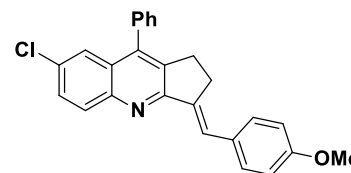
White solid, mp 182–183°C, 86% yield. ¹H NMR (400 MHz, CDCl₃+DMSOd₆) δ 7.95 (s, 1H), 7.89 (d, *J* = 10.4 Hz, 3H), 7.78 (d, *J* = 14.8 Hz, 1H), 7.71–7.64 (m, 5H), 7.42 (d, *J* = 6.4 Hz, 3H), 7.28 (d, *J* = 5.6 Hz, 2H), 2.29 (s, 3H); ¹³C NMR (100 MHz, CDCl₃+ DMSOd₆) δ 162.7, 145.3, 142.9, 140.8, 136.5, 136.3, 135.2, 133.9, 133.6, 132.0, 131.1, 130.2, 129.5, 129.1, 128.4, 127.4, 125.8, 124.6, 122.7, 120.7, 119.5, 113.5, 110.8, 17.7; HRMS (ESI, m/z): Calcd. For C₂₆H₁₉ClN₂H⁺ 395.1310, found 395.1314; IR (KBr, thin film, cm⁻¹): ν_{\max} 3301, 3078, 2951, 1651, 1272, 1246, 1075, 742.

7-Chloro-3-(4-methylbenzylidene)-9-phenyl-2,3-dihydro-1H-cyclopenta[b]quinoline (7a):



Yellow solid, mp 229–230°C, 89% yield. ¹H NMR (500 MHz, CDCl₃) δ 8.06 (d, *J* = 9.0 Hz, 1H), 7.81 (s, 1H), 7.55–7.49 (m, 7H), 7.35 (d, *J* = 7.5 Hz, 2H), 7.24–7.20 (m, 2H), 3.15 (s, 2H), 3.0–2.98 (m, 2H), 2.38 (s, 3H); ¹³C NMR (125 MHz, CDCl₃) δ 162.2, 147.2, 142.7, 139.7, 137.6, 136.0, 135.9, 134.5, 131.4, 130.8, 129.5, 129.4, 129.3, 129.1, 128.8, 128.3, 127.8, 125.4, 124.4, 28.8, 27.7, 21.4; HRMS (ESI, m/z): Calcd. For C₂₆H₂₀ClNH⁺ 382.1357, found 382.1353; IR (KBr, thin film, cm⁻¹): ν_{\max} 3030, 2917, 1600, 1585, 1163, 1075, 826.

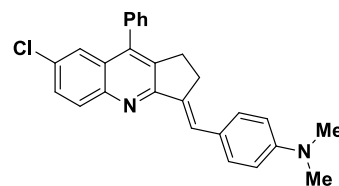
7-Chloro-3-(4-methoxybenzylidene)-9-phenyl-2,3-dihydro-1H-cyclopenta[b]quinoline (7b):



White solid, mp 168–169°C, 85% yield. ¹H NMR (400 MHz, CDCl₃) δ 8.06 (d, *J* = 8.8 Hz, 1H), 7.79 (s, 1H), 7.58–7.49 (m, 7H), 7.36 (d, *J* = 6.8 Hz, 2H), 6.96 (d, *J* = 8.4 Hz, 2H), 3.85 (s, 3H), 3.17–3.14 (m, 2H), 3.03–3.00 (m, 2H); ¹³C NMR (100 MHz, CDCl₃) δ 162.3, 159.1, 147.2, 142.6, 138.4, 136.0, 132.0, 131.2, 130.9, 130.7, 130.2, 129.4, 129.1, 128.8, 128.3, 127.8, 125.0, 124.3, 114.0, 55.3, 28.7, 27.7; HRMS (ESI, m/z): Calcd. For C₂₆H₂₀ClNOH⁺ 398.1306, found 398.1312; IR (KBr, thin film, cm⁻¹): ν_{\max} 2974, 2835, 1632, 1604, 1252, 1128, 1028, 830.

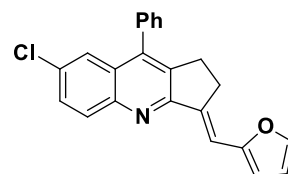
4-((7-Chloro-9-phenyl-1H-cyclopenta[b]quinolin-3(2H)-ylidene)methyl)-N,N-dimethylaniline

(7c): White solid, mp 218–219°C, 85% yield. ¹H NMR (500 MHz, CDCl₃) δ 8.14 (s, 1H), 8.03 (d, *J* = 9.0 Hz, 1H), 7.54–7.50 (m, 3H), 7.49–7.46 (m, 3H), 7.27–7.23 (m, 3H), 6.75 (d, *J* = 9.0 Hz, 2H), 3.01 (s, 6H), 2.63 (t, *J* = 5.5 Hz, 2H), 1.79 (t, *J* = 6.0 Hz, 2H); ¹³C NMR (125MHz, CDCl₃) δ 155.5, 149.5, 145.2, 144.8, 136.6, 132.3, 130.9, 130.6, 129.7, 129.3, 129.2, 128.7, 128.0, 127.4, 126.0, 124.5, 111.8, 40.3, 28.5, 28.5, 22.9; HRMS (ESI, *m/z*): Calcd. For C₂₇H₂₃ClN₂H⁺ 411.1623, found 411.162; IR (KBr, thin film, cm⁻¹): ν_{max} 3385, 3101, 2932, 1613, 1566, 1265, 1163, 822.



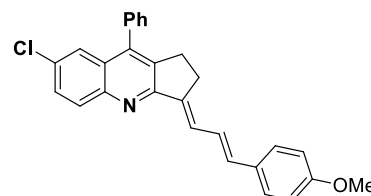
6-Chloro-2-(furan-2-ylmethylene)-8-phenyl-1,2-dihydrocyclobuta [b] quinoline (7d): Brown

solid, mp 198–199°C, 88% yield. ¹H NMR (400 MHz, CDCl₃) δ 8.02 (d, *J* = 8.8 Hz, 1H), 7.63 (t, *J* = 2.4 Hz, 1H), 7.57–7.447 (m, 6H), 7.36 (d, *J* = 6.8 Hz, 2H), 6.53–6.49 (m, 2H), 3.17 – 3.16 (m, 2H), 3.02–2.99 (m, 2H); ¹³C NMR (100 MHz, CDCl₃) δ 161.5, 153.8, 143.0, 142.7, 138.8, 136.8, 135.9, 131.4, 130.7, 129.4, 129.0, 128.8, 128.3, 127.8, 124.3, 112.7, 112.6, 112.0, 111.7, 28.4, 27.4; HRMS (ESI, *m/z*): Calcd. For C₂₃H₁₆ClNOH⁺ 358.0993, found: 358.0990; IR (KBr, thin film, cm⁻¹): ν_{max} 3059, 2942, 2884, 1683, 1537, 1268, 1073, 829.



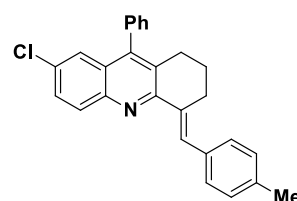
7-Chloro-3-((E)-3-(4-methoxyphenyl)allylidene)-9-phenyl-2,3-dihydro-1H-cyclopenta

[b]quinoline (7e): Yellow solid, mp 170–171°C, 85% yield. ¹H NMR (400 MHz, CDCl₃) δ 8.13–7.92 (m, 2H), 7.62 (d, *J* = 8.0 Hz, 2H), 7.58–7.39 (m, 5H), 7.25 (d, *J* = 7.6 Hz, 4H), 6.94 (d, *J* = 8.0 Hz, 2H), 3.75 (s, 3H), 2.95 (d, *J* = 7.3 Hz, 2H), 2.19 (t, *J* = 7.0 Hz, 2H); ¹³C NMR (100 MHz, CDCl₃) δ 171.22, 160.5, 145.6, 145.0, 141.2, 134.3, 133.2, 132.6, 131.7, 129.5, 129.3, 129.1, 128.9, 128.6, 128.2, 127.6, 124.8, 124.7, 123.0, 114.3, 97.4, 55.3, 27.5, 26.5; HRMS (ESI, *m/z*): Calcd. For C₂₈H₂₂ClNOH⁺ 424.1463, found 424.1467; IR (KBr, thin film, cm⁻¹): ν_{max} 3068, 2932, 1599, 1583, 1509, 1253, 1173, 818.



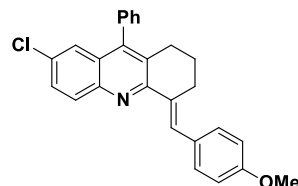
7-Chloro-4-(4-methylbenzylidene)-9-phenyl-1, 2, 3, 4-tetrahydroacridine (7f): White solid, mp

185–186°C, 88% yield. ¹H NMR (500 MHz, CDCl₃) δ 8.20 (s, 1H), 8.04 (d, *J* = 9.0 Hz, 1H), 7.55–7.47 (m, 5H), 7.41 (d, *J* = 8.0 Hz, 2H), 7.29 (d, *J* = 2.5 Hz, 1H), 7.25–7.20 (m, 3H), 2.97 (t, *J* = 5.5 Hz, 2H), 2.65 (t, *J* = 6.0 Hz, 3H), 2.38 (s, 3H), 1.81–1.76 (m, 2H); ¹³C NMR (125 MHz,

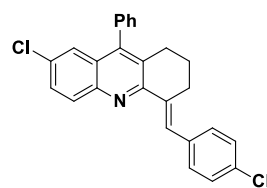


CDCl₃) δ 154.7, 145.3, 145.1, 137.0, 136.5, 135.4, 134.9, 131.4, 131.0, 130.0, 129.9, 129.8, 129.4, 129.2, 128.9, 128.8, 128.1, 127.6, 124.5, 28.6, 28.2, 22.9, 21.3; HRMS (ESI, m/z): Calcd. For C₂₇H₂₂ClNH⁺ 396.1518, found 396.1514; IR (KBr, thin film, cm⁻¹): ν_{max} 3102, 2958, 2863, 1602, 1540, 1169, 820.

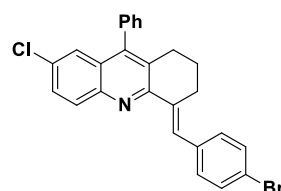
7-Chloro-4-(4-methoxybenzylidene)-9-phenyl-1,2,3,4-tetrahydroacridine (7g): White solid, mp 174–175 °C, 85% yield. ¹H NMR (500 MHz, CDCl₃) δ 8.17 (s, 1H), 8.03 (d, *J* = 9.0 Hz, 1H), 7.54–7.46 (m, 7H), 7.28–7.24 (m, 2H), 6.94 (d, *J* = 8.0 Hz, 2H), 3.84 (s, 3H), 2.96 (t, *J* = 5.5 Hz, 2H), 2.64 (t, *J* = 6.0 Hz, 2H), 1.80 (p, *J* = 6.0, 5.5 Hz, 2H); ¹³C NMR (125 MHz, CDCl₃) δ 162.3, 159.1, 158.6, 147.2, 142.6, 138.4, 136.0, 135.9, 131.2, 130.9, 130.7, 130.2, 129.4, 129.1, 128.8, 128.3, 127.8, 125.0, 124.3, 114.0, 55.3, 28.7, 27.7; HRMS (ESI, m/z): Calcd. For C₂₇H₂₂ClNOH⁺ 412.1463, found 412.1467; IR (KBr, thin film, cm⁻¹): ν_{max} 3069, 2948, 1602, 1536, 1167, 1031, 832.



7-Chloro-4-(4-chlorobenzylidene)-9-phenyl-1,2,3,4-tetrahydroacridine (7h): White solid, mp 221–222 °C, 90% yield. ¹H NMR (500 MHz, CDCl₃) δ 8.17 (s, 1H), 8.03 (d, *J* = 9.0 Hz, 1H), 7.55–7.52 (m, 3H), 7.51–7.47 (m, 2H), 7.36 (d, *J* = 8.0 Hz, 2H), 7.30 (d, *J* = 2.0 Hz, 1H), 7.25–7.23 (m, 2H), 2.93 (t, *J* = 7.0 Hz, 2H), 2.66 (t, *J* = 6.5 Hz, 2H), 1.82–1.77 (m, 2H); ¹³C NMR (125 MHz, CDCl₃) δ 154.2, 145.5, 145.1, 136.7, 136.4, 136.2, 132.8, 131.6, 131.1, 129.8, 129.5, 129.2, 129.0, 128.8, 128.6, 128.4, 128.1, 127.7, 124.6, 28.5, 28.1, 22.9; HRMS (ESI, m/z): Calcd. For C₂₆H₁₉Cl₂NH⁺ 416.0967, found 416.0968; IR (KBr, thin film, cm⁻¹): ν_{max} 3080, 2940, 1565, 1474, 829, 820.

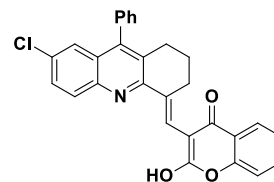


4-(4-Bromobenzylidene)-7-chloro-9-phenyl-1,2,3,4-tetrahydroacridine (7i): White solid, mp 237–238 °C, 95% yield. ¹H NMR (500 MHz, CDCl₃) δ 8.16 (s, 1H), 8.02 (d, *J* = 9.0 Hz, 1H), 7.54–7.46 (m, 4H), 7.42–7.33 (m, 4H), 7.28 (d, *J* = 2.0 Hz, 1H), 7.24–7.21 (m, 2H), 2.92–2.90 (m, 2H), 2.64 (t, *J* = 6.5 Hz, 2H), 1.81–1.76 (m, 2H); ¹³C NMR (125 MHz, CDCl₃) δ 155.2, 149.0, 146.1, 139.3, 137.7, 137.2, 133.8, 132.6, 132.1, 131.3, 130.5, 130.2, 129.8, 129.6, 129.4, 129.1, 128.7, 128.0, 125.6, 29.5, 29.1, 23.9; HRMS (ESI, m/z): Calcd. For C₂₆H₁₉BrClNH₂⁺ 461.0535, found 461.9387; IR (KBr, thin film, cm⁻¹): ν_{max} 3051, 2938, 1620, 1566, 1071, 830, 708.



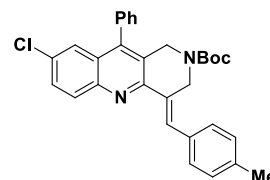
3-((7-Chloro-9-phenyl-2,3-dihydroacridin-4(1H)-ylidene)methyl)-2-hydroxy-4H-chromen-4-

one (7j): Yellow solid, mp 205–206 °C, 85% yield. ¹H NMR (400 MHz, CDCl₃) δ 8.24 (s, 1H), 8.19 (d, *J* = 8.8 Hz, 2H), 7.58 (d, *J* = 8.4 Hz, 2H), 7.52–7.44 (m, 4H), 7.26 (d, *J* = 1.6 Hz, 1H), 7.18 (d, *J* = 6.8 Hz, 3H), 2.89 (t, *J* = 5.2 Hz, 2H), 2.63 (t, *J* = 6.0 Hz, 2H), 1.80–1.74 (m, 2H); ¹³C NMR (100 MHz, CDCl₃) δ 183.4, 172.6, 137.2, 136.3, 135.4, 134.2, 133.9, 133.7, 132.6, 132.3, 132.0, 131.8, 129.9, 129.3, 129.0, 128.9, 128.5, 128.5, 128.6, 127.1, 126.1, 125.8, 122.8, 120.4, 26.6, 22.7, 22.8; HRMS (ESI, *m/z*): Calcd. For C₂₉H₂₀ClNO₃ 465.1132, found 463.9975 (M-1); IR (KBr, thin film, cm⁻¹): ν_{max} 3420, 3050, 2931, 1651, 1291, 1271, 703.



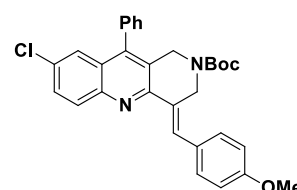
Tert-butyl-8-chloro-4-(4-methylbenzylidene)-10-phenyl-3,4-dihydrobenzo[*b*][1,6] naphthyridin

-2(1H)-carboxylate (8a): Pale yellow solid, mp 155–156 °C, 88% yield. ¹H NMR (400 MHz, CDCl₃) δ 8.10 (s, 1H), 8.02 (d, *J* = 8.8 Hz, 1H), 7.53–7.43 (m, 4H), 7.31–7.28 (m, 3H), 7.22–7.14 (m, 4H), 4.70 (s, 2H), 4.39 (s, 2H), 2.31 (s, 3H), 1.21 (s, 9H); ¹³C NMR (100 MHz, CDCl₃) δ 154.6, 145.6, 145.0, 139.3, 137.8, 134.9, 133.6, 132.0, 131.9, 131.0, 130.1, 129.7, 129.1, 128.7, 128.7, 128.6, 128.3, 127.3, 126.0, 124.6, 80.2, 53.8, 44.5, 28.3, 21.3; HRMS (ESI, *m/z*): Calcd. For C₃₁H₂₉ClN₂O₂H⁺ 497.1990, found 497.1991; IR (KBr, thin film, cm⁻¹): ν_{max} 3345, 2976, 1689, 1623, 1259, 1148, 832.



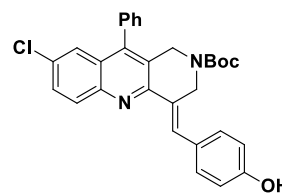
Tert-butyl-8-chloro-4-(4-methoxybenzylidene)-10-phenyl-3,4-dihydrobenzo[*b*][1,6]

naphthyridine-2(1H)-carboxylate (8b): White solid, mp 165–166 °C, 86% yield. ¹H NMR (400 MHz, CDCl₃) δ 8.11 (s, 1H), 7.55–7.36 (m, 6H), 7.29 (d, *J* = 2.0 Hz, 1H), 7.23–7.18 (m, 3H), 6.89 (d, *J* = 8.8 Hz, 2H), 4.72 (s, 2H), 4.39 (s, 2H), 3.78 (s, 3H), 1.22 (s, 9H); ¹³C NMR (100 MHz, CDCl₃+DMSO-*d*₆) δ 163.3, 159.6, 152.9, 148.6, 146.8, 144.5, 139.1, 134.3, 132.5, 131.7, 130.1, 129.4, 128.3, 127.8, 126.7, 124.8, 122.7, 121.6, 117.8, 71.0, 57.7, 55.7, 50.3, 44.8, 28.1; HRMS (ESI, *m/z*): Calcd. For C₃₁H₂₉ClN₂O₃H⁺ 513.1939, found 513.0981; IR (KBr, thin film, cm⁻¹): ν_{max} 3411, 2921, 1604, 1254, 1165, 1032, 830.



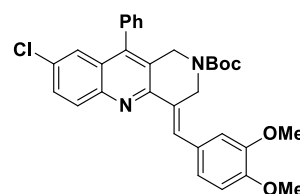
Tert-butyl-8-chloro-4-(4-hydroxybenzylidene)-10-phenyl-3,4-dihydrobenzo[b][1,6]

naphthyridine-2(1H)-carboxylate (8c): Yellow solid, mp 172–173 °C, 86% yield. ¹H NMR (400 MHz, CDCl₃) δ 8.08–7.93 (m, 2H), 7.54–7.49 (m, 6H), 7.47 (s, 2H), 7.29–7.16 (m, 3H), 4.64 (s, 2H), 4.41 (s, 2H), 1.18 (s, 9H); ¹³C NMR (100 MHz, CDCl₃) δ 154.5, 150.3, 145.4, 144.6, 138.8, 136.3, 134.6, 132.1, 131.8, 131.0, 130.9, 130.1, 130.0, 129.0, 128.9, 128.7, 127.2, 125.9, 124.6, 115.6, 80.1, 64.1, 44.5, 28.3; HRMS (ESI, m/z): Calcd. For C₃₀H₂₇ClN₂O₃H⁺ 499.1783, found 499.1799; IR (KBr, thin film, cm⁻¹): ν_{max} 3778, 3348, 3024, 2975, 1633, 1570, 1170, 955, 829.



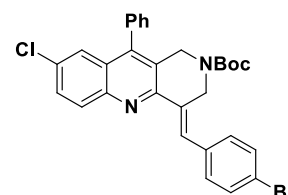
Tert-butyl-8-chloro-4-(3,4-dimethoxybenzylidene)-10-phenyl-3,4-dihydrobenzo[b][1,6]

naphthyridine-2(1H)-carboxylate (8d): Pale yellow solid, mp 140–141 °C, 85% yield. ¹H NMR (400 MHz, CDCl₃) δ 8.08 (s, 2H), 7.54–7.45 (m, 4H), 7.29–7.21 (m, 3H), 7.03–6.96 (m, 2H), 6.86 (d, *J* = 8.4 Hz, 1H), 4.73 (s, 2H), 4.40 (s, 2H), 3.86 (d, *J* = 4.4 Hz, 6H), 1.23 (s, 9H); ¹³C NMR (100 MHz, CDCl₃) δ 154.6, 148.9, 148.7, 145.6, 141.3, 134.6, 134.1, 133.2, 131.9, 131.0, 130.1, 130.1, 129.1, 128.7, 128.7, 128.3, 127.3, 126.0, 122.7, 118.4, 114.7, 111.0, 80.2, 55.9, 50.8, 45.0, 28.3; HRMS (ESI, m/z): Calcd. For C₃₂H₃₁ClN₂O₄H⁺ 543.2045, found 543.2054; IR (KBr, thin film, cm⁻¹): ν_{max} 3345, 3066, 2976, 1683, 1578, 1260, 1160, 1143, 1077, 827.



Tert-butyl-4-(4-bromobenzylidene)-8-chloro-10-phenyl-3,4-dihydrobenzo[b][1,6]

naphthyridine-2(1H)-carboxylate (8e): White solid, mp 168–169°C, 90% yield. ¹H NMR (400 MHz, CDCl₃) δ 8.04 (s, 1H), 7.99–7.88 (m 1H), 7.53–7.45 (m, 4H), 7.28–7.25 (m, 3H), 7.21–7.15 (m, 3H), 4.63 (s, 2H), 4.39–3.34 (m, 2H), 1.17 (s, 9H); ¹³C NMR (100 MHz, CDCl₃) δ 156.5, 151.2, 147.0, 141.6, 139.9, 136.6, 136.3, 134.2, 133.9, 133.6, 133.0, 132.2, 132.1, 131.1, 131.0, 130.7, 130.3, 129.3, 128.0, 126.6, 82.4, 60.6, 46.6, 30.3; HRMS (ESI, thin film, m/z): Calcd. For C₃₀H₂₆BrClN₂O₂H₂⁺ 562.1012, found 562.9716; IR (KBr, cm⁻¹): ν_{max} 3410, 3030, 2974, 1689, 1242, 1149, 832, 703.



Tert-butyl-8-chloro-4-(3-nitrobenzylidene)-10-phenyl-3,4-dihydrobenzo[*b*][1,6]-naphthyridine-

2(1H)-carboxylate (8f): White solid, mp 185–186 °C, 85% yield. ¹H

NMR (400 MHz, CDCl₃) δ 8.22 (d, *J* = 8.8 Hz, 3H), 8.01 (d, *J* = 8.8

Hz, 1H), 7.51–7.54 (m, 3H), 7.52–7.46 (m, 3H), 7.31 (s, 1H), 7.22–

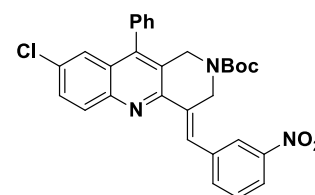
7.18 (m, 2H), 4.65 (s, 2H), 4.44 (s, 2H), 1.18 (s, 9H); ¹³C NMR (100

MHz, CDCl₃) δ 153, 146.5, 145.3, 140.4, 134.9, 134.4, 132.4, 131.5, 131.0, 130.2, 129.7, 129.0,

128.7, 128.7, 128.6, 128.1, 127.4, 127.0, 126.2, 124.4, 123.5, 121.1, 80.3, 55.1, 44.3, 27.9; HRMS

(ESI, *m/z*): Calcd. For C₃₀H₂₆ClN₃O₄H⁺ 528.1685, found 528.1698; IR (KBr, thin film, cm⁻¹): ν_{max}

3350, 3060, 2974, 2841, 1693, 1645, 1514, 1150, 834.



Tert-butyl-8-chloro-4-(4-(dimethylamino)benzylidene)-10-phenyl-3,4-dihydrobenzo[*b*][1,6]

1naphthyridine-2(1H)-carboxylate (8g): Yellow solid, mp 201–202 °C, 85% yield. ¹H NMR (400

MHz, CDCl₃) δ 8.08 (d, *J* = 8.8 Hz, 1H), 8.00 (d, *J* = 8.8 Hz, 1H), 7.59–

7.56 (m, 6H), 7.44 (d, *J* = 6.0 Hz, 1H), 7.37 (s, 1H), 7.32 (t, *J* = 6.8 Hz

1H), 6.77–6.71 (m, 2H), 4.85 (s, 2H), 4.46 (s, 2H), 3.04 (s, 6H), 1.34

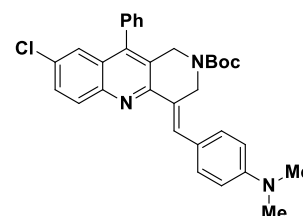
(s, 9H); ¹³C NMR (100 MHz, CDCl₃) δ 154.5, 150.0, 145.7, 134.1,

131.9, 131.4, 130.8, 130.1, 130.0, 129.8, 129.1, 128.9, 128.7, 128.7,

128.5, 128.3, 126.0, 124.6, 111.9, 111.0, 80.1, 45.3, 44.3, 40.3, 28.2; HRMS (ESI, *m/z*): Calcd.

For C₃₂H₃₂ClN₃O₂NH₄⁺ 543.2256, found 543.1048; IR (KBr, thin film, cm⁻¹): ν_{max} 3382, 2979,

2917, 1693, 1602, 1568, 1169, 818.



(E)-Ethyl 6-chloro-2-(3-(((4-nitrophenyl)sulfonyl)oxy)styryl)-4-phenylquinoline-3-carboxylate

11a: Pale yellow solid, mp 192–193 °C, 88% yield. ¹H NMR (400 MHz, CDCl₃+DMSO-*d*₆) δ

8.18 (s, 1H), 8.04–7.97 (m, 3H), 7.85 (d, *J* = 10.4 Hz, 1H), 7.74 (d, *J* = 8.4 Hz, 1H), 7.69–7.32 (m,

11H), 6.81 (d, *J* = 15.6 Hz, 1H), 4.03 (q, *J* = 8.0, 7.2 Hz, 2H), 0.90 (t, *J* = 7.2 Hz, 3H); ¹³C NMR

(100 MHz, CDCl₃+DMSO-*d*₆) δ 166.35, 156.95, 156.67,

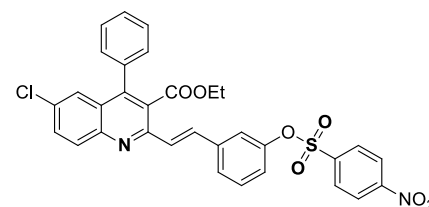
156.24, 151.62, 150.76, 150.58, 145.79, 144.42, 142.84,

140.13, 139.39, 137.67, 137.56, 134.97, 134.84, 133.59,

133.42, 129.15, 128.54, 125.46, 124.11, 123.41, 120.08,

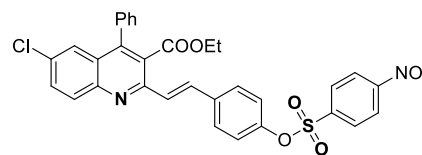
117.03, 116.18, 60.79, 26.61; HRMS (ESI, *m/z*): calcd. For C₃₂H₂₃ClN₂O₇SH⁺ 615.0987, found

615.0998; IR (KBr thin film, cm⁻¹): ν_{max} 3053, 2986, 1729, 1502, 1366, 1213, 858.



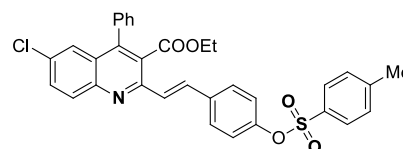
(E)-Ethyl 6-chloro-2-(4-((4-nitrophenyl)sulfonyl)oxy)styryl)-4-phenylquinoline-3-carboxylate

(11b): Pale green solid, mp 158–159°C, 95% yield. ^1H NMR (400 MHz, DMSO- d_6 + CDCl_3) δ 8.38 (d, J = 8.8 Hz, 2H), 8.06–7.82 (m, 5H), 7.64 (d, J = 8.8 Hz, 1H), 7.55–7.40 (m, 6H), 7.28–7.14 (m, 3H), 7.00 (d, J = 8.4 Hz, 1H), 4.01 (q, J = 14.4, 6.8 Hz 2H), 0.85 (t, J = 6.8 Hz, 3H); ^{13}C NMR (100 MHz, DMSO- d_6 + CDCl_3) δ 167.46, 151.16, 150.52, 149.22, 146.24, 146.05, 140.46, 135.85, 134.92, 134.81, 132.64, 131.61, 131.29, 130.19, 129.26, 129.12, 128.63, 127.69, 126.44, 125.15, 124.91, 124.80, 122.95, 122.66, 61.74, 13.67; HRMS (ESI, m/z): calcd. For $\text{C}_{32}\text{H}_{23}\text{ClN}_2\text{O}_7\text{SH}^+$ 615.0987, found 615.0431; IR (KBr thin film, cm^{-1}): ν_{max} 2972, 1724, 1557, 1368, 1214, 860.



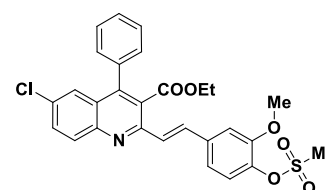
(E)-Ethyl 6-chloro-4-phenyl-2-(4-(tosyloxy)styryl)quinoline-3-carboxylate (11c): White solid,

mp 201–202°C, 85% yield. ^1H NMR (400 MHz, CDCl_3) δ 7.99–7.092 (m, 2H), 7.63–7.16 (m, 14H), 6.92 (s, 2H), 4.00 (d, J = 3.6 Hz, 2H), 2.37 (s, 3H), 0.85 (s, 3H); ^{13}C NMR (100 MHz, CDCl_3) δ 167.95, 150.92, 149.76, 146.48, 146.13, 145.49, 135.46, 135.07, 132.79, 132.29, 131.56, 129.78, 129.28, 128.87, 128.75, 128.73, 128.58, 128.51, 127.63, 126.53, 125.25, 124.94, 122.83, 122.65, 61.75, 21.67, 13.56; HRMS (ESI, m/z): calcd. For $\text{C}_{33}\text{H}_{26}\text{ClNO}_5\text{SH}^+$ 584.1293, found 584.1301; IR (KBr thin film, cm^{-1}): ν_{max} 3067, 2972, 1731, 1504, 1373, 1231, 857.



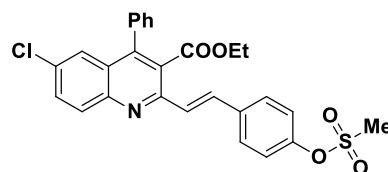
(E)-Ethyl-6-chloro-2-(3-methoxy-4-((methylsulfonyl)oxy)styryl)-4-phenylquinoline-3-carboxylate (11d): White solid, mp 162–163°C, 86% yield. ^1H NMR

(400 MHz, CDCl_3) δ 8.32 (d, J = 15.6 Hz, 1H), 8.04 (d, J = 8.8 Hz, 1H), 7.59 (dd, J = 9.2, 2.4 Hz, 1H), 7.44–7.16 (m, 9H), 6.90 (d, J = 8.0 Hz, 1H), 4.01 (q, J = 14.4, 7.2 Hz, 2H), 3.85 (s, 3H), 3.31 (s, 3H), 0.85 (t, J = 7.2 Hz, 3H); ^{13}C NMR (100 MHz, CDCl_3) δ 167.87, 152.58, 150.71, 146.40, 146.16, 137.52, 135.11, 132.90, 132.22, 130.30, 129.36, 129.14, 128.82, 128.64, 128.48, 127.69, 127.58, 127.37, 126.60, 125.16, 119.04, 112.81, 61.75, 56.23, 40.12, 13.60; HRMS (ESI, m/z): calcd. For $\text{C}_{28}\text{H}_{24}\text{ClNO}_6\text{SH}^+$ 538.1086, found 538.0567; IR (KBr thin film, cm^{-1}): ν_{max} 3061, 2972, 1729, 1514, 1365, 1221, 865.



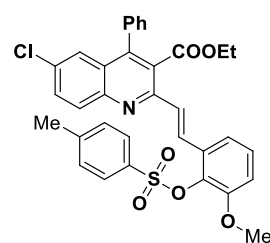
(E)-Ethyl 6-chloro-2-(4-((methylsulfonyl)oxy)styryl)-4-phenylquinoline-3-carboxylate (11e):

White solid, mp 183–184°C, 88% yield. ^1H NMR (400 MHz, $\text{DMSO-d}_6+\text{CDCl}_3$) δ 8.24 (d, J = 15.6 Hz, 1H), 8.08 (d, J = 8.8 Hz, 1H), 7.70–7.61 (m, 2H), 7.47–7.28 (m, 10H), 4.03 (q, J = 14.2, 7.2 Hz, 2H), 3.21 (s, 3H), 0.85 (t, J = 6.8 Hz, 3H); ^{13}C NMR (100 MHz, $\text{DMSO-d}_6+\text{CDCl}_3$) δ 167.55, 150.45, 147.45, 146.44, 145.95, 134.72, 132.99, 131.72, 131.08, 130.24, 129.66, 129.21, 129.05, 128.57, 128.19, 127.71, 126.88, 126.58, 125.17, 123.38, 61.88, 38.26, 13.59; HRMS (ESI, m/z): calcd. For $\text{C}_{27}\text{H}_{22}\text{ClNO}_5\text{SH}^+$ 508.0980, found 508.0475; IR (KBr thin film, cm^{-1}): ν_{max} 2980, 1725, 1485, 1358, 1222, 1082, 886.



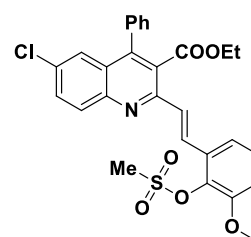
(E)-Ethyl 6-chloro-2-(3-methoxy-2-(tosyloxy)styryl)-4-phenylquinoline-3-carboxylate (11f):

White solid, mp 199–200 °C, 85% yield. ^1H NMR (400 MHz, CDCl_3) δ 7.89 (d, J = 8.2 Hz, 1H), 7.75–7.42 (m, 10H), 7.16–6.85 (m, 6H), 3.99 (d, J = 6.4 Hz, 2H), 3.72 (s, 3H), 1.84 (s, 3H), 0.85 (s, 3H); ^{13}C NMR (100 MHz, CDCl_3) δ 167.77, 153.32, 150.55, 146.24, 145.65, 144.56, 137.77, 135.00, 133.99, 132.79, 131.84, 131.41, 130.54, 129.45, 129.29, 128.89, 128.54, 128.46, 128.42, 127.56, 126.36, 126.10, 125.14, 119.40, 118.45, 112.81, 61.73, 56.02, 21.25, 13.73; HRMS (ESI, m/z): calcd. For $\text{C}_{34}\text{H}_{28}\text{ClNO}_6\text{SH}^+$ 614.1399, found 614.0845; IR (KBr thin film, cm^{-1}): ν_{max} 3050, 2962, 1724, 1511, 1368, 1156, 858.



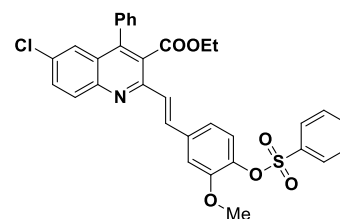
(E)-Ethyl 6-chloro-2-(3-methoxy-2-((methylsulfonyl)oxy)styryl)-4-phenylquinoline-3-carboxylate (11g):

Yellow solid, mp 203–204°C, 85% yield. ^1H NMR (400 MHz, CDCl_3) δ 8.31 (d, J = 15.6 Hz, 1H), 8.02 (d, J = 8.8 Hz, 1H), 7.57 (d, J = 7.6 Hz, 1H), 7.43–7.15 (m, 9H), 6.89 (d, J = 7.6 Hz, 1H), 4.00 (q, J = 14.0, 6.8 Hz, 2H), 3.84 (s, 3H), 3.30 (s, 3H), 0.84 (t, J = 7.2 Hz, 3H); ^{13}C NMR (100 MHz, CDCl_3) δ 167.91, 152.58, 150.74, 146.52, 146.05, 137.53, 135.14, 132.86, 132.25, 131.56, 131.44, 130.17, 129.37, 128.80, 128.47, 127.69, 127.57, 127.47, 126.59, 125.14, 119.00, 112.80, 61.73, 56.22, 39.83, 13.60; HRMS (ESI, m/z): calcd. For $\text{C}_{28}\text{H}_{24}\text{ClNO}_6\text{SH}^+$ 538.1086, found 538.0561; IR (KBr thin film, cm^{-1}): ν_{max} 3030, 2972, 1730, 1546 1378, 1156, 857.



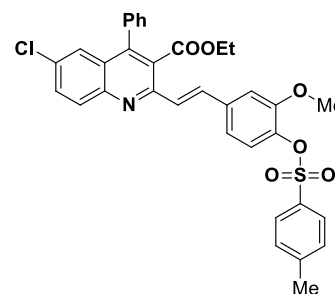
(E)-Ethyl 6-chloro-2-(3-methoxy-4-((phenylsulfonyl)oxy)styryl)-4-phenylquinoline-3-carboxylate (11h): Pale yellow solid, mp 219–220 °C, 85% yield. ¹H

NMR (400 MHz, CDCl₃) δ 7.82–7.78 (m, 4H), 7.62–7.10 (m, 12H), 6.85 (d, *J* = 4.0 Hz, 1H), 4.00 (d, *J* = 6.0 Hz, 2H), 3.68 (s, 3H), 0.86 (s, 3H); ¹³C NMR (100 MHz, CDCl₃) δ 167.81, 153.09, 150.63, 146.27, 145.82, 137.66, 137.02, 135.09, 133.31, 132.81, 132.05, 131.41, 130.55, 129.40, 129.36, 128.86, 128.78, 128.73, 128.53, 128.40, 127.63, 127.50, 126.45, 125.17, 125.15, 118.49, 61.72, 55.95, 13.72; HRMS (ESI, *m/z*): calcd. For C₃₃H₂₆ClNO₆SH⁺ 600.1242, found 600.1250; IR (KBr thin film, cm⁻¹): ν_{max} 3012, 2986, 1712, 1509, 1385, 1232, 862.



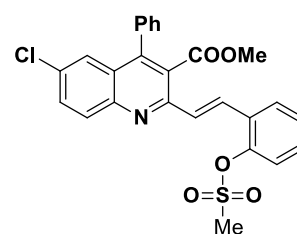
(E)-Ethyl 6-chloro-2-(3-methoxy-4-(tosyloxy)styryl)-4-phenylquinoline-3-carboxylate (11i):

Pale green powder, mp 198–199 °C, 88% yield. ¹H NMR (400 MHz, DMSO-*d*₆+CDCl₃) δ 8.03–7.97 (m, 2H), 7.68–7.62 (m, 3H), 7.49–7.48 (m, 3H), 7.34–7.29 (m, 5H), 7.18–7.05 (m, 4H), 4.04 (q, *J* = 14.2, 6.8 Hz, 2H), 3.54 (s, 3H), 2.40 (s, 3H), 0.88 (t, *J* = 6.8 Hz, 3H); ¹³C NMR (100 MHz, DMSO-*d*₆+CDCl₃) δ 167.38, 151.95, 150.69, 146.33, 145.94, 145.56, 138.46, 136.43, 135.67, 134.81, 132.81, 132.49, 131.67, 131.44, 129.80, 129.35, 129.15, 128.72, 128.58, 127.76, 126.42, 125.10, 124.98, 124.20, 119.64, 112.41, 61.75, 55.78, 21.70, 13.78; HRMS (ESI, *m/z*): calcd. For C₃₄H₂₈ClNO₆SH⁺ 614.1399, found 614.1406; IR (KBr thin film, cm⁻¹): ν_{max} 3067, 2972, 1731, 1504, 1373, 1231, 857.



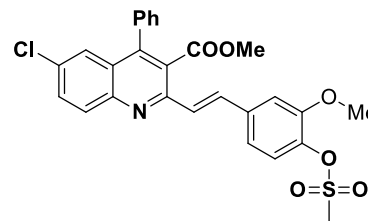
(E)-Methyl 6-chloro-2-(4-((methylsulfonyl)oxy)styryl)-4-phenylquinoline-3-carboxylate (11j):

White solid, mp 166–167 °C, 86% yield. ¹H NMR (400 MHz, CDCl₃) δ 8.01–7.96 (m, 2H), 7.59–7.42 (m, 8H), 7.23–7.14 (m, 4H), 3.52 (s, 3H), 3.09 (s, 3H); ¹³C NMR (100 MHz, CDCl₃) δ 168.49, 150.80, 149.32, 146.54, 146.30, 135.84, 135.19, 135.00, 132.89, 131.66, 131.22, 131.11, 129.11, 128.93, 128.91, 128.57, 127.53, 126.49, 125.30, 125.20, 122.41, 122.33, 52.55, 37.48; HRMS (ESI, *m/z*): calcd. For C₂₆H₂₀ClNO₅SH⁺ 494.0823, found 494.0837; IR (KBr thin film, cm⁻¹): ν_{max} 2980, 1711, 1485, 1354, 1228, 1085, 882.



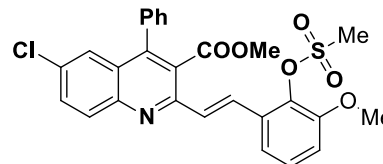
(E)-Methyl 6-chloro-2-(3-methoxy-4-((methylsulfonyl)oxy)styryl)-4-phenylquinoline-3-carboxylate (11k): Light yellow solid, mp 186–187 °C, 92% yield.

¹H NMR (400 MHz, CDCl₃) δ 8.39 (d, *J* = 15.6 Hz, 1H), 8.12 (d, *J* = 9.2 Hz, 1H), 7.68 (d, *J* = 9.6 Hz, 1H), 7.55–7.52 (m, 4H), 7.39–7.26 (m, 5H), 7.00 (d, *J* = 8.0 Hz, 1H), 3.94 (s, 3H), 3.60 (s, 3H), 3.40 (s, 3H); ¹³C NMR (100 MHz, DMSO-*d*₆+CDCl₃) δ 165.10, 160.98, 150.62, 147.41, 145.90, 145.17, 140.60, 135.74, 130.71, 130.15, 129.74, 129.05, 128.93, 128.77, 128.23, 128.06, 125.22, 124.29, 123.83, 121.87, 118.53, 116.34, 57.06, 51.06, 36.29; HRMS (ESI, *m/z*): calcd. For C₂₇H₂₂ClNO₆SH⁺ 524.0929, found 524.0926; IR (KBr thin film, cm⁻¹): ν_{max} 2972, 1714, 1480, 1375, 1214, 1156, 832.



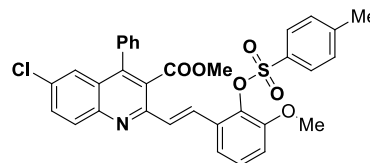
(E)-Methyl 6-chloro-2-(3-methoxy-2-((methylsulfonyl)oxy)styryl)-4-phenylquinoline-3-carboxylate (11l): White solid, 85% mp 197–198 °C, yield.

¹H NMR (400 MHz, CDCl₃) δ 8.30 (d, *J* = 15.6 Hz, 1H), 8.02 (d, *J* = 9.0 Hz, 1H), 7.60–7.57 (m, 1H), 7.45–7.42 (m, 4H), 7.29–7.16 (m, 5H), 6.90 (d, *J* = 8.0 Hz, 1H), 3.85 (s, 3H), 3.51 (s, 3H), 3.31 (s, 3H); ¹³C NMR (100 MHz, DMSO-*d*₆+CDCl₃) δ 168.01, 158.71, 149.77, 146.08, 142.07, 134.67, 132.83, 131.88, 131.45, 131.17, 130.00, 129.67, 129.18, 128.75, 128.58, 128.19, 127.82, 126.64, 126.27, 124.44, 118.79, 113.76, 56.32, 52.68, 36.07; HRMS (ESI, *m/z*): calcd. For C₂₇H₂₂ClNO₆SH⁺ 524.0929, found 524.0930; IR (KBr thin film, cm⁻¹): ν_{max} 3050, 2952, 1724, 1621, 1214, 1156, 832.



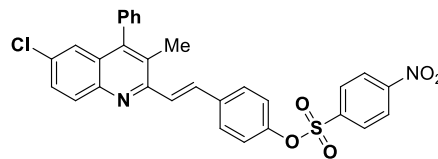
(E)-Methyl 6-chloro-2-(3-methoxy-2-(tosyloxy)styryl)-4-phenylquinoline-3-carboxylate (11m): White solid, mp 210–211 °C, 85% yield.

¹H NMR (400 MHz, DMSO-*d*₆+CDCl₃) δ 8.01 (d, *J* = 8.8 Hz, 1H), 7.87 (d, *J* = 15.6 Hz, 1H), 7.75–7.69 (m, 4H), 7.56–7.51 (m, 4H), 7.36 (d, *J* = 7.2 Hz, 3H), 7.12–6.98 (m, 4H), 3.75 (s, 3H), 3.60 (s, 3H), 2.01 (s, 3H); ¹³C NMR (100 MHz, DMSO-*d*₆+CDCl₃) δ 187.82, 168.05, 153.10, 150.27, 146.18, 145.82, 144.93, 137.47, 134.73, 133.72, 132.78, 131.57, 131.39, 130.30, 129.71, 129.52, 129.06, 128.66, 128.26, 127.79, 127.46, 126.25, 126.07, 125.10, 118.42, 113.14, 56.05, 52.52, 21.27; HRMS (ESI, *m/z*): calcd. For C₃₃H₂₆ClNO₆SH⁺ 599.1169, found 600.0698; IR (KBr thin film, cm⁻¹): ν_{max} 2943, 117, 1561, 1375, 1278, 760.



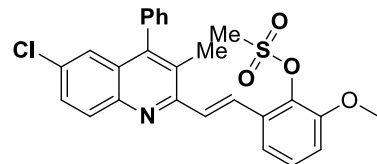
(E)-4-(2-(6-Chloro-3-methyl-4-phenylquinolin-2-yl)vinyl)phenyl 4-nitrobenzenesulfonate

(12a): White solid, mp 172–173 °C, 95% yield. ¹H NMR (400 MHz, DMSO-*d*₆+CDCl₃) δ 8.38 (d, *J* = 8.8 Hz, 2H), 8.05 (d, *J* = 8.8 Hz, 2H), 7.84–7.82 (m, 1H), 7.68 (s, 1H), 7.63–7.46 (m, 7H), 7.20–7.15 (m, 3H), 7.00 (d, *J* = 8.4 Hz, 2H), 2.28 (s, 3H); ¹³C NMR (100 MHz, DMSO-*d*₆+CDCl₃) δ 161.68, 156.93, 151.13, 148.76, 143.88, 140.53, 139.19, 131.59, 130.13, 129.25, 129.10, 129.01, 128.57, 128.00, 126.99, 126.10, 124.92, 124.82, 124.70, 123.77, 122.90, 122.57, 116.73, 16.81; HRMS (ESI, *m/z*): calcd. For C₃₀H₂₁ClN₂O₅SH⁺ 557.0932, found 557.0403; IR (KBr thin film, cm⁻¹): ν_{max} 2982, 1524, 1369, 1214, 1159, 869.

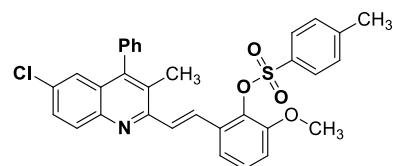


(E)-2-(2-(6-Chloro-3-methyl-4-phenylquinolin-2-yl)vinyl)-6-methoxyphenyl methanesulfonate

(12b): White solid, mp 221–222 °C, 85% yield. ¹H NMR (400 MHz, DMSO-*d*₆+CDCl₃) δ 8.20 (d, *J* = 15.6 Hz, 1H), 7.93 (d, *J* = 8.8 Hz, 1H), 7.64–7.36 (m, 7H), 7.24–7.14 (m, 3H), 6.97 (d, *J* = 8.0 Hz, 1H), 3.87 (s, 3H), 3.37 (s, 3H), 2.26 (s, 3H); ¹³C NMR (100 MHz, DMSO-*d*₆+CDCl₃) δ 153.55, 151.43, 145.36, 143.67, 136.35, 135.69, 131.51, 130.58, 130.16, 128.57, 128.48, 128.28, 128.06, 127.88, 127.25, 127.17, 126.94, 126.73, 123.71, 117.93, 111.75, 55.22, 39.01, 15.74; HRMS (ESI, *m/z*): calcd. For C₂₆H₂₂ClNO₄SH⁺ 480.1031, found 524.0934; IR (KBr thin film, cm⁻¹): ν_{max} 2993, 1502, 1476, 1370, 1152, 878.

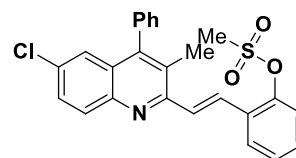


(E)-2-(2-(6-Chloro-3-methyl-4-phenylquinolin-2-yl)vinyl)-6-methoxyphenyl 4-methylbenzenesulfonate (12c): White powder, mp 191–192 °C, 88% yield. ¹H NMR (400 MHz, DMSO-*d*₆+CDCl₃) δ 7.90 (s, *J* = 9.2 Hz, 1H), 7.78 (d, *J* = 15.2 Hz, 1H), 7.69 (d, *J* = 8.4 Hz, 2H), 7.58–7.45 (m, 4H), 7.38–7.16 (m, 6H), 7.05 (d, *J* = 8.0 Hz, 2H), 6.89 (d, *J* = 7.2 Hz, 1H), 3.65 (s, 3H), 2.22 (s, 3H), 1.98 (s, 3H); ¹³C NMR (100 MHz, DMSO-*d*₆+CDCl₃) δ 154.23, 152.99, 146.48, 144.85, 144.22, 137.42, 136.56, 133.90, 132.12, 131.72, 130.81, 130.03, 129.45, 129.22, 128.93, 128.33, 128.24, 127.98, 127.89, 127.84, 127.70, 126.72, 124.76, 118.60, 112.78, 55.97, 21.31, 16.75; HRMS (ESI, *m/z*): calcd. For C₃₂H₂₆ClNO₄SH⁺ 556.1344, found 556.0813; IR (KBr thin film, cm⁻¹): ν_{max} 2952, 1424, 1368, 1214, 1156, 862.



(E)-2-(2-(6-Chloro-3-methyl-4-phenylquinolin-2-yl)vinyl)phenyl methanesulfonate (12d):

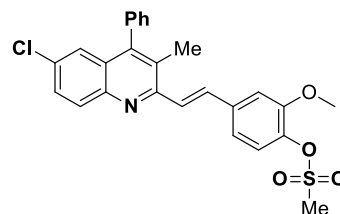
White powder, mp 152–153 °C, 85% yield. ^1H NMR (400 MHz, $\text{DMSO}-d_6+\text{CDCl}_3$) δ 7.99–7.94 (m, 2H), 7.69 (d, J = 8.4 Hz, 2H), 7.53–7.45 (m, 5H), 7.29 (d, J = 8.6 Hz, 2H), 7.20–7.15 (m, 3H), 3.18 (s, 3H), 2.26 (s, 3H); ^{13}C NMR (100 MHz, $\text{DMSO}-d_6+\text{CDCl}_3$) δ



154.58, 149.27, 146.48, 144.55, 136.65, 136.10, 134.65, 131.53, 130.82, 130.22, 129.41, 129.26, 129.01, 128.91, 128.71, 128.30, 128.11, 127.93, 125.63, 124.77, 122.54, 37.60, 16.77; HRMS (ESI, m/z): calcd. For $\text{C}_{25}\text{H}_{20}\text{ClNO}_3\text{SH}^+$ 450.0925, found 450.0449; IR (KBr thin film, cm^{-1}): ν_{max} 2993, 1505, 1480, 1365, 1156, 876.

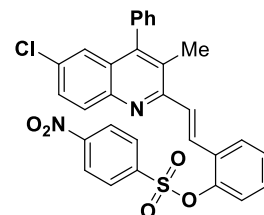
(E)-4-(2-(6-Chloro-3-methyl-4-phenylquinolin-2-yl)vinyl)-2-methoxyphenyl methanesulfonate

(12e): White powder, mp 202–203 °C, 85% yield. ^1H NMR (400 MHz, CDCl_3) δ 8.19 (d, J = 15.6 Hz, 1H), 7.96 (d, J = 8.8 Hz, 1H), 7.57–7.41 (m, 5H), 7.33–7.15 (m, 5H), 6.90 (d, J = 7.6 Hz, 1H), 3.85 (s, 3H), 3.32 (s, 3H), 2.25 (s, 3H); ^{13}C NMR (100 MHz, CDCl_3) δ 154.71, 152.53, 146.44, 144.89, 137.46, 136.95, 132.83, 131.85, 131.19, 129.76, 129.39, 129.35, 128.79, 128.44, 128.10, 128.08, 128.04, 127.55, 124.80, 119.16, 112.48, 56.20, 39.87, 16.78; HRMS (ESI, m/z): calcd. For $\text{C}_{26}\text{H}_{22}\text{ClNO}_4\text{SNa}^+$ 502.0850, found 502.0739; IR (KBr thin film, cm^{-1}): ν_{max} 2980, 1556, 1495, 1370, 1160, 866.



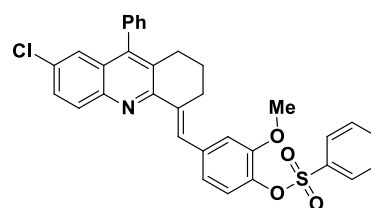
(E)-2-(2-(6-Chloro-3-methyl-4-phenylquinolin-2-yl)vinyl)phenyl 4-nitrobenzenesulfonate

(12f): Pale yellow powder, mp 186–187 °C, 95% yield. ^1H NMR (400 MHz, $\text{CDCl}_3+\text{DMSO}-d_6$) δ 7.96 (d, J = 2.8 Hz, 5H), 7.71 (d, J = 7.2 Hz, 1H), 7.58–7.46 (m, 5H), 7.38–7.29 (m, 3H), 7.22–7.12 (m, 4H), 2.12 (s, 3H); ^{13}C NMR (100 MHz, $\text{CDCl}_3+\text{DMSO}-d_6$) δ 153.47, 153.45, 150.59, 147.25, 146.48, 144.55, 140.52, 136.63, 131.63, 131.13, 130.28, 130.26, 130.15, 129.65, 129.29, 128.99, 128.39, 128.31, 127.87, 127.64, 126.77, 124.79, 124.54, 124.46, 124.18, 16.50; HRMS (ESI, m/z): calcd. For $\text{C}_{30}\text{H}_{21}\text{ClN}_2\text{O}_5\text{SH}^+$ 557.0932, found 557.0991; IR (KBr thin film, cm^{-1}): ν_{max} 2975, 1545, 1480, 1375, 1156, 856.



(E)-4-((7-Chloro-9-phenyl-2,3-dihydroacridin-4(1H)-ylidene)methyl)-2-methoxyphenyl benzenesulfonate (12g):

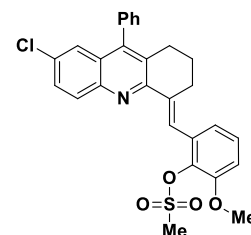
White powder, mp 206–207 °C, 90% yield. ^1H NMR (400 MHz, CDCl_3) δ 8.11 (s, 1H), 7.98 (d, J = 8.2 Hz, 1H), 7.86 (d, J = 7.6 Hz, 2H), 7.63–7.45 (m, 8H), 7.20–7.15 (m, 3H), 7.00 (d, J = 8.0 Hz, 1H), 6.90 (s, 1H), 3.51 (s, 3H), 2.88



(s, 2H), 2.62 (t, $J = 5.6$ Hz, 2H), 1.77 (t, $J = 5.6$ Hz, 2H); ^{13}C NMR (100 MHz, CDCl_3) δ 154.01, 151.34, 145.64, 145.08, 137.98, 137.18, 137.06, 136.33, 133.94, 131.73, 131.06, 129.83, 129.56, 129.19, 128.86, 128.74, 128.64, 128.21, 127.77, 124.60, 123.74, 122.00, 114.29, 55.56, 28.50, 28.16, 22.87; HRMS (ESI, m/z): calcd. For $\text{C}_{33}\text{H}_{25}\text{ClNO}_4\text{SH}^+$ 569.0892 found 569.2999; IR (KBr thin film, cm^{-1}): ν_{max} 2976, 1570, 1486, 1365, 1155, 850.

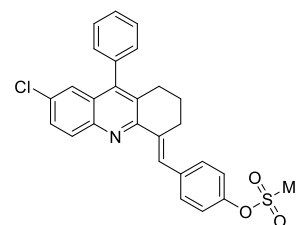
(Z)-2-((7-Chloro-9-phenyl-2,3-dihydroacridin-4(1H)-ylidene)methyl)-6-methoxyphenyl

methanesulfonate (12h): White solid, mp 152–153 °C, 88% yield. ^1H NMR (400 MHz, $\text{CDCl}_3 + \text{DMSO}-d_6$) δ 8.08 (d, $J = 15.6$ Hz, 1H), 7.83 (d, $J = 8.4$ Hz, 1H), 7.57–7.27 (m, 6H), 7.14–7.02 (m, 4H), 6.87 (d, $J = 8.0$ Hz, 1H), 3.75 (s, 3H), 3.25 (s, 3H), 3.14 (s, 2H), 2.38 (s, 2H), 2.15 (s, 2H); ^{13}C NMR (100 MHz, $\text{DMSO}-d_6 + \text{CDCl}_3$) δ 154.95, 153.70, 145.55, 138.13, 137.29, 134.61, 132.85, 132.41, 131.56, 131.14, 130.68, 130.15, 129.93, 129.63, 128.95, 128.55, 128.40, 127.48, 125.46, 119.30, 113.46, 56.68, 28.89, 28.23, 27.43, 22.02; HRMS (ESI, m/z): calcd. For $\text{C}_{28}\text{H}_{24}\text{ClNO}_4\text{SH}^+$ 506.1187, found 506.1165; IR (KBr thin film, cm^{-1}): ν_{max} 3050, 2986, 1719, 1550, 1358, 1146, 868.



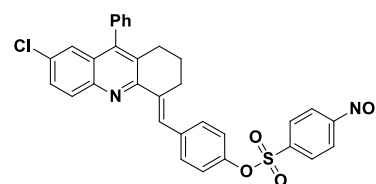
(E)-4-((7-Chloro-9-phenyl-2,3-dihydroacridin-4(1H)-ylidene)methyl)phenyl methanesulfonate

(12i): White powder, mp 212–213 °C, 88% yield. ^1H NMR (400 MHz, CDCl_3) δ 8.14 (s, 1H), 7.97 (d, $J = 8.8$ Hz, 1H), 7.49–7.42 (m, 6H), 7.25–7.16 (m, 5H), 3.10 (s, 3H), 2.86 (t, $J = 5.2$ Hz, 2H), 2.60 (t, $J = 5.2$ Hz, 2H), 1.76–1.70 (m, 2H); ^{13}C NMR (100 MHz, CDCl_3) δ 153.99, 147.94, 145.69, 145.09, 137.22, 136.35, 131.77, 131.35, 131.08, 129.81, 129.59, 129.18, 128.92, 128.86, 128.20, 127.79, 124.59, 121.76, 37.47, 28.51, 28.07, 22.87; HRMS (ESI, m/z): calcd. For $\text{C}_{27}\text{H}_{23}\text{ClNO}_3\text{SH}^+$ 476.1082, found 476.0964; IR (KBr thin film, cm^{-1}): ν_{max} 2975, 1565, 1488, 1375, 1148, 860.



(E)-4-((7-Chloro-9-phenyl-2,3-dihydroacridin-4(1H)-ylidene)methyl)phenyl 4-nitrobenzene

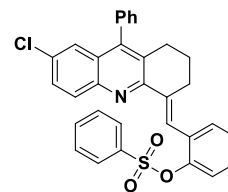
sulfonate (12j): White solid, mp 180–181 °C, 95% yield. ^1H NMR (400 MHz, CDCl_3) δ 8.35 (d, $J = 8.4$ Hz, 2H), 8.12–7.91 (m, 4H), 7.52–7.46 (m, 4H), 7.41 (d, $J = 8.4$ Hz, 2H), 7.22–7.19 (m, 3H), 6.99 (d, $J = 8.4$ Hz, 2H), 3.45 (s, 2H), 2.86 (s, 2H), 2.63 (t, $J = 5.6$ Hz, 2H); ^{13}C NMR (100 MHz, CDCl_3) δ 153.84, 151.05, 147.82, 145.72, 145.07, 141.09, 137.53, 137.42, 136.29, 131.83, 131.29, 131.05, 129.94, 129.79, 129.63, 129.17, 128.86, 128.22,



127.93, 127.80, 124.60, 124.37, 121.85, 28.46, 28.07, 22.85; HRMS (ESI, m/z): calcd. For $C_{32}H_{23}ClN_2O_5SH^+$ 583.1089, found 583.1314; IR (KBr thin film, cm^{-1}): ν_{max} 2956, 1545, 1490, 1368, 1158, 852.

(E)-2-((7-Chloro-9-phenyl-2,3-dihydroacridin-4(1H)-ylidene)methyl)phenyl benzenesulfonate

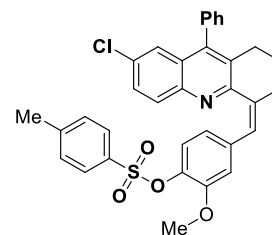
(12k): White powder, mp 177–178 °C, 90% yield. 1H NMR (400 MHz, $CDCl_3$) δ 7.94 (d, J = 8.8 Hz, 1H), 7.76–7.72 (m, 3H), 7.51–7.41 (m, 4H), 7.33–7.09 (m, 10H), 2.55–2.51 (m, 4H), 1.60–1.57 (m, 2H); ^{13}C NMR (100 MHz, $CDCl_3$) δ 153.44, 147.75, 145.57, 144.99, 138.00, 136.41, 135.97,



133.68, 131.75, 131.73, 131.21, 130.82, 129.61, 129.54, 129.16, 128.89, 128.81, 128.57, 128.50, 128.20, 127.73, 126.77, 124.59, 123.67, 123.36, 28.57, 27.86, 22.68; HRMS (ESI, m/z): calcd. For $C_{32}H_{24}ClNO_3SH^+$ 538.1238, found 538.1298; IR (KBr thin film, cm^{-1}): ν_{max} 3085, 2975, 1544, 1486, 1368, 1156, 860.

(Z)-4-((7-Chloro-9-phenyl-2,3-dihydroacridin-4(1H)-ylidene)methyl)-2-methoxyphenyl 4-methylbenzenesulfonate (12l):

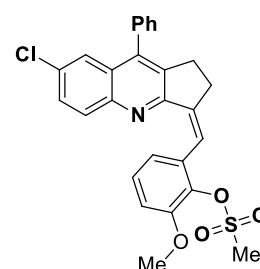
White solid, mp 169–170 °C, 86% yield. 1H NMR (400 MHz, $DMSO-d_6+CDCl_3$) δ 8.09 (s, 1H), 7.96 (d, J = 8.8 Hz, 1H), 7.65 (d, J = 8.4 Hz, 2H), 7.55–7.41 (m, 4H), 7.27–7.16 (m, 5H), 7.06 (d, J = 8.4 Hz, 1H), 6.97–6.90 (m, 2H), 3.50 (s, 3H), 2.90–2.81 (t, J = 5.2 Hz, 2H), 2.59 (t, J = 6.4 Hz, 2H), 2.38 (s, 3H), 1.76–1.70



(m, 2H); ^{13}C NMR (100 MHz, $DMSO-d_6+CDCl_3$) δ 153.86, 151.31, 145.70, 145.65, 145.31, 144.76, 137.80, 137.08, 136.81, 136.75, 136.07, 132.90, 131.51, 130.95, 129.96, 129.48, 129.10, 128.91, 128.52, 128.30, 127.64, 124.46, 123.49, 121.93, 114.29, 55.57, 28.40, 28.08, 22.71, 21.68; HRMS (ESI, m/z): calcd. For $C_{34}H_{28}ClNO_4S$ 581.1428, found 581.0699; IR (KBr thin film, cm^{-1}): ν_{max} 2968, 1595, 1505, 1370, 1176, 843.

(Z)-2-((7-Chloro-9-phenyl-1H-cyclopenta[b]quinolin-3(2H)-ylidene)methyl)-6-methoxyphenyl methanesulfonate (12m):

Light brown solid, mp 180–181 °C, 85% yield. 1H NMR (400 MHz, $DMSO-d_6+CDCl_3$) δ 8.19 (s, 1H), 8.02 (d, J = 6.4 Hz, 1H), 7.72 (s, 1H), 7.52–7.43 (m, 4H), 7.23–7.18 (m, 3H), 7.00–6.96 (m, 2H), 3.88 (s, 3H), 3.26 (s, 3H), 2.81–2.70 (t, J = 5.2 Hz, 2H), 2.62 (t, J = 6.0 Hz, 2H); ^{13}C NMR (100 MHz, $DMSO-d_6+CDCl_3$) δ 153.32, 152.33, 144.13, 137.40, 135.94, 135.89, 133.38, 131.76, 131.71, 130.07, 129.81, 129.44, 129.19,



129.02, 128.46, 128.16, 127.80, 127.31, 124.47, 122.33, 112.18, 56.22, 28.52, 27.97, 22.61; HRMS (ESI, m/z): calcd. For $C_{27}H_{22}ClNO_4SH^+$ 492.1031, found 492.1014; IR (KBr thin film, cm^{-1}): ν_{max} 2952, 1524, 1381, 1214, 1156, 832.

2.12. References

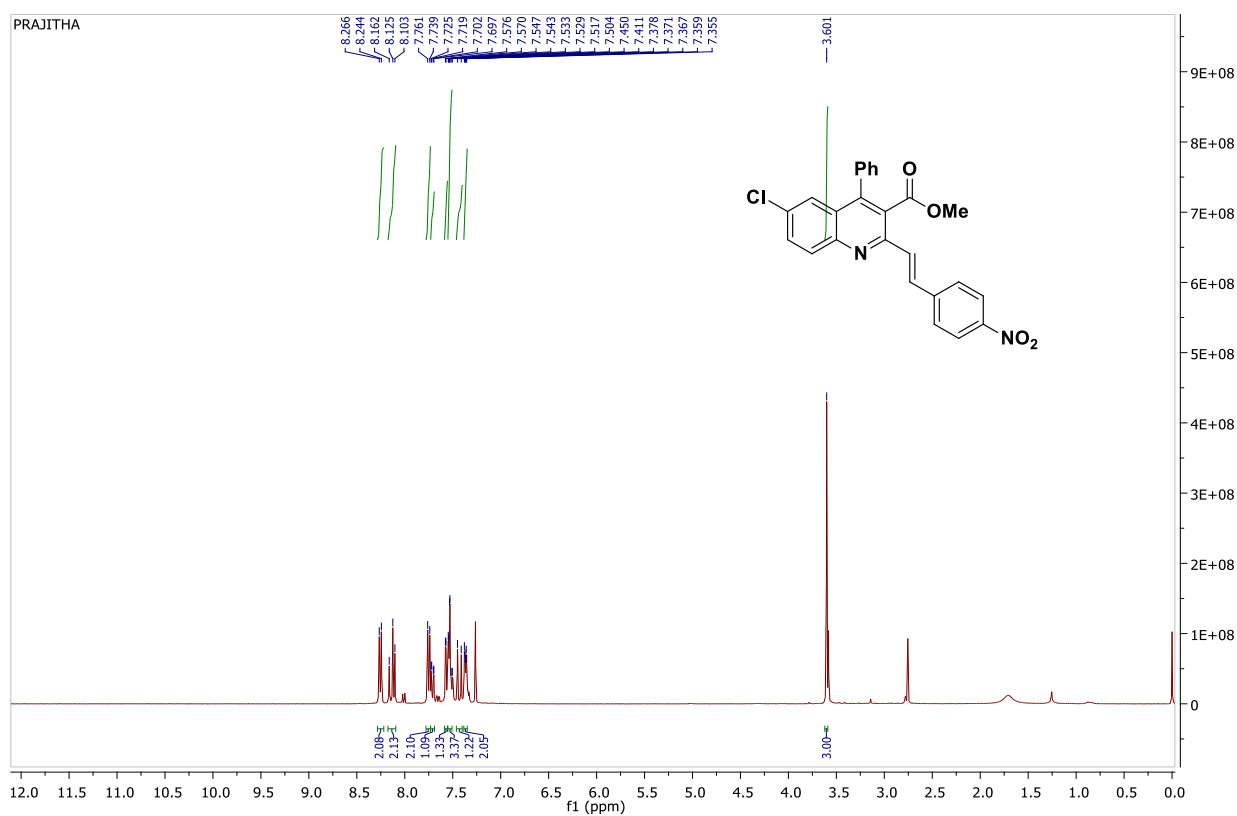
- 1 (a) Morimoto, Y.; Matsuda, F.; Shirahama, H. *Synlett* **1991**, 3, 201-202. (b) Katritzky, A. R.; Rees, C. W.; Scriven, E. F. V. *Eds. Pergamon, New York*, **1996**, 5, 245. (c) Michael, J. P. *Nat. Prod. Rep.* **1997**, 14, 605–618. (d) Maguire, M. P.; Sheets, K. R.; McVety, K.; Spada, A. P.; Zilberstein, A. *J. Med. Chem.* **1994**, 37, 2129–2137. (e) Kalluraya, B.; Sreenivasa, S. *Farmaco*, **1998**, 53, 399–404.
- 2 (a) Bharate, J. B.; Vishwakarma, R. A.; Bharate, S. B. *RSC Adv.* **2015**, 5, 42020–42053. (b) Nainwal, L. M.; Tasneem, S.; Akhtar, W.; Verma, G.; Khan, M. F.; Parvez, S.; Shaquiquzzaman, M.; Akhter, M.; Alam, M. M. *Eur. J. Med. Chem.* **2019**, 164, 121–170.
- 3 (a) Kaur, K.; Jain, M.; Reddy, R. P.; Jain, R. *Eur. J. Med. Chem.* **2010**, 45, 3245–3264. (b) Jain, S.; Chandra, V.; Jain, P. K.; Pathak, K.; Pathak, D.; Vaidya, A. *Arabian J. Chem.* **2019**, 12, 4920–4946. (c) Mukherjee, S.; Pal, M. *Curr. Med. Chem.* **2013**, 20, 4386–4410.
- 4 (a) Bharate, J. B.; Vishwakarma, R. A. and Bharate, S. B. *RSC Adv.* **2015**, 5, 42020–42053. (b) Sangshetti, J. N.; Zambare, A. S.; Gonjari, I.; Shinde, D. B. *Mini-Rev. Org. Chem.* **2014**, 11, 225–250.
- 5 (a) Roberts, B. F.; Zheng, Y. S.; Cleavele, J.; Lee, S.; Lee, E.; Ayong, L.; Yuan, Y.; Chakrabarti, D. *Int. J. Parasitol. Drugs Drug Resist.* **2017**, 7, 120–129. (b) El-Sayed, M. A.-A.; El-Husseiny, W. M.; Abdel-Aziz, N. I.; El-Azab, A. S.; Abuelizz, H. A.; Abdel-Aziz, A. -M. *J. Enzyme Inhib. Med. Chem.* **2018**, 33, 199–209. (c) Mrozek-Wilczkiewicz, A.; Spaczynska, E.; Malarz, K.; Cieslik, W.; Rams-Baron, M.; Kryštof, V.; Musiol, R. *PloS One* **2015**, 10 (11), 1–14. (d) Wang, X. Q.; Zhao, C. P.; Zhong, L. C.; Zhu, D. L.; Mai, D. H.; Liang, M. G.; He, M. H. *Molecules* **2018**, 23, 3100.
- 6 (a) Liu, Z.; Li, G.; Wang, Y.; Li, J.; Mi, Y.; Zou, D.; Li, T.; Wua, Y. *Talanta* **2019**, 192, 6–13. (b) Cinar, R.; Nordmann, J.; Dirksen, E.; Müller, T. J. J. *Org. Biomol. Chem.* **2013**, 11, 2597–2604.
- 7 Manickam, S.; Balijapalli, U.; Sawminathan, S.; Samuelrajamani, P.; Kamaraj, S.; Shanmugam, V.; Ramalingam, S.; Iyer, S. K. *Eur. J. Org. Chem.* **2018**, 45, 6204–6216.
- 8 (a) Ramalingam, B. M.; Ramakrishna, I. and Baidya, M. *J. Org. Chem.* **2019**, 84 (15), 9819–9825. (b) Das, J.; Vellakkaran, M.; Banerjee, D. *Chem. Commun.* **2019**, 55, 7530–7533. (c)

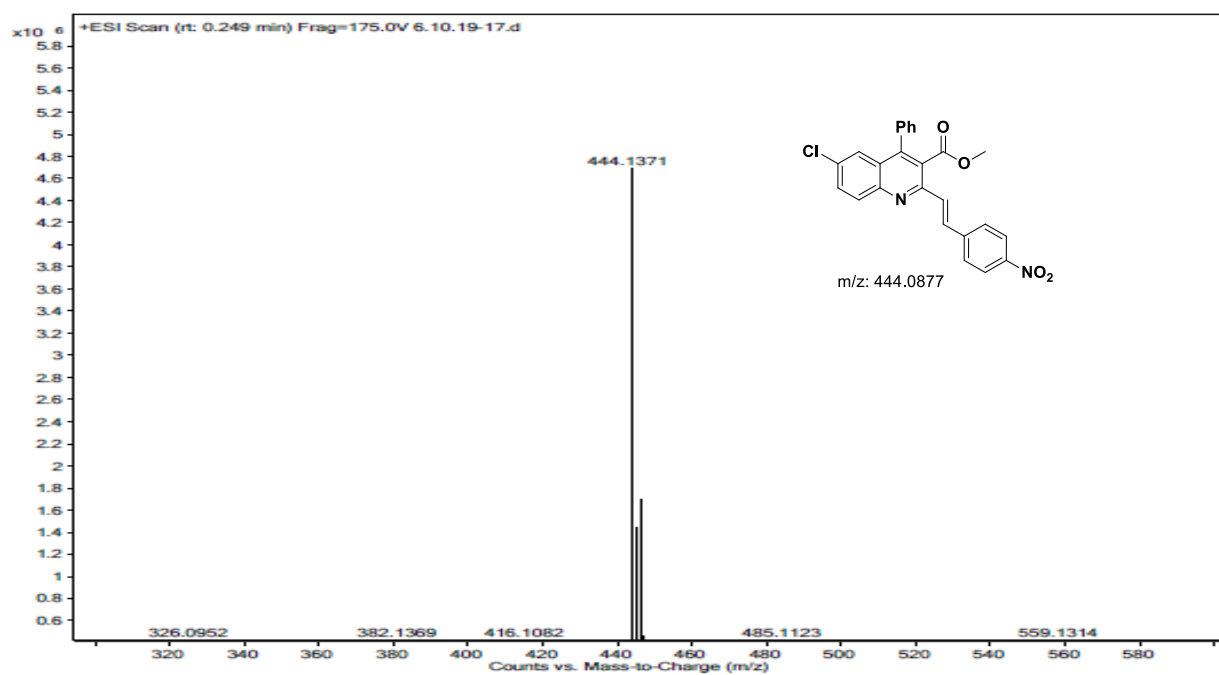
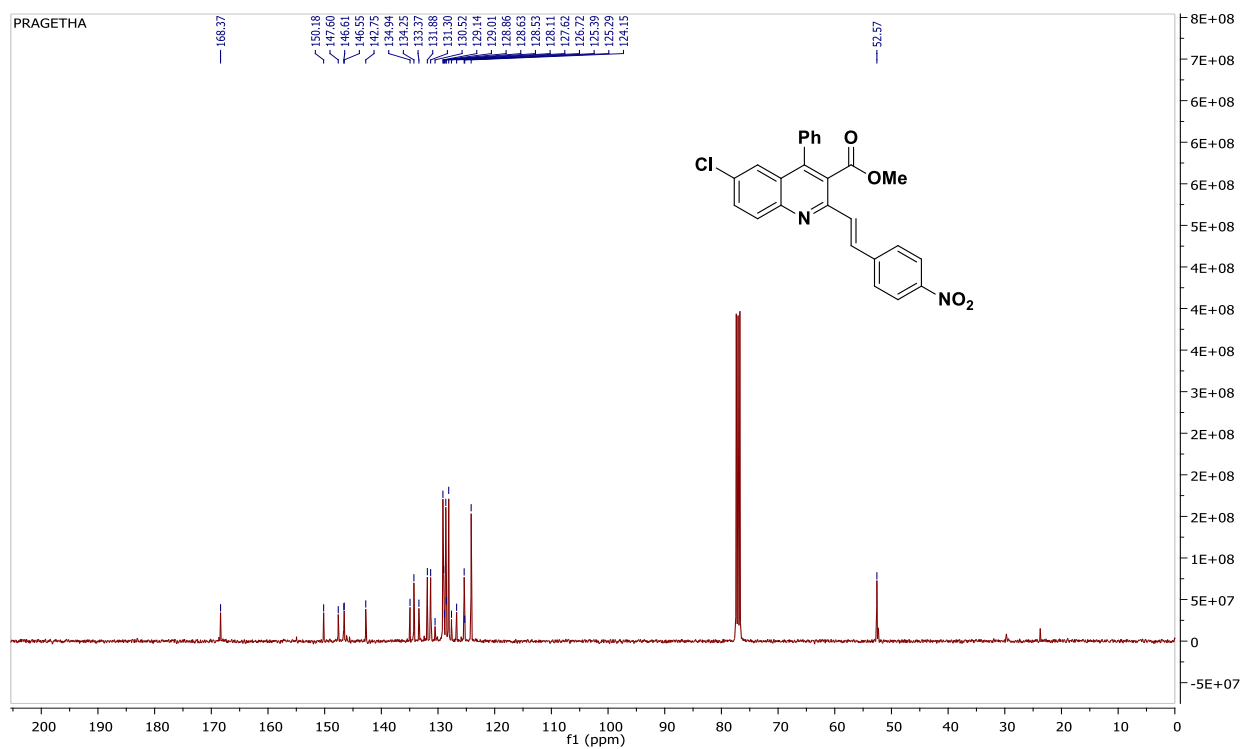
- Barman, M. K.; Waiba, S.; Maji, B. *Angew. Chem. Int. Ed.* **2018**, *57*, 9126–9130. (d) Pi, D.; Jiang, K.; Zhou, H.; Sui, Y.; Uozumi, Y.; Zoua, K. *RSC Adv.* **2014**, *4*, 57875–57884. (e) Jamal, Z.; Teo, Y.-C.; Lim, G. S. *Tetrahedron* **2016**, *72*, 2132–2138. (f) Jamal, Z.; Teo, Y.-C. *Synlett* **2014**, 2049–2053. (g) Yaragorla, S.; Singh, G.; Dada, R. *Tetrahedron Lett.* **2015**, *56*, 5924–5929. (h) Dang, H. T.; Lieu, T. N.; Truong, T.; Phan, N. T. S. *J. Mol. Catal. A: Chem.* **2016**, *420*, 237–245. (i) Chaudhari, C.; Siddiki, S. M. A. H.; Shimizu, K. *Tetrahedron Lett.* **2013**, *54*, 6490–6493. (j) Qian, B.; Xie, P.; Xie, Y.; Huang, H. *Org. Lett.* **2011**, *13*, 2580–2583. (k) Gong, L.; Xing, L.-J.; Xu, T.; Zhu, X.-P.; Zhou, W.; Kang, N.; Wang, B. *Org. Biomol. Chem.* **2014**, *12*, 6557–6560.
- 9 (a) Xu, L.; Shao, Z.; Wang, L.; Zhao, H.; Xiao, J. *Tetrahedron Lett.* **2014**, *55*, 6856–6860. (b) Fu, S.; Wang, L.; Dong, H.; Yu, J.; Xu, L.; Xiao, J. *Tetrahedron Lett.* **2016**, *57*, 4533–4536.
- 10 (a) Dabiri, M.; Salehi, P.; Baghbanzadeh, M.; Nikcheg, M. S. *Tetrahedron Lett.* **2008**, *49*, 5366–5368. (b) Sarma, P.; Saikia, S.; Borah, R. *Synth. Commun.* **2016**, *46*, 1187–1196.
- 11 Kumar, D.; Kumar, A.; Qadri, M. M.; Ansari, Md. I.; Gautam, A.; Chakraborti, A. K. *RSC Adv.* **2015**, *5*, 2920–2927.
- 12 (a) Prameela, S.; Khan, F.-R. N. *Eur. J. Org. Chem.* **2020**, 2888–2903. (b) Prameela, S.; Khan, F.-R. N. *Eur. J. Org. Chem.* **2020**, 5394–5410.
- 13 (a) Singh, G.; Yaragorla, S. *RSC Adv.* **2017**, *7*, 18874–18882. (b) Jin, J.; Wang, D.; Niu, H.; Wu, S.; Qu, G.; Zhang, Z.; Guo, H. *Tetrahedron* **2013**, *69*, 6579–6584.
- 14 Zhang, Q.; De Oliveira, V. K.; Royer, S.; Je'ro'me, F. *Chem. Soc. Rev.* **2012**, *41*, 7108–7146.
- 15 Smith, E. L.; Abbott, A. P.; Ryder, K. S. *Chem. Rev.* **2014**, *114*, 11060–11082.
- 16 Alonso, D. A.; Baeza, A.; Chinchilla, R.; Guillena, G.; Pastor, I. M.; Ramón, D. J. *Eur. J. Org. Chem.* **2016**, 612–632.
- 17 Liu, P.; Hao, J.-W.; Mo, L.-P.; Zhang, Z.-H. *RSC Adv.* **2015**, *5*, 48675–48704.
- 18 Xu, P.; Zheng, G.-W.; Zong, M.-H.; Li, N.; Lou, W.-Y. *Bioresour. Bioprocess.* **2017**, *4*, 34.
- 19 (a) Becke, A. D. *J. Chem. Phys.* **1993**, *98*, 5648–5652. (b) Lee, C.; Yang, W.; Parr, R. G. *Phys. Rev. B.* **1988**, *37*, 785–789. (c) Grimme, S.; Ehrlich, S.; Goerigk, L. *J. Comp. Chem.* **2011**, *32*, 1456–65. (d) Boys, S. F.; Bernardi, F. *Mol. Phys.* **1970**, *19*, 553.
- 20 (a) Becke, A. D. *J. Chem. Phys.* **1993**, *98*, 5648–5652. (b) Lee, C.; Yang, W.; Parr, R. G. *Phys. Rev. B.* **1988**, *37*, 785–789. (c) Grimme, S.; Ehrlich, S.; Goerigk, L. *J. Comp. Chem.* **2011**, *32*, 1456–65.
- 21 (a) Farhad, P.; Reza, Y.; Mohammad, H. M.; Ali, K.-N. *Carbohydr. Res.* **2013**, *380*, 81–91. (b) Berna, E.; Amarila, M.; Purwa, I. S.; Bianca, L. *Int. J. Pharm. Tech. Res.* **2012**,

- 4(4), 1667-1671. (c) Zhenhua, Y.; Wei, Z.; Fajin, F.; Yong, Z.; Wenyi, K. *Food Sci. Hum. Wellness*. **2014**, *3*, 136–174.
- 22 (a) Kumar, D.; Kumar, A.; Qadri, M. M.; Ansari, Md, I.; Gautam, A.; Chakraborti, A. K. *RSC Adv*. **2015**, *5*, 2920–2927. (b) Sarma, P.; Saikia, S.; Borah, R. *Synth. Commun*. **2016**, *46*, 1187–1196.

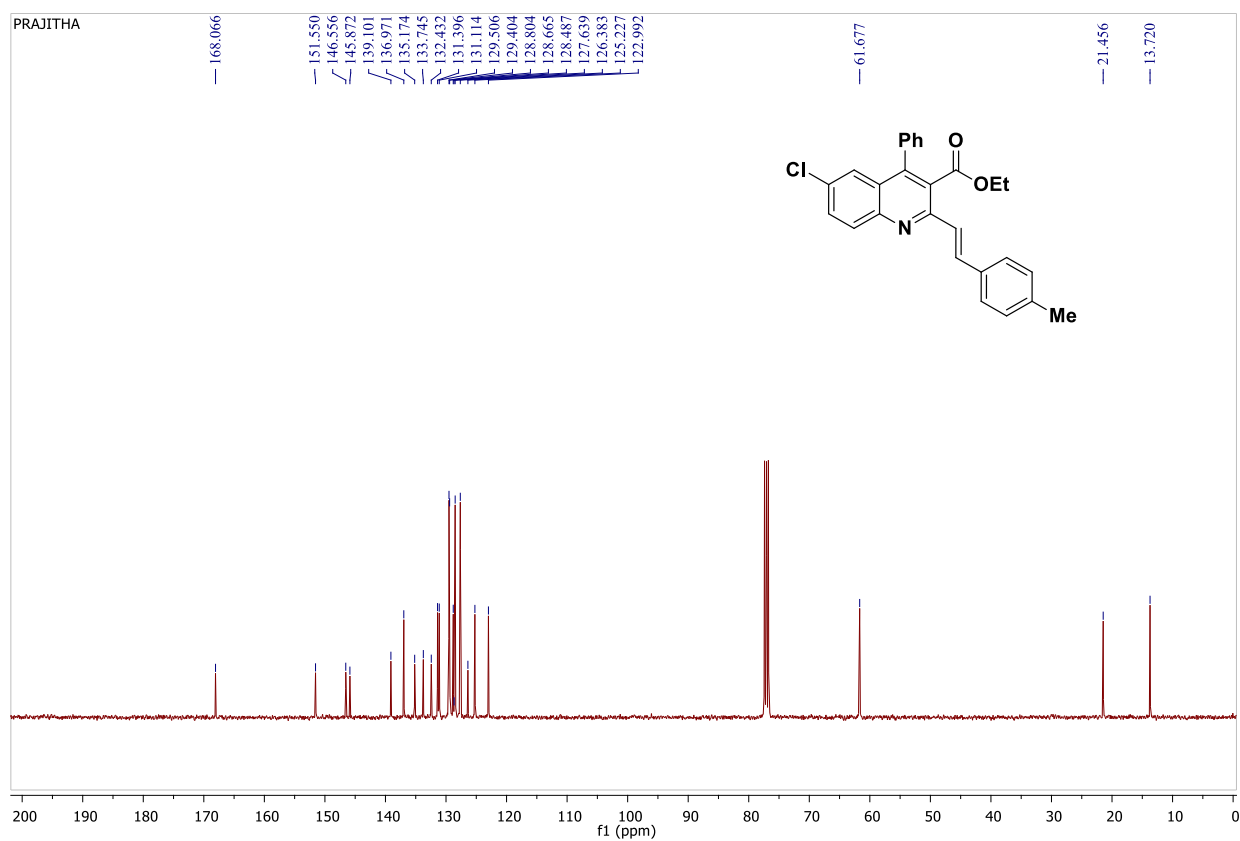
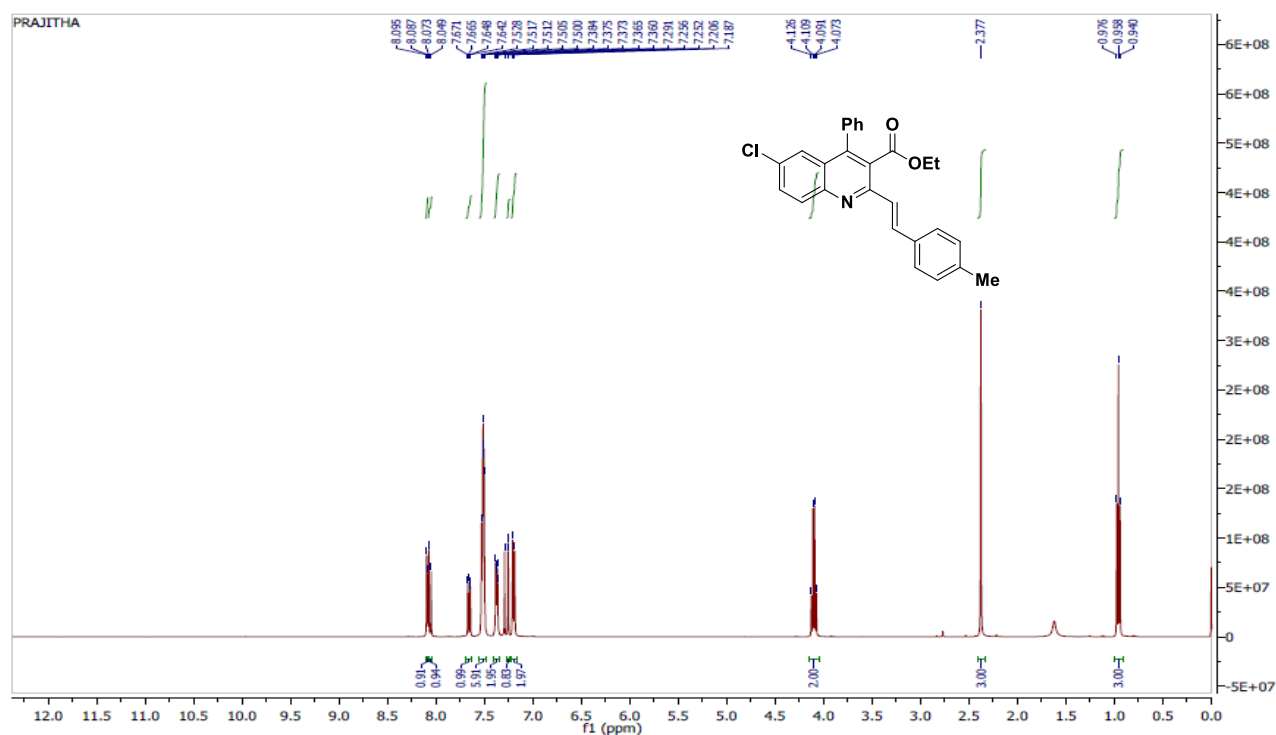
2.13. Selected Spectral data

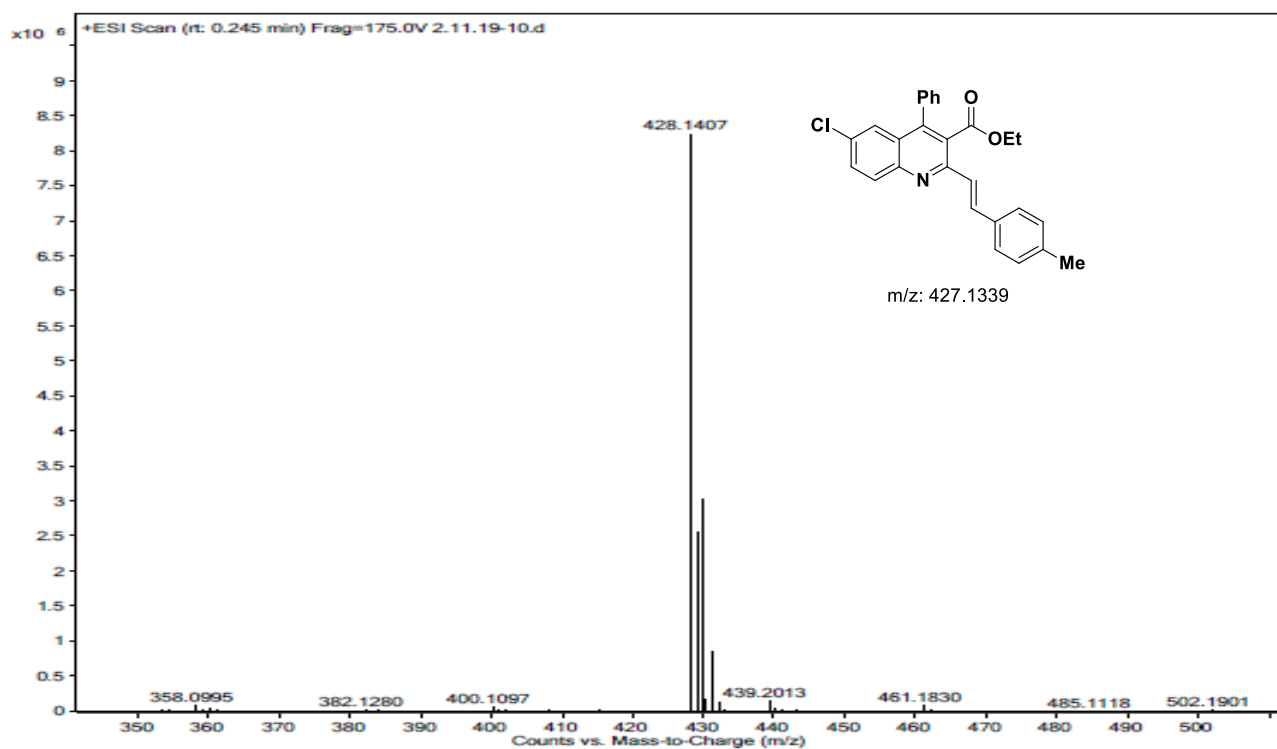
Methyl- 6-chloro-2-(3-nitrostyryl)-4-phenylquinoline-3-carboxylate (5b):



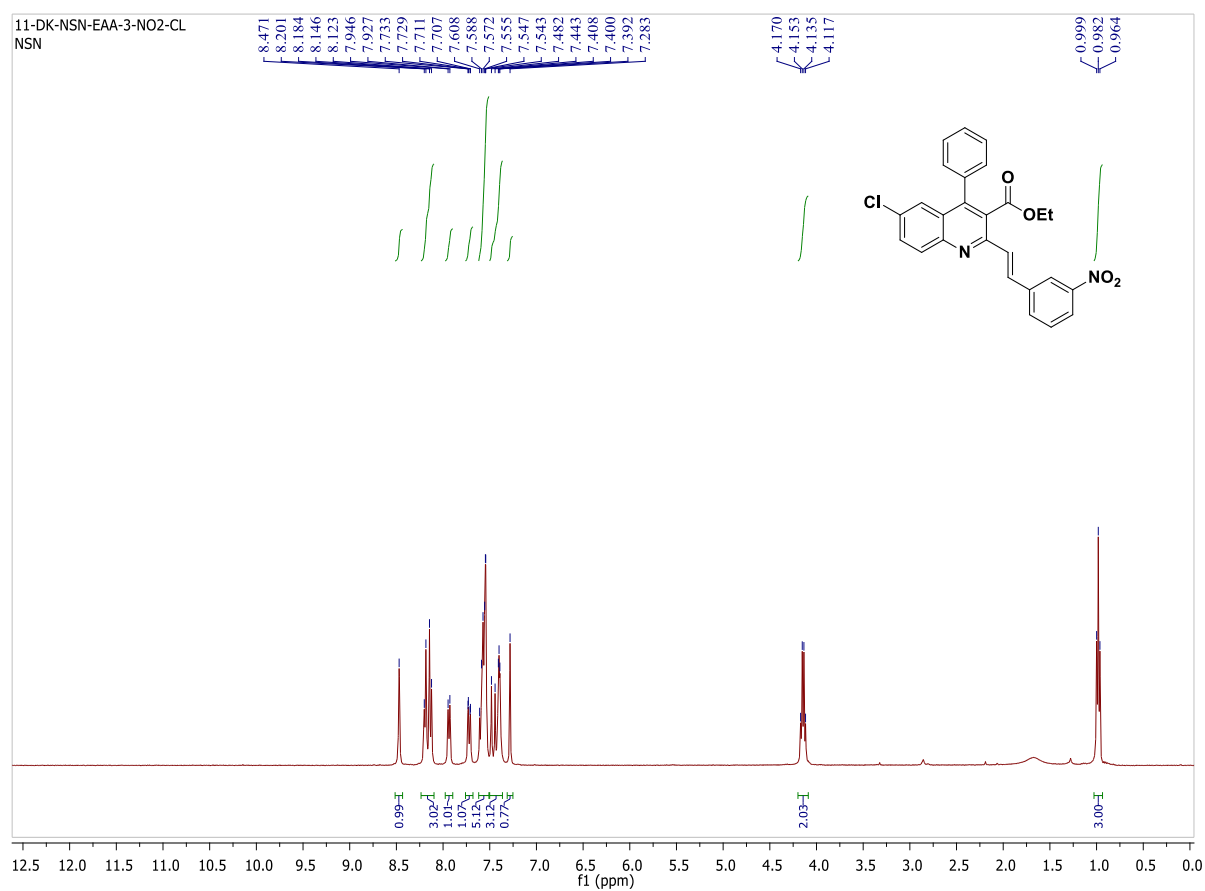


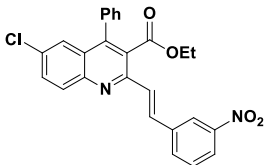
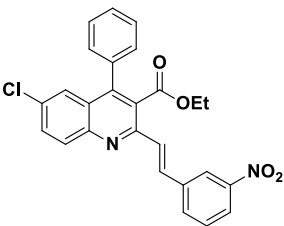
Ethyl 6-chloro-2-(4-methylstyryl)-4-phenylquinoline-3-carboxylate (5h):



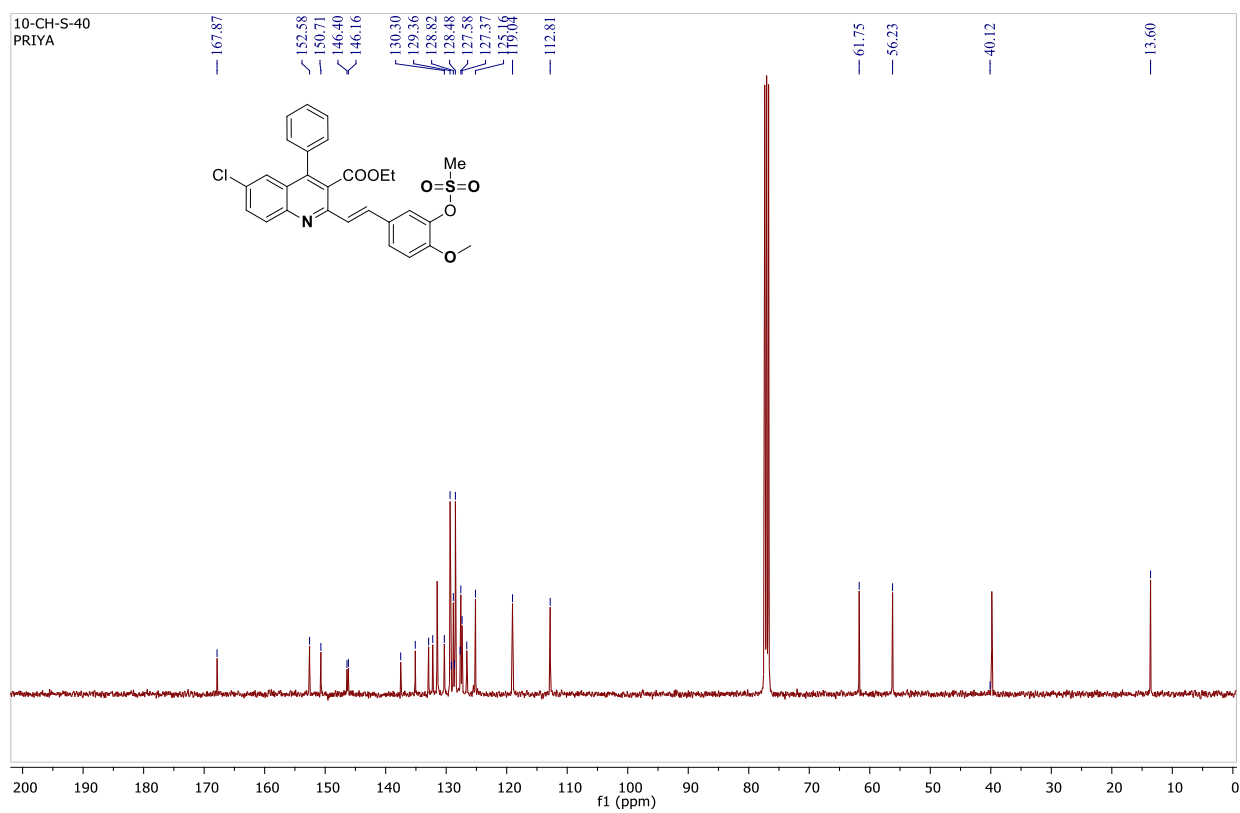
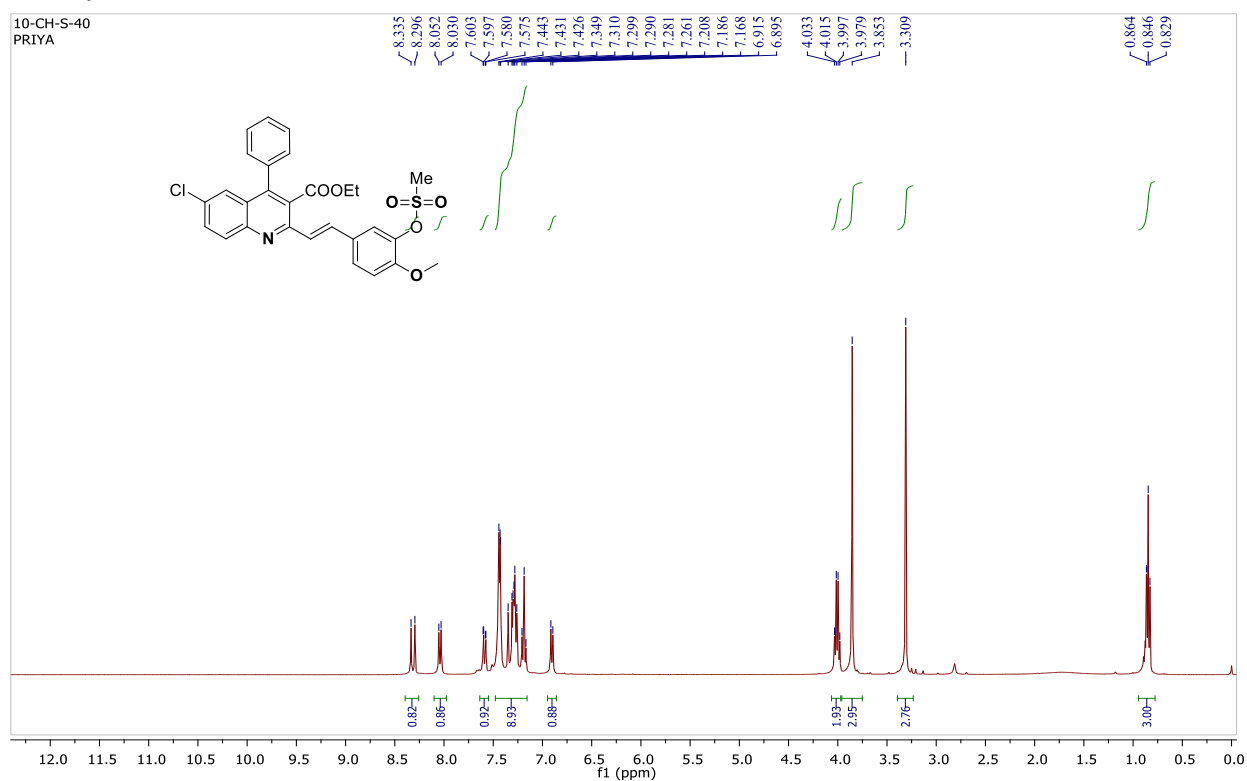


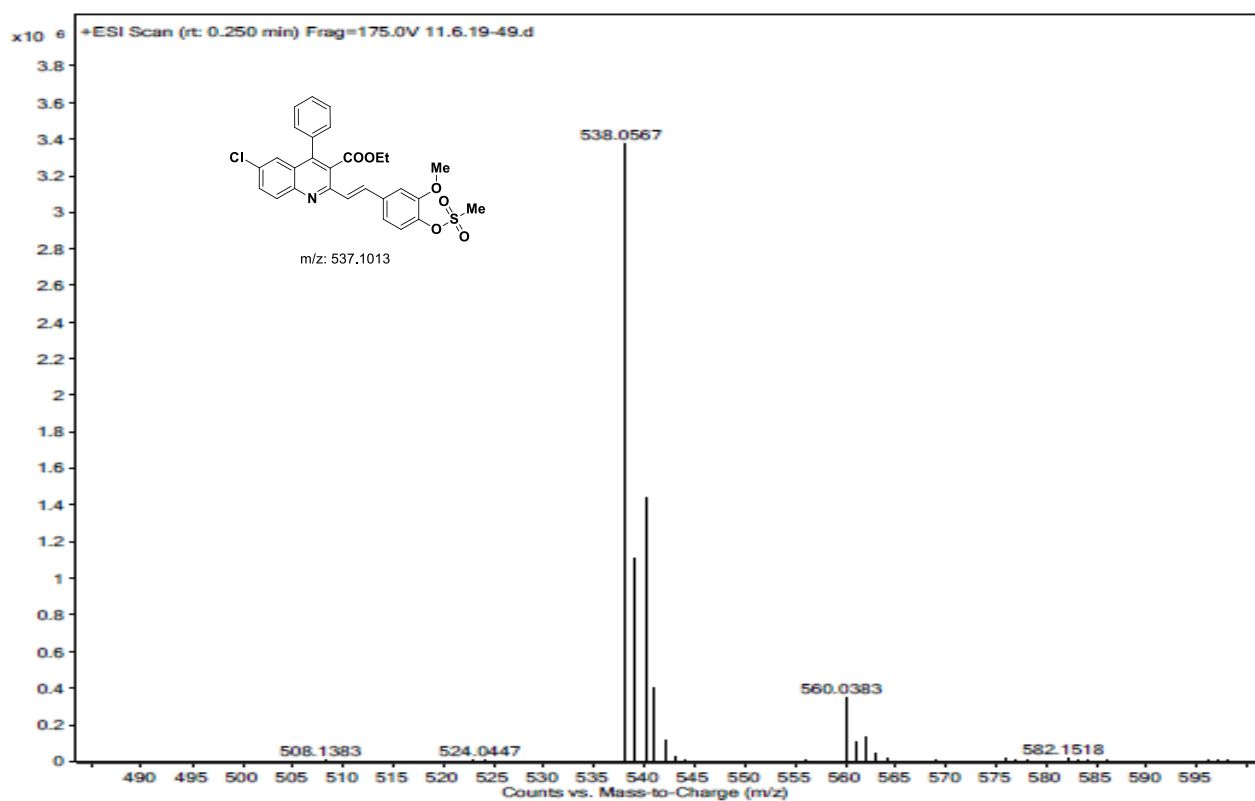
Ethyl 6-chloro-2-(3-nitrostyryl)-4-phenylquinoline-3-carboxylate (5m):



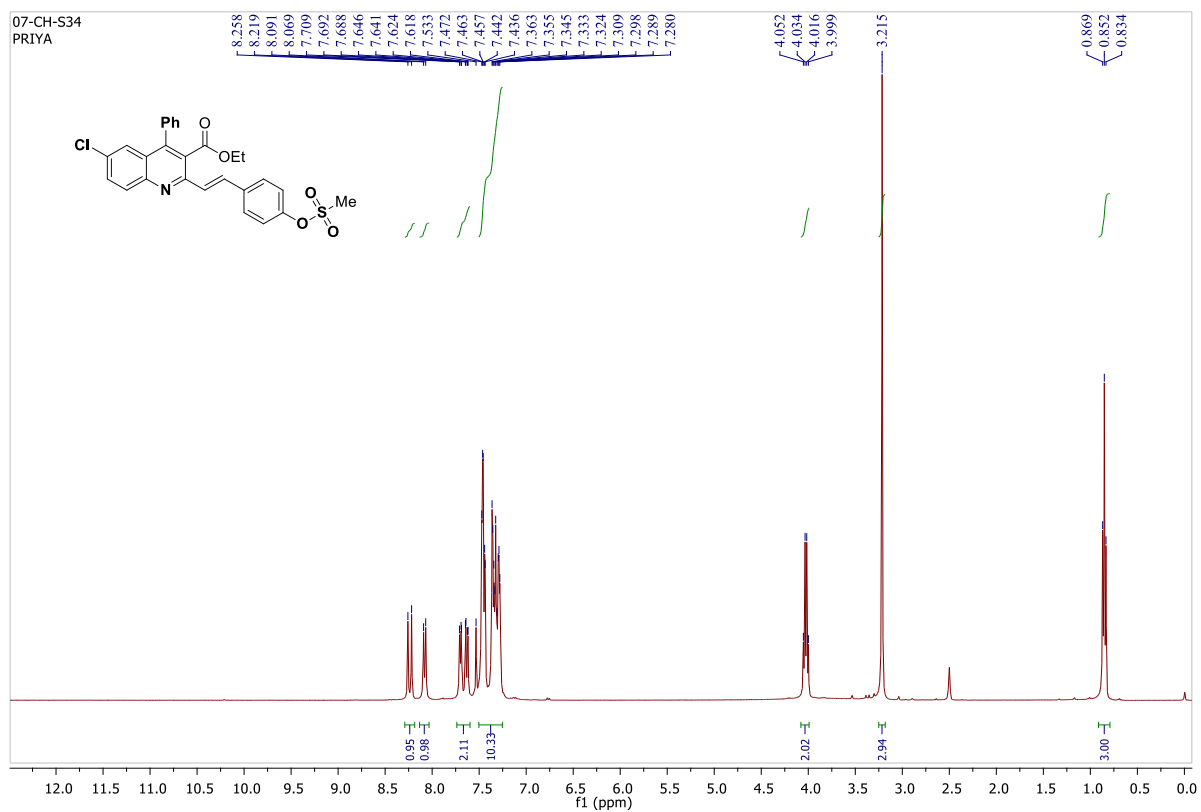


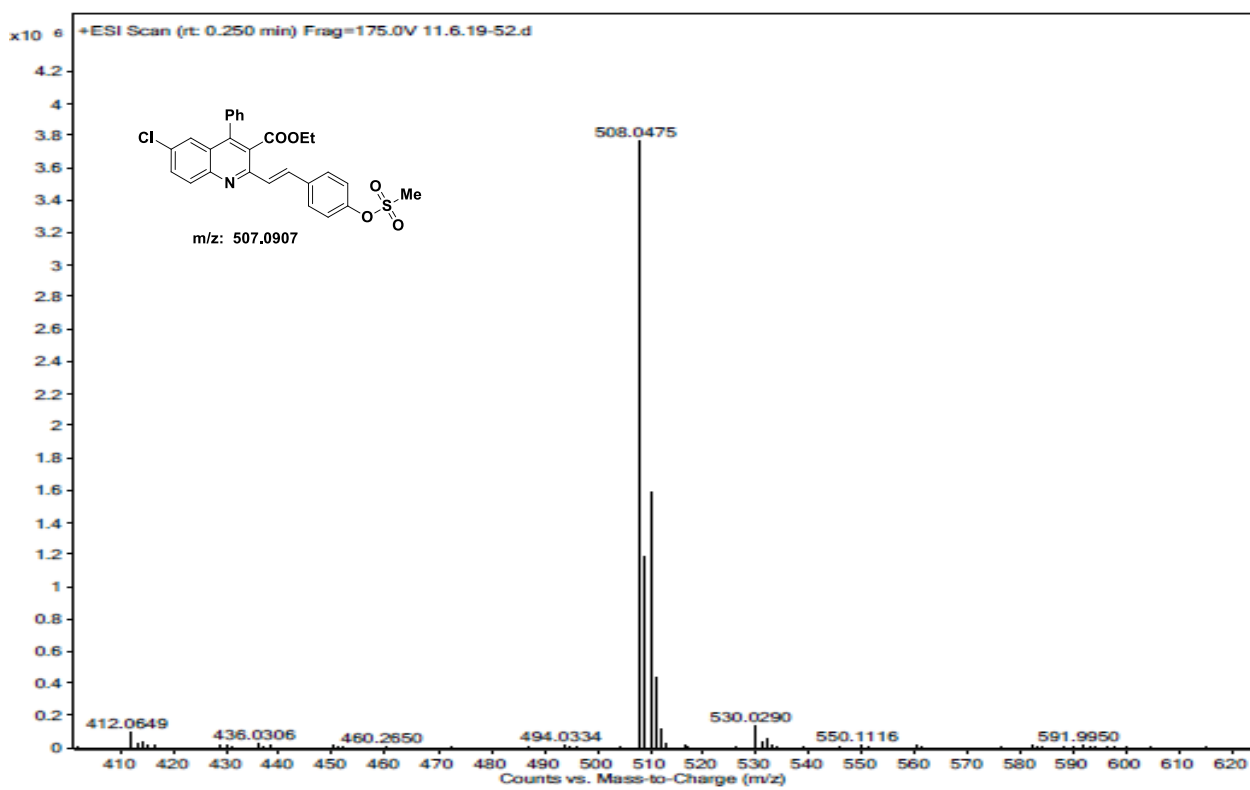
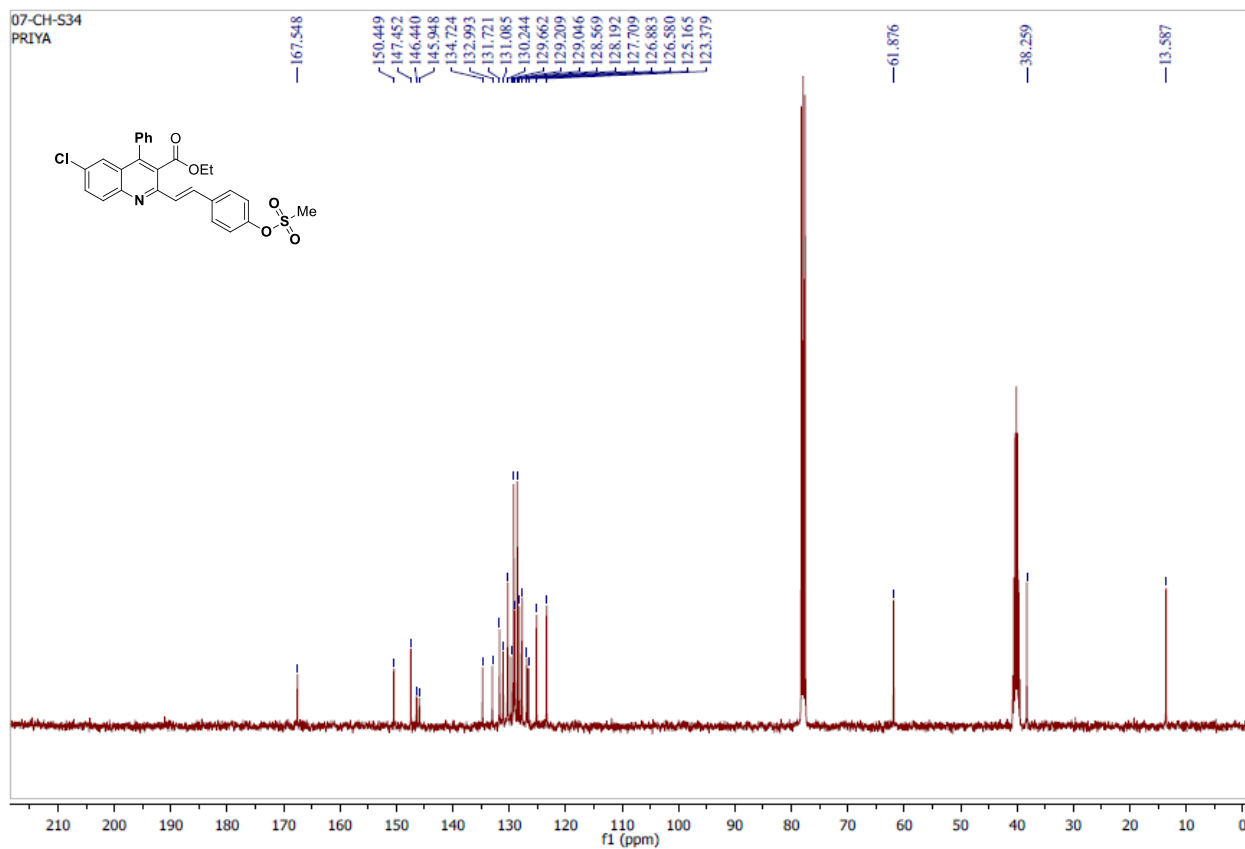
(E)-Ethyl 6-chloro-2-(4-methoxy-3-((methylsulfonyl)oxy)styryl)-4-phenylquinoline-3-carboxylate (11d):





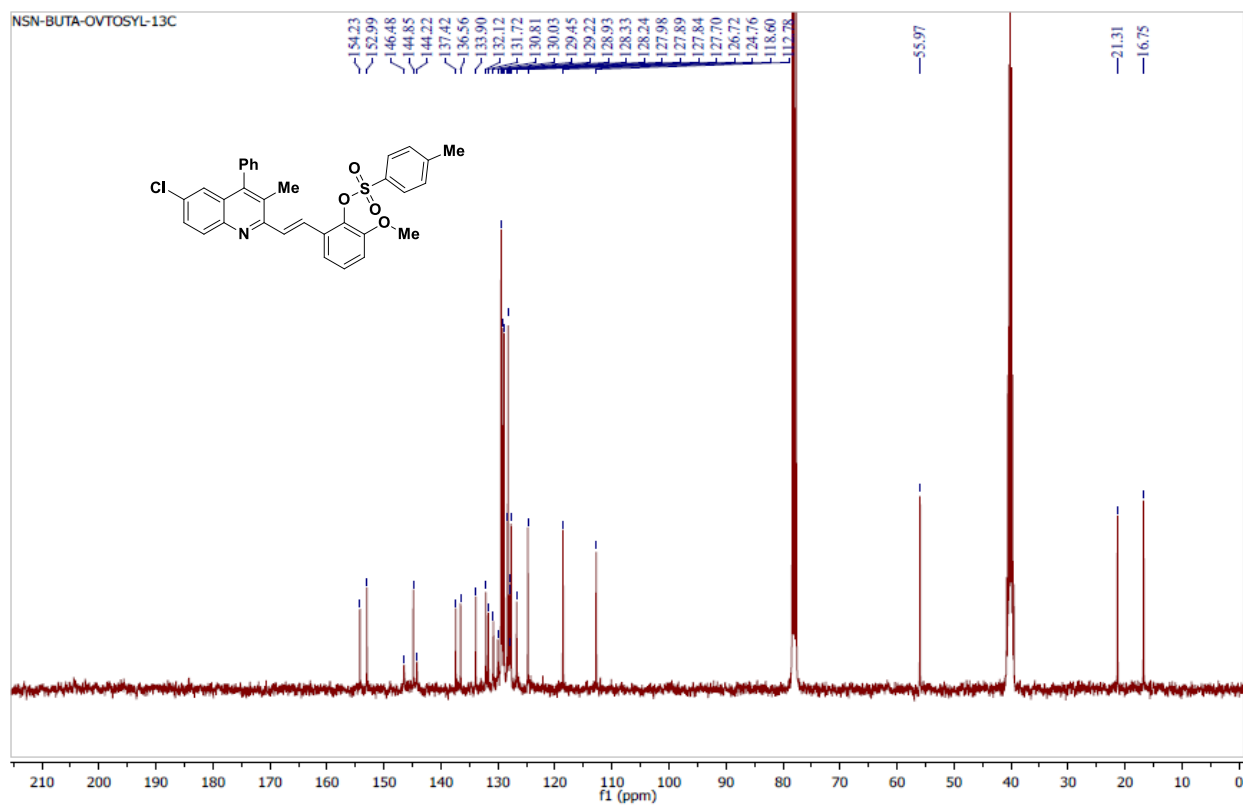
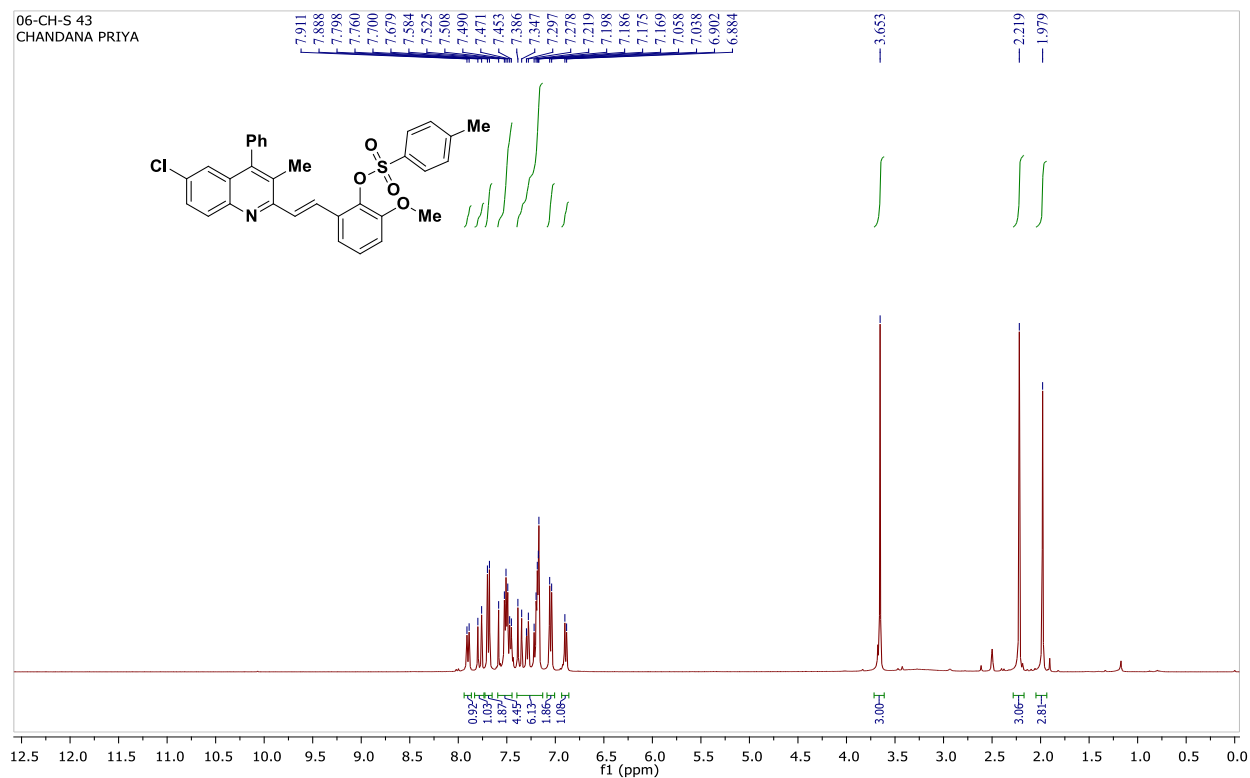
(E)-Ethyl 6-chloro-2-(4-((methylsulfonyl)oxy)styryl)-4-phenylquinoline-3-carboxylate (11e):

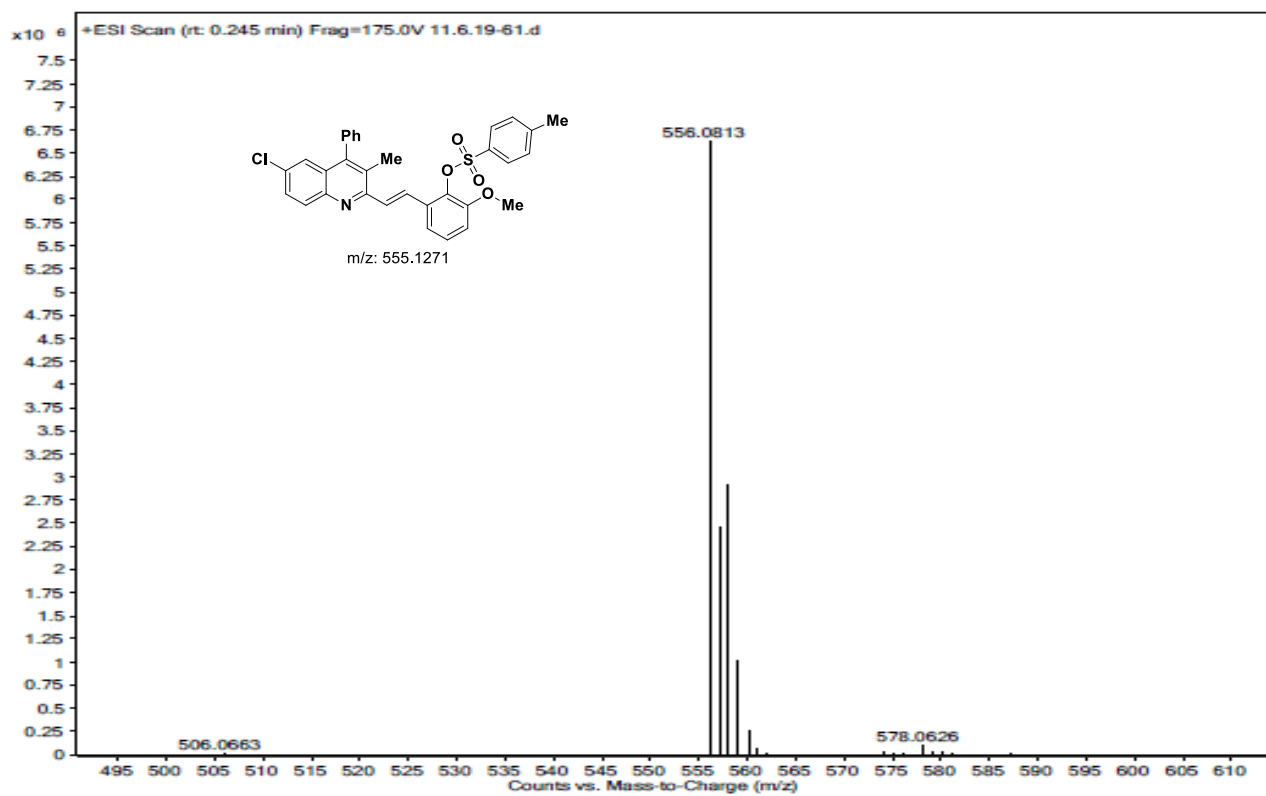




(E)-2-(2-(6-Chloro-3-methyl-4-phenylquinolin-2-yl)vinyl)-6-methoxyphenyl methylbenzenesulfonate (12c):

4-





CHAPTER-3

Facile synthesis of quinoxaline, quinoxaline-2-one, quinazoline-based styryls, and their sulfonate-styryls via sp^3 C-H activation and their evaluation as α -glucosidase inhibitors

Abstract

Quinoxaline and quinazoline derivatives play significant role in medicinal, natural product chemistry and are part of many commercial drugs. The synthetic compounds well explored in materials chemistry for photoluminescent properties. Considering these, the synthesis of quinazoline, quinoxaline styryls, bis-quinoxaline styryls and sulfonate ester conjugates is reported via sp^3 C-H activation at 2nd and 3rd positions of quinazoline, quinoxaline. The photo physical properties of resulting compounds studied along with their evaluation for α -glucosidase inhibition. A detailed study (synthesis, photo physical and biological) is described in this chapter.

3.1 Introduction

3.1.1 Reported methods for the synthesis of 3-styryl quinoxaline-2-ones, 2-styryl quinazolines

Isomeric structures quinazoline and quinoxaline belong to the benzodiazepine class (1,3-diazanaphthalenes and 1,4-diazanaphthalene) of molecules and considered privileged structures in medicinal chemistry.^{1a-d} Quinazolines show antimicrobial,^{2a,b} COX-2 inhibitory,^{2c} anti-leishmanial,^{2d} anticonvulsant,^{2e} antihypertensive^{2f}, and anti-cancer^{2g} properties. The derivatives of quinazolines play a specific role in the inhibition of P13ka,^{3a} tyrosine kinase^{3b}, and acetyl/butyryl cholinesterase (AChE/BChE),^{3c} and are used in the redox switching reactions.^{3d} Many of the quinazoline-based molecules are in clinical trials for different diseases.^{3e}

Quinoxaline derivatives are known for their antibacterial,^{4a} antiviral,^{4b} anticancer,^{4c,d} anti-inflammatory,^{4e} antimicrobial,^{4f} anti-analgesic,^{4g} and anti-diabetic properties.^{4h} The quinoxaline unit is present in the molecules used for P38a MAP kinase inhibition,^{5a} PDGF receptor tyrosine kinase inhibition,^{5b} glucagon receptor antagonists,^{5c} tyrosine kinase c-Met inhibition,^{5d} and cholinesterase inhibition.^{5e} These compounds play a significant role in chemotherapy,^{5f} also used in the development of organic luminescent materials^{6a} and organic solar cells.^{6b}

2-Styryl-quinolines are structurally similar to 2-styryl-quinazolines and 3-styryl-quinoxalines and exhibit many biological and material properties.^{7a-c} 2-Styryl-quinolines are prepared by the condensation of the methyl group of 2-methyl quinoline with an aldehyde in the presence of a base.^{7d} Recently this trend has shifted towards sp³ C–H activation under metal and metal-free (one-pot) green conditions.⁷

The sulfonates are well-known for anticancer,^{8a} monoamine oxidase inhibition,^{8b} antioxidant,^{8c} aldose reductase,^{8d} and PTP1B (anti-hyperglycemic) inhibition activity.^{8e} The aromatic sulfonate derivatives of 2-styryl-quinazolines are also known to show better anticancer activity compared to reference compounds.^{8f} α -Glucosidase inhibition is one of the important and attractive targets for the treatment of type-1 and type-2 diabetes. Inhibition of α -glucosidase helps in the prevention of diabetes by lowering the absorption of glucose in the digestive system.⁹ Many plant-based compounds (such as flavonoids, 7-geranyloxy-6-methoxy coumarin, apigenin, β -Amyrin, vitexin, isovitexin, 3-O- β -D-rutinoside, β -sitosterol, salacinol, terpenes, and dicaffeoylquinic acids),^{10a-b} and synthetic molecules (pyrrole, pyrrolidine,

pyrazole, indole, *bis*-diindolylmethane, oxindoles) are known for the purposes.^{11a-b} Along with these, the quinazoline and quinoxaline derivatives have been reported for α -glucosidase inhibition. Based on the literature reports on various approaches for the synthesis of 3-styrylquinoxaline derivatives we have found that the Knoevenagel condensation is the simple method for the construction of titled compounds, which are derived from the coupling of 3-methylquinoxaline-2-one/2-methylquinazoline with aromatic aldehydes under mild conditions. In many previous reports, the Knoevenagel condensation products were the key intermediates for the construction of 2-styryl of quinazoline/ quinoxalines/ methylquinazoline/ bis-quinoxaline derivatives *via* intermolecular-aldol reactions.

In the reported methods, *o*-phenylenediamine (OPDA) (**1a**) was initially treated with 2-oxopropanoic acid (**2a**) in the presence of different catalysts such as piperidine,^{12a-b} acetic acid,^{12c} acetic anhydride,^{12d-e} to generate 3-methylquinoxaline-2-one intermediate which is reacted with benzaldehyde (**3a**) to access (*E*) 3-styrylquinoxaline-2-one (**4a**) with moderate to good yields as shown in **Figure-1**. Similarly, ethyl pyruvate (**2b**) is combined with OPDA (**1a**) and benzaldehyde under acidic catalysts [e.g., 20 mol% HCl,^{12f} sulfuric acid^{12g}] to give corresponding (*E*) 3-styryl quinoxaline-2-one (**4a**) and its 4-methoxy derivative (**4c**) under refluxing conditions. In addition, (*E*)-styryl quinoxaline-2-one (**4a**) synthesized from the reaction of benzaldehyde (**2a**) with various reagents such as sodium salt of diethyl oxalacetate (1,4-diethoxy-1,3,4-trioxobutan-2-ide),^{12h} under basic medium (NaOH) or sodium pyruvate¹²ⁱ (**2d**) using AcONa and AcOH *via* cyclization and aldol reaction as represented in the **Figure-1**.

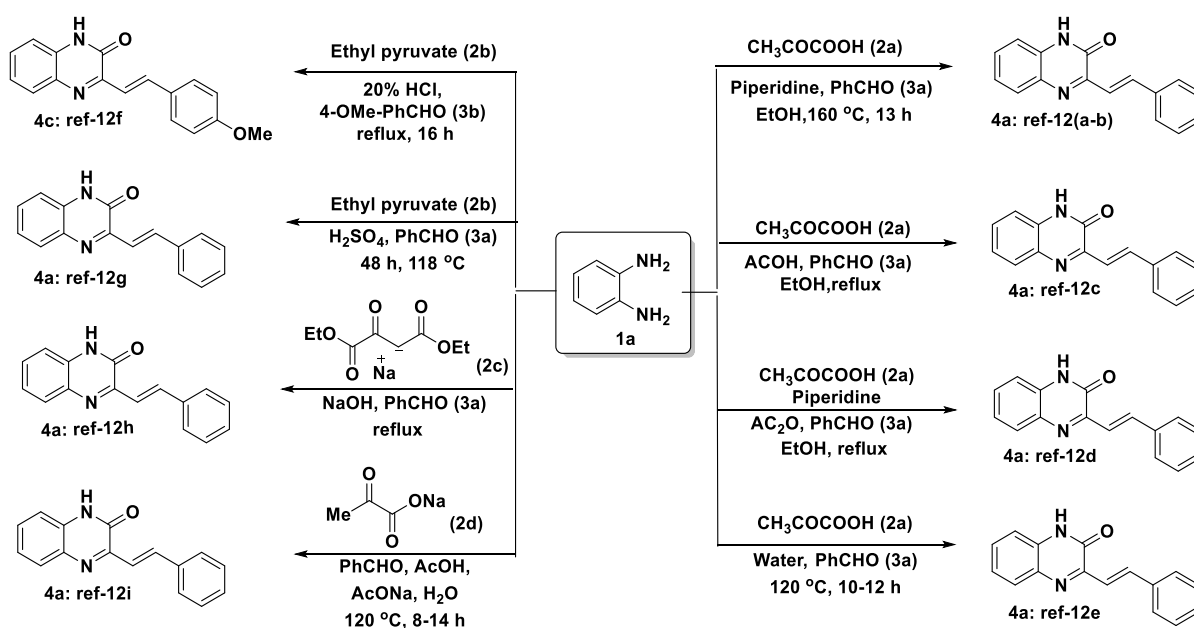
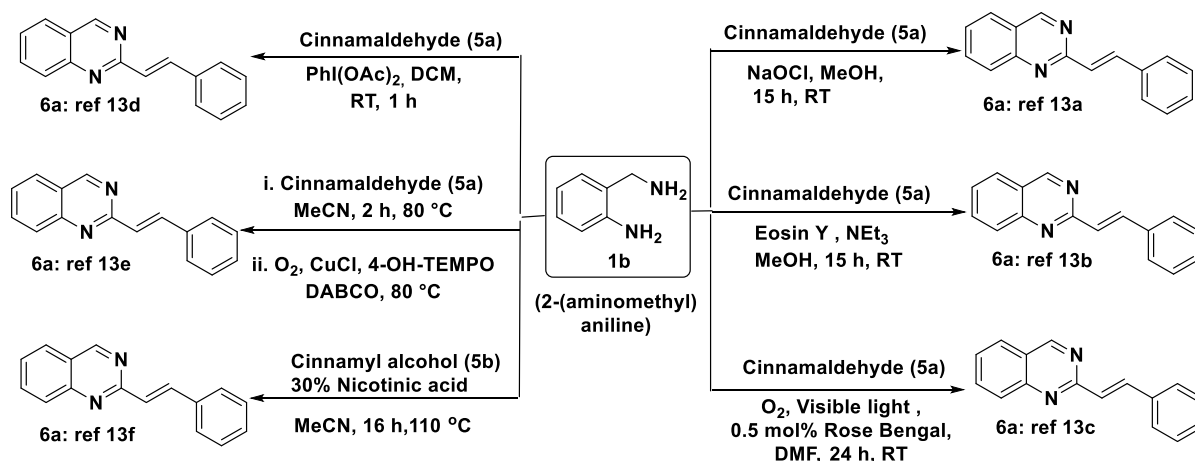


Figure-1: Reported methods for the synthesis of 3-styryl quinoxaline-2-ones.

Also, 2-styrylquinazoline (**6a**) was synthesized by the coupling of 2-(aminomethyl) aniline (**1b**) and cinnamaldehyde (**5a**) by using catalytic transformations like NaOCl,^{13a} Eosin Y+NEt₃,^{13b} rose Bengal (0.5 mol%/visible light by aerobic oxidation),^{13c} phenyliodine (III)-diacetate (PIDA),^{13d} and Lewis acids (CuCl+4-OH-TEMPO) catalyzed oxidative cyclization,^{13e} from cinnamyl alcohol (**5b**) in presence of 30% nicotinic acid^{13f} under reflux conditions. Similarly, the titled molecules were prepared *via* cyclization followed by intramolecular aldol reaction of N-benzylaniline (**1c**) with 2-methylquinazoline (**1d**) in presence of DDQ (catalytic amount).^{13g} Sodium acetate mediated reaction of 2-aminobenzoic acid (**1e**), thiourea (**7**) with 4-chlorobenzaldehyde (**3c**) affords desired (*E*)-2-(4-chlorostyryl) quinazolin-4-ol (**6b**) in good yields^{13h} has shown in the **Figure-2**.

Bin et al. reported the synthesis of (*E*)-2-methyl-3-styrylquinoxaline derivatives (**10a-10b**) from phenyl methenamine (**8**), 2-methylquinoxaline (**9a**)/ 2,3-dimethylquinoxaline (**9b**), and tert-butyl hydroperoxide (TBHP) under reflux conditions using the catalyst N-bromosuccinamide (NBS) via oxidative olefination of primary amines followed by direct deamination and C–H bond activation,^{14a} also Shim et al. described the synthesis of 2-methyl-3-styrylquinoxaline (**10b**) via sp³ C-H activation of 2-methyl-quinoxaline (**9a**) under basic medium.^{14b} Moreover, Barluenga et al. also reported the one-pot synthesis of substituted propargyl alcohol (**11**) with OPDA (**1a**) in presence of the catalytic amount of mercuric acetate to give the titled compound (**10b**) via oxidative aminomercuration of alcohol.^{14c} Recently, alkenylazaarenes (**10b**) were prepared from the activation of 2,3-dimethylquinoxaline (**9b**) with benzyl alcohol^{14d} using CsOH-mediated aerobic oxidative dehydrogenation as shown in the **Figure-3**.



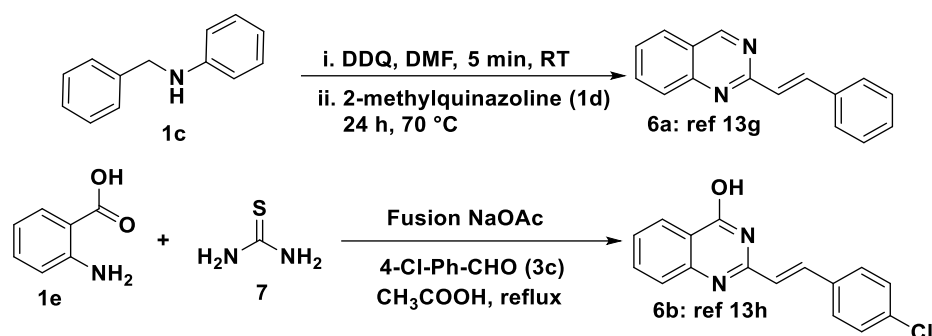


Figure-2: Reported methods for the synthesis of 2-styrylquinazolines.

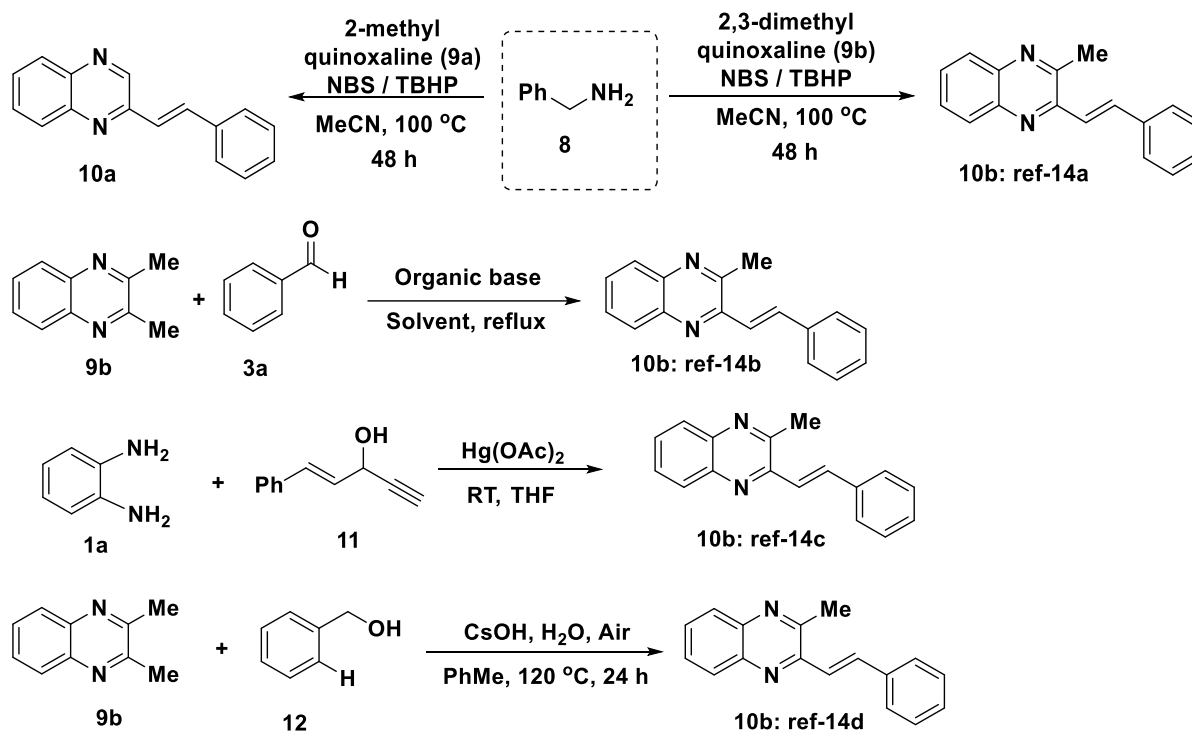


Figure-3: Reported methods for the synthesis of substituted (*E*)-2-methyl-3-styrylquinoxaline.

2,3-Bis-tyrylquinoxalines (**14a-14c**) are potential biologically active molecules^{14d} for the treatment of cancer, neurodegenerative disorders and display diversified medicinal properties. Based on the significance of these compounds, the 2,3-di(*E*-styryl) quinoxaline (**14a**) is prepared from the coupling of 2,3-dimethylquinoxaline (**9b**) with the use of benzylalcohol (2 equiv.)^{14d} in basic medium (CsOH). Recently, catalyst-free conditions (solvents as catalysts) like water,^{15a} methanol^{15b} were reported for direct coupling of OPDA (**1a**) with 1,6-diphenylhexa-1,5-diene-3,4-dione (**13a-13c**). Along with this palladium acetate catalyzed Heck cross-coupling reaction of 2,3-dichloroquinoxaline (**9c**) with styrene (**13d**) in TEA^{15c} also provides desired product (**14a**) in good yields.

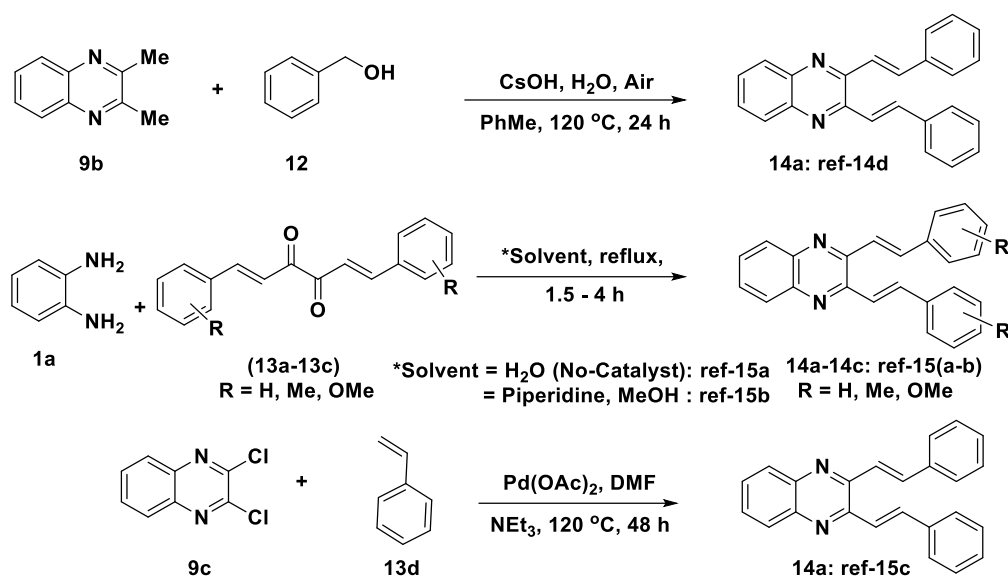
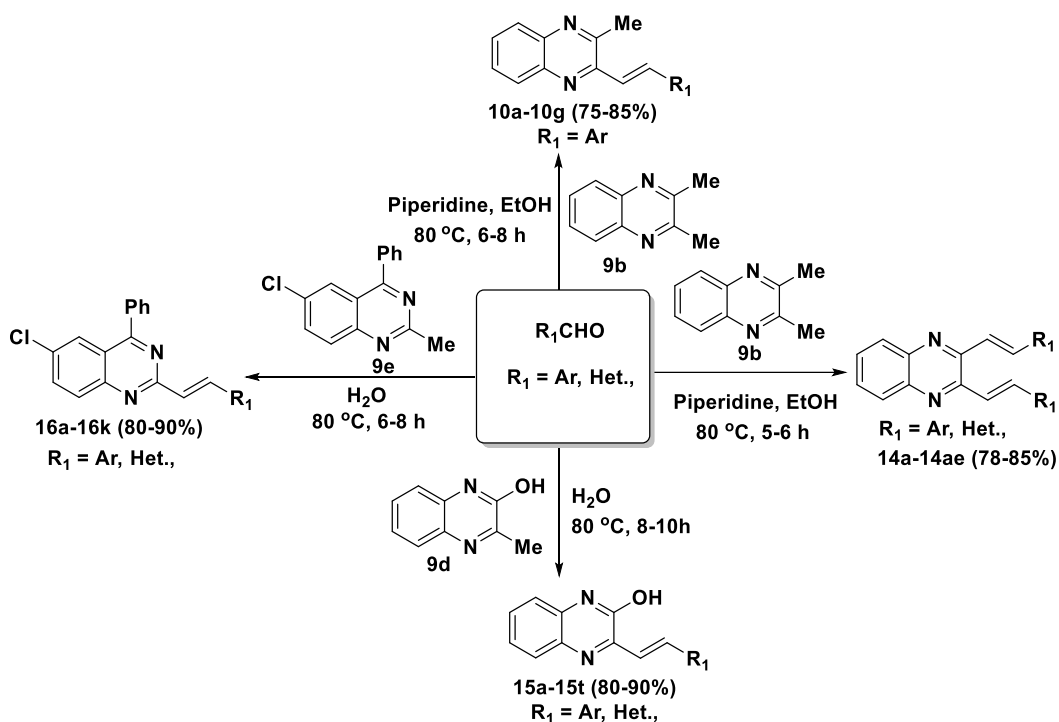


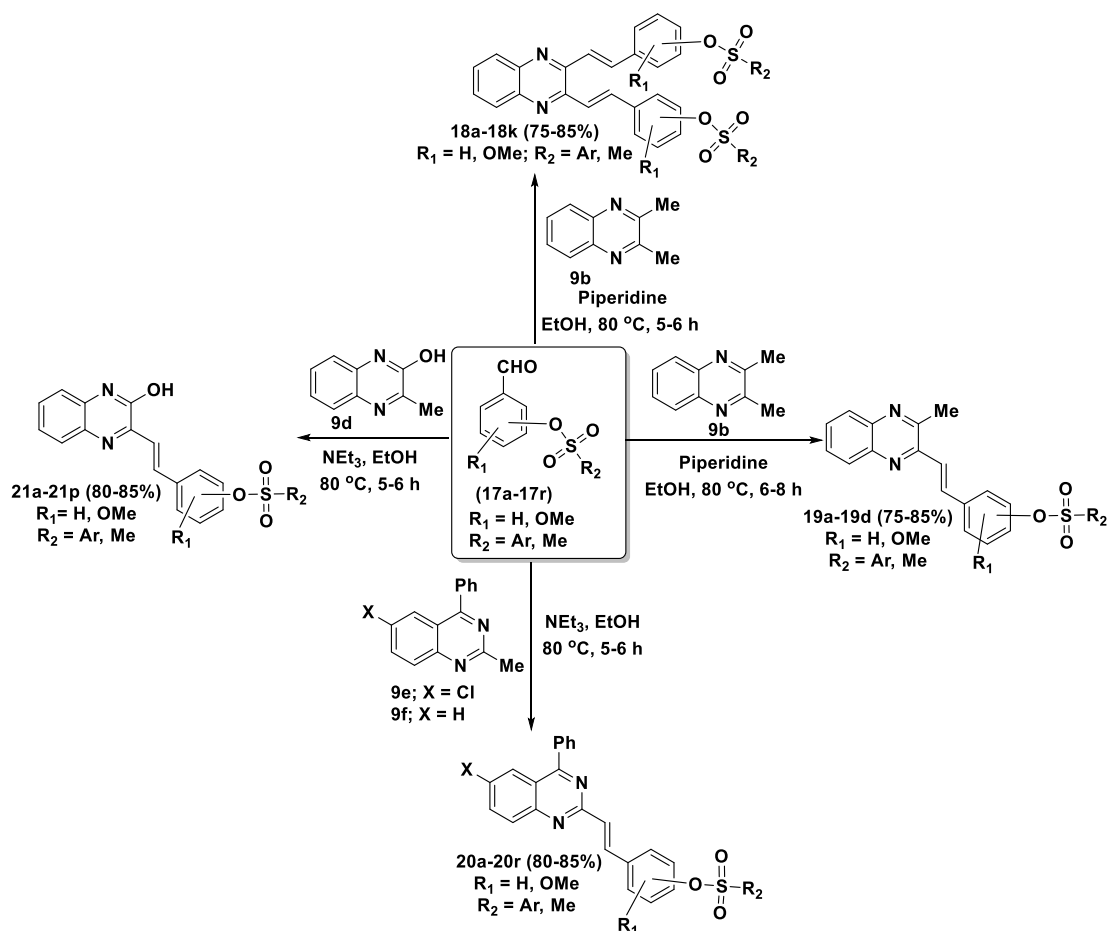
Figure-4: Reported methods for the synthesis of 2,3-distyrylquinoxalines.

3.2 Present Study

Based on the discussions in the introduction (chapter-1) of this thesis and this chapter, considering the biological, materials importance of the quinoxaline and quinazoline based molecules (especially styrenes), we envisaged the development of a general and metal-free, one-pot method for the synthesis of quinoxaline and quinazoline styrenes and sulphonate derivatives *via* sp^3 C-H functionalization as shown in **Scheme-1**. This synthetic methodology for new class of sulfonate esters based 2,3-di-styrylquinoxaline (**18a-18t**), 3-methyl-2-styrylquinoxaline (**19a-19d**), 2-styrylquinazoline (**20a-20r**), and 3-styrylquinoxaline-2-ol (**21a-21p**) analogs as shown in **Scheme-2**.



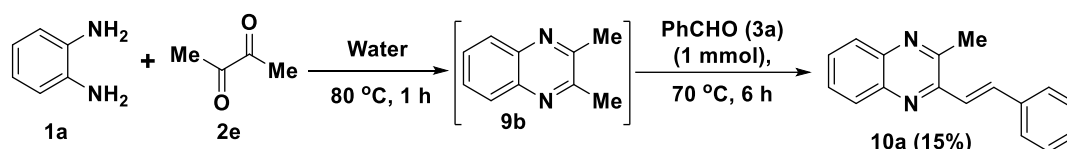
Scheme-1: Synthetic strategy of various quinoxaline and quinazoline styryl derivatives (**10**, **14**, **15** and **16** series).



Scheme-2: Synthetic strategy of various sulfonate ester-based quinoxaline and quinazoline styryl derivatives (**18**, **19**, **20** and **21** series).

3.3 Results and Discussion

From the literature, it is clear that quinoxalines play important role in medicinal and materials chemistry. It is noteworthy to mention that there are limited reports for the synthesis of the quinoxaline derivatives type **10** and **14** (especially the compound **10**).^{14a-d, 15a-c} Considering this, we have started our investigation for the preparation of the (*E*)-2-methyl-3-styrylquinoxaline (**10**) by adopting a catalyst-free, one-pot approach. Thus, the 2,3-dimethylquinoxaline (**9b**) was prepared (*in situ*) by the reaction of *o*-phenylenediamine (**1a**) and pyruvic acid (**2e**) [equimolar ratio] in water at 80 °C for 1 h. To the same reaction pot, benzaldehyde (**3a**) was added and heated for 6 h to give the expected product (**10a**) in 15% yield (**Scheme-3a**).



Scheme-3a: Initial attempt for synthesis of 3-methyl-2-styrylquinoxaline (**10a**).

Encouraged by this result, attempts were made to improve the yields by performing the reactions in the presence of different bases (TEA, DIPEA, pyridine, and piperidine) and solvents (water, MeCN, and EtOH) as indicated in **Table-1**. All the reactions were performed by controlled addition of the aldehyde to get the required product selectivity. Among the screened, a combination of piperidine (10 mol%) in EtOH gave the desired product **10a** in 80% yield along with *bis*-coupled product **14a** (12%) as shown in **Scheme-3b** (**Entry-7; Table-2**).

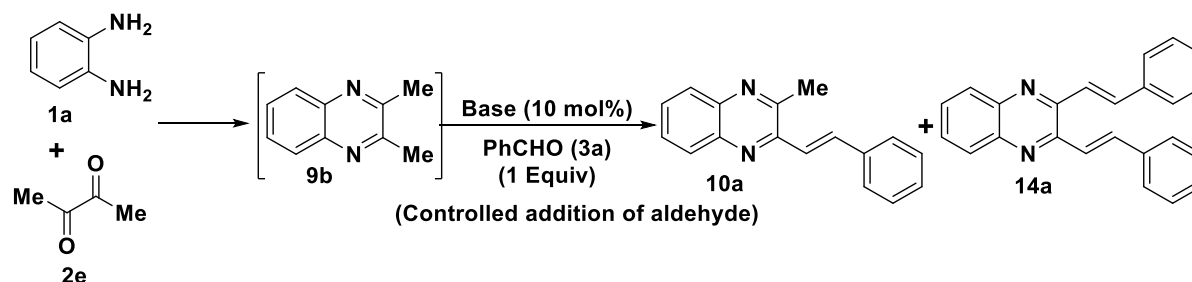


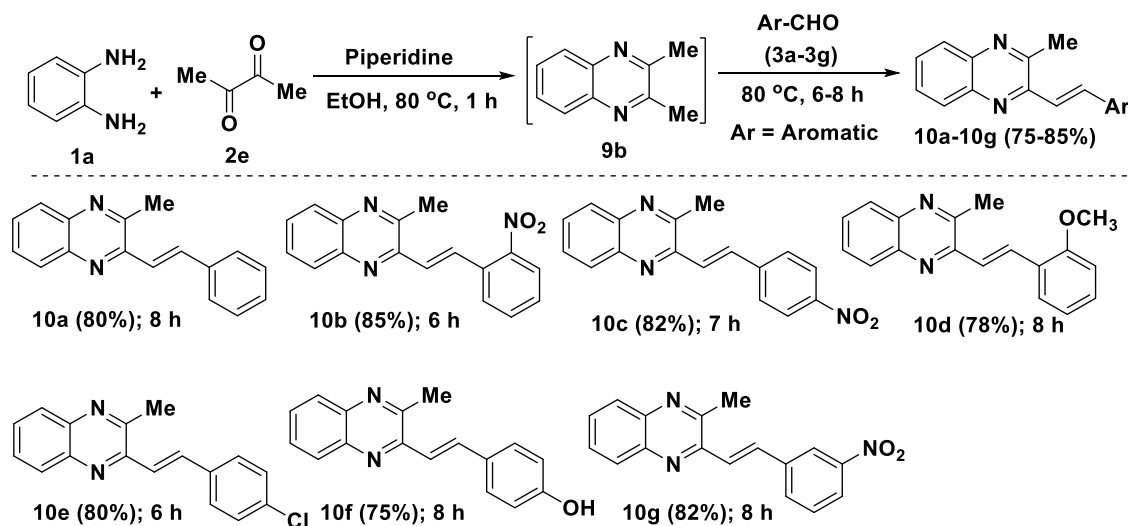
Table-2: Optimization condition^[a]

Entry	Base (10mol%)	Solvent	Temp (°C) for 1 st & 2 nd steps	Time (h)	Yield (%) 10a	Yield (%) 14a
1	Catalyst free	Water	80	12	15	ND
2	Catalyst free	EtOH	80	10	35	ND
3	DIPEA	EtOH	80	12	20	Trace
4	NEt ₃ (TEA)	CH ₃ CN	80	10	35	4%

5	NEt ₃ (TEA)	EtOH	70	8	55	10%
6	Piperidine	EtOH	70	8	60	10%
7	Piperidine	EtOH	80	8	80	12%
8	DABCO	EtOH	80	8	45	8%
9	Pyridine	EtOH	80	8	20	Trace
10	Piperidine	Water	80	8	50	10%
11	DABCO	Water	80	8	35	8%
12	pyridine	Water	80	8	trace	ND

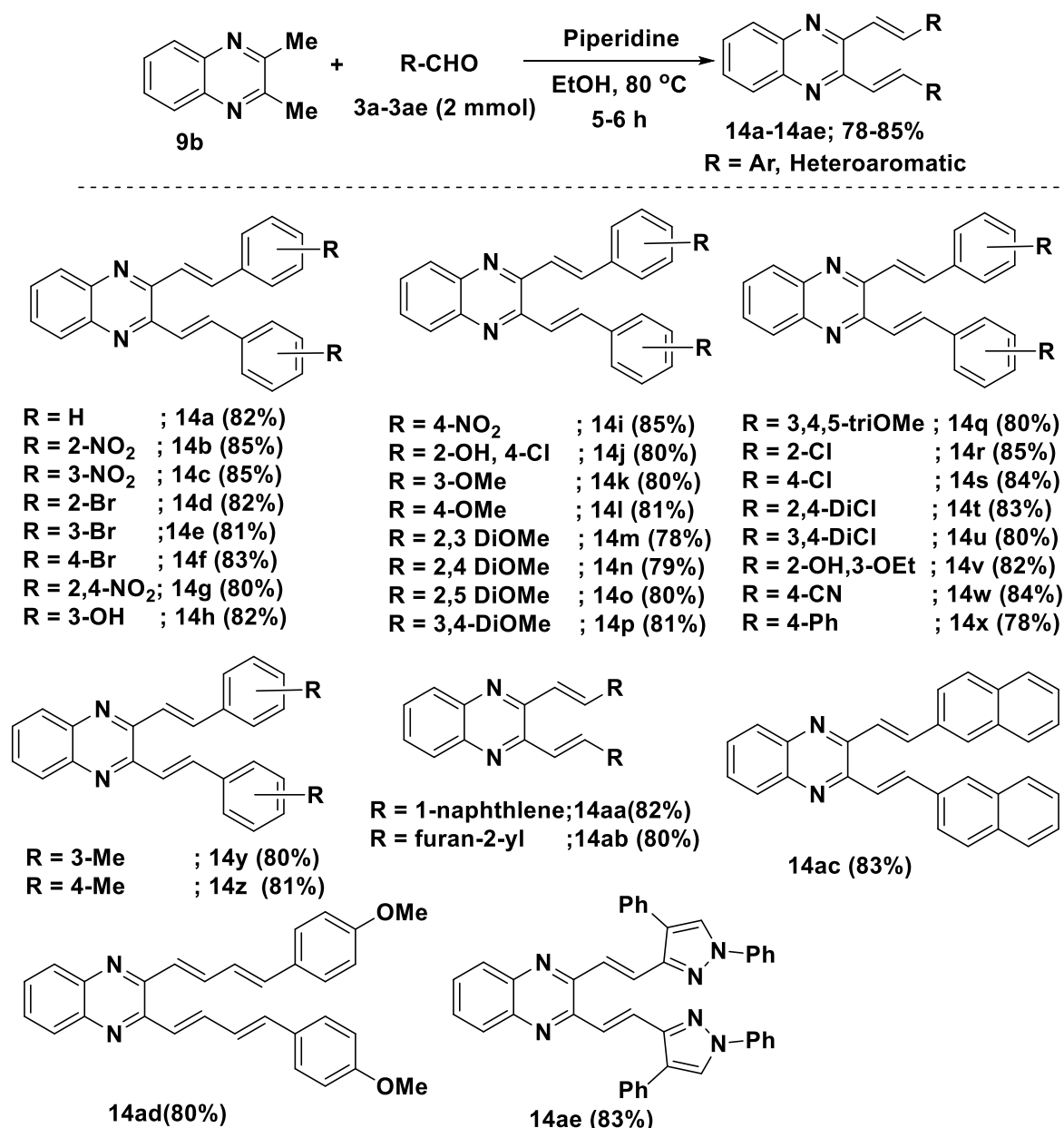
^[a]Reaction conditions: All the reactions were conducted with **1a** (1.0 mmol), **2e** (1.0 mmol), **3a** (1.0 mmol), base (10 mol%) in 5 mL of solvent at 80 °C for 6-8 h; ND = Not detected

Having optimized the reaction conditions, next attention was turned towards testing the substrate scope. Thus, different aromatic aldehydes (**3b-3g**) were treated with 2,3-dimethylquinoxaline (**9b**) using optimized conditions, to give desired (**10b-10g**) via sp³ C-H functionalization of 2,3-dimethylquinoxaline with moderate yields (**78-85%**) (**Scheme-3b**). All the synthesized products were characterized using complementary spectral data. Though the *bis*-styryl quinoxalines (**14a**) are undesired products in the present investigation, they have the biological and materials (photo physical) relevance.^{16a} Considering this, above developed method is extended to the generation of *bis*-styryl quinoxalines (**14a-14ae**) from dimethylquinoxaline (**9b**). Hence, dimethylquinoxaline (**9b**) was treated with different aldehydes (2 mmol) in the presence of piperidine (10 mol%) in EtOH at 80 °C, 5-6 h to give functionalized *bis*-styryl quinoxalines (**14a-14ae**) in moderate yields (**78-85%**) (**Scheme-4**).



Reaction conditions: Reactions were conducted with **1a** (1.0 mmol), **2e** (1.0 mmol), (**3a-3g**) (1.0 mmol), piperidine (10 mol%) in 5 mL of EtOH at 80 °C for 6-8 h

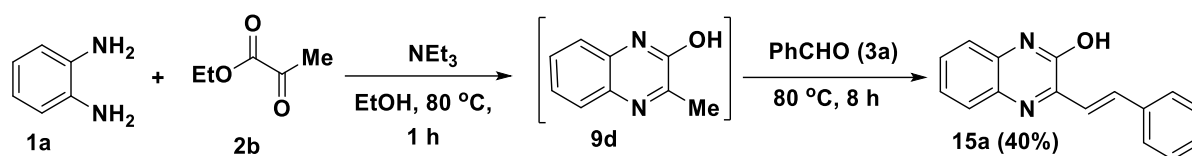
Scheme-3b: Synthesis of 3-methyl-2-styrylquinoxaline analogues (**10a-10g**).



Reaction conditions: Reactions were conducted with **9b** (1.0 mmol), (**3a-3ae**) (2.0 mmol), piperidine (10 mol%) in 5 mL of EtOH at 80 °C for 6-8 h.

Scheme-4: Synthesis of functionalized *bis*-styryl quinoxalines (**14a-14ae**).

The compounds (*E*)-3-styrylquinoxalin-2-ols (**15**) are known to show antitumor properties as inhibitors of FGFR1.^{4c} These compounds are usually prepared by using **9d** or **1a**.^{5e,12g} Based on this, we planned for the preparation of these compounds using above described method. To achieve this goal, we started the reaction of *o*-phenylenediamine (OPDA) (1.0 Equiv.) (**1a**) and ethyl pyruvate (1.0 Equiv.) (**2b**) using NEt₃ (0.1 Equiv.) in EtOH at 80 °C for 1 h to generate intermediate (**9d**; *in situ*) which was reacted with benzaldehyde (**3a**) for 8 h to give desired product 3-styrylquinoxaline-2-one (**15a**) in 40% yield (**Scheme-5a**).



Scheme-5a: Initial attempt for the synthesis of 3-styrylquinoxaline-2-ol derivative (**15a**).

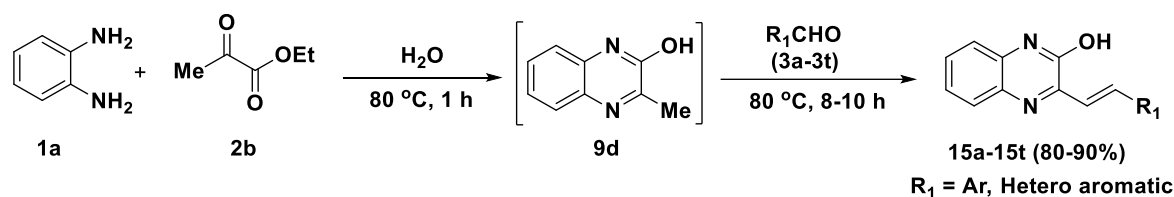
To improve the yields, experiments were performed in presence of different bases (NHEt₂, DIPEA, pyridine, piperidine, DABCO) and solvents (MeOH, EtOH, water, DMSO, DMF) but the results were not encouraging (**Entries-1 to 7; Table-1**). Later catalyst-free approach attempted. Thus, the same reaction was performed by changing the solvents to water at 80 °C. Surprisingly this condition gave the desired in 80% yield in 8 h of total reaction time (**Entry-13; Table-1**). The same reaction was repeated at 100 °C for 6 h strangely, there was no improvement in the yield of the product (**Entry-14; Table-1**).

Table- 1: Optimization conditions^[a]

Entry	Catalyst	Solvent	Temp (°C)	Time (h) 1 st step	Time (h) 2 nd step	Yield (%)
1	NEt ₃	EtOH	80	1	12	40
2	NHEt ₂	EtOH	80	1	10	35
3	Piperidine	EtOH	80	1	10	55
4	Piperidine	MeOH	65	1	8	58
5	Piperidine	DMSO	80	1	12	30
6	DIPEA	EtOH	80	1	12	20
7	Pyridine	EtOH	80	1	10	30
8	DABCO	EtOH	80	1	8	45
9	Catalyst free	DMSO	80	1	12	20
10	Catalyst free	DMF	80	1	12	20
11	Catalyst free	EtOH	80	1	12	35
12	Catalyst free	MeOH	65	1	12	20
13	Catalyst free	Water	80	1	8	80
14	Catalyst free	Water	100	1	6	80

^[a]Reaction conditions: reactions were conducted with **1a** (1.0 mmol), **2b** (1.0 mmol), catalyst: (0.1 mmol) in 5 mL of Water, Total reaction time: 1st and 2nd steps.

After confirmation of desired product by complementary spectral data, the optimized conditions were applied for substrate scope. Thus, the reaction of *o*-phenylenediamine (OPDA) (**1a**) (1.0 Equiv.) and ethyl pyruvate (**2b**) (1.0 Equiv) in water at 80 °C for 1 h gave the intermediate **9d** (*in situ*) which was treated with different aldehydes (aromatic, heteroaromatic) (**3b-3t**) for 8-10 h to give 3-styrylquinoxaline-2-ol derivatives (**15b-15t**) in 80-90% (**Scheme-3b**).

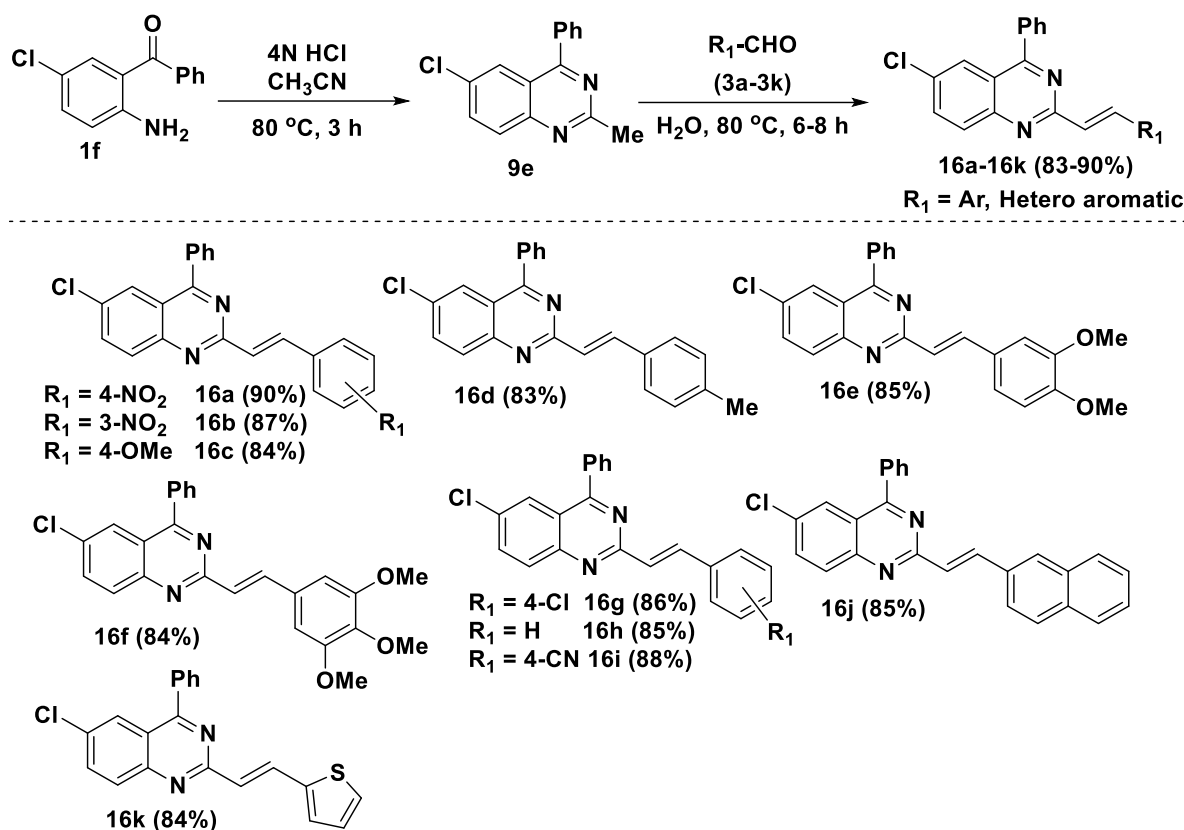


R₁ = H ;15a (80%); 8 h 3-NO₂ ;15b (88%); 8 h 3-OH ;15c (81%); 8.5 h 4-Br ;15d (90%); 8 h 2-OH,3-OMe ;15e (80%); 10 h 2-Br ;15f (85%); 8 h 2-F ;15g (82%); 8 h 2,4 Di-OH ;15h (81%); 9 h	R₁ = 4-F ;15i (80%); 10 h 3,4,5-triOMe ;15j (85%); 10 h 3,4 Di-OMe ;15k (86%); 10 h 4-OMe ;15l (85%); 9.5 h 4-N,NDiMe ;15m (82%); 10 h 4-OH,3-OMe ;15n (80%); 9 h 2,4-Di-Cl ;15o (88%); 9 h 4-NO₂ ;15p (85%); 8 h 2-Cl ;15q (85%); 8 h	R₁ = 2-furyl ;15r (82%); 8 h 2-thiophenyl ;15s (85%); 10 h 2-naphthyl ;15t (88%); 9 h

Reaction conditions: Reactions were conducted with **1a** (1.0 mmol), **2b** (1.0 mmol), **3a-3t** (1.0 mmol) in 5 mL of water, 1st step reaction time for 1 h, 2nd step reaction time 8-10 h.

Scheme-5b: Synthesis of 3-styrylquinoxaline-2-ol analogues **15b-15t**.

Similar to quinoxalines, the quinoxaline based compounds are important in biology and materials science. There are many methods for the preparation of styrene-based quinoxalines as shown in **Figures 1** and **2** (in the introduction part of this chapter). Some of the reported methods require expensive reagents. Considering this, we wish to develop a cheap and general/catalyst-free method for the synthesis of 2-styrylquinazoline hybrids (**16a-16k**) using above method. Towards this, 6-chloro-2-methyl-4-phenylquinazoline (**9e**) was prepared from (2-amino-5-chlorophenyl) (phenyl)methanone (**1f**) using known procedure^{16b} and reacted with different aldehydes (**3a-3k**) in water to give 2-styrylquinazoline hybrids (**16a-16k**) with 83–90% yield (as shown in **Scheme-6**).

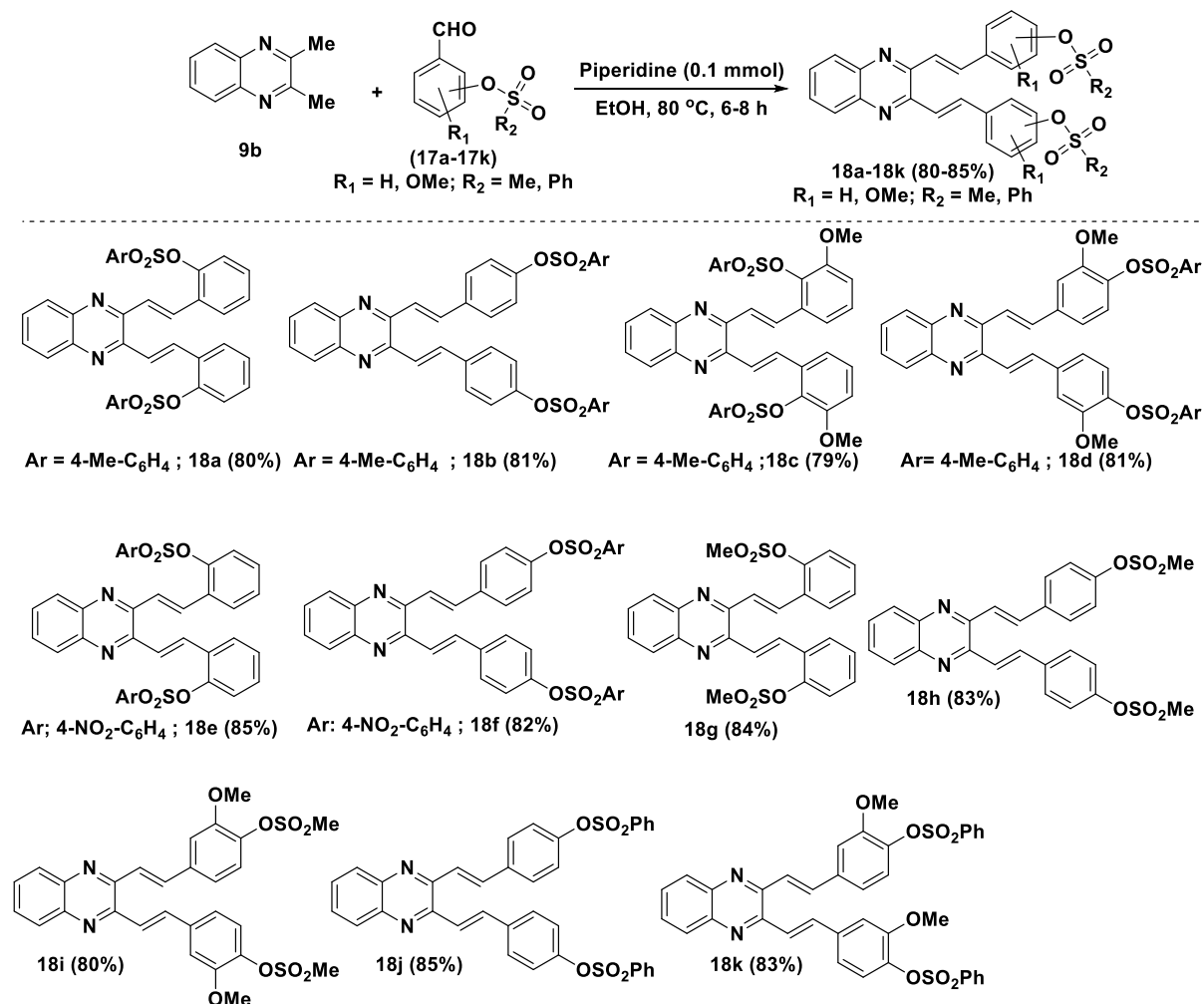


Reaction conditions: Reactions were conducted with **1f** (1.0 mmol), CH_3CN (3.0 mmol), 4N HCl (3.0 mmol), **14b** (1.0 mmol), **3a-3k** (1.0 mmol) in 5 mL of water, 6-8 h.

Scheme-6: Synthesis of substituted 2-styrylquinazoline analogs (**16a-16k**).

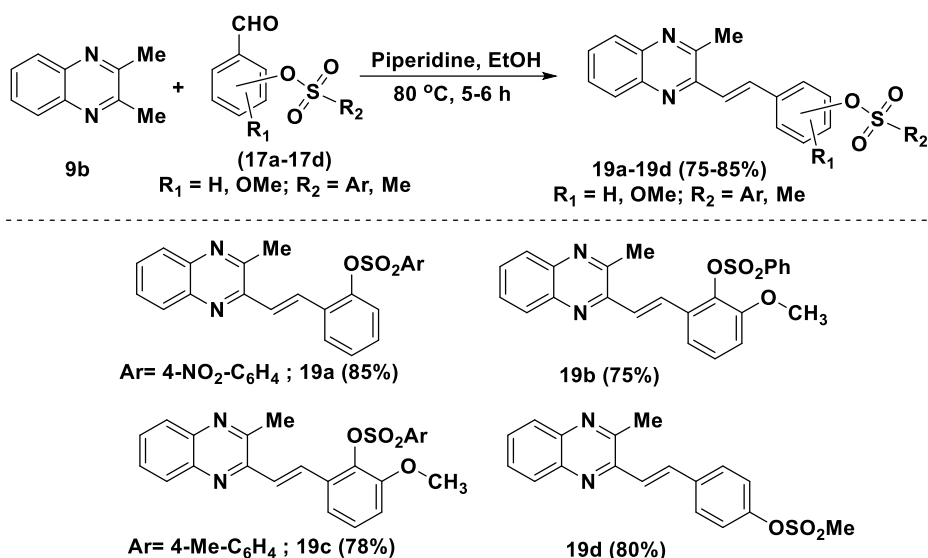
Benzene sulfonate esters are known to show the biological activity such as STAT 3 inhibitors and P2X7 antagonists.^{16c} Sulfonate moiety can also be used as bioisostere to carboxylic esters in medicinal chemistry.^{16d} Considering the biological activity of the benzene sulfonate esters the synthesis and biological activity of quinoline-based sulfonate esters is described in **Chapter-2**. In continuation with our efforts, we planned for the extension of above methods for the hierarchical activation sp^3 C-H activation of compound **9b** as key step using above-described conditions and sulfonate-based aldehydes **17a-17k**. Towards achieving this, 2,3-dimethylquinoxaline (**9b**) was simultaneously reacted with sulfonate-based aldehydes **17a-17k** by varying the stoichiometry (i.e., 2.0 mmol and 1.0 mmol) of aldehyde partner. Hence, the reaction of 2,3-dimethylquinoxaline (**9b**) (1.0 mmol) and sulfonate ester aldehydes (**17a-17k**) (2.0 mmol) in the presence of piperidine (10 mol%) in EtOH at 80 °C for 6-8 h gave desired products (**18a-18k**) with good yields (**80-85%**) (**Scheme-7**). Similarly, selective sp^3 C-H functionalization of one methyl group of 2,3-dimethylquinoxaline (**9b**) was achieved by performing the reaction of **9b** (1.0 mmol) with sulfonate ester aldehydes (**17a-17d**) (1.0 mmol) in similar conditions [i.e., piperidine

(10 mol%), EtOH, 80 °C)] in 5-6 h to produce 3-methyl-2-styrylquinoxaline sulfonate ester hybrids with good yields (**75-85%**) as shown in **Scheme-8**.



Reagents and conditions: All the reactions were conducted with **9b** (1.0 mmol), (**17a-17k**) (2.0 mmol), piperidine (0.1 mmol) in 5 mL of EtOH at 80 °C for 6-8 h.

Scheme-7: Synthesis of 3-methyl-2 styryl-quinoxaline-based benzenesulfonate ester analogs.



Reagents and conditions: All the reactions were conducted with **9b** (1.0 mmol), Piperidine (0.1 mmol), **17a-17d** (1.0 mmol) in 5 mL of EtOH at 80 °C for 5-6 h.

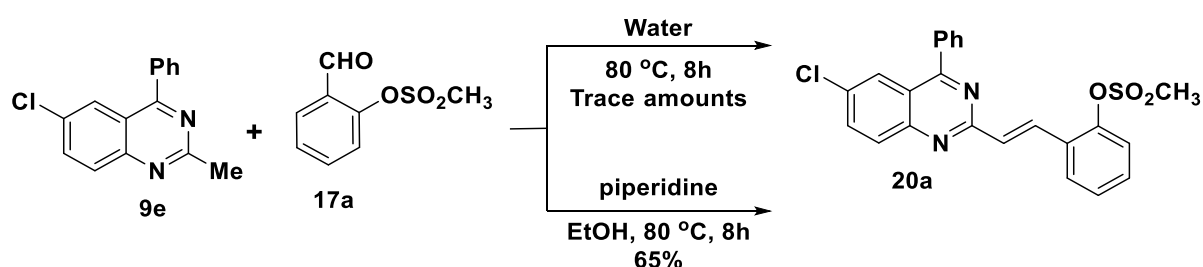
Scheme-8: Synthesis of 3-methyl-2 styryl-quinoxaline-based sulfonate ester analogs.

Further, our efforts were continued for the preparation of 2-styryl-quinazoline-based sulfonate esters based on above described strategy (**Scheme-6**). For this, initially, the reactions of 6-chloro-2-methyl-4-phenylquinazoline (**9e**) and 2-formyl phenyl methyl sulfonate (**17a**) were carried out under catalyst-free and piperidine (10 mol%) conditions. Strangely, catalyst-free reactions could not give the product but the piperidine conditions gave the desired product **20a** in 65% yield (in EtOH, 80 °C 6 h) (**Entries-1-3; Table-3**). Further to improve the yield of the desired compound, experiments were performed in different combinations of solvents (EtOH, MeOH, Water) and bases (NHEt_2 , NEt_3 , DIPEA, piperidine, DABCO, DBU, DMAP, KOH, K_2CO_3 , Cs_2CO_3) and it was found that a combination of EtOH and NEt_3 is the best suitable condition for the success of the reaction giving the desired product in 85% yield at 80 °C in 6h (**Entry-4; Table-3**).

Having optimized the reaction conditions, different sulfonate ester aldehydes (**17a-17r**) were treated with 6-chloro-2-methyl-4-phenyl quinazoline (**9e**) under optimized conditions to provide corresponding 2-styryl-quinazoline sulfonate esters (**20a-20r**) with 80–85% yield (**Scheme-9b**). Based on the above results and considering the biological importance of quinoxaline-based sulfonates, the strategy was extended for the synthesis of a new class of 3-styrylquinoxaline sulfonates. Thus, 3-methyl quinoxaline-2-ol (**14a**) was treated with sulfonate-based aldehydes (**17a-17p**) under optimized conditions to give the desired products (**21a-21p**) with 75–85% yield (**Scheme-10**). It is noteworthy to mention that the sulfonate aldehydes

containing electron-withdrawing groups ($-\text{NO}_2$) gave better yields (up to **85%**) compared to the substrates with electron-donating groups.

Based on the experimental observations, a plausible reaction mechanism is proposed, as shown in **Figure 5**. As per the literature^{17,18} and current experimental condition, first the methyl group of quinoxalines or quinazoline undergoes imine-enamine type tautomerism to provide intermediate (**A**) and then the proton abstraction takes place on the enamine part by base. After that, the enamine (nucleophile) attacks at the electrophilic site of the aldehyde (**B**), which further undergo intermolecular aldol reaction followed by dehydration to provide the desired product (**D**) (**Figure 5**).



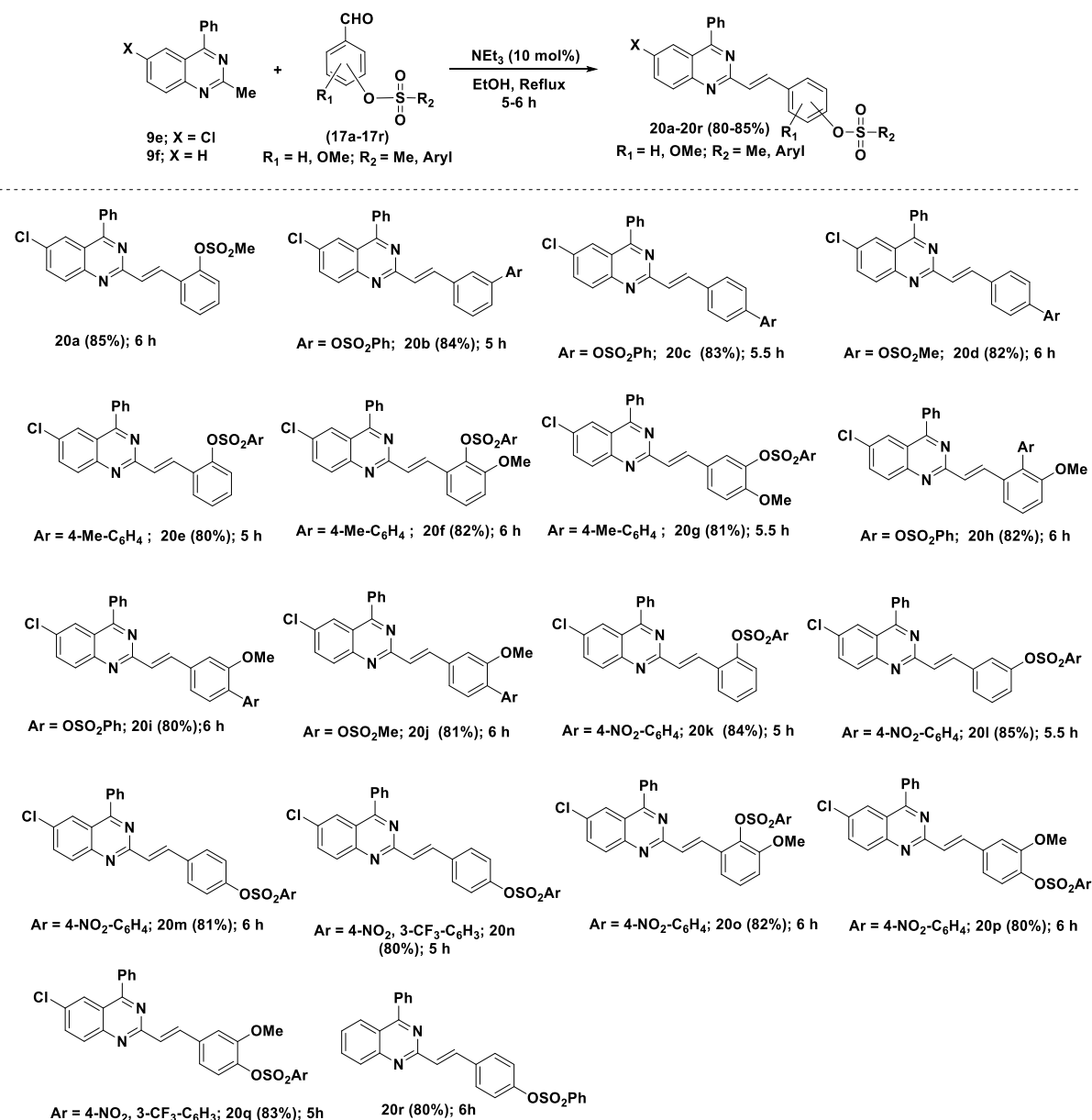
Scheme-9a: Initial attempt for sp^3 C-H activation of compound (**9e**).

Table -3: Optimization conditions^[a]

Entry	Catalyst (Base) (10 mol%)	Solvent (3 mL)	Temp (°C)	Time (h)	Yield ^[b] (%)
1	Catalyst-free	Water	80	8	Trace
2	Catalyst-free	H ₂ O	100	8	Trace
3	Piperidine	EtOH	80	6	65
4	NEt₃	EtOH	80	6	85
5	DABCO	EtOH	80	6	40
6	DBU	EtOH	80	6	65
7	DMAP	EtOH	80	8	75
8	DIPEA	EtOH	80	8	50
9	NHEt ₂	EtOH	80	6	60
10	KOH	EtOH	80	6	20
11	K ₂ CO ₃	EtOH	80	8	25
12	CS ₂ CO ₃	EtOH	80	8	30

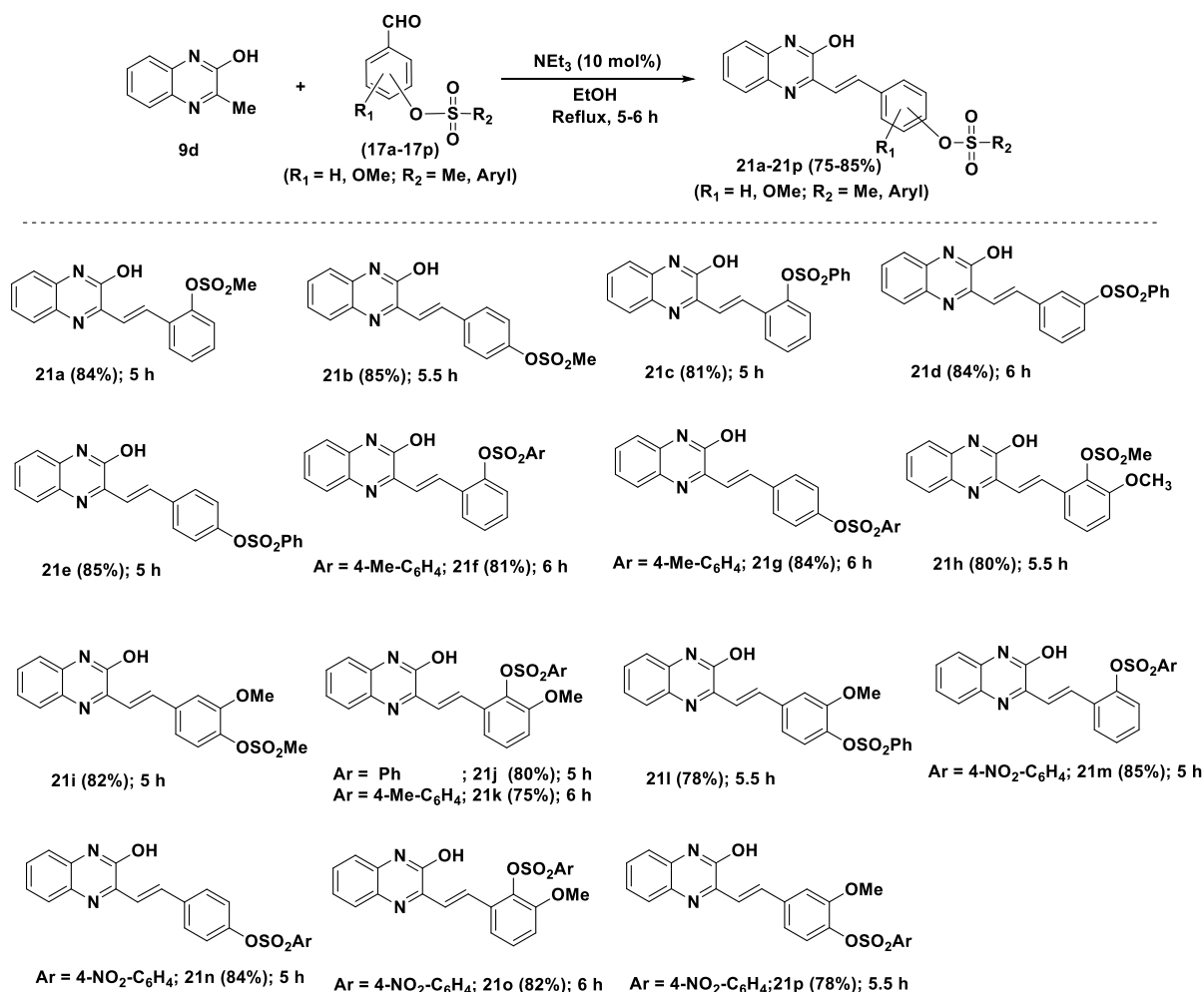
^[a]**Reaction conditions:** All the reactions were conducted with **9e** (1.0 mmol), and **17a** (1.0 mmol) in 5 mL of EtOH.

^[b]Isolated yield.



Reaction conditions: 9e-9f (1.0 mmol), 17a-17r (1.0 mmol), NEt₃ (10 mol%), EtOH (5 mL), 80 °C, 5-6 h.

Scheme-9b: Synthesis of 2-styryl-quinazoline sulfonate derivatives (20a-20r).



Reaction Conditions: 9d (1.0 mmol), 17a-17p (1.0 mmol), NEt₃ (10 mol%), EtOH (5 mL), 80 °C, 5-6 h.

Scheme-10: Synthesis of 2-styrylquinoxaline-2-ol sulfonate derivatives (21a-21p).

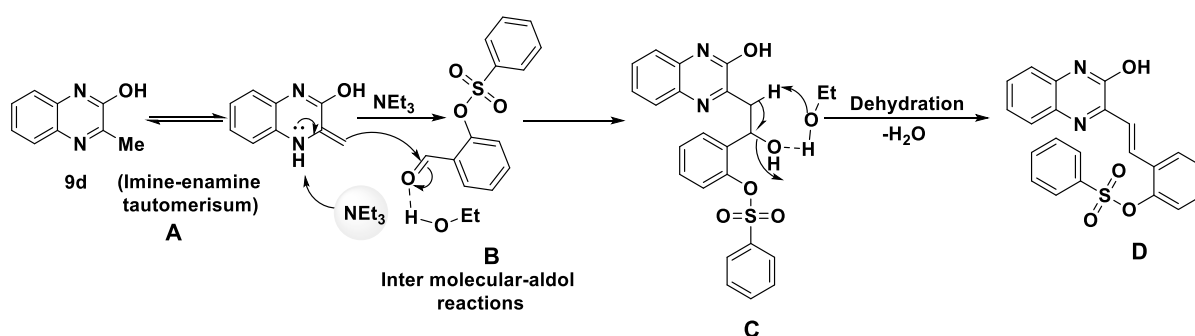


Figure-5: Plausible reaction mechanism for compound 21c.

3.4 Photo physical properties

3.4.1 Fluorescent properties of 3-styrylquinoxaline-2-ol and 2-styrylquinazoline hybrids

The chromophores, donor, and acceptor containing π -conjugated organic compounds with unique photophysical properties play great role in optoelectronic and biological applications.^{19a} In

this context, 3-styrylquinoxaline-2-ol motifs are well explored for the development of electroluminescent material^{19b} and OLEDs.^{19c} After the successful synthesis of these molecules, next, our focus was shifted to investigate the photoluminescent properties (absorption and emission spectra) of the synthesized 3-methyl-2-styrylquinoxaline (**10a-10d**), 3-styrylquinoxaline-2-ol (**15d-15t**), 2-styryl-quinazolines (**16b-16k**). Towards this, absorption and emission spectra were studied in EtOAc (100 μ M) at room temperature. For the compounds **15d-15t**, absorption bands were found in the range of 383-452 nm as shown in **Figure-6(A)** and corresponding emission spectra were observed in the range around 470-579 nm as represented in **Figure 6(B)**. Interestingly, the compound **15m** with an electron-donating group (i.e., 4-*N,N*-dimethyl) is responsible for the intramolecular charge transfer (ICT) and exhibits an emission band at 579 nm (bathochromic shift) (**Table-4**). Similarly, for the styryl-quinazolines (**16b-16k**) the absorption peaks were seen at 406-450nm and their corresponding emission spectra were observed in the range of 466-520 nm (**Table-5**). In these series, the emission band of the compound (**16e**) shifted towards 546 nm (bathochromic). Interestingly, compound (**15n**) with an electron donor group (i.e., 4-OH,3-OMe) has been found to show a strong $n-\pi^*$ transition with a stokes shift at 172 nm. The derivatives (**15d-15t**) and (**16b-16k**) display distinct color properties in CHCl_3 in a Long-Wave UV lamp (as shown in **Figure-7**).

The absorption bands of the 2-methyl-3-styrylquinoxaline (**10a-10e**) and sulfonates (**19a-19d**) were noticed at 425-461nm (**Table-6**) and their spectra were noticed at 466-520 nm as represented in **Figure-6(F)**. In this series compound (**19d**) has an electron donor group (methyl sulfonate) associated with its aromatic ring, which promotes the emission wavelength towards the bathochromic shift at 512 nm compared to benzene sulfonates containing aromatic ring compounds (**19a and 19c**) as represented in **Figure-6(E)**. In conclusion, the series (**10a-10e**) and (**19a-19d**) derivatives exhibit smaller absorption, emission band maxima and stokes shifts compare to the compounds **15d-15t** and **16b-16k**.

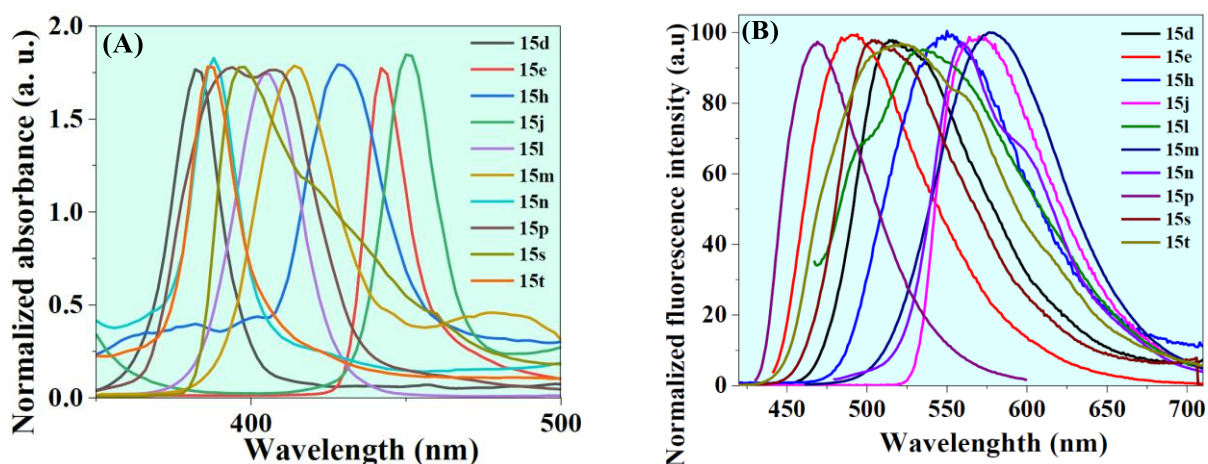


Table-4: Photo physical properties data of the resultant compounds (15d-15t).

Compound	λ_{Abs} (nm)	λ_{em} (nm)	Stokes shift ($\Delta\lambda$ nm)
15d	383	516	133
15e	443	491	48
15h	429	549	120
15j	452	569	102
15l	405	538	133
15m	414	579	165
15n	388	560	172
15p	408	470	62
15s	398	510	112
15t	387	519	132

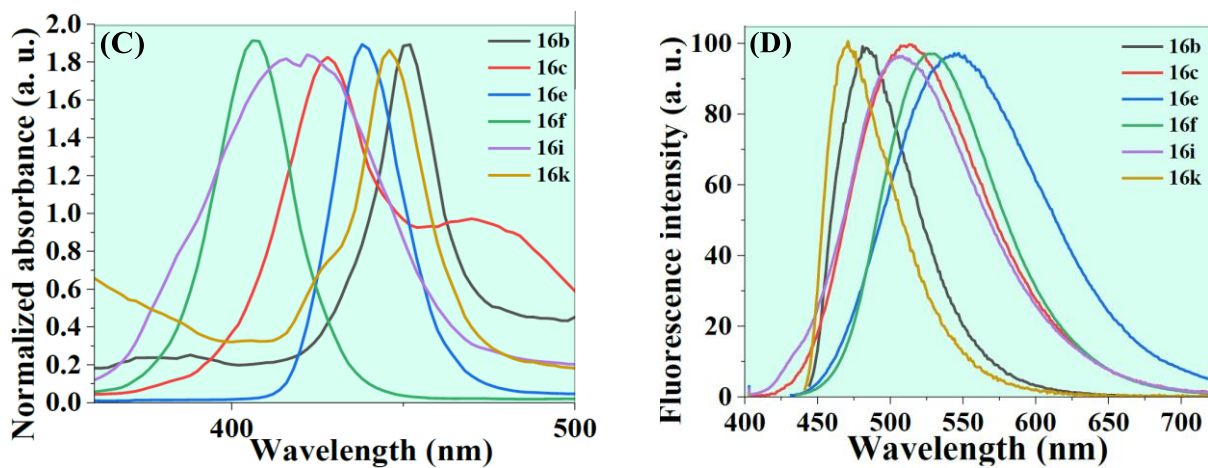


Table-5: Photo physical properties data of the compounds (16b-16k).

Compound	λ_{Abs} (nm)	λ_{em} (nm)	Stokes shift ($\Delta\lambda$ nm)
16b	450	484	34
16c	428	515	87
16e	438	546	108
16f	406	529	123

16i	416	509	93
16k	444	470	26

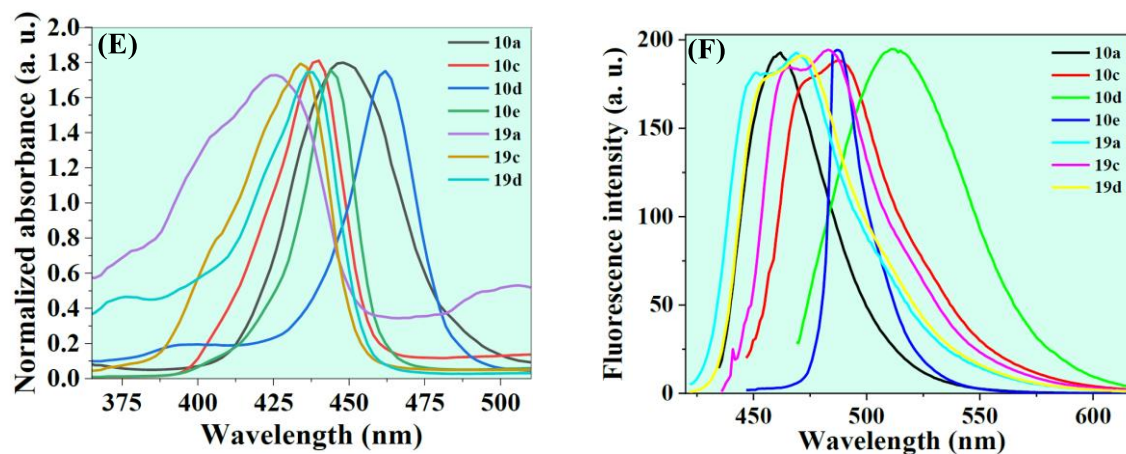


Table-6: Photo physical properties data of the resultant (**10a-10e**) - (**19a-19d**) compounds.

Compound	λ_{Abs} (nm)	λ_{em} (nm)	Stokes shift ($\Delta\lambda$ nm)
10a	444	466	22
10c	438	487	49
10d	461	520	51
10e	443	488	45
19a	425	470	45
19c	433	471	37
19d	437	472	35

Figure-6: (A) Absorption (B) Emission spectra of the compounds (**15d-15t**) (C) Absorption (D) Emission spectra of the compounds (**16b-16k**) (E) Absorption (F) Emission spectra of the compounds (**10a-10e**) & (**19a-19d**).

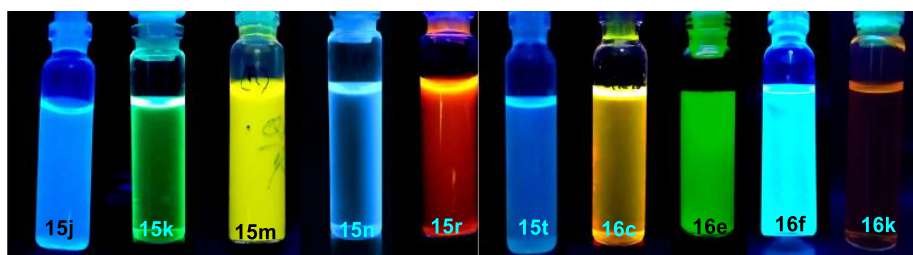


Figure-7: Different color display (in CHCl_3) under UV lamp (long wave) by the selected compounds (**15j-15t**) and (**16c-16k**).

Among all the compounds, **15j**, **15l**, **15m**, and **15n** (with electron donating groups) displayed highest emission band maxima at 569, 538, 579, and 560 nm respectively with intramolecular charge transfer (ITC).^{19d} Also, molecules **15n**, **15m**, and **15l** showed the highest stokes shifts at 172, 165 and 132 nm respectively. Later, we examined the solvatochromic effect of

the compound **16f** in various solvent systems (i.e., non-polar to polar; *n*-hexane to DMSO) at room temperature at 100 μ M concentration as shown in **Figures-8a and 8B (Table-7)**. It was observed that the compound **16f** shows an absorption bands in the range of 387-450 nm and emission in the range of 475-625 nm indicate strong solvatochromism with bathochromic shift from non-polar to polar solvents (*n*-Hexane, DCM, CHCl_3 , EtOAc, Acetone, MeOH, MeCN, DMF and DMSO) **Figure-8 (C)**.^{19e} Due to the ICT effect^{19e} this compound displays distinct color pattern under UV lamp (long-wave range) as shown in **Figure -8 (C)**.

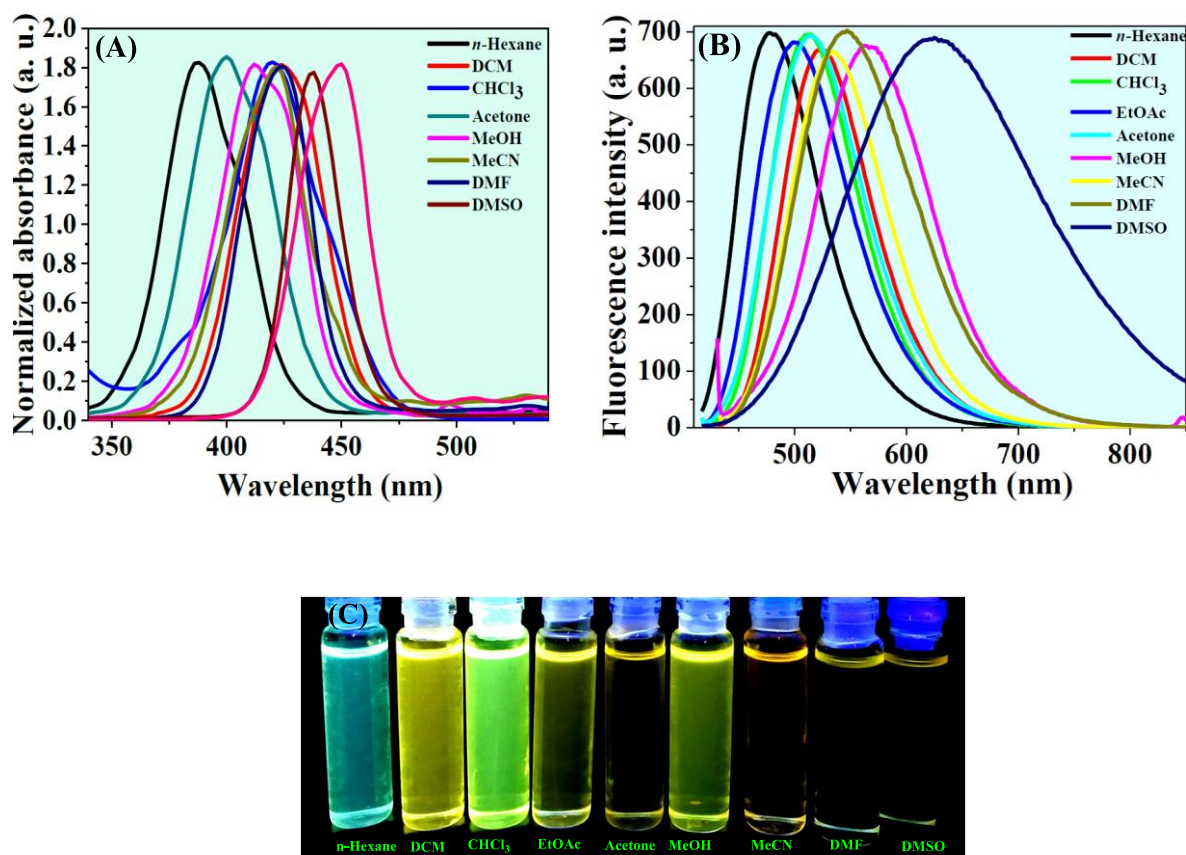


Figure 8: (A) Absorption (B) Emission spectra of the compound (**16f**) in non-polar to polar solvents (*n*-Hexane to DMSO) at 100 μ M. (C) Solvatochromic effect of compound (**16f**) in different solvents (non-polar to polar) irradiated under long-wave UV-lamp.

Table-7: Solvatochromic effect data of the resultant compound (**16f**).

Solvent	λ_{Abs} (nm)	λ_{em} (nm)	Stokes shift ($\Delta\lambda$ nm)
<i>n</i> -Hexane	387	475	88
DCM	425	525	100
CHCl_3	420	512	87
EtOAc	406	529	103
Acetone	412	515	103
MeOH	419	568	149
MeCN	424	538	114
DMF	437	548	111
DMSO	450	625	175

3.5 Biological activity

3.5.1 Biological activity of 2,3-di(*E*-styryl) quinoxalines (14a-14ae) and their sulfonate derivatives (18a-18k)

3.5.1.2 α -D-glucosidase assay, materials, and methods

The α -glucosidase activity was determined calorimetrically with 4-nitrophenyl D-glucopyranoside (4-NPG) as the substrate. The enzymatic reaction was performed by adding 40 μ l of 4-NPG (substrate stock of 2mg/ml made in 0.1M Tris- HCl pH 7.5) and 10 μ l of α -glucosidase (1mg/ml made in 0.1M Tris- HCl pH 7.5) to 150 μ l 0.1M Tris- HCl pH 7.5 and the reaction mixture was incubated at 37°C for 5 min. The activity was estimated by reading the absorbance of 4-nitrophenol formed at 410 nm against an enzyme-free blank. For studying inhibition kinetics, the enzyme was incubated with the inhibitors, (14a-14ae) and (18a-18k) (compounds (1mg/ml in DMSO) for 15 min at room temperature before the addition of substrate. 1 Unit of glycolytic activity is defined as the quantity of enzyme required to liberate 1 μ g of 4-nitrophenol per minute under standard assay conditions.

3.5.1.3 Determination of IC₅₀ values of the 2,3-di(*E*-styryl) quinoxaline and their sulfonate derivatives (14a-ae) and (18a-18k)

IC₅₀ values of inhibitors were calculated based on the concentration of inhibitor required to inhibit 50% of α -glucosidase activity under the standard assay conditions. For quantification of IC₅₀ values, the enzyme inhibition assays were carried out at different concentrations (20 to 100 μ g) of inhibitors, without varying concentrations of enzyme. The enzyme reaction was performed by pre-incubating the enzyme with an inhibitor at room temperature for 15 min and inhibitory activity was determined under standard assay conditions. For those molecules which showed significant inhibition, the mode of inhibition exhibited by the inhibitor was examined by carrying out Michaelis-Menten enzyme kinetics by varying substrate (4-NPG) concentration (8, 16, 32, 40, and 80 μ g) in the absence and presence of the inhibitor molecules at three different concentrations (20, 40 and 100 μ g). Mode of inhibition was determined by Lineweaver-Burk plot analysis of the data obtained. All IC₅₀ values are represented as Mean \pm Standard Deviation.

Insilico - Ligand Preparation

The 2D structures of all 32 synthetic inhibitor molecules (14a-ae) and (18a-18k) were sketched using VLife MDS software v.4.6 and saved in .mol format. The 3D coordinate files were generated and saved in .mol2 format. The geometry of the ligand

molecules was optimized using the MMFF force field until a gradient of 0.001 kcal/mol/Å was achieved.

Homology Modelling

As the structure of *Saccharomyces cerevisiae*, α -glucosidase MAL12 (UniProt ID P53341) is not available in the public domain, its theoretical model was built by homology modelling. It was accomplished by retrieving the sequence of the MAL12 protein from the UniProt database (Sequence ID P53341). A potential template with PDB ID 3AJ7 was identified by BLAST analysis using the BLOSUM62 matrix in the PDB database, based on the sequence identity. The template had 72% identical residues, 85% positive residues, and negligible gaps. Its coordinates were further modified to make it suitable for automated homology modelling and a model was generated by the Biopredicta module of the VLife® program. Superimposing the template and the generated protein model yielded an RMSD value of 0.251094.

Docking method Validation and GRIP Docking

Molecular docking simulations were carried out using the GRIP docking method in the VLife® Biopredicta module. The largest cavity with greater volume was chosen for docking the compounds. Scoring of the docked poses was done by the PLP method and dock score. The docking interactions were critically analyzed and the analysis revealed the key amino acid residues within the binding pocket contributing to α -glucosidase inhibition.

Results and discussions

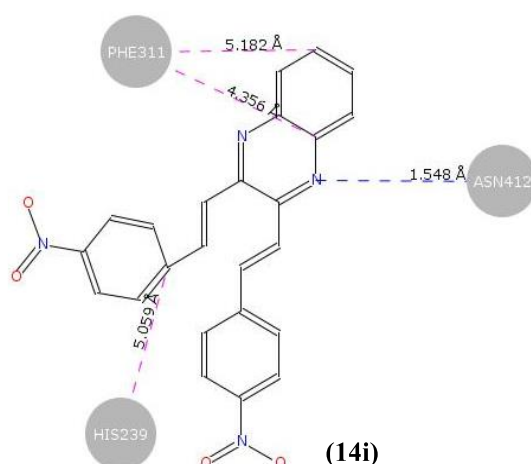
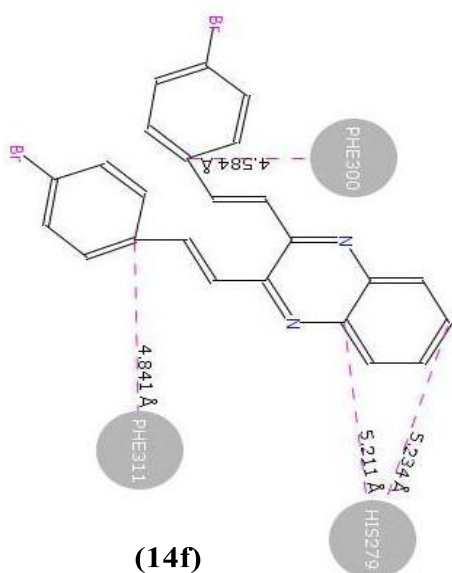
The α -glucosidase inhibition activity of 2,3-di((E)-styryl) quinoxaline (**14a-ae**) and their sulfonate derivatives(**18a-18k**) showed varying degrees of inhibition with IC₅₀ values ranging from 36 μ M to 154 μ M (**Table-8**). Acarbose was selected as a control inhibitor, the IC₅₀ value of which was found to be 33.36 μ M under the same assay conditions. Among the tested compounds, the compound (**14t**) showed a minimal/lowest IC₅₀ value of 36 μ M, and the compound (**14s**) showed a maximum IC₅₀ value of 154 μ M. The compounds (**14f**), (**14i**), and (**14t**) which showed minimal IC₅₀ values among the tested compounds against α -glucosidase activity were chosen for determining the mode of inhibition against MAL12 (**Table-10**). It was achieved by comparing the Michaelis-Menten kinetic constants obtained from the experimental investigation carried out in the presence of varying concentrations of substrate and inhibitors. Results of K_m and V_{max} of α -

glucosidase in the presence of tested compounds were shown in **Table-9**. By studying the kinetics of α -glucosidase it was observed that the presence of inhibitor/ligand greatly affected the K_m and V_{max} values. From the Line weaver–Burk double reciprocal plot for the inhibition of α -glucosidase by compound (**14f**), it was observed that the mode of inhibition is mixed uncompetitive type. **Deng et al.** recently reported a similar type of mixed inhibition of α -glucosidase by pu-erh tea polysaccharide.^{20a} Increase in the concentration of compounds (**14i**) and (**14t**) showed corresponding decreases in the value of kinetic constants K_m and V_{max} . This reveals that the ligands (**14i**) and (**14t**) bind to α -glucosidase competitively. Different modes of inhibition were studied by varying the inhibitors and reported for α -glucosidase activity by **Jaikai et al.** and **Berna et al.** reported that α -glucosidase was competitively inhibited by *Antidesma bunius* L plant extract.^{20b} In contrast to our findings, **Farhad et al.** reported that their pyrimidine-fused derivatives inhibited the activity of α -glucosidase in a mixed-competitive mode.^{20c} **Zhenhua et al.** reported inhibition profiles of various medicinal plant extracts having different modes of inhibition like competitive, uncompetitive and mixed competitive.^{20d}

Table-8: In-vitro α -D-glucosidase inhibition studies of synthesized derivatives (**14a-14ae**) and (**18a-18k**).

S. No.	Compound code/ ligand	IC ₅₀ (μ M)
1	14a	99.23 \pm 2.51
2	14b	83.43 \pm 2.81
3	14c	57.30 \pm 2.06
4	14d	107.97 \pm 2.02
5	14f	38.75 \pm 2.57
6	14g	90.16 \pm 2.01
7	14h	108.55 \pm 1.81
8	14i	41.82 \pm 3.53
9	14j	46.58 \pm 2.47
10	14m	51.24 \pm 2.65
11	14p	60.20 \pm 2.62
12	14r	132.21 \pm 7.16
13	14s	154.36 \pm 6.57
14	14t	36.23 \pm 2.78
15	14v	94.08 \pm 3.97

16	14w	61.65 ± 2.46
17	14x	100.45 ± 3.53
18	14z	49.68 ± 2.09
19	14a2	75.34 ± 2.88
20	14a4	83.50 ± 3.72
31	14a5	48.88 ± 2.51
21	18a	69.32 ± 3.14
22	18b	49.54 ± 2.11
23	18c	43.11 ± 4.91
24	18d	75.86 ± 4.81
25	18e	144.3 ± 8.33
26	18f	69.37 ± 4.61
27	18g	43.40 ± 5.37
28	18h	81.15 ± 4.74
29	18i	68.11 ± 3.11
30	18j	80.40 ± 4.91
32	18k	42.45 ± 5.65
33	Acarbose	33.36 ± 1.22



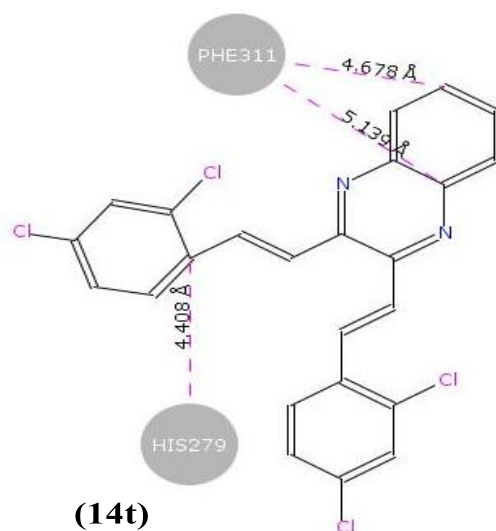


Figure-9: 2D docking interactions of compounds **14f**, **14i**, and **14t** with MAL12 protein model using rigid docking, PLP scoring function (GRIP docking algorithm).

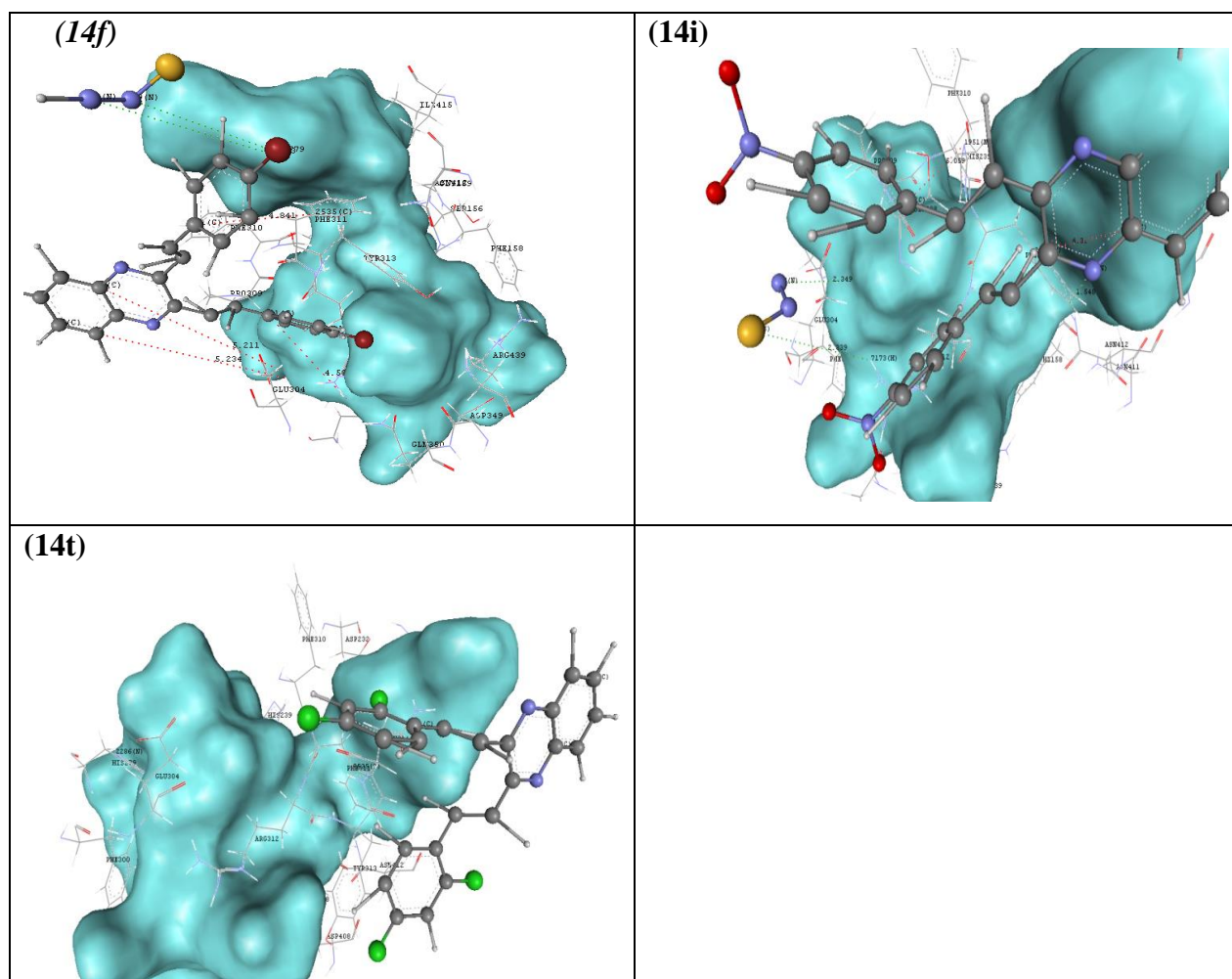


Figure-10: 3D docking interactions of compounds (**14f**, **14i**, and **14t**) with MAL12 protein model using rigid docking, PLP scoring function (GRIP docking algorithm).

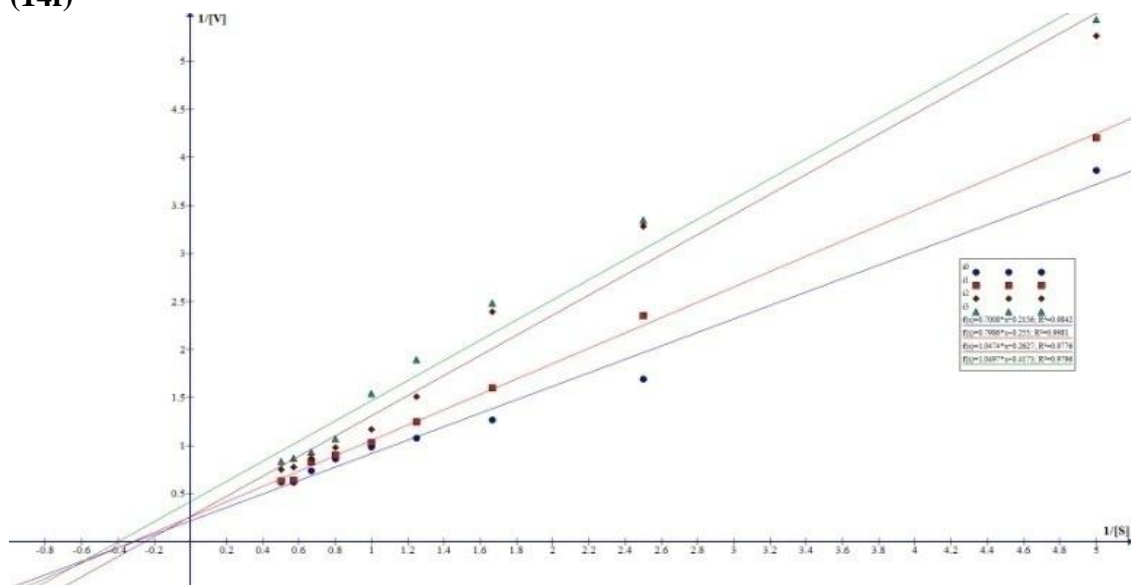
Compound	IC ₅₀ (μM)	K _{im} (μM)	V _{max} (μM/min)	Mode of inhibition
		Inhibitor concentration of 25 μg		
14f	38.75 ± 2.57	2.94	3.48	Mixed-Uncompetitive
14i	41.82 ± 3.53	4.10	4.61	Mixed-inhibition
14t	36.23 ± 2.78	3.15	4.53	Mixed-inhibition

Table-9: IC₅₀, K_{im}, V_{max}, and modes of inhibition of selected synthetic molecules (**14f**, **14i**, and **14t**). K_m and V_{max} values of α-D-glycosidase for 4-NPG without inhibitor were 3.24 μM and 4.64 μM/min respectively.

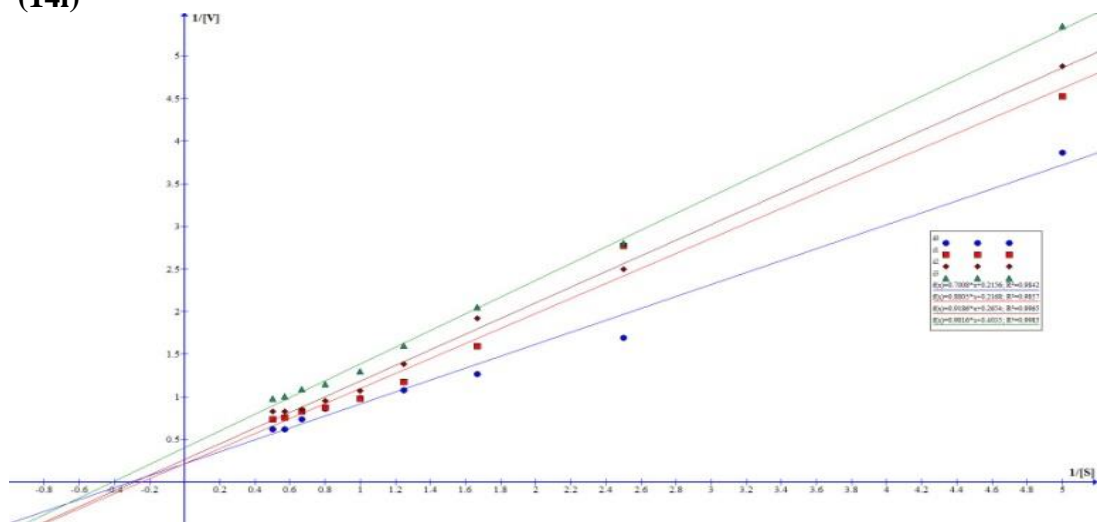
Compound	Residue Atom		Ligand Atom	Distance Å	Interaction
14f	HIS279	2286N	1C	5.234	π-STACKING
	HIS279	2286N	4C	5.211	π-STACKING
	PHE300	2449C	21C	4.584	π-STACKING
	PHE311	2535C	11C	4.841	π-STACKING
	LYS155	5989H	29N	1.779	H-BOND
	LYS155	5989H	31N	2.523	H-BOND
14i	HIS239	1951N	20C	5.059	π-STACKING
	PHE311	2535C	1C	5.182	π-STACKING
	PHE311	2535C	4C	4.356	π-STACKING
	HIS279	6938H	35N	2.349	H-BOND
	ARG312	7173H	34S	2.339	H-BOND
	ASN412	7977H	7N	1.548	H-BOND
14t	HIS279	2286N	21C	4.408	π-STACKING
	PHE311	2535C	1C	4.678	π-STACKING
	PHE311	2535C	4C	5.139	π-STACKING
	ASN314	7190H	33N	2.475	H-BOND

Table-9: Molecular docking interactions between the MAL12 protein model and the most potent compounds (**14f**, **14i**, and **14t**).

(14f)



(14i)



(14t)

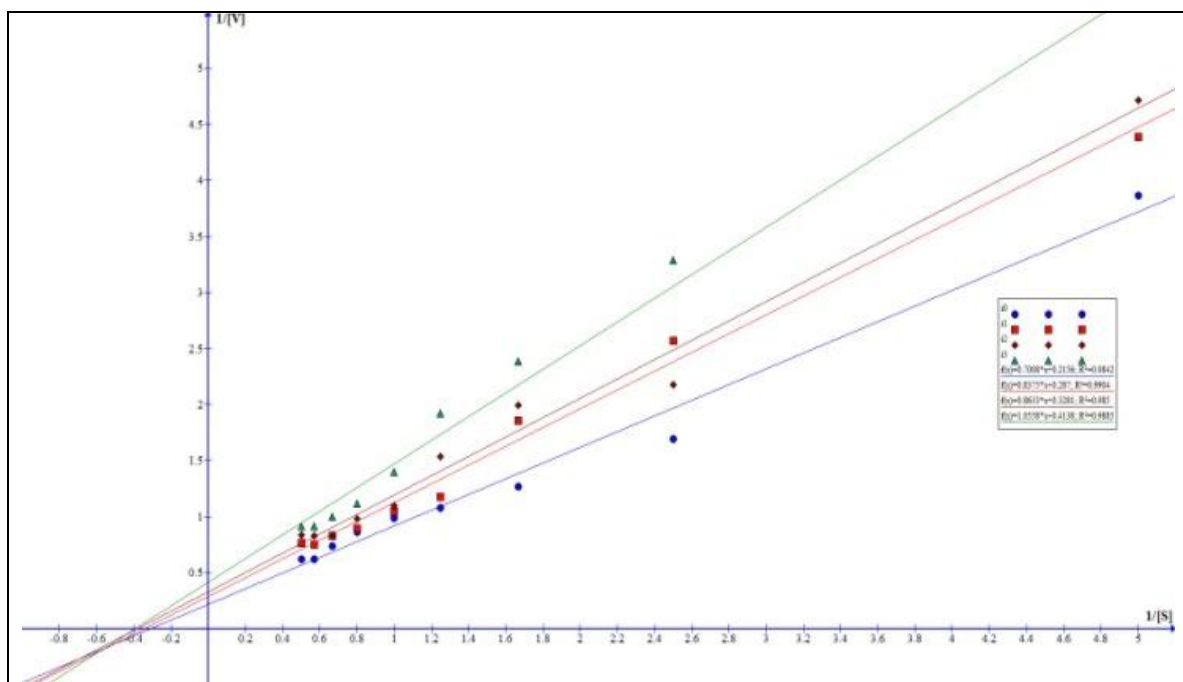


Figure-11: Lineweaver-Burk plot for an understanding of the mode of Inhibition of α -D-glucosidase by compounds (**14f**, **14i**, and **14t**).

3.5.2 Biological activity of 2-styryl-quinazoline (**20a-20r**) and 3-styryl-quinoxaline based sulfonate ester derivatives (**21a-21p**)

3.5.2.1 α -Glucosidase assay, materials, and methods

The enzymatic activity of α -glucosidase was determined by the colorimetric method using 4-nitrophenyl glucopyranoside (4-NPG) as a substrate. The enzymatic reaction was started by the addition of 25 mL of 4-NPG (substrate stock solution) to 25 mL of α -glucosidase (2 mg dissolved in 1 mL of 10 mM Tris-HCl pH 7.0) and 950 mL deionized H₂O and the reaction mixture was incubated at 37°C for 10 min. The catalytic activity was calculated by measuring the absorbance of the liberated 4-nitrophenol against an enzyme-free blank at 410 nm. For inhibition kinetics experiments, the enzyme was incubated with inhibitors (**20a-20r** and **21a-21p**) for 30 min before adding substrate solution. 1 unit (U) of glycolytic activity was defined as the amount of enzyme needed to release 1 mg of 4-nitrophenol per min under standard assay conditions.

Table 10: Statistical parameters of the GA-LDA

Parameters	Training set	Test set
No. of compounds	34	14

Sensitivity (%)	76.3	64.2
Specificity (%)	72.1	75.4
Accuracy (%)	84.0	83.3
Precision (%)	65.2	68.5
MCC	0.632	0.411
AUROC	0.893	0.732

Determination of the IC₅₀ values

IC₅₀ values of inhibitors were calculated based on the concentration of inhibitor molecule required to inhibit 50% of α -glucosidase activity under the standard assay conditions. For quantification of the IC₅₀ value of the enzyme, the enzyme inhibition assays were carried out at different concentrations (10 to 500 mg) of inhibitors, without changing the enzyme concentration. The enzyme reaction was performed by preincubating the enzyme with inhibitor at 37 °C for 30 min and inhibitory activity was determined under standard assay conditions. For those molecules which showed significant inhibition, the mode of inhibition exhibited by the inhibitor was examined by carrying out Michaelis–Menten enzyme kinetics by varying the substrate (4NPG) concentration (0.25, 0.4, 0.6, 0.8, 1.0, 1.25, 1.5 and 2.0 mM) in the absence or presence of the inhibitor molecules at two different concentrations (25 and 50 mg). The mode of inhibition was determined by Lineweaver–Burk plot analysis of the data obtained through Michaelis–Menten kinetics values. All IC₅₀ values are represented as mean-standard deviation.

In silico ligand preparation

The 2D structures of all 2-styryl-quinazoline sulfonates (**20a–20r**) and 3-styrylquinoxaline sulfonates (**21a–21p**) were sketched using VLife MDS software v.4.6 and saved in .mol format and the 3D coordinate files were generated and stored as .mol2 format. The ligand molecule geometry was optimized by using the MMFF force field until a gradient of 0.001 kcal mol⁻¹ Å⁻¹ was reached.

Homology modelling

The experimentally solved structure of *Saccharomyces cerevisiae* α -glucosidase MAL12 (uniprot id P53341) is not available in the public domain. So, the theoretical structure model of the MAL12 protein was built by the homology modelling approach. The sequence of the target protein

Saccharomyces cerevisiae α -glucosidase MAL12 was retrieved from the uniprot database (Seq id P53341). BLAST analysis was performed using the BLOSUM62 matrix to identify possible templates available in the PDB database. Based on the sequence identity, PDB ID 3AJ7 was selected as a potential template. The chosen template had 72% identity (423/587) residues, 85% positives (499/587) residues, and 0% literally negligible gaps (5/587). The coordinates of the 3AJ7 (PDB ID) were retrieved from the RCSB PDB database and modified, missing, and cis-cross residues were identified, rectified, and cleared to make the structure suitable for automated homology modelling. The homology model for MAL12 was generated by automated homology model building in the Biopredicta module of the Vlifex program. RMSD was calculated as 0.251094 by superimposing the template and the generated protein model.

Method validation and GRIP docking

Molecular docking simulations were carried out using the GRIP docking method in the Vlifex Biopredicta module. The largest cavity with a higher volume was chosen for docking the compounds. Scoring of the docked poses was done by the PLP method and dock score. The docking interactions were critically analysed and the analysis revealed the key amino acid residues within the binding pocket contributing toward α -glucosidase inhibition.

QSAR analysis

QSAR analysis was performed using the open-source tool QSAR-Co. A model was developed using linear discriminant analysis (LDA). The following model parameters were considered for evaluating the generated model accuracy, sensitivity, specificity, precision, MCC (Matthews Correlation Coefficient), and AUROC (Area Under the Receiver Operating Characteristic curve), as shown in **Table-10**. The molecular descriptors used were calculated using the PaDEL tool. The Monte Carlo optimization method as implemented in the correlation and logic (CORAL) tool was used for the analysis of fragments that influence the inhibitory activity of the compounds.

Results and discussions

The inhibition of α -glucosidase activity tested by 2-styrylquinazoline sulfonates (**20a–20r**) and 3-styryl-quinoxaline sulfonate esters (**21a–21p**) showed varying degrees of α -glucosidase inhibition with IC₅₀ values ranging from 28 mM to 662 mM (**Table-11**). Acarbose was selected as a control inhibitor, and the IC₅₀ value of acarbose under the same assay

conditions was found to be 33 mM. Among the tested compounds (**20a–20p** and **21a–21o**), compound (**20o**) showed the lowest IC₅₀ value of 28 mM and compound (**20n**) showed the maximum IC₅₀ value of 662 mM. Compounds (**20o**), (**21n**), and (**21o**) showed minimal IC₅₀ values against α -glucosidase activity, so were chosen for determining the mode of inhibition of these ligands against MAL12. The mode of inhibition of selected inhibitors was determined by comparing the Michaelis–Menten kinetic constants obtained from the experimental investigation carried out in the presence of varying concentrations of substrate and inhibitors. The results of K_m and V_{max} of α -glucosidase in the presence of the tested ligands are shown in **Table-12**. The molecular docking interactions between the selected most potent inhibitor molecules (**20o**, **21n**, and **21o**) and the MAL12 protein model are represented in **Table-12 (Fig. 12 and 13)**. Among them, compound (**21n**) shows hydrogen interactions with the highest bond distance of 2.500 Å observed between atom 6637H and ligand atom 29O by the residue ASN241. Moreover, in the p-stacking interactions, compound (**20o**) displayed an impressive bond distance of 5.372 Å with the linking atom 2286N and ligand atom 1C by using a histidine (HIS239) residue. Docking studies were performed for similar structures to predict the biological significance. The QSAR model was generated and the docking score was obtained for a series of compounds with similar structural/functional groups and was used for biological activity. The presence of a combination of sulfonate and nitro groups in the molecule showed a good correlation with the inhibitory effect. The fragments with methoxy and methyl-sulfonated groups also showed a positive effect (if the sulfonate moiety is *ortho* to the double bond present in the structure). However, the compounds with the sulfonyl and nitro group combination showed more positive effects and are most influential to possess inhibitory properties. The molecules with high TPSA and low hydrophobicity showed better interaction with the proteins. Based on interactions obtained in docking studies and predictions made through QSAR studies, it can be interpreted that these functional groups show inhibitory effects due to the nature of amino acids (hydrophilic basic amino acids HIS239, HIS279, LYS155, ARG312) present in the core binding cavity of α -glucosidase. The presence of the electron-withdrawing group also showed improved inhibitory activity. Therefore, these groups positioned near HIS or LYS residues in the binding pocket were desirable (**Figure-12 and 13**).

Different sulfonate esters exhibited different enzyme inhibitory activities. The sulfonate substitution with a hydrogen bond acceptor and the electron-withdrawing nitro group appeared to be vital for enzyme inhibitory activity. The inhibitory effect was maximum when the substitution was at the para position (**20o**, **20p**, **21n**, **21o**). These results are synchronous with the literature

reports.^{21(a,b)} Also equal inhibitory activity was found with methyl sulfonated substitution at the *ortho* position (20a, 21h). An electron-donating methoxy group at the meta position in combination with *ortho* substitution of sulfonyl (with a nitro group, a hydrogen bond acceptor) favoured the inhibitory activity (20o, 20p, 21n, 21o). The K_m and V_{max} values (Table-13) and the Lineweaver–Burk double reciprocal plot (kinetic studies) (Figure- 14) for the compound (21o) indicate a mixed uncompetitive mode of inhibition towards α -glucosidase, which is similar to the observation by Deng et al.^{20a} for pu-erh tea polysaccharide. Whereas, for the compounds (20o) and (21n), an increase in the concentration of the compounds showed a decrease in the value of K_m and V_{max} . This reveals that (20o) and (21n) bind to α -glucosidase competitively in the active site. These observations are similar to the results of various types of inhibitors for α -glucosidase activity as reported by Zhang et al.^{20e} and Berna et al.^{20b} for *Antidesma bunius* L plant extract. This is also supported (for compound 20o) by the work of Moghadam et al. in which they observe competitive inhibition for the 2,4- diarylquinazoline derivatives.²² In contrast to our findings, Farhad et al.^{20c} reported that the selected pyrimidine-fused decrease in the value of K_m and V_{max} . This reveals that (20o) and derivatives inhibited the activity of α -glucosidase by mixed competitive mode and Zhenhua et al.^{20d} reported competitive, uncompetitive, and mixed competitive mode of inhibition profiles of plant extracts. This may be due to the different binding modes/energies of the compounds 21n and 21o where they show different kinetics toward α -glucosidase enzyme inhibition.

Table-11: In vitro α -D-glucosidase inhibition studies of 2-styryl-quinazoline and 3-styryl-quinoxaline sulfonate esters (20a–20p and 21a–21o).

S. No	Compound	IC ₅₀ (mM)
1	20a	37 ± 2.07
2	20b	38 ± 2.05
3	20c	111± 6.07
4	20d	222± 11.35
5	20e	44 ± 1.15
6	20f	154 ± 8.97
7	20g	154 ± 8.35

8	20h	154 ± 10.24
9	20i	76 ± 3.24
10	20j	46 ± 3.24
11	20k	201 ± 10.35
12	20l	185 ± 6.84
13	20m	93 ± 6.03
14	20n	662 ± 18.64
15	20o	28 ± 1.99
16	20p	36 ± 9.78
17	21a	48 ± 1.12
18	21b	42 ± 2.11
19	21c	194 ± 8.61
20	21d	58 ± 3.29
21	21e	38 ± 2.20
22	21f	83 ± 6.24
23	21g	194 ± 5.37
24	21h	33 ± 1.68
25	21i	194 ± 9.08
26	21j	104 ± 6.78
27	21k	139 ± 7.25
28	21l	145 ± 7.91
29	21m	193 ± 9.32
30	21n	32 ± 2.11
31	21o	33 ± 1.37
32	Acarbose	33 ± 2.65

Figure-12: 2D docking interactions of compounds (**20o**, **21n** and **21o**) with MAL12 protein model using rigid docking, PLP scoring function (GRIP docking algorithm).

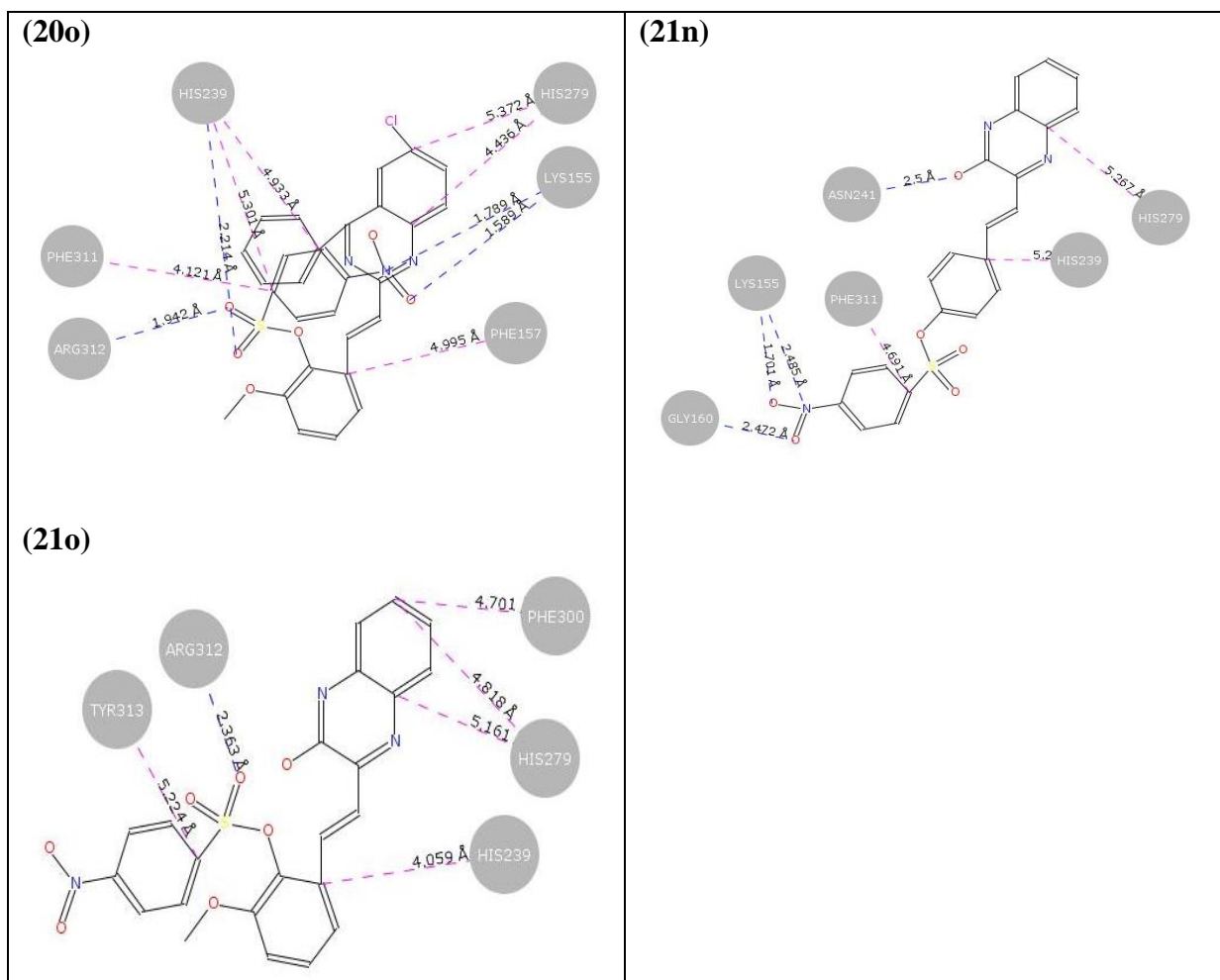
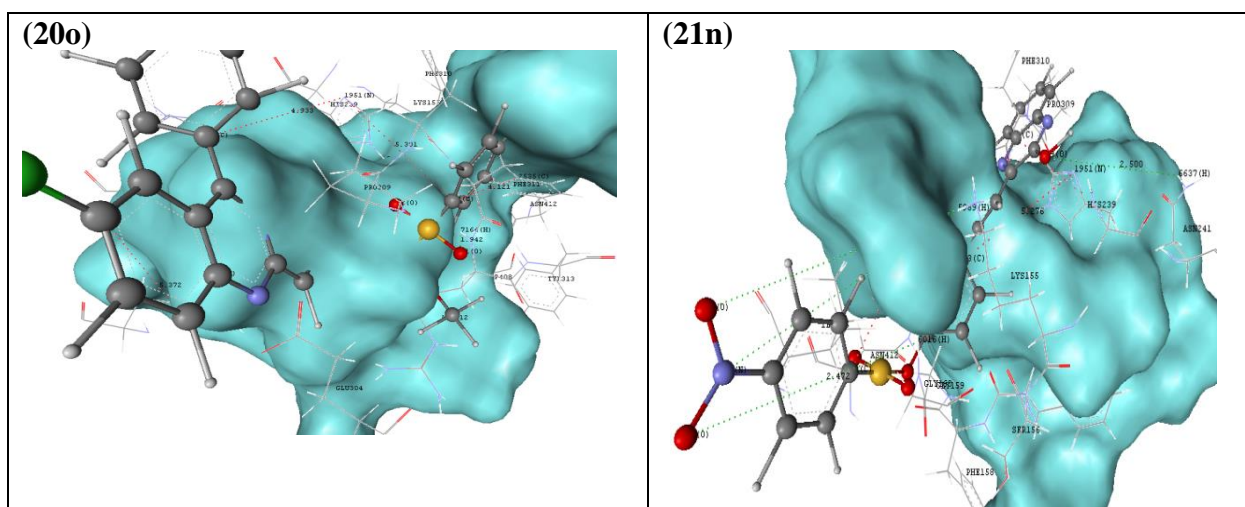


Figure-13: 3D docking interactions of compounds **20o**, **21n** and **21o** with MAL12 protein model using rigid docking, PLP scoring function (GRIP docking algorithm)



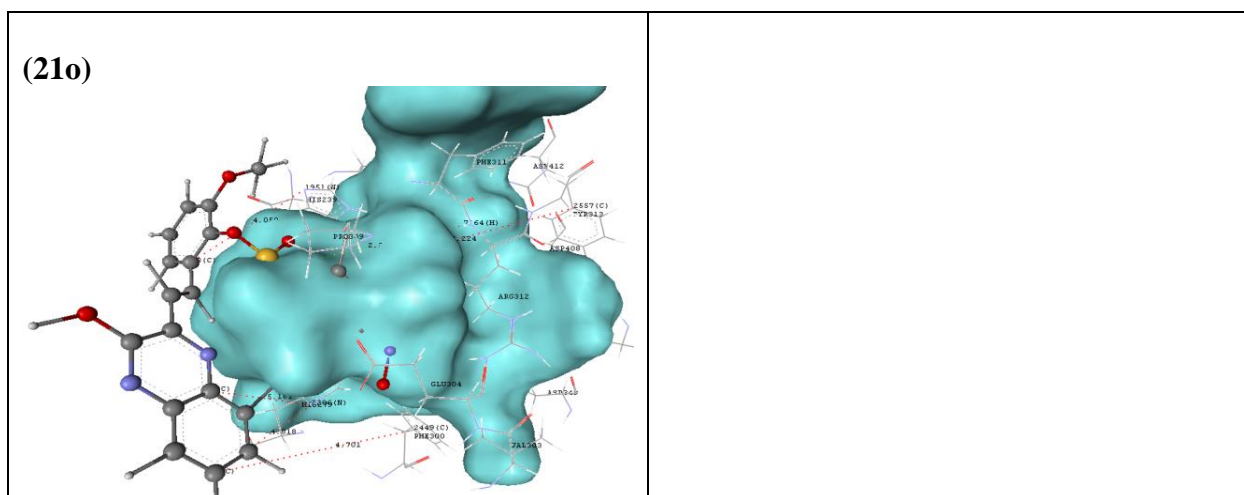


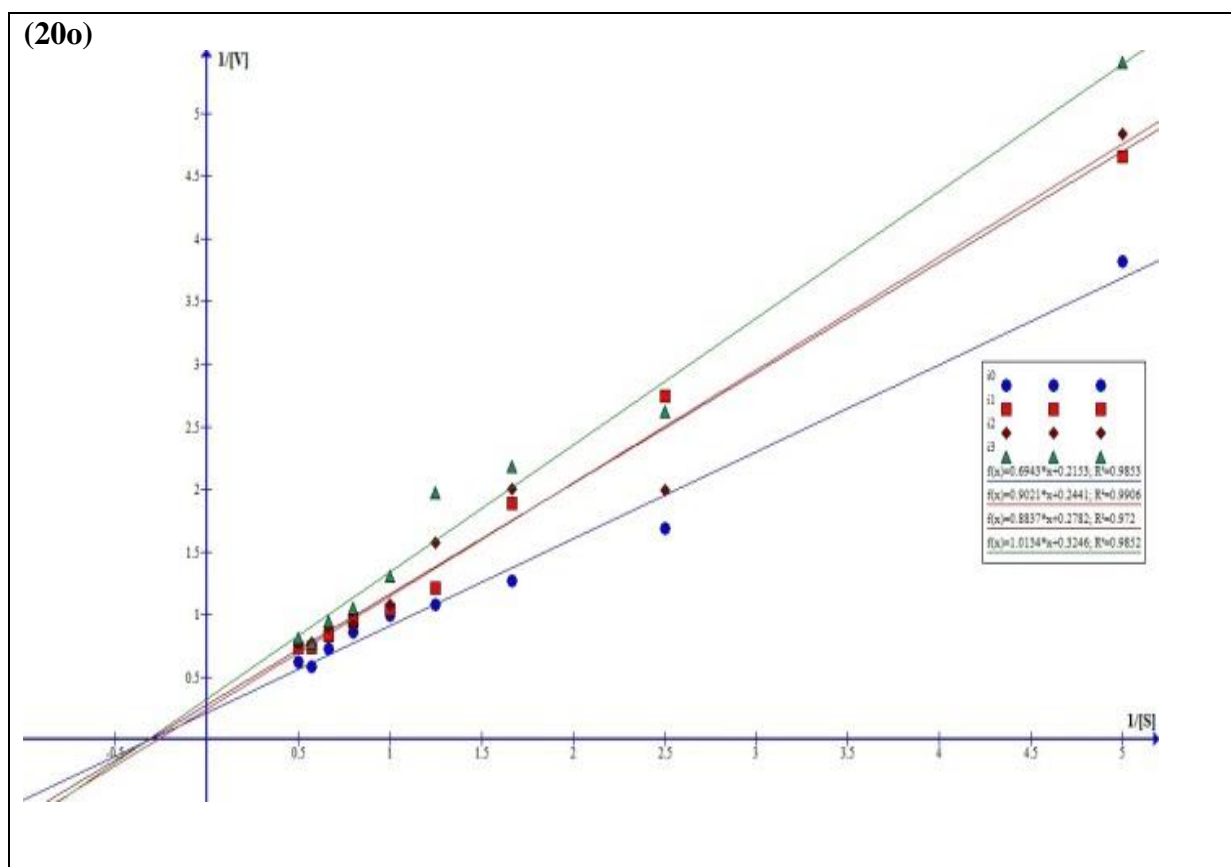
Table 12: Molecular docking interactions between the MAL12 protein model and the most potent inhibitor compounds (**20o**, **21n**, and **21o**).

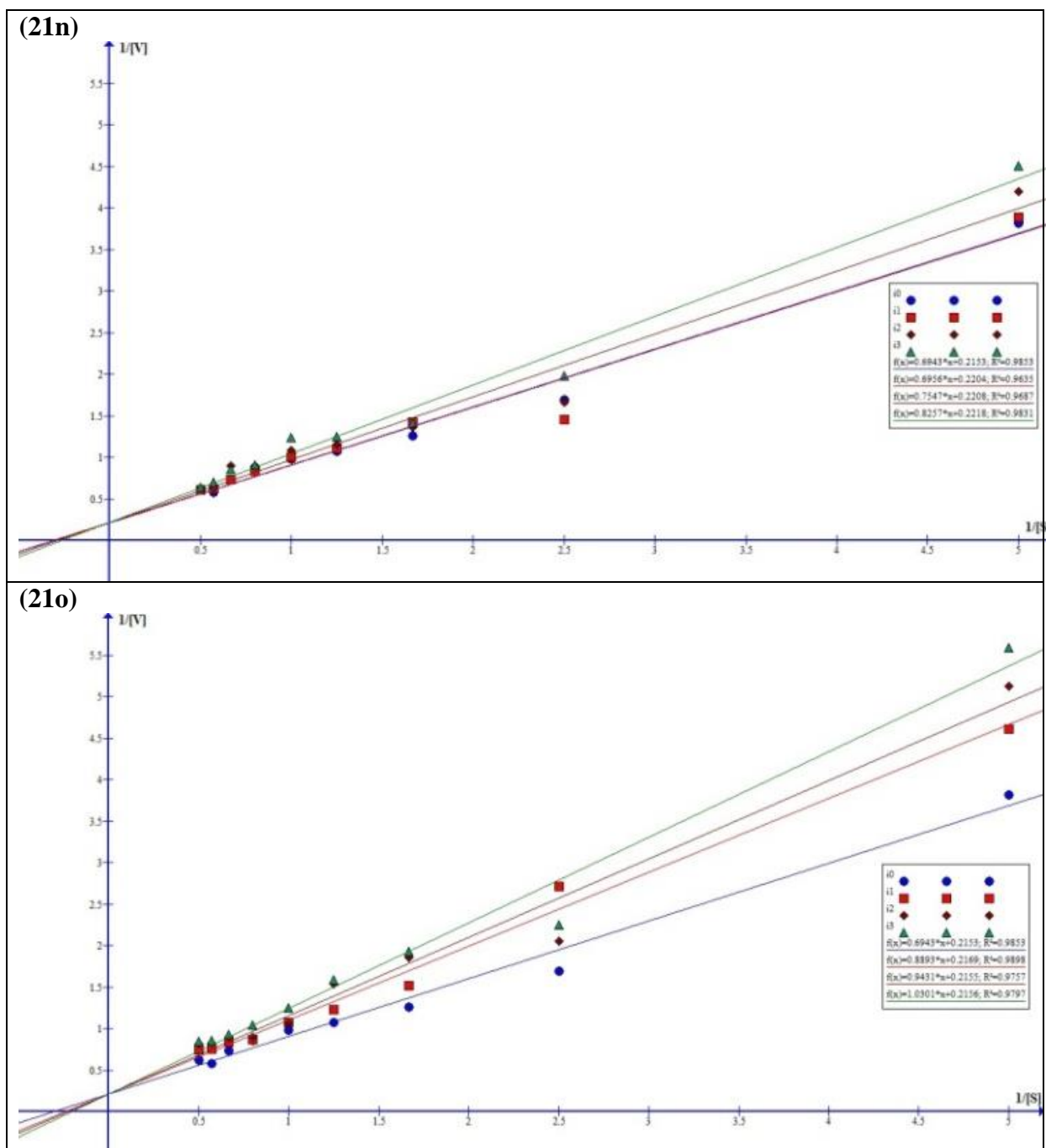
Compound	Residue	Atom	Ligand Atom	Distance Å	Interaction
20o	PHE157	1281C	13C	4.995	π -STACKING
	HIS239	1951N	23C	5.301	π -STACKING
	HIS239	1951N	29C	4.933	π -STACKING
	HIS279	2286N	1C	5.372	π -STACKING
	HIS279	2286N	4C	4.436	π -STACKING
	PHE311	2535C	23C	4.121	π -STACKING
	LYS155	5989H	38N	1.789	H-BOND
	LYS155	5989H	39O	1.589	H-BOND
	HIS239	6622H	22O	2.214	H-BOND
	ARG312	7164H	21O	1.942	H-BOND
21n	LYS155	5989H	30N	2.485	H-BOND
	LYS155	5989H	32O	1.701	H-BOND
	GLY160	6016H	31O	2.472	H-BOND
	ASN241	6637H	29O	2.500	H-BOND
21o	HIS239	1951N	13C	4.059	π -STACKING
	HIS279	2286N	1C	4.818	π -STACKING
	HIS279	2286N	4C	5.161	π -STACKING
	PHE300	2449C	1C	4.701	π -STACKING
	TYR313	2557C	23C	5.224	π -STACKING
	ARG312	7164H	22O	2.363	H-BOND
	HIS239	1951N	13C	5.276	π -STACKING
	HIS279	2286N	4C	5.267	π -STACKING
	PHE311	2535C	23C	4.691	π -STACKING

Table-13: IC₅₀, K_m, and inhibition mode of **20o**, **21n** and **21o**. The K_m and V_{max} values of α -D-glycosidase for 4-NGP without inhibitor were 3.24 mM and 4.64 mM min⁻¹, respectively.

Ligand	IC ₅₀ (μ M)	K _{im} (μ M)	V _{max} (μ M/min)	Mode of inhibition
20o	28 \pm 1.99	4.10	4.61	Competitive
21n	32 \pm 2.11	3.15	4.53	Competitive
21o	33 \pm 1.37	2.94	3.48	Mixed-Uncompetitive

Figure-14: Lineweaver-Burk plot for an understanding mode of Inhibition of α -D-glucosidase by compounds (**20o**, **21n** and **21o**)





Density functional theory (DFT) calculation

To explore the stability of the cis vs trans isomers of the compound **21g**, the energy was calculated by density functional theory (DFT) using Becke's three-parameter hybrid exchange functional and the Lee-Yang-Parr correlation functional (B3LYP) employing the TZP basis set. A similar level of theory was used to calculate the frequencies. All the geometries were found to yield the minimum energy structure on the corresponding potential energy surfaces by frequency analysis. All these calculations were carried out using the SCM-ADF simulation package.²³ The difference in the total energy of both the conformers DE ($E_{\text{trans}} - E_{\text{cis}}$) is (-) 85.67 kcal mol⁻¹. It is

found that the *trans* isomer is more stable as compared to the *cis* isomer. The calculated frontier highest occupied molecular orbital (HOMO) and lowest unoccupied molecular orbital (LUMO) of the *cis* and *trans* isomers are shown in **Figure-15**. It is interesting to note that the HOMO orbital of the *trans* isomer is spread all over the molecule, whereas the LUMO orbital is mostly concentrated on the SO₃ of the molecule. The HOMO and LUMO energies in the *trans* isomer are found to be -6.56 eV and -5.13 eV, respectively.

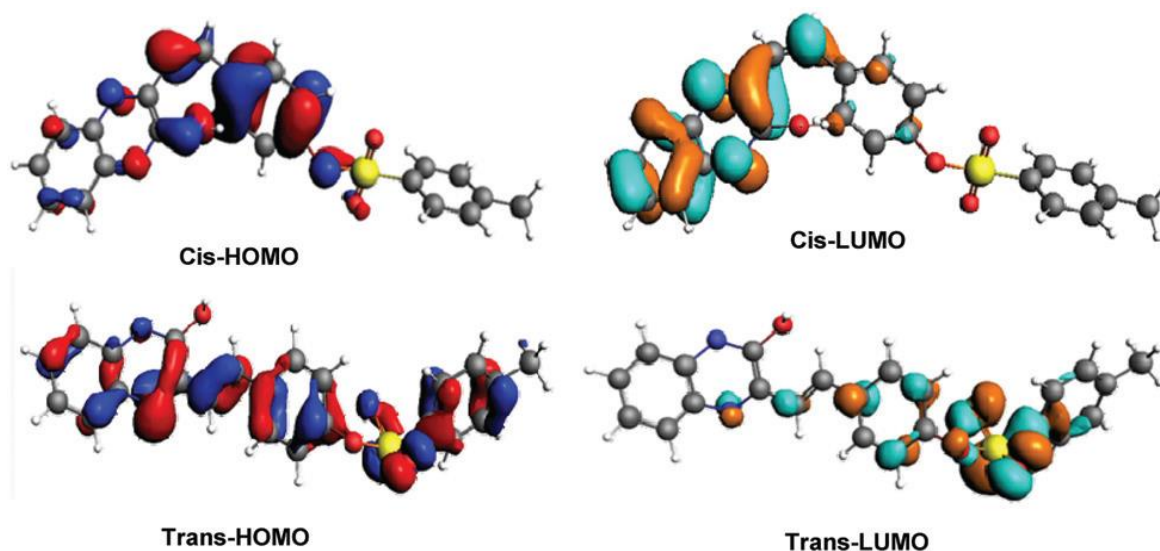


Figure-15: B3LYP/TZP calculated frontier HOMO and LUMO orbitals of *cis* and *trans* isomers of compound **21g**.

3.6 Experimental section

3.6.1 General:

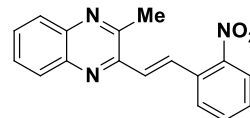
The starting materials were purchased from Sigma-Aldrich, SRL, Spectrochem, and SD-Fine and used as they are received. ¹H and ¹³C-NMR spectra are recorded on Bruker 400 MHz spectrometer using CDCl₃ or DMSO-d₆ as solvents and reported in δ ppm. The mass spectra were recorded on Shimadzu LCMS-2020 and Agilent QTOF machine. Melting points were recorded on the Stuart melting point apparatus. UV-visible spectra were taken using Agilent-Cary 100 UV-Visible spectrometer. Emission spectra were recorded by Horiba FluoroLog spectrophotometer.

3.6.2 Representative procedure for the one-pot synthesis of 2-methyl-styrylquinoxaline (**10a**):

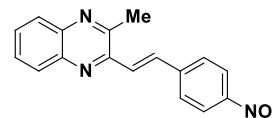
To solution of *o*-phenylenediamine (OPDA) (1.0 mmol) (**1a**) in EtOH (5mL) butane-2,3-dione (**2e**) (1.0 mmol), piperidine (10 mol%) were added and the mixture was refluxed at 80 °C for 1 hour to provide intermediate 2,3-dimethylquinoxaline (**9b**). After that benzaldehyde (**3a**) (1 Equiv.) and heating continued for 8 h. After completion of the reaction (monitored by TLC), the mixture was cooled to room temperature and extracted with EtOAc (2X10mL). The combined

organic layers were washed with brine, water and dried over sodium sulphate. Solvent was evaporated under reduced pressure to give the crude product which was purified by silica gel column chromatography. Elution of the column with EtOAc and *n*-hexane (3:1v/v) gave the desired product **10a** (80%).

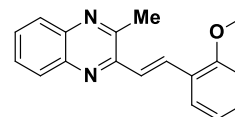
(E)-2-Methyl-3-(2-nitrostyryl)quinoxaline (10b): White solid, mp 218–219 °C, 85% yield. ¹H NMR (400 MHz, DMSO+CDCl₃) δ 8.29 (dd, *J* = 15.4, 4.0 Hz, 1H), 8.02–7.90 (m, 4H), 7.81–7.78 (m, 1H), 7.71–7.63 (m, 2H), 7.52–7.45 (m, 2H), 2.83 (s, 3H); ¹³C NMR (100 MHz, DMSO+CDCl₃) δ 152.76, 148.59, 148.13, 141.71, 141.20, 133.60, 132.54, 131.92, 130.38, 129.79, 129.60, 129.43, 129.16, 128.31, 127.41, 124.77, 22.98; HRMS (ESI, *m/z*): Calcd. For C₁₇H₁₃N₃O₂H⁺ 292.1081, found 292.0709.



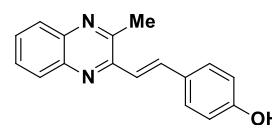
(E)-2-Methyl-3-(4-nitrostyryl)-quinoxaline (10c): White powder, mp 201–202 °C, 82 % yield. ¹H NMR (400 MHz, DMSO+CDCl₃) δ 8.26 (d, *J* = 8.8 Hz, 2H), 8.09 (s, 1H), 8.05 (s, 1H), 7.97–7.94 (m, 3H), 7.78 (d, *J* = 15.6 Hz, 1H), 7.76–7.71 (m, 2H), 2.91 (s, 3H); ¹³C NMR (100 MHz, DMSO+CDCl₃) δ 153.10, 147.53, 142.92, 141.49, 141.21, 134.59, 129.86, 129.50, 129.10, 128.98, 128.63, 128.39, 127.42, 124.17, 23.01; HRMS (ESI, *m/z*): Calcd. For C₁₇H₁₃N₃O₂H⁺ 292.1081, found 292.0710; IR (KBr, thin film, cm⁻¹): ν_{max} 2968, 1547, 1504, 1423, 1231, 820.



(E)-2-(2-Methoxystyryl)-3-methylquinoxaline (10d): Pale yellow solid, mp 121–122 °C, 78% yield. ¹H NMR (400 MHz, DMSO+CDCl₃) δ 8.21 (d, *J* = 15.6 Hz, 1H), 7.99 (d, *J* = 7.2 Hz, 1H), 7.92 (d, *J* = 15.6 Hz, 1H), 7.60–7.56 (m, 3H), 7.16 (dd, *J* = 6.0, 3.2 Hz, 1H), 6.79–6.77 (m, 3H), 3.84 (s, 3H), 2.80 (s, 3H); ¹³C NMR (100 MHz, DMSO+CDCl₃) δ 145.71, 142.41, 140.59, 140.47, 136.61, 128.74, 124.51, 124.40, 124.05, 122.92, 118.50, 116.66, 116.00, 114.71, 114.62, 106.36, 51.43, 17.97; IR (KBr, thin film, cm⁻¹): ν_{max} 3053, 2965, 1504, 1403, 1801, 857.



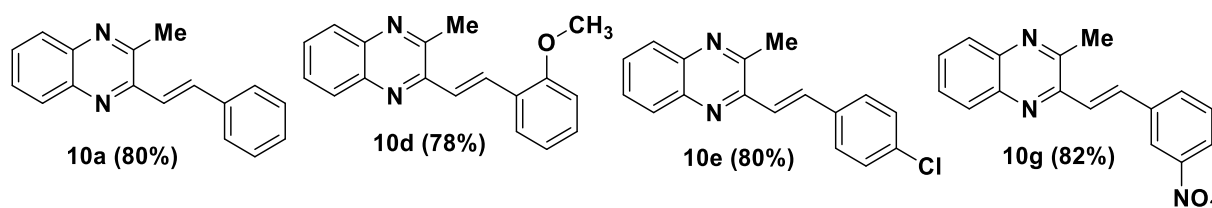
(E)-4-(2-(3-Methylquinoxalin-2-yl)vinyl)phenol (10f): Yellow solid, mp 196–197 °C, 75% yield. ¹H NMR (400 MHz, DMSO+CDCl₃) δ 7.97–7.94 (m, 1H), 7.98–7.85 (m, 2H), 7.61–7.58 (m, 2H), 7.36 (d, *J* = 15.2 Hz, 1H), 7.14 (d, *J* = 8.0 Hz, 1H), 7.08–7.06 (m, 2H), 6.79–6.76 (m, 1H), 2.80 (s, 3H); ¹³C NMR (100 MHz, DMSO+CDCl₃) δ 157.76, 152.51, 149.75, 141.35, 140.95, 137.76, 129.78, 129.19, 128.83, 128.11, 122.32, 119.02, 116.68, 114.31, 22.97; HRMS (ESI, *m/z*): Calcd. For C₁₇H₁₄N₂O



262.1106, found 261.0952; IR (KBr, thin film, cm^{-1}): ν_{max} 3395, 3067, 2956, 1522, 1420, 1126, 833.

Confirmation of reported molecules by using melting points:

S. No.	Compound (code) No.	MP °C (Found)	MP °C (Reported) ^{24(a,b,c)}
1	10a	137-138	136-138
2	10d	121-122	122-124
3	10e	110-111	109-111
4	10g	185-186	184-186

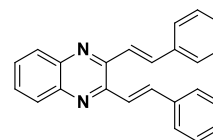


3.6.3 A representative procedure for the synthesis of 2,3-di((E)-styryl)quinoxaline (14a):

To a solution of *o*-phenyldiamine **1a** (1mmol, 0.1g) in ethanol (5 mL) were added butane-2,3-dione (**2e**) (1mmol) and piperidine (10 mol%) and the mixture was heated at 80 °C for 30 min to generate a 2,3-dimethyl quinoxaline (**9b**). To this, benzaldehyde (**3a**) (2 mmol) was added and heating continued 6h. After completion of the reaction (monitored by TLC), the reaction mixture was cooled to room temperature. Solvent was evaporated extracted with EtOAc (2X20mL). Combined organic layers were washed with water, dried over sodium sulphate. Evaporation of the solvent gave the crude product which was purified by silica gel column chromatography. Elution of the column with EtOAc+*n*-hexane mixture gave the desired product **14a** in 82% yield.

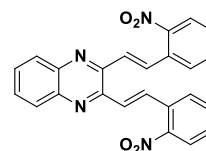
2,3-Di((E)-styryl)quinoxaline (14a): Yellow solid, mp 333–334 °C, 82%

yield. ¹H NMR (400 MHz, CDCl₃+DMSO) δ 8.04–7.93 (m, 6H), 7.85 (d, J = 7.2 Hz, 4H), 7.73–7.72 (m, 2H), 7.46–7.35 (m, 6H); ¹³C NMR (100 MHz, CDCl₃+DMSO) δ 148.98, 141.53, 137.77, 136.56, 129.83, 129.29, 129.05, 128.97, 128.21, 122.73.



2,3-Bis((E)-2-nitrostyryl)quinoxaline (14b): Light green solid, mp 181–182

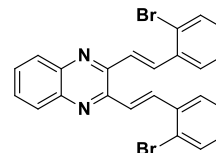
°C, 85% yield. ¹H NMR (400 MHz, DMSO) δ 8.35–8.23 (m, 2H), 8.18 (d, J = 16.8 Hz, 2H), 8.14–8.04 (m, 2H), 7.96 (m, 2H), 7.83 (d, J = 8.4 Hz, 4H), 7.75–



7.61 (m, 2H), 7.49 (d, $J = 7.6$ Hz, 2H); ^{13}C NMR (100 MHz, DMSO) δ 153.67, 149.31, 141.60, 133.97, 131.89, 129.76, 129.32, 128.78, 128.46, 127.66, 124.99, 124.07; IR (KBr, thin film, cm^{-1}): ν_{max} 3062, 2929, 1519, 1348, 1127, 963, 734.

2,3-Bis((E)-2-bromostyryl)quinoxaline (14d): Pale green powder, mp 160–161 °C, 82% yield.

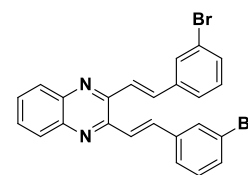
^1H NMR (400 MHz, CDCl_3) δ 7.97 (dd, $J = 24.8, 15.6$ Hz, 2H), 7.88 (d, $J = 15.6$ Hz, 2H), 7.63 (m, 2H), 7.57–7.49 (m, 4H), 7.33 (d, $J = 8.0$ Hz, 4H), 7.19 (s, 2H); ^{13}C NMR (100 MHz, $\text{CDCl}_3+\text{DMSO}$) δ 153.24, 141.65, 136.20, 133.26, 130.41, 130.01, 129.62, 129.12, 128.10, 127.98, 125.67, 124.90;



HRMS (ESI, m/z): Calcd. For $\text{C}_{24}\text{H}_{16}\text{Br}_2\text{N}_2\text{H}_2^{+2}$ 491.9826, found 492.9654; IR (KBr, thin film, cm^{-1}): ν_{max} 3051, 2905, 1625, 1464, 1024, 964, 746.

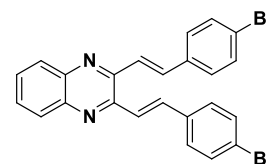
2,3-Bis((E)-3-bromostyryl)quinoxaline (14e):

Yellow solid, mp 209–210 °C, 81% yield. ^1H NMR (400 MHz, $\text{CDCl}_3+\text{DMSO}$) δ 8.01 (dd, $J = 6.4, 3.2$ Hz, 2H), 7.90 (d, $J = 15.6$ Hz, 2H), 7.80 (s, 2H), 7.68 (dd, $J = 6.4, 3.2$ Hz, 2H), 7.58–7.54 (m, 4H), 7.48 (d, $J = 7.6$ Hz, 2H), 7.30 (d, $J = 7.6$ Hz, 2H); ^{13}C NMR (100 MHz, $\text{CDCl}_3+\text{DMSO}$) δ 148.36, 141.67, 138.51, 136.39, 131.86, 130.35, 130.15, 129.83, 128.95, 126.25, 123.64, 122.99; HRMS (ESI, m/z): Calcd. For $\text{C}_{24}\text{H}_{16}\text{Br}_2\text{N}_2\text{H}_2^{+2}$ 491.9826, found 492.9698; IR (KBr, thin film, cm^{-1}): ν_{max} 3058, 1625, 1417, 1193, 966, 751.



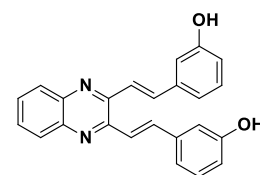
2,3-Bis((E)-4-bromostyryl)quinoxaline (14f): Yellow solid, mp 206–207

°C, 83% yield. ^1H NMR (400 MHz, $\text{CDCl}_3+\text{DMSO}$) δ 7.99 (s, 6H), 7.80–7.72 (m, 6H), 7.59 (d, $J = 7.6$ Hz, 2H); ^{13}C NMR (100 MHz, $\text{CDCl}_3+\text{DMSO}$) δ 148.72, 141.57, 136.41, 135.74, 131.98, 130.03, 129.99, 128.99, 123.53, 122.72; HRMS (ESI, m/z): Calcd. For $\text{C}_{24}\text{H}_{16}\text{Br}_2\text{N}_2\text{H}_2^{+2}$ 491.9826, found 492.9727; IR (KBr, thin film, cm^{-1}): ν_{max} 3056, 2960, 1625, 1487, 1404, 1072, 971, 751.



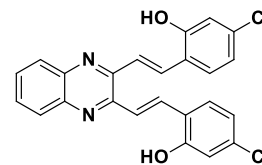
3,3'-((1E,1'E)-Quinoxaline-2,3-diylbis(ethene-2,1-diyl))diphenol (14h): Pale brown solid, mp 249–250 °C, 82% yield. ^1H NMR (400 MHz, $\text{CDCl}_3+\text{DMSO}$) δ 9.35 (s, 2H),

8.11 (dd, $J = 6.4, 3.6$ Hz, 2H), 8.01 (d, $J = 15.6$ Hz, 2H), 7.80–7.74 (m, 4H), 7.36–7.25 (m, 6H), 6.95 (dd, $J = 7.8, 1.4$ Hz, 2H); ^{13}C NMR (100 MHz, $\text{CDCl}_3+\text{DMSO}$) δ 162.65, 153.70, 146.24, 142.72, 142.43, 134.64, 134.30, 133.60, 127.09, 124.09, 121.47, 118.74; HRMS (ESI, m/z): Calcd. For $\text{C}_{24}\text{H}_{18}\text{N}_2\text{O}_2\text{H}^+$ 367.1441,

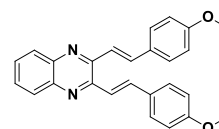


found 367.1220; IR (KBr, thin film, cm^{-1}): ν_{max} 3395, 3157, 3070, 1625, 1580, 1270 H^+ , 1129, 978, 762.

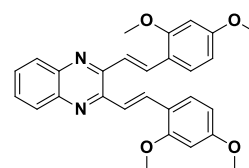
6,6'-((1E,1'E)-Quinoxaline-2,3-diylbis(ethene-2,1-diyl))bis(3-chlorophenol) (14j): Light green powder, mp 259–260 °C, 82% yield. ^1H NMR (400 MHz, CDCl_3 +DMSO) δ 8.21 (dd, J = 15.2, 11.2 Hz, 2H), 8.02–7.91 (m, 4H), 7.69–7.62 (m, 4H), 7.13 (d, J = 7.6 Hz, 2H), 6.94 (d, J = 7.6 Hz, 1H); ^{13}C NMR (100 MHz, DMSO) δ 155.33, 153.06, 141.30, 131.66, 129.64, 129.26, 128.92, 128.35, 127.34, 125.10, 123.80, 117.87; HRMS (ESI, m/z): Calcd. For $\text{C}_{24}\text{H}_{16}\text{Cl}_2\text{N}_2\text{O}_2\text{H}_2^{+2}$ 436.0734, found 436.0670; IR (KBr, thin film, cm^{-1}): ν_{max} 3410, 3680, 2964, 1595, 1479, 1320, 1113, 960, 750.



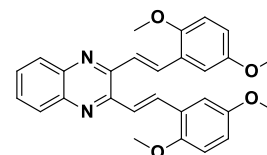
2,3-Bis((E)-4-methoxystyryl)quinoxaline (14l): Red sticky solid, mp 181–182 °C, 81% yield. ^1H NMR (400 MHz, CDCl_3 +DMSO) δ 7.98–7.96 (m, 4H), 7.82 (d, J = 6.4 Hz, 6H), 7.70 (s, 2H), 7.00 (s, 4H), 3.84 (s, 6H).



2,3-Bis((E)-2,4-dimethoxystyryl)quinoxaline (14n): Light brick red solid, mp 156–157 °C, 79% yield. ^1H NMR (400 MHz, CDCl_3 +DMSO) δ 8.18 (d, J = 15.6 Hz, 2H), 7.99–7.97 (m, 2H), 7.70–7.63 (m, 6H), 6.59–6.54 (m, 4H), 3.95 (s, 6H), 3.86 (s, 6H); ^{13}C NMR (100 MHz, CDCl_3 +DMSO) δ 161.80, 159.24, 149.86, 141.34, 132.72, 129.36, 128.97, 128.70, 120.84, 118.47, 105.71, 98.43, 55.70, 55.51; HRMS (ESI, m/z): Calcd. For $\text{C}_{28}\text{H}_{26}\text{N}_2\text{O}_4\text{H}^+$ 455.1965, found 455.1978; IR (KBr, thin film, cm^{-1}): ν_{max} 2960, 2838, 1626, 1513, 1263, 1135, 985, 764.



2,3-Bis((E)-2,5-dimethoxystyryl)quinoxaline (14o): Yellow solid, mp 190–191 °C, 80% yield. ^1H NMR (400 MHz, CDCl_3 +DMSO) δ 7.99–7.95 (m, 4H), 7.83 (d, J = 15.6 Hz, 2H), 7.68 (s, 2H), 7.49 (s, 2H), 7.32 (d, J = 8.0 Hz, 2H), 6.96 (d, J = 8.0 Hz, 2H), 3.95 (s, 6H), 3.88 (s, 6H); ^{13}C NMR (100 MHz, CDCl_3 +DMSO) δ 150.26, 149.33, 149.20, 141.43, 137.67, 129.70, 129.36, 128.77, 122.26, 120.69, 111.69, 110.60, 56.03, 55.95; HRMS (ESI, m/z): Calcd. For $\text{C}_{28}\text{H}_{26}\text{N}_2\text{O}_4\text{H}^+$ 455.1965, found 455.2956; IR (KBr, thin film, cm^{-1}): ν_{max} 3105, 2960, 1605, 1289, 1210, 749.



2,3-Bis((E)-3,4,5-trimethoxystyryl)quinoxaline (14q): Yellow solid, mp

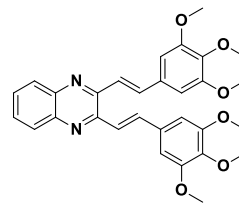
207–208 °C, 80% yield. ¹H NMR (400 MHz, CDCl₃+DMSO) δ 8.04–8.01

(m, 4H), 7.98–7.94 (m, 3H), 7.79–7.75 (m, 3H), 7.62 (d, J = 15.6 Hz, 1H),

7.16 (s, 1H), 3.89 (s, 18H); ¹³C NMR (100 MHz, CDCl₃+DMSO) δ 158.33,

153.89, 146.23, 143.74, 142.59, 136.98, 135.05, 133.70, 127.16, 110.73,

65.36, 61.16. HRMS (ESI, m/z): Calcd. For C₃₀H₃₀N₂O₆H⁺ 515.2177, found 515.2191; IR (KBr, thin film, cm⁻¹): ν_{max} 3078, 2941, 1629, 1578, 1504, 1420, 1239, 1128, 994, 811.

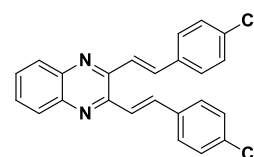


2,3-Bis((E)-4-chlorostyryl)quinoxaline (14s): Pale yellow powder, 84%

yield, mp 215–216 °C. ¹H NMR (400 MHz, CDCl₃+DMSO) δ 7.995 (s, 6H),

7.89 (d, J = 7.6 Hz, 4H), 7.74 (s, 2H), 7.45 (d, J = 7.6 Hz, 4H); IR (KBr, thin

film, cm⁻¹): ν_{max} 3043, 2895, 1626, 1490, 1196, 1095, 804, 752.



2,3-Bis((E)-2,4-dichlorostyryl)quinoxaline (14u): Greenish yellow powder, mp 193–194 °C,

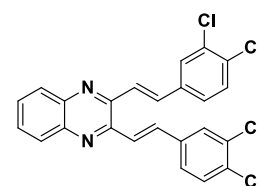
yield = 80%. ¹H NMR (400 MHz, CDCl₃+DMSO) δ 8.27 (d, J = 8.4 Hz, 2H),

8.21–8.12 (m, 1H), 8.07–7.96 (m, 4H), 7.91–7.68 (m, 4H); ¹³C NMR (100

MHz, CDCl₃+DMSO) δ 156.47, 140.94, 133.99, 129.88, 129.04, 128.93,

128.85, 128.77, 126.35, 123.18, 119.59, 116.40. HRMS (ESI, m/z): Calcd.

For C₂₄H₁₄Cl₄N₂H⁺ 470.9984, found 471.0871; IR (KBr, thin film, cm⁻¹): ν_{max} 3074, 2926, 1592, 1511, 1337, 1107, 761, 747.



6,6'-((1E,1'E)-Quinoxaline-2,3-diylbis(ethene-2,1-diyl))bis(2-

ethoxyphenol (14v): Yellow solid, mp 179–180 °C, 82% yield. ¹H NMR (400

MHz, CDCl₃+DMSO) δ 8.66 (s, 2H), 8.28 (d, J = 16.0 Hz, 2H), 8.01 (dd, J =

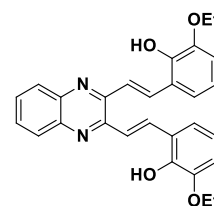
6.4, 3.6 Hz, 2H), 7.91 (d, J = 15.6 Hz, 2H), 7.67 (dd, J = 6.4, 3.6 Hz, 2H), 7.32

(d, J = 8.4 Hz, 2H), 6.88–6.80 (m, 4H), 4.11 (q, J = 13.8, 6.8 Hz, 4H), 1.44 (t, J = 6.8 Hz, 6H); ¹³C

NMR (100 MHz, CDCl₃+DMSO) δ 154.44, 151.95, 150.83, 146.20, 138.21, 134.13, 133.62,

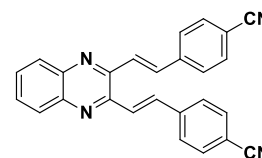
128.40, 127.55, 125.13, 124.13, 117.86, 69.49, 19.78; HRMS (ESI, m/z): Calcd. For

C₂₈H₂₆N₂O₄H⁺ 455.1965, found 455.1890; IR (KBr, thin film, cm⁻¹): ν_{max} 3494, 3055, 2977, 1620, 1467, 1229, 1062, 981, 762.

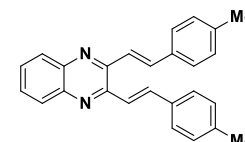


4,4'-((1E,1'E)-Quinoxaline-2,3-diylbis(ethene-2,1-diyl))dibenzonitrile (14w):

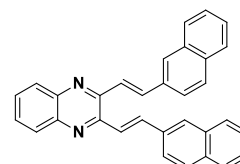
Pale green powder, mp 210–211 °C, 84% yield. ¹H NMR (400 MHz, CDCl₃+DMSO) δ 8.23 (d, J = 15.2 Hz, 2H), 8.10–8.03 (m, 8H), 7.87 (d, J = 7.6 Hz, 4H), 7.80 (s, 2H); ¹³C NMR (100 MHz, DMSO+CDCl₃) δ 155.52, 145.45, 138.61, 131.86, 129.86, 129.56, 128.63, 128.52, 123.24, 117.74, 111.22; HRMS (ESI, m/z): Calcd. For C₂₆H₁₆N₄H⁺ 385.1448, found 385.1442; IR (KBr, thin film, cm⁻¹): ν_{max} 3098, 2965, 2220, 1603, 1501, 1322, 1129, 974, 817.



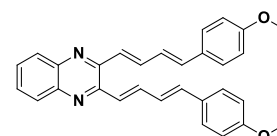
2,3-Bis((E)-4-methylstyryl)quinoxaline (14z): Pale yellow solid, mp 365–366 °C, 81% yield. ¹H NMR (400 MHz, CDCl₃+DMSO) δ 7.99–7.95 (m, 4H), 7.87–7.80 (m, 2H), 7.70 (s, 6H), 7.24 (d, J = 7.2 Hz, 4H), 2.39 (s, 6H).



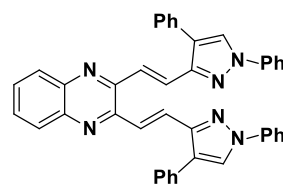
2,3-Bis((E)-2-(naphthalen-2-yl)vinyl)quinoxaline (14ac): White solid, mp 198–199 °C, 83% yield. ¹H NMR (400 MHz, CDCl₃) δ 8.77 (d, J = 15.2 Hz, 2H), 8.38 (d, J = 8.4 Hz, 2H), 8.07 (dd, J = 6.4, 3.2 Hz, 2H), 7.82 (dd, J = 12.4, 6.8 Hz, 6H), 7.79–7.74 (m, 4H), 7.59–7.51 (m, 6H); ¹³C NMR (100 MHz, DMSO) δ 153.28, 147.42, 135.62, 134.08, 133.84, 133.48, 131.55, 130.14, 129.66, 129.04, 128.47, 127.06, 126.46, 126.11, 125.53, 123.66; HRMS (ESI, m/z): Calcd. For C₃₂H₂₂N₂H⁺ 435.1856, found 435.1851; IR (KBr, thin film, cm⁻¹): ν_{max} 3044, 3006, 1612, 1402, 1130, 959, 760.



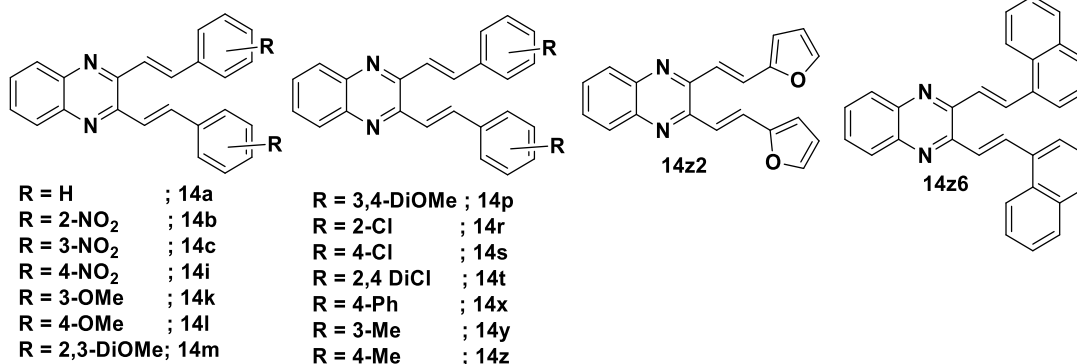
2,3-Bis((1E,3E)-4-(4-methoxyphenyl)buta-1,3-dien-1-yl)quinoxaline (14ad): Red sticky solid, mp 175–176 °C, 80% yield. ¹H NMR (400 MHz, DMSO+CDCl₃) δ 7.97 (d, J = 16.0 Hz, 2H), 7.67 (d, J = 7.2 Hz, 2H), 7.61 (d, J = 7.2 Hz, 3H), 7.49 (d, J = 16.0 Hz, 2H), 7.32 (d, J = 7.2 Hz, 2H), 7.24–7.16 (m, 4H), 7.08–7.02 (m, 5H), 3.50 (s, 6H); ¹³C NMR (100 MHz, CDCl₃+DMSO) δ 159.60, 146.37, 144.03, 141.32, 135.89, 132.85, 130.78, 129.06, 127.15, 125.68, 122.33, 116.91, 56.29; HRMS (ESI, m/z): Calcd. For C₃₀H₂₆N₂O₂ 446.1918, found 445.1994; IR (KBr, thin film, cm⁻¹): ν_{max} 3063, 3076, 1599, 1306, 1257, 1023, 990, 760.



2,3-Bis((E)-2-(1,4-diphenyl-1H-pyrazol-3-yl)vinyl)quinoxaline (14ae): Yellow powder, mp 190–191 °C, 83% yield. ¹H NMR (400 MHz, CDCl₃+DMSO) δ 8.83 (s, 2H), 8.03 (d, J = 15.2 Hz, 1H), 7.93–7.90 (m, 2H), 7.88–7.86 (m, 8H), 7.80 (d, J = 6.8 Hz, 2H), 7.65–7.61 (m, 2H), 7.53–7.45 (m, 14H), 7.40–7.33 (m, 4H); ¹³C NMR (100 MHz, CDCl₃+DMSO) δ 158.59, 153.56, 143.71, 137.72, 136.26, 134.44, 134.33, 134.01, 133.69, 133.50, 133.39, 132.62, 132.37, 131.64, 127.22, 124.33, 123.75; HRMS (ESI, m/z): Calcd. For C₄₂H₃₀N₆H⁺ 619.2605, found 619.2592; IR (KBr, thin film, cm⁻¹): ν_{max} 3124, 3057, 1671, 1524, 1449, 1227, 1056, 752.



Confirmation of reported molecules by using melting points:



S. No.	Compound No.	M.P °C (Found)	M.P °C (Reported) ²⁵
1	14a	333-334	334-336
2	14b	195-196	194-196
3	14c	204-205	204-206
14	14i	196-197	195-197
6	14k	127-228	126-228
7	14l	136-137	136-138
8	14m	210-211	211-213
9	14p	209-210	208-210
10	14r	189-190	189-191
11	14s	215-216	216-218
12	14t	189-190	188-190
13	14x	204-205	203-205
4	14y	202-203	203-205
5	14z	365-366	364-366
15	14aa	215-216	214-216
16	14ae	170-171	169-171

4.6.4 General procedure for the one-pot synthesis of 3-(4-nitrostyryl) quinoxaline-2-ol (15a):

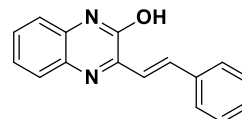
The reaction of *ortho* phenyl-1,2-diamine (OPDA) (1.0 mmol) (**1a**), ethyl pyruvate (1.0 mmol) (**2b**) were reacted under aqueous medium (5 mL) at 80 °C. And continue the stirring for up to 60 min, gave intermediate 2-methyl quinoxaline-2-ol (**14a**), then (in situ) add benzaldehyde (**3a**) (1.0 mmol) in the same reaction condition and stir up to 8 h. After complete conversion of precursors (checked by TLC) the reaction mixture was cool to room temperature. Further, add 30 ml of EtOAc and 50 ml of water to the reaction mixture, then separated organic layer was dried over sodium sulfate. Evaporation of the solvent under reduced pressure gave the crude product which was purified by silica gel column chromatography. Elution of the column with EtOAc + n-hexane mixture gave the desired product (**15a**) in good yield.

3.6.5 Representative procedure for the synthesis of 2-styrylquinoxaline hybrid (**16a**):

To a solution of 2-amino-5-chloro benzophenone (**1c**) (1.0 mmol), was added acetonitrile (3.0 mmol, synthesis grade) followed by 4N HCl (5 volume) under N₂ atmosphere and heated at 80°C for 3h. After completion of the reaction, aq. sodium bicarbonate (10 mL) was added to it. The solid obtained was washed with ethanol and dried under a high vacuum to give the 6-chloro-2-methyl,4-phenylquinoxaline (**14b**).

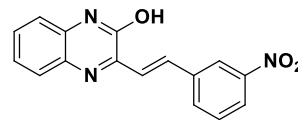
In a separate reaction vessel, to a solution of 6-chloro-2-methyl,4-phenylquinoxaline (**14b**) (1.0 mmol) in water (5 mL) was added 4-nitrobenzaldehyde (**3a**) (1.0 mmol) and the mixture was heated at 80 °C for 6h. After completion of the reaction (checked by TLC), the reaction mixture was cooled to room temperature and extracted with EtOAc (2X10 mL). Combined organic layers were dried over sodium sulfate. Evaporation of the solvent under reduced pressure gave the crude product, which was purified by silica gel column chromatography (Hexane/EtOAc) gave the desired product (**16a**).

3-Styrylquinoxalin-2-ol (15a): Yellow crystalline solid, mp 221–222 °C, 85% yield. ¹H NMR (400 MHz, CDCl₃) δ 11.26 (s, 1H), 8.12 (d, J = 16.4 Hz, 1H), 7.81 (dd, J = 8.0, 1.2 Hz, 1H), 7.70–7.64 (m, 3H), 7.44–7.40 (m, 1H), 7.37–7.33 (m, 2H), 7.31–7.27 (d, J = 7.2 Hz, 2H), 7.26 (d, J = 8.0 Hz, 1H); ¹³C NMR (100 MHz, CDCl₃+DMSO) δ 168.03, 155.51, 140.93, 137.21, 136.58, 135.85, 130.48, 128.41, 125.29, 124.17, 123.66, 122.49, 120.26, 115.54; HRMS (ESI, m/z): Calcd. For C₁₆H₁₂N₂OH⁺ 249.1022, found 249.1027; IR (KBr, thin film, cm⁻¹): ν_{max} 3080, 2971, 2842, 1655, 1588, 1449, 1147, 974, 771.

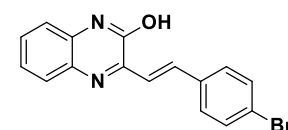


3-(3-Nitrostyryl) quinoxalin-2-ol (15b): Yellow solid, mp 234–235 °C, 88% yield. ¹H NMR (400 MHz, CDCl₃+DMSO) δ 12.53 (s, 1H), 8.46 (s, 1H), 8.18–8.08 (m, 3H), 7.77 (s, 1H), 7.67 (t, J =

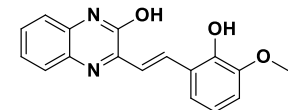
7.6 Hz, 1H), 7.46 (t, $J = 7.2$ Hz, 1H), 7.33–7.27 (m, 2H), 7.15 (d, $J = 7.2$ Hz, 1H); ^{13}C NMR (100 MHz, $\text{CDCl}_3 + \text{DMSO}$) δ 155.29, 152.74, 148.75, 138.33, 134.84, 133.80, 132.82, 132.22, 130.47, 130.35, 128.91, 125.17, 123.78, 123.54, 121.97, 115.76; HRMS (ESI, m/z): Calcd. For $\text{C}_{16}\text{H}_{11}\text{N}_3\text{O}_3\text{H}^+$ 294.0873, found 294.0875; IR (KBr, thin film, cm^{-1}): ν_{max} 3092, 2972, 2891, 1662, 1524, 1353, 1187, 972, 756.



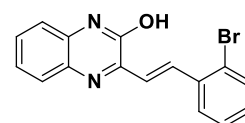
3-(4-Bromostyryl) quinoxalin-2-ol (15d): Pale green powder, mp 250–251 °C, 90% yield. ^1H NMR (400 MHz, $\text{CDCl}_3 + \text{DMSO}$) δ 12.45 (s, 1H), 8.05 (d, $J = 16.0$ Hz, 1H), 7.76 (d, $J = 8.0$ Hz, 1H), 7.66–7.54 (m, 4H), 7.44 (t, $J = 7.6$ Hz, 1H), 7.33–7.28 (m, 2H), 7.16 (t, $J = 8.8$ Hz, 1H); ^{13}C NMR (100 MHz, $\text{CDCl}_3 + \text{DMSO}$) δ 154.36, 147.67, 144.51, 142.39, 137.86, 136.35, 136.15, 135.83, 134.95, 132.25, 129.64, 128.99; HRMS (ESI, m/z): Calcd. For $\text{C}_{16}\text{H}_{11}\text{N}_3\text{O}_3\text{H}^+$ 327.0128; found: 327.0125.



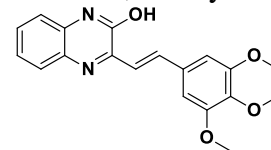
3-(2-Hydroxy-3-methoxystyryl)quinoxalin-2-ol (15e): White powder, mp 202–203 °C, 80% yield. ^1H NMR (400 MHz, $\text{CDCl}_3 + \text{DMSO}$) δ 12.31 (s, 1H), 8.00 (d, $J = 16.0$ Hz, 1H), 7.90 (s, 1H), 7.78–7.67 (m, 1H), 7.56–7.43 (m, 3H), 7.33 (d, $J = 6.8$ Hz, 1H), 7.25–7.20 (m, 1H), 6.89 (d, $J = 6.4$ Hz, 1H), 4.89 (s, 1H), 3.79 (s, 3H); ^{13}C NMR (100 MHz, $\text{CDCl}_3 + \text{DMSO}$) δ 171.25, 160.86, 155.43, 153.87, 152.71, 140.88, 135.89, 134.11, 133.19, 132.53, 131.30, 129.64, 128.16, 125.88, 123.66, 118.13, 60.74; HRMS (ESI, m/z): Calcd. For $\text{C}_{17}\text{H}_{14}\text{N}_2\text{O}_3\text{H}^+$ 295.1077, found 295.1076.



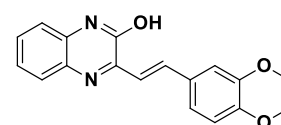
3-(2-Bromostyryl)quinoxalin-2-ol (15f): Pale yellow solid, mp 216–217 °C, 85% yield. ^1H NMR (400 MHz, $\text{CDCl}_3 + \text{DMSO}$) δ 12.50 (s, 1H), 8.41 (d, $J = 16.4$ Hz, 1H), 7.90 (d, $J = 7.6$ Hz, 1H), 7.79 (d, $J = 8.0$ Hz, 1H), 7.67 (d, $J = 8.0$ Hz, 1H), 7.60 (d, $J = 16.0$ Hz, 1H), 7.49–7.41 (m, 2H), 7.36–7.28 (m, 3H); ^{13}C NMR (100 MHz, $\text{CDCl}_3 + \text{DMSO}$) δ 155.25, 153.03, 136.09, 135.42, 133.53, 132.82, 132.24, 130.97, 130.34, 128.98, 128.47, 127.84, 125.43, 124.96, 123.80, 115.74; HRMS (ESI, m/z): Calcd. For $\text{C}_{16}\text{H}_{11}\text{N}_3\text{O}_3\text{H}^+$ 327.0133, found 327.0123; IR (KBr, thin film, cm^{-1}): ν_{max} 3093, 2968, 2882, 1659, 1552, 1428, 1159, 971.



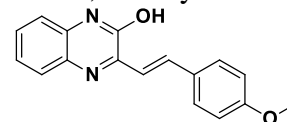
3-(3,4,5-Trimethoxystyryl)quinoxalin-2-ol (15j): Yellow solid, mp 230–231 °C, 85% yield. ¹H NMR (400 MHz, CDCl₃+DMSO) δ 12.47 (s, 1H), 8.05 (d, J = 16.0 Hz, 1H), 7.73 (d, J = 8.0 Hz, 1H), 7.56 (d, J = 16.4 Hz, 1H), 7.44 (t, J = 7.6 Hz, 1H), 7.31–7.25 (m, 2H), 6.99 (s, 2H), 3.89 (s, 6H), 3.76 (s, 3H); ¹³C NMR (100 MHz, CDCl₃+DMSO) δ 155.34, 153.55, 153.41, 139.19, 137.87, 132.94, 132.13, 131.99, 129.79, 128.57, 123.72, 121.68, 115.66, 105.29, 60.53, 56.30; HRMS (ESI, m/z): Calcd. For C₁₉H₁₈N₂O₄H⁺ 339.1339, found 339.1341; IR (KBr, thin film, cm⁻¹): ν_{max} 2976, 231, 1664, 1506, 1333, 1248, 1233, 1133, 999, 751.



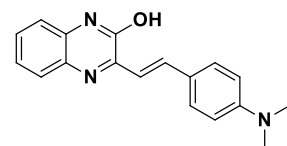
3-(3,4-Dimethoxystyryl)quinoxalin-2-ol (15k): Yellow powder, mp 221–222 °C, 86% yield. ¹H NMR (400 MHz, CDCl₃+DMSO) δ 12.00 (s, 1H), 8.04 (d, J = 16.0 Hz, 1H), 7.71 (d, J = 7.6 Hz, 1H), 7.50 (d, J = 16.0 Hz, 1H), 7.33–7.27 (m, 1H), 7.23–7.14 (m, 4H), 6.81 (d, J = 8.0 Hz, 1H), 3.86 (s, 3H), 3.84 (s, 3H); ¹³C NMR (100 MHz, CDCl₃) δ 169.14, 162.75, 151.93, 150.89, 140.59, 138.69, 136.30, 133.95, 131.92, 131.59, 130.94, 130.51, 127.67, 123.70, 112.80, 110.99, 57.66, 57.57; HRMS (ESI, m/z): Calcd. For C₁₈H₁₆N₂O₃H⁺ 309.1234, found 309.1232; IR (KBr, thin film, cm⁻¹): ν_{max} 3060, 2933, 2837, 1662, 1517, 1438, 1266, 1234, 1134, 746.



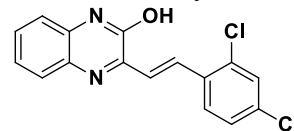
3-(4-Methoxystyryl)quinoxalin-2-ol (15l): Pale yellow solid, mp 242–243 °C, 85% yield. ¹H NMR (400 MHz, CDCl₃+DMSO) δ 12.22 (s, 1H), 8.01 (d, J = 16.0 Hz, 1H), 7.69 (d, J = 6.4 Hz, 1H), 7.60–7.45 (m, 3H), 7.31–7.19 (m, 3H), 6.86 (d, J = 6.4 Hz, 2H), 3.77 (s, 3H); ¹³C NMR (100 MHz, CDCl₃+DMSO) δ 169.04, 158.53, 137.60, 134.83, 133.87, 132.15, 130.46, 128.76, 127.71, 126.71, 125.71, 123.74, 121.35, 117.55, 53.90; HRMS (ESI, m/z): Calcd. For C₁₇H₁₄N₂O₂H⁺ 279.1128, found 279.1123; IR (KBr, thin film, cm⁻¹): ν_{max} 3010, 2923, 1652, 1602, 1511, 1173, 1017, 822, 757.



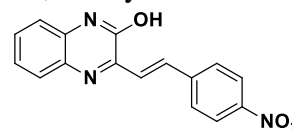
3-(4-(Dimethylamino)styryl)quinoxalin-2-ol (15m): Brown solid, mp 226–227 °C, 82% yield. ¹H NMR (400 MHz, CDCl₃+DMSO) δ 11.99 (s, 1H), 7.57 (d, J = 8.8 Hz, 2H), 7.29–7.23 (m, 3H), 7.15–7.08 (m, 3H), 6.60 (d, J = 8.4 Hz, 2H), 3.29 (s, 6H); ¹³C NMR (100 MHz, CDCl₃+DMSO) δ 161.13, 155.50, 149.22, 133.51, 132.27, 131.93, 129.35, 128.48, 128.40, 128.36, 126.11, 123.14, 115.51, 112.77, 39.18; HRMS (ESI, m/z): Calcd. For C₁₈H₁₇N₃O⁺ 292.1444, found 292.1447; IR (KBr, thin film, cm⁻¹): ν_{max} 3098, 2963, 2843, 1653, 1522, 1430, 587.



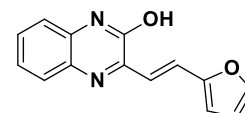
3-(2,4-Dichlorostyryl)quinoxalin-2-ol (15o): Pale green solid, mp 245–246 °C, 88% yield. ¹H NMR (400 MHz, CDCl₃+DMSO) δ 12.56 (s, 1H), 8.39 (d, J = 16.4 Hz, 1H), 8.01 (d, J = 8.4 Hz, 1H), 7.80 (d, J = 8.0 Hz, 1H), 7.69–7.62 (m, 2H), 7.53–7.46 (m, 2H), 7.33 (d, J = 8.0 Hz, 2H); ¹³C NMR (100 MHz, CDCl₃+DMSO) δ 168.68, 155.35, 139.34, 138.10, 136.07, 135.66, 134.26, 132.90, 132.11, 130.99, 129.95, 129.52, 128.74, 123.69, 123.07, 122.91; HRMS (ESI, m/z): Calcd. For C₁₆H₁₀Cl₂N₂OH⁺ 317.0243, found 317.0245; IR (KBr, thin film, cm⁻¹): ν_{max} 3095, 2966, 2883, 1659, 1584, 1462, 1191, 975, 862, 755.



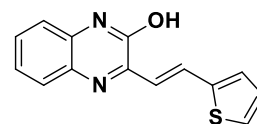
3-(4-Nitrostyryl) quinoxalin-2-ol (15p): Pale yellow solid, mp 284–285 °C, 90% yield. ¹H NMR (400 MHz, CDCl₃+DMSO) δ 12.57 (s, 1H), 8.23 (d, J = 8.4 Hz, 2H), 8.16 (d, J = 16.0 Hz, 1H), 7.96 (d, J = 8.4 Hz, 2H), 7.80–7.76 (m, 2H), 7.49 (t, J = 7.2 Hz, 1H), 7.32 (d, J = 8.8 Hz, 2H); ¹³C NMR (100 MHz, CDCl₃+DMSO) δ 155.25, 152.78, 147.63, 143.05, 134.90, 132.83, 132.36, 130.70, 129.04, 128.88, 126.83, 124.40, 123.93, 115.82; HRMS (ESI, m/z): Calcd. For C₁₆H₁₁N₃O₃H⁺ 294.0873, found 294.0877; IR (KBr, thin film, cm⁻¹): ν_{max} 3101, 2930, 1665, 1590, 1511, 1344, 976, 748.



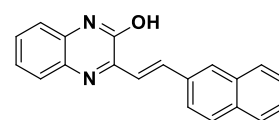
3-(2-(Furan-2-yl)vinyl)quinoxalin-2-ol (15r): Brown powder, mp 202–203 °C, 82% yield. ¹H NMR (400 MHz, CDCl₃+DMSO) δ 12.38 (s, 1H), 7.92 (d, J = 16.0 Hz, 1H), 7.72 (d, J = 8.0 Hz, 1H), 7.64 (s, 1H), 7.44–7.39 (m, 2H), 7.31–7.24 (m, 2H), 6.72 (d, J = 2.4 Hz, 1H), 6.54 (s, 1H); ¹³C NMR (100 MHz, DMSO) δ 170.48, 155.34, 153.09, 152.79, 144.54, 131.87, 129.64, 128.55, 124.58, 123.62, 120.40, 115.60, 113.47, 112.73; HRMS (ESI, m/z): Calcd. For C₁₄H₁₀N₂O₂H⁺ 239.0815, found 239.0820.



3-(2-(Thiophen-2-yl)vinyl)quinoxalin-2-ol (15s): Light brown solid, mp 195–196 °C, 85% yield. ¹H NMR (400 MHz, CDCl₃+DMSO) δ 12.32 (s, 1H), 8.29 (d, J = 16.0 Hz, 1H), 7.75 (d, J = 8.0 Hz, 1H), 7.44–7.39 (m, 3H), 7.33–7.30 (m, 3H), 7.10–7.07 (m, 1H); ¹³C NMR (100 MHz, CDCl₃+DMSO) δ 155.48, 152.95, 142.26, 133.06, 131.67, 130.64, 129.60, 129.55, 128.48, 128.24, 127.37, 123.65, 121.59, 115.59; HRMS (ESI, m/z): Calcd. For C₁₄H₁₀N₂OSH⁺ 255.0587, found 255.0591; IR (KBr, thin film, cm⁻¹): ν_{max} 2970, 2879, 1656, 1613, 1550, 1449, 1226, 759.



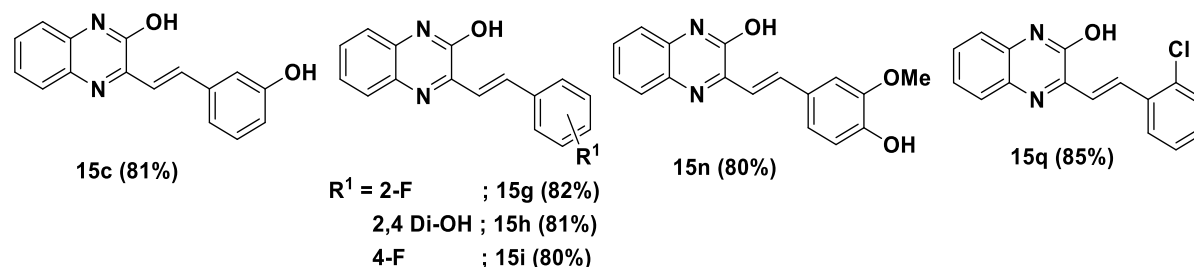
3-(2-(Naphthalen-2-yl)vinyl)quinoxalin-2-ol (15t): Yellow solid, mp 254–255 °C, 88% yield. ¹H NMR (400 MHz, CDCl₃+DMSO) δ 12.52 (s, 1H), 8.97 (d, J = 16.0 Hz, 1H), 8.32 (d, J = 8.0 Hz, 1H), 7.97 (d, J = 7.2 Hz, 3H), 7.83 (d, J = 7.6 Hz, 1H), 7.7–7.57 (m, 4H), 7.48 (t, J = 6.8 Hz, 1H), 7.35–7.29 (m, 2H); ¹³C NMR (100 MHz, CDCl₃+DMSO) δ 155.28, 152.82, 147.62, 134.95, 134.89, 132.89, 132.19, 130.47, 130.35, 130.22, 129.70, 129.66, 128.99, 128.70, 128.07, 127.29, 124.37, 123.85, 123.79, 115.81; IR (KBr, thin film, cm⁻¹): ν_{max} 3120, 2980, 1670, 1601, 1515, 1410, 1250, 985, 760, 660.



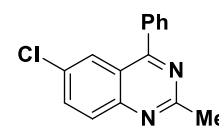
Melting points of the Reported molecules²⁶:

Compound	Experimental M.P	Reported M.P	Compound	Experimental M.P	Reported ²⁶ M.P
(15c)	248-249	248-250	(15i)	167-168	168-169
(15g)	260-261	260-262	(15n)	243-244	243-245
(15h)	250-251	249-251	(15q)	248-249	249-251

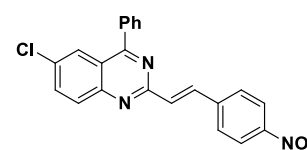
Reported molecules²⁶



6-Chloro-2-methyl-4-phenylquinazoline (9e): White powder, 90% yield. ¹H NMR (400 MHz, CDCl₃) δ 7.91–7.85 (m, 2H), 7.70–7.63 (m, 3H), 7.49 (s, 3H), 2.84 (s, 3H); HRMS (ESI, m/z): Calcd. For C₁₅H₁₁ClN₂H⁺ 255.0684, found 255.0680.



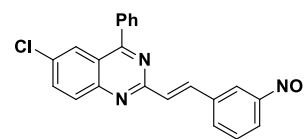
6-Chloro-2-(3-nitrostyryl)-4-phenylquinazoline (16a): Light green powder, mp 156–157 °C, 90% yield. ¹H NMR (400 MHz, CDCl₃+DMSO) δ 8.55 (s, 1H), 8.24–8.18 (m, 3H), 8.07 (d, J = 9.6 Hz, 1H), 7.98 (s, 2H), 7.85 (s, 2H), 7.72–7.59 (m, 5H); ¹³C NMR (100 MHz, CDCl₃+DMSO) δ 159.99, 148.81, 137.95, 136.71, 136.32, 135.15, 133.89, 132.61, 131.02, 130.95, 130.66, 130.61, 130.22, 129.10, 125.92, 123.73, 122.53, 122.15; HRMS (ESI, m/z): Calcd. For



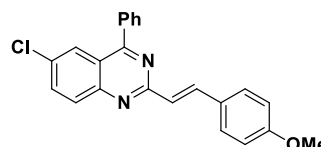
$C_{22}H_{14}ClN_3O_2H^+$ 388.0847, found 388.0852; IR (KBr, thin film, cm^{-1}): ν_{max} 3406, 3071, 1639, 1527, 1330, 1077, 836.

6-Chloro-2-(3-nitrostyryl)-4-phenylquinazoline (16b): Yellow

powder, mp 201–202 °C, 87% yield. 1H NMR (400 MHz, $CDCl_3$ +DMSO) δ 8.25–8.15 (m, 3H), 8.06 (d, J = 8.8 Hz, 1H), 7.98–7.93 (m, 4H), 7.83 (s, 2H), 7.66–7.59 (m, 4H); ^{13}C NMR (100 MHz, DMSO+ $CDCl_3$) δ 164.99, 152.40, 145.56, 141.65, 140.63, 136.51, 135.71, 132.58, 130.17, 129.51, 128.80, 128.47, 127.87, 125.75, 124.26, 124.12, 123.94, 123.05, 122.36, 118.31; HRMS (ESI, m/z): Calcd. For $C_{22}H_{14}ClN_3O_2H^+$ 388.0847, found 388.0851; IR (KBr, thin film, cm^{-1}): ν_{max} 3410, 3029, 2875, 1596, 1519, 1340, 1107, 844.

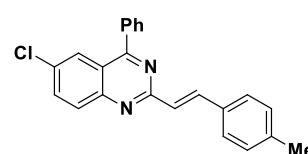


6-Chloro-2-(4-methoxystyryl)-4-phenylquinazoline (16c): Red sticky solid, mp 242–243 °C, 84% yield. 1H NMR (400 MHz, $CDCl_3$) δ 8.17 (d, J = 16.0 Hz 1H), 8.01 (d, J = 2.0 Hz, 1H), 7.98 (d, J = 8.8 Hz, 1H), 7.82–7.77 (m, 3H), 7.63–7.61 (m, 5H), 7.31 (d, J = 16.0 Hz, 1H), 6.94 (d, J = 8.8 Hz, 2H), 3.85 (s, 3H); HRMS (ESI, m/z): Calcd. For $C_{23}H_{17}ClN_2OH^+$ 373.1102, found 373.0870; IR (KBr, thin film, cm^{-1}): ν_{max} 3010, 2923, 1652, 1602, 1511, 1173, 1017, 822, 757.

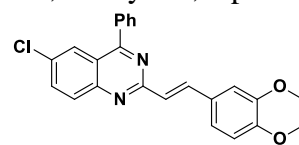


6-Chloro-2-(4-methylstyryl)-4-phenylquinazoline (16d): White

powder, mp 154–155 °C, 83% yield. 1H NMR (400 MHz, $CDCl_3$) δ 8.19 (d, 1H), 8.00–7.98 (m, 2H), 7.82–7.77 (m, 3H), 7.62–7.56 (m, 5H), 7.39 (d, J = 16.0 Hz 1H), 7.22 (d, J = 7.6 Hz, 2H), 2.38 (s, 3H); ^{13}C NMR (100 MHz, DMSO+ $CDCl_3$) δ 167.37, 157.81, 147.55, 141.30, 136.24, 133.73, 131.14, 130.69, 130.29, 129.91, 129.13, 128.75, 127.87, 127.55, 124.87, 124.22, 123.54, 120.63, 22.30; HRMS (ESI, m/z): Calcd. For $C_{23}H_{17}ClN_2H^+$ 357.1153, found 357.1150; IR (KBr, thin film, cm^{-1}): ν_{max} 3390, 3021, 2892, 1636, 1535, 1389, 970, 836, 701.



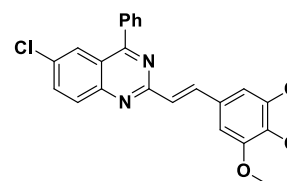
6-Chloro-2-(3,4-dimethoxystyryl)-4-phenylquinazoline (16e): White solid, 85% yield, mp 169–170 °C. 1H NMR (400 MHz, $CDCl_3$) δ 8.06 (d, J = 16.0 Hz, 1H), 7.91–7.86 (m, 2H), 7.72–7.67 (m, 3H), 7.52 (s, 3H), 7.23–7.10 (m, 3H), 6.80 (d, J = 8.0 Hz, 1H), 3.85 (s, 3H), 3.83 (s, 3H); ^{13}C NMR (100 MHz, $CDCl_3$) δ 167.44, 161.05, 150.30, 150.23, 149.19, 138.89, 136.99, 134.60, 132.25, 130.22, 130.21, 129.89, 129.24, 128.81, 125.97, 125.70, 122.00, 111.10, 109.29, 55.96, 55.87; HRMS (ESI, m/z):



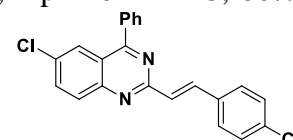
Calcd. For $C_{24}H_{19}ClN_2O_2H^+$ 403.1208, found 403.1214; IR (KBr, thin film, cm^{-1}): ν_{max} 3395, 3060, 2958, 1633, 1534, 1435, 1266, 1253, 1138, 1024, 839.

6-Chloro-4-phenyl-2-(3,4,5-trimethoxystyryl)quinazoline (16f):

Pale yellow solid, mp 195–196 °C, 84% yield. 1H NMR (400 MHz, $CDCl_3$ +DMSO) δ 7.96–7.94 (m, 2H), 7.83 (d, J = 3.2 Hz, 2H), 7.75 (d, J = 3.2 Hz, 2H), 7.66 (s, 2H), 7.63 (s, 2H), 7.44 (d, J = 16.0 Hz, 1H), 7.08 (s, 1H), 3.88 (s, 6H), 3.74 (s, 3H); ^{13}C NMR (100 MHz, $CDCl_3$ +DMSO) δ 167.42, 153.57, 149.98, 139.08, 136.86, 136.69, 135.03, 134.84, 131.88, 131.73, 130.83, 130.59, 130.53, 130.13, 129.08, 127.41, 125.90, 125.61, 105.50, 60.51, 56.37; HRMS (ESI, m/z): Calcd. For $C_{25}H_{21}ClN_2O_3H^+$ 433.1313, found 433.1317; IR (KBr, thin film, cm^{-1}): ν_{max} 3410, 3110, 2928, 1635, 1548, 1420, 1139, 1151, 1251, 1151, 836.

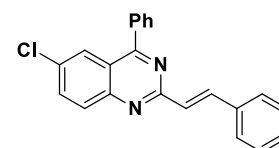


6-Chloro-2-(4-chlorostyryl)-4-phenylquinazoline (16g): White powder, mp 210–211 °C, 86% yield. 1H NMR (400 MHz, $CDCl_3$ +DMSO) δ 8.11–7.94 (m, 4H), 7.84 (s, 4H), 7.68 (s, 3H), 7.48 (d, J = 6.0 Hz, 3H); HRMS (ESI, m/z): Calcd. For $C_{22}H_{14}Cl_2N_2H^+$ 377.0607, found 377.0605; IR (KBr, thin film, cm^{-1}): ν_{max} 3412, 3089, 2915, 1633, 1535, 1386, 1076, 836, 695.



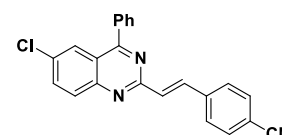
6-Chloro-4-phenyl-2-styrylquinazoline (16h): White powder, mp

179–180 °C, 85% yield. 1H NMR (400 MHz, $CDCl_3$) δ 8.21 (d, J = 16.0 Hz, 1H), 8.03–7.99 (m, 2H), 7.81 (s, 3H), 7.72–7.53 (m, 5H), 7.49–7.31 (m, 4H); ^{13}C NMR (100 MHz, $CDCl_3$) δ 167.49, 155.36, 146.30, 141.43, 140.04, 137.29, 136.37, 135.21, 131.70, 131.47, 130.31, 129.72, 129.03, 128.74, 128.12, 126.79, 125.66, 124.43; HRMS (ESI, m/z): Calcd. For $C_{22}H_{15}ClN_2H^+$ 343.0997, found 343.0993; IR (KBr, thin film, cm^{-1}): ν_{max} 3369, 3070, 2998, 1640, 1528, 1386, 1072, 969, 844, 763.

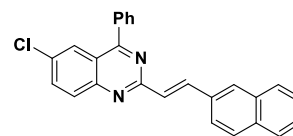


4-(2-(6-Chloro-4-phenylquinazolin-2-yl)vinyl)benzonitrile (16i): Yellow solid, mp 206–207

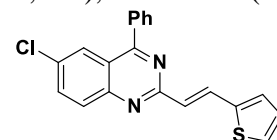
°C, 88% yield. 1H NMR (400 MHz, $CDCl_3$ +DMSO) δ 8.14 (d, J = 16.0 Hz, 1H), 8.07 (d, J = 9.2 Hz, 1H), 7.98–7.93 (m, 4H), 7.82–7.80 (m, 4H), 7.66–7.57 (m, 4H). HRMS (ESI, m/z): Calcd. For $C_{23}H_{14}ClN_3H^+$ 368.0949, found 368.0954; IR (KBr, thin film, cm^{-1}): ν_{max} 3402, 3049, 2223, 1602, 1534, 1420, 1387, 1076, 840, 695.



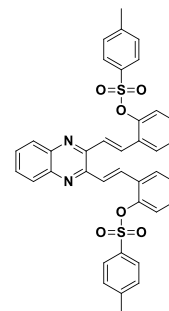
6-Chloro-2-(2-(naphthalen-2-yl)vinyl)-4-phenylquinazoline (16j): Pale yellow solid, mp 158–159 °C, 85% yield. ^1H NMR (400 MHz, CDCl_3 +DMSO) δ 8.94 (d, J = 15.6 Hz, 1H), 8.28 (d, J = 8.4 Hz, 1H), 8.07 (d, J = 9.2 Hz, 1H), 8.01–7.79 (m, 5H), 7.87 (d, J = 3.6 Hz, 2H), 7.67 (s, 3H), 7.61–7.54 (m, 3H), 7.47 (d, J = 15.6 Hz, 1H); ^{13}C NMR (100 MHz, CDCl_3 +DMSO) δ 167.38, 160.48, 150.27, 136.87, 135.02, 134.96, 133.83, 133.09, 132.31, 131.36, 130.94, 130.65, 130.57, 130.17, 129.78, 129.09, 129.01, 127.08, 126.43, 126.11, 125.88, 124.78, 123.57, 122.06; HRMS (ESI, m/z): Calcd. For $\text{C}_{16}\text{H}_{11}\text{N}_3\text{O}_3\text{H}^+$ 393.1153, found 393.1158; IR (KBr, thin film, cm^{-1}): ν_{max} 3390, 3038, 1635, 1534, 1383, 1153, 962, 788.



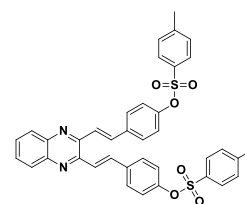
(E)-6-Chloro-4-phenyl-2-(2-(thiophen-2-yl)vinyl)quinazoline (16k): Light brown powder, mp 171–172 °C, 84% yield. ^1H NMR (400 MHz, CDCl_3) δ 8.31 (d, J = 15.2 Hz, 1H), 8.00–7.95 (m, 2H), 7.80 (s, 3H), 7.61 (s, 3H), 7.32–7.21 (m, 3H), 7.06 (s, 1H); ^{13}C NMR (100 MHz, DMSO+ CDCl_3) δ 167.76, 153.71, 146.29, 143.51, 141.23, 137.27, 134.03, 132.44, 130.23, 129.93, 129.42, 129.00, 128.94, 128.44, 127.71, 124.57, 124.05, 122.35, 114.63; HRMS (ESI, m/z): Calcd. For $\text{C}_{20}\text{H}_{13}\text{ClN}_2\text{SH}^+$ 349.0561, found 349.0563; IR (KBr, thin film, cm^{-1}): ν_{max} 3396, 3095, 2901, 1629, 1536, 1387, 1204, 1072, 840, 696.



((1E,1'E)-Quinoxaline-2,3-diylbis(ethene-2,1-diyl))bis(2,1-phenylene) bis(4-methylbenzene sulfonate) (18a): Yellow solid, mp 175–176 °C, 80% yield. ^1H NMR (400 MHz, CDCl_3 +DMSO- d_6) δ 8.06 (dd, J = 6.4, 3.6 Hz, 2H), 8.03–7.99 (m, 2H), 7.86–7.82 (m, 4H), 7.71 (d, J = 8.4 Hz, 4H), 7.65 (d, J = 15.6 Hz, 2H), 7.42–7.39 (m, 4H), 7.27–7.24 (m, 2H), 7.14 (d, J = 8.0 Hz, 4H), 2.11 (s, 6H); ^{13}C NMR (100 MHz, CDCl_3 +DMSO- d_6) δ 152.80, 152.41, 150.48, 146.23, 136.95, 135.08, 134.98, 134.90, 134.83, 134.24, 133.83, 133.20, 132.90, 132.52, 129.12, 128.42, 26.15; HRMS (ESI, m/z): Calcd. For $\text{C}_{38}\text{H}_{30}\text{N}_2\text{O}_6\text{S}_2\text{H}^+$ 675.1618, found 675.1616; IR (KBr, thin film, cm^{-1}): ν_{max} 2979, 1588, 1507, 1375, 1086, 851, 1037, 866.



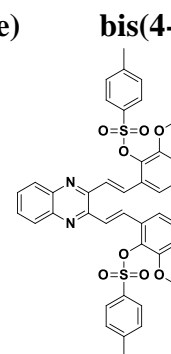
((1E,1'E)-Quinoxaline-2,3-diylbis(ethene-2,1-diyl))bis(4,1-phenylene) bis(4-methylbenzene sulfonate) (18b): Yellow solid, mp 184–186 °C, 81% yield. ^1H NMR (400 MHz, DMSO- d_6) δ 7.99 (dd, J = 6.2, 4.0 Hz, 2H), 7.94 (d, J = 3.2 Hz, 4H), 7.83 (d, J = 8.8 Hz, 4H), 7.74 (d, J = 8.4 Hz, 6H), 7.44 (d, J = 8.0 Hz, 4H), 7.05 (d, J = 8.8 Hz, 4H), 2.46 (s, 6H); ^{13}C NMR (100 MHz, DMSO- d_6) δ 149.67, 148.62, 145.95, 141.54, 136.07, 135.69, 132.04, 130.37, 130.03, 129.63, 128.98, 128.58,



123.74, 122.74, 21.73; HRMS (ESI, m/z): Calcd. For $C_{38}H_{30}N_2O_6S_2H^+$ 675.1618, found 675.1608; IR (KBr, thin film, cm^{-1}): ν_{max} 2981, 1594, 1501, 1381, 1094, 844, 1026, 861.

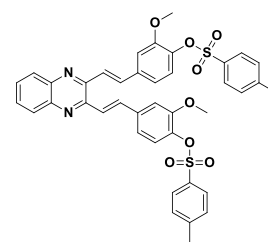
((1E,1'E)-Quinoxaline-2,3-diylbis(ethene-2,1-diyl))bis(2-methoxy-6,1-phenylene methylbenzenesulfonate) (18c): Pale yellow powder, mp 184–185 °C, 79% yield.

1H NMR (400 MHz, $CDCl_3$ +DMSO- d_6) δ 7.92–7.90 (m, 2H), 7.75–7.62 (m, 8H), 7.49 (d, J = 5.2 Hz, 1H), 7.35 (d, J = 7.8 Hz, 2H), 7.26–7.22 (m, 2H), 7.01 (d, J = 8.0 Hz, 4H), 6.93 (d, J = 8.0 Hz, 2H), 3.68 (s, 6H), 1.93 (s, 6H); ^{13}C NMR (100 MHz, $CDCl_3$ +DMSO- d_6) δ 157.85, 153.08, 150.23, 146.12, 142.15, 138.43, 136.28, 135.39, 135.19, 134.93, 134.01, 133.62, 133.12, 130.02, 124.10, 118.84, 61.16, 25.90; HRMS (ESI, m/z): Calcd. For $C_{40}H_{34}N_2O_8S_2H^+$ 735.1829, found 735.1709; IR (KBr, thin film, cm^{-1}): ν_{max} 2930, 1576, 1477, 1382, 1273, 1176, 1062, 547.



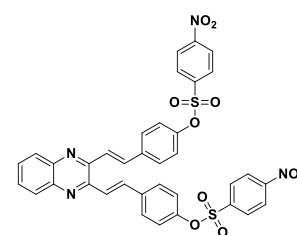
((1E,1'E)-Quinoxaline-2,3-diylbis(ethene-2,1-diyl))bis(2-methoxy-5,1-phenylene bis(4-methylbenzene sulfonate) (18d): Yellow powder, mp 152–153 °C, 81% yield.

1H NMR (400 MHz, $CDCl_3$ +DMSO- d_6) δ 7.84 (dd, J = 6.2, 3.6 Hz, 2H), 7.79 (d, J = 3.6 Hz, 4H), 7.57 (d, J = 8.0 Hz, 6H), 7.27–7.19 (m, 8H), 6.99 (d, J = 8.4 Hz, 2H), 3.49 (s, 6H), 2.31 (s, 6H); ^{13}C NMR (100 MHz, $CDCl_3$ +DMSO- d_6) δ 156.66, 153.34, 150.26, 146.34, 143.21, 141.49, 141.31, 137.61, 134.65, 134.51, 133.68, 133.32, 128.74, 128.56, 125.43, 117.13, 60.61, 26.45; HRMS (ESI, m/z): Calcd. For $C_{40}H_{34}N_2O_8S_2H^+$ 735.1829, Found 735.1705; IR (KBr, thin film, cm^{-1}): ν_{max} 3120, 2950, 1595, 1379, 1258, 1175, 1030, 851.



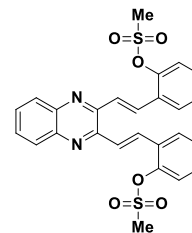
((1E,1'E)-Quinoxaline-2,3-diylbis(ethene-2,1-diyl)) bis(4,1-phenylene) bis(4-nitrobenzene sulfonate) (18f): Greenish yellow powder, mp 206–207 °C, 82% yield.

1H NMR (400 MHz, $CDCl_3$ +DMSO- d_6) δ 8.48 (d, J = 8.8 Hz, 4H), 8.17 (d, J = 8.8 Hz, 4H), 8.04–7.91 (m, 6H), 7.86 (d, J = 8.6 Hz, 4H), 7.73 (dd, J = 6.4, 3.4 Hz, 2H), 7.11 (d, J = 8.6 Hz, 4H); ^{13}C NMR (100 MHz, DMSO- d_6) δ 151.58, 149.33, 148.80, 141.50, 139.93, 136.00, 132.11, 130.58, 130.22, 129.98, 129.09, 125.54, 124.31, 122.92; HRMS (ESI, m/z): Calcd. For $C_{36}H_{24}N_4O_{10}S_2H^+$ 737.1007, found 737.0934; IR (KBr, thin film, cm^{-1}): ν_{max} 3150, 2950, 1695, 1525, 1390, 1279, 1049, 850.



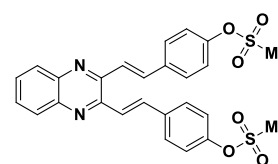
((1E,1'E)-Quinoxaline-2,3-diylbis(ethene-2,1-diyl))bis(2,1-phenylene)

dimethanesulfonate (18g) : White solid, mp 124–125 °C, 84% yield. ¹H NMR (400 MHz, CDCl₃+DMSO-d₆) δ 8.01 (d, J = 5.6 Hz, 5H), 7.96 (d, J = 8.8 Hz, 5H), 7.74 (dd, J = 6.4, 3.2 Hz, 2H), 7.41 (d, J = 8.4 Hz, 4H), 3.34 (s, 6H); ¹³C NMR (100 MHz, CDCl₃+DMSO-d₆) δ 154.44, 153.45, 146.33, 140.93, 140.57, 134.76, 134.53, 134.23, 133.74, 130.55, 128.60, 127.57, 42.54; HRMS (ESI, m/z): Calcd. For C₂₆H₂₂N₂O₆S₂H⁺ 523.0992, found 523.0908.



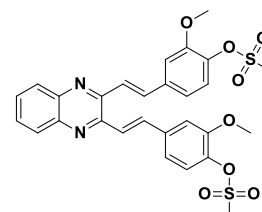
((1E,1'E)-Quinoxaline-2,3-diylbis(ethene-2,1-diyl))bis(4,1-phenylene) dimethanesulfonate

(18h): White solid, mp 192–193 °C, 83% yield. ¹H NMR (400 MHz, CDCl₃+DMSO-d₆) δ 8.27–8.22 (m, 4H), 8.10–8.03 (m, 4H), 7.77 (dd, J = 6.4, 3.2 Hz, 2H), 7.17–7.45 (m, 6H), 3.46 (s, 6H); ¹³C NMR (100 MHz, CDCl₃+ DMSO-d₆) δ 153.46, 152.42, 146.39, 135.36, 134.95, 133.98, 133.42, 132.59, 130.29, 128.12, 43.48; HRMS (ESI, m/z): Calcd. For C₂₆H₂₂N₂O₆S₂H⁺ 523.0992, found 523.0996; IR (KBr, thin film, cm⁻¹): ν_{max} 3110, 2952, 1610, 1509, 1355, 1152, 832.



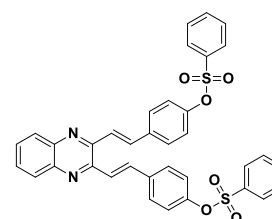
((1E,1'E)-Quinoxaline-2,3-diylbis(ethene-2,1-diyl))bis(2-methoxy-5,1-phenylene) dimethane

sulfonate (18i): Pale yellow solid, mp 198–199 °C, 80% yield. ¹H NMR (400 MHz, CDCl₃+DMSO-d₆) δ 8.05 (dd, J = 6.4, 3.2 Hz, 2H), 7.97 (d, J = 15.6 Hz, 2H), 7.72 (dd, J = 6.4, 3.2 Hz, 2H), 7.63 (d, J = 15.6 Hz, 2H), 7.37–7.34 (m, 4H), 7.30 (s, 2H), 3.99 (s, 6H), 3.24 (s, 6H); ¹³C NMR (100 MHz, CDCl₃+DMSO-d₆) δ 151.61, 148.43, 141.61, 138.57, 136.77, 136.68, 129.84, 128.86, 124.74, 123.80, 120.03, 112.14, 56.13, 38.43; HRMS (ESI, m/z): Calcd. For C₂₈H₂₆N₂O₈S₂H⁺ 583.1203, found 457. 6405; IR (KBr, thin film, cm⁻¹): ν_{max} 3110, 2968, 1598, 1508, 1363, 1259, 1026, 861.



Quinoxaline-2,3-diylbis(ethene-2,1-diyl))bis(4,1-phenylene) dibenzene sulfonate (18j): Pale

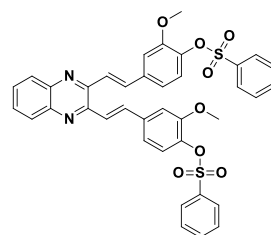
green powder, mp 158–159 °C, 85% yield. ¹H NMR (400 MHz, CDCl₃) δ 8.03 (s, 2H), 7.94–7.86 (m, 6H), 7.71 (d, J = 6.4 Hz, 4H), 7.59–7.52 (m, 10H), 7.05 (d, J = 8.0 Hz, 4H); ¹³C NMR (100 MHz, CDCl₃+ DMSO-d₆) δ 154.33, 153.24, 146.29, 140.77, 140.44, 139.77, 139.63, 134.61, 134.42, 134.13, 133.68, 133.21, 128.37, 127.43. HRMS (ESI, m/z): Calcd. For



$C_{36}H_{26}N_2O_6S_2H^+$ 647.1305, found 647.1286; IR (KBr, thin film, cm^{-1}): ν_{max} 2981, 1594, 1501, 1381, 1094, 844, 1026, 861.

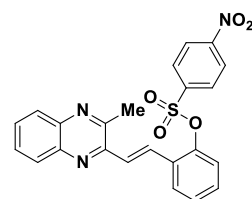
((1E,1'E)-Quinoxaline-2,3-diylbis(ethene-2,1-diyl))bis(2-methoxy-5,1-phenylene) dibenzene sulfonate (18k): Yellow solid, mp 180–181 °C, 83% yield.

1H NMR (400 MHz, $CDCl_3$ +DMSO) δ 8.00 (dd, J = 6.4, 3.2 Hz, 2H), 7.94 (d, J = 6.8 Hz, 4H), 7.88–7.85 (m, 4H), 7.78–7.70 (m, 4H), 7.62 (t, J = 8.0 Hz, 4H), 7.41 (d, J = 1.6 Hz, 2H), 7.37 (dd, J = 8.4, 1.6 Hz, 2H), 7.19 (d, J = 8.4 Hz, 2H), 3.61 (s, 6H); ^{13}C NMR (100 MHz, $CDCl_3$ +DMSO- d_6) δ 156.59, 153.31, 146.34, 143.13, 141.58, 141.26, 140.59, 139.32, 134.63, 133.96, 133.68, 133.27, 128.83, 128.60, 125.41, 117.03, 60.57; HRMS (ESI, m/z): Calcd. For $C_{38}H_{30}N_2O_8S_2H^+$ 707.1516, found 707.1518; IR (KBr, thin film, cm^{-1}): ν_{max} 3130, 1606, 1524, 1346, 1192, 1012, 854.



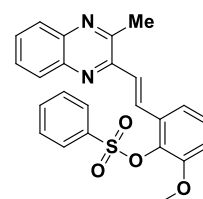
(E)-2-(2-(3-Methylquinoxalin-2-yl) vinyl)phenyl 4-nitrobenzenesulfonate (19a): Light green solid, mp 190–191 °C, 85% yield.

1H NMR (400 MHz, DMSO+ $CDCl_3$) δ 8.07–7.99 (m, 5H), 7.97–7.91 (m, 2H), 7.74–7.67 (m, 3H), 7.65 (s, 1H), 7.39–7.34 (m, 2H), 7.21 (d, J = 15.6 Hz, 1H), 2.73 (s, 3H); ^{13}C NMR (100 MHz, DMSO+ $CDCl_3$) δ 152.29, 150.80, 148.47, 147.27, 140.91, 140.64, 130.41, 130.08, 129.85, 129.80, 129.67, 129.37, 128.85, 128.20, 128.15, 127.67, 125.05, 124.41, 123.76, 123.60, 22.65; HRMS (ESI, m/z): Calcd. For $C_{23}H_{17}N_3O_5SH^+$ 448.0962, found 448.0965; IR (KBr, thin film, cm^{-1}): ν_{max} 3067, 2972, 1553, 1450, 1373, 1131, 850.



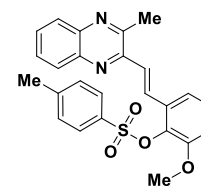
(E)-2-Methoxy-6-(2-(3-methylquinoxalin-2-yl)vinyl)phenyl benzenesulfonate (19b): Yellow solid, mp 209–210 °C, 75% yield.

1H NMR (400 MHz, $CDCl_3$ +DMSO) δ 8.24–8.13 (m, 5H), 7.93–7.86 (m, 2H), 7.76–7.72 (m, 3H), 7.55–7.49 (m, 2H), 7.38 (t, J = 7.6 Hz, 1H), 7.13 (d, J = 8.0 Hz, 1H), 3.72 (s, 3H), 2.84 (s, 3H); ^{13}C NMR (100 MHz, DMSO+ $CDCl_3$) δ 152.60, 151.81, 149.25, 148.47, 141.58, 138.44, 136.60, 136.12, 135.87, 134.38, 129.80, 129.28, 129.00, 128.48, 128.21, 124.22, 123.67, 119.95, 112.11, 111.78, 55.67, 22.99; HRMS (ESI, m/z): Calcd. For $C_{24}H_{20}N_2O_4SH^+$ 433.1217, found 433.0756; IR (KBr, thin film, cm^{-1}): ν_{max} 3022, 2972, 1731, 1368, 1223, 987.



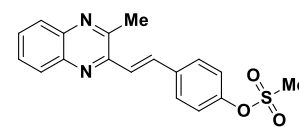
(E)-2-Methoxy-6-(2-(3-methylquinoxalin-2-yl)vinyl)phenyl 4-methylbenzenesulfonate (19c):

Yellow solid, mp 155–156 °C, 78 % yield. ^1H NMR (400 MHz, DMSO- d_6 +CDCl $_3$) δ 8.11 (d, J = 4.4 Hz, 2H), 7.93–7.86 (m, 3H), 7.53 (s, 1H), 7.49–7.42 (m, 2H), 7.24–7.21 (m, 2H), 7.16 (d, J = 8.0 Hz, 1H), 3.89 (s, 3H), 2.98 (s, 3H), 2.09 (s, 3H); ^{13}C NMR (100 MHz, DMSO- d_6 +CDCl $_3$) δ 154.09, 153.45, 150.01, 149.16, 145.96, 142.41, 142.13, 142.02, 138.49, 134.86, 131.79, 130.53, 130.34, 130.08, 129.20, 128.83, 126.18, 120.14, 119.63, 114.24, 57.05, 23.92, 22.14; HRMS (ESI, m/z): Calcd. For C $_{25}$ H $_{22}$ N $_2$ O $_4$ SH $^+$ 447.1373, found 447.0905; IR (KBr, thin film, cm $^{-1}$): ν_{max} 3027, 2956, 1514, 1365, 1158.



(E)-4-(2-(3-Methylquinoxalin-2-yl)vinyl)phenyl methanesulfonate (19d): Pale yellow solid,

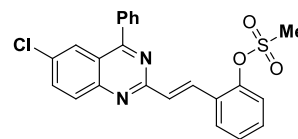
mp 175–176 °C, 80% yield. ^1H NMR (400 MHz, DMSO- d_6 +CDCl $_3$) δ 7.83–7.80 (m, 2H), 7.77 (d, J = 1.6 Hz, 1H), 7.58 (s, 1H), 7.57–7.48 (m, 2H), 7.40 (s, 1H), 7.20 (d, J = 1.6 Hz, 1H), 7.15–7.13 (m, 1H), 7.11 (s, 1H), 3.79 (s, 3H), 3.04 (s, 3H); ^{13}C NMR (100 MHz, DMSO- d_6 +CDCl $_3$) δ 147.49, 146.50, 140.67, 129.79, 129.30, 129.06, 128.99, 128.40, 128.10, 127.51, 127.09, 126.75, 124.58, 122.21, 37.41, 21.88; HRMS (ESI, m/z): Calcd. For C $_{18}$ H $_{16}$ N $_2$ O $_3$ SH $^+$ 341.0954, found 341.0553.



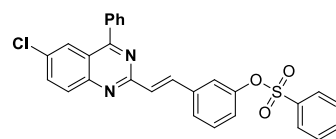
4.6.6 General procedure for the synthesis of sulfonates ester based 6-chloro-4-phenyl-2-styrylquinazoline (20a): To a solution of 6-chloro-2-methyl-4-phenylquinazoline (**9e**) (1mmol) in EtOH (5 mL) were added sulfonate aldehyde (**17a**) (1 mmol), NEt $_3$ (10 mol%). The mixture was stirred at 80 °C for 5.5 h till the completion of the reaction (TLC monitoring) and cooled to room temperature. The solvent was removed under reduced pressure to give the crude product which was purified by silica gel column chromatography. Elution of the column with EtOAc:hexanes (30/70 v/v) as afford pure product **20a** (0.3488 g, 80%).

4.6.7 General procedure for the synthesis of sulfonates ester-based 3-styrylquinoxaline-2-ol (21a): To a solution of 3-methyl quinoxaline-2-ol (**9d**) (1 mmol) in EtOH (5 mL), sulfonate aldehyde (**17a**) (1 mmol), NEt $_3$ (10 mol%) were added and the mixture was refluxed at 80 °C for 5 h. After the completion of the reaction (monitored by TLC), the mixture was cooled to room temperature. Evaporation of the solvent gave the crude product which was purified by silica gel column chromatography. Elution of the column using EtOAc:hexanes (30:70 v/v) gave desire product **21a** (287 mg, 84 %).

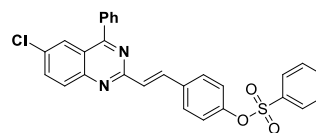
2-(2-(6-Chloro-4-phenylquinazolin-2-yl)vinyl)phenyl methanesulfonate (20a): White solid, mp 173–174 °C, 85% yield. ^1H NMR (400 MHz, CDCl_3) δ 8.25 (d, J = 8.8 Hz, 2H), 8.11 (d, J = 8.8 Hz, 1H), 7.75–7.69 (m, 3H), 7.57–7.49 (m, 5H), 7.43 (d, J = 15.6 Hz, 1H), 7.37–7.35 (m, 2H), 3.60 (s, 3H); ^{13}C NMR (100 MHz, $\text{CDCl}_3+\text{DMSO}-d_6$) δ 160.13, 155.23, 152.96, 147.34, 137.61, 132.85, 131.92, 130.42, 130.26, 129.44, 128.98, 128.21, 127.94, 127.60, 125.62, 123.73, 123.06, 122.20, 115.70, 115.42, 26.80; HRMS (ESI, m/z): calcd. For $\text{C}_{23}\text{H}_{17}\text{ClN}_2\text{O}_3\text{SH}^+$ 437.0732, found 437.0728; IR (KBr thin film, cm^{-1}): ν_{max} 3085, 2958, 1650, 1421, 1370, 1205, 971, 880.



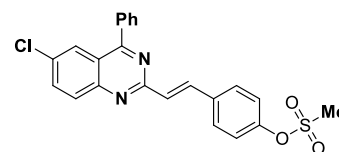
3-(2-(6-Chloro-4-phenylquinazolin-2-yl)vinyl)phenyl benzenesulfonate (20b): White solid, mp 180–181 °C, 84% yield. ^1H NMR (400 MHz, CDCl_3) δ 8.12–8.00 (m, 3H), 7.89–7.82 (m, 5H), 7.69–7.56 (m, 7H), 7.36–7.28 (m, 3H), 6.99 (d, J = 7.2 Hz, 1H); ^{13}C NMR (100 MHz, $\text{CDCl}_3+\text{DMSO}-d_6$) δ 160.81, 156.29, 156.15, 153.74, 149.75, 139.33, 135.84, 134.80, 133.82, 133.22, 132.95, 132.90, 131.47, 131.35, 130.56, 129.91, 129.31, 126.17, 124.78, 124.54, 124.17, 122.97, 116.76, 116.51; HRMS (ESI, m/z): calcd. For $\text{C}_{28}\text{H}_{19}\text{ClN}_2\text{O}_3\text{SH}^+$ 499.0889, found 499.0893; IR (KBr thin film, cm^{-1}): ν_{max} 3392, 2963, 1667, 1434, 1368, 1258, 1036, 829.



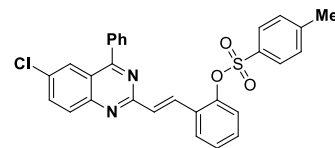
4-(2-(6-Chloro-4-phenylquinazolin-2-yl)vinyl)phenyl benzenesulfonate (20c): White solid, mp 215–216 °C, 83% yield. ^1H NMR (400 MHz, CDCl_3) δ 8.13 (d, J = 15.6 Hz, 1H), 8.03–7.98 (m, 2H), 7.87–7.79 (m, 5H), 7.70–7.52 (m, 8H), 7.36 (d, J = 16.0 Hz, 1H), 7.03 (d, J = 8.4 Hz, 2H); ^{13}C NMR (100 MHz, $\text{CDCl}_3+\text{DMSO}-d_6$) δ 166.27, 159.37, 149.16, 135.76, 133.85, 132.72, 131.98, 131.20, 130.25, 129.83, 129.54, 129.46, 129.06, 128.67, 127.98, 125.97, 125.32, 125.00, 124.77, 123.67, 122.46, 120.95; HRMS (ESI, m/z): calcd. For $\text{C}_{28}\text{H}_{19}\text{ClN}_2\text{O}_3\text{SH}^+$ 499.0889, found 499.0888; IR (KBr thin film, cm^{-1}): ν_{max} 3420, 2905, 1661, 1416, 1346, 1246, 1025, 827.



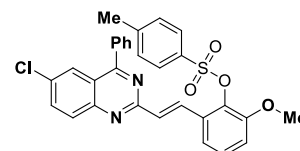
4-(2-(6-Chloro-4-phenylquinazolin-2-yl)vinyl)phenyl methanesulfonate (20d): White solid, mp 230–231 °C, 82% yield. ^1H NMR (400 MHz, CDCl_3) δ 8.11 (d, J = 16 Hz, 1H), 7.95–7.90 (m, 2H), 7.76–7.70 (m, 3H), 7.56–7.54 (m, 5H), 7.21 (d, J = 10.0 Hz, 1H), 6.87 (d, J = 8.8 Hz, 2H), 3.79 (s, 3H); ^{13}C NMR (100 MHz, $\text{CDCl}_3+\text{DMSO}-d_6$) δ 167.44, 160.35, 150.21, 149.91, 137.21, 136.79, 135.30, 135.06, 132.33, 130.93, 130.58, 130.14, 129.67, 129.13, 129.07, 125.90, 123.05, 122.07, 37.89; HRMS (ESI, m/z): calcd. For $\text{C}_{30}\text{H}_{23}\text{ClN}_2\text{O}_4\text{SH}^+$ 437.0732, found 437.0727; IR (KBr thin film, cm^{-1}): ν_{max} 3396, 2999, 2894, 1651, 1558, 1352, 1149, 896, 780.



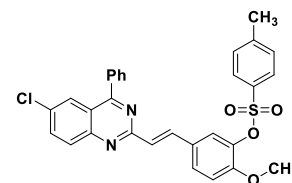
2-(2-(6-Chloro-4-phenylquinazolin-2-yl)vinyl)phenyl-4-methylbenzenesulfonate (20e): Pale green powder, mp 199–200 °C, 80% yield. ¹H NMR (400 MHz, CDCl₃+DMSO-d₆) δ 8.05–7.91 (m, 4H), 7.84 (s, 3H), 7.70 (s, 3H), 7.64 (d, J = 8.0 Hz, 2H), 7.44–7.39 (m, 2H), 7.29 (d, J = 7.2 Hz, 1H), 7.17 (d, J = 15.6 Hz, 1H), 7.01 (d, J = 7.6 Hz, 2H), 2.13 (s, 3H); ¹³C NMR (100 MHz, CDCl₃+DMSO-d₆) δ 167.32, 155.52, 147.32, 145.85, 143.87, 136.87, 134.96, 132.60, 131.90, 131.11, 130.84, 130.59, 130.44, 130.10, 130.02, 129.08, 128.40, 127.99, 127.49, 125.88, 123.83, 121.99, 118.12, 116.79, 21.50; HRMS (ESI, m/z): calcd. For C₂₉H₂₁ClN₂O₃SH⁺ 513.1045, found 513.1040; IR (KBr thin film, cm⁻¹): ν_{max} 3395, 2950, 1636, 1562, 1348, 1154, 975, 856, 765.



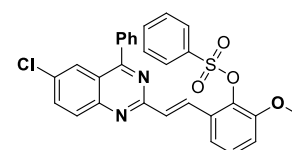
2-(2-(6-Chloro-4-phenylquinazolin-2-yl)vinyl)-6-methoxyphenyl-4-methylbenzenesulfonate (20f): Yellow powder, mp 173–174 °C, 82% yield. ¹H NMR (400 MHz, DMSO-d₆) δ 8.06–8.03 (m, 4H), 7.89–7.86 (m, 2H), 7.73–7.70 (m, 5H), 7.57 (d, J = 7.6 Hz, 1H), 7.37–7.30 (m, 3H), 7.22–7.15 (m, 3H), 3.64 (s, 3H), 2.08 (s, 3H); ¹³C NMR (100 MHz, DMSO-d₆) δ 167.25, 160.11, 153.02, 150.13, 145.68, 137.00, 136.69, 135.32, 133.40, 132.38, 131.87, 131.37, 131.16, 130.93, 130.70, 130.38, 130.25, 129.31, 128.56, 128.47, 125.99, 121.97, 118.87, 114.30, 56.33, 21.36; HRMS (ESI, m/z): calcd. For C₃₀H₂₃ClN₂O₄SH⁺ 543.1151, found 543.1142; IR (KBr thin film, cm⁻¹): ν_{max} 3396, 2980, 1650, 1534, 1328, 1150, 1070, 862.



5-(2-(6-Chloro-4-phenylquinazolin-2-yl)vinyl)-2-methoxyphenyl 4-methylbenzenesulfonate (20g): White powder, mp 210–211 °C, 81% yield. ¹H NMR (400 MHz, CDCl₃) δ 8.13 (d, J = 16.0 Hz, 1H), 8.04–8.01 (m, 2H), 7.83–7.76 (m, 5H), 7.63–7.61 (m, 3H), 7.39–7.30 (m, 3H), 7.18 (s, 1H), 7.15 (s, 1H), 3.62 (s, 3H), 2.45 (s, 3H); ¹³C NMR (100 MHz, CDCl₃+DMSO-d₆) δ 155.46, 153.29, 147.03, 145.47, 138.14, 137.46, 135.48, 133.16, 132.21, 132.15, 131.37, 130.17, 129.82, 129.77, 129.57, 129.20, 129.16, 129.11, 128.63, 126.48, 125.41, 119.68, 113.91, 57.10, 17.53; HRMS (ESI, m/z): calcd. For C₃₀H₂₃ClN₂O₄SH⁺ 543.1151, found 543.1146; IR (KBr thin film, cm⁻¹): ν_{max} 3396, 2980, 1650, 1534, 1328, 1150, 1070, 862.



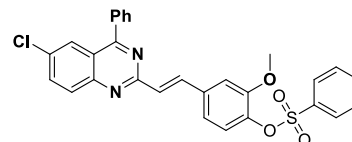
2-(2-(6-Chloro-4-phenylquinazolin-2-yl)vinyl)-6-methoxyphenyl benzenesulfonate (20h): Yellow powder, mp 225–226 °C, 82% yield. ¹H NMR (400 MHz, CDCl₃+DMSO-d₆) δ 8.14 (s, 1H), 8.10 (s, 1H), 8.06–8.03 (m, 1H), 7.98–7.94 (m, 3H), 7.84–7.82 (m, 2H), 7.67–7.62 (m, 2H), 7.55 (s, 1H), 7.51 (s, 1H), 7.39–7.31 (m, 3H), 3.97 (s, 3H); ¹³C NMR (100 MHz, CDCl₃+DMSO-d₆) δ 168.04, 154.67, 152.53, 146.29, 144.73, 137.39, 136.67, 135.21, 134.15, 133.50, 132.44, 131.40, 129.46, 129.39, 129.04, 128.41, 128.35, 127.90, 127.85, 126.50, 125.70,



124.68, 118.92, 113.06, 56.33; HRMS (ESI, m/z): calcd. For $C_{29}H_{21}ClN_2O_4SH^+$ 529.0994, found 529.0915; IR (KBr thin film, cm^{-1}): ν_{max} 3400, 2969, 1650, 1486, 1362, 1147, 1024, 874.

5-(2-(6-Chloro-4-phenylquinazolin-2-yl)vinyl)-2-methoxyphenyl benzenesulfonate (20i):

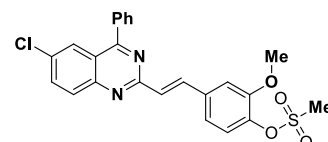
Pale yellow powder, mp 205–206 °C, 80% yield. 1H NMR (400 MHz, $CDCl_3$) δ 8.14–7.91 (m, 8H), 7.63–7.54 (m, 6H), 7.37 (d, J = 15.6 Hz, 1H), 7.28–7.15 (m, 3H), 3.59 (s, 3H); ^{13}C NMR (100 MHz, $CDCl_3$)



δ 170.37, 152.18, 149.60, 148.61, 148.55, 144.75, 136.94, 136.25, 135.37, 133.88, 133.30, 132.52, 131.14, 131.01, 130.86, 130.63, 130.53, 130.14, 130.11, 129.62, 128.72, 127.39, 127.29, 126.15, 54.57; HRMS (ESI, m/z): calcd. For $C_{29}H_{21}ClN_2O_4SH^+$ 529.0994, found 529.2456. IR (KBr thin film, cm^{-1}): ν_{max} 3080, 2985, 1660, 1490, 1370, 1130, 1010, 835.

5-(2-(6-Chloro-4-phenylquinazolin-2-yl)vinyl)-2-methoxyphenyl methanesulfonate (20j):

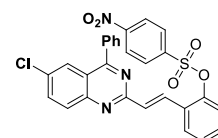
White solid, mp 264–265 °C, 82% yield. 1H NMR (400 MHz, $CDCl_3+DMSO-d_6$) δ 8.27 (d, J = 15.6 Hz, 1H), 8.01 (d, J = 7.6 Hz, 1H), 7.70–7.50 (m, 7H), 7.35–7.26 (m, 2H), 7.19 (s, 1H), 7.10 (d, J = 7.6 Hz, 1H), 3.94 (s, 3H), 3.48 (s, 3H); ^{13}C NMR (100 MHz, $CDCl_3+DMSO-d_6$) δ 168.24, 161.17, 152.86, 150.95, 139.56, 138.46, 137.53, 137.16, 135.87, 133.04, 131.68, 131.36, 130.91, 130.01, 129.85, 126.67, 125.36, 122.82, 121.64, 113.40, 57.31, 39.54; HRMS



(ESI, m/z): calcd. For $C_{24}H_{19}ClN_2O_4SH^+$ 467.0838, found 467.0841; IR (KBr thin film, cm^{-1}): ν_{max} 3394, 1662, 1508, 1325, 1153, 970, 873.

2-(2-(6-Chloro-4-phenylquinazolin-2-yl)vinyl)phenyl-4-nitrobenzene sulfonate (20k):

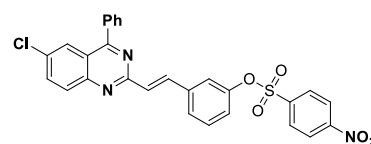
Yellow crystalline solid, mp 236–237 °C, 84% yield. 1H NMR (400 MHz, $CDCl_3+DMSO-d_6$) δ 8.04–7.94 (m, 3H), 7.80–7.74 (m, 4H), 7.63–7.45 (m, 7H), 7.29–7.19 (m, 3H), 6.90 (d, J = 8.0 Hz, 1H); ^{13}C NMR (100 MHz,



$CDCl_3+DMSO-d_6$) δ 167.66, 160.31, 153.03, 151.67, 150.12, 149.45, 139.91, 139.61, 137.09, 136.71, 135.68, 135.35, 132.11, 131.06, 130.56, 130.27, 130.03, 129.51, 129.24, 126.01, 125.62, 125.54, 123.45, 123.03; HRMS (ESI, m/z): calcd. For $C_{28}H_{18}ClN_3O_5SH^+$ 544.0728, found 544.0744; IR (KBr thin film, cm^{-1}): ν_{max} 3400, 3105, 1651, 1538, 1347, 1191, 1088, 900, 779.

3-(2-(6-Chloro-4-phenylquinazolin-2-yl)vinyl)phenyl 4-nitrobenzenesulfonate (20l):

Pale yellow solid, mp 201–203 °C, 85% yield. 1H NMR (400 MHz, $CDCl_3$) δ 8.22 (d, J = 16.0 Hz, 1H), 8.04–7.99 (m, 2H), 7.82 (s, 4H), 7.69–7.62 (m, 6H), 7.46–7.35 (m, 5H); ^{13}C NMR (100 MHz,

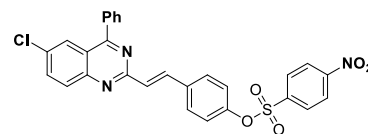


$CDCl_3+DMSO-d_6$) δ 168.50, 154.58, 152.70, 149.83, 142.20, 138.93, 136.70, 134.88, 134.68, 133.14, 131.72, 130.67, 130.43, 130.38, 129.98, 128.93, 128.15, 127.61, 126.25, 125.75, 125.45,

121.31, 119.89, 118.11; HRMS (ESI, m/z): calcd. For $C_{28}H_{18}ClN_3O_5SNH_4^+$ 561.0994, found 561.0738.

4-(2-(6-Chloro-4-phenylquinazolin-2-yl)vinyl)phenyl 4-nitrobenzenesulfonate (20m): Pale

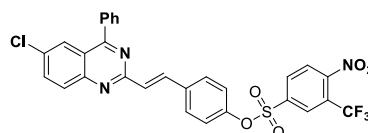
yellow solid, mp 218–219 °C, 81% yield. 1H NMR (400 MHz, $CDCl_3$) δ 8.04–7.95 (m, 3H), 7.80–7.73 (m, 5H), 7.61–7.55 (m, 4H), 7.48–7.45 (m, 3H), 7.24–7.18 (m, 2H), 6.90 (d, J = 8.0 Hz, 1H); ^{13}C



NMR (100 MHz, $CDCl_3$ +DMSO- d_6) δ 154.03, 151.78, 149.38, 148.75, 137.42, 134.47, 134.06, 133.66, 131.61, 131.02, 129.50, 129.09, 128.80, 128.25, 127.66, 127.44, 125.73, 122.96, 122.59, 121.59, 119.92, 114.54; HRMS (ESI, m/z): calcd. For $C_{28}H_{18}ClN_3O_5SH^+$ 544.0728, found 544.0746; IR (KBr thin film, cm^{-1}): ν_{max} 3395, 3098, 1650, 1557, 1536, 1364, 1202, 1090, 839.

4-(2-(6-Chloro-4-phenylquinazolin-2-yl)vinyl)phenyl-4-nitro-3-(trifluoromethyl) benzene sulfonate (20n): Light Brown solid, mp 175–176 °C, 80% yield. 1H NMR (400 MHz,

$CDCl_3$ +DMSO- d_6) δ 8.57 (s, 1H), 8.26–8.20 (m, 4H), 8.09 (d, J = 9.6 Hz, 1H), 8.00 (s, 2H), 7.87 (s, 3H), 7.74–7.61 (m, 5H); ^{13}C NMR (100 MHz, DMSO- d_6) δ 155.33, 153.06, 150.08, 149.44, 141.49,

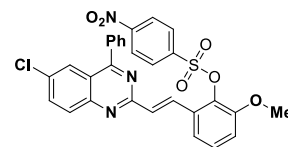


141.30, 141.10, 132.10, 131.66, 129.64, 129.61, 129.26, 129.16, 128.92, 128.35, 127.52, 127.34, 125.29, 125.10, 123.84, 123.80, 123.62, 123.40, 117.87, 117.83; HRMS (ESI, m/z): calcd. For $C_{29}H_{17}ClF_3N_3O_5S$ 611.0530, found 610.1852; IR (KBr thin film, cm^{-1}): ν_{max} 3390, 2901, 1650, 1532, 1345, 1115, 1031, 865.

2-(2-(6-Chloro-4-phenylquinazolin-2-yl)vinyl)-6-methoxyphenyl-4-nitrobenzenesulfonate (20o):

Yellow solid, mp 184–185 °C, 82% yield. 1H NMR (400 MHz, DMSO- d_6)

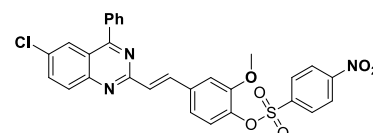
δ 8.37 (d, J = 7.6 Hz, 2H), 8.07–7.75 (m, 8H), 7.58 (s, 3H), 7.37–7.13 (m, 4H), 3.54 (s, 3H); ^{13}C NMR (100 MHz, DMSO- d_6) δ 167.34, 159.81,



152.71, 150.81, 150.05, 141.78, 136.88, 136.56, 135.36, 132.53, 131.33, 131.12, 130.95, 130.70, 130.32, 130.24, 129.30, 129.24, 129.01, 125.93, 125.03, 121.93, 119.19, 114.44, 56.39; HRMS (ESI, m/z): calcd. For $C_{29}H_{20}ClN_3O_6SH^+$ 574.0834, found 574.0863; IR (KBr thin film, cm^{-1}): ν_{max} 3396, 2989, 1649, 1566, 1346, 1279, 1148, 1066, 833.

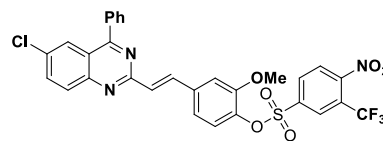
5-(2-(6-Chloro-4-phenylquinazolin-2-yl)vinyl)-2-methoxyphenyl-4-nitrobenzenesulfonate (20p): Yellow powder, mp 190–191 °C, 80% yield. 1H NMR (400

MHz, $CDCl_3$) δ 8.39 (d, J = 8.0 Hz, 2H), 8.14–8.00 (m, 5H), 7.83 (s, 3H), 7.64 (s, 3H), 7.39 (d, J = 16.0 Hz, 1H), 7.28 (s, 1H), 7.17 (s, 1H),

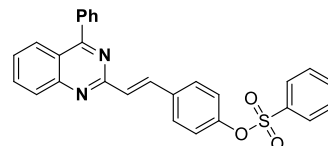


3.61 (s, 3H); ^{13}C NMR (100 MHz, DMSO- d_6) δ 167.70, 160.39, 151.76, 151.42, 150.14, 140.90, 138.13, 137.62, 136.97, 136.72, 135.38, 132.30, 131.04, 130.77, 130.46, 130.27, 129.65, 129.23, 126.03, 125.11, 124.45, 122.12, 121.06, 112.87, 56.24; HRMS (ESI, m/z): calcd. For $\text{C}_{29}\text{H}_{20}\text{ClN}_3\text{O}_6\text{SH}^+$ 574.0834, found 574.0864; IR (KBr thin film, cm^{-1}): ν_{max} 3401, 2960, 1630, 1508, 1348, 1154, 1074, 846.

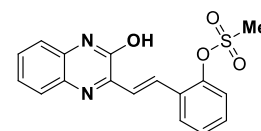
5-(2-(6-Chloro-4-phenylquinazolin-2-yl)vinyl)-2-methoxyphenyl-4-nitro-3-(trifluoromethyl) benzenesulfonate (20q): Light brown powder, mp 185–186 °C, 83% yield. ^1H NMR (400 MHz, CDCl_3) δ 8.37 (d, J = 8.4 Hz, 2H), 8.07–7.74 (m, 7H), 7.57 (s, 3H), 7.37–7.12 (m, 4H), 3.53 (s, 3H); ^{13}C NMR (100 MHz, CDCl_3 +DMSO- d_6) δ 166.24, 162.85, 159.61, 152.41, 149.11, 148.83, 137.93, 135.70, 135.53, 133.88, 133.68, 130.86, 130.72, 130.57, 130.43, 129.67, 129.43, 129.41, 129.38, 128.98, 128.95, 127.93, 127.89, 126.26, 124.75, 124.45, 104.35, 55.22; HRMS (ESI, m/z): calcd. For $\text{C}_{30}\text{H}_{19}\text{ClF}_3\text{N}_3\text{O}_6\text{S}$ 641.2635, found 641.2272.



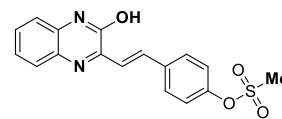
(E)-4-(2-(4-Phenylquinazolin-2-yl)vinyl)phenyl benzenesulfonate (20r): pale yellow solid, mp 196–197 °C, 80% yield. ^1H NMR (400 MHz, CDCl_3) δ 8.12 (d, J = 16.0 Hz, 1H), 8.02–7.97 (dd, J = 16.9, 5.2 Hz, 2H), 7.86–7.78 (m, 5H), 7.69–7.51 (m, 8H), 7.35 (d, J = 16.0 Hz, 1H), 7.02 (d, J = 8.4 Hz, 2H); ^{13}C NMR (100 MHz, CDCl_3) δ 167.52, 160.41, 150.22, 149.81, 137.17, 136.83, 135.39, 135.32, 134.71, 134.33, 132.75, 130.37, 130.32, 129.88, 129.21, 128.89, 128.84, 128.53, 125.97, 122.77, 122.16. IR (KBr thin film, cm^{-1}): ν_{max} 2982, 1615, 1512, 1375, 1185, 1068.



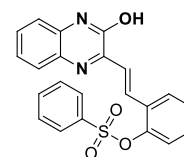
(E)-2-(2-(3-Hydroxyquinoxalin-2-yl)vinyl)phenyl methanesulfonate (21a): Yellow solid, mp 230–231 °C, 84% yield. ^1H NMR (400 MHz, DMSO- d_6 + CDCl_3) δ 12.39 (s, 1H), 8.06–7.94 (m, 1H), 7.70 (d, J = 7.2 Hz, 3H), 7.57 (d, J = 16.4 Hz, 1H), 7.44–7.14 (m, 5H), 3.24 (s, 3H); ^{13}C NMR (100Hz, CDCl_3 +DMSO- d_6) δ 168.98, 144.03, 142.60, 141.66, 139.56, 137.24, 135.89, 134.53, 133.16, 131.49, 128.53, 127.15, 125.68, 123.99, 122.33, 115.91, 38.53; HRMS (ESI, m/z): calcd. For $\text{C}_{17}\text{H}_{14}\text{N}_2\text{O}_4\text{SNa}^+$ 365.0566, found 365.0756; IR (KBr thin film, cm^{-1}): ν_{max} 3400, 2910, 283, 1640, 1574, 1366, 1151, 1067, 861.



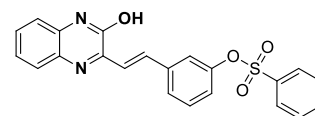
4-(2-(3-Hydroxyquinoxalin-2-yl)vinyl)phenyl methanesulfonate (21b): Pale red solid, mp 237–238 °C, 85% yield. ¹H NMR (400 MHz, CDCl₃+ DMSO-d₆) δ 12.23 (s, 1H), 8.01 (d, J = 16.0 Hz, 1H), 7.69–7.17 (m, 7H), 6.86 (d, J = 8.4 Hz, 2H), 3.77 (s, 3H); ¹³C NMR (100 MHz, CDCl₃+DMSO-d₆) δ 168.34, 148.65, 144.32, 138.86, 135.75, 134.21, 133.43, 131.71, 130.18, 128.72, 126.99, 126.00, 123.89, 113.10, 36.28; HRMS (ESI, m/z): calcd. For C₁₇H₁₄N₂O₄SNa⁺ 365.0566, found 365.0756; IR (KBr thin film, cm⁻¹): ν_{max} 3400, 3017, 2966, 1651, 1525, 1415, 1336, 1148, 992, 839.



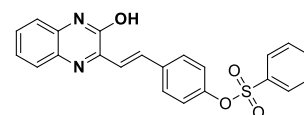
2-(2-(3-Hydroxyquinoxalin-2-yl)vinyl)phenyl benzenesulfonate (21c): Light green solid, mp 235–236 °C, 81% yield. ¹H NMR (400 MHz, DMSO-d₆) δ 12.54 (s, 1H), 7.96–7.82 (m, 5H), 7.69–7.65 (m, 1H), 7.56–7.27 (m, 9H); ¹³C NMR (100 MHz, CDCl₃+DMSO-d₆) δ 169.35, 158.32, 145.23, 138.19, 136.71, 136.30, 135.32, 134.44, 133.38, 132.39, 132.13, 129.50, 127.65, 127.30, 125.17, 124.22, 123.38, 121.11, 119.92, 118.67; HRMS (ESI, m/z): calcd. For C₂₂H₁₆N₂O₄SH⁺ 405.0904, found 405.0913; IR (KBr thin film, cm⁻¹): ν_{max} 3403, 2926, 2886, 1625, 1558, 1372, 1192, 1081, 880, 771.



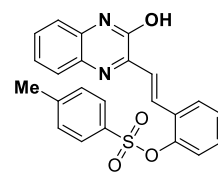
3-(2-(3-Hydroxyquinoxalin-2-yl)vinyl)phenyl benzenesulfonate (21d): Pale yellow solid, mp 221–222 °C, 84% yield. ¹H NMR (400 MHz, CDCl₃+DMSO-d₆) δ 12.31 (s, 1H), 9.58 (s, 1H), 8.02–7.92 (m, 2H), 7.71 (d, J = 6.8 Hz, 2H), 7.49–7.23 (m, 8H), 6.81 (d, J = 4.8 Hz, 2H); ¹³C NMR (100 MHz, CDCl₃+DMSO-d₆) δ 156.18, 153.72, 148.52, 135.85, 135.79, 133.79, 133.09, 131.38, 131.25, 131.13, 130.60, 130.56, 129.89, 129.61, 128.97, 128.19, 125.27, 124.75, 124.69, 116.71; HRMS (ESI, m/z): calcd. For C₂₂H₁₆N₂O₄SH⁺ 405.0904, found 405.0920; IR (KBr thin film, cm⁻¹): ν_{max} 3400, 2980, 1644, 1536, 1355, 1185, 958, 810, 762.



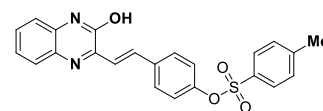
4-(2-(3-Hydroxyquinoxalin-2-yl)vinyl)phenyl benzenesulfonate (21e): Yellow solid, mp 202–203 °C, 85% yield. ¹H NMR (400 MHz, CDCl₃) δ 11.99 (s, 1H), 8.04 (d, J = 16.4 Hz, 1H), 7.80 (d, J = 7.6 Hz, 3H), 7.64–7.60 (m, 1H), 7.59–7.52 (m, 2H), 7.51–7.40 (m, 3H), 7.30–7.27 (m, 2H), 7.19 (s, 1H), 6.96 (d, J = 8.4 Hz, 2H); ¹³C NMR (100 MHz, CDCl₃+DMSO-d₆) δ 168.64, 150.50, 143.64, 139.53, 137.22, 135.86, 134.52, 133.16, 132.15, 130.13, 129.05, 127.06, 125.71, 124.68, 124.00, 122.62, 121.00, 117.96; HRMS (ESI, m/z): calcd. For C₂₂H₁₆N₂O₄SH⁺ 405.0904, found 405.0921.



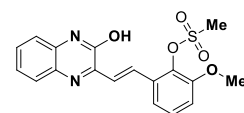
2-(2-(3-Hydroxyquinoxalin-2-yl)vinyl)phenyl 4-methylbenzenesulfonate (21f): Pale yellow powder, mp 224–225 °C, 81% yield. ¹H NMR (400 MHz, CDCl₃+DMSO-d₆) δ 12.30 (s, 1H), 7.85 (d, J = 16.0 Hz, 1H), 7.76 (d, J = 8.0 Hz, 1H), 7.69–7.62 (m, 4H), 7.45–7.42 (m, 1H), 7.37–7.28 (m, 5H), 7.11 (d, J = 8.0 Hz, 2H), 2.16 (s, 3H); ¹³C NMR (100 MHz, CDCl₃+ DMSO-d₆) δ 160.64, 154.42, 144.41, 141.13, 139.69, 138.66, 137.16, 135.98, 134.75, 134.05, 133.50, 132.96, 131.97, 130.41, 129.39, 127.81, 127.50, 126.56, 126.01, 119.71, 21.54; HRMS (ESI, m/z): calcd. For C₂₃H₁₈N₂O₄SH⁺ 419.1060, found 419.1082; IR (KBr thin film, cm⁻¹): ν_{max} 3395, 2986, 2877, 1665, 1527, 1353, 1374, 1196, 1083, 880.



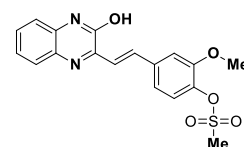
4-(2-(3-Hydroxyquinoxalin-2-yl)vinyl)phenyl-4-methylbenzenesulfonate (21g): Yellow solid, mp 229–230 °C, 84% yield. ¹H NMR (400 MHz, DMSO-d₆+CDCl₃) δ 12.32 (s, 1H), 7.99 (d, J = 16.0 Hz, 1H), 7.70–7.20 (m, 12H), 6.93 (d, J = 5.2 Hz, 1H), 2.40 (s, 3H); ¹³C NMR (100 MHz, CDCl₃+DMSO-d₆) δ 155.29, 153.08, 149.77, 145.92, 135.77, 135.65, 132.85, 132.09, 132.00, 130.31, 129.99, 129.15, 128.75, 128.53, 123.67, 123.44, 122.89, 115.67, 21.72; HRMS (ESI, m/z): calcd. For C₂₃H₁₈N₂O₄SH⁺ 418.0987, found 419.1079; IR (KBr thin film, cm⁻¹): ν_{max} 3396, 2932, 2893, 1666, 1590, 1430, 1372, 1176, 1091, 828.



2-(2-(3-Hydroxyquinoxalin-2-yl)vinyl)-6-methoxyphenyl methanesulfonate (21h): White solid, mp 243–244 °C, 80% yield. ¹H NMR (400 MHz, CDCl₃+DMSO-d₆) δ 12.50 (s, 1H), 8.35 (d, J = 16.0 Hz, 1H), 7.76 (d, J = 8.0 Hz, 1H), 7.64 (d, J = 16.4 Hz, 1H), 7.512–7.455 (m, 2H), 7.39–7.26 (m, 3H), 7.17 (d, J = 8.0 Hz, 1H), 3.91 (s, 3H), 3.49 (s, 3H); ¹³C NMR (100 MHz, CDCl₃) δ 168.44, 162.05, 151.23, 150.19, 139.89, 137.99, 135.60, 133.25, 131.22, 130.89, 130.24, 129.81, 126.70, 123.00, 112.10, 110.3, 56.87, 30.73; HRMS (ESI, m/z): calcd. For C₁₈H₁₆N₂O₅SH⁺ 373.0853, found 373.0870; IR (KBr thin film, cm⁻¹): ν_{max} 3400, 2910, 283, 1640, 1574, 1366, 1151, 1067, 861.

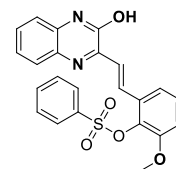


5-(2-(3-Hydroxyquinoxalin-2-yl)vinyl)-2-methoxyphenyl methane sulfonate (21i): Yellow crystalline solid, mp 207–208 °C, 82% yield. ¹H NMR (400 MHz, CDCl₃+ DMSO-d₆) δ 12.27 (s, 1H), 8.04 (d, J = 16.0 Hz, 1H), 7.74 (d, J = 8.0 Hz, 1H), 7.64 (d, J = 8.0 Hz, 2H), 7.56–7.44 (m, 1H), 7.37–7.33 (m, 1H), 7.24–7.23 (m, 1H), 7.10–7.06 (m, 2H), 3.52 (s, 3H), 2.38 (s, 3H); ¹³C NMR (100 MHz, CDCl₃+ DMSO-d₆) δ 161.41, 158.70, 157.57, 151.10, 144.39, 142.42, 138.52, 137.48, 135.56, 135.20, 134.34, 129.45,

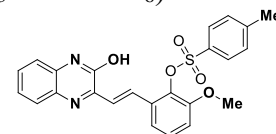


128.90, 126.35, 121.35, 116.76, 61.32, 27.41; HRMS (ESI, m/z): calcd. For $C_{18}H_{16}N_2O_5SNa^+$ 395.0672, found 395.0689; IR (KBr thin film, cm^{-1}): ν_{max} 3401, 2935, 2884, 1655, 1587, 1415, 1347, 1154, 1090, 843.

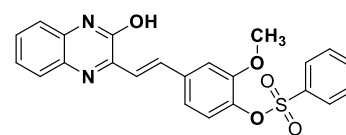
2-(2-(3-Hydroxyquinoxalin-2-yl)vinyl)-6-methoxyphenyl benzenesulfonate (21j): Pale green solid, mp 223–224 °C, 80% yield. 1H NMR (400 MHz, $CDCl_3$ +DMSO- d_6) δ 8.13–8.03 (m, 2H), 8.01–7.82 (m, 2H), 7.84–7.82 (m, 2H), 7.67–7.62 (m, 4H), 7.56 (s, 1H), 7.52 (s, 1H), 7.39–7.31 (m, 2H), 3.97 (s, 3H); ^{13}C NMR (100 MHz, $CDCl_3$ +DMSO- d_6) δ 159.95, 157.57, 142.05, 141.40, 138.97, 137.49, 136.89, 136.71, 134.96, 134.82, 134.06, 133.71, 133.09, 132.85, 129.08, 128.42, 123.05, 120.43, 118.21, 60.70; HRMS (ESI, m/z): calcd. For $C_{23}H_{18}N_2O_5SH^+$ 435.1009, found 435.1017; IR (KBr thin film, cm^{-1}): ν_{max} 3398, 1666, 1576, 1449, 1376, 1205, 1084, 766.



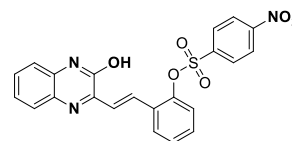
2-(2-(3-Hydroxyquinoxalin-2-yl)vinyl)-6-methoxyphenyl 4-methylbenzenesulfonate (21k): Light brown solid, mp 222–223 °C, 75% yield. 1H NMR (400 MHz, $CDCl_3$ +DMSO- d_6) δ 12.39 (s, 1H), 7.94–7.81 (m, 1H), 7.73–7.69 (m, 3H), 7.49–7.43 (m, 2H), 7.36–7.27 (m, 4H), 7.22 (d, J = 8.0 Hz, 2H), 7.03 (d, J = 7.6 Hz, 1H), 3.72 (s, 3H), 2.12 (s, 3H); ^{13}C NMR (100 MHz, $CDCl_3$ +DMSO- d_6) δ 159.88, 157.83, 157.51, 149.94, 142.16, 138.41, 137.46, 136.85, 136.54, 135.02, 134.81, 134.57, 133.66, 133.12, 132.76, 128.74, 128.43, 123.05, 120.40, 118.29, 60.84, 26.06; HRMS (ESI, m/z): calcd. For $C_{24}H_{20}N_2O_5SH^+$ 449.1166, found 449.1187; IR (KBr thin film, cm^{-1}): ν_{max} 3389, 2835, 1650, 1573, 1354, 1083, 811.



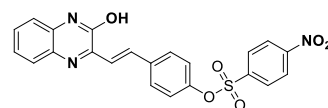
(E)-4-(2-(3-Hydroxyquinoxalin-2-yl)vinyl)-2-methoxyphenyl benzenesulfonate (21l): Yellow solid, mp 197–198 °C, 78 % yield. 1H NMR (400 MHz, DMSO- d_6 + $CDCl_3$) δ 12.29 (s, 1H), 7.89–7.82 (m, 3H), 7.68–7.63 (m, 1H), 7.50–7.20 (m, 9H), 6.92 (d, J = 6.8 Hz, 1H), 3.61 (s, 3H); ^{13}C NMR (100 MHz, $CDCl_3$ +DMSO- d_6) δ 157.95, 155.57, 140.05, 139.40, 136.97, 135.49, 134.89, 134.71, 132.96, 132.82, 132.06, 131.71, 131.09, 130.85, 127.08, 126.42, 121.05, 118.43, 116.21, 58.70; HRMS (ESI, m/z): calcd. For $C_{23}H_{18}N_2O_5SH^+$ 435.1009, found 435.1026; IR (KBr thin film, cm^{-1}): ν_{max} 3410, 2928, 2845, 1659, 1504, 1355, 1114, 1030, 839.



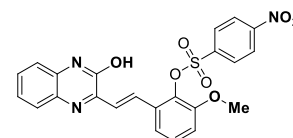
2-(2-(3-Hydroxyquinoxalin-2-yl)vinyl)phenyl-4-nitrobenzenesulfonate (21m): Pale yellow solid, mp 238–239 °C, 85% yield. ¹H NMR (400 MHz, CDCl₃+DMSO-d₆) δ 12.53 (s, 1H), 8.22 (d, J = 8.4 Hz, 2H), 8.08 (d, J = 8.4 Hz, 2H), 7.86–7.78 (m, 2H), 7.66 (d, J = 16.4 Hz, 1H), 7.59–7.43 (m, 3H), 7.42–7.23 (m, 4H); ¹³C NMR (100 MHz, CDCl₃+DMSO-d₆) δ 157.74, 155.10, 153.82, 149.96, 142.83, 135.43, 134.88, 133.47, 133.34, 133.17, 132.88, 131.89, 131.66, 131.28, 130.65, 130.42, 127.63, 126.82, 126.57, 118.50; HRMS (ESI, m/z): calcd. For Calculated Formula: C₂₂H₁₅N₃O₆SH⁺ 450.0754, found 450.0769; IR (KBr thin film, cm⁻¹): ν_{max} 3395, 2950, 2840, 1160, 1531, 1356, 1189, 1074, 821.



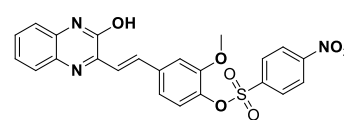
4-(2-(3-Hydroxyquinoxalin-2-yl)vinyl)phenyl-4-nitrobenzenesulfonate (21n): Yellow solid, mp 233–234 °C, 84% yield. ¹H NMR (400 MHz, CDCl₃+DMSO-d₆) δ 8.45–8.41 (m, 2H), 8.13–8.09 (m, 2H), 8.04–7.98 (m, 1H), 7.72 (dd, J = 7.6, 1.0 Hz, 1H), 7.64 (d, J = 8.4 Hz, 2H), 7.56 (d, J = 16.4 Hz, 1H), 7.43–7.38 (m, 1H), 7.29–7.22 (m, 2H), 7.05 (d, J = 8.4 Hz, 2H); ¹³C NMR (100 MHz, CDCl₃+DMSO-d₆) δ 160.08, 157.71, 155.98, 154.05, 145.09, 140.91, 140.28, 137.60, 136.80, 135.06, 134.75, 134.05, 133.50, 129.70, 128.49, 128.41, 127.50, 120.41; HRMS (ESI, m/z): calcd. For C₂₂H₁₅N₃O₆SH⁺ 450.0754, found 450.0756; IR (KBr thin film, cm⁻¹): ν_{max} 3396, 2886, 1664, 1532, 1405, 1360, 1149, 977, 855.



2-(2-(3-Hydroxyquinoxalin-2-yl)vinyl)-6-methoxyphenyl 4-nitrobenzenesulfonate (21o): Yellow solid, mp 229–230 °C, 82% yield. ¹H NMR (400 MHz, DMSO-d₆+CDCl₃) δ 12.49 (s, 1H), 8.33 (d, J = 7.8 Hz, 2H), 8.20 (t, J = 14.6 Hz, 2H), 7.77 (d, J = 16.0 Hz, 1H), 7.67 (d, J = 7.2 Hz, 1H), 7.51–7.28 (m, 6H), 7.18 (d, J = 8.0 Hz, 1H), 3.72 (s, 3H); ¹³C NMR (100 MHz, CDCl₃+DMSO-d₆) δ 159.72, 157.56, 157.29, 155.62, 146.63, 141.89, 137.28, 136.97, 136.21, 135.27, 134.97, 134.36, 133.61, 133.56, 129.69, 129.63, 128.64, 123.39, 120.50, 118.89, 61.07; HRMS (ESI, m/z): calcd. For C₂₃H₁₇N₃O₇SH⁺ 480.0860, found 480.0880; IR (KBr thin film, cm⁻¹): ν_{max} 3390, 3102, 2892, 1666, 1573, 1347, 1140, 1063, 887, 754.



5-(2-(3-Hydroxyquinoxalin-2-yl)vinyl)-2-methoxyphenyl-4-nitrobenzenesulfonate (21p): White solid, mp 218–219 °C, 78% yield. ¹H NMR (400 MHz, CDCl₃+DMSO-d₆) δ 12.33 (s, 1H), 8.35 (d, J = 8.8 Hz, 2H), 8.06–7.97 (m, 3H), 7.73–7.67 (m, 1H), 7.53 (d, J = 16.0 Hz, 1H), 7.38–7.33 (m, 1H), 7.26–7.13 (m, 5H), 3.53 (s, 3H); ¹³C NMR (100 MHz, CDCl₃+DMSO-d₆) δ 155.86, 153.71, 153.57, 153.44, 151.79, 142.73, 138.02, 133.41, 133.12, 132.32, 131.48, 131.13, 130.50, 129.77, 125.89, 125.79, 124.84, 119.56, 116.66, 115.12, 57.25; HRMS (ESI, m/z): calcd. For



C₂₃H₁₇N₃O₇SH⁺ 480.0860, found 480.0866; IR (KBr thin film, cm⁻¹): ν_{max} 3405, 2976, 2844, 1661, 1532, 1347, 1115, 851.

3.7 References

1. (a) Thomas, M.; Attila, A. P.; Farzaneh, P.; Santos, F and Prakash, G. K. S. *Chem. Soc. Rev.* **2017**, *46*, 3060–3094. (b) He. L.; Li, H.; Chen, J and Wu, X. F. *RSC Adv.* **2014**, *4*, 12065–12077. (c) Alagarsamy, V.; Chitra, K.; Saravanan, G.; Solomon, V. R.; Sulthana, M. T and Narendhar, B. *Eur. J. Med. Chem.* **2018**, *151*, 628–685. (d) Palem, J. D.; Alugubelli, G. R., Bantu, R; Nagarapu, L., Polepalli, S., Nishanth. J., S.; Bathini, R. and Manga. V. *Bioorg. Med. Chem. Lett.* **2016**, *26*, 3014–3018.
2. (a) Khan, I.; Zaib, S.; Batool, S.; Abbas, N.; Ashraf, Z.; Iqbal and, J.; Saeed, A. *Bioorg. Med. Chem. Lett.* **2016**, *24*, 2361–2381. (b) Yang, L.; Ge, S.; Huang, J and Bao, X. *Mol. Diversity.* **2018**, *22*, 71–82. (c) Hayun, S. H.; Hanafi, M. and Yanuar, A. *Pharmaceuticals*, **2012**, *5*, 1282–1290. (d) Tesfahunegn, R. G.; Bekhit, A. A and Hymete, A. *EC Pharm. Sci.* **2015**, *1*, 153–164. (e) Ugale, V. G and Bari, S. B. *Eur. J. Med. Chem.* **2014**, *80*, 447–501. (f) Jain, K. S.; Bariwal, J. B., Kathiravan, M. K.; Phoujdar, M. S.; Sahne, R. S.; Chauhan, B. S.; Shah, A. K and Yadav, M. R. *Bioorg. Med. Chem.* **2008**, *16*, 4759–4800. (g) Jiang, J. B.; Hesson, D. P.; Dusak, B. A.; Dexter, D. L.; Kang, G. J and Hamel, E. *J. Med. Chem.* **1990**, *33*, 1721–1728.
3. (a) Xin, M.; Hei, Y. -Y.; Zhang, H.; Shen, Y. and Zhang, S.-Q. *Bioorg. Med. Chem. Lett.* **2017**, *27*, 1972–1977. (b) Cruz- López, O.; Conejo-García, A.; Núñez M. C.; Kimatrai, M.; García-Rubín, M. E.; Morales, F.; Gómez-Pérez, V and Campos, J. M. *Curr. Med. Chem.* **2011**, *18*, 943–963. (c) Decker, M. *Eur. J. Med. Chem.*, **2005**, *40*, 305–313. (d) Li, S. -C.; Jhang, W. -F.; Liou, T.-J. and Yang, D. -Y. *Dyes Pigm.*, **2015**, *114*, 259–266. (e) Auti, P. S.; George, G and Paul, A. T. *RSC Adv.* **2020**, *10*, 41353–41392.
4. (a) Jiang, W., Beier, R. C., Wang, Z., Wu, Y and Shen, J. *J. Agric. Food Chem.* **2013**, *61*, 10018–10025. (b) Sehlstedt, U.; Aich, P.; Bergman, J.; Vallberg, H.; Nordén, B and Gräslund, A. *J. Mol. Biol.*, **1998**, *278*, 31–56. (c) Liu, Z.; Yu, S.; Di Chen, G. S.; Wang, Y.; Hou, L.; Lin, D.; Zhang, J and Ye, F. *Drug Des., Dev. Ther.* **2016**, *10*, 1489–1500. (d) Noolvi, M. N.; Patel, H. M.; Bhardwaj, V and Chauhan, A. *Eur. J. Med. Chem.* **2011**, *46*, 2327–2346. (e) Vieira, M.; Pinheiro, C.; Fernandes, R.; Noronha, J. P and Prudêncio, C. *Microbiol. Res.* **2014**, *169*, 287–293. (f) Rodrigues, F. A. R.; Bomfim, I. S.; Cavalcanti,

- B. C.; Pessoa, C. Ó.; Wardell, J. L.; Wardell, S. M. S. V.; Pinheiro, A. C.; Kaiser, C. R., Nogueira, T. C. M., Low, J. N.; Gomes, L. R and Souza, M. V. N. *Bioorg. Med. Chem.* **2014**, *24*, 934–939. (g) Hashem, A. A. A.; Gouda, M. A and Badria, F. A. *Eur. J. Med. Chem.*, 2010, *45*, 1976–1981 (h) Shintre, S. A.; Ramjugernath, D.; Islam, M. S.; Mopuri, R.; Mocktar, C. and Koorbanally, N. A. *Med. Chem. Res.* **2017**, *26*, 2141–2151.
5. (a) Tariq, S.; Alam, O and Amir, M. *Bioorg. Chem.* **2018**, *76*, 343–358. (b) He, W. Myers, M. R.; Hanney, B.; Spada, A. P.; Bilder, G.; Galzcinski, H.; Amin, D.; Needle, S.; Page, K.; Jayyosi, Z and Perrone, M. H. *Bioorg. Med. Chem. Lett.* **2003**, *13*, 3097–3100. (c) Guillon, J., Dallemagne, P.; Pfeiffer, B., Renard, P.; Manechez, D.; Kervran, A and Rault, S. *Eur. J. Med. Chem* **1998**, *33*, 293–308. (d) Wu, K.; Ai, J.; Liu, Q.; Chen, T. T.; X, Zhao, A.; Peng, Y. W.; Ji, Y.; Yao, Y. Q.; Xu, M. G. and Zhang, A. *Bioorg. Med. Chem. Lett.* **2012**, *22*, 6368–6372. (e) Mahajan, S.; Slathia, N.; Nuthakki, V. K.; Bharate, S. B and Kapoor, K. K. *RSC Adv.* **2020**, *10*, 15966–15975. (f) Rodrigues, J. H. S.; Ueda–Nakamura, T.; Correa, A. G.; Sangi, D. P and Nakamura, C. V. *PLoS One.* **2014**, *9*, 85706.
6. (a) Szydłowska, J.; Krzyczkowska, P.; Salamonczyk, M.; Gorecka, E.; Pocięcha, D.; Maranowski, B and Krowczyński A. *J. Mater. Chem. C*, **2013**, *1*, 6883–6889. (b) L.-N. Yang, S.-C. Li, Z.-S. Li and Q.-S. Li, *RSC Adv.* **2015**, *5*, 25079–25088.
7. (a) El-Sayed, M. A.-A.; El-Husseiny, W. M.; Abdel-Aziz, N. I.; El-Azab, A. S.; Abuelizz, H. A and Abdel-Aziz A. A. -M. *J. Enzyme Inhib. Med. Chem.* **2018**, *33*, 199–209. (b) Mrozek-Wilczkiewicz, A.; Kuczak, M.; Malarz, K.; Cieslik, W.; Spaczynska, E and Musiol, R. *Eur. J. Med. Chem.* **2019**, *117*, 338–349; (c) Latha, D. S and Yaragorla, S. *Eur. J. Org. Chem.* **2020**, *15*, 2155–2179. (d) Satyanarayana, N.; Sathish, K.; Nagaraju, S.; Pawar, R.; Faizan, M.; Arumugavel, M.; Shirisha, T and Kashinath, D. *New J. Chem.* **2022**, *46*, 1637–1642.
8. (a) Gao, J.; Pan, X.; Liu, J.; Lai, J.; Chang, L and Yuan, G. *RSC Adv.* **2015**, *5*, 27439–27442. (b) Pisani, L.; Bareletta, M.; Soto-Otero, R.; Nicolotti, O.; Mendez-Alvarez, E.; Catto, M.; Introcaso, A.; Stefanachi, A.; Cellamare, S.; Altomare, C and Carotti, A. *J. Med. Chem.* **2013**, *56*, 2651–2664. (c) El-Mekabaty, A and Habib, O. M. O. *Pet. Sci.* **2014**, *11*, 161–173. (c) Andleeb, H.; Tehseen, Y.; Jabeen, F.; Khan, I.; Iqbal, J and Hameed, S. *Bioorg. Chem.*, **2017**, *75*, 1–15. (e) Mahapatra, M. K.; Kumar, R. and Kumar, M. *Med. Chem. Res.* **2018**, *27*, 476–487. (f) Malarz, K.; Mularski, J.; Kuczak, M.; Mrozek-Wilczkiewicz, A and Musiol, R. *Cancers.* **2021**, *13*, 1790, DOI: 10.3390/cancers13081790.

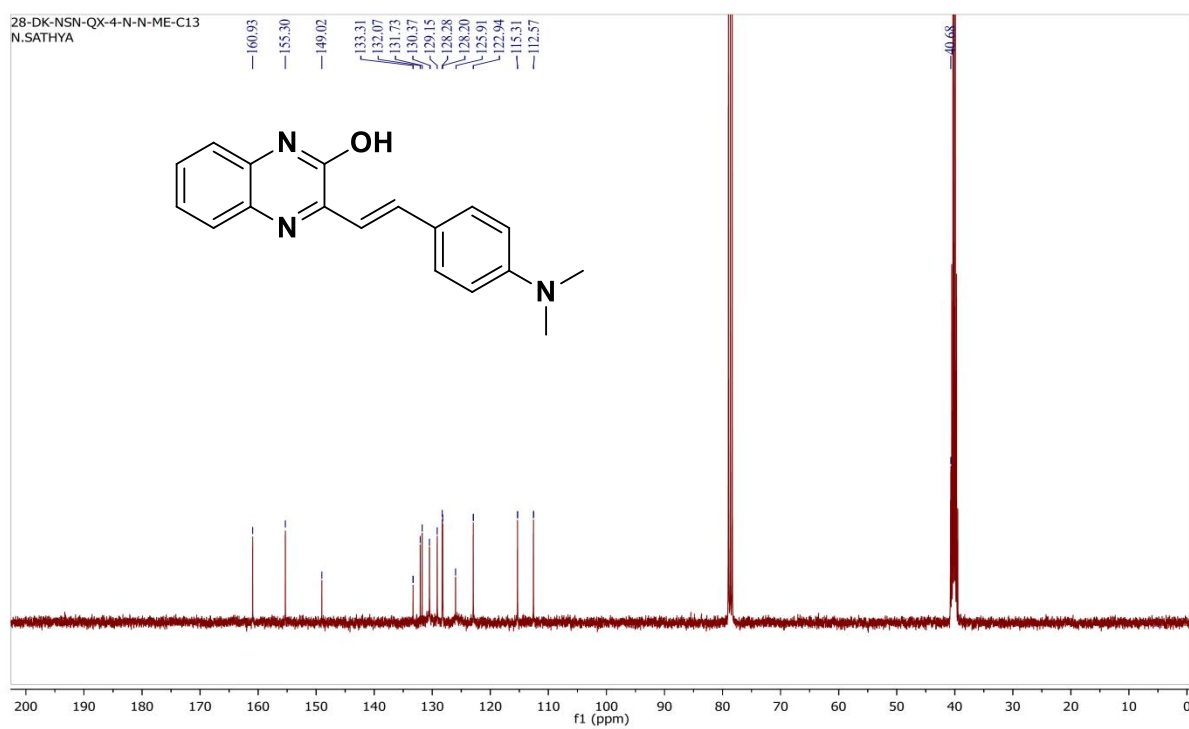
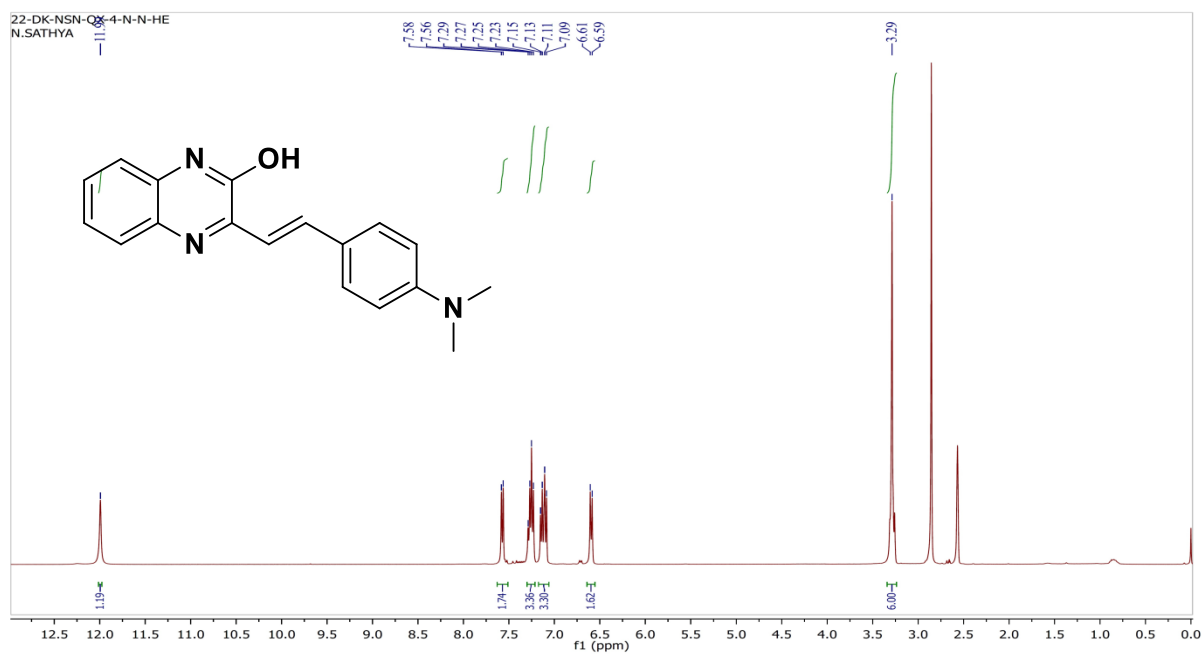
9. Ghani, U. *Alpha-Glucosidase inhibitors Clinically Promising Candidates for Antidiabetic Drug Discovery*, Elsevier, Amsterdam, Netherlands, **2020**.
10. (a) Abbas, G.; Al-Harrasi, A. S and Hussain, H. *Discovery and Development of Antidiabetic Agents from Natural Products Natural Product Drug Discovery*, ed. Brahmachari, G. Elsevier, Amsterdam, Netherlands, **2017**, 251–269. (b) Dirir, A. M.; Daou, M.; Yousef, A. F and Yousef, L. F. *Phytochem. Rev.* DOI: 10.1007/s11101-021-09773-1.
11. (a) Dhameja, M and Gupta P, *Eur. J. Med. Chem.*, **2019**, 176, 343–377. (b) Ghani, U. *Eur. J. Med. Chem.* **2015**, 103, 133–162.
12. (a) Sain, D. K.; Thadhaney, B.; Joshi, A.; Hussain, N & Talesara, G. L *Indian J. Chem.*, **2010**, 49B, 818-825. (b) Asif, H.; Diwakar, M.; Mohd, R.; Aftab, A. and Shah, A. Khan. *J. Enzyme Inhib. Med. Chem.* **2016**, 31(6), 1682–1689. (c) Krishnan, V. S. H.; Chowdary, K. S.; Dubey, P. K & Vijaya, S. *Indian J. Chem.* **2001**, 408, 565-573. (d) Sherif, M. H.; Assy, M. G.; Zahran, F and Khalil, A. *AFINIDAD LXV*, **2008**, 534, 156-162. (e) Fu, S.; Wang, L.; Dong, H.; Yu, J.; Xu, L.; Xiao, J. *Tetrahedron Lett.* **2016**, 57, 4533-4536. (f) El-Aoufir, Y.; Lgaz, H.; Bourazmi, H.; Kerroum, Y.; Ramli, Y.; Guenbour, A.; alghi, R. S.; El-Hajjaji, F.; Hammouti, B.; Oudda H. *J. Mater. Environ. Sci.* **2016**, 7 (12), 4330-4347. (g) Erivaldo, P. d. C.; Sara, E. C.; André, H. d. O.; Renata, M. A.; Livia, N. C.; Josiel, B. D.; Fabrício, G. M. *Tetrahedron Lett.* **2018**, 59, 3961–3964. (h) Kurasawa, Y.; Muramatsu, M.; Yamazaki, K.; Okamoto, Y.; Takada, A. *J. Heterocyclic Chem.* **1997**, 34 (1), 39-42. (i) da Costa, E. P.; Coelho, S. E.; de Oliveira, A. H.; Araujo, R. M.; Cavalcanti, L. N.; Domingos, J. B. and Menezes, F. G. *Tetrahedron Lett.* **2018**, 59 (44), 3961–3964.
13. (a) Maheswari, C. U.; Kumar, G. S.; Venkateshwar, M.; Kumar, R. A.; Kantam, M. L.; Reddy, K. R. *Adv. Synth. Catal.* **2010**, 352, 341-346. (b) Li-Zhu. W.; Xiu-Long, Y.; Qing-Yuan, Meng.; Xue-Wang, Gao.; Tao, Lei.; Cheng-Juan, W.; Bin, C. and Chen-Ho, T. *Asian J. Org. Chem.* **2016**, DOI: 10.1002/ajoc.201600550. (c) Tomoaki, Y.; Yukina, S.; Eiji, Y.; Norihiro, T. and Akichika, I. *Asian J. Org. Chem.* **2016**, 10.1002/ajoc.201600431. (d) Moumita, S.; Prasun, M.; Asish, R. D. *Tetrahedron Lett.* **2017**, 58, 2044–2049. (e) Han, B.; Yang, X.-L.; Wang, C.; Bai, Y.-W.; Pan, T.-C.; Chen, X.; Yu, W. *J. Org. Chem.* **2012**, 77, 1136-1142. (f) Chandi, C. M.; Raghuram, G.; Suvik, K. M.; Chinmoy, K. H.; Nagaraju, V.; Shiv, D.; Anil, K. and Uwe, B. *Eur. J. Org. Chem.* **2018**, 33, 4628-4638. (g) Zhang, Y.-G.; Xu, J.-K.; Li, X.-M.; Tian, S. -K. *Euro. J. Org. Chem.*, **2013**, 18, 3648-3652. (h) Aisha, Y. H. H.; Marwa, T. M. S.; Makarem, M. S.K.; Mona, S. F. E. -Z. *Open J. Med. Chem.* **2014**, 4, 12-37.

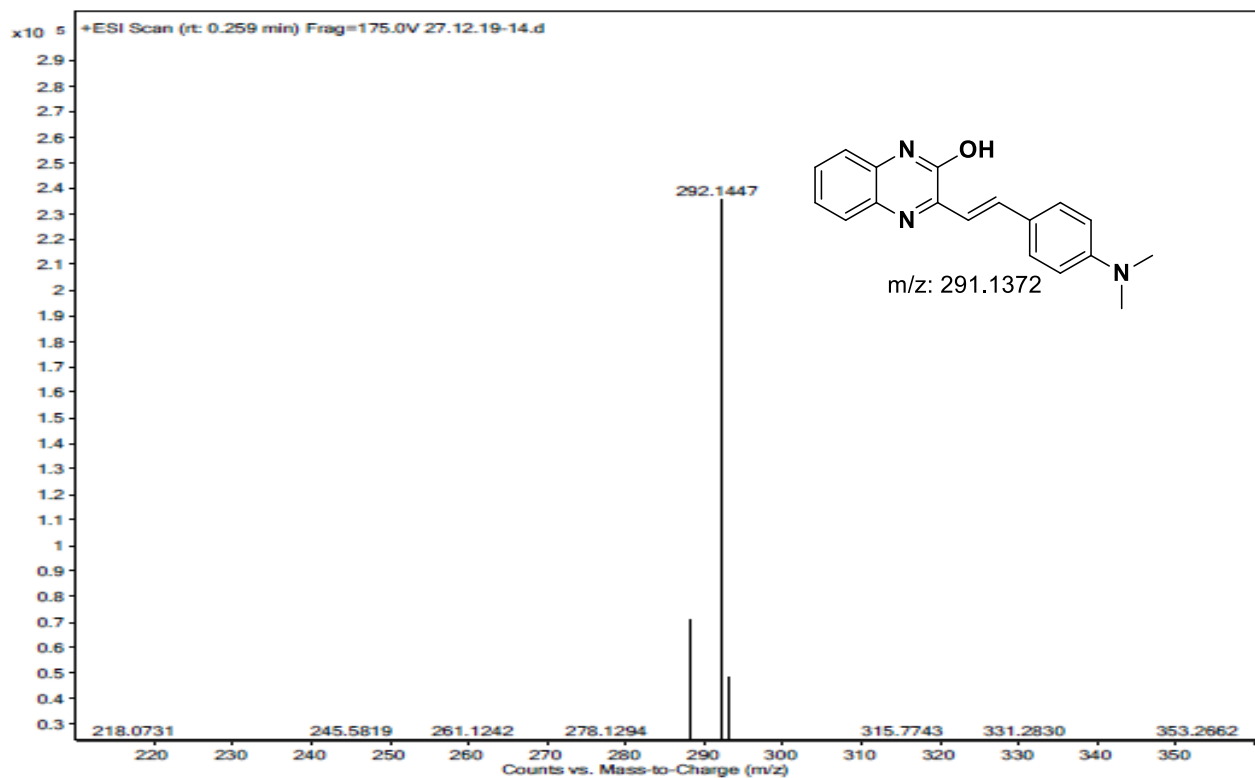
14. (a) Liang, G.; Li-Juan, Xing.; Tong, Xu.; Xue-Ping, Z.; Wen, Z.; Ning, K and Bin, W. *Org. Biomol. Chem.* **2014**, *12*, 6557-6560. (b) Sang, C. S.; Ki, T. L. and Maeng, S. K. *J. Org. Chem.* **1990**, *55*, 4316-4321. (c) José, B.; Fernando, Aznar.; Ramón, Liz.; María-Paz, C. *Synthesis*. **1985**, *3*, 313-314. (d) Dipak, J. D.; Aritra, G.; Sanjay, B. *Euro. J. Org. Chem.*, **2021**, *19*, 2746-2751.
15. (a) Prakasam, T.; Duraisamy, M.; Paramasivan, T. P. *Dyes Pigm.* **2009**, *81*, 245–253; (b) Luo, X and Lim, L. T. *Molecules*, **2019**, *24* (20), 3673.; (c) Imran, M.; Munawar, H.; Asad, A.; Serge-Mitthe, T. T.; Fatima, Z. B.; Christine, F.; Peter, L. *Tetrahedron*. **2010**, *66*, 1637–1642.
16. (a) P. Thirumurugan, D. Muralidharan, P. T. Perumal, *Dyes Pigm.* **2009**, *81*, 245–253. (b) Ujwal P. S.; Geetika, B.; Pallab, P. *Euro. J. org. Chem.*, **2018**, *10*, 1211-1217. (c) Jin-Hee, Park.; Darren, R. W.; Ji-Hyung, Lee.; So-Deok, L.; Je-Heon, L.; Hyojin, K.; Ga-Eun, L.; Sujin, K.; Jeong-Min, L.; Aliaa, A.; Christa, E. M.; Da-Woon, J and Yong-Chul, K. *J. Med. Chem.* **2016**, *59*, 16, 7410–7430. (d) Kato, B.; Silke, G.; Dorien, C.; Karolien, D. B. and Matthias, D. *J. Chem.* **2022**, *21*, ID 2164558. DOI: org/10.1155/2022/2164558.
17. Xu, H and Zhang, J. L. *Bioorg. Med. Chem. Lett.* **2011**, *21*, 5177–5180.
18. Xu, L.; Shao, Z.; Wang, L.; Zhao, H and Xiao, J. *Tetrahedron Lett.* **2014**, *55*, 6856–6860.
19. (a) Jagadish, K.; Bidhan, H.; Mrigank, S.; Verma, V. P.; Nagaraju, S.; Manabendra, C and Sriram, K. *Chemistry Select.* **2018**, *3*, 7416–7421. (b) Justin, T. K. R.; Velusamy, M.; Lin, J. T.; Chuen, C. H.; Tao, Y.-T. *Chem. Mater.* **2005**, *17*, 1860. (c) Rajeshkumar, R. M.; Si, H. H.; Jun, Y. L., Sung, Y. S. *Dyes Pigm.* **2018**, *153*, 132–136. (d) Kulkarni, A.P.; Zhu Y.; Jenekhe, S. A. *Macromolecules*, **2005**, *38*, 1553. (e) Lee, C.; Yang, W.; Parr, R. G. *Phys. Rev. B.* **1988**, *37*, 785–789.
20. (a) Deng, W.; Babu, I.; Su, R.; Yin, S. D.; Begley, T. J.; Dedon P. C. *LoS Genet.* **2015** *11*(12), 1005706. (b) Berna, E.; Amarila, M.; Purwa, I. S. M.; Bianca, L. *Int. J. Pharmtech Res.* **2012**, *4*, 1667-1671. (c) Farhad, P.; Reza, Yousefi.; Mohammad, H. M.; Ali, K. -N. *Carbohydr. Res.* **2013**, *380*, 81–91. (d) Zhenhua, Y.; Wei, Z.; Fajin, F.; Yong, Z.; Wenyi, K. *Food Sci. Hum. Wellness.* **2014**, *3*, 136–174. (e) Zhang, b. L.; Hogan, S.; Li, J.; Sun, S.; Canning, C.; Zheng, S. J. and Zhou, K. *Food Chem.* **2011**, *126*, 466–471.
21. (a) Kaur, R.; Kumar, R.; Dogra, N and Yadav, A. K. *J. Mol. Struct.* **2022**, *1247*, 131266. (b) Tavani, C.; Bianchi, L.; Palma, A. D.; Passeri, G. I.; Punzi, G.; Pierri, C. L.; Lovece, A.; Cavalluzzi, M. M.; Franchini, C.; Lentini, G and Petrillo, G. *Bioorg. Med. Chem. Lett.*, **2017**, *27*, 3980–3986.
22. Moghadam, E. S.; Faramarzi, M. A.; Imanparast, S and Amini, M. *Curr. Enzyme Inhib.*, **2020**, *16*, 155–161.

23. AMS DFTB, SCM, *Theoretical Chemistry*. Vrije Universiteit, Amsterdam, The Netherlands, 2020, <http://www.scm.com>.

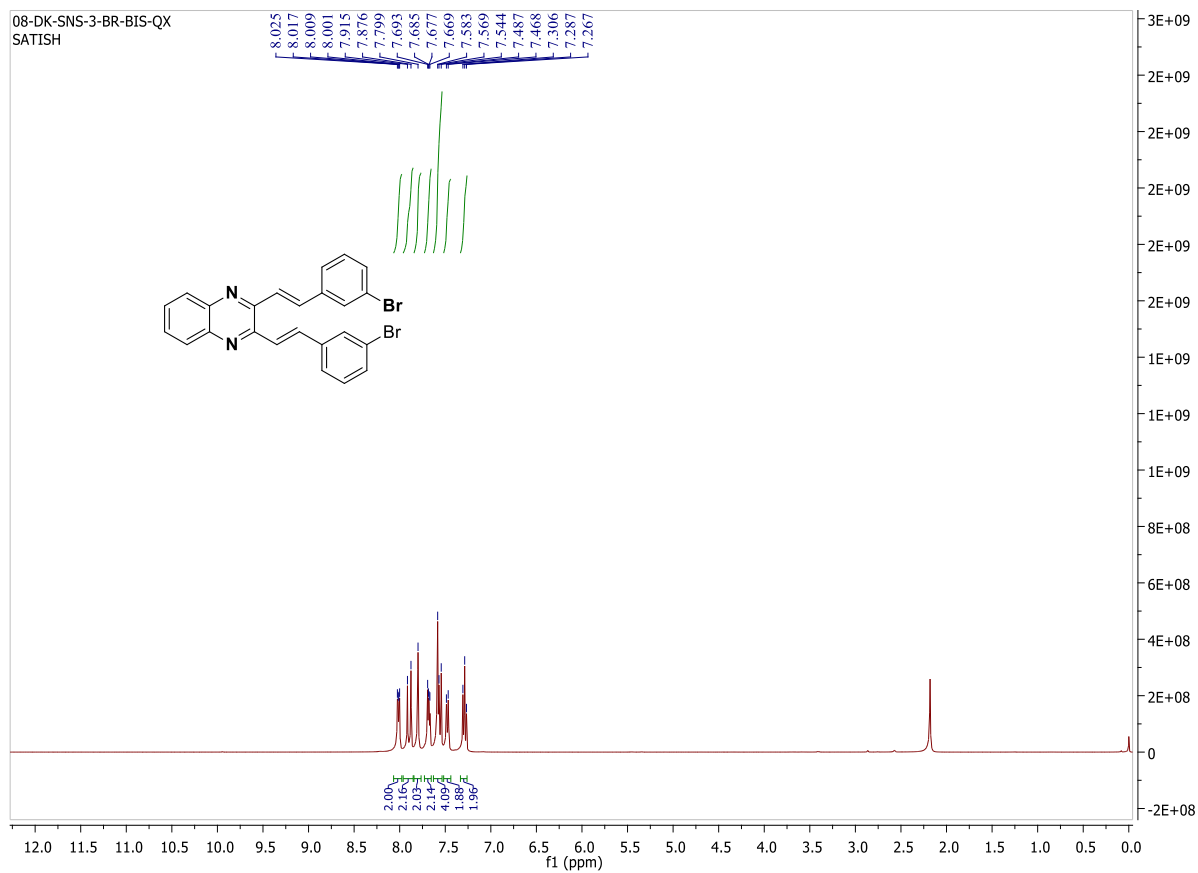
3.8 Selected spectral data:

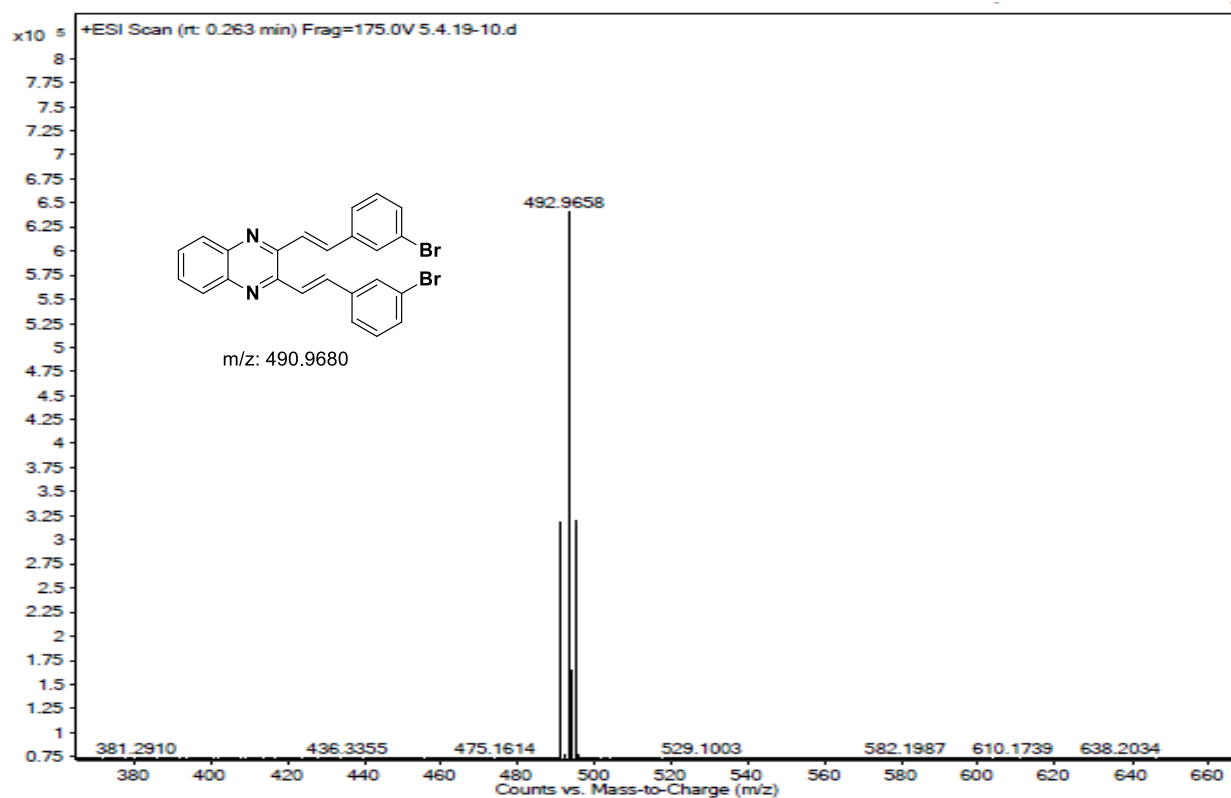
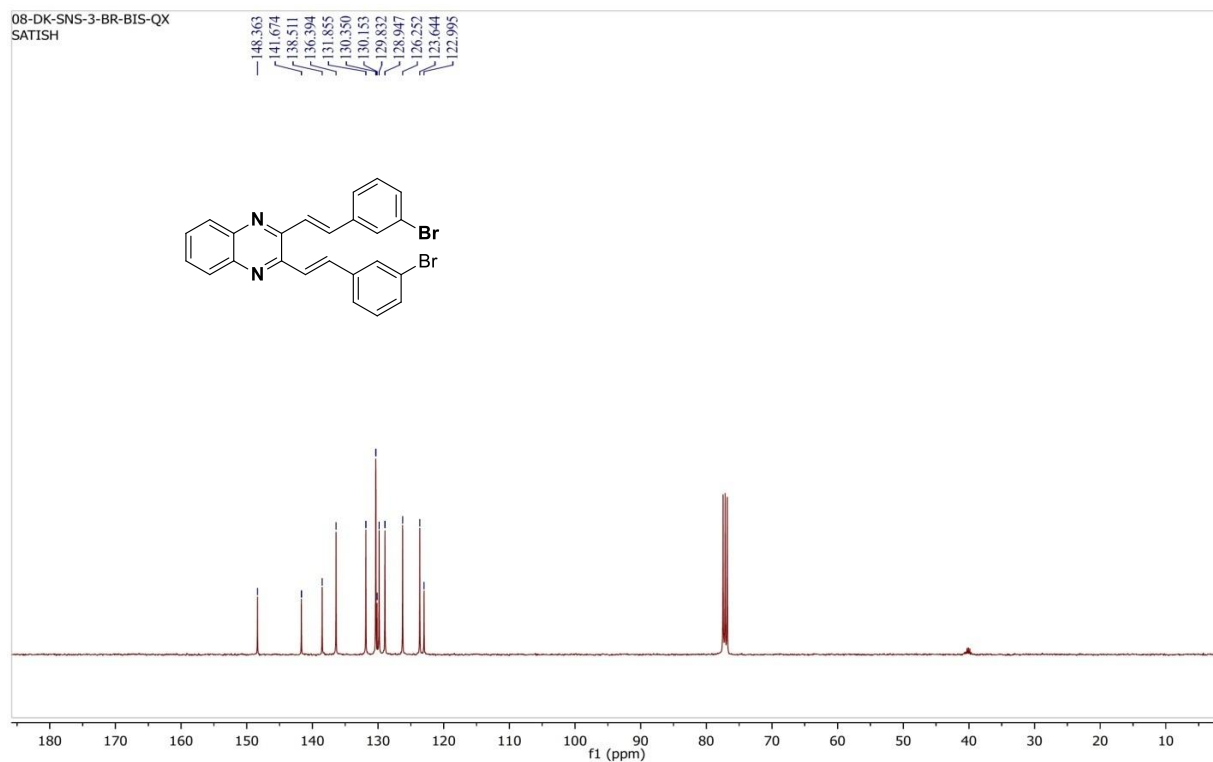
(E)-3-(4-(Dimethylamino)styryl)quinoxalin-2-ol (15m):



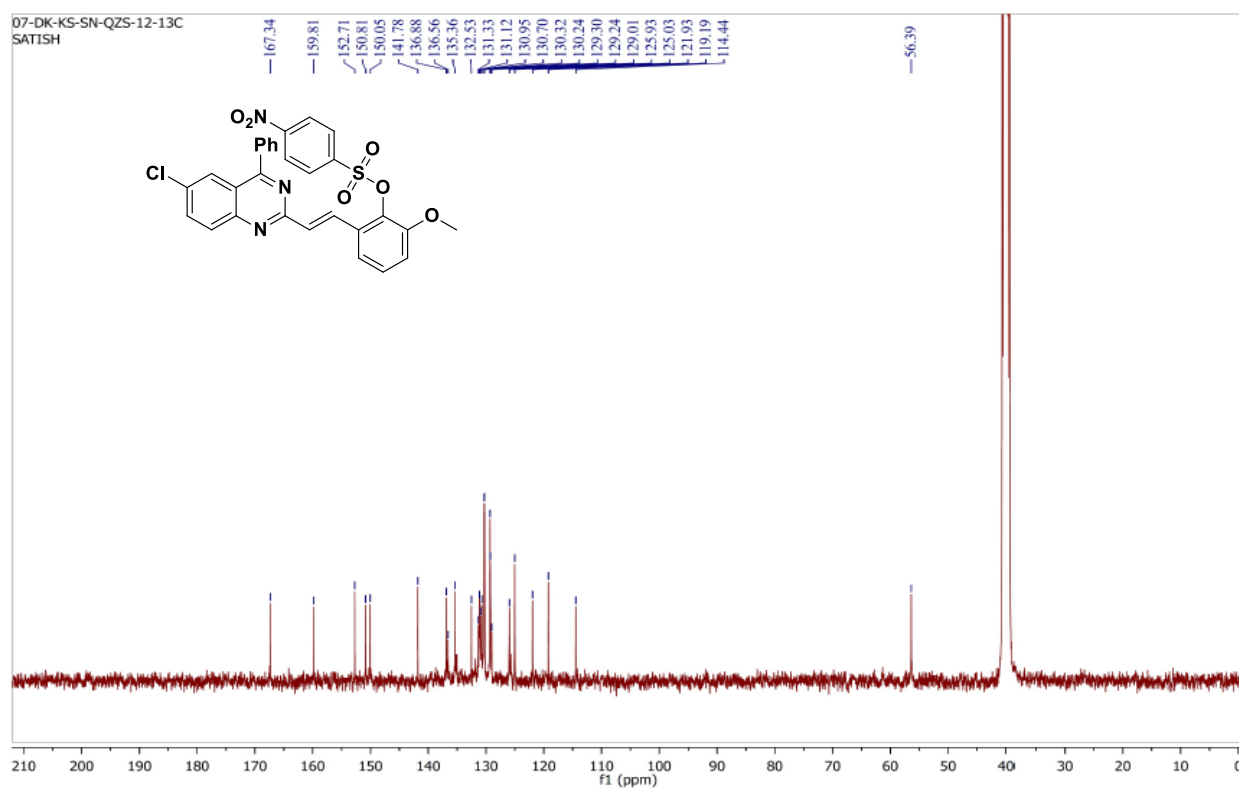
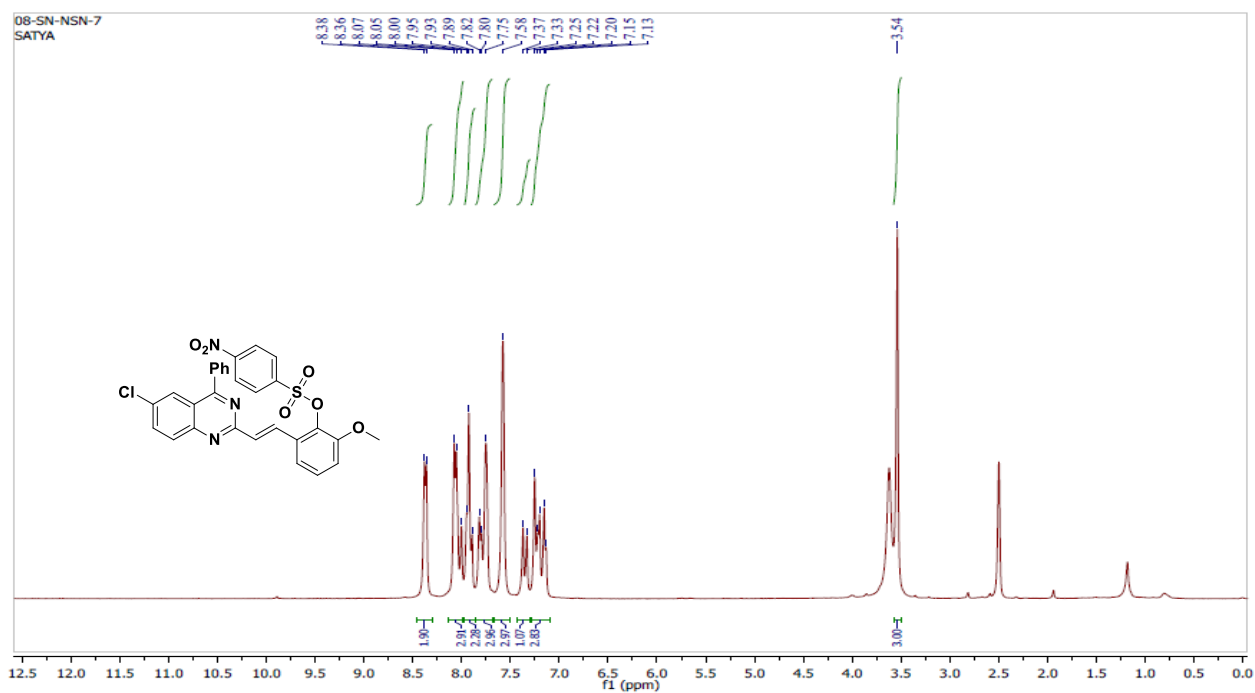


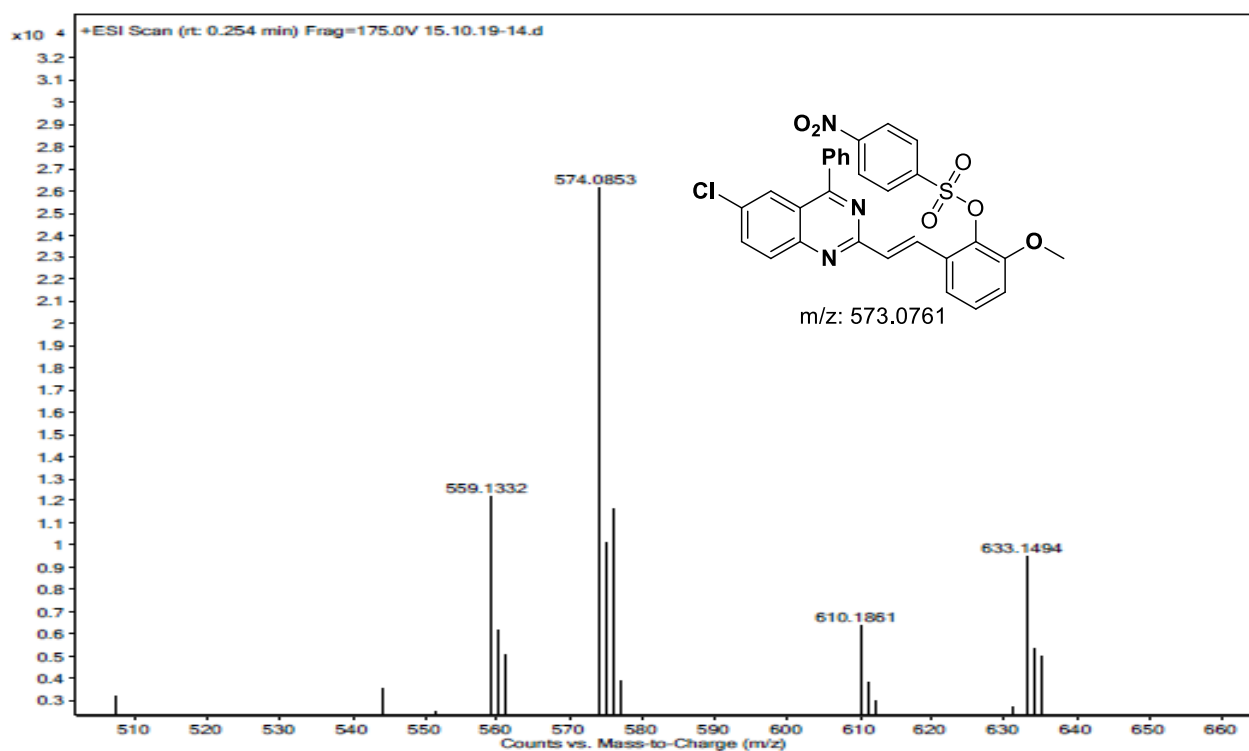
2,3-Bis((E)-3-bromostyryl)quinoxaline (14e):



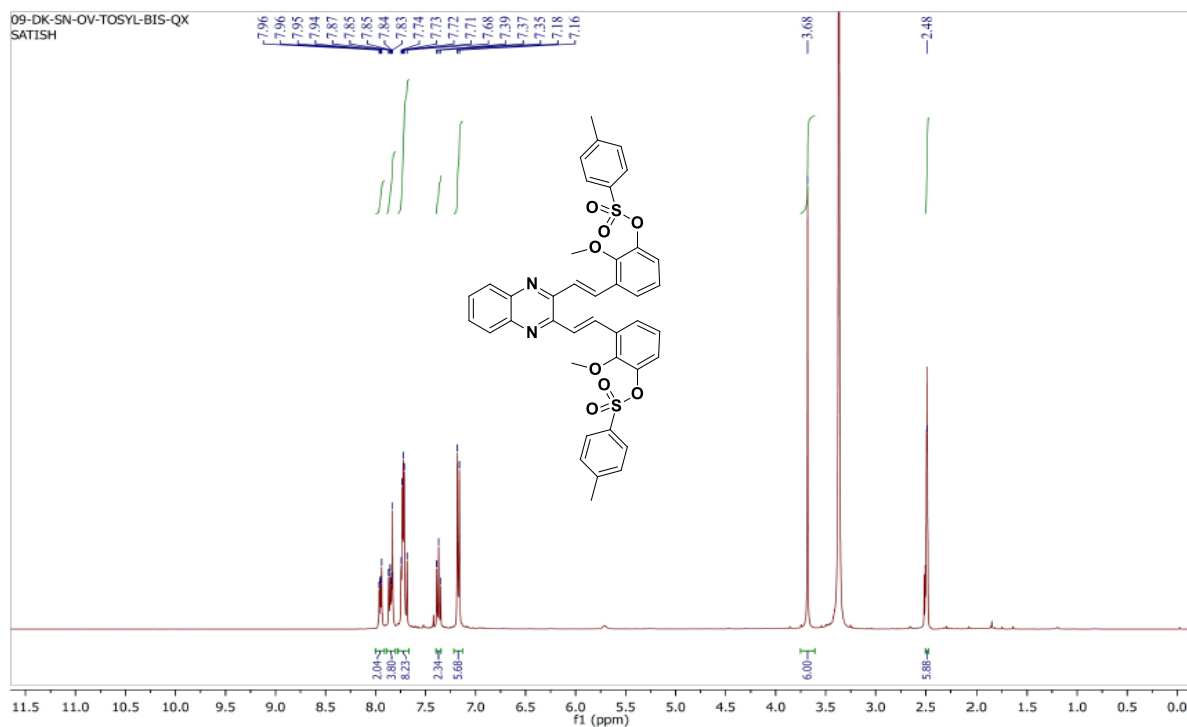


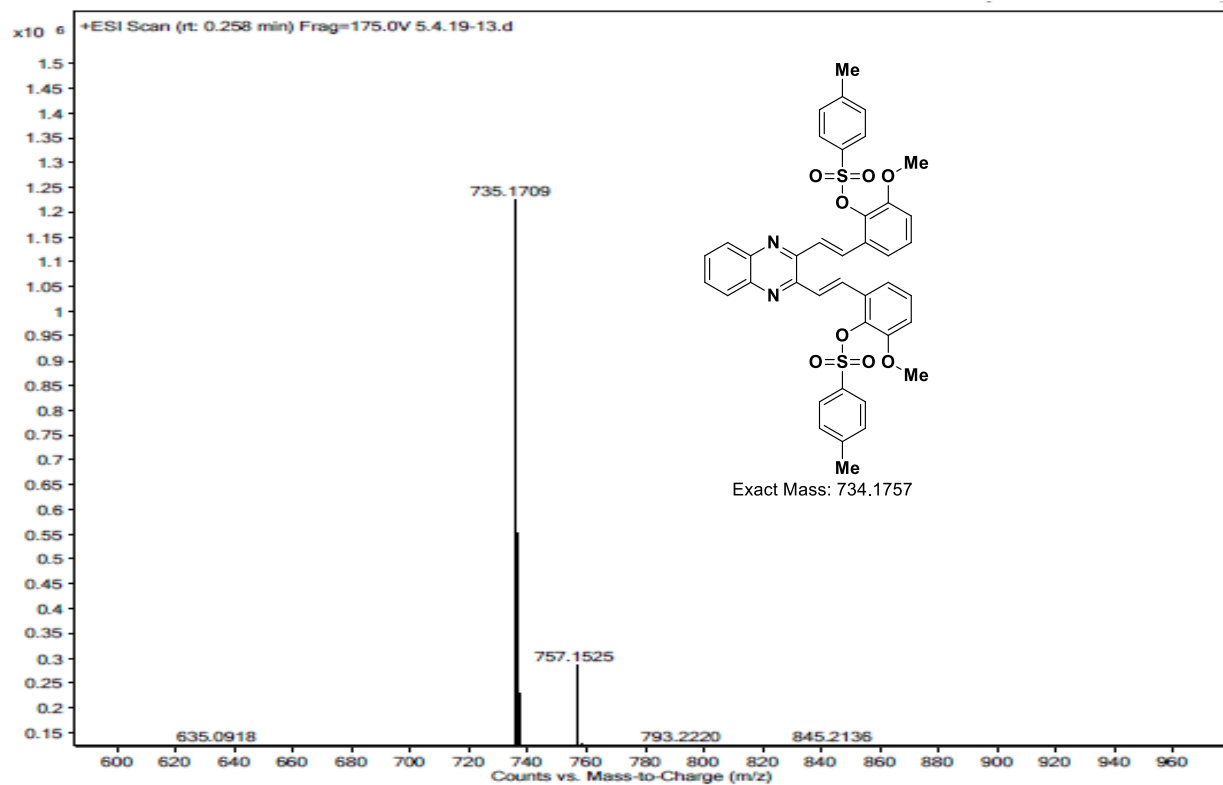
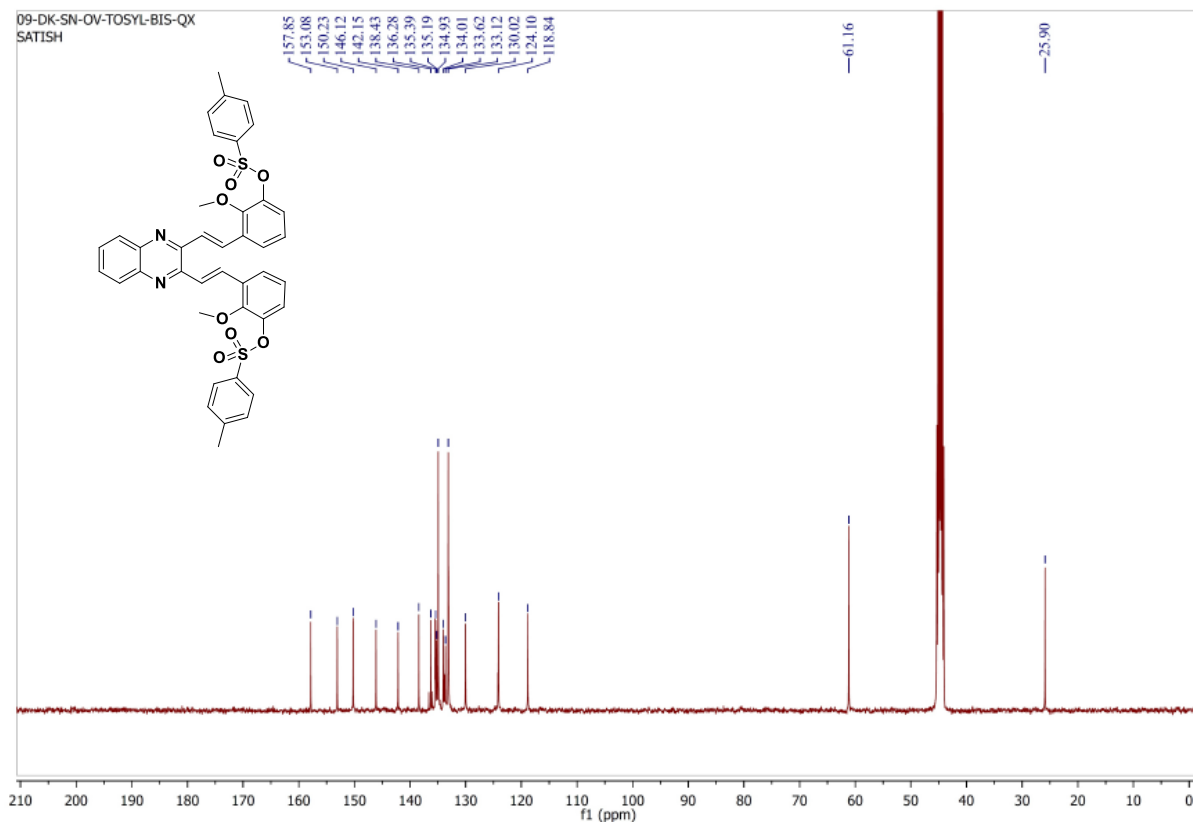
2-(2-(6-Chloro-4-phenylquinazolin-2-yl)vinyl)-6-methoxyphenyl 4-nitrobenzenesulfonate (20d):



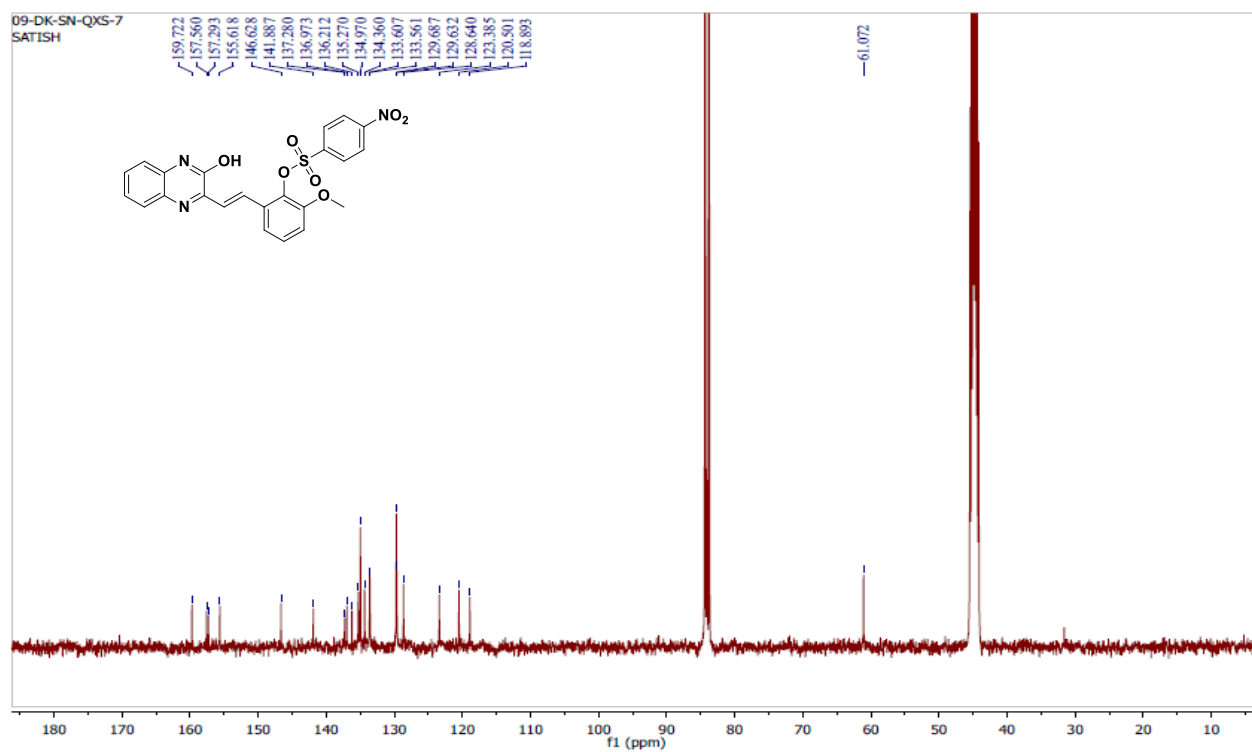
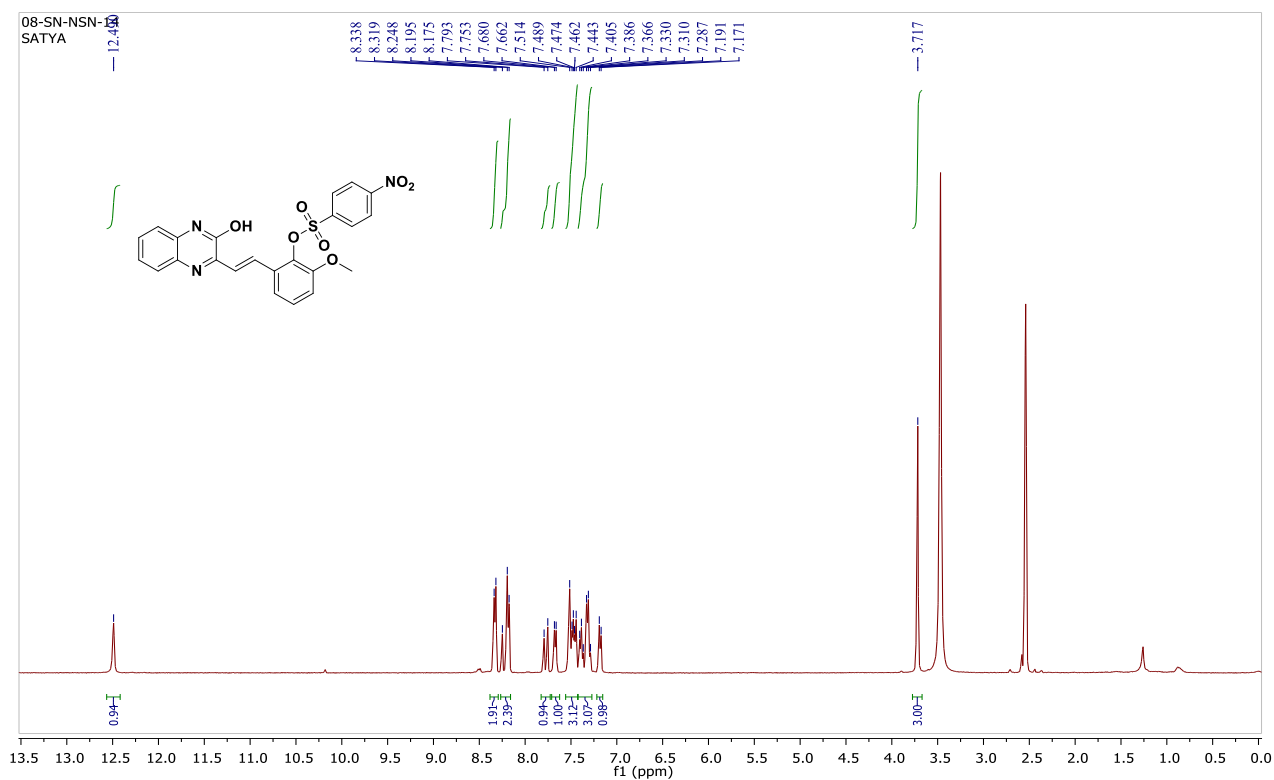


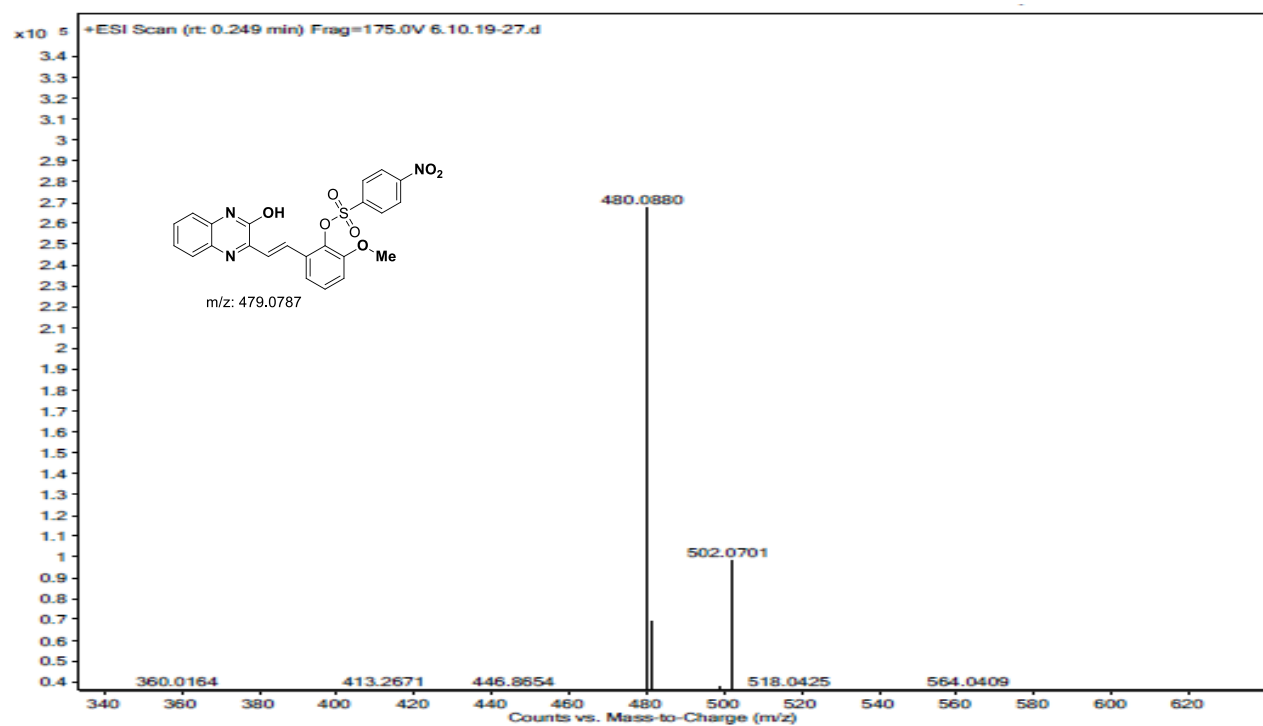
((1E,1'E)-Quinoxaline-2,3-diylbis(ethene-2,1-diyl))bis(2-methoxy-6,1-phenylene) bis(4-methylbenzenesulfonate) (18c):





2-(2-(3-Hydroxyquinoxalin-2-yl)vinyl)-6-methoxyphenyl 4-nitrobenzenesulfonate (21g):





CHAPTER-4

Synthesis of spiro and bicyclic thiolane derivatives via 1,4-Michael addition followed by intramolecular aldol reactions

Abstract

The substituted 2,4-thiazolidinedione, 3-nitro-2-phenyl-[2H]-chromene, and rhodamine motifs exhibit good biological activity. Particularly, tetrahydrothiophenes are part of coenzymes (e.g., biotin). Considering this, the synthesis of new spiro- and bicyclic 2,4-thiazolidinedione, rhodanine(2,4-thioxothiazolidinone), substituted 2-amino-4-one-thiazolidinedione and 3-nitro-[2H]-chromene–thiolane derivatives is described in this chapter. To achieve our goal, 1,4-dithiane-2,5-diol is used as a precursor with 2,4-thiazolidinedione and rhodanine via Knoevenagel condensation followed by 1,4-Sulfa-Michael addition and intramolecular Aldol reaction gave desired products.

4.1 Introduction

4.1.1 Synthetic methods for the tetrahydrothiophenes

Tetrahydrothiophenes (THT), a rare class of compounds found in natural products,^{1a} penicillins,^{1b} coenzymes (biotin)^{1c} and display inhibition activity for phosphodiesterase B,^{1d} antagonists for cholecystokinin type-B receptor,^{1e} FSH-receptor^{1f} and glucosidase inhibition (salacinol),^{1g} These moieties are also part of the drugs used for Hepatitis-B,^{2a} HIV,^{2b} arrhythmic^{2c} and diabetic activities.^{2d}

Limited synthetic approaches are known in the literature for the construction of tetrahydrothiophene derivatives. In 1992, Effenberger et al.^{2e} used 1,4-dithiane-2,5-diol (**1**; dimer of α -mercaptoacetaldehyde/2-sulfanylacetaldehyde) for the synthesis of substituted tetrahydrothiophenes by the action of α -mercaptoacetaldehyde and dihydroxyacetone phosphate by rabbit muscle aldolase (RAMA) as a catalyst. Since the applications of 1,4-dithiane-2,5-diol (**1**) got attention for the development of domino sulfa-Michael/aldol reactions to give tetrahydrothiophene rings^{2f} as a result many simple/complex, spiro- tetrahydrothiophene derivatives were synthesized in combinations with oxindole,^{2g} and chromanone as core structures.^{2h}

The bifunctionality of 1,4-dithiane-2,5-diol (electrophile (-CHO) and nucleophile (-SH)) was used for the preparation of thiazoles by Gewald and co-workers.^{3a} Later, Belleau^{3b} and Spino^{3c} groups used this molecule for the preparation of cyclic thia derivatives *via* Michael type addition and intramolecular aldol reactions which were further exploited for the diene generation. In 2006, Pollini and co-workers explored the bifunctional nature of 1,4-dithiane-2,5-diol (**1**) (-CHO as electrophile and -SH as nucleophile) for the tandem Michael–Henry or Michael–Michael reactions resulting in 3,4-disubstituted tetrahydrothiophenes.^{3d} Therefore, 1,4-dithiane-2,5-diol (**1**) leads to the development of tetrahydrothiophenes with three stereogenic centers which have been employed to construct additional C-C and C-S bonds. Particularly, monomeric α -mercaptaldehyde was used for this-Michael additions, domino reactions, [3+3]/[3+2]-cycloadditions, and aldol reactions. In addition, dithiane-2,5-diol (**1**) was used as an intermediate and key precursor for the synthesis of substituted tetrahydrothiophene hybrids like lamivudine /Epivir (antiviral agent-relative drug molecule)^{3e} **Figure-2**.

The reaction of 1,4-dithiane-2,5-diol (**1**) with simple chalcones (**2**) in presence of organocatalysts such as chiral squaramide^{4a} (as shown in **Figure-1**, catalyst-III, IV) gave (*E*)-2-benzylidenebenzofuran-3(2H)-one (**4**),^{4b} 2-arylidene-1,3-indandiones^{4(c-d)} (**6**) in enantioselective fashion.^{4e} (**3**, **5**, and **7**). These reactions proceed *via* Michael's addition followed by intramolecular aldol reactions. Similarly, 3-nitro-2-substituted thiophenes (**11**) were synthesized by the combination of 1,4-dithiane-2,5-diol (**1**) and nitrostyrene (**10**) using a catalytic amount of DDQ.^{5a} The DIPEA mediated diastereoselective sulfa-Michael/aldol domino reaction of arylidenepyrazolones (**8**) and 1,4-dithiane-2,5-diol (**1**) provided spiro[pyrazolone-4,3'-tetrahydrothiophenes (**9**).^{5b} In addition, asymmetric synthesis of spiro-tetrahydrothiophene-indan-1,3-diones were also achieved *via* squaramide-catalyzed^{5c} sulfa-Michael/Aldol domino reactions. In a similar report, polyacrylonitrile fiber (tertiary amine) was used as a catalyst for the reaction of 1,4-dithiane-2,5-diol (**1**) to result in functionalized tetrahydrothiophenes in a diastereoselective manner.^{5c} The derivatives of bicyclic pyrrolidone and thiophenes were synthesized *via* [3+2]-cycloaddition^{5d} reaction of maleimide (**12**) and 1,4-dithiane-2,5-diol (**1**) with excellent diastereoselectivity.

Similar to above reports, Lewis acid (BF₃·OEt₂)^{5e} catalyzed synthesis of 2,3-disubstituted thiophenes (**15**) from 2-aryl-3-nitro-cyclopropane-1,1-dicarboxylates (**14**) and 1,4-dithiane-2,5-diol (**1**) *via* ring-opening followed by rearrangement ([3+3]-annulation), Nef reaction, and subsequent tandem thia-Michael addition/aldol reactions is reported.^{5f} The stereoselective domino synthesis of spiro-tetrahydrothiophene containing chromanones^{5g} (**15,19**) using NEt₃^{5h} DBU,⁵ⁱ fused

oxindole-thiolane hybrids (**17**) using chiral squaramide, and quinine are known **Figure-1**.^{5j} Similarly, Rui Wang, et al.^{5k} described the application of chiral quinine-derived squaramide for asymmetric vinylogous 1,6-Michael addition of α,β -unsaturated γ -butyrolactone starting from 3-methyl-4-nitro-5-alkenyl-isoxazoles and trichloromethyl ketones. Our group also reported the synthesis of isoxazole-thiolane derivatives (**21**) via 1,6-Michael/ direct vinylogous reaction of substituted isoxazole with 1,4-dithiane-2,5-diol (**1**).^{5l}

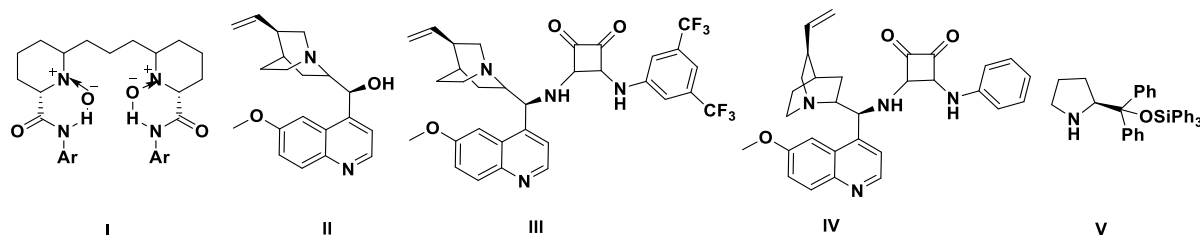
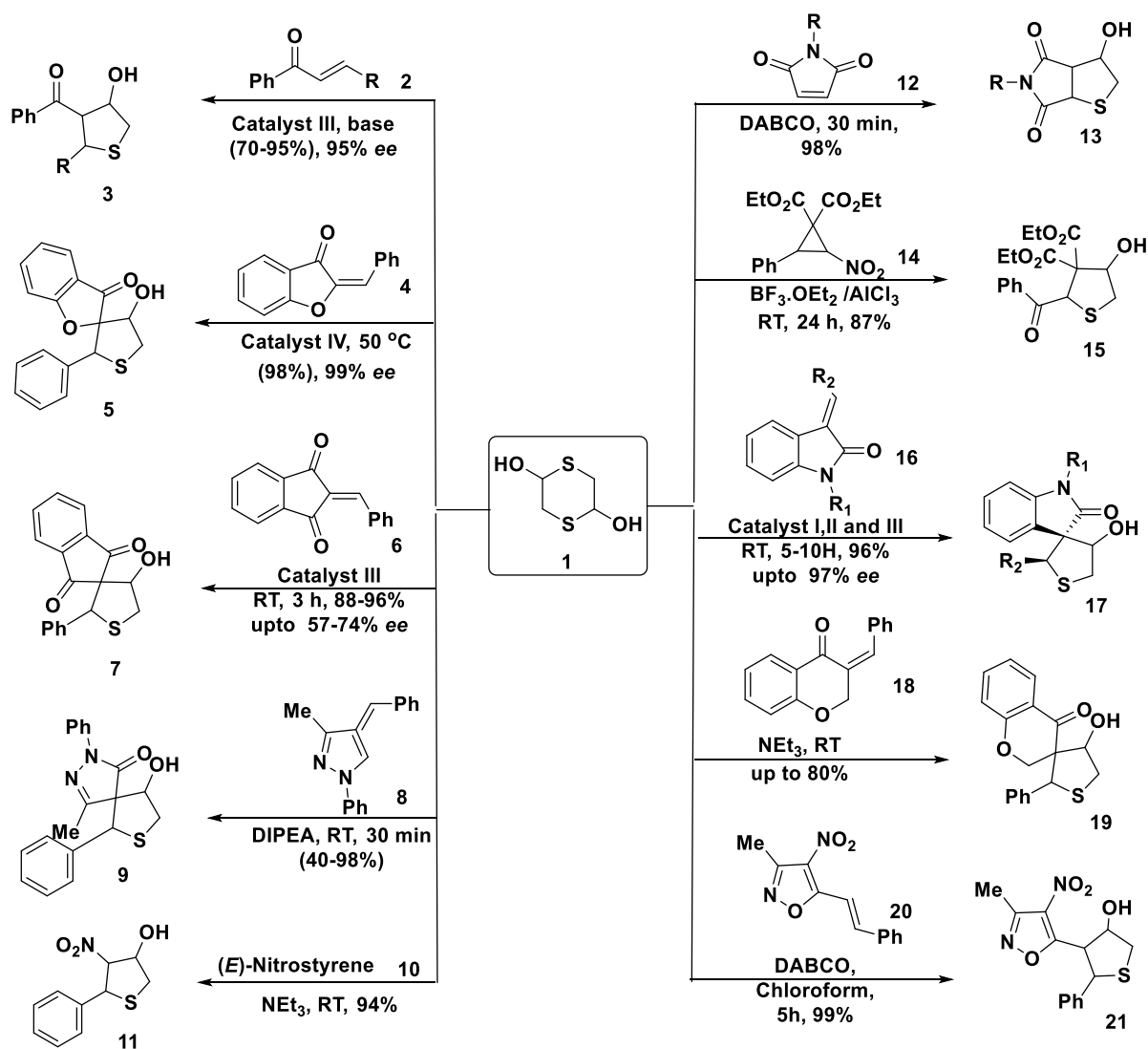


Figure-1: Some of the chiral catalysts used for the synthesis of tetrahydrothiophenes.



Note: Catalyst I, II, III & IV as shown in Figure-1

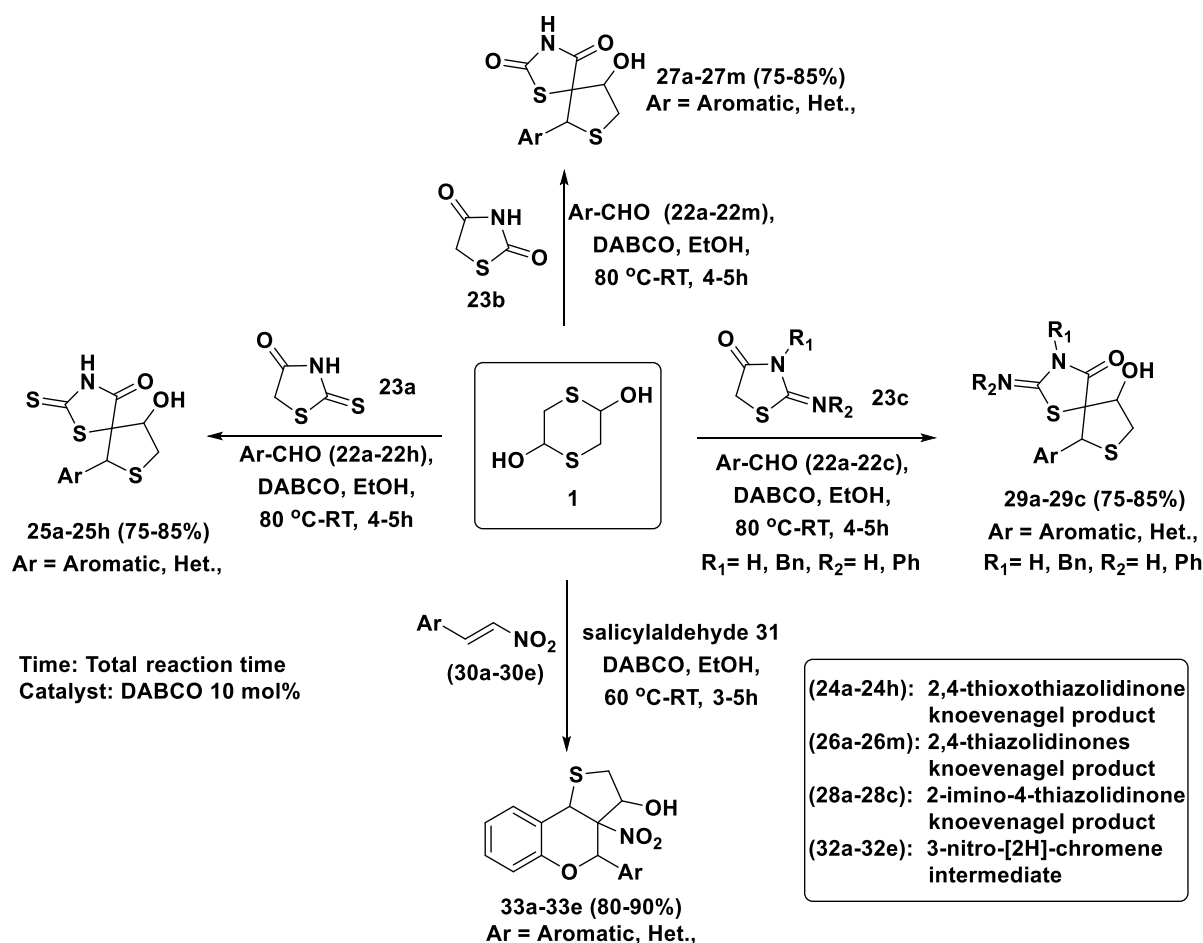


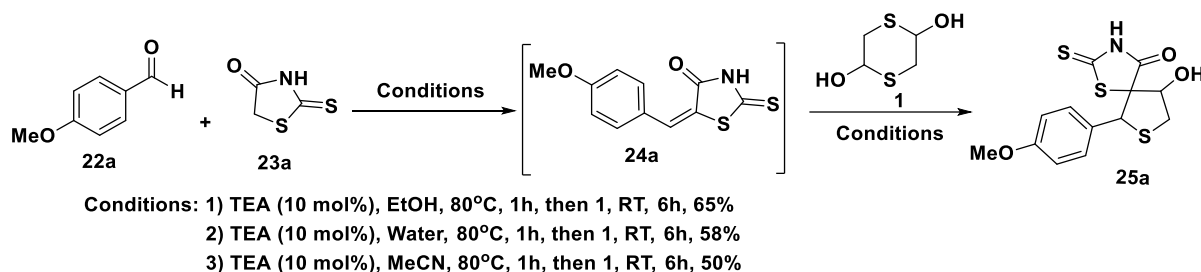
Figure-3: Present strategy of the 2, 4-thioxothiazolidinone, 2-imino-4-thiazolidinedione, 3-nitro-chromene, and 2, 4-thiazolidinedione-thiolane hybrids.

4.3 Results and discussions

4.3.1 One-pot synthesis of spiro-tetrahydrothiophene (thiolanes) hybrids:

To achieve our goal and based on our previous results in catalyst-free reactions, we started the investigation using 4-methoxy benzaldehyde (**22a**) (1.0 mmol) and 2,4-thioxothiazolidinone (rhodanine) (**23a**) (1.0 mmol) without catalyst in EtOH, water, and ACN at 80 °C, 5 h. But the formation of intermediate (**24a**) was not observed. Then the same reaction was performed in presence of TEA (10 mol%) to give intermediate (**24a**) which was subsequently treated with 1,4-dithiane-2,5-diol (**1**) (1.0 mmol) at RT for 6 h to give the desired product (**25a**) in 65%, 58% and 50% respectively (**Scheme-1; Entry-1 to 3; Table-1**). Encouraged by these results and to improve the yield, many experiments were conducted by varying the base, solvent, and reaction time. All the results are summarized in **Table-1**. Among the screened conditions, DABCO in EtOH was found to be the best suitable condition for obtaining the desired product in good yield (up to **85%**) (**Entry-18; Table-1**). Having optimized reaction conditions, different aldehydes (**22a-22h**) were

treated with 2,4-thioxothiazolidinone (rhodanine) (**23a**) (1.0 mmol) in EtOH at 80°C (first step) to generate the intermediates (*in situ*) and 1,4-dithiane-2-5-diol (**1**) (1.0 mmol) were added at RT to give the spiro thioxothiazolidinone-thiolane hybrids (**25b-25h**) in moderate to good yields (**75-90%**). All the newly synthesized compounds are characterized using ¹H-NMR, ¹³C-NMR, and mass spectra.

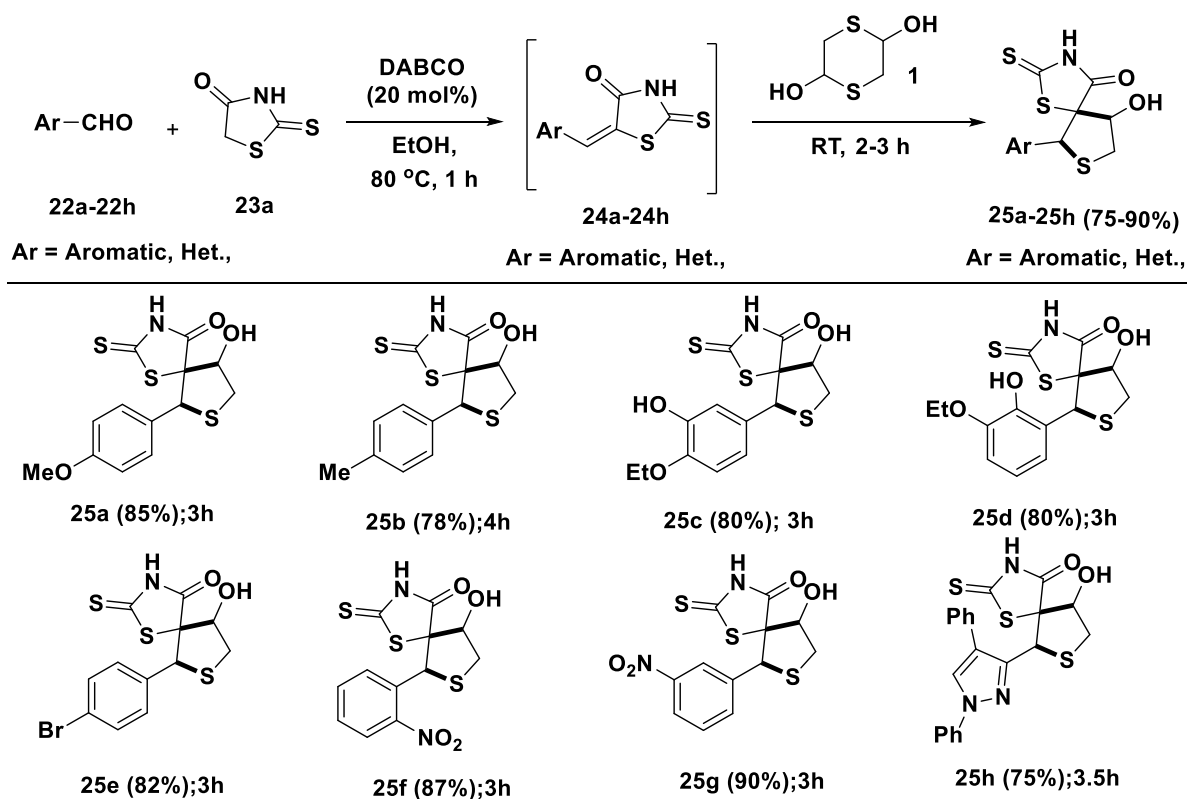


Scheme-1: Initial attempts for synthesis of 2,4-thioxothiazolidinone-thiolane hybrid **25a**.

Table-1: Optimization Conditions^[a]

Entry	Base	Solvent/Temp (°C)	Time (h) 1 st Step	Time (h) 2 nd Step (RT)	Yield ^[b] (%)
1	TEA (10 mol%)	EtOH/80 °C	1	6	65
2	TEA (10 mol%)	Water/80 °C	1	6	58
3	TEA (10 mol%)	ACN/80 °C	1	6	50
4	DABCO (10 mol%)	EtOH/80 °C	1	2	78
5	DABCO (10mol%)	Water/80 °C	1	7	65
6	DABCO (10mol%)	DMF/80 °C	1	3	60
7	DABCO (10mol%)	DMSO/80 °C	1	5	68
8	DABCO (10mol%)	CHCl ₃ /65 °C	1	5	70
9	DEA (10mol%)	EtOH/80 °C	1	5	50
10	Piperidine (10 mol%)	EtOH/80 °C	1	5	50
11	DIPEA (10mol%)	EtOH/80 °C	1	5	55
12	DBU (10mol%)	EtOH/80 °C	1	5	50
13	DMAP (10mol%)	EtOH/80 °C	1	5	50
14	NaOH (10mol%)	EtOH/80 °C	1	5	40
15	KOH (10mol%)	EtOH/80 °C	1	5	15
16	K ₂ CO ₃ (10mol%)	EtOH/80 °C	1	5	trace
17	Cs ₂ CO ₃ (10mol%)	EtOH/80 °C	1	5	15
18	DABCO (20 mol%)	EtOH/80 °C	1	2	85

^[a]Unless otherwise indicated, all reactions were carried out using aldehyde (**22a**, 1.0 mmol), thiazolidine-2,4-dione (**23a**, 1.0 mmol), and 1,4-dithiane-2,5-diol (**1**, 1.0 mmol), catalyst (20 mol%) in the specified solvent (5.0 mL) under argon at the specified temperature (1st step at 80°C and 2nd step at RT) and total time 3h. ^[b]Isolated yields after purification (for both steps).

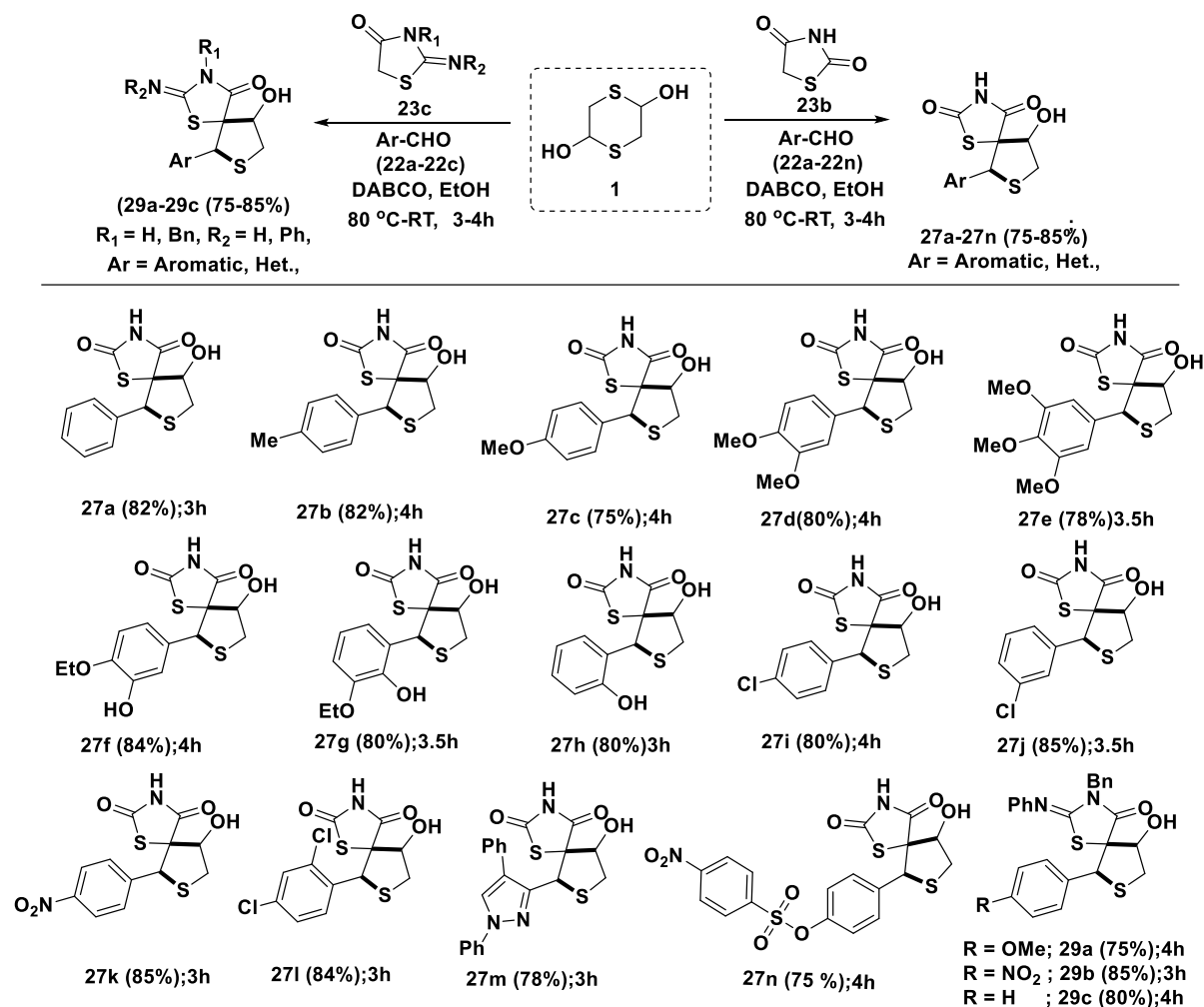


^a**Reagent and condition:** (**22a-22h**) (1.0 mmol) **23a** (1.0 mmol) **1** (1.0 mmol) DABCO (20 mol%), EtOH (5 mL) at 80 °C for 1h then RT up to 2-3 h.

Scheme-2: Synthesis of 2,4-thioxothiazolidinone-thiolane hybrids (**25a-25h**) via 1,4-Michael addition followed by intramolecular aldol reaction.

Based on the above results and considering the biological importance of 2,4-thiazolidinedione (**23b**) and 2-imino-4-thiazolidinedione (**23c**), the synthetic strategy was extended for the synthesis of a new class of 2,4-thiazolidinedione, 2-imino-4-thiazolidinedione thiolane derivatives (**27a-27n**)/ (**29a-29c**). Thus, 2,4-thiazolidinedione (**23b**)/2-imino-4-thiazolidinedione (**23c**) were treated with various aromatic, heteroaromatic aldehydes (**22a-22n**) in presence of DABCO (20 mol%) in EtOH at 80°C to give the unsaturated systems (*in situ*) followed by the treatment of the intermediates with 1,4-dithiane-2-5-diol (**1**) at RT to provide corresponding the desired products (**27a-27n**)/(**29a-29c**) with good yield 75–85% yield (**Scheme 3**). All these three reactions proceed *via* sulfa-1,4-Michael addition followed by intramolecular aldol reaction in a one-pot approach. It is noteworthy to mention that the aldehydes containing

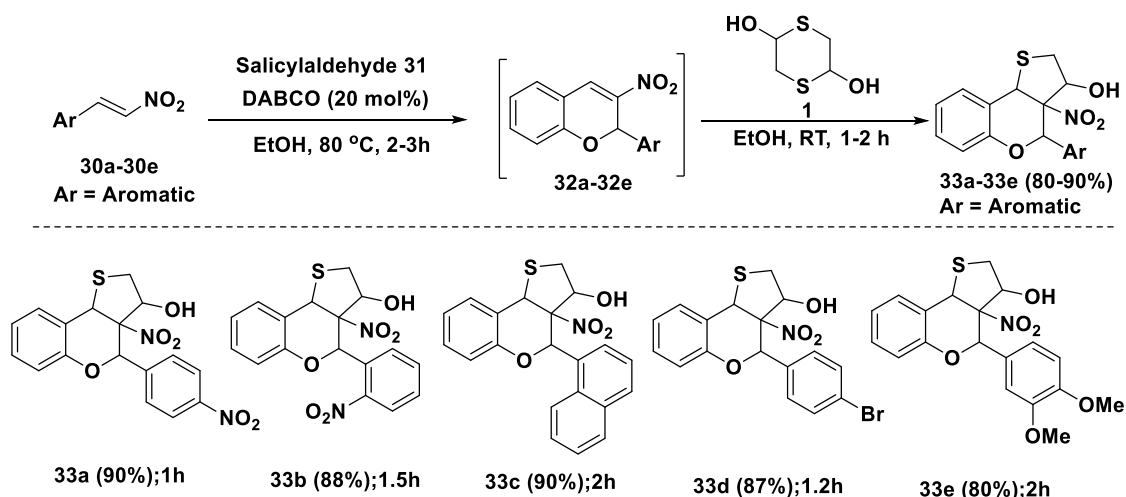
electron-withdrawing groups (e.g., $-\text{NO}_2$) provide better yields (up to 85%) compared to the substrates containing electron-donating groups.



^a**Reagent and conditions:** **23b-23c** (1.0 mmol), **22a-22n** (1.0 mmol), **1** (1.0 mmol) DABCO (20 mol%), EtOH 5 mL and stirred at 80 °C for 1 h and RT for 3-4 h.

Scheme-3: Substrate scope of 2,4-thiazolidinediones and 2-imino-4-thiazolidinedione thiolanes

From the discussion, it is clear that chromene-based molecules play an important role in medicinal chemistry. However, there are no reports on the fusion of chromene moiety with thiolane. With this background, to explore the complexity of the reaction and substrate scope, β -nitrostyrene (**30a-30e**) was explored for this purpose. Towards this, various β -nitrostyrene (**30a-30e**) were treated with salicylaldehyde (**31**) in presence of DABCO (20 mol%) in EtOH at 80°C for 2-3h to give 3-nitro-[2H]-chromenes (**32a-32e**) (*in situ*). These generated 3-nitro-[2H]-chromenes (**32a-32e**) were reacted 1,4-dithiane-2,5-diol (α -mercaptaldehyde) (**1**) at room temperature for 1-2 h to provide substituted 3-nitro-[2H]-chromene-thiolanes derivatives (**33a-33e**) with good to excellent yields (80-90%). This reaction proceeds *via* 1,4-*aza*-Michael addition followed by intramolecular Aldol reactions as shown in **Scheme-4**.



Reagent and condition: **30a-30e** (1.0 mmol), **31** (1.0 mmol), **1** (1.0 mmol), DABCO (20 mol%), EtOH 5 mL and stirred at 80 °C for 2-3 h, then RT, 1-2 h for 2nd step.

Scheme-4: Synthesis of 3-nitro-chromene-[2H]-thiolane hybrids (**33a-33e**)

4.4 Plausible reaction mechanism:

Based on the experimental observations and above literature reports,⁶ a plausible reaction mechanism is proposed as shown in **Figure-4**. The unsaturated system (**I**) (Knoevenagel condensation product) is formed from the reaction of aldehyde and 2,4-thiazolidinedione in the presence of DABCO which is further reacted with α -mercaptoacetaldehyde *via* sulfa 1,4-Michael addition (**II**) and intramolecular aldol reaction (**III**) to give the expected cyclic spiro-thiophene compound **27a**.

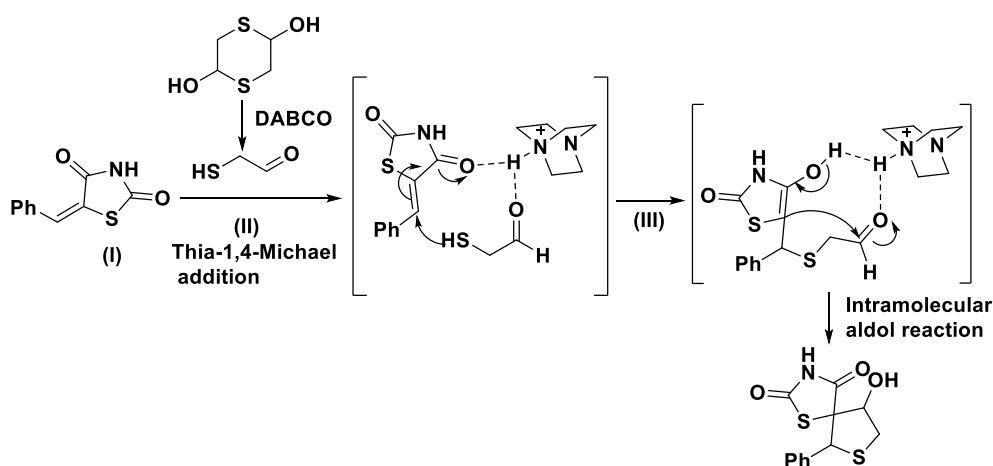


Figure-4: Plausible reaction mechanism of spiro based- 2,4-thioxothiazolidinone-thiolane hybrid **27a**.

4.5 Conclusion

In conclusion, we successfully synthesized novel spiro-based 2,4-thioxothiazolidinone, 2,4-thiazolidinedione, substituted 2-imino-4-thiazolidinedione thiolane derivatives using 20 mol% of DABCO as a catalyst with moderate to good yields in one-pot MCR approach. The key steps for the reaction include Knoevenagel condensation followed by 1,4-sulfa-Michael reactions and intramolecular-aldol reactions which lead to cyclization and formation of a new C-S bond for the construction of thiolane hybrids.

4.6 Experimental Section

4.6.1 General: All the commercial compounds were bought from Spectrochem, SRL, SD-Fine, and Sigma-Aldrich. ^1H and ^{13}C -NMR spectra were recorded on Bruker 400 MHz spectrometer using CDCl_3 or $\text{DMSO}-d_6$ solvents (reported in δ ppm). The mass spectra were recorded on Shimadzu LCMS-2020 or Agilent 6530 QTOF with a 1290 quaternary UHPLC system. IR spectra were recorded using the Perkin Elmer FTIR instrument and melting points are recorded using the Stuart melting point apparatus.

General procedure for the synthesis of 2,4-thiazolidine-thiolane derivatives (25a-25h): To a solution of aldehydes (**22a-22h**) (1 mmol) in EtOH (5 mL) was added 2,4-thiazolidine (**23a**) (1 mmol) followed by DABCO (20 mol%). The mixture was heated at 80 °C for 1h to form Knoevenagel condensation (*in-situ*) (conformed on TLC). To this, 1,4-dithiane-2,5-diol (**1**) (1 mmol) was added and the mixture was allowed to stir for 2h. After the completion of the reaction (on TLC), aq. NH_4Cl solution (5ml) was added and extracted with EtOAc (2X10ml). The combined organic layers were dried over sodium sulfate. Evaporation of the solvent gave the crude mixture which was purified by silica gel column chromatography. Elution of the column with hexane-EtOAc mixture gave the desired products (**25a-25h**) in moderate to good yields of (75-90%).

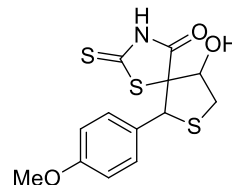
General procedure for the synthesis of 2,4-thiazolidine-thiolane derivatives (27a-27n): To a solution of aldehydes (**22a-22n**) (1 mmol) in EtOH (5 mL) was added 2,4-thiazolidine (**23b**) (1 mmol) followed by DABCO (20 mol%). The mixture was heated at 80 °C for 1h to form Knoevenagel condensation (*in-situ*) (conformed on TLC). To this, 1,4-dithiane-2,5-diol (**1**) (1 mmol) was added and the mixture was allowed to stir for 2h. After the completion of the reaction (on TLC), aq. NH_4Cl solution (5ml) was added and extracted with EtOAc (2X10ml). The combined organic layers were dried over sodium sulfate. Evaporation of the solvent gave the crude mixture which was purified by silica gel column chromatography. Elution of the column with

hexane-EtOAc mixture gave the desired products (**27a-27n**) in moderate to good yields of 75-85%.

General procedures for the synthesis of spiro- 3-nitro-[2H]-chromene-thiolane derivatives (33a-33e): To a solution of β -nitro-styrenes (**30a-30e**) (1mmol) in EtOH (5 mL) was added 2-hydroxy benzaldehyde (**31**) (1 mmol) and DABCO (20 mol%). The mixture was heated at 80 °C for 2-3 h to give 3-nitro 2-phenyl-[2H]-chromenes (**32a-32e**). To this, 1,4-dithiane-2,5-diol (**1**) (1mmol) was added, and stirring continued at RT for 1-2 h till the completion of the reaction (confirmed by TLC). Then the reaction mixture was quenched with aq. NH₄Cl (10 mL) and extracted with EtOAc (2X10ml). The combined organic layers were washed with brine, and water and dried over Na₂SO₄. Evaporation of the solvent under reduced pressure gave the crude product which was purified by silica gel column chromatography. Elution of the column with EtOAc + *n*-hexane mixture gave the desired product **33a-33e** in good to excellent yields (80-90%).

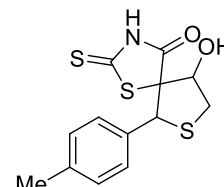
4.6.2 Spectral data of the synthesized compounds

9-Hydroxy-6-(4-methoxyphenyl)-4-thioxo-1,7-dithia-3-azaspiro [4.4] nonan-2-one (25a): Pale yellow solid, mp 156–157 °C, 85% yield. ¹H NMR (400 MHz, CDCl₃+DMSO-*d*₆) δ 12.68 (s, 1H), 7.32 (d, *J* = 8.8 Hz, 2H), 6.82 (t, *J* = 8.8 Hz, 2H), 5.13 (s, 1H), 4.87 (dd, *J* = 10.0, 7.4 Hz, 1H), 3.79 (s, 3H), 3.24–3.19 (m, 1H), 2.89 (s, 1H), 2.59 (t, *J* = 10.4 Hz, 1H); ¹³C NMR (100 MHz, CDCl₃+DMSO-*d*₆) δ 199.2, 178.4, 146.4, 136.3, 131.4, 118.9, 85.1, 76.1, 57.6, 45.1, 35.5; HRMS (ESI, *m/z*): Calcd. for C₁₃H₁₃NO₃S₃H⁺ 328.0130, found 328.0134; IR (KBr, thin film, cm⁻¹): ν_{\max} 3410, 3202, 3002, 2927, 1715, 1603, 1510, 1223, 1026, 832.



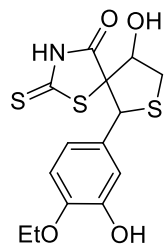
9-Hydroxy-2-thioxo-6-(*p*-tolyl)-1,7-dithia-3-azaspiro [4.4] nonan-4-one (25b):

White sticky solid, mp 180–181 °C, 78% yield. ¹H NMR (400 MHz, CDCl₃) δ 9.40 (s, 1H), 7.20 (d, *J* = 8.4 Hz, 2H), 7.05 (d, *J* = 8.0 Hz, 2H), 5.13 (s, 1H), 4.95–4.90 (m, 1H), 3.27 (dd, *J* = 10.8, 7.6 Hz, 1H), 2.78 (t, *J* = 10.4 Hz, 1H), 2.25 (s, 3H); ¹³C NMR (100 MHz, CDCl₃) δ 198.0, 175.7, 139.1, 130.2, 129.2, 128.9, 82.6, 79.7, 52.1, 34.0, 21.1; HRMS (ESI, *m/z*): Calcd. for C₁₃H₁₃NO₂S₃H⁺ 312.0181, found 312.0173; IR (KBr, thin film, cm⁻¹): ν_{\max} 3520, 3402, 2956, 1710, 1602, 1520, 1210, 1022, 821.



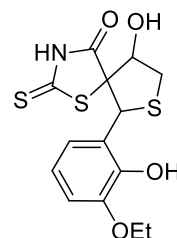
6-(4-Ethoxy-3-hydroxyphenyl)-9-hydroxy-2-thioxo-1,7-dithia-3-azaspiro [4.4] nonan-4-one

(25c): Pale yellow sticky solid, mp 160–161 °C, 80% yield. ¹H NMR (400 MHz, CDCl₃) δ 9.00 (s, 1H), 6.92 (s, 1H), 6.78 (s, 2H), 5.66 (s, 1H), 5.09 (s, 1H), 4.93–4.87 (m, 1H), 4.03 (q, J = 3.6 Hz, 2H), 3.30–3.25 (m, 1H), 3.09 (d, J = 12.0 Hz, 1H), 2.75 (t, J = 10.0 Hz, 1H), 1.37 (t, J = 6.8 Hz, 1H); ¹³C NMR (100 MHz, CDCl₃+DMSO-*d*₆) δ 189.7, 180.1, 158.8, 138.8, 133.5, 130.1, 128.7, 117.2, 80.0, 65.6, 55.2, 48.5, 41.0, 13.5; HRMS (ESI, m/z): Calcd. for C₁₄H₁₅NO₄S₃H⁺ 358.0236, found 358.0247; IR (KBr, thin film, cm⁻¹): ν_{max} 3506, 4714, 3070, 2932, 2854, 1700, 1515, 1438, 1105, 800.



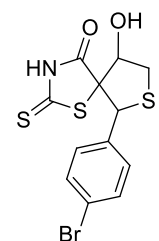
6-(4-Ethoxy-3-hydroxyphenyl)-9-hydroxy-2-thioxo-1,7-dithia-3-azaspiro[4.4]nonan-4-one

(25d): Yellow solid, mp 135–136 °C, 80% yield. ¹H NMR (400 MHz, CDCl₃+DMSO-*d*₆) δ 12.77 (s, 1H), 6.86 (s, 1H), 6.68 (s, 2H), 4.99 (s, 1H), 4.76 (t, J = 8.4 Hz, 1H), 3.99 (d, J = 6.0 Hz, 2H), 3.12 (t, J = 8.8 Hz, 1H), 2.76 (t, J = 10.0 Hz, 1H), 1.34 (t, J = 6.4 Hz, 3H); ¹³C NMR (100 MHz, CDCl₃+DMSO-*d*₆) δ 197.8, 175.7, 146.4, 145.5, 124.9, 122.1, 114.3, 112.5, 82.9, 79.4, 64.7, 52.3, 34.0, 14.7; HRMS (ESI, m/z): Calcd. for C₁₄H₁₅NO₄S₃H⁺ 358.0236, found 358.0252; IR (KBr, thin film, cm⁻¹): ν_{max} 3490, 3313, 1632, 1515, 1439, 1278, 1077, 756.



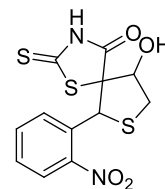
6-(4-Bromophenyl)-9-hydroxy-2-thioxo-1,7-dithia-3-azaspiro [4.4] nonan-4-one (25e):

Yellow solid, mp 179–180 °C, 82% yield. ¹H NMR (400 MHz, CDCl₃+DMSO-*d*₆) δ 12.98 (s, 1H), 7.47 (d, J = 8.0 Hz, 2H), 7.29 (d, J = 7.6 Hz, 2H), 6.36 (s, 1H), 5.13 (s, 1H), 4.90–4.80 (m, 1H), 3.21 (t, J = 9.6 Hz, 1H), 2.86 (t, J = 10.4 Hz, 1H); ¹³C NMR (100 MHz, CDCl₃+DMSO-*d*₆) δ 183.4, 176.8, 135.0, 133.8, 132.6, 126.6, 53.2, 52.7, 29.0, 26.8; HRMS (ESI, m/z): Calcd. for C₁₂H₁₀BrNO₂S₃H₂⁺ 376.9203, found 377.9112; IR (KBr, thin film, cm⁻¹): ν_{max} 3455, 3065, 2985, 1715, 1540, 1420, 1220, 580.

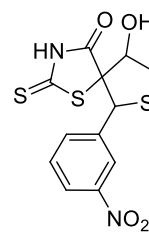


9-Hydroxy-6-(2-nitrophenyl)-2-thioxo-1,7-dithia-3-azaspiro [4.4] nonan-4-one (25f):

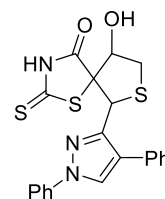
White sticky solid, mp 178–179 °C, 87% yield. ¹H NMR (400 MHz, CDCl₃+DMSO-*d*₆) δ 12.77 (s, 1H), 8.08 (d, J = 7.2 Hz, 2H), 7.54–7.49 (m, 2H), 5.20 (s, 1H), 4.85 (dd, J = 10.2, 7.2 Hz, 1H), 3.83 (s, 1H), 3.19 (dd, J = 10.8, 7.2 Hz, 1H), 2.88 (t, J = 10.4 Hz, 1H); ¹³C NMR (100 MHz, CDCl₃+DMSO-*d*₆) δ 200.7, 176.9, 147.8, 14.3, 130.3, 123.3, 81.7, 79.6, 51.5, 34.0; HRMS (ESI, m/z): Calcd. for C₁₂H₁₀N₂O₄S₃H⁺ 342.9875, found 342.9860; IR (KBr, thin film, cm⁻¹): ν_{max} 3430, 2986, 1705, 1620, 1540, 1012, 865.



9-Hydroxy-6-(3-nitrophenyl)-2-thioxo-1,7-dithia-3-azaspiro [4.4] nonan-4-one (25g): White solid, mp 140–141 °C, 90% yield. ^1H NMR (400 MHz, $\text{CDCl}_3+\text{DMSO}-d_6$) δ 12.88 (s, 1H), 8.19 (s, 1H), 8.11 (d, $J = 7.6$ Hz, 1H), 7.70 (d, $J = 7.2$ Hz, 1H), 7.49 (t, $J = 7.6$ Hz, 1H), 6.27 (s, 1H), 5.22 (s, 1H), 4.86 (t, $J = 8.4$ Hz, 1H), 3.21 (t, $J = 9.2$ Hz, 1H), 2.90 (t, $J = 10.4$ Hz, 1H); ^{13}C NMR (100 MHz, $\text{CDCl}_3+\text{DMSO}-d_6$) δ 198.6, 174.9, 145.9, 135.2, 133.53, 127.5, 122.0, 121.7, 79.8, 77.4, 49.4, 32.1; HRMS (ESI, m/z): Calcd. For $\text{C}_{14}\text{H}_{15}\text{N}_2\text{O}_4\text{S}_3\text{H}^+$ 342.9875, found 342.9880; IR (KBr, thin film, cm^{-1}): ν_{max} 3408, 3110, 2920, 2850, 1711, 1524, 1462, 1227, 1077, 797.

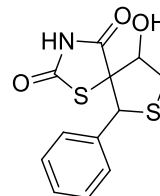


6-(1,4-Diphenyl-1H-pyrazol-3-yl)-9-hydroxy-4-thioxo-1,7-dithia-3-azaspiro [4.4] nonan-2-one (25h): White solid, mp 201–202 °C, 75% yield. ^1H NMR (400 MHz, $\text{CDCl}_3+\text{DMSO}-d_6$) δ 12.88 (s, 1H), 8.48 (s, 1H), 7.79 (s, 1H), 7.76–7.74 (m, 2H), 7.61–7.57 (m, 2H), 7.50–7.43 (m, 5H), 7.33 (t, $J = 7.6$ Hz, 1H), 5.24 (s, 1H), 4.80 (dd, $J = 9.6, 7.4$ Hz, 1H), 3.24–3.19 (m, 1H), 2.88 (t, $J = 10.4$ Hz, 1H); ^{13}C NMR (100 MHz, $\text{CDCl}_3+\text{DMSO}-d_6$) δ 176.6, 172.7, 154.7, 141.6, 134.3, 131.5, 131.4, 130.7, 130.5, 130.3, 128.8, 121.0, 117.4, 80.9, 80.7, 44.4, 31.5; HRMS (ESI, m/z): Calcd. for $\text{C}_{21}\text{H}_{17}\text{N}_3\text{O}_2\text{S}_3\text{H}^+$ 440.0556, found 440.0562; IR (KBr, thin film, cm^{-1}): ν_{max} 3397, 3230, 3101, 2925, 1719, 1597, 1198, 1073, 758.



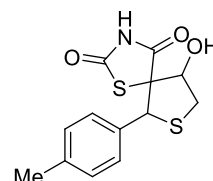
9-Hydroxy-6-phenyl-1,7-dithia-3-azaspiro [4.4]nonane-2,4-dione (27a):

White solid, mp 205–206 °C, 82% yield. ^1H NMR (400 MHz, CDCl_3) δ 8.86 (s, 1H), 7.27–7.19 (m, 5H), 5.14 (s, 1H), 4.92–4.88 (m, 1H), 3.28–3.23 (m, 1H), 2.77 (t, $J = 10.4$ Hz, 1H); ^{13}C NMR (100 MHz, CDCl_3) δ 174.0, 135.0, 132.1, 130.8, 130.5, 128.7, 82.0, 79.3, 51.5, 33.8; HRMS (ESI, m/z): Calcd. for $\text{C}_{12}\text{H}_{11}\text{NO}_3\text{S}_2\text{H}^+$ 282.0253, found 282.0250; IR (KBr, thin film, cm^{-1}): ν_{max} 3402, 3052, 2975, 1710, 1563, 1220, 1120, 815.

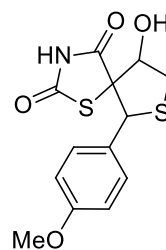


9-Hydroxy-6-(p-tolyl)-1,7-dithia-3-azaspiro [4.4] nonane-2,4-dione (27b):

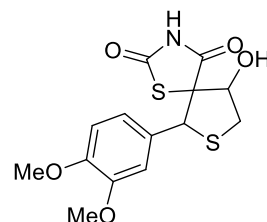
White solid, mp 196–197 °C, 82% yield. ^1H NMR (400 MHz, $\text{CDCl}_3+\text{DMSO}-d_6$) δ 11.24 (s, 1H), 7.27–7.20 (m, 2H), 7.02 (d, $J = 8.0$ Hz, 2H), 5.55 (s, 1H), 5.13 (s, 1H), 4.86–4.80 (m, 1H), 3.15 (dd, $J = 10.4, 7.2$ Hz, 1H), 2.79 (t, $J = 10.4$ Hz, 1H), 2.25 (s, 3H); ^{13}C NMR (100 MHz, $\text{CDCl}_3+\text{DMSO}-d_6$) δ 175.3, 170.8, 138.3, 131.3, 129.1, 128.8, 79.7, 79.0, 52.0, 33.7, 21.1; HRMS (ESI, m/z): Calcd. for $\text{C}_{13}\text{H}_{13}\text{NO}_3\text{S}_2\text{H}^+$ 296.0410, found 296.0407; IR (KBr, thin film, cm^{-1}): ν_{max} 3480, 3056, 2966, 1595, 1520, 1210, 1005, 835.



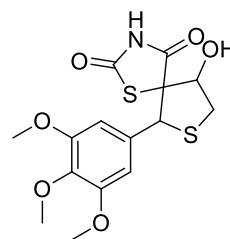
9-Hydroxy-6-(4-methoxyphenyl)-1,7-dithia-3-azaspiro[4.4]nonane-2,4-dione (27c): Pale yellow solid, mp 185–186 °C, 75% yield. ¹H NMR (400 MHz, CDCl₃) δ 8.12 (s, 1H), 7.41 (d, J = 8.0 Hz, 1H), 7.35 (d, J = 8.0 Hz, 1H), 6.87 (d, J = 8.4 Hz, 2H), 5.51 (s, 1H), 5.25 (s, 1H), 4.99 (dd, J = 16.6, 8.4 Hz, 1H), 3.82 (s, 3H), 3.39–3.34 (m, 1H), 2.82 (t, J = 10.0 Hz, 1H); ¹³C NMR (100 MHz, CDCl₃) δ 178.8, 168.3, 160.2, 132.2, 124.1, 117.2, 82.7, 71.8, 61.0, 47.8, 40.0; HRMS (ESI, m/z): Calcd. For C₁₃H₁₃NO₄S₂H⁺ 312.0359, found 312.0350; IR (KBr, thin film, cm⁻¹): ν_{max} 3469, 2929, 2790, 1687, 1609, 1502, 1177, 841.



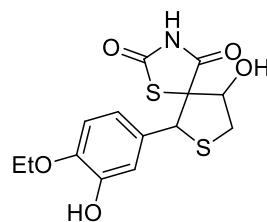
6-(3,4-Dimethoxyphenyl)-9-hydroxy-1,7-dithia-3-azaspiro [4.4] nonane-2,4-dione (27d): Pale yellow solid, 80% yield, mp 176–177 °C. ¹H NMR (400 MHz, CDCl₃+DMSO-*d*₆) δ 11.63 (s, 1H), 6.97 (s, 1H), 6.93 (d, J = 8.0 Hz, 1H), 6.80 (d, J = 8.0 Hz, 1H), 5.18 (s, 1H), 4.89 (dd, J = 10.0, 7.4 Hz, 1H), 3.86 (s, 6H), 3.21 (t, J = 10.4, 1H), 2.86 (t, J = 10.4 Hz, 1H), 2.60 (s, 1H); ¹³C NMR (100 MHz, CDCl₃+DMSO-*d*₆) δ 175.5, 170.9, 149.0, 148.2, 126.8, 121.7, 112.5, 110.7, 79.8, 78.7, 55.8, 55.8, 52.1, 33.7; HRMS (ESI, m/z): Calcd. For C₁₄H₁₅NO₅S₂ 341.0392, found 341.0390; IR (KBr, thin film, cm⁻¹): ν_{max} 3417, 3211, 3069, 2934, 2763, 1696, 1514, 1267, 1254, 1022.



6-(3,4,5-Trimethoxyphenyl)-9-hydroxy-1,7-dithia-3-azaspiro [4.4] nonane-2,4-dione (27e): White solid, mp 192–193 °C, 78% yield. ¹H NMR (400 MHz, CDCl₃) δ 10.04 (s, 1H), 6.69–6.61 (m, 2H), 5.14 (s, 1H), 4.96–4.94 (m, 1H), 3.80 (s, 3H), 3.80 (s, 6H), 3.29 (dd, J = 10.6, 7.2 Hz, 1H), 2.86 (t, J = 10.4 Hz, 1H); ¹³C NMR (100 MHz, CDCl₃) δ 198.3, 176.2, 152.9, 138.3, 132.4, 131.07, 129.1, 106.3, 82.5, 79.5, 60.8, 56.3, 52.4, 33.8, 29.6; HRMS (ESI, m/z): Calcd. for C₁₄H₁₅NO₅S₂H⁺ 372.0570, found 372.0560; IR (KBr, thin film, cm⁻¹): ν_{max} 3480, 2985, 1720, 1595, 1511, 1198, 1011, 860.

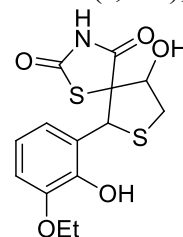


6-(4-Ethoxy-3-hydroxyphenyl)-9-hydroxy-1,7-dithia-3-azaspiro [4.4] nonane-2,4-dione (27f): Pale brown solid, mp 155–156 °C, 84% yield. ¹H NMR (400 MHz, CDCl₃+DMSO-*d*₆) δ 11.69 (s, 1H), 6.96 (d, J = 14.8 Hz, 1H), 6.76 (s, 2H), 5.11 (s, 1H), 4.84 (dd, J = 17.0, 8.6 Hz, 1H), 4.07 (d, J = 6.4 Hz, 2H), 3.18 (t, J = 9.6 Hz, 1H), 3.08 (d, J = 11.2 Hz, 1H), 2.81 (t, J = 10.0 Hz, 1H), 1.42 (t, J = 6.8 Hz, 3H); ¹³C NMR (100 MHz, CDCl₃+DMSO-*d*₆) δ 175.5, 170.9, 147.1, 146.1, 125.3, 121.9, 115.0, 114.2, 80.0, 64.3, 52.2, 37.0, 33.7, 14.9; HRMS (ESI, m/z): Calcd. for C₁₄H₁₅NO₅S₂H⁺ 342.0464, found 342.0454; IR (KBr, thin film, cm⁻¹): ν_{max} 3794, 3403, 3129, 2937, 2753, 1734, 1698, 1518, 1173, 820.

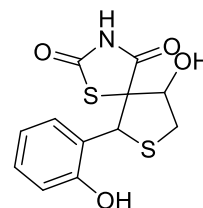


6-(3-Ethoxy-2-hydroxyphenyl)-9-hydroxy-1,7-dithia-3-azaspiro [4.4] nonane-2,4-dione (27g):

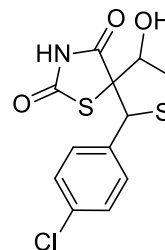
Yellow sticky solid, mp 181–182 °C, 80% yield. ¹H NMR (400 MHz, CDCl₃) δ 9.48 (s, 1H), 6.88 (s, 1H), 6.77 (s, 2H), 5.71 (s, 1H), 5.08 (s, 1H), 4.93–4.88 (m, 1H), 4.03 (q, *J* = 3.2 Hz, 2H), 3.26 (dd, *J* = 10.8, 7.6 Hz, 1H), 2.76 (t, *J* = 10.4 Hz, 1H), 1.36 (t, *J* = 6.8 Hz, 3H); ¹³C NMR (100 MHz, CDCl₃+DMSO-*d*₆) δ 176.5, 171.9, 147.9, 147.0, 126.4, 123.0, 115.8, 115.0, 80.9, 65.4, 53.3, 34.7, 30.5, 15.8; HRMS (ESI, *m/z*): Calcd. for C₁₄H₁₅NO₅S₂H⁺ 341.0392, found 342.0460; IR (KBr, thin film, cm⁻¹): ν_{max} 3520, 3429, 3086, 2956, 1702, 1590, 1240, 1120, 860.



9-Hydroxy-6-(2-hydroxyphenyl)-1,7-dithia-3-azaspiro [4.4] nonane-2,4-dione (27h): White sticky solid, mp 192–193 °C, 80% yield. ¹H NMR (400 MHz, CDCl₃+DMSO-*d*₆) δ 11.57 (s, 1H), 7.60 (s, 1H), 7.12 (d, *J* = 8.4 Hz, 1H), 6.66 (d, *J* = 8.4 Hz, 2H), 5.04 (s, 1H), 4.83–4.76 (dd, *J* = 10.2, 7.6 Hz, 1H), 3.99 (d, *J* = 6.8 Hz, 1H), 3.12 (d, *J* = 7.6 Hz, 1H), 2.75 (t, *J* = 10.0 Hz, 1H); ¹³C NMR (100 MHz, CDCl₃+DMSO-*d*₆) δ 174.1, 169.1, 146.9, 136.3, 134.6, 128.4, 123.2, 122.6, 78.1, 78.0, 50.3, 33.0; HRMS (ESI, *m/z*): Calcd. for C₁₂H₁₁NO₄S₂H⁺ 298.0202, found 298.0202; IR (KBr, thin film, cm⁻¹): ν_{max} 3380, 2924, 2852, 1693, 1610, 1513, 1023, 834.

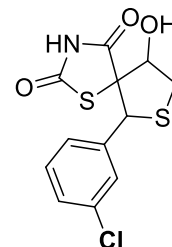


6-(4-Chlorophenyl)-9-hydroxy-1,7-dithia-3-azaspiro [4.4] nonane-2,4-dione (27i): White solid, 80% yield, mp 134–135 °C. ¹H NMR (400 MHz, CDCl₃) δ 8.55 (s, 1H), 7.39 (d, *J* = 8.4 Hz, 2H), 7.19 (s, 2H), 5.15 (s, 1H), 4.91 (dd, *J* = 15.6, 7.6 Hz, 1H), 3.31–3.26 (m, 1H), 3.03 (d, *J* = 12.4 Hz, 1H), 2.77 (t, *J* = 10.4 Hz, 1H); ¹³C NMR (100 MHz, CDCl₃+DMSO-*d*₆) δ 201.1, 177.1, 134.3, 133.0, 130.6, 128.3, 82.1, 79.5, 51.6, 33.9; HRMS (ESI, *m/z*): Calcd. for C₁₂H₁₀ClNO₃S₂H⁺ 315.9863, found 315.9803; IR (KBr, thin film, cm⁻¹): ν_{max} 3401, 3447, 3064, 2951, 2778, 1774, 1588, 1064, 795.

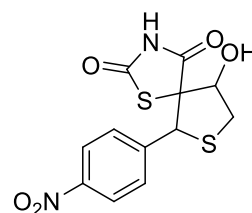


6-(3-Chlorophenyl)-9-hydroxy-1,7-dithia-3-azaspiro [4.4] nonane-2,4-dione (27j):

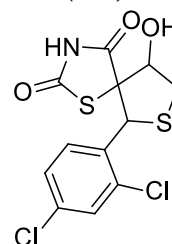
Yellow solid, mp 169–170 °C, 85% yield. ¹H NMR (400 MHz, CDCl₃) δ 8.45 (s, 1H), 7.39 (d, *J* = 8.4 Hz, 2H), 7.29–7.19 (m, 2H), 5.15 (s, 1H), 4.90 (dd, *J* = 10.0, 2.4 Hz, 1H), 3.31–3.26 (m, 1H), 3.10 (d, *J* = 12.4 Hz, 1H), 2.77 (t, *J* = 10.4 Hz, 1H); ¹³C NMR (100 MHz, CDCl₃+DMSO-*d*₆) δ 180.0, 175.3, 138.7, 136.2, 136.0, 136.0, 135.8, 127.1, 86.9, 84.1, 56.2, 38.5; IR (KBr, thin film, cm⁻¹): ν_{max} 3515, 3389, 3077, 2924, 1709, 1608, 1253, 1176, 835; HRMS (ESI, *m/z*): Calcd. for C₁₂H₁₀NO₃S₂H⁺ 314.9791, found 315.9855; IR (KBr, thin film, cm⁻¹).



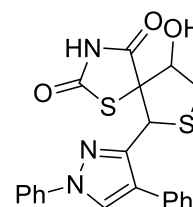
9-Hydroxy-6-(4-nitrophenyl)-1,7-dithia-3-azaspiro [4.4] nonane-2,4-dione (27k): White solid, mp 202–203 °C, 85% yield. ¹H NMR (400 MHz, CDCl₃+DMSO-*d*₆) δ 7.98 (d, *J* = 8.8 Hz, 2H), 7.51–7.42 (m, 2H), 5.15 (s, 1H), 4.78–4.72 (m, 1H), 3.08 (dd, *J* = 10.6, 7.2 Hz, 1H), 2.99 (dd, *J* = 11.8, 2.4 Hz, 1H), 2.76 (t, *J* = 10.4 Hz, 1H); ¹³C NMR (100 MHz, CDCl₃+DMSO-*d*₆) δ 175.0, 170.0, 147.8, 142.4, 130.4, 123.2, 79.1, 51.4, 33.9, 29.5; HRMS (ESI, *m/z*): Calcd. for C₁₂H₁₀N₂O₅S₂H⁺ 327.0104, found 327.0100; IR (KBr, thin film, cm⁻¹): ν_{max} 3390, 3068, 2985, 1610, 1540, 1190, 840.



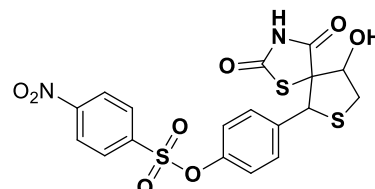
6-(2,4-Dichlorophenyl)-9-hydroxy-1,7-dithia-3-azaspiro [4.4] nonane-2,4-dione (27l): White solid, mp 171–172 °C, 84% yield. ¹H NMR (400 MHz, CDCl₃+DMSO-*d*₆) δ 11.76 (s, 1H), 7.42 (d, *J* = 8.4 Hz, 2H), 7.29 (s, 1H), 5.16 (s, 1H), 4.87 (d, *J* = 10.4 Hz, 1H), 4.83 (d, *J* = 8.4 Hz, 1H), 3.20 (t, *J* = 7.2 Hz, 1H), 2.85 (t, *J* = 10.4 Hz, 3H); ¹³C NMR (100 MHz, CDCl₃+DMSO-*d*₆) δ 193.6, 169.9, 140.8, 130.1, 128.4, 122.5, 117.0, 116.6, 74.7, 72.4, 44.3, 27.0; HRMS (ESI, *m/z*): Calcd. For C₁₂H₉Cl₂NO₃S₂H⁺ 349.9474, found 349.9412; IR (KBr, thin film, cm⁻¹): ν_{max} 3446, 3400, 3064, 2951, 2778, 1417, 1558, 1158, 1063, 795, 730.



6-(1,4-Diphenyl-1H-pyrazol-3-yl)-9-hydroxy-1,7-dithia-3-azaspiro [4.4] nonane-2,4-dione (27m): Yellow solid, mp 195–196 °C, 78% yield. ¹H NMR (400 MHz, CDCl₃+DMSO-*d*₆) δ 11.93 (s, 1H), 8.61 (s, 1H), 7.84 (d, *J* = 8.0 Hz, 2H), 7.60–7.42 (m, 7H), 7.33 (t, *J* = 7.4 Hz, 1H), 5.28 (s, 1H), 4.75 (dd, *J* = 9.6, 7.6 Hz, 1H), 3.21–3.17 (m, 1H), 2.80 (t, *J* = 10.0 Hz, 1H); ¹³C NMR (100 MHz, DMSO-*d*₆+CDCl₃) δ 161.7, 152.7, 149.0, 145.0, 134.8, 134.4, 133.0, 132.1, 131.7, 129.6, 127.4, 121.7, 116.7, 82.1, 72.39, 59.3, 55.6; HRMS (ESI, *m/z*): Calcd. for C₂₁H₁₇N₃O₃S₂NH₄⁺ 441.1050, found 441.0702; IR (KBr, thin film, cm⁻¹): ν_{max} 3397, 3230, 3101, 2925, 1719, 1597, 1198, 1073, 758.

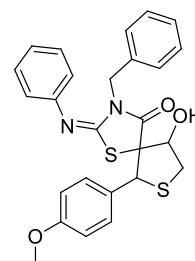


4-((5*S*,6*R*,9*S*)-9-Hydroxy-2,4-dioxo-1,7-dithia-3-azaspiro [4.4] nonan-6-yl) phenyl 4-nitrobenzene sulfonate (27n): Light brown solid, mp 209–210 °C, 75% yield. ¹H NMR (400 MHz, CDCl₃+DMSO) δ 8.39 (d, *J* = 8.8 Hz, 2H), 7.96 (d, *J* = 8.0 Hz, 2H), 7.34 (d, *J* = 8.4 Hz, 2H), 6.96 (d, *J* = 7.6 Hz, 2H), 5.14 (s, 1H), 4.85–4.81 (m, 1H), 4.23 (t, *J* = 6.4 Hz, 1H), 3.18 (dd, *J* = 10.2, 7.2 Hz, 1H), 2.79 (t, *J* = 10.4 Hz, 1H); ¹³C NMR (100 MHz, CDCl₃+DMSO-*d*₆) δ 176.7, 172.0, 152.7, 150.5, 141.4, 136.1, 132.4, 131.6, 126.3, 123.4, 81.1, 53.1, 35.4, 31.0. HRMS (ESI, *m/z*): Calcd. for C₁₈H₁₄N₂O₈S₃H⁺ 482.9985, found 482.9943. IR (KBr, thin film, cm⁻¹): ν_{max} 3485, 3322, 1662, 1540, 1432, 1375, 1283, 1056, 765.



2-(Benzylimino)-9-hydroxy-6-(4-methoxyphenyl)-3-phenyl-1,7-dithia-3-azaspiro [4.4] nonan-4-one (29a): Pale yellow sticky solid, mp 158–159 °C, 75% yield. ¹H NMR

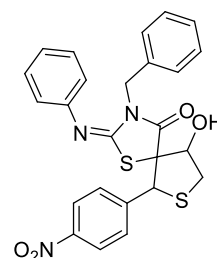
(400 MHz, CDCl₃) δ 7.32 (t, *J* = 7.6 Hz, 2H), 7.26–7.25 (m, 3H), 7.20–7.12 (m, 5H), 6.74 (d, *J* = 7.6 Hz, 2H), 6.67 (d, *J* = 8.4 Hz, 2H), 5.18 (s, 1H), 4.97 (d, *J* = 14.0 Hz, 1H), 4.86 (d, *J* = 14.4 Hz, 1H), 4.74 (dd, *J* = 14.2, 6.8 Hz, 1H), 3.79 (s, 1H), 3.29–3.25 (m, 1H), 2.66 (t, *J* = 10.4 Hz, 1H); ¹³C NMR (100



MHz, CDCl₃) δ 172.3, 147.8, 147.6, 129.3, 129.3, 129.1, 128.5, 128.5, 128.4, 127.9, 125.0, 124.5, 123.6, 120.7, 78.3, 75.6, 55.8, 52.2, 46.4, 34.2; HRMS (ESI, *m/z*): Calcd. for C₂₆H₂₄N₂O₃S₂H⁺ 477.1301, found 477.1296; IR (KBr, thin film, cm⁻¹): ν_{max} 3412, 2931, 2850, 1637, 1384, 1034, 750.

2-(Benzylimino)-9-hydroxy-6-(4-nitrophenyl)-3-phenyl-1,7-dithia-3-azaspiro [4.4] nonan-4-one (29b): White solid, mp 173–174 °C, 85% yield. ¹H NMR (400 MHz,

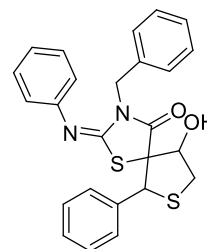
CDCl₃+DMSO-*d*₆) δ 7.23–7.17 (m, 8H), 7.11 (d, *J* = 6.8 Hz, 3H), 7.02 (t, *J* = 7.6 Hz, 1H), 6.66 (d, *J* = 7.6 Hz, 2H), 5.13 (s, 1H), 4.93–4.87 (m, 2H), 4.79 (d, *J* = 14.8 Hz, 1H), 4.01 (d, *J* = 6.0 Hz, 1H), 3.13 (t, *J* = 8.4 Hz, 1H), 2.73 (t, *J* = 9.6 Hz, 1H); ¹³C NMR (100 MHz, CDCl₃) δ 173.6, 148.6, 136.3, 134.7,



130.5, 130.2, 130.2, 129.6, 129.4, 129.2, 129.1, 129.0, 128.6, 125.8, 121.9, 79.6, 77.3, 54.0, 47.4, 35.2; HRMS (ESI, *m/z*): Calcd. for C₂₅H₂₁N₃O₄S₂H⁺ 492.1046, found 492.0952; IR (KBr, thin film, cm⁻¹): ν_{max} 3346, 1634, 1384, 1520, 1162, 675.

(E)-3-Benzyl-9-hydroxy-6-phenyl-2-(phenylimino)-1,7-dithia-3-azaspiro[4.4]nonan-4-one (29c): Light brown solid, mp 201–202 °C, 80% yield. ¹H NMR (400 MHz,

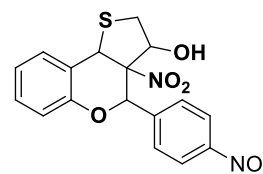
CDCl₃) δ 7.24–7.17 (m, 9H), 7.14–7.05 (m, 6H), 6.64 (d, *J* = 7.2 Hz, 2H), 5.18 (s, 1H), 4.96–4.93 (m, 1H), 4.91 (d, *J* = 2.8 Hz, 1H), 4.81 (d, *J* = 15.6 Hz, 1H), 3.22 (dd, *J* = 10.6, 7.2 Hz, 1H), 2.62 (t, *J* = 10.4 Hz, 1H); ¹³C NMR (100 MHz, CDCl₃+DMSO-*d*₆) δ 173.4, 152.5, 148.4, 136.1, 134.9, 129.8,



129.6, 129.0, 128.8, 128.5, 128.1, 127.8, 125.0, 121.5, 76.7, 53.3, 46.3, 34.1, 30.0; HRMS (ESI, *m/z*): Calcd. for C₂₅H₂₂N₂O₂S₂H⁺ 447.1195, found 477.0905; IR (KBr, thin film, cm⁻¹): ν_{max} 3456, 1642, 1322, 1542, 1122, 652.

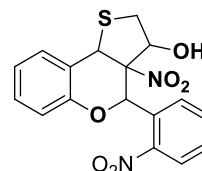
3a-Nitro-4-(4-nitrophenyl) - 3, 3a, 4, 9b-tetrahydro-2H-thieno [3, 2-c] chromen-3-ol (33a): White Crystalline solid, mp 177–178 °C, 90% yield. ¹H NMR (400 MHz, CDCl₃): δ 7.49 (d, = 5.6

Hz, 3H), 7.36 (d, *J* = 6.4 Hz, 2H), 7.29 (d, *J* = 7.6 Hz, 1H), 7.08 (t, *J* = 7.2 Hz, 1H), 7.02 (d, *J* = 8.4 Hz, 1H), 5.56 (s, 1H), 5.36 (s, 1H), 4.75 (s, 1H), 3.53 (d, *J* = 10.8 Hz, 1H), 3.13 (d, *J* = 12.0 Hz, 1H); ¹³C NMR (100 MHz, CDCl₃): δ 152.38, 133.66, 129.88, 129.26, 128.81, 128.71,

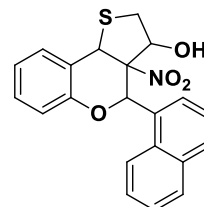


127.14, 122.58, 121.63, 117.39, 98.56, 76.46, 75.87, 42.97, 33.50; HRMS (ESI, m/z): Calcd. for $C_{18}H_{18}N_2O_6SNH_4^+$ 392.0911, found 392.0600; IR (KBr, thin film, cm^{-1}): ν_{max} 3425, 3062, 2937, 1610, 1554, 1259, 1239, 1111, 810, 757.

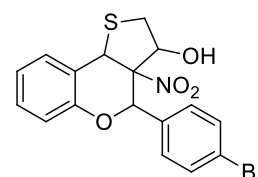
3a-Nitro-4-(2-nitrophenyl)-3, 3a, 4, 9b-tetrahydro-2H-thieno [3, 2-c] chromen-3-ol (33b): Pale yellow solid, mp 183–184 °C, 88% yield. 1H NMR (400 MHz, $CDCl_3$) δ 7.45 (s, 3H), 7.32 (d, J = 6.0 Hz, 2H), 7.23 (d, J = 4.4 Hz, 1H), 7.04 (t, J = 7.6 Hz, 1H), 6.98 (d, J = 8.4 Hz, 1H), 5.53 (s, 1H), 5.32 (s, 1H), 4.72 (s, 1H), 3.49 (dd, J = 12.0, 4.0 Hz, 1H), 3.10 (d, J = 12.0 Hz, 1H), 2.77 (s, 1H); ^{13}C NMR (100 MHz, $DMSO-d_6+CDCl_3$) δ 157.12, 140.60, 135.74, 130.71, 130.15, 129.05, 128.93, 128.23, 125.22, 121.87, 118.53, 116.34, 114.60, 75.55, 70.59, 46.86, 42.77; IR (KBr, thin film, cm^{-1}): ν_{max} 3425, 3062, 2937, 1610, 1554, 1259, 1239, 1111, 810, 757.



4-(Naphthalen-1-yl)-3a-nitro-3, 3a, 4, 9b-tetrahydro-2H-thieno [3, 2-c] chromen-3-ol (33c): Yellow solid, mp 183–184 °C, 90% yield. 1H NMR (400 MHz, $CDCl_3$) δ 8.09 (d, J = 7.6 Hz, 1H), 7.95 (d, J = 7.2 Hz, 2H), 7.56–7.50 (m, 4H), 7.20–7.28 (m, 1H), 7.23–7.21 (m, 1H), 7.08–7.04 (m, 1H), 6.97 (d, J = 8.0 Hz, 1H), 5.42 (s, 1H), 4.49 (s, 1H), 4.12 (q, J = 7.2 Hz, 1H), 3.56 (dd, J = 12.4, 5.2 Hz, 1H), 3.04 (dd, J = 12.4, 2.4 Hz, 1H); ^{13}C NMR (100 MHz, $CDCl_3$) δ 152.59, 133.74, 131.30, 130.41, 129.53, 129.24, 129.17, 129.06, 128.85, 126.96, 126.68, 126.01, 125.20, 122.61, 121.73, 117.51, 99.35, 76.20, 60.47, 44.26, 33.77; HRMS (ESI, m/z): Calcd. for $C_{21}H_{17}NO_4SNa^+$ 402.0770, found 402.0765; IR (KBr, thin film, cm^{-1}): ν_{max} 3429, 3046, 2924, 1585, 1547, 1230, 1170, 783.

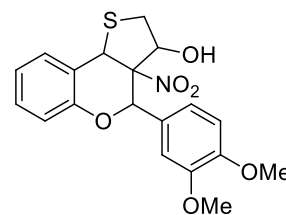


4-(4-Bromophenyl)-3a-nitro-3, 3a, 4, 9b-tetrahydro-2H-thieno [3, 2-c] chromen-3-ol (33d): White solid, mp 186–187 °C, 87% yield. 1H NMR (400 MHz, $CDCl_3$) δ 7.58 (d, J = 8.4 Hz, 2H), 7.24–7.22 (m, 2H), 7.20 (d, J = 8.4 Hz, 2H), 7.07–7.03 (m, 1H), 6.97–6.95 (m, 1H), 5.50 (s, 1H), 5.32 (s, 1H), 4.69 (s, 1H), 3.45 (dd, J = 12.2, 4.4 Hz, 1H), 3.11 (dd, J = 12.2, 1.6 Hz, 1H); ^{13}C NMR (100 MHz, $CDCl_3$) δ 152.16, 132.73, 131.89, 129.28, 128.89, 128.76, 124.09, 122.77, 121.47, 117.36, 98.42, 76.42, 75.35, 42.90, 33.47; IR (KBr, thin film, cm^{-1}): ν_{max} 3414, 2957, 1654, 1545, 1264, 1212, 768.



4-(3,4-Dimethoxyphenyl)-3a-nitro-3,3a,4,9b-tetrahydro-2H-thieno[3,2-c] chromen-3-ol (33e):

Pale yellow solid, mp 155–156 °C, 80% yield. ¹H NMR (400 MHz, CDCl₃+DMSO-*d*₆) δ 7.22 (d, *J* = 8.8 Hz, 2H), 6.88 (d, *J* = 8.4 Hz, 3H), 6.76 (t, *J* = 6.8 Hz, 2H), 5.45 (s, 1H), 5.26 (s, 1H), 4.47 (d, *J* = 2.8 Hz, 1H), 3.77 (s, 3H), 3.72 (s, 3H), 3.46 (dd, *J* = 12.0, 3.6 Hz, 1H), 2.93 (d, *J* = 11.6 Hz, 1H); ¹³C NMR (100 MHz, CDCl₃) δ 161.06, 149.08, 143.37, 143.03, 129.57, 126.99, 124.07, 122.93, 122.64, 121.65, 114.43, 111.75, 99.05, 76.76, 76.47, 56.70, 56.15, 44.00, 35.63; Mass (ESI, *m/z*): Calcd. for C₁₉H₁₉NO₆SN⁺ 412, found 412; IR (KBr, thin film, cm⁻¹): ν_{max} 3423, 2937, 1664, 1550, 1257, 1226, 1024, 766.



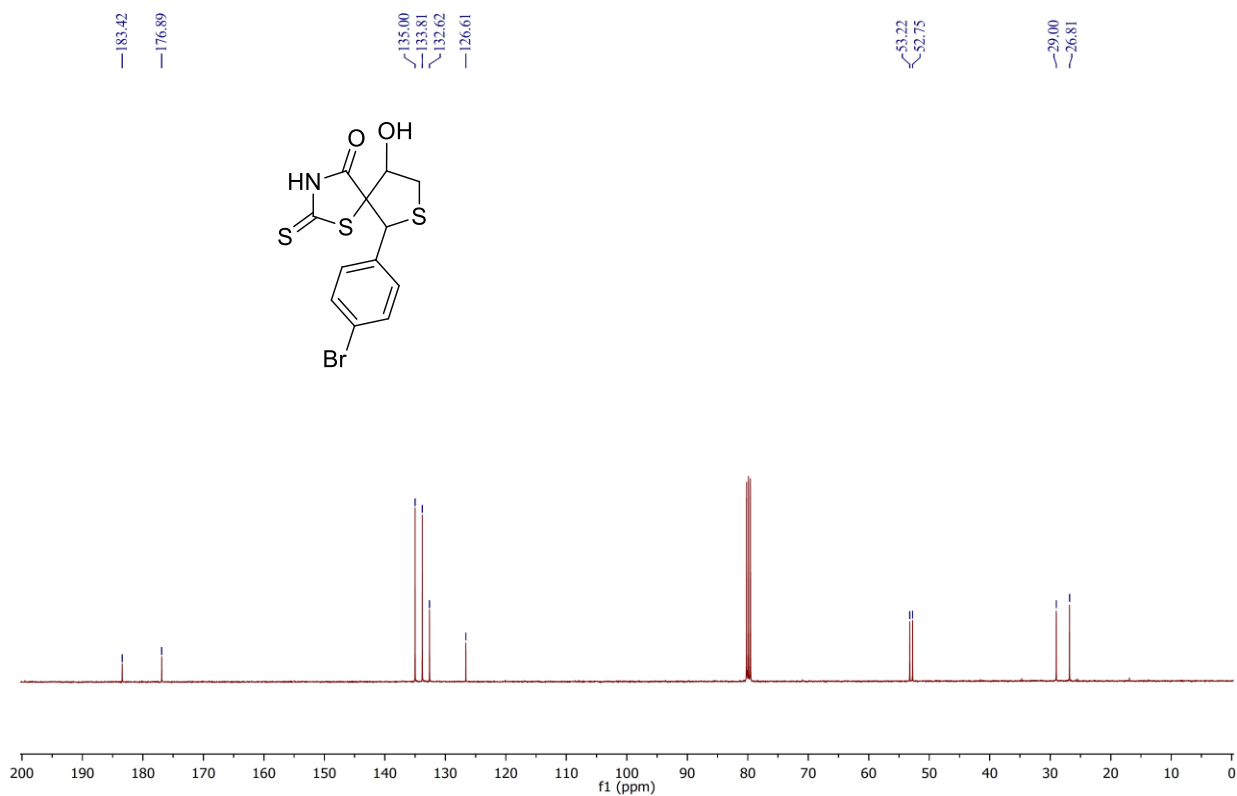
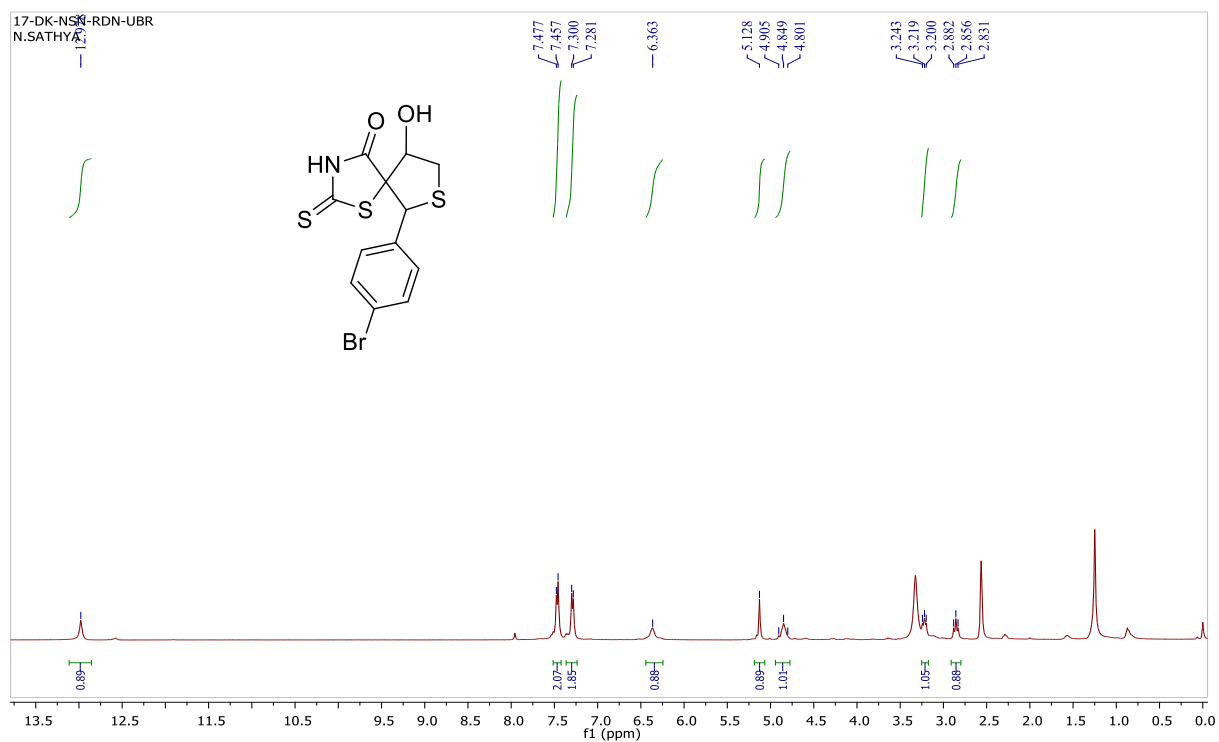
4.7 References

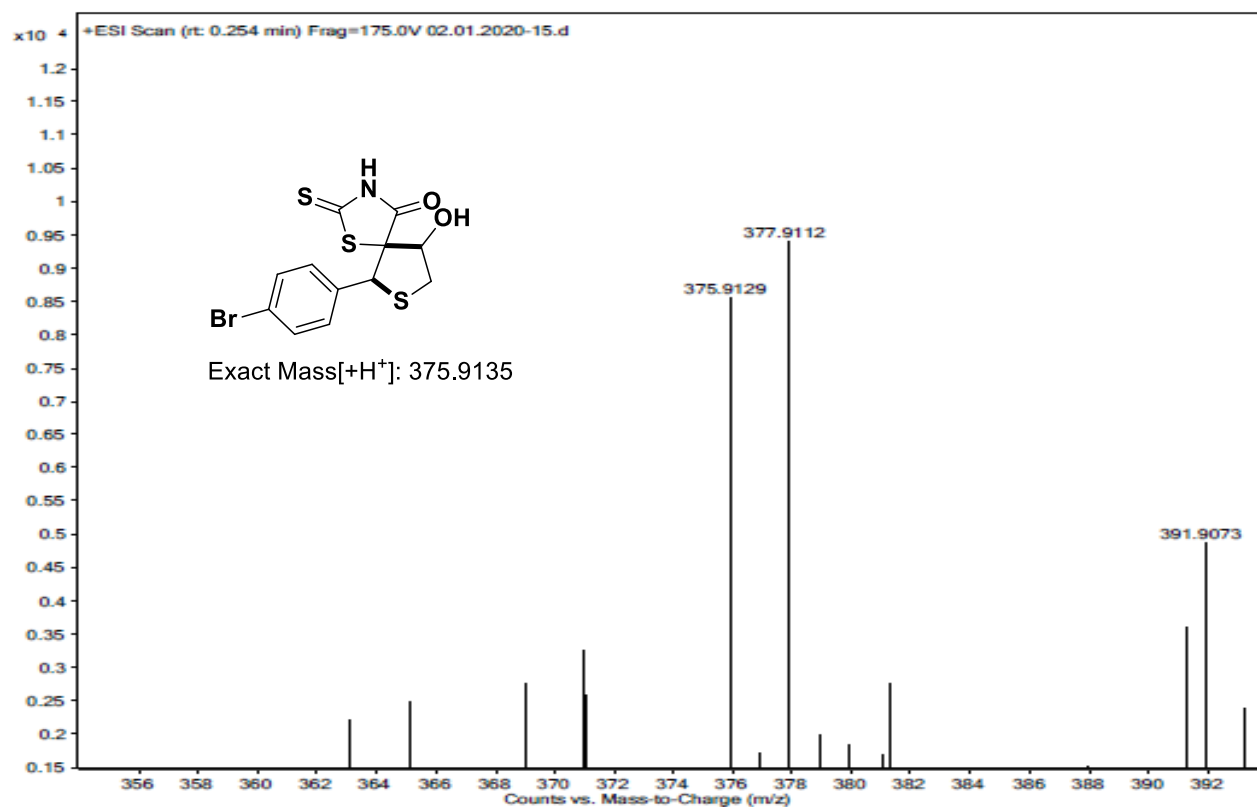
- (a) Wirsching, J.; Voss, J.; Adiwidjaja, G.; Giesler, A.; Kopf. *J. Eur. J. Org. Chem.* **2001**, 6, 1077-1087. (b) Johnson, J. W.; Evanoff, D. P.; Savard, M. E.; Lange, G.; Ramadhar, T. R.; Assoud, A.; Taylor, N. J.; Dmitrienko, G. I. *J. Org. Chem.* **2008**, 73, 6970. (c) Zempleni, J.; Wijeratne, S. S. K.; Hassan, Y. I. *Biofactors*. **2009**, 35(1), 36-46. (d) Ibrahim, P. N.; Cho, H.; England, B.; Gillette, S.; Artis, D. R.; Zuckerman, R. and Zhang, C. *US Patent.*, 8, 470, 821 B2, **2013**. (e) Ohtsuka, T.; Kotaki, H.; Nakayama, N.; Itezono, Y.; Shimma, N.; Kudoh, T.; Kuwahara, T.; Arisawa, M and Yokose, K. *J. Antibiotics*. **1993**, 46, 11–17. (f) Smith, P. W.; Sollis, S. L.; Howes, P. D.; Cherry, P. C.; Starkey, I. D.; Cobley, K. N.; Weston, H.; Scicinski, J.; Merritt, A.; Whittington, A.; Wyatt, P.; Taylor, N.; Green, D.; Bethell, R.; Madar, S.; Fenton, R. J.; Morley, P. J.; Pateman, T. and Beresford, A. *J. Med. Chem.* **1998**, 41, 787. (g) Yuasa, H.; Takada, J and Hashimoto, H. *Bioorg. Med. Chem. Lett.* **2001**, 11, 1137–1139.
- (a) Almond, C. M.; D., Liotta, D. C.; Painter, G. R. and Soria, J.; WO 2000009494 A1. **2000**. (b) Maclean, D.; Holden, F.; Davis, A. M.; Scheuerman, R. A.; Yanofsky, S.; Holmes, C. P.; Fitch, W. L.; Tsutsui, K.; Barrett, R. W.; Gallop, M. A. *J. Comb. Chem.* **2004**, 6, 196. (c) Raghav, M.; Jha, K. K.; Sachinm, K.; Isha, T. *Der Pharma Chemica*. **2011**, 3 (4), 38-54. (d) Maccari, R.; Corso, A. D.; Giglio, M.; Moschini, R.; Mura, U.; Ottana, R. *Bioorg. Med. Chem. Lett.* **2011**, 21, 200-119. (e) Effenberger, F.; Straub, A.; Null, V. *Justus Liebigs Ann. Chem.* **1992**, 1297–1301. (f) Chauhan, P.; Mahajan, S.; Enders, D. *Chem. Rev.* **2014**, 114, 8807. (g) Duan, S.-W.; Li, Y.; Liu, Y.-Y.; Zou, Y.-Q.; Shi, D.-Q.; Xiao, W.-J. *Chem. Commun.* **2012**, 48, 5160. (h) Hu, Y.-J.; Wang, X.-B.; Li, S.-Y.; Xie, S.-S.; Wang, K. D. G.; Kong, L.-Y. *Tetrahedron Lett.* **2015**, 56, 105.

3. (a) Gewald, K.; Schinke, E.; Böttcher, H. *Chem. Ber.* **1966**, *99*, 94–100. (b) Honek, J. F.; Mancini, M. L. and Belleau, B. *Synth. Comm.* **1984**, *14*, 483–491. (c) Spino, C.; Crawford, J. and Bishop, J. *J. Org. Chem.* **1995**, *60*, 844–851; (d) Barco, A.; Baricordi, N.; Benetti, S.; De Risi, C. and Pollinib, G. P. *Tetrahedron Lett.* **2006**, *47*, 8087–8090. (e) Stefan, S.; Erna, Z.; Luca, S.; Kurt, F.; Christoph, K. W. and Wolfgang, K. *Chem. Rev.* **2022**, *122*, 1052–1126.
4. (a) Ling, J.-B.; Su, Y.; Zhu, H.-L.; Wang, G.-Y.; Xu, P.-F. *Org. Lett.* **2012**, *14*, 1090. (b) Kowalczyk, D.; Wojciechowski, J.; Albrecht, Ł. *Tetrahedron Lett.* **2016**, *57*, 2533. (c) Kumar, S.-V.; Prasanna, P.; Perumal, S. *Tetrahedron Lett.* **2013**, *54*, 6651. (d) Kayaa, U.; Mahajana, S.; Schöbela, J.-H.; Valkonenb, A.; Rissanenb, K.; Enders, D.; *Synthesis* **2016**, *48*, 4091. (e) Liang, J.-J.; Pan, J.-Y.; Xu, D.-C. Xie, J.-W. *Tetrahedron Lett.* **2014**, *55*, 6335.
5. (a) Connor, C. J. O.; Roydhouse, M. D.; Przybyz, A. M.; Wall, M. D.; Southern, J. M. *J. Org. Chem.* **2010**, *75*, 2534. (b) Kaya, U.; Mahajan, S.; Schöbel, J. H.; Valkonen, A.; Rissanen, K.; Enders, D. *Synthesis*. **2016**, *48*, 4091–4098. (c) Suruchi, M.; Pankaj, C.; Marcus, B.; Rakesh, P.; Kari, R.; Gerhard, R.; Dieter, E. *Synthesis*, **2016**, *48*, 1131–1138. (d) McNabola, N.; O'Connor, C. J.; Roydhouse, M. D.; Wall, M. D.; Southern, J. M. *Tetrahedron*. **2015**, *71*, 4598. (e) Fang, X.; Jun, L.; Tao, H.-Y and Wang, C. -J. *Org. Lett.* **2013**, *15*, 5554–5557. (f) Zhong, Y.; Ma, S.; Li, B.; Jiang, X.; Wang, R.; *J. Org. Chem.* **2015**, *80*, 6870. (g) Selvi, T.; Vanmathi, G.; Srinivasan, K. *RSC Adv.* **2015**, *5*, 49326. (h) Hu, Y.-J.; Wang, X.-B.; Li, S.-Y.; Xie, S.-S.; Wang, K. D. G.; Kong, L.-Y. *Tetrahedron Lett.* **2015**, *56*, 105. (i) Sathishkannan, G.; Srinivasan, K. *Chem. Commun.* **2014**, *50*, 4062. (j) Evdokimov, N. M.; Kireev, A. S.; Yakovenko, A. A.; Antipin, M. Y.; Magedov, I. V.; Kornienko, A. *J. Org. Chem.* **2007**, *72*, 3443. (k) Zhang, J.-L.; Liu, X.-H.; Ma, X.-J and Wang, R. *Chem. Commun.*, **2013**, *49*, 9329–9331. (l) Sakkani, N.; Neeli, S.; Banoth, P.; Anuji, K. V.; Sriram, K.; Balasubramanian, S.; Prabhakar, S and Dhurke, K., *RSC Adv.* **2015**, *5*, 94474. (m) Azath, I. A.; Puthiaraj, P.; Pitchumani, K. *ACS Sustainable Chem. Eng.* **2013**, *1*, 174.
6. Kaya, U.; Mahajan, S.; Schöbel, J. H.; Valkonen, A.; Rissanen, K.; Enders, D. *Synthesis* **2016**, *48*, 4091–4098.

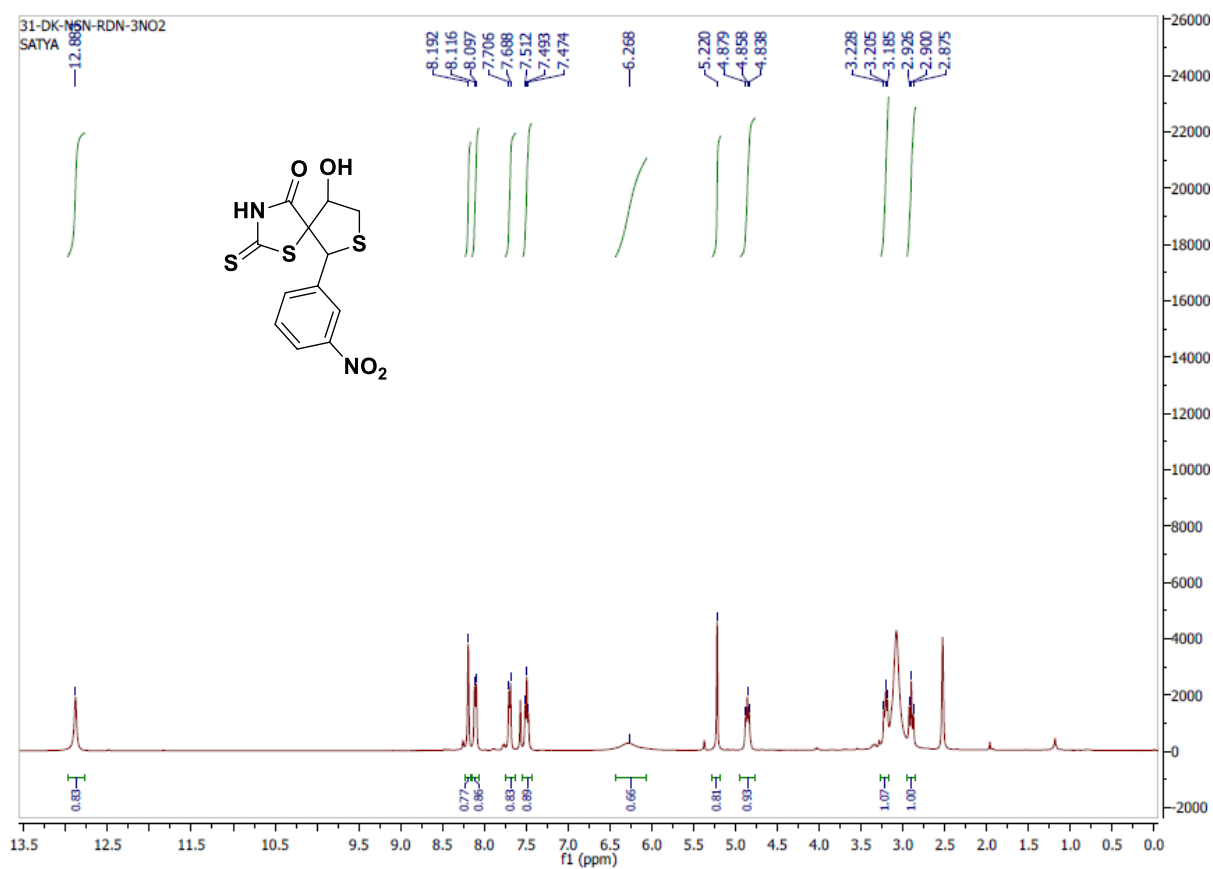
4.7 Selected Spectral data

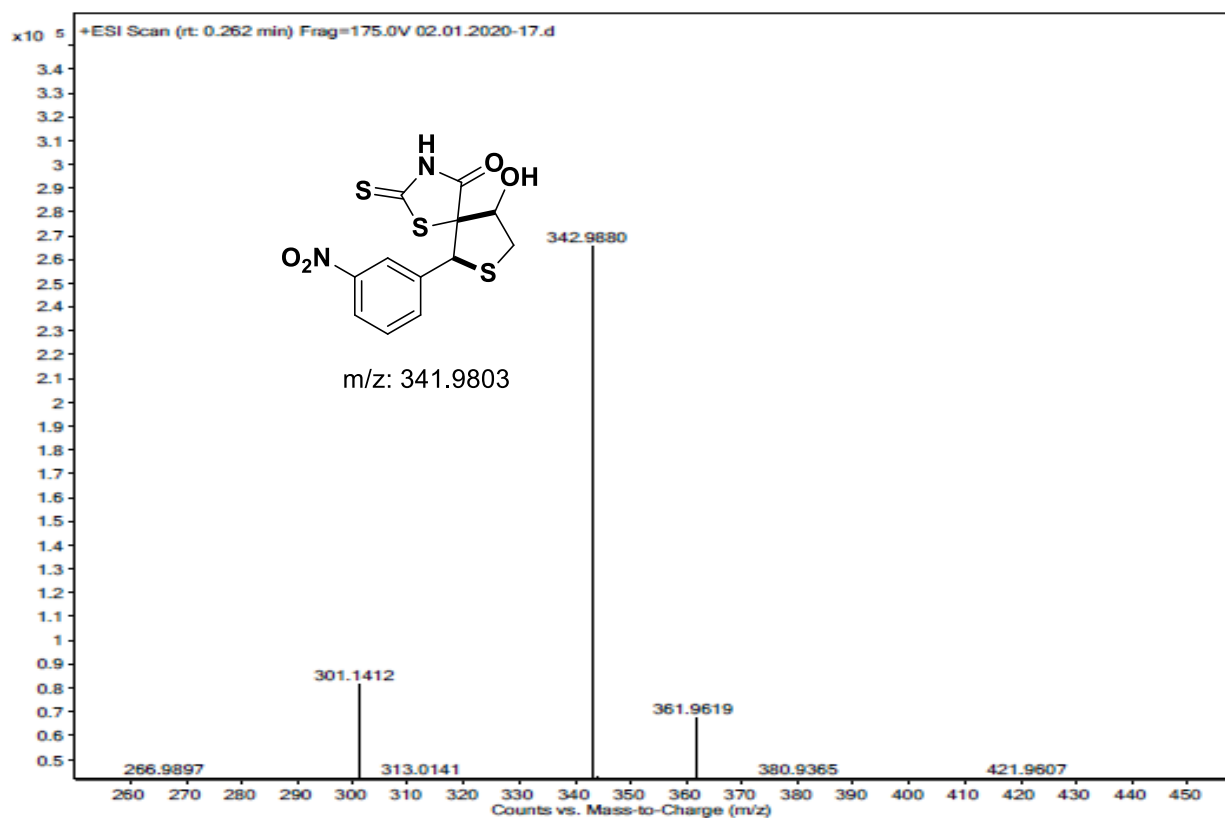
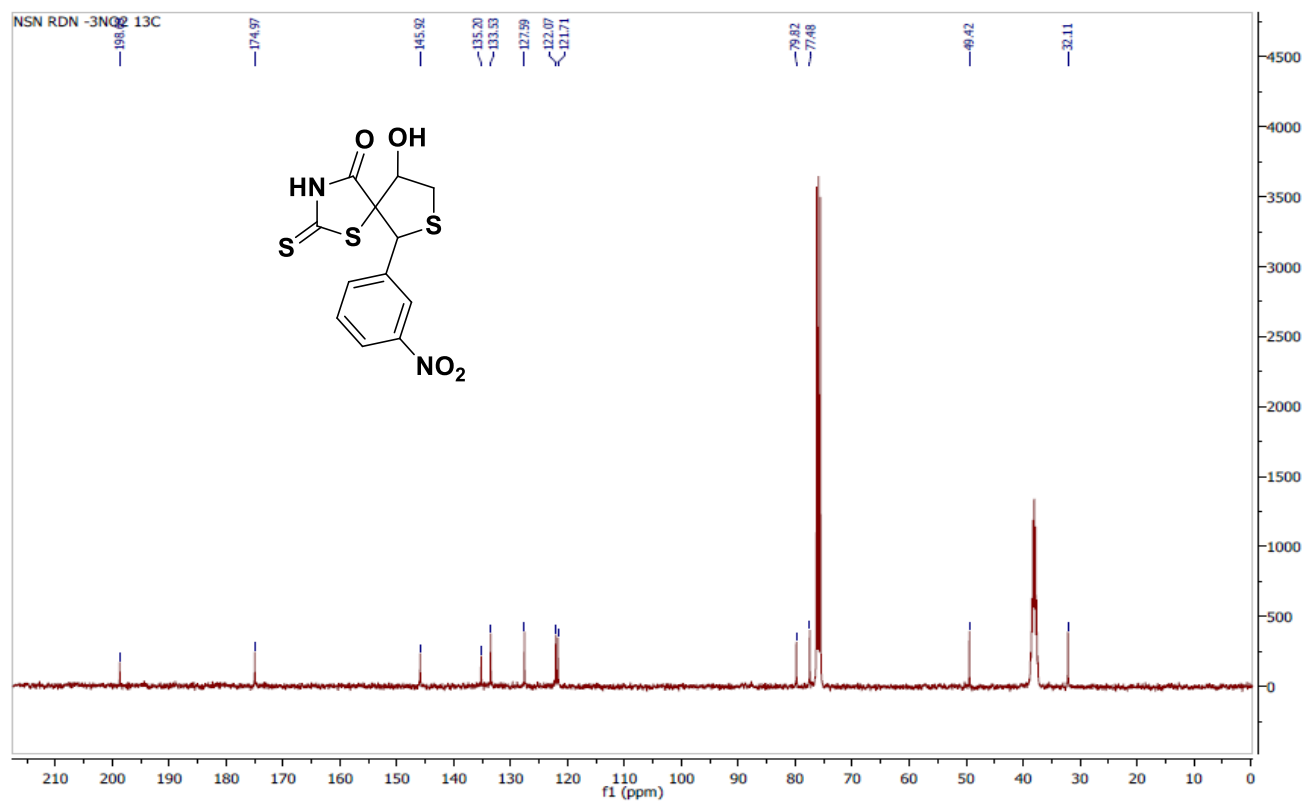
6-(4-Bromophenyl)-9-hydroxy-2-thioxo-1,7-dithia-3-azaspiro[4.4]nonan-4-one (25e):



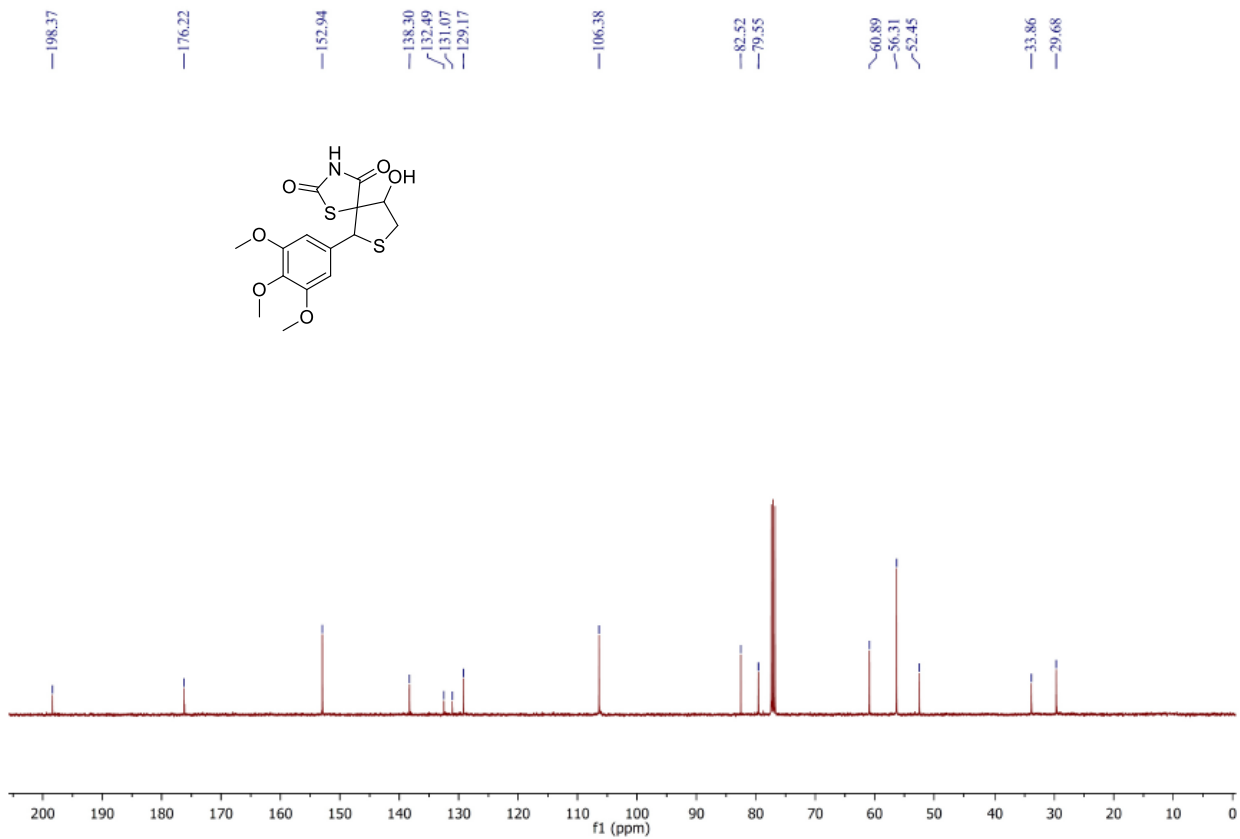
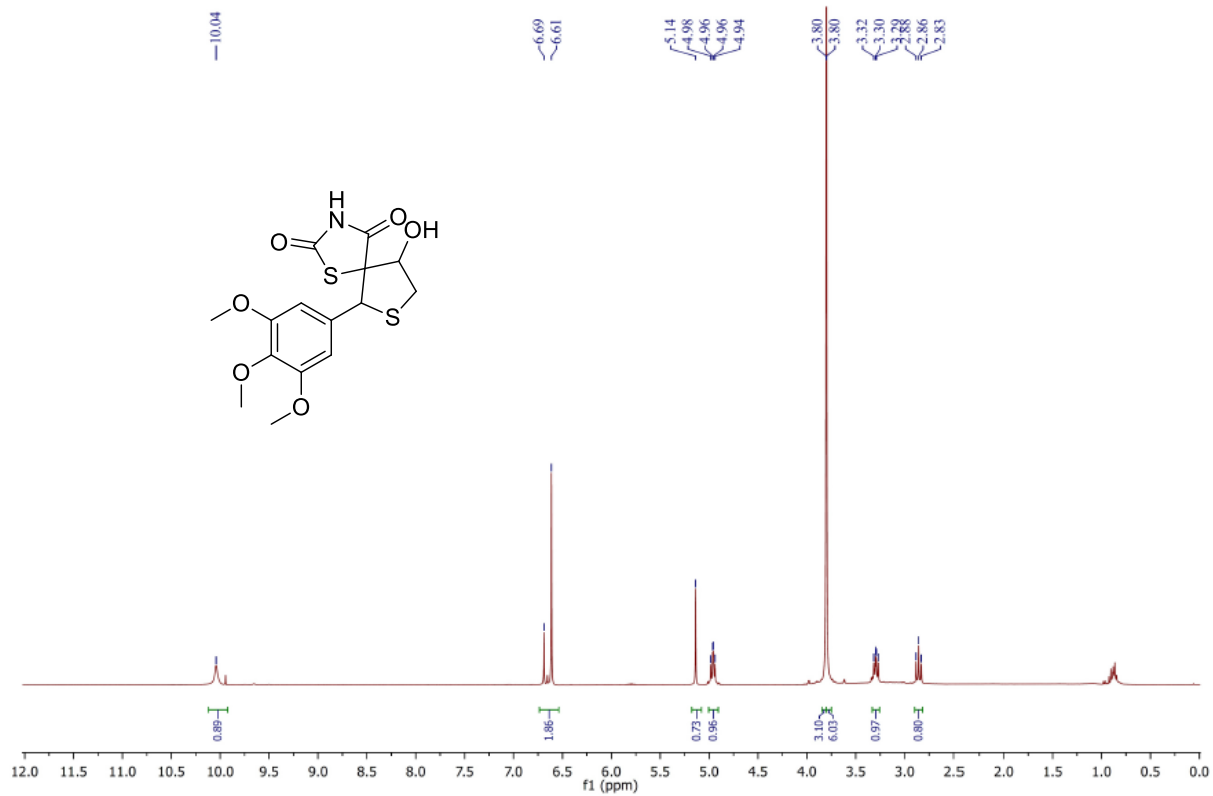


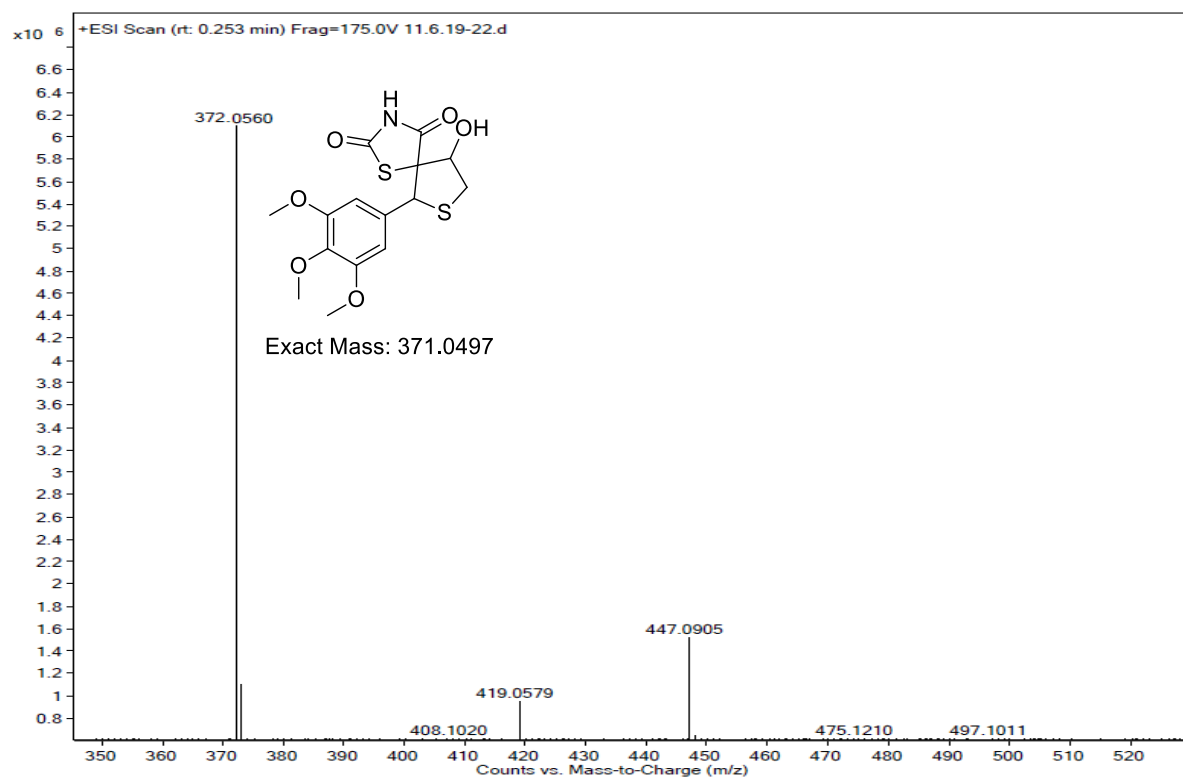
9-Hydroxy-6-(3-nitrophenyl)-2-thioxo-1,7-dithia-3-azaspiro[4.4]nonan-4-one (25g):



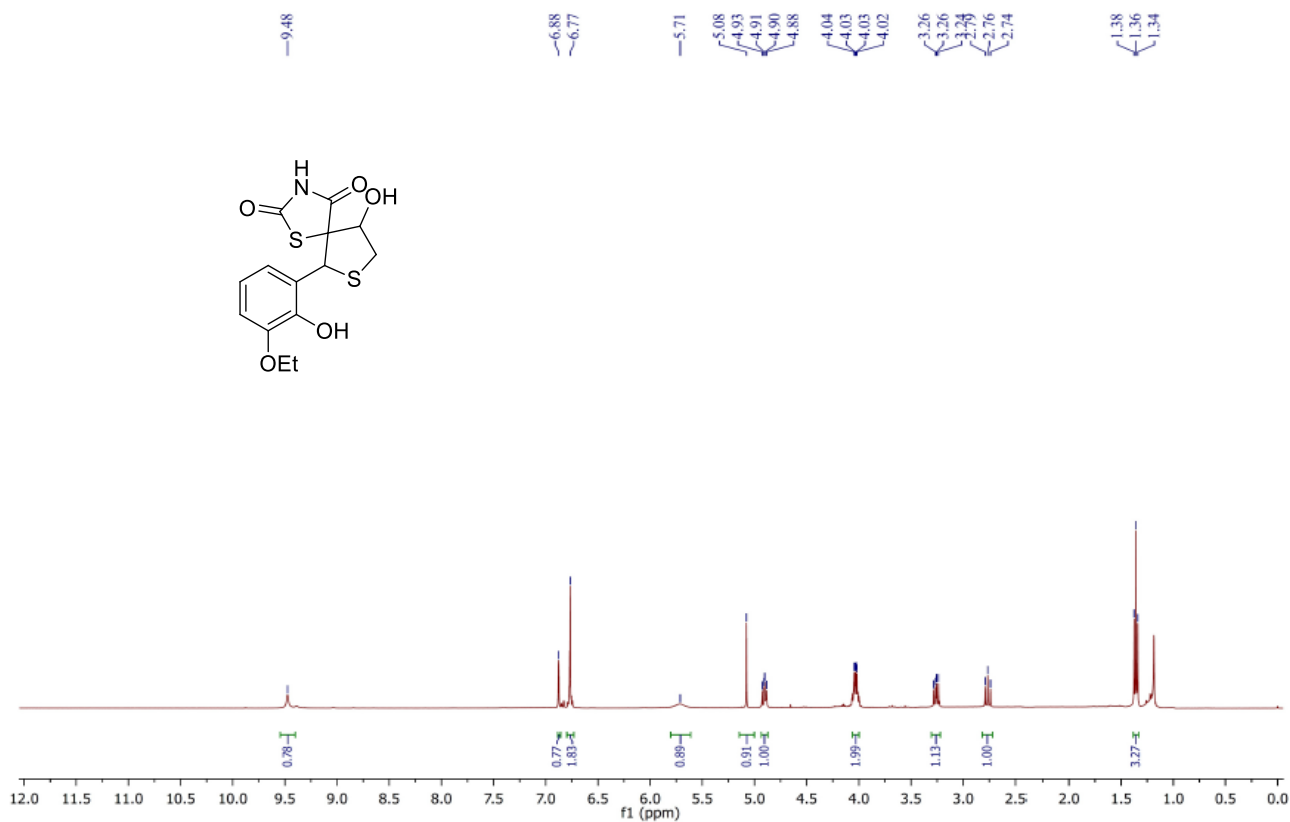


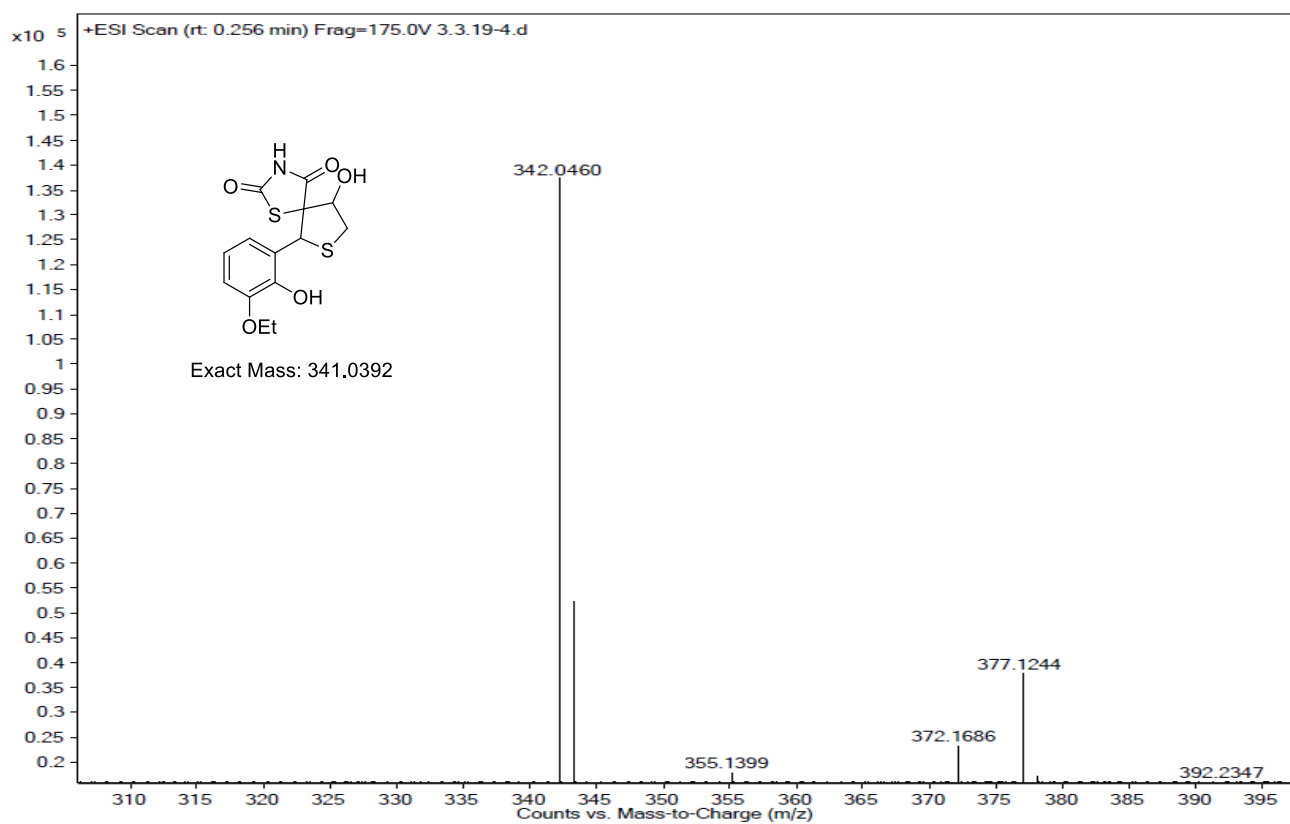
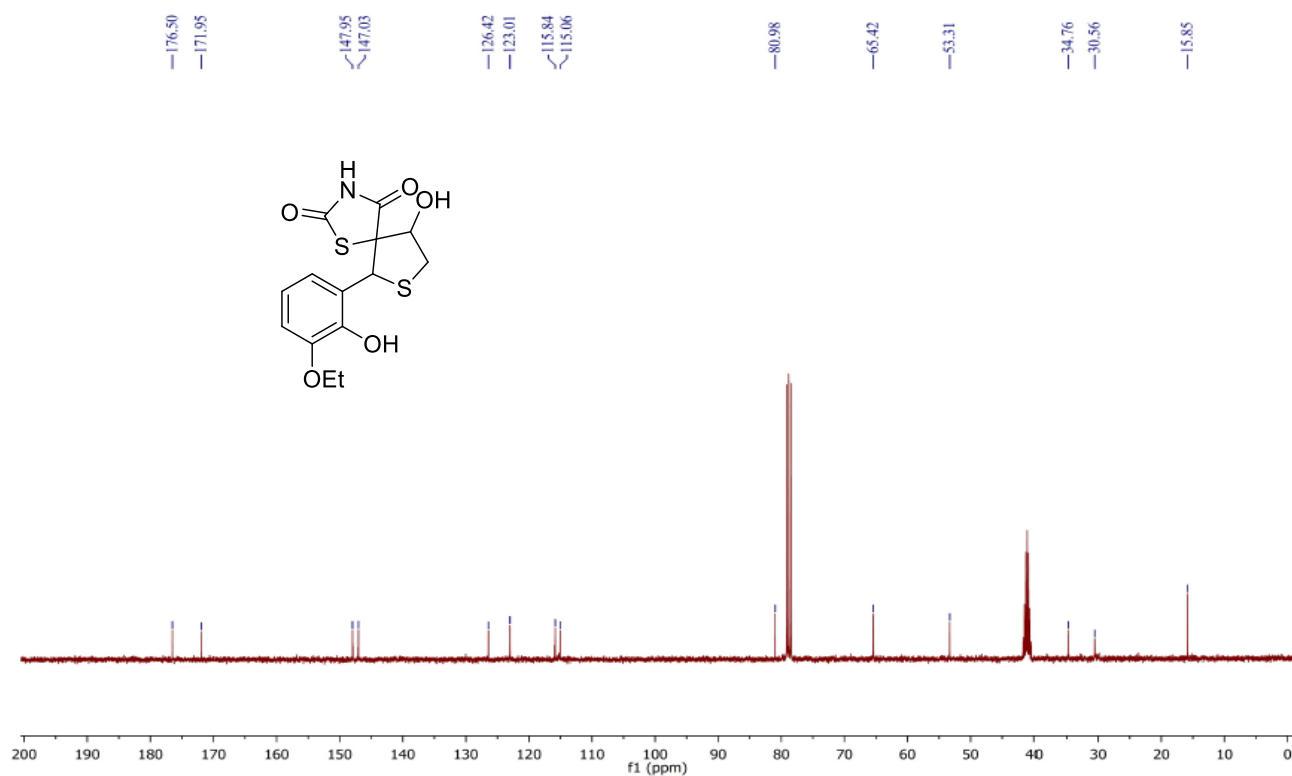
6-(3,4,5-Trimethoxyphenyl)-9-hydroxy-1,7-dithia-3-azaspiro[4.4]nonane-2,4-dione (27e):



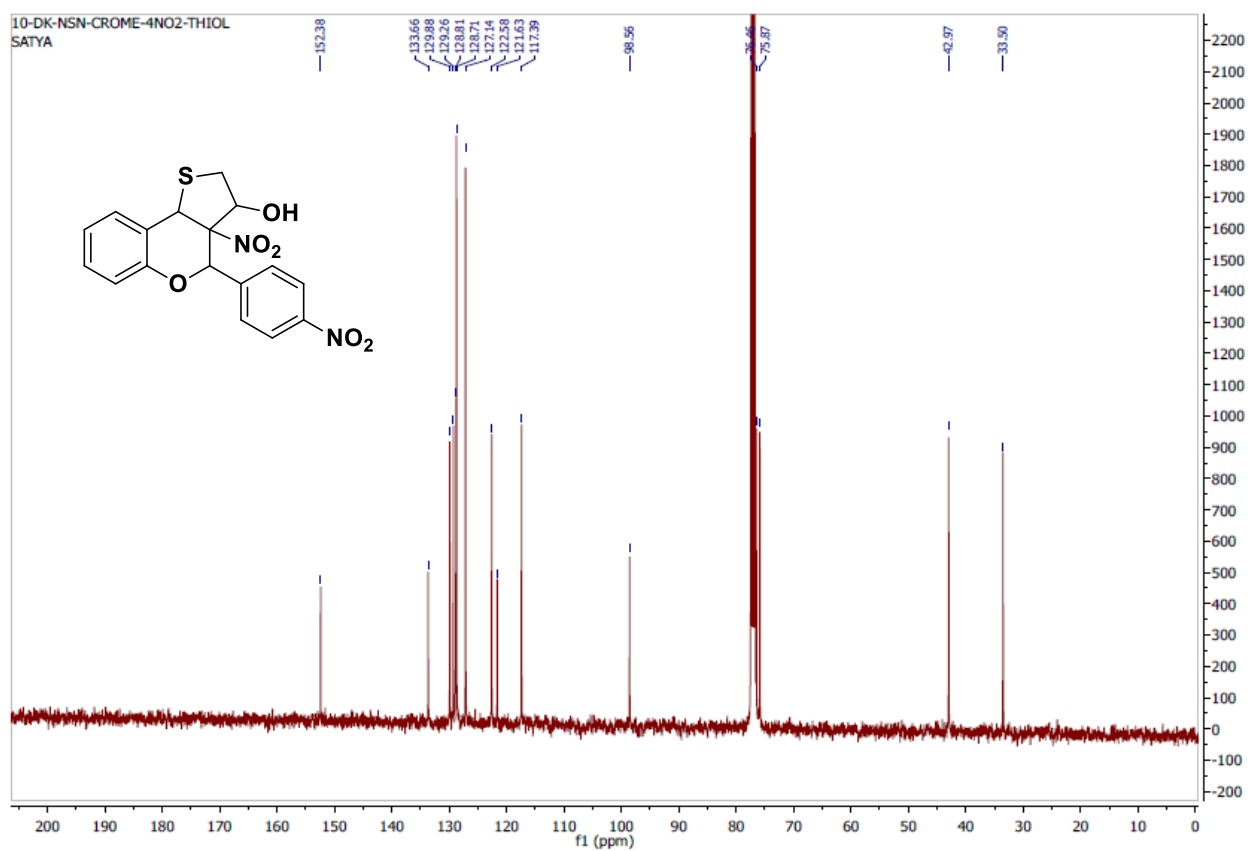
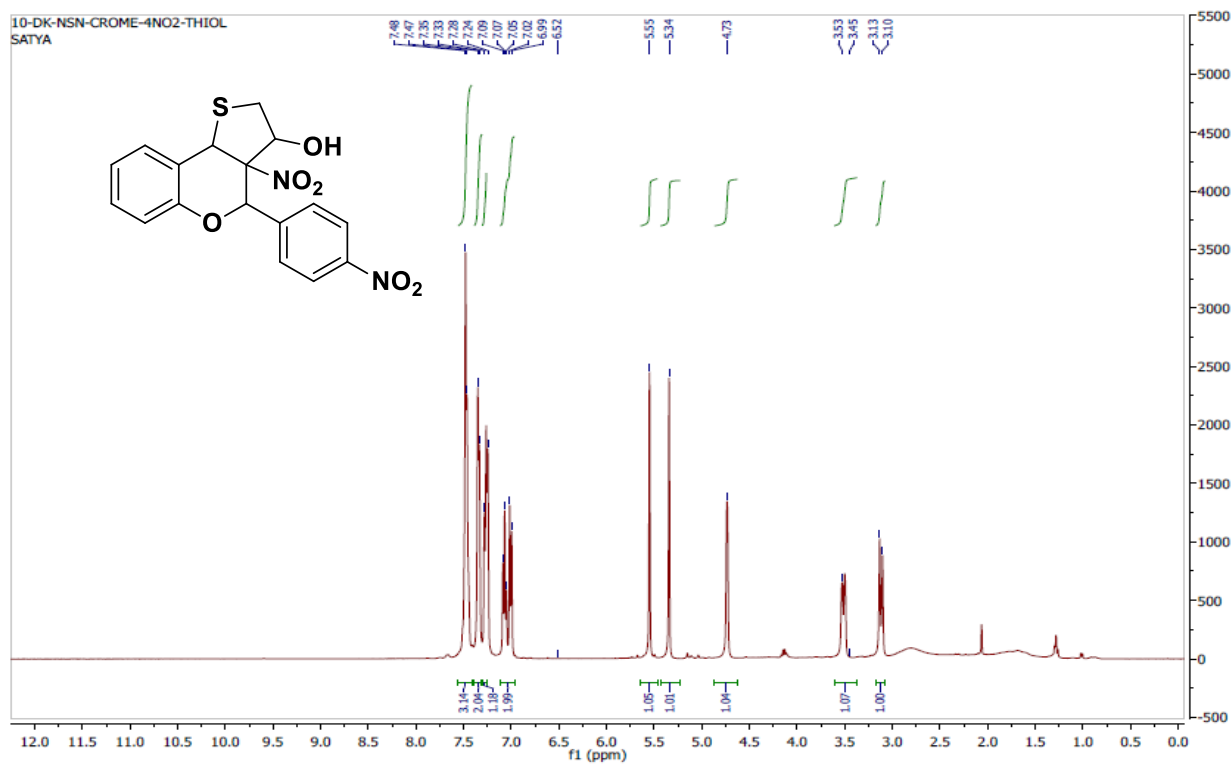


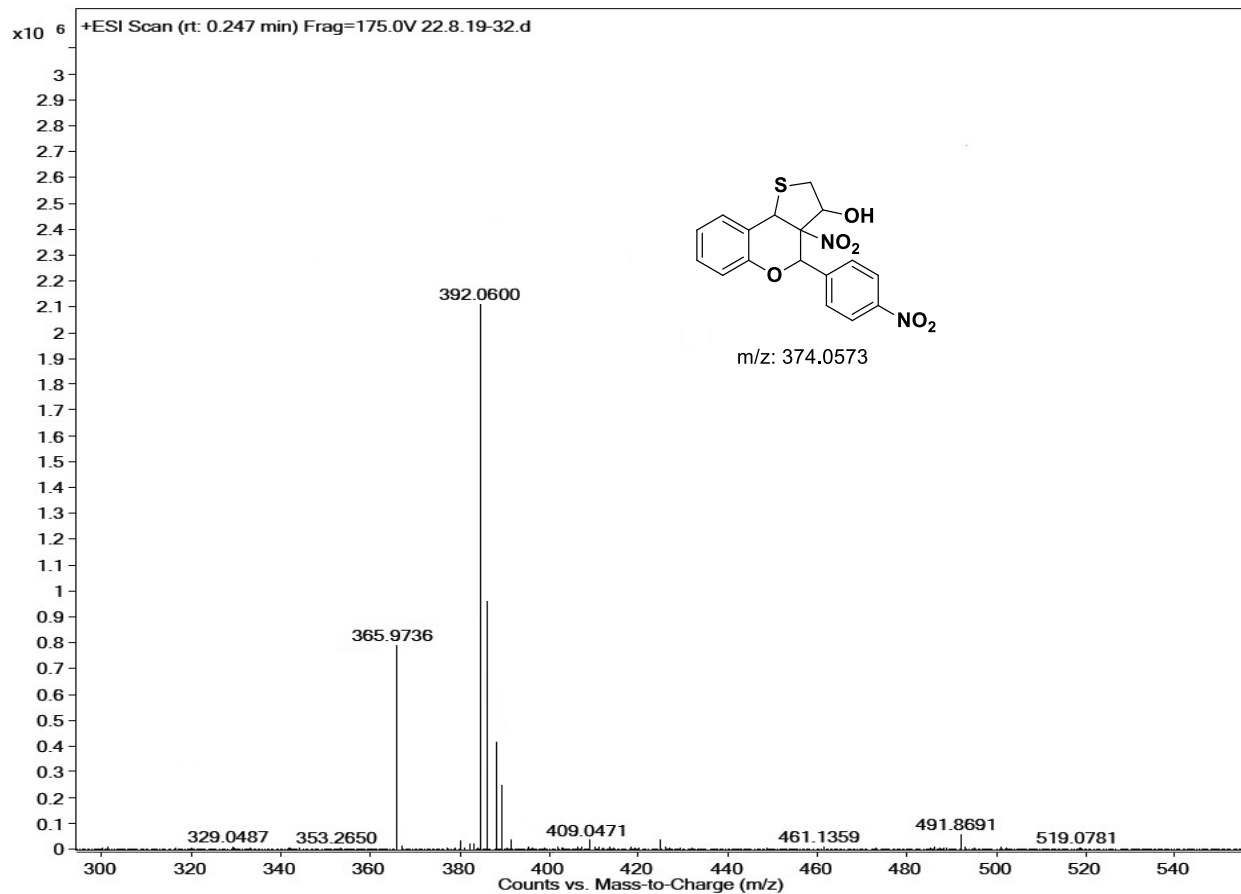
6-(3-Ethoxy-2-hydroxyphenyl)-9-hydroxy-1,7-dithia-3-azaspiro[4.4]nonane-2,4-dione (27g):





3a-Nitro-4-(4-nitrophenyl)-3,3a,4,9b-tetrahydro-2H-thieno[3,2-c]chromen-3-ol (33a):





CHAPTER-5

SnCl₂-catalyzed synthesis of dibenzo-[1,4]-diazepin-1-one, phenyl quinazoline, and pyridine-1,3,4-oxadiazole based sulfonate esters and their evaluation as α -glucosidase inhibitors

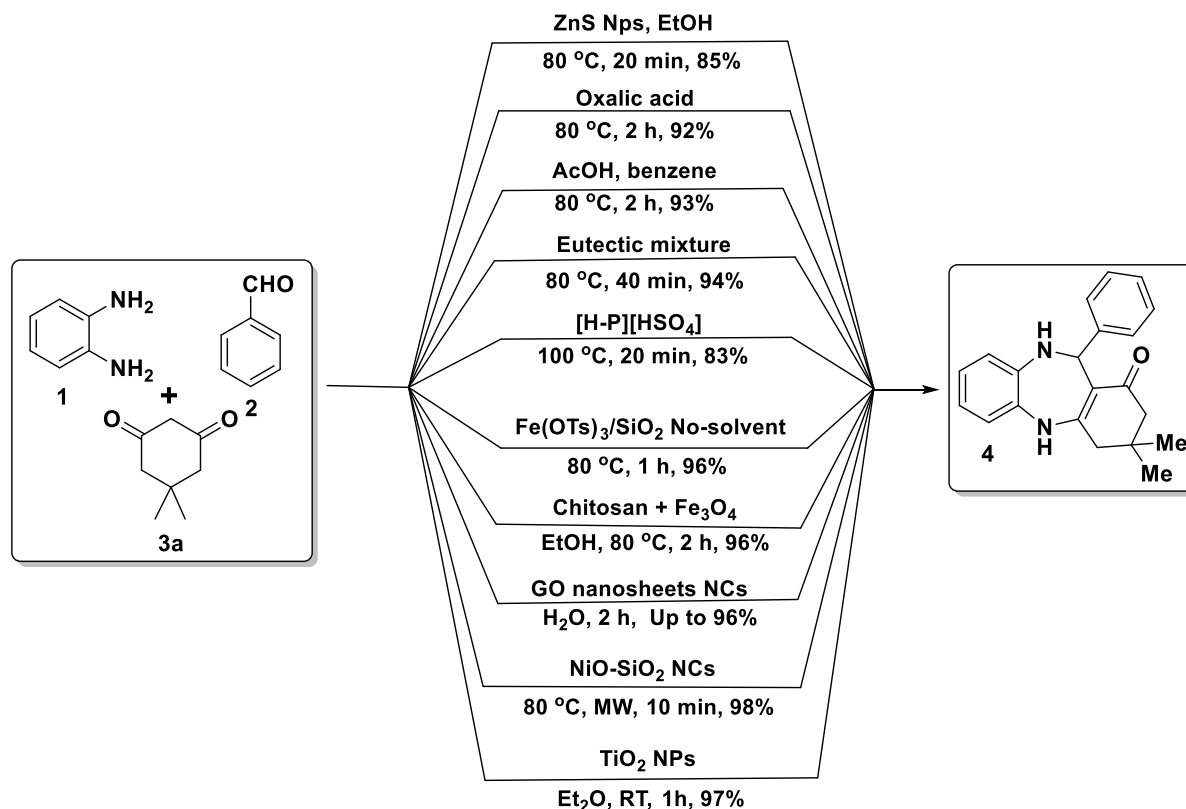
Abstract

Benzodiazepines are well known in the rheumatoid arthritis and neurological diseases. The synthetic derivatives of these compounds are used for protease and hepatitis-C-virus (HCV) NS5B polymerase inhibition. The quinazolines are used in different therapeutic areas. Similarly, the applications of functionalized 1,3,4-oxadiazoles are explored in medicinal, material chemistry. Considering the importance of title related compounds, in this chapter, we have described the synthesis of substituted dibenzo-[1,4]-diazepin-1-ones, phenyl quinazolines, and pyridine-1,3,4-oxadiazole sulfonate using SnCl₂ (catalytic amount). The newly benzodiazepine derivatives were evaluated for α -glucosidase enzyme inhibition activity against acarbose as a standard drug. A detailed discussion on the synthesis biological study is discussed in this chapter.

5.1 Introduction

5.1.1 Biologically active dibenzo-[1,4]-diazepin-1-ones and their synthetic methods

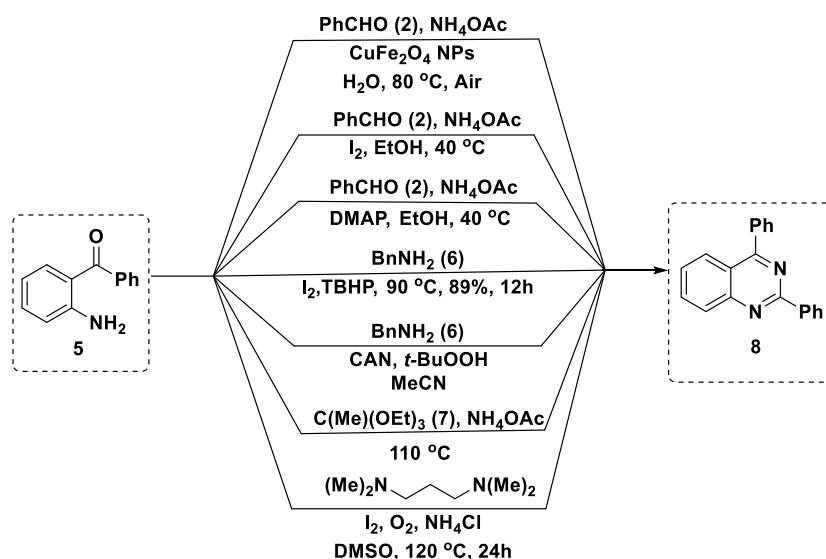
Benzodiazepine received great attention in medicinal chemistry^{1a} particularly in central nervous system (CNS) as depressants.^{1b} psychotropics^{1c} anti-anxiety drugs (chlordiazepoxide)^{1a} and schizophrenia (clozapine)^{1d} and rheumatoid arthritis,^{1e} inflammatory.^{1f} The dibenzo-[1,4]-diazepinone derivatives play important role as platelet-activating factors, inhibition of phosphodiesterase,^{2a} protease,^{2b} and hepatitis-C-virus polymerize.^{2c} Some of the synthetic derivatives of benzodiazepins are known as metabotropic receptor-2 antagonists,^{3a} histamine receptor antagonists,^{3b} and muscarinic receptor-M1 antagonist (pirenzepine).^{3c} Dibenzo-[1,4]-diazepin-1-ones (**4**) are usually prepared from *o*-phenylenediamine (**1**), benzaldehyde (**2**), and dimedone (**3**). The reaction conditions are oxalic acid^{4a} or AcOH^{4b} in benzene. The use of deep eutectic mixtures (ChCl + urea),^{4c} ionic liquids like *N*-methyl-2-pyrrolidonium hydrogen sulfate [H-NMP][HSO₄].^{4d} has also been reported to give good yields. Also, chitosan-supported Fe₃O₄, graphene oxide nanosheets,^{4e} ZnS nanoparticles,^{4f} TiO₂ nanoparticles,^{4g} silica-supported Fe(OTf)₃,^{5a} silica supported NiO nanoparticles^{5b} are also known for this purpose. Recently our group^{5c} also reported L-proline catalyzed water-mediated reaction for preparation of dibenzo-[1,4]-diazepin-1-one derivatives with good yields (**Scheme-1**).



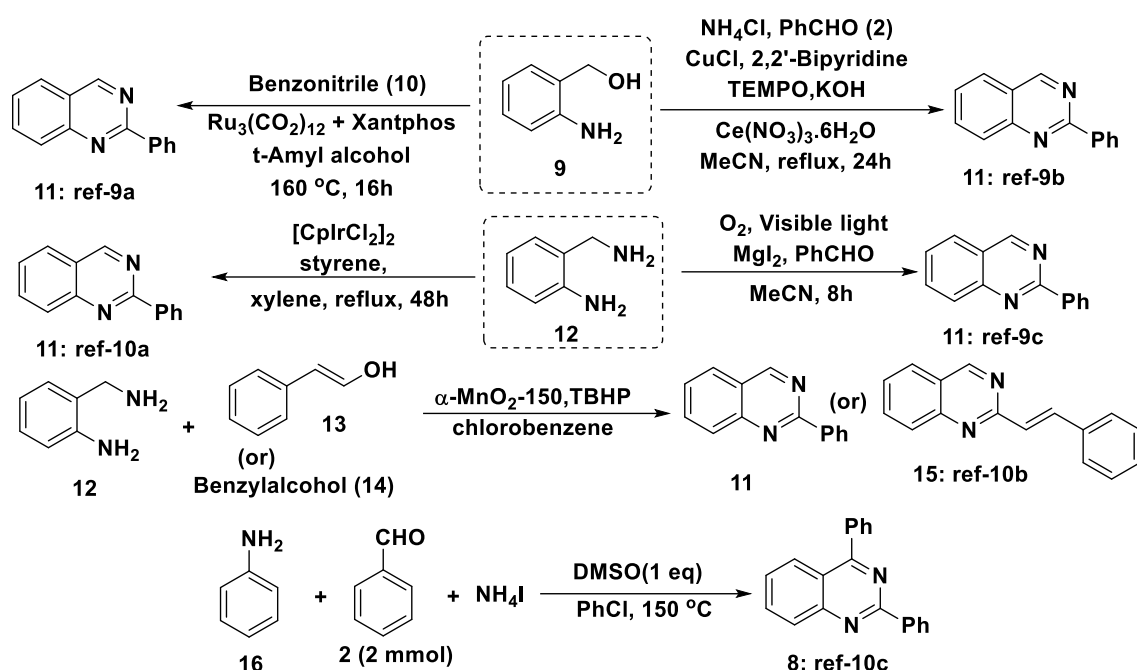
Scheme-1: Reported methods of the synthesis of dibenzo-[1,4]-diazepin-1-one.

5.1.2 Bioactive quinazolines and their synthetic methods

Quinazoline based drugs like erlotinib,^{6a} used for pancreatic cancer and as $\alpha 1$ -AR antagonists (prazosin, doxazosin, terazosin),^{6b} inhibitors of tubulin polymerization,^{7a} PI3k/Akt/mTOR, topoisomerase-I,^{7b} protein kinase,^{7c} RTK/EGFR,^{7d} tyrosine kinase activity, and apoptotic inhibition activity.^{7e} The synthesis of 2,4-diphenylquinazolines is relatively easy and can be achieved from 2-amino benzophenone (**5**) and benzyl amines (**6**) *via* sp^3 C-H functionalization. This was achieved using iodine^{8a} and CAN as catalysts.^{8b} Other methods applied for this purpose include CuFeO₄ nanopartials^{8c} DMAP,^{8d} catalyst-free conditions,^{8e} oxidative sp^3 C-H amination in DMSO at 120 °C as shown in **Scheme-2**. Along with these, there are few multi-step methods reported based on the ruthenium mediated dehydrogenative condensation,^{9a} cerium nitrate mediated oxidative condensation of 2-amino benzyl alcohol (**9**) with benzonitrile,^{9b} (**Scheme-3a**) are known. Similarly, Itoh group reported magnesium iodide (MgI₂)^{9c} mediated coupling 2-aminobenzylamine (**12**) and benzaldehyde (**2**) *via* an aerobic photooxidation and Iridium ([CpIrCl₂]₂) catalyzed^{10a} reaction of 2-amino benzylamine (**12**) and styrene to generate 2-substituted quinazoline (**11**). In addition, *Feng et al.*,^{10b} also developed α -MnO₂-150/TBHP catalyzed cascade reaction of 2-amino benzylamine with benzyl alcohol (**13**) (or) styryl alcohol (**14**) in chlorobenzene to provide 2-substituted quinazoline (**11**) or 2-phenyl styrylquinazolines (**15**). Recently, Fuhong and co-workers^{10c} described a four-component synthesis of substituted quinazolines from aniline (**16**), aromatic aldehyde (**2**), and ammonium iodide (NH₄I) in presence of DMSO. This reaction proceeds *via* C–H bond activation of the amino group of aniline moieties under metal-free conditions.



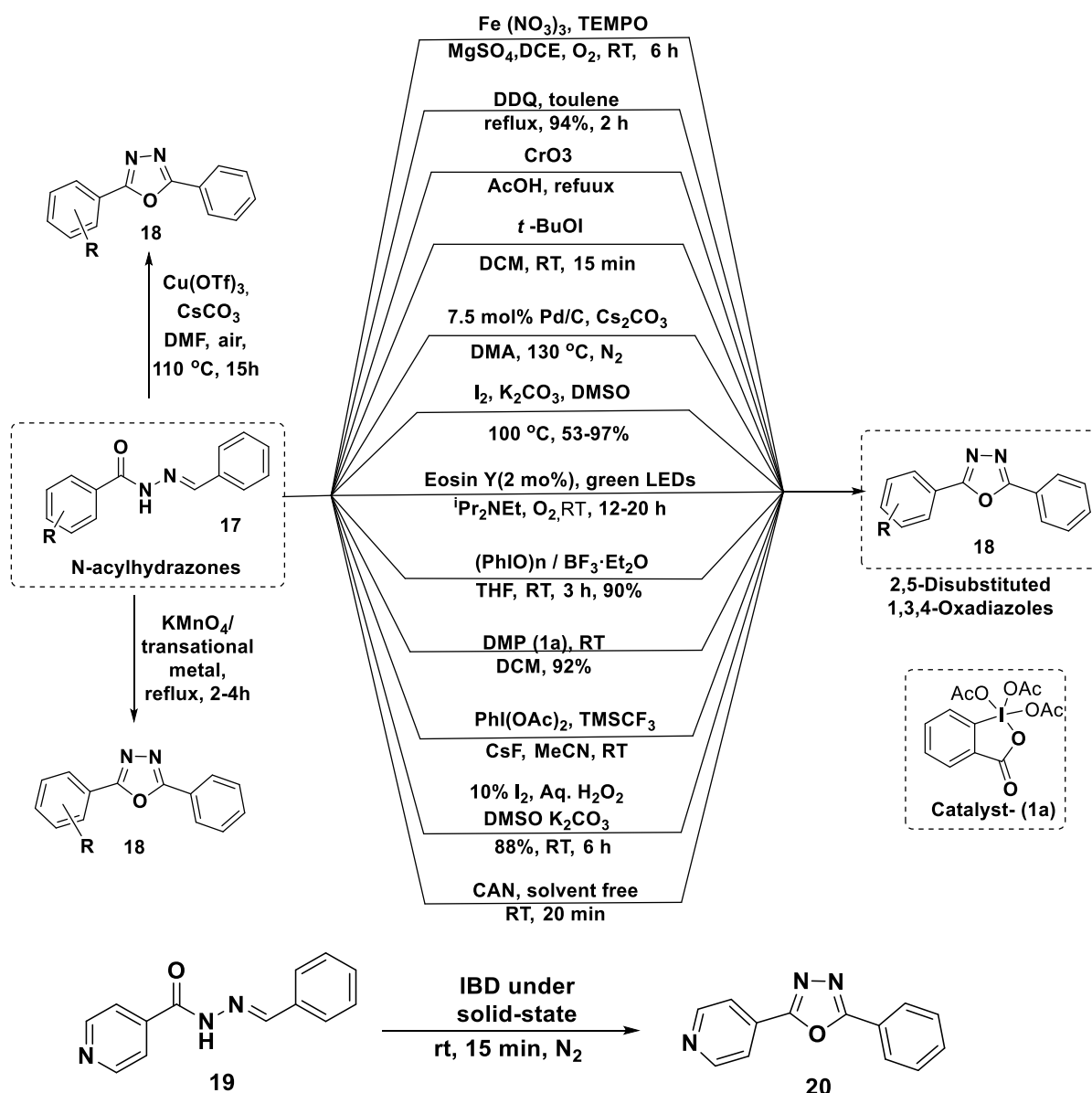
Scheme-2: Reported methods for the synthesis of substituted 2,4-diphenylquinazolines.



Scheme-3(a): Other approaches for the synthesis of substituted-2-phenylquinazolines.

5.1.4 Bioactive 1,3,4-oxadiazoles and their synthetic methods.

The 1,3,4-oxadiazoles as bioisosteres in medicinal chemistry and part of many drugs with antimicrobial,^{11a} antisedative,^{11b} insecticidal,^{11c} anti-TB,^{11d} antiepileptic,^{11e} and anti-inflammatory^{11f} properties. Also, there are reports of oxadiazoles for photochemical and electrochemical applications and^{11g} and agrochemistry.^{11h} General methods for the synthesis of disubstituted 1,3,4-oxadiazoles (**18**) is either by dehydrative cyclization or oxidative reduction of 1,2-diacylhydrazines. The dehydrative cyclization (decarboxylative reduction) was achieved by the oxidation of N, N'-acyl hydrazones (**17**) using different oxidants such as CrO_3 ,^{12a} DDQ,^{12b} $\text{Fe}(\text{NO}_3)_3/\text{TEMPO}$,^{12c} $t\text{-BuOI}$,^{12d} eosin-Y/Green LED,^{12e} Dess-martin periodinane,^{12f} CAN,^{12g} KMnO_4 ,^{12h} transitional metals¹²ⁱ and $\text{Cu}(\text{OTf})_3$.^{12j} The oxidant and H-acceptor free, Pd/C mediated^{13a} cyclization of acyl hydrazones, $(\text{PhIO})_n/\text{BF}_3 \cdot \text{Et}_2\text{O}$ mediated synthesis is also applied effectively for the generation of disubstituted-1,3,5-oxadiazoles *via* oxidative cyclization of acyl hydrazones (**Scheme-3b**). Additionally, the cyclization of *N*-acyl hydrazones is achieved using $\text{I}_2/\text{H}_2\text{O}_2$ catalyst,^{13b} transition-metal free I_2/CsCO_3 .^{13c} (**Scheme-3b**). Alternatively, the iodobenzene diacetate (IBD)^{13d} catalyzed synthesis of 2-phenyl-5-(pyridine-4-yl)-1,3,4-oxadiazole (**20**) has been developed *via* cyclization of (E)-N'-benzylidene isonicotinohydrazide (**19**).

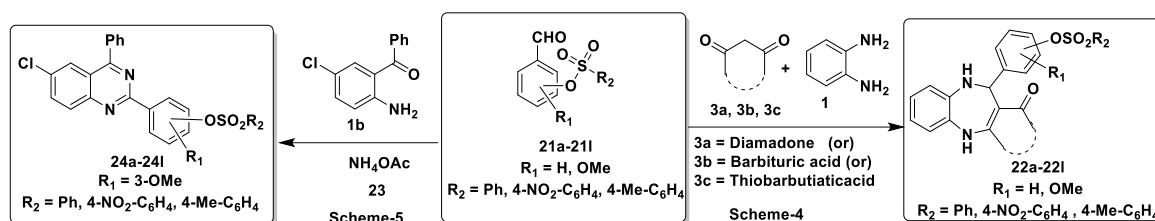


Scheme-3b: Reported methods for 2,5 substituted 1,3,4-oxadiazoles via oxidative reduction strategy.

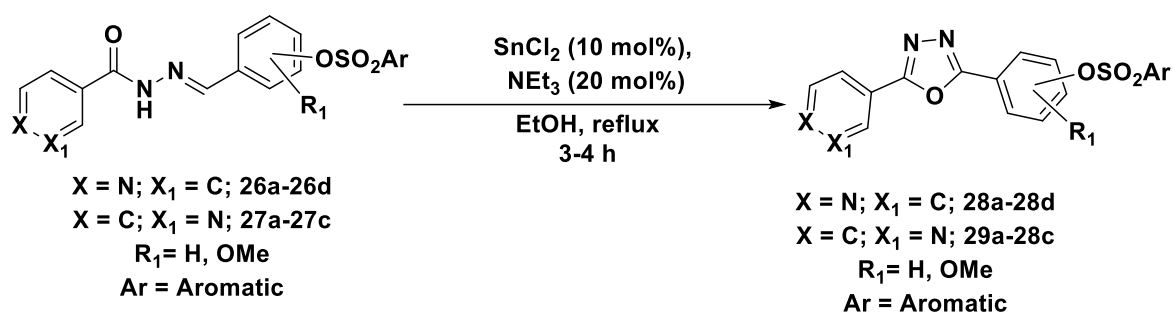
5.2 Present study

Based on above (Chapter-1) discussions regarding the biological importance of the dibenzo-[1,4]-diazepin-1-ones, 2-phenylquinazolines and 1,3,4-oxadiazole derivatives and after thorough literature survey (sulfonate aldehydes), we propose a simple protocol for the synthesis of dibenzo-[1,4]-diazepin-1-one sulfonates, 2-phenylquinazolines sulfonates *via* MCR approach by using OPDA (**1**), various sulfonate aldehydes (**21a-21i**) and different active methylene groups moiety (**3a-3c**) under Lewis acid (SnCl₂) condition in EtOH (**Schemes-4** and **5**). Using the same reagent, an oxidative cyclization is planned for substituted 1,3,4-oxadiazoles from N'-benzylideneisonicotinohydrazide/N'-benzylideneisonicotinohydrazide sulfonates (**26a-26d/27a-**

27c) (or) Schiff-base sulfonates in presence of catalytic SnCl₂ and organic base (TEA) as shown **Scheme-6**.



Scheme-4 and 5: Strategy for sulfonate ester-based dibenzo-[1,4]-diazepin-1-ones and 2-phenylquinazolines.

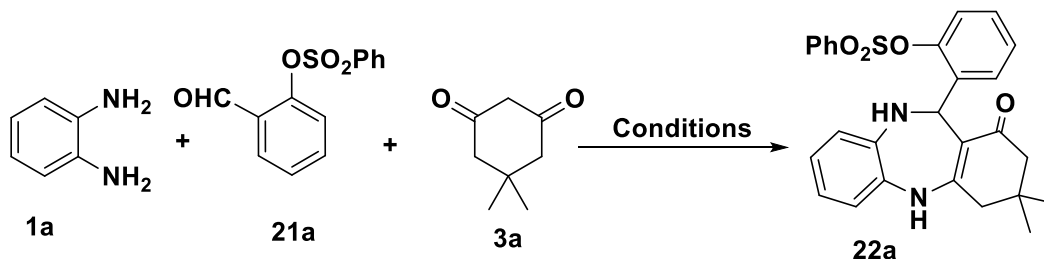


Scheme-6: Strategy for substituted-1,3,4-oxadiazole sulfonate synthesis.

5.3 Results and Discussion

The methods discussed in above section for the synthesis of dibenzo-[1,4]-diazepin-1-ones may be good. But, they are not explored for the aldehydes with sulphonate functional groups. In 2017, we have reported the synthesis of dibenzo-[1,4]-diazepin-1-ones (L-proline as catalyst and catalyst-free conditions) for α -glucosidase inhibition.^{13e} Also, the synthesis and biological evaluation (α -glucosidase inhibition) of functionalized sulfonate esters is discussed in other chapters in the present thesis. With this background, we planned the synthesis of hybrid molecules containing dibenzo-[1,4]-diazepin-1-one and a sulfonate. Towards this, the initial investigation was started with the treatment of *o*-phenyl diamine (OPDA) (**1a**) (1.0 mmol), dimedone (**3a**) (1.0 mmol), and formylphenylbenzenesulfonates (**21a**) (1.0 mmol) in water (catalyst-free, 100 °C and L-proline as catalyst, 60 °C) for 2 h to give the desired product **22a** only in trace amounts. Same reaction was also attempted in the presence of AcOH (1 equiv), MeOH at 65 °C for 2 h to give the product 20% of the desired product was obtained (**Scheme-7a**). To find the optimized reaction condition, experiments were conducted in the presence of different acids like SnCl₂, SnCl₄, FeCl₂, FeCl₃, and ZnCl₂, organic acids (PTSA), and inorganic bases K₂CO₃, Cs₂CO₃, and I₂-K₂CO₃ and solvents like MeOH, EtOH, DMF, MeCN, water, toluene, EtOH+Water (1:1) and DMSO). Among

all, a combination of SnCl₂ (10 mol%) and EtOH, 80 °C, 30 min (**Entry-8; Table-1**) gave better yield (90%) of the desired product. Reaction was also performed using 1,3-dimethylurea + L-tartaric acid, (3:1 ratio) as deep eutectic solvent. But it could give only 28% desired product (**Entry-18; Table 1**).



Initial attempts (Conditions): i) Catalyst-free, Water, 100 °C, 2h, trace amounts
 ii) L-proline (30 mol%), Water, 60 °C, 2h, trace amounts
 iii) AcOH (1eq.), MeOH, 65 °C, 2h: 20% yield

Scheme-7a: Initial attempts for the synthesis of sulfonate ester based dibenzo-[1,4]-diazepin-1-one derivative **22a**.

Table-1: Optimization of reaction conditions ^[a]

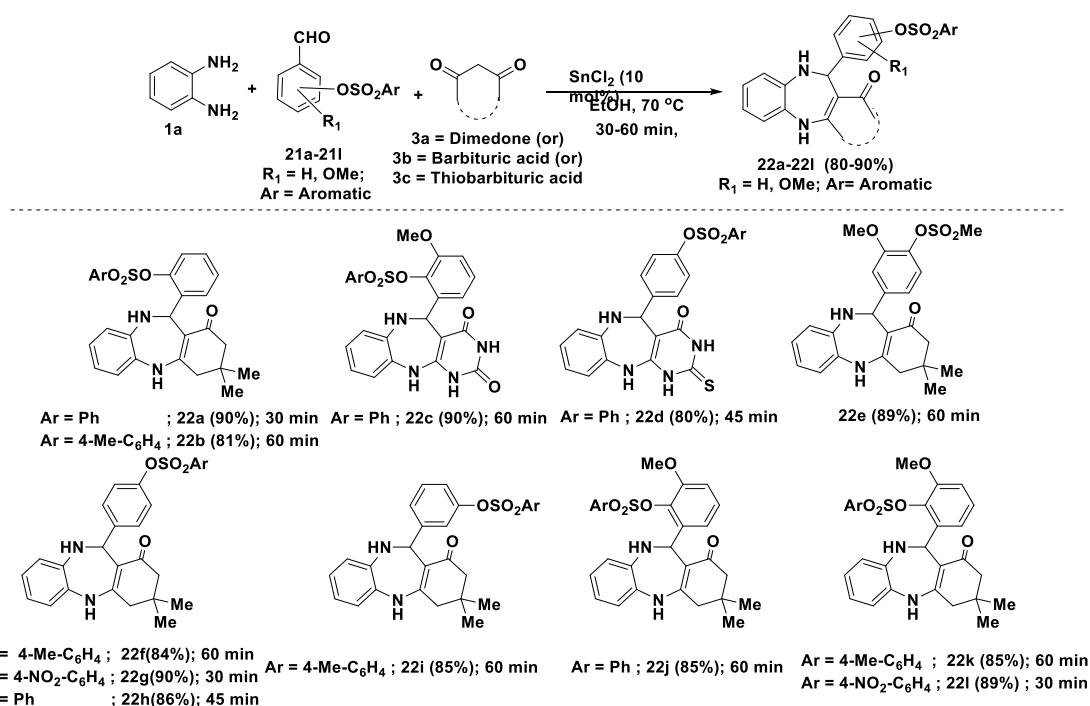
Entry	Catalyst	Solvent	Temp. (°C)	Time (h)	Yield ^[b] (%)
1	AcOH	MeOH	65	2	20
2	NaOH	MeOH	65	2	30
3	HCl	EtOH	80	2	48
4	K ₂ CO ₃	CH ₃ CN	80	2	40
5	Cs ₂ CO ₃	DMF	80	2	42
6	I ₂ / K ₂ CO ₃	CHCl ₃	65	5	50
7	SnCl ₂ (5 mol%)	EtOH	80	1	70
8	SnCl₂ (10 mol%)	EtOH	80	0.5	90
9	SnCl ₂ (10 mol%)	Water	80	0.5	60
10	SnCl ₂ (10 mol%)	EtOH+Water (1:1)	80	0.5	30
11	SnCl ₂ (20 mol%)	EtOH	80	1	90
12	SnCl ₄ (10 mol%)	EtOH	80	1	55
13	SnCl ₄ (20 mol%)	EtOH	80	2	40
14	FeCl ₃ (10 mol%)	EtOH	80	2	trace
15	FeCl ₂ (10 mol%)	EtOH	80	2	trace
16	ZnCl ₂ (10 mol%)	EtOH	80	2	35
17	PTSA	DMSO	80	2	trace
18	DMU + L-(+)-TA (3:1)	--	80	2	28

^[a]Reaction conditions: All reactions were conducted with **1a** (1.0 mmol), **2a** (1.0 mmol), **3a** (1.0 mmol),

^[b]Isolated yields.

After confirmation of the desired product by complementary spectra data, our next task was to check the substrate scope for the reaction. Thus, the sulfonate aldehydes (**21a-21l**) were

reacted with OPDA (**1a**) and dimedone (**3a**)/barbituric acid (**3b**)/thiobarbituric acid (**3c**) under optimized conditions to provide corresponding sulfonate ester-based dibenzo-[1,4]-diazepin-one (**22a-22i**) with good yields (80-90%) in shorter times (30-60 min) as shown in **Scheme-7b**. Based on the experimental procedure and observations, a possible mechanism is proposed as shown in **Figure-1**. Initially, SnCl_2 reacts with OPDA (**1a**) and dimedone (**3a**) to give imine (**A**) which undergoes imine-enamine tautomerism to give intermediate (**B**). Subsequently, another amine group of OPDA reacts with 2-formyl phenyl benzene sulfonate (**21c**) in presence of SnCl_2 to provide activated intermediate (**D**), proton migration and promote the formation of the seven-member ring (**E**), which further facilitates intramolecular proton migration, followed by cyclization leads to the desired product (**F**).



Reaction conditions: All reactions were conducted using **1a** (1.0 mmol), **21a-21i** (1.0 mmol), (**3a/3b/3c**) (1.0 mmol), SnCl_2 (10 mol %), 5 mL of EtOH at 80 °C for 30-60 min.

Scheme-7b: Synthesis of some of sulfonate ester based dibenzo- [1,4]-diazepin-1-one derivatives.

Plausible reaction mechanism:

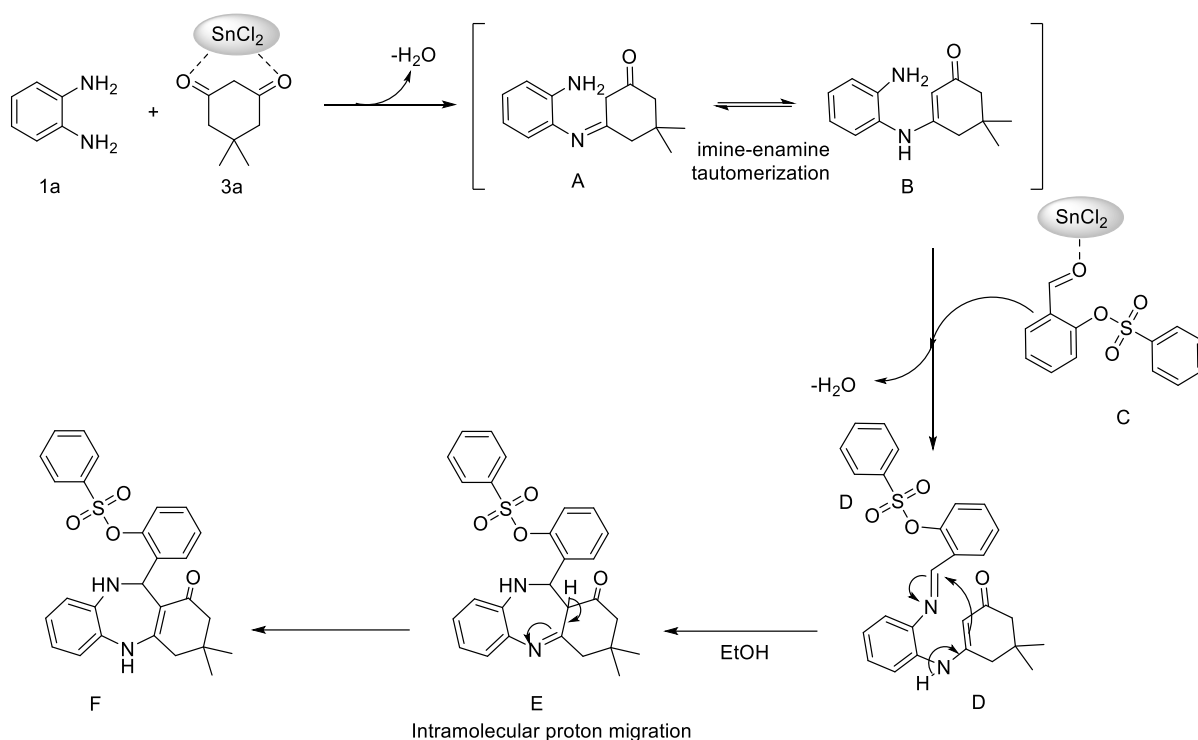
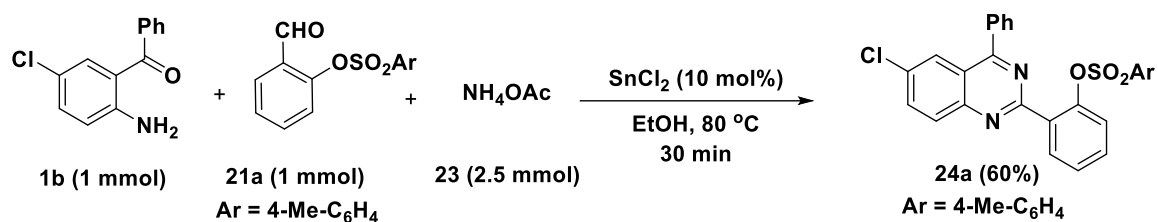


Figure-1: Plausible reaction mechanism for the preparation of sulfonate ester based dibenzo-[1,4]-diazepin-1-ones (**22a-22l**).

After successful synthesis of sulfonate ester based dibenzo-[1,4]-diazepin-1-ones (**22a-22l**), and as indicated in the introduction, focus was shifted towards the utilization of above reaction conditions for the synthesis of substituted phenylquinazoline sulfonates using a combination of 5-chloro-2-aminobenzophenone, formylpheyyl benzenesulfonates, and NH_4OAc . In this context, the reaction of 5-chloro-2-amino benzophenone (**1b**) (1 mmol) with 2-formylpheyyl benzenesulfonate (**21a**) (1.0 mmol) and ammonium acetate (**23**) (2.5 mmol) was carried out using optimized conditions [SnCl_2 (10 mol%), EtOH , 80 °C, 30 min) to give the desired phenylquinazoline sulfonate (**24a**) in 60% yield (**Scheme-8a**). After confirming the structure of the product, the reactions conditions were optimized by increasing the reaction time up to 6 h. Strangely the reaction is working well in 3 hours giving 85% of the desired product. Increasing the reaction time did not help to improve the yield. Later, different phenylbenzenesulfonate aldehyde **21b-21i** were treated with 5-chloro-2-aminobenzophenone (**1b**) and NH_4OAc (**23**) to give **24b-24i** with moderate to good yields (75-95%) (**Scheme-8b**).

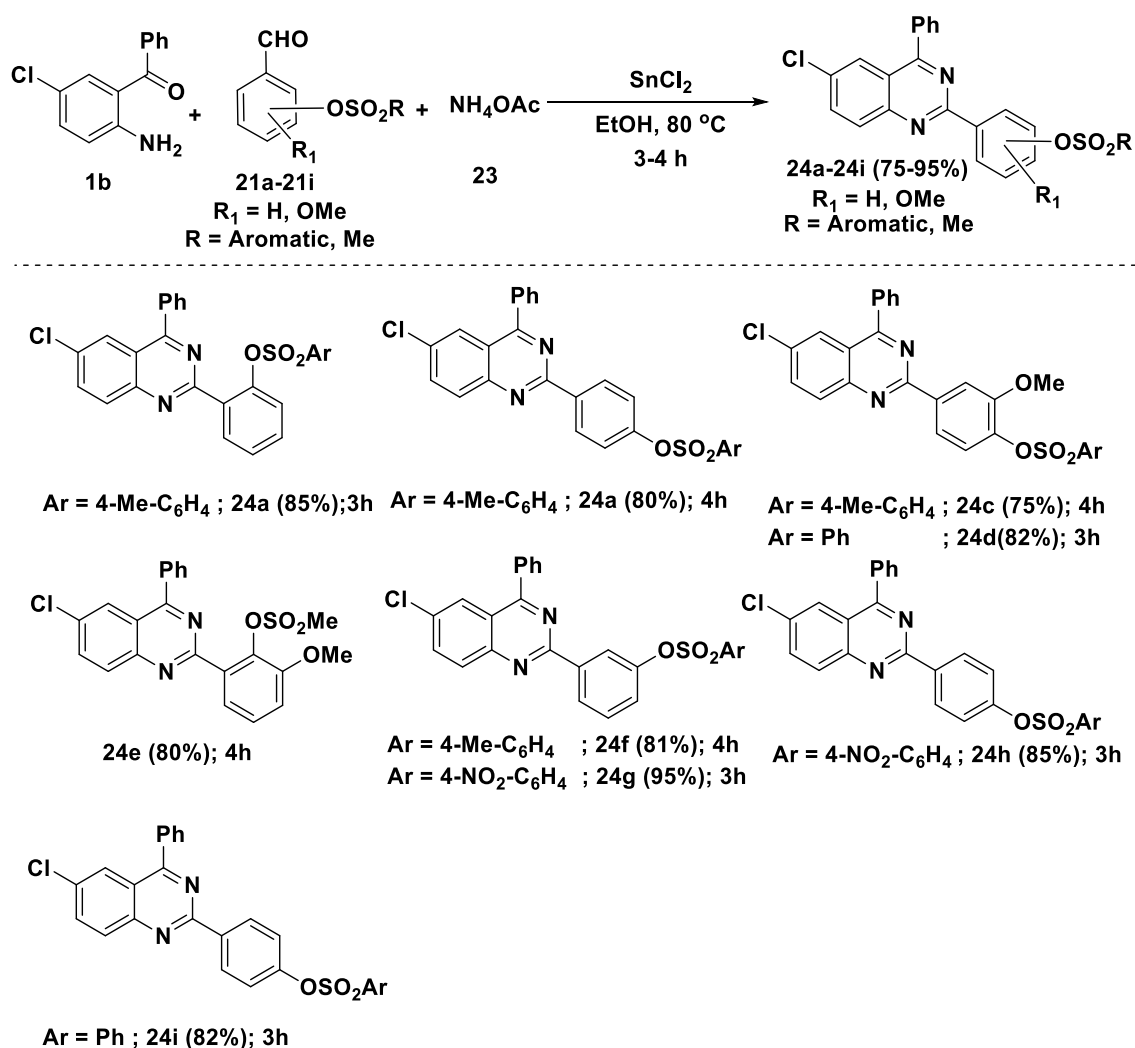


Scheme-8a. Synthesis of phenylquinazoline sulfonates.

Table-2: Optimization of reaction conditions^[a]

Entry	Catalyst	Solvent	Temp (°C)	Time (h)	Yield (%)
1	SnCl ₂ (10 mol %)	EtOH	80	1	65
2	SnCl ₂ (10 mol %)	EtOH	80	2	70
3	SnCl₂ (10 mol %)	EtOH	80	3	85
4	SnCl ₂ (10 mol %)	EtOH	80	5	80
5	SnCl ₂ (10 mol %)	EtOH	80	6	80

Reaction conditions: Reactions were conducted at with **1b** (1.0 mmol), **21a** (1.0 mmol), **23** (2.5 mmol), SnCl₂(10 mol%), 5 mL of EtOH at 80 °C for 3 h.



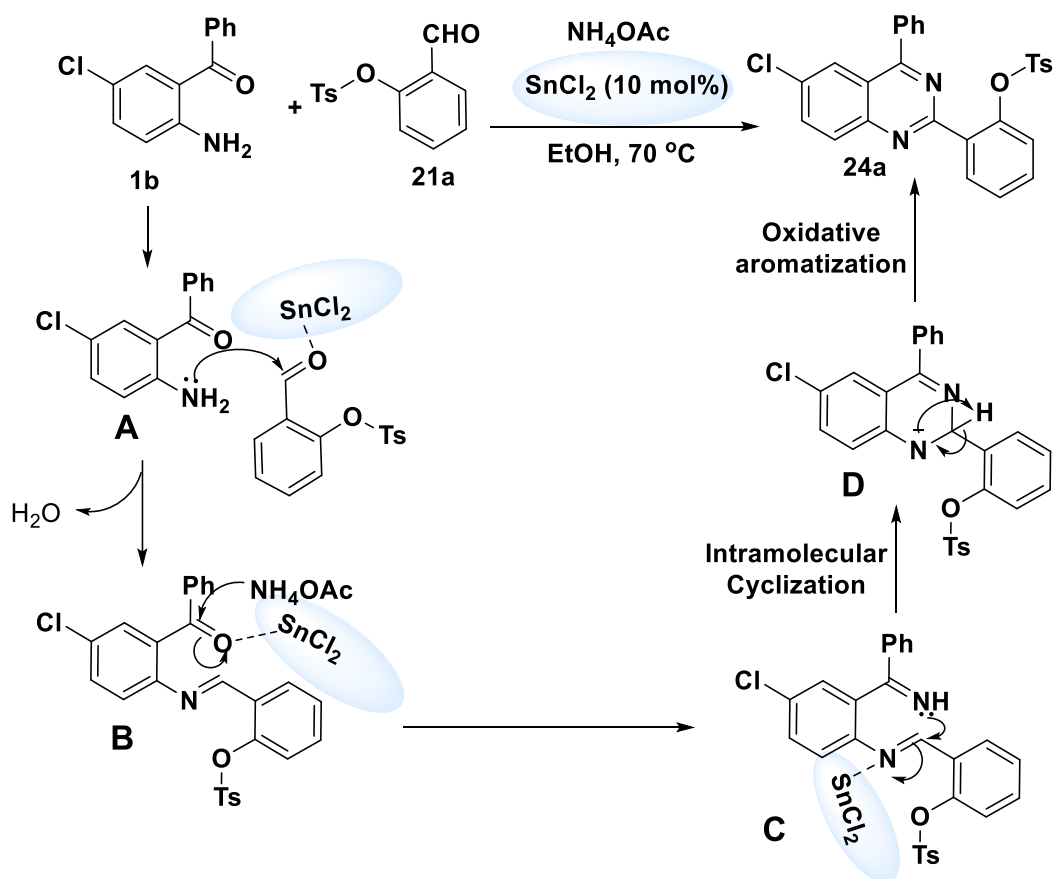
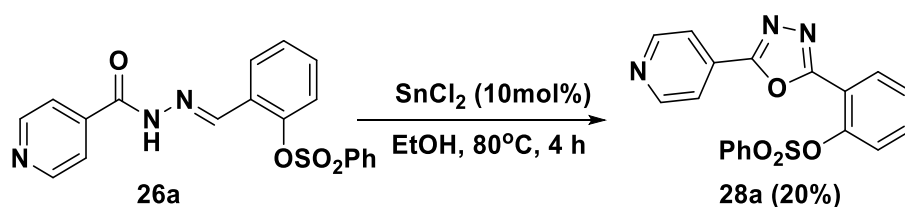


Figure-2: Plausible reaction mechanism for the preparation of phenylquinazoline sulfonate (24a) hybrid.

After getting the fruitful results of phenylquinazoline sulfonates, we have extended the above synthetic strategy for Schiff-base sulfonates used for the generation of substituted-1,3,4-oxadiazole sulfonates *via* oxidative cyclization. Towards this, the sulfonate ester Schiff-base (26a-26d and 27a-27c) were prepared from hydrazones (25a and 25b) and sulfonate aldehydes (21a-21d) using known procedure. In an initial attempt Schiff-base (26a) was reacted with SnCl_2 (10 mol%) in EtOH at 80°C for 4 h to give the desired product in 20% yield (Scheme-9a).



Scheme-9a: Initial attempt for the preparation of 1,3,4-oxadiazole sulfonate ester (28a).

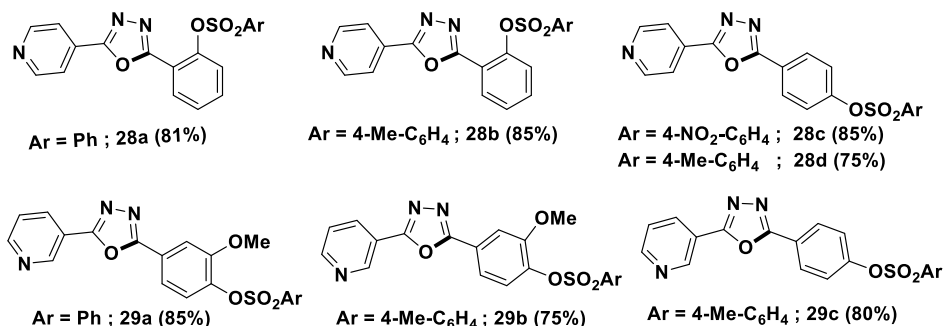
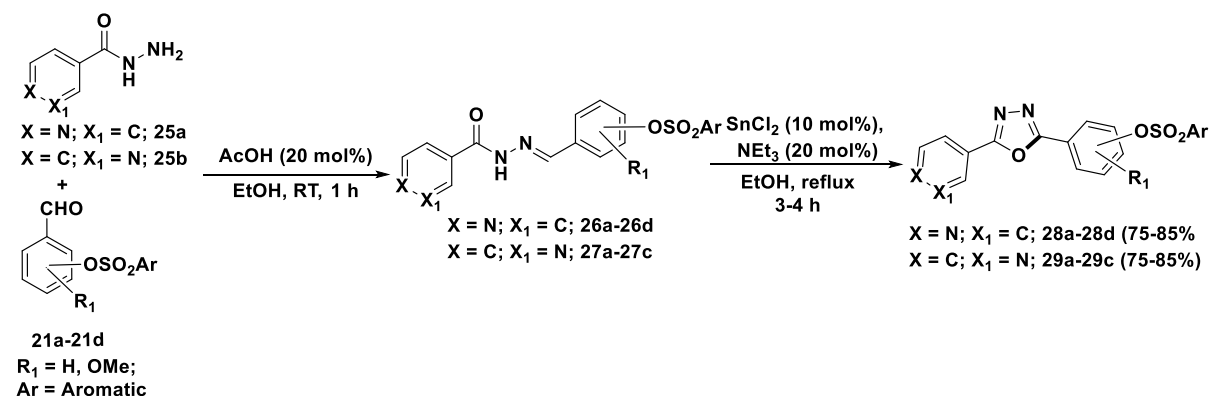
To improve the yield further, experiments were performed in different combinations of SnCl_2 in EtOH by varying the concentrations of SnCl_2 and bases (K_2CO_3 , Cs_2CO_3 , piperidine, and NEt_3) and found that the combination of SnCl_2 (10 mol%) and NEt_3 (20 mol%) was suitable

condition to give the desired product in 81% yield in 3h (**Entry-5; Table-1**). Later, other sulfonate ester Schiff-bases (**26b-26d/ 27a-27c**) were prepared from isonicotinohydrazide (**25a**)/nicotinohydrazide (**25b**) and sulfonate ester aldehydes (**21b-21d**) treated with optimized conditions [i.e. SnCl_2 (10 mol%), TEA (20 mol%) in EtOH at 80 °C] to give disubstituted-1,3,4-oxadiazole sulfonate (**28b-28d/ 29a-29c**) with moderate to good yield (75-85%) (**Scheme-9**). Based on the experimental results, a plausible reaction mechanism as shown in **Figure-3**.

Table-3: Optimization of reaction conditions ^[a]

Entry	Catalyst /Bases	Solvent	Temp (°C)	Time (h)	Yield (%)
1	SnCl_2	EtOH	80	4	25
2	$\text{SnCl}_2/\text{K}_2\text{CO}_3$	MeCN	80	4	35
3	$\text{SnCl}_2/\text{Cs}_2\text{CO}_3$	DMSO	80	4	50
4	SnCl_2 /Piperidine	EtOH	80	4	70
5	$\text{SnCl}_2/\text{NEt}_3$	EtOH	80	3	81

^[a]**Reaction conditions:** Reactions were conducted using **26a** (1.0 mmol), catalyst SnCl_2 (10 mol %), NEt_3 (20 mol%), 5 mL of EtOH at 80 °C for 3 h.



Reaction conditions: Reactions were conducted using **25a-25b** (1.0 mmol), and **21a-21d** (1.0 mmol), 1st step catalyst: AcOH (20 mol%) at RT for 1 h, 2nd step Catalyst: SnCl_2 (10 mol %), NEt_3 (20 mol%), 5mL of EtOH at 80 oC for 3-4 h. (total reaction time-4 h-5 h).

Scheme-9b: Substrate scope of pyridine containing substituted-1,3,4-oxadiazole sulfonates.

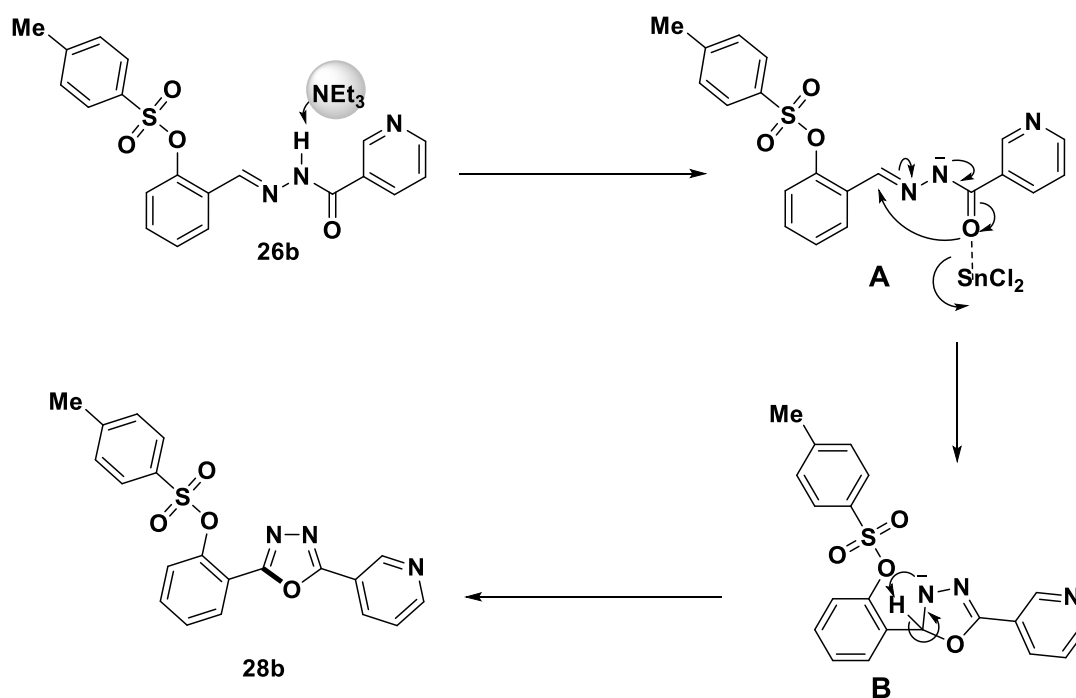


Figure-3: Plausible reaction mechanism for the compound (**28b**).

5.5 Photophysical properties

Quinazolines are reported for photoluminescent properties and show second-order nonlinear optical characteristics by push-pull mechanism.^{14a} Similarly 1,3,4-oxadiazoles used for electron-injection for OLEDs, with good thermal and chemical stability.^{14(b-c)} Based on these reports, our task was to study the photophysical (absorption and emission) of the phenylquinazolines **24a-24g**, 1,3,4-oxadiazole sulfonates **26a-27c**. Towards this, absorption spectra were recorded in DMSO (100 μ M) and the absorption bands were observed in the range of 385-438 nm (for **24a-24g**), (**Figure-3: A**; **Table-4**). Among **24a-24g**, compound **24g** showed λ_{max} at 438 nm. The emission (λ_{em}) for these compounds was seen in the range of 456-518 nm (**Figure-3: B**). Interestingly, compound **24f** showing a strong bathochromic shift at 518 nm with stokes shift at 133 nm due to ICT effect.^{14d} Similarly compounds **24a** and **24g** show better emission bands at 486 nm and 500 nm (all data are represented in **Table-4**).

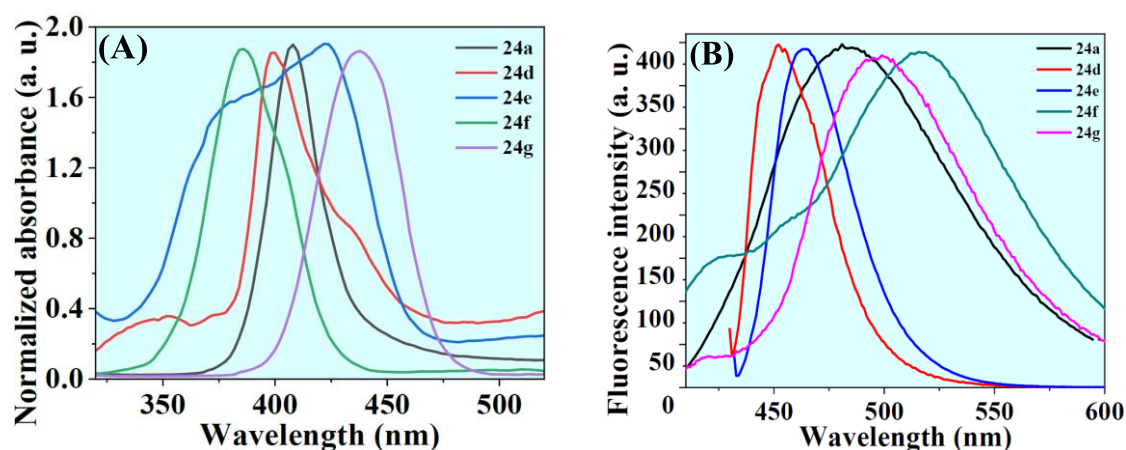


Figure-3: (A) Absorption and (B) Emission spectra of the compounds **24a-24g** in DMSO.

Table-4: Photo physical properties data of the resultant compounds (**24a-24g**).

Compound code	λ_{Abs} (nm)	λ_{em} (nm)	Stokes shift ($\Delta\lambda$ nm)
24a	408	486	78
24d	400	456	56
24e	422	463	41
24f	385	518	133
24g	438	500	62

Similar to above, absorption bands (λ_{abs}) of pyridine-based-1,3,4-oxadiazole sulfonate esters **26a-27c** was seen in the range of **377-415 nm**, and their corresponding emission spectra (λ_{em}) at **525-585 nm** (**Figure-5: B**). Among these molecules, compounds **26a**, **27c** showed emission bands at **558** and **585 nm** respectively (**Table-5**). The Stokes shifts for the compounds **27c**, **26a**, and **26d** were observed at **208**, **180** and **153 nm** respectively because of the intramolecular charge transfer effect (ICT) as shown in **Table-5**.

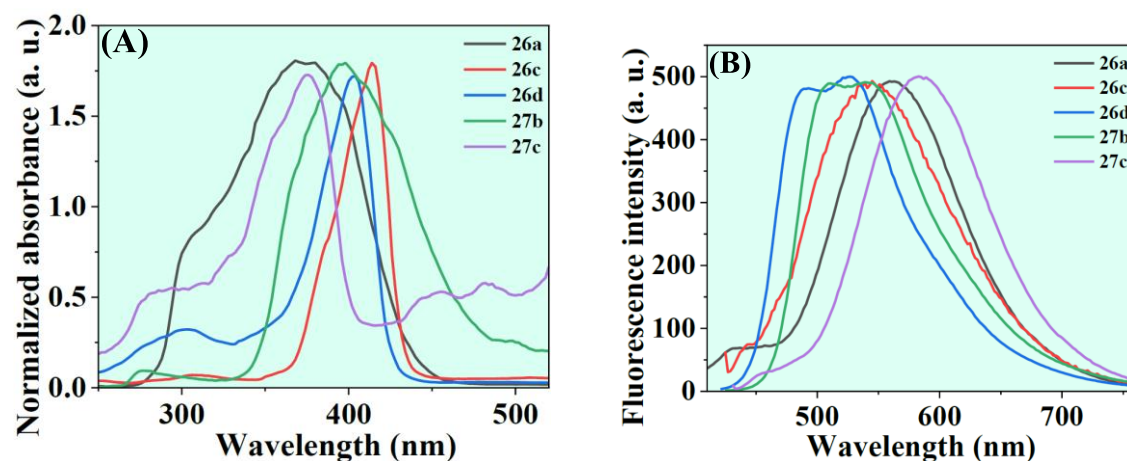


Figure-4: (A) Absorption (B) Emission spectra of the compounds (26a-27c) in DMSO.

Table-5: Photo physical properties data of the resultant compounds (26a-27c).

Compound code	λ_{Abs} (nm)	λ_{em} (nm)	Stokes shift ($\Delta\lambda$ nm)
26a	378	558	180
26c	415	545	130
26d	402	525	153
27b	396	541	145
27c	377	585	208

5.5 Biological activity

5.5.1 α -glucosidase assay

The catalytic activity of α -glucosidase was measured by calorimetric assay using 4-nitrophenyl glucopyranoside (4-NPG). The enzymatic reaction was started by adding 25 μ l of 4-NPG (substrate stock solution) to 25 μ l of α -glucosidase (2mg dissolved in 1ml of 10mM cTris-HCl pH 7.0 and 25 μ l of 4-NPG (substrate stock solution), 950 μ l deionised H₂O and the reaction mixture was incubated at 37°C for 10 min. The enzyme activity was quantified by measuring the absorbance of the liberated 4-nitrophenol against an enzyme-free blank at 410nm. For enzyme inhibition experiments, the enzyme was incubated with benzodiazophine derivatives for 30 min before adding substrate solution. 1U (I Unit) of glycolytic activity was defined as the amount of enzyme needed to release 1 μ g of 4-nitrophenol per min. under standard assay conditions.

Determination of IC₅₀ values

IC₅₀ value of inhibitors were calculated based on concentration of inhibitor molecule required to inhibit 50% of α -glucosidase activity under the standard assay conditions. For quantification of enzymes IC₅₀ values, the enzyme inhibition assays were carried at different concentration (10 to 500 μ g) of inhibitors, without changing enzyme concentration. The enzyme reaction was performed by pre-incubating the incubating the enzyme with inhibitor at 37 °C for 30 min and inhibitory activity was determined under standard assay conditions. For those molecules which showed significant inhibition, the mode of inhibition exhibited by inhibitor was examined by carrying out Michalies-Menten enzyme kinetics by varying substrate (4NPG) concentration (0.25, 0.4, 0.6, 0.8, 1.0, 1.25, 1.5 and 2.0 mM) in the absence or presence of the inhibitor molecules at two different concentrations (25 and 50 μ g). Mode of inhibition of was determined by Lineweaver-

Burk plot analysis of the data calculated following Michaelis-Menten kinetics values. All IC₅₀ values are represented as Mean \pm Standard Deviation.

Results

The inhibition of α -glucosidase activity by a series of tested twenty-seven (**27**) sulfonate compounds (22a-22l, 24-24i, 26a-26d and 27a-27c) showed varying degree of α -glucosidase inhibition with IC₅₀ values ranging from 33 μ M to 134 μ M (**Table-6**). Acarbose was selected as a control inhibitor, IC₅₀ value of acarbose under the same assay conditions was found to be 32.65 μ M. Among the tested compounds, **compound 22g** showed a minimum IC₅₀ value of **33.1 \pm 1.51** μ M and the ligand 24g showed a maximum IC₅₀ value of 134.09 μ M. The compounds 22b, 22g and 24h which showed minimal IC₅₀ values among the tested ligands against α -glucosidase activity were selected for studying the mode of inhibition of these compounds against yeast α -glucosidase. The mode of inhibition of selected inhibitors was determined by comparing the Michaelis-Menten Kinetic constants obtained from the experimental investigation carried out in the presence of a varying concentration of substrate and inhibitors. The tested compounds **22b, 22g and 24h** showed competitive mode of inhibition. Results of K_m and V_{max} of α -glucosidase in the presence of tested compounds were shown in **Table-8**.

Discussions

By studying the kinetics of α -glucosidase it was observed that the presence of compound **22g** greatly affected the K_m and V_{max} values. Lineweaver-Burk double reciprocal plot for the inhibition of α -glucosidase shows that there is increasing trend for k_m value for increase in the concentration of the tested compounds **22b, 22g and 24h** but there is no significant change was observed for V_{max} (**Figure-7**). This reveals that the tested compounds exhibit competitive mode of inhibition against α -glucosidase. Berna et al.^{15a} (2012) reported that mode of inhibition of by a natural compound extracted from *Antidesma bunius* L plant. Similarly, isoacarbose, a derivative of acarbose also reported to bind and inhibit the α -glucosidase through competitive mode. (Kimura et al.^{15b} 2009). A similar competitive mode of inhibition against glucosidase was reported competitive for benzodithiophene derivatives (Abbas et al.^{15c} 2018) and pyrimidine derivatives (Mohammed et al.^{15d} 2020)

The molecular docking studies revealed that the tested compounds (**22b, 22g and 24h**) are interacting with target protein by hydrogen bonding and aromatic (π - π stacking) interactions. The interactions are between amino acids of the α -glucosidase enzyme, a nitro group and the aromatic ring of the compound. It was observed that the amino acid LYS155 and HIS239 in the active site

of α -glucosidase play a role in interaction with all the tested inhibitors. The compound 22b is forming π - π stacking interaction with PHE311 and hydrogen bonding interaction with LYS155 residue present in the α -glucosidase active site region. Similarly, the compound 22g is also forming π - π stacking interaction with PHE311 and hydrogen bonding interaction with LYS155. An interaction between NO₂ group of compounds (22b and 22g) with LYS155 was observed. The presence of NO₂ substitute in the benzodiazophine played a key role in inhibiting the α -glucosidase activity.

Table 6: In-vitro α -D-glucosidase inhibition by sulfonate ester compounds 22a-22l, 24a-24i, 26a-26d and 27a-27c.

S. No.	Compound code	IC ₅₀ (μ M)
1	22a	56.91 \pm 2.55
2	22b	36.81\pm1.05
3	22c	53.26 \pm 2.63
4	22d	66.34 \pm 3.17
5	22e	97.83 \pm 4.15
6	22f	59.77 \pm 2.85
7	22g	33.1 \pm1.51
8	22h	79.46 \pm 3.31
9	22i	96.21 \pm 5.05
10	22j	102.48 \pm 5.14
11	22k	95.63 \pm 4.15
12	22l	41.85 \pm 4.25
13	24a	136.31 \pm 7.01
14	24b	83.24 \pm 4.62
15	24c	122.04 \pm 6.02
16	24d	105.43 \pm 5.15
17	24h	37.97\pm1.69
18	24f	114.65 \pm 5.32
19	24g	134.09 \pm 5.45

Figure-5: 2D docking interactions of Compound 22b, 22g, and 24h with MAL12 protein model using rigid docking, PLP scoring function (GRIP docking algorithm)

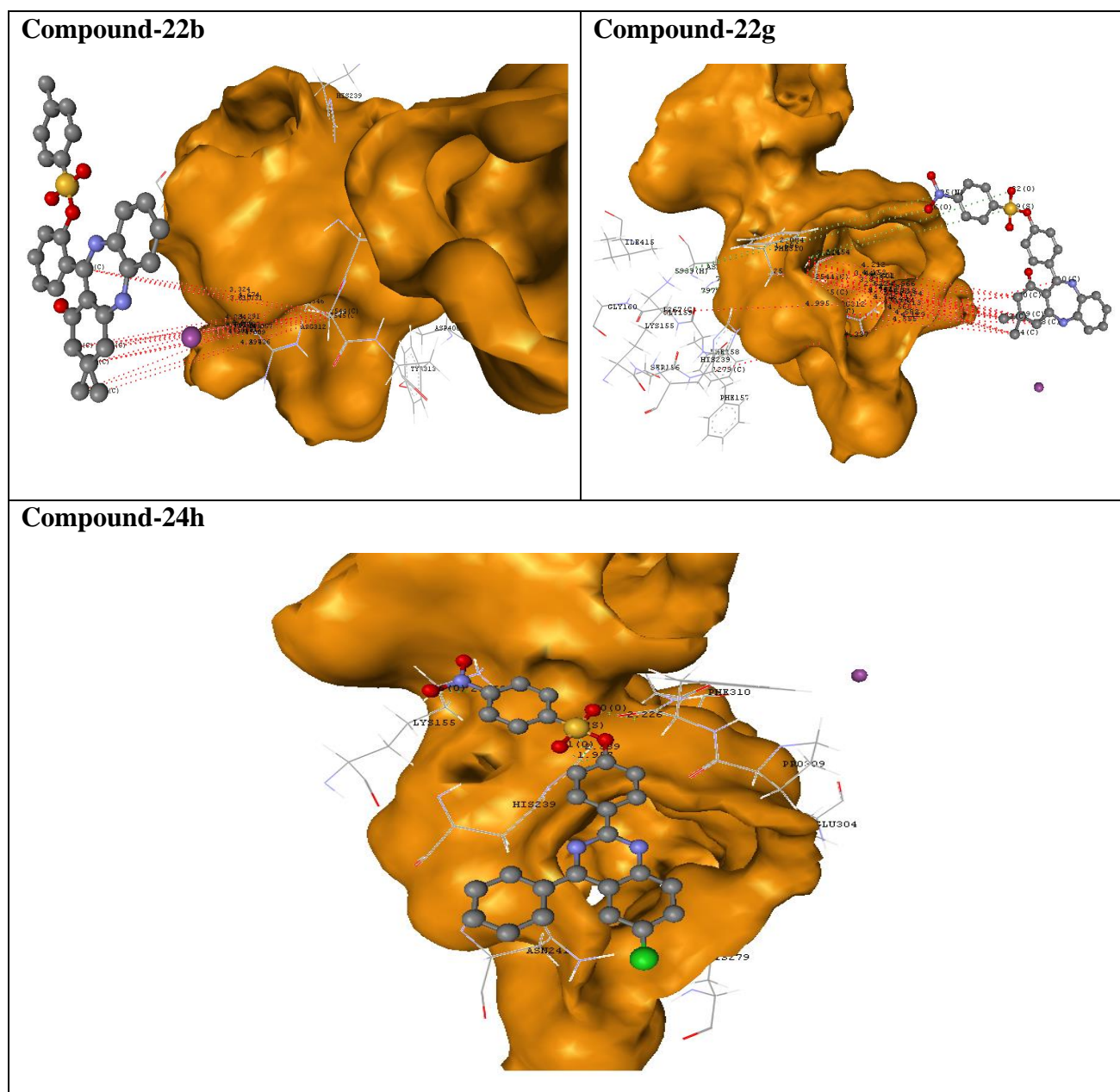


Figure-6: Molecular 3D docking interactions of compounds 22b, 22g, and 24h with MAL12 protein model using rigid docking, PLP scoring function (GRIP docking algorithm)

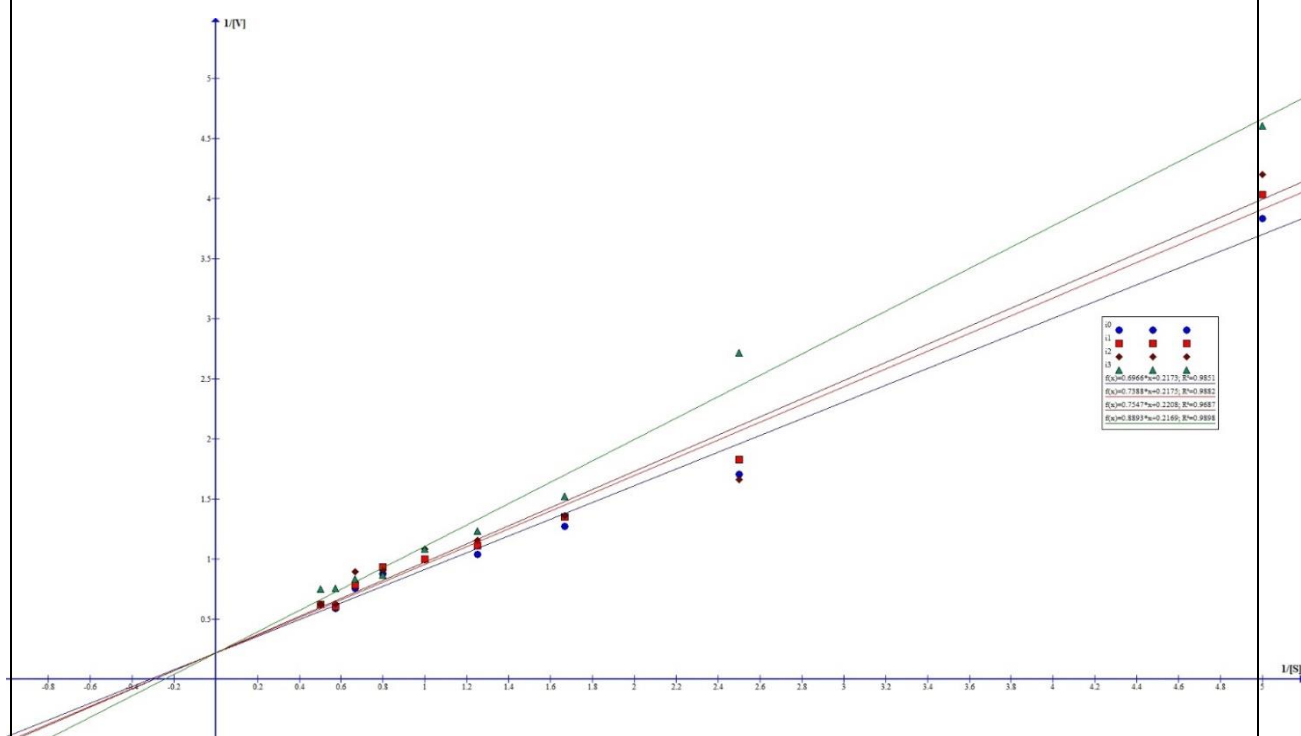
Table-7: Molecular docking interactions between the MAL12 protein model and the most potent compounds **22b**, **22g**, and **24h**

Compound	Residue	Ligand Atom	Distance Å	Interaction
22b	PHE311	12C	4.547	PI-STACKING
	PHE311	20C	4.272	PI-STACKING
	PHE420	20C	5.075	PI-STACKING
	LYS155	21O	1.844	H-BOND
22g	HIS239	12C	5.014	PI-STACKING
	PHE311	12C	3.976	PI-STACKING
	PHE311	20C	5.248	PI-STACKING
	PHE420	20C	4.501	PI-STACKING
	LYS155	18O	2.030	H-BOND
	LYS155	21O	1.967	H-BOND
24h	HIS239	1C	4.321	PI-STACKING
	PHE300	20C	4.881	PI-STACKING
	TYR313	12C	4.952	PI-STACKING
	HIS239	45H	2.340	H-BOND

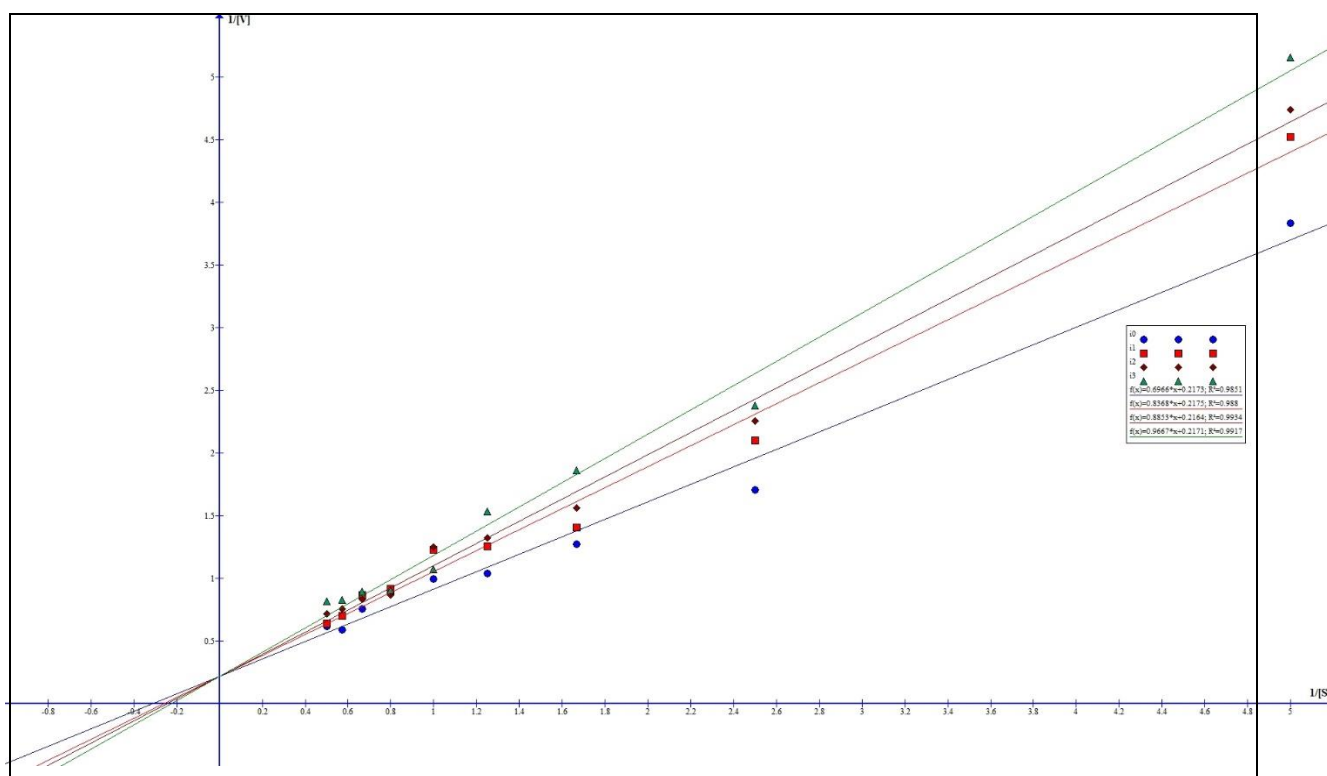
Table 8: IC_{50} , K_{im} , V_{max} and modes of inhibition of selected synthetic ligands. K_m and V_{max} values of α -D-glycosidase for 4-NPG without inhibitor were 3.14 μ M and 4.52 μ M/min respectively.

Ligand	IC ₅₀ (μM)	K _{im} (μM)	V _{max} (μM/min)	Mode of inhibition
		Inhibitor concentration of 25 μg		
24b	36.81±1.05	3.39	4.59	Competitive
22g	33.58±1.51	3.84	4.59	Competitive
24h	37.97±1.69	3.41	4.53	Competitive

Compound 22b



Compound 22g



Compound 24h

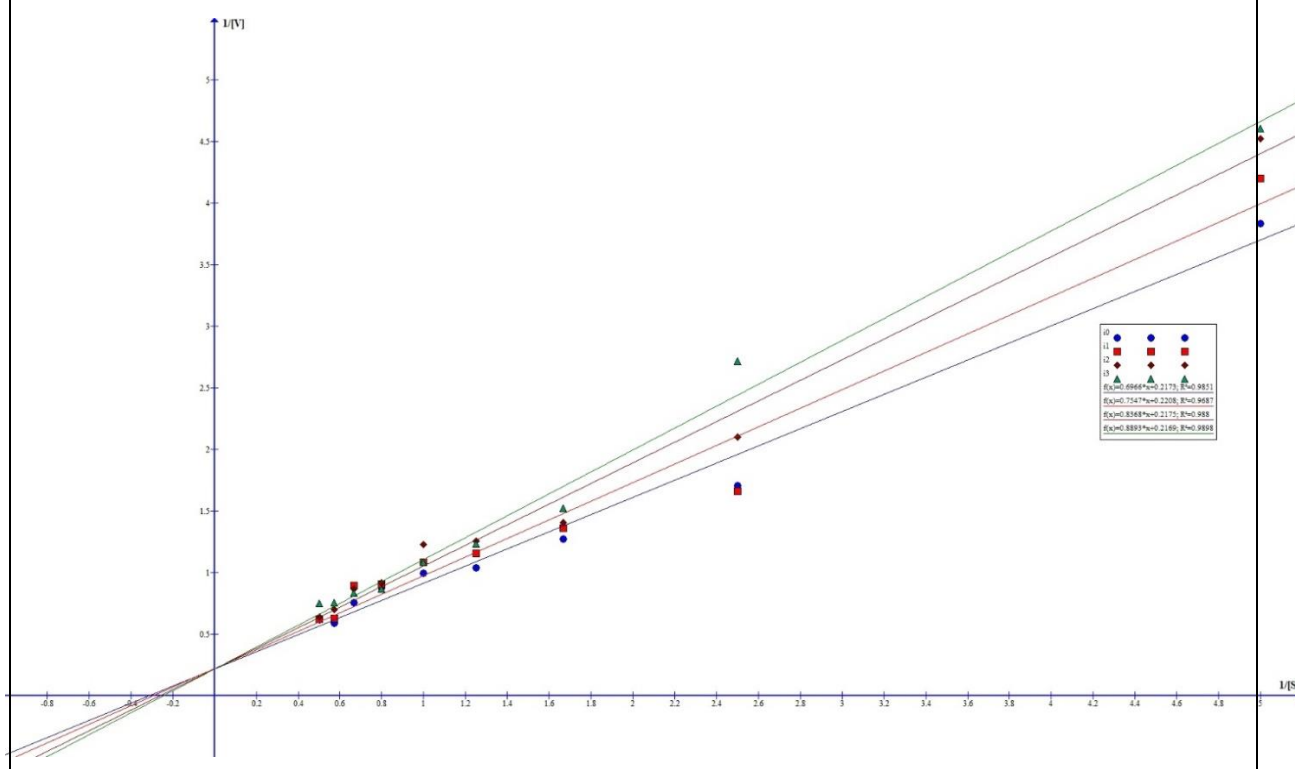


Figure 7: Lineweaver-Burk plot for understanding mode of Inhibition of α -D-glucosidase by compounds 22b, 22g, and 24h.

5.5 Conclusion

In conclusion, we have successfully synthesized sulfonate-based dibenzo-[1,4]-diazepin-1-ones, quinazolines and oxadiazoles using SnCl_2 as catalyst. The resultant molecules were tested α -glucosidase enzyme inhibition activity against acarbose as a standard drug (IC_{50} **33.4 \pm 2.654**) and found that the compounds **22g**, **22b**, and **24h** showed the activity with IC_{50} values **33.1 \pm 1.51** mM, **36.81 \pm 1.05**, mM, and **37.97 \pm 1.69** mM respectively.

The enzyme inhibition kinetics studies of these compounds exhibiting competitive mode of inhibition against α -glucosidase inhibition. Also, the absorption and emission spectra of the resulting phenyl quinazolines and substituted-1,3,4-oxadiazoles was recorded and found that compound **27c** showed the highest emission band maximum (585 nm) due to intramolecular charge transfer and compounds **26a** and **26c** exhibited a larger bathochromic shift at 558 nm and 545 nm, respectively. The compound **27c** showed the highest Stokes shift (at 208 nm).

5.6 Experimental section

5.6.1 General: In this work, we bought all starting materials from the SD-Fine, Sigma-Aldrich, and Spectrochem are used. ^1H and ^{13}C -NMR were recorded under Bruker 400 MHz spectrometer using CDCl_3 or DMSO-d_6 solvents (reported in δ ppm). The mass spectrums are recorded on Shimadzu LCMS-2020 and melting points are recorded using the Stuart melting point apparatus.

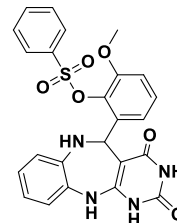
5.6.2 Experimental procedures

General procedure for the synthesis of sulfonates ester based [1,4]-benzodiazepine derivative (22a-22l):

To a solution of *o*-phenyl diamine **1a** (1 mmol) in EtOH (5 mL), was added active methylene compound (**3a/3b/3c**) (1 mmol) followed by sulfonate aldehyde **21a-21l** (1.0 mmol) and SnCl_2 (10 mol%) heated at 80 °C for 3-4 h. After the specified time, reaction mixture was cooled to room temperature and extracted using EtOAc (2X10 mL). Combined organic layers were washed with water, brine and dried with sodium sulphate. Evaporation of the solvent under reduced pressure gave the crude product which was purified by silica gel column chromatography. Elution of the column with EtOAc+*n*-hexane (3:1 ratio) gave desired products **22a-22l** with good yields.

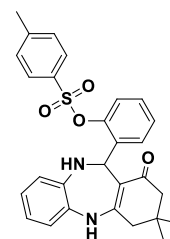
2-(2,4-Dioxo-2,3,4,5,6,11-hexahydro-1H-benzo[b]pyrimido[4,5-e][1,4]diazepin-5-yl)-6-methoxyphenyl benzenesulfonate (22a): Pale yellow solid, mp 192–193 °C,

90% yield. ¹H NMR (400 MHz, CDCl₃+DMSO-*d*₆) δ 8.01 (d, *J* = 7.6 Hz, 2H), 7.74 (d, *J* = 7.6 Hz, 1H), 7.64 (t, *J* = 8.0 Hz, 2H), 7.48 (d, *J* = 7.2 Hz, 1H), 7.37 (t, *J* = 8.0 Hz, 1H), 7.25 (t, *J* = 8.0 Hz, 2H), 7.13 (d, *J* = 8.0 Hz, 2H), 7.00 (d, *J* = 8.8 Hz, 1H), 6.62 (d, *J* = 7.6 Hz, 2H), 6.00 (s, 1H), 5.75 (s, 1H), 3.50 (s, 3H); ¹³C NMR (100 MHz, CDCl₃+DMSO-*d*₆) δ 161.70, 157.66, 152.32, 150.03, 143.42, 137.60, 137.50, 137.29, 135.39, 135.15, 132.57, 129.89, 129.05, 128.88, 127.75, 125.85, 121.75, 117.30, 113.42, 83.57, 56.36, 46.66; HRMS (ESI, *m/z*): calcd. For C₂₄H₂₀N₄O₆SH⁺ 493.1176, found 493.1170; IR (KBr thin film, cm⁻¹): ν_{max} 3391, 3018, 2955, 1607, 1507, 1478, 1383, 1124, 876.



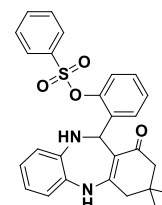
2-(3,3-Dimethyl-1-oxo-2,3,4,5,10,11-hexahydro-1H-dibenzo[b,e][1,4]diazepin-11-yl)phenyl 4-methylbenzenesulfonate (22b): White solid, mp 157–158 °C, 81% yield. ¹H NMR (400 MHz,

CDCl₃+DMSO-*d*₆) δ 8.78 (s, 1H), 7.96 (d, *J* = 8.0 Hz, 2H), 7.49 (d, *J* = 8.0 Hz, 2H), 7.06 (d, *J* = 7.6 Hz, 1H), 7.00–6.96 (m, 1H), 6.87–6.81 (m, 2H), 6.74–6.64 (m, 2H), 6.44–6.41 (m, 1H), 6.11 (d, *J* = 5.2 Hz, 1H), 4.96 (d, *J* = 5.2 Hz, 1H), 2.63 (s, 2H), 2.51 (s, 3H), 2.13 (dd, *J* = 16.0, 10.8 Hz, 2H), 1.13 (s, 3H), 1.03 (s, 3H); ¹³C NMR (100 MHz, CDCl₃+DMSO-*d*₆) δ 197.66, 159.80, 152.48, 150.76, 142.50, 142.03, 137.64, 136.82, 135.14, 133.11, 132.87, 132.40, 131.14, 128.30, 126.32, 125.98, 125.91, 125.37, 114.21, 57.39, 54.78, 49.85, 36.93, 33.48, 32.64, 26.54; HRMS (ESI, *m/z*): calcd. For C₂₈H₂₈N₂O₄SH⁺ 489.1843, found 489.1759; IR (KBr thin film, cm⁻¹): ν_{max} 3346, 3040, 2850, 1588, 1505, 1344, 1176, 834.



2-(3,3-Dimethyl-1-oxo-2,3,4,5,10,11-hexahydro-1H-dibenzo[b,e][1,4]diazepin-11-yl)phenyl benzenesulfonate (22c): Light brown, mp 181–182 °C, 88% yield. ¹H NMR (400 MHz,

CDCl₃+DMSO-*d*₆) δ 8.61 (s, 1H), 8.10 (d, *J* = 5.6 Hz, 2H), 7.79–7.66 (m, 4H), 7.05–6.67 (m, 6H), 6.46 (d, *J* = 6.8 Hz, 1H), 6.14 (s, 1H), 4.97 (d, *J* = 1.6 Hz, 1H), 2.63 (s, 2H), 2.23–2.07 (m, 2H), 1.14 (s, 3H), 1.04 (s, 3H); ¹³C NMR (100 MHz, CDCl₃+DMSO-*d*₆) δ 193.06, 155.73, 147.80, 137.56, 137.33, 135.69, 135.37, 132.10, 130.24, 128.43, 128.25, 128.06, 126.65, 123.70, 121.53, 121.35, 121.22, 120.77, 120.74, 109.32, 52.53, 49.90, 44.83, 32.22, 28.66, 27.91; HRMS (ESI, *m/z*): calcd. For C₂₇H₂₆N₂O₄SH⁺ 475.1686, found 475.1603; IR (KBr thin film, cm⁻¹): ν_{max} 3372, 3079, 2985, 1603, 1527, 1382, 1156, 776.

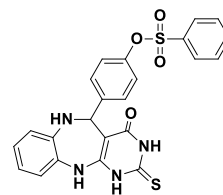


4-(4-Oxo-2-thioxo-2,3,4,5,6,11-hexahydro-1H-benzo[b]pyrimido[4,5-e][1,4]diazepin-5-yl)

phenyl benzenesulfonate (22d): White solid, mp 175–176 °C, 80% yield.

¹H NMR (400 MHz, CDCl₃+DMSO-*d*₆) δ 8.16 (d, *J* = 8.4 Hz, 2H), 7.89–7.74 (m, 4H), 7.69–7.60 (m, 5H), 7.25 (d, *J* = 2.4 Hz, 2H), 7.13 (d, *J* = 8.0 Hz, 2H), 6.70 (d, *J* = 7.2 Hz, 1H); ¹³C NMR (100 MHz, CDCl₃+DMSO-*d*₆)

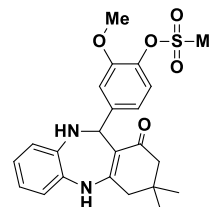
δ 161.24, 157.57, 156.60, 149.65, 144.15, 141.26, 140.37, 138.41, 138.01, 137.62, 137.12, 136.68, 136.10, 135.98, 135.91, 133.67, 132.90, 79.20, 51.32; HRMS (ESI, *m/z*): calcd. For C₂₃H₁₈N₄O₄S₂H⁺ 479.0842, found: 479.0840; IR (KBr thin film, cm⁻¹): ν_{max} 3370, 3063, 2971, 1583, 1372, 1197, 1092.



4-(3,3-Dimethyl-1-oxo-2,3,4,5,10,11-hexahydro-1H-dibenzo[b,e][1,4]diazepin-11-yl)-2-methoxyphenyl methanesulfonate (22e): White solid, mp 165–166 °C, 89% yield.

¹H NMR (400 MHz, CDCl₃+DMSO-*d*₆) δ 8.71 (s, 1H), 6.99–6.95 (m, 3H), 6.69–6.59 (m, 4H), 6.60 (d, *J* = 7.2 Hz, 1H), 5.86 (d, *J* = 12.8 Hz, 2H), 3.73 (s, 3H), 3.11 (s, 3H), 2.62 (s, 2H), 2.30–2.16 (m, 2H), 1.17 (s, 3H), 1.11 (s, 3H); ¹³C NMR (100 MHz, CDCl₃+DMSO-*d*₆) δ 193.13,

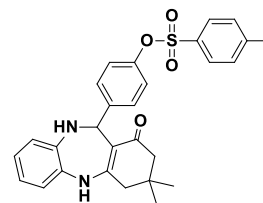
155.51, 150.82, 145.54, 138.38, 136.29, 131.43, 123.34, 123.25, 121.26, 120.63, 120.45, 119.77, 112.79, 110.39, 56.73, 55.84, 50.02, 44.98, 38.11, 32.18, 29.11, 27.75; HRMS (ESI, *m/z*): calcd. For C₂₃H₂₆N₂O₅SH⁺ 443.1635, found 443.1564; IR (KBr thin film, cm⁻¹): ν_{max} 339, 3018, 2965, 1609, 1509, 1479, 1373, 1123, 877.



4-(3,3-Dimethyl-1-oxo-2,3,4,5,10,11-hexahydro-1H-dibenzo[b,e][1,4]diazepin-11-yl)phenyl 4-methylbenzenesulfonate (22f): White powder, mp 160–161 °C, 84% yield.

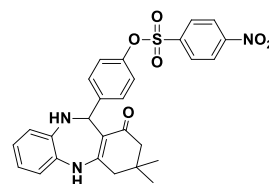
¹H NMR (400 MHz, CDCl₃+DMSO-*d*₆) δ 8.76 (s, 1H), 7.50 (d, *J* = 7.6 Hz, 2H), 7.33 (d, *J* = 7.2 Hz, 2H), 7.05–6.91 (m, 3H), 6.68–6.48 (m, 5H), 6.04 (d, *J* = 4.0 Hz, 1H), 5.71 (d, *J* = 4.4 Hz, 1H), 2.58 (s, 2H), 2.42 (s, 3H), 2.21–2.08 (m, 2H), 1.10 (s, 3H), 1.04 (s, 3H); ¹³C NMR (100 MHz, CDCl₃+DMSO-*d*₆)

δ 192.89, 155.83, 147.46, 145.90, 144.31, 138.67, 131.71, 131.58, 130.39, 128.95, 128.43, 123.26, 121.61, 121.16, 120.35, 109.99, 56.01, 49.83, 44.52, 43.41, 32.20, 28.66, 28.11, 21.64; HRMS (ESI, *m/z*): calcd. For C₂₈H₂₈N₂O₄SH⁺ 489.1843, found 489.1759; IR (KBr thin film, cm⁻¹): ν_{max} 3341, 047, 2964, 1601, 1530, 1361, 1174, 873.



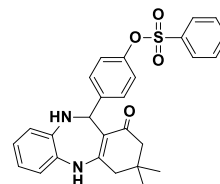
4-(3,3-Dimethyl-1-oxo-2,3,4,5,10,11-hexahydro-1H-dibenzo[b,e][1,4]diazepin-11-yl)phenyl 4-nitrobenzenesulfonate (22g): Yellow solid, mp 152–153 °C, 90% yield.

¹H NMR (400 MHz, CDCl₃+DMSO-*d*₆) δ 8.60 (s, 1H), 8.27 (d, *J* = 8.8 Hz, 2H), 7.79 (d, *J* = 8.4 Hz, 2H), 7.09 (d, *J* = 8.4 Hz, 2H), 6.96 (d, *J* = 8.8 Hz, 1H), 6.70 (d, *J* = 8.0 Hz, 3H), 6.50 (d, *J* = 4.8 Hz, 1H), 5.88 (s, 1H), 5.58 (s, 1H), 2.60 (s, 2H), 2.29–2.15 (m, 2H), 1.15 (s, 3H), 1.08 (s, 3H); ¹³C NMR (100 MHz, CDCl₃+DMSO-*d*₆) δ 193.10, 155.55, 150.84, 147.22, 144.51, 140.06, 138.24, 131.70, 130.00, 128.97, 124.44, 123.12, 121.41, 121.26, 120.57, 120.50, 109.95, 56.45, 49.95, 44.92, 32.14, 28.87, 27.99; HRMS (ESI, *m/z*): calcd. For C₂₇H₂₅N₃O₆SH⁺ 520.1537, found 520.1445; IR (KBr thin film, cm⁻¹): ν_{max} 3388, 3029, 2948, 1884, 1524, 1377, 1197, 868.



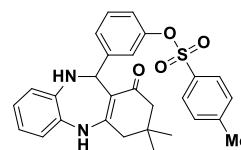
4-(3,3-Dimethyl-1-oxo-2,3,4,5,10,11-hexahydro-1H-dibenzo[b,e][1,4]diazepin-11-yl)phenyl benzenesulfonate (22h): White solid, mp 234–235 °C, 86% yield. ¹H NMR

(400 MHz, CDCl₃+DMSO-*d*₆) δ 8.61 (s, 1H), 7.92–7.35 (m, 5H), 7.06–6.95 (m, 3H), 6.66–6.49 (m, 4H), 5.84 (s, 1H), 5.63 (s, 1H), 2.59 (s, 2H), 2.27–2.14 (m, 2H), 1.15 (s, 3H), 1.08 (s, 3H); ¹³C NMR (100 MHz, CDCl₃+DMSO-*d*₆) δ 193.22, 156.25, 147.37, 144.24, 138.58, 135.14, 134.49, 131.55, 129.90, 128.95, 128.34, 123.38, 121.59, 121.24, 120.59, 120.53, 109.82, 56.06, 49.72, 44.51, 32.18, 28.59, 28.08; HRMS (ESI, *m/z*): calcd. For C₂₇H₂₆N₂O₄SH⁺ 475.1686, found 475.1603; IR (KBr thin film, cm⁻¹): ν_{max} 3356, 2946, 1601, 1586, 1372, 1197.

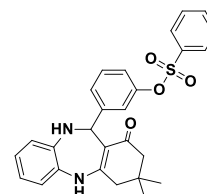


4-(3,3-Dimethyl-1-oxo-2,3,4,5,10,11-hexahydro-1H-dibenzo[b,e][1,4]diazepin-11-yl)-2-

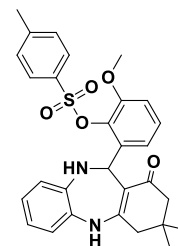
methoxyphenyl 4-methylbenzenesulfonate (22i): White solid, mp 180–181 °C, 85% yield. ¹H NMR (400 MHz, CDCl₃+DMSO-*d*₆) δ 8.67 (s, 1H), 7.79 (d, *J* = 8.8 Hz, 1H), 7.54–7.30 (m, 4H), 7.04–6.61 (m, 6H), 5.91 (s, 1H), 5.61 (d, *J* = 4.0 Hz, 1H), 2.66 (s, 2H), 2.51 (s, 3H), 2.31 (d, *J* = 23.4 Hz, 2H), 1.22 (s, 3H), 1.16 (s, 3H); ¹³C NMR (100 MHz, CDCl₃+DMSO-*d*₆) 193.12, 155.41, 150.83, 145.28, 138.31, 136.02, 135.53, 134.07, 131.56, 128.80, 128.34, 123.19, 123.00, 121.27, 120.51, 119.50, 112.19, 110.25, 56.79, 55.21, 49.98, 45.00, 32.15, 29.12, 27.64; HRMS (ESI, *m/z*): calcd. For C₂₈H₂₈N₂O₄SH⁺ 489.1843, found 489.1961; IR (KBr thin film, cm⁻¹): ν_{max} 3405, 3341, 3090, 2986, 1619, 1450, 1382, 1178, 1082.



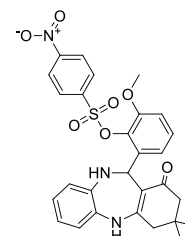
3-(3,3-Dimethyl-1-oxo-2,3,4,5,10,11-hexahydro-1H-dibenzo[b,e][1,4]diazepin-11-yl)phenyl benzenesulfonate (22j): White solid, mp 181–182 °C, 85% yield. ¹H NMR (400 MHz, CDCl₃+DMSO-*d*₆) δ 8.52 (s, 1H), 7.58–7.52 (m, 3H), 7.40–7.39 (m, 2H), 6.90 (s, 1H), 6.78 (d, *J* = 7.6 Hz, 1H), 6.64–6.47 (m, 5H), 5.78 (s, 1H), 5.50 (d, *J* = 1.2 Hz, 1H), 2.53 (s, 2H), 2.24–2.10 (m, 2H), 1.09 (s, 3H), 1.02 (s, 3H); ¹³C NMR (100 MHz, CDCl₃+DMSO-*d*₆) δ 187.58, 151.51, 149.85, 143.67, 139.64, 136.15, 132.62, 130.51, 129.95, 129.25, 128.64, 127.27, 125.18, 124.23, 123.59, 120.21, 117.80, 114.80, 106.02, 53.62, 51.20, 44.47, 33.60, 28.38, 27.17; HRMS (ESI, *m/z*): calcd. For C₂₇H₂₆N₂O₄SH⁺ 475.1686, found 475.1680; IR (KBr thin film, cm⁻¹): ν_{max} 3464, 3391, 2979, 1715, 1591, 1510, 1359, 1030.



2-(3,3-Dimethyl-1-oxo-2,3,4,5,10,11-hexahydro-1H-dibenzo[b,e][1,4]diazepin-11-yl)-6-methoxyphenyl 4-methylbenzenesulfonate (22k): Light red solid, mp 180–181 °C, 85% yield. ¹H NMR (400 MHz, CDCl₃+DMSO-*d*₆) δ 8.87 (s, 1H), 7.99 (d, *J* = 8.0 Hz, 2H), 7.49–7.38 (m, 2H), 7.09 (d, *J* = 7.6 Hz, 1H), 6.84 (t, *J* = 8.0 Hz, 1H), 6.73–6.67 (m, 3H), 6.52 (d, *J* = 7.2 Hz, 1H), 6.36 (d, *J* = 7.6 Hz, 1H), 6.13 (d, *J* = 5.2 Hz, 1H), 5.13 (d, *J* = 5.6 Hz, 1H), 3.51 (s, 3H), 2.65 (d, *J* = 2.8 Hz, 2H), 2.51 (s, 3H), 2.22–2.04 (m, 2H), 1.14 (s, 3H), 1.04 (s, 3H); ¹³C NMR (100 MHz, CDCl₃+DMSO-*d*₆) δ 192.80, 155.44, 151.74, 145.64, 139.47, 137.44, 137.34, 133.84, 132.17, 130.01, 128.47, 128.03, 126.91, 123.58, 121.14, 120.65, 119.46, 111.59, 109.78, 55.62, 52.69, 49.96, 44.80, 32.25, 28.76, 27.80, 21.72; HRMS (ESI, *m/z*): calcd. For C₂₉H₃₀N₂O₅SH⁺ 519.1948, found 519.1859; IR (KBr thin film, cm⁻¹): ν_{max} 3407, 3340, 3089, 2985, 1618, 1449, 1380, 1177, 1081.



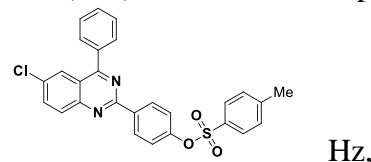
2-(3,3-Dimethyl-1-oxo-2,3,4,5,10,11-hexahydro-1H-dibenzo[b,e][1,4]diazepin-11-yl)-6-methoxy phenyl 4-nitrobenzenesulfonate (22l): White solid, mp 176–177 °C, 89% yield. ¹H NMR (400 MHz, CDCl₃+DMSO-*d*₆) δ 8.42 (s, 1H), 8.12 (s, 1H), 6.78 (d, *J* = 2.0 Hz, 1H), 6.58–6.33 (m, 8H), 5.59 (s, 1H), 5.45 (s, 1H), 3.50 (s, 3H), 2.41 (s, 2H), 2.11–1.97 (m, 2H), 0.96 (d, *J* = 17.8 Hz, 6H); ¹³C NMR (100 MHz, CDCl₃+DMSO-*d*₆) δ 191.72, 154.13, 146.16, 143.61, 137.80, 137.79, 134.97, 134.94, 130.57, 121.93, 120.17, 119.33, 119.29, 118.99, 118.96, 118.83, 113.75, 110.82, 110.06, 55.36, 54.61, 49.00, 43.80, 31.08, 28.17, 26.57; HRMS (ESI, *m/z*): calcd. For C₂₈H₂₇N₃O₇SH⁺ 550.1642, found 550.1551; IR (KBr thin film, cm⁻¹): ν_{max} 3409, 3347, 2928, 1606, 1532, 1381, 1280, 1059.



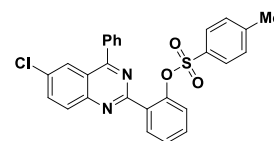
General procedure for the synthesis 2-(6-chloro-4-phenylquinazolin-2-yl)phenyl sulfonate ester scaffolds (24a-24i):

To a solution of 2-amino 5-chloro benzophenone **1b** (1.0 mmol) in EtOH (5 mL) was added sulfonate ester aldehyde substrates (**21a-21i**) (1.0 mmol), ammonium acetate **23** (2.5 mmol) SnCl₂ (10 mol%). The mixture was heated at 80 °C for 3-4h. After that it was cooled to room temperature, extracted with EtOAc (2X10 mL). Combined organic layers were washed with water, brine and dried over sodium sulphate. Evaporation of the solvent gave the crude product which was purified by silica gel column chromatography. Elution of the column with EtOAc+n-Hexane (1:4) gave the pure products **24a-24i** in 75-95% yields.

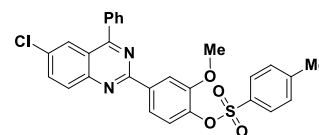
4-(6-Chloro-4-phenylquinazolin-2-yl)phenyl 4-methylbenzenesulfonate (24a): Yellow solid, mp 334–335 °C, 80% yield. ¹H NMR (400 MHz, CDCl₃+DMSO-*d*₆) δ 8.57 (d, *J* = 8.6 Hz, 2H), 8.13 (d, *J* = 8.8 Hz, 1H), 8.02 (s, 1H), 7.87–7.85 (m, 2H), 7.77 (d, *J* = 8.4 Hz, 2H), 7.67 (s, 3H), 7.46 (d, *J* = 8.0 Hz, 3H), 7.19 (d, *J* = 8.8 Hz, 2H), 2.44 (s, 3H); ¹³C NMR (100 MHz, CDCl₃+DMSO-*d*₆) δ 158.06, 155.73, 150.58, 148.98, 135.75, 135.12, 134.82, 133.53, 133.35, 133.25, 132.72, 131.93, 131.61, 131.09, 130.35, 127.40, 127.33, 126.96, 126.83, 118.71, 24.44; HRMS (ESI, *m/z*): calcd. For C₂₇H₁₉ClN₂O₃SH⁺ 487.0878, found 487.0815; IR (KBr thin film, cm⁻¹): ν_{max} 2975, 1537, 1375, 1305, 1150, 109, 547.



2-(6-Chloro-4-phenylquinazolin-2-yl)phenyl 4-methylbenzenesulfonate (24b): Yellow solid, mp 246–247 °C, 82 % yield. ¹H NMR (400 MHz, CDCl₃+DMSO-*d*₆) δ 8.05 (s, 1H), 7.79 (d, *J* = 8.4 Hz, 2H), 7.68–7.66 (m, 1H), 7.47 (d, *J* = 7.6 Hz, 2H), 7.43–7.35 (m, 5H), 7.27 (dd, *J* = 8.8, 2.0 Hz, 1H), 7.17 (d, *J* = 8.4 Hz, 1H), 6.94 (d, *J* = 1.8 Hz, 1H), 6.81 (d, *J* = 8.6 Hz, 1H), 6.71 (s, 1H), 2.39 (s, 3H); ¹³C NMR (100 MHz, CDCl₃+DMSO-*d*₆) δ 151.32, 149.85, 147.87, 140.87, 138.96, 136.60, 135.90, 135.11, 134.84, 134.59, 134.44, 134.10, 134.07, 134.02, 133.99, 133.08, 132.40, 131.99, 131.49, 129.88, 127.83, 127.80, 25.50; HRMS (ESI, *m/z*): calcd. For C₂₇H₁₉ClN₂O₃SH⁺ 487.0878, found 487.0870.



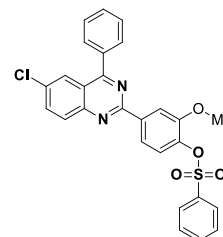
4-(6-Chloro-4-phenylquinazolin-2-yl)-2-methoxyphenyl 4-methylbenzenesulfonate (24c): White solid, mp 312–313 °C, 75 % yield. ¹H NMR (400 MHz, CDCl₃+DMSO-*d*₆) δ 8.19–8.13 (m, 2H), 8.01 (s, 1H), 7.88 (d, *J* = 3.6 Hz, 1H), 7.74–7.67 (m, 4H), 7.48–7.42 (m, 4H), 7.29–7.19 (m,



2H), 7.09–7.04 (m, 1H), 3.65 (s, 3H), 2.43 (s, 3H); ^{13}C NMR (100 MHz, DMSO- d_6) δ 166.00, 158.86, 151.77, 148.88, 144.43, 135.75, 135.44, 134.07, 132.15, 131.13, 130.62, 130.12, 129.91, 129.68, 129.13, 129.00, 128.06, 127.22, 124.74, 120.72, 117.62, 113.05, 55.08, 20.11; HRMS (ESI, m/z): calcd. For $\text{C}_{28}\text{H}_{21}\text{ClN}_2\text{O}_4\text{SH}^+$ 517.0983, found 517.0913; IR (KBr thin film, cm^{-1}): ν_{max} 2974, 1598, 1504, 1348, 1175, 1091, 840, 701.

4-(6-Chloro-4-phenylquinazolin-2-yl)-2-methoxyphenyl benzenesulfonate (24d): Pale yellow solid, mp 252–253 °C, 82% yield. ^1H NMR (400 MHz, CDCl_3 +DMSO- d_6)

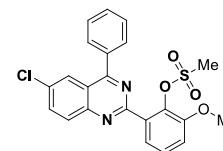
δ 8.20–8.14 (m, 3H), 8.02 (s, 2H), 7.87–7.78 (m, 5H), 7.67 (d, J = 6.4 Hz, 5H), 7.31 (d, J = 8.4 Hz, 1H), 3.62 (s, 3H); ^{13}C NMR (100 MHz, CDCl_3 +DMSO- d_6) δ 153.13, 151.82, 150.74, 140.67, 138.63, 138.49, 136.13, 136.09, 135.69, 130.81, 130.77, 130.59, 130.54, 129.80, 129.52,



129.42, 129.31, 128.68, 124.59, 124.04, 122.38, 116.11, 57.01; HRMS (ESI, m/z): calcd. For $\text{C}_{27}\text{H}_{19}\text{ClN}_2\text{O}_4\text{SH}^+$ 503.0827, Found 503.1768; IR (KBr thin film, cm^{-1}): ν_{max} 2973, 1557, 1504, 1345, 1317, 11.9, 838, 701.

2-(6-Chloro-4-phenylquinazolin-2-yl)-6-methoxyphenyl methanesulfonate (24e): White solid, mp 225–226 °C, 80% yield. ^1H NMR (400 MHz, CDCl_3 +DMSO) δ 8.24 (s,

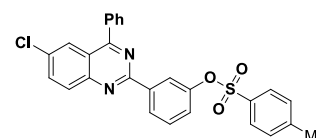
1H), 7.47 (s, 4H), 7.30 (d, J = 8.0 Hz, 1H), 7.24 (d, J = 8.4 Hz, 2H), 7.16 (d, J = 8.0 Hz, 1H), 6.96 (d, J = 2.0 Hz, 1H), 6.84–6.80 (m, 2H), 3.90 (s, 3H), 3.51 (s, 3H); ^{13}C NMR (100 MHz, CDCl_3 +DMSO- d_6) δ 160.25,



154.31, 152.09, 148.79, 144.71, 140.62, 134.83, 132.26, 131.08, 128.99, 128.38, 127.75, 125.52, 123.62, 123.34, 122.69, 121.93, 114.68, 57.69, 36.80; HRMS (ESI, m/z): calcd. For $\text{C}_{22}\text{H}_{17}\text{ClN}_2\text{O}_4\text{SH}^+$ 441.0670, found 441.0665; IR (KBr thin film, cm^{-1}): ν_{max} 3009, 2980, 1621, 1478, 1363, 1149, 505.

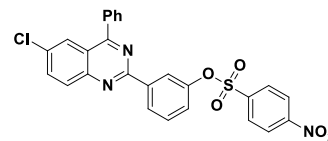
3-(6-Chloro-4-phenylquinazolin-2-yl)phenyl 4-methylbenzenesulfonate (24f): White solid, mp

198–199 °C, 81% yield. ^1H NMR (400 MHz, CDCl_3 +DMSO) δ 7.86 (s, 1H), 7.82–7.78 (m, 3H), 7.67 (d, J = 8.0 Hz, 2H), 7.51 (t, J = 7.2 Hz, 1H), 7.46–7.39 (m, 2H), 7.35–7.33 (m, 3H), 7.28 (d, J =

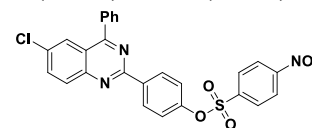


8.0 Hz, 2H), 7.23 (d, J = 8.0 Hz, 2H), 2.17 (s, 3H); ^{13}C NMR (100 MHz, CDCl_3 +DMSO- d_6) δ 155.06, 152.73, 147.58, 145.98, 132.75, 132.12, 131.82, 130.53, 130.35, 130.25, 129.83, 129.72, 128.93, 128.61, 128.09, 127.39, 127.35, 126.81, 124.40, 123.96, 123.83, 115.71, 21.44; HRMS (ESI, m/z): calcd. For $\text{C}_{27}\text{H}_{19}\text{ClN}_2\text{O}_3\text{SH}^+$ 487.0878, found 487.0860; IR (KBr thin film, cm^{-1}): ν_{max} 3378, 3106, 2944, 1665, 1610, 1527, 1352, 1196, 852.

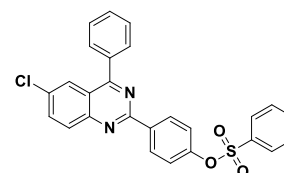
3-(6-Chloro-4-phenylquinazolin-2-yl)phenyl 4-nitrobenzenesulfonate (24g): White solid, mp 216–217 °C, 95% yield. ¹H NMR (400 MHz, CDCl₃+DMSO-*d*₆) δ 8.55 (d, *J* = 8.0 Hz, 1H), 8.20 (s, 1H), 8.14 (d, *J* = 8.4 Hz, 2H), 8.04–7.99 (m, 2H), 7.90 (d, *J* = 7.6 Hz, 1H), 7.83–7.81 (m, 2H), 7.77 (d, *J* = 7.6 Hz, 1H), 7.69–7.63 (m, 4H), 7.55 (t, *J* = 8.0 Hz, 1H), 7.19–7.17 (m, 1H); ¹³C NMR (100 MHz, CDCl₃+DMSO-*d*₆) δ 156.03, 153.78, 150.75, 139.42, 136.47, 136.06, 135.66, 133.94, 133.61, 133.02, 131.50, 131.09, 131.05, 130.80, 129.66, 129.44, 127.73, 124.96, 124.59, 123.59, 121.92, 116.54; HRMS (ESI, *m/z*): calcd. For C₂₆H₁₆ClN₃O₅SH⁺ 518.0572, found 518.1531.



4-(6-Chloro-4-phenylquinazolin-2-yl)phenyl 4-nitrobenzenesulfonate (24h): White solid, mp 228–229 °C, 85% yield. ¹H NMR (400 MHz, CDCl₃+DMSO-*d*₆) δ 9.35 (s, 1H), 8.86 (s, 1H), 8.56 (d, *J* = 8.4 Hz, 2H), 8.28 (s, 1H), 8.16–8.13 (m, 1H), 8.06–8.02 (m, 2H), 7.89–7.87 (m, 2H), 7.68–7.64 (m, 3H), 7.59 (d, *J* = 8.8 Hz, 1H), 7.19 (d, *J* = 8.8 Hz, 1H), 6.87 (d, *J* = 8.8 Hz, 1H); ¹³C NMR (100 MHz, CDCl₃+DMSO-*d*₆) δ 158.02, 155.56, 150.36, 137.69, 137.63, 135.63, 134.93, 133.21, 133.09, 132.96, 132.44, 132.40, 131.73, 131.44, 130.81, 130.03, 127.11, 126.59, 126.53, 118.55; HRMS (ESI, *m/z*): calcd. For C₂₆H₁₆ClN₃O₅SH⁺ 518.0572, found 518.0421; IR (KBr thin film, cm⁻¹): ν_{max} 3380, 3101, 2956, 1659, 1609, 1519, 1360, 1185, 859.



4-(6-Chloro-4-phenylquinazolin-2-yl)phenyl benzenesulfonate (24i): White solid, mp 175–176 °C, 82% yield. ¹H NMR (400 MHz, CDCl₃+DMSO-*d*₆) δ 8.55 (d, *J* = 8.8 Hz, 2H), 8.10 (d, *J* = 9.6 Hz, 1H), 8.00 (s, 2H), 7.89–7.79 (m, 5H), 7.68–7.64 (m, 5H), 7.19 (d, *J* = 8.8 Hz, 2H); ¹³C NMR (100 MHz, CDCl₃+DMSO-*d*₆) δ 167.78, 158.67, 151.43, 150.25, 136.73, 136.70, 135.29, 135.27, 134.80, 132.78, 131.29, 130.75, 130.29, 130.25, 130.04, 129.10, 128.63, 125.83, 122.66, 122.15; HRMS (ESI, *m/z*): calcd. For C₂₆H₁₇ClN₂O₃SH⁺ 473.0721, found 473.0767.

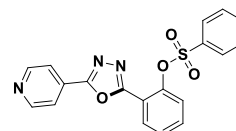


1.3 General procedure for the synthesis of 2,5-substituted-1,3,4-oxadiazol-2-yl)phenyl benzenesulfonates (28a-28d/ 29a-29c): To a solution of isonicotinohydrazide **25a**/nicotinohydrazide **25b** (1.0 mmol) in EtOH (5 mL) was added sulfonate ester aldehyde (**21a-21d**) (1.0 mmol) and AcOH (20 mol%). The mixture was heated at 80 °C, 1 h to give the sulfonate ester Schiff-bases (**26a-26d/27a-27c**).

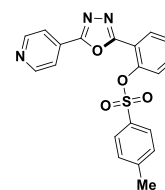
To a solution of sulfonate ester Schiff-base **26a-26d/ 27a-27c** (1mmol) in EtOH (5 mL) was added SnCl₂ (10 mol%) and TEA (20 mol%) and the mixture was heated at 80 °C for 3-4 h. After the

completion of the reaction (monitored by TLC), it was cooled to room temperature and extracted with ethyl acetate (2X10 mL). Combined organic layers were washed with water, brine, dried over sodium sulphate. Solvent was evaporated under reduced pressure to give the crude product which was purified by silica gel column chromatography. Elution of the column using ethyl acetate+*n*-hexane (1:4 ratio) gave the desired products **28a-28d/29a-29c** in 75-85% yields.

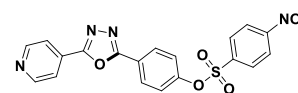
2-(5-(Pyridin-4-yl)-1,3,4-oxadiazol-2-yl)phenyl benzenesulfonate (28a): White solid, mp 201–202 °C, 81% yield. ¹H NMR (400 MHz, CDCl₃+DMSO-*d*₆) δ 8.90 (s, 2H), 8.04 (s, 2H), 7.77–7.71 (m, 3H), 7.56 (d, *J* = 7.6 Hz, 1H), 7.48 (s, 1H), 7.44 (t, *J* = 8.0 Hz, 2H), 7.37 (t, *J* = 8.0 Hz, 1H), 7.06 (d, *J* = 8.0 Hz, 1H); ¹³C NMR (100 MHz, DMSO-*d*₆) δ 161.02, 158.77, 158.47, 150.22, 140.14, 138.41, 137.55, 135.32, 134.23, 130.26, 129.30, 126.08, 121.28, 119.15, 118.41; HRMS (ESI, *m/z*): calcd. For C₁₉H₁₃N₃O₄SH⁺ 380.0700, found 380.0707; IR (KBr thin film, cm⁻¹): ν_{max} 3110, 2983, 1642, 1612, 1532, 1340, 1150, 855.



2-(5-(Pyridin-4-yl)-1,3,4-oxadiazol-2-yl)phenyl 4-methylbenzenesulfonate (28b): White solid, mp 192–193 °C, 85 % yield. ¹H NMR (400 MHz, CDCl₃) δ 8.81 (s, 2H), 8.14 (dd, *J* = 7.8, 1.2, Hz, 1H), 7.96 (s, 2H), 7.58 (d, *J* = 8.0 Hz, 2H), 7.49–7.45 (m, 1H), 7.39 (t, *J* = 7.6 Hz, 1H), 7.19–7.10 (m, 3H), 2.31 (s, 3H); ¹³C NMR (100 MHz, CDCl₃) δ 163.32, 162.79, 150.87, 146.89, 145.98, 133.33, 132.30, 130.78, 129.91, 128.31, 127.77, 124.06, 120.56, 118.21, 21.71; HRMS (ESI, *m/z*): calcd. For C₂₀H₁₅N₃O₄SH⁺ 394.0856, found 394.0854; IR (KBr thin film, cm⁻¹): ν_{max} 3385, 3109, 2962, 1665, 1611, 1526, 1355, 1170, 861.

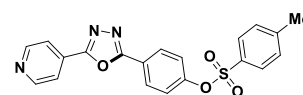


4-(5-(Pyridin-4-yl)-1,3,4-oxadiazol-2-yl)phenyl 4-nitrobenzenesulfonate (28c): Light brown solid, mp 219–220 °C, 85 % yield. ¹H NMR (400 MHz, CDCl₃) δ 8.83 (d, *J* = 7.2 Hz, 2H), 8.42 (d, *J* = 7.6 Hz, 2H), 7.85 (d, *J* = 7.6 Hz, 2H), 7.47 (d, *J* = 8.0 Hz, 2H), 7.14 (d, *J* = 8.4 Hz, 2H), 7.04 (d, *J* = 7.6 Hz, 2H); ¹³C NMR (100 MHz, CDCl₃+DMSO-*d*₆) δ 160.00, 157.53, 152.38, 147.80, 139.65, 137.58, 137.11, 135.45, 133.63, 131.58, 129.15, 128.68, 120.57; HRMS (ESI, *m/z*): calcd. For C₁H₁₂N₄O₆S 424.0478, found 424.0954; IR (KBr thin film, cm⁻¹): ν_{max} 3355, 3110, 2956, 1609, 1550, 1516, 1349, 1190, 855.



4-(5-(Pyridin-4-yl)-1,3,4-oxadiazol-2-yl)phenyl

4-

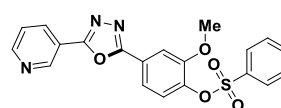


4-methylbenzenesulfonate (28d): White powder, mp 199–200 °C, 75 %

yield. ¹H NMR (400 MHz, CDCl₃+DMSO-*d*₆) δ 8.87 (s, 2H), 8.12 (d, *J* = 8.0 Hz, 2H), 7.99 (s, 2H), 7.73 (d, *J* = 7.6 Hz, 2H), 7.37 (d, *J* = 7.2 Hz, 2H), 7.20 (d, *J* = 7.6 Hz, 2H), 2.48 (s, 3H); ¹³C NMR (100 MHz, CDCl₃+DMSO-*d*₆) δ 164.23, 162.85, 152.06, 145.92, 131.59, 130.53, 129.91, 128.61, 128.28, 123.22, 122.06, 120.19, 120.04, 21.60; HRMS (ESI, *m/z*): calcd. For C₂₀H₁₅N₃O₄SH⁺ 394.0856 found 394.0857; IR (KBr thin film, cm⁻¹): ν_{max} 3100, 2955, 1665, 1605, 1529, 1372, 1165, 862.

2-Methoxy-4-(5-(pyridin-3-yl)-1,3,4-oxadiazol-2-yl)phenyl benzenesulfonate (29a): White solid,

mp 129–130 °C, 85% yield. ¹H NMR (400 MHz, CDCl₃) δ 9.31 (s, 1H),

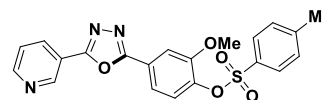


8.78 (d, *J* = 8.4 Hz, 1H), 8.35 (d, *J* = 8.0 Hz, 1H), 7.82 (d, *J* = 7.6 Hz,

2H), 7.62–7.54 (m, 3H), 7.47 (t, *J* = 7.6 Hz, 1H), 7.29 (d, *J* = 8.4 Hz, 1H), 3.57 (s, 3H); ¹³C NMR (100 MHz, CDCl₃) δ 164.21, 162.85, 152.48, 152.39, 147.79, 141.07, 135.90, 134.31, 128.93, 128.74, 128.60, 128.56, 125.07, 124.98, 123.18, 119.61, 111.04, 56.02; HRMS (ESI, *m/z*): calcd. For C₂₀H₁₅N₃O₅SH⁺ 410.0805, found 410.0815; IR (KBr thin film, cm⁻¹): ν_{max} 3112, 2986, 1662, 1619, 1525, 1372, 1162, 851.

2-Methoxy-4-(5-(pyridin-3-yl)-1,3,4-oxadiazol-2-yl)phenyl 4-methylbenzenesulfonate (29b):

Pale yellow solid, 75% yield, mp 204–205 °C; ¹H NMR (400 MHz,

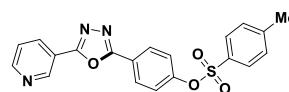


CDCl₃) δ 8.86 (s, 2H), 8.00 (d, *J* = 4.0 Hz, 2H), 7.78 (d, *J* = 8.0 Hz,

2H), 7.65 (s, 2H), 7.37–7.32 (m, 3H), 3.70 (s, 3H), 2.46 (s, 3H); ¹³C NMR (100 MHz, CDCl₃+DMSO-*d*₆) δ 164.51, 162.99, 152.38, 150.82, 145.71, 141.12, 132.55, 130.75, 129.62, 129.52, 128.52, 128.46, 124.84, 122.95, 120.39, 119.73, 111.14, 55.97, 21.70; HRMS (ESI, *m/z*): calcd. For C₂₁H₁₇N₃O₅SH⁺ 424.0962, found 424.0967; IR (KBr thin film, cm⁻¹): ν_{max} 3110, 2986, 16540, 1612, 1553, 1165, 863.

4-(5-(Pyridin-3-yl)-1,3,4-oxadiazol-2-yl)phenyl 4-methylbenzenesulfonate (29c): White solid,

mp 169–170 °C, 80% yield. ¹H NMR (400 MHz, CDCl₃+DMSO-*d*₆) δ



9.32 (s, 1H), 8.81 (d, *J* = 4.4 Hz, 2H), 8.12 (d, *J* = 8.4 Hz, 2H), 7.96

(d, *J* = 8.4 Hz, 1H), 7.72 (d, *J* = 8.0 Hz, 2H), 7.40 (d, *J* = 8.0 Hz, 2H), 7.20 (d, *J* = 8.4 Hz, 2H), 2.48 (s, 3H); ¹³C NMR (100 MHz, CDCl₃+DMSO-*d*₆) δ 162.04, 157.35, 155.12, 138.07, 137.66, 134.90, 134.11, 134.05, 131.96, 131.52, 130.74, 125.69, 125.08, 124.91, 117.68, 28.77; HRMS

(ESI, m/z): calcd. For $C_{20}H_{15}N_3O_4S$ 394.0856, found 394.0857; IR (KBr thin film, cm^{-1}): ν_{max} 3113, 2979, 1655, 1614, 1353, 1176, 866.

5.7 References

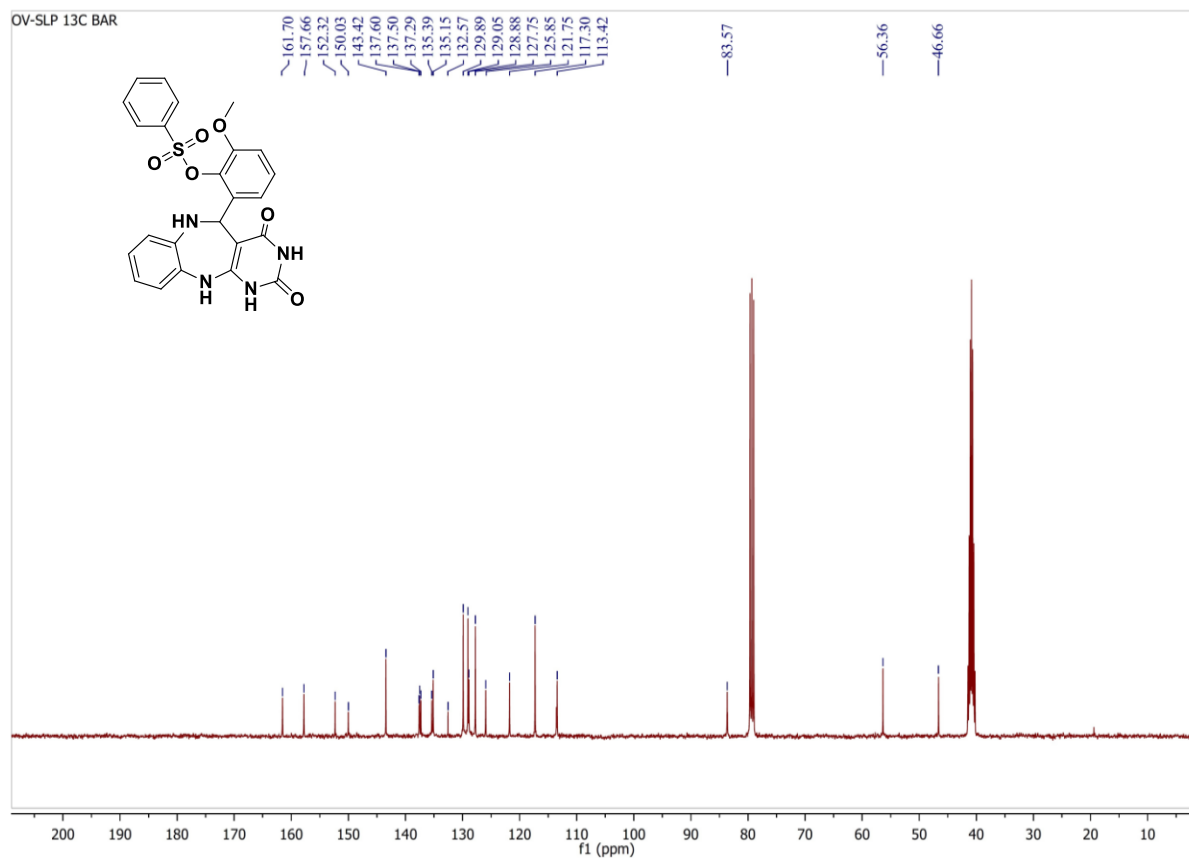
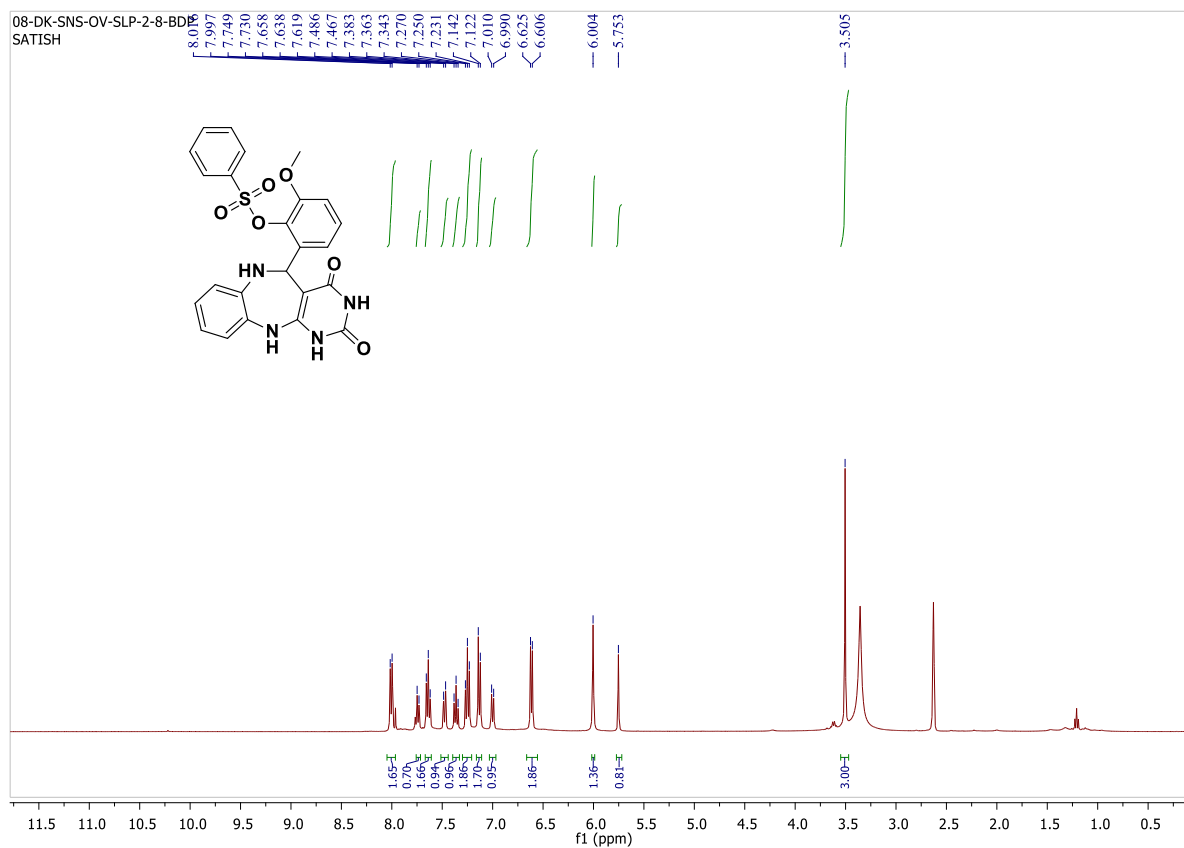
1. (a) Cortés, E. C.; Ana, L. V. C.; Olivia, G. M. *J. Heterocycl Chem.* **2007**, *44*, 183–187. (b) Kumar, R.; Chaudhary, P.; Nimesh, S.; Verma A. K.; Chandra, R. *Green Chem.* **2006**, *8*, 519–521. (c) Ookura, R.; Kito, K.; Ooi, T.; Namikoshi, M.; Kusumi, T. *J. Org. Chem.* **2008**, *73*, 4245–4247. (d) Klaubert, D. H.; Flemington, N. J.; Stanley, C. B.; Pattison, T.W and Rees, R. W., *US Pat.* 4 495101, **1985**. (e) Bader, A. A. S.; Omar, A.H.; El-Odemi, M. H. *J. Clin. Epigenet.* **2017**, *3*, (2). (f) Torres, S. R.; Fröde, T.S.; Nardi, G.M.; Vita, N.; Reeb, R.; Ferrara, P.; Ribeiro-do-Valle, R. M and Farges, R. C. *Eur. J. Pharmacol.* **2000**, *408* (2), 199–211. doi: 10.1016/s0014-2999(00)00760-3.
2. (a) Collado, M. C.; Beleta, J.; Martinez, E.; Miralpeix, M.; Dome`nech, T.; Palacios, J. M and Herna´ndez, J. *J. Pharmacol.* **1998**, *123*, 1047–1054. (b) De Corte, B. L. *J. Med. Chem.* **2005**, *48*, 1689–1696. (c) Vandyck, K.; Cumming, M. D.; Nyanguile, O.; Boutton, C.W.; Vendeville, S.; McGowan, D.; Devogelaere, B.; Amssoms, K.; Last, S.; Rombauts, K.; Tahri, A.; Lory, P.; Hu, L.; Beauchamp, D. A.; Simmen, K and Raboisson, P. *J. Med. Chem.* **2009**, *52*, 4099–4102.
3. (a) Wang, Y.; Konkoy, C. S.; Ilyin, V. I.; Vanover, K. E.; Carter, R. B.; Weber, E.; Keana; J. F. W.; Woodward, R. M. and Cai, S. X. *J. Med. Chem.*, **1998**, *41*, 2621–2625. (b) Smits, R. A.; Lim, H. D.; Stegink, B.; Bakker, R. A.; de Esch, I. J. P. and Leurs, R. *J. Med. Chem.*, **2006**, *49*, 4512–4516. (c) Naeimi, H.; Foroughi, H. *New J. Chem.* **2015**, *39*, 1228–1236.
4. (a) Cortés, E. C.; Sanabria, A. M. H.; Mellado, O. G. *J. Heterocyclic Chem.* **2002**, *39*, 55. (b) Cortés, E. C.; Baños, M. A.; de Cortés, O. G.-M. *J. Heterocyclic Chem.* **2004**, *41*, 277. (c) Shaabani, A.; Hooshmand, S. E.; Nazeri, M. T.; Afshari, R.; Ghasemi, S. *Tetrahedron Lett.* **2016**, *57*, 3727. (d) Naeimi, H.; Foroughi, H. *Chinese J. Catal.* **2015**, *36*, 734. (e) Nazia, K.; Prasun, M and Asish, R. D. *RSC Adv.* **2016**, *6*, 88904–88910. (f) Naeimi, H.; Foroughi, H. *New J. Chem.* **2015**, *39*, 1228. (g) Shoeb, M.; Mobin, M.; Ali, A.; Zaman, S.; Naqvi, A. H. *Appl Organometal Chem.* DOI: 10.1002/aoc.3945.
5. (a) Tarannum, S.; Siddiqui, Z. N. *RSC Adv.* **2015**, *5*, 74242; (b) Nasir, Z.; Ali, A.; Shakir, M.; Wahab, R.; Shamsuzzaman, Lutfullah. *New J. Chem.* **2017**, *41*, 5893. (c) Sakkani, N.; Onkara, P. P.; Divakar, K.; Banoth, P and Dhurke, K. *New J. Chem.* **2017**, *41*, 8993;

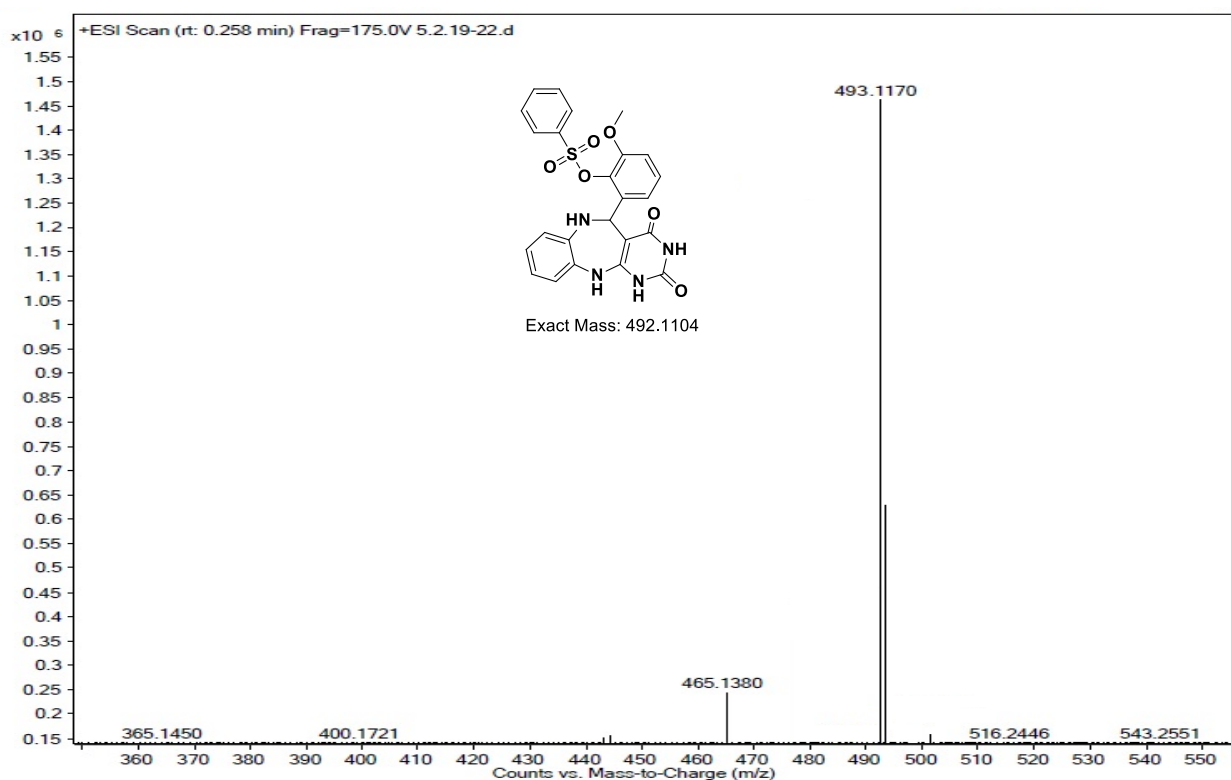
6. (a) Gundla, R.; Kazemi, R.; Sanam, R.; Muttineni, R.; Sarma, J. A. R. P.; Dayam, R. and Neamati, N. *J. Med. Chem.* **2008**, *51*, 3367. (b) Desiniotis, A. & Kyprianou, N. *Expert Opin. Ther. Targets*, **2011**, *15* (12), 14051418. <https://doi.org/10.1517/14728222.2011.641534>.
7. (a) Siemann, D. W. *Cancer Treat. Rev.*, **2011**, *37*, 63–74. (b) Pommier, Y. *ACS Chem. Biol.*, **2013**, *8*, 82–95. (c) Ismail, R. S. M.; Ismail, N. S. M.; Abuserii, S and Abou El Ella, D. A. *Future J. Pharm. Sci.* **2016**, *2*, 9–19. (d) Kris, M. G.; Natale, R. B.; Herbst, R. S.; Lynch, Jr, T. J.; Prager, D.; Belani, C. P.; Schiller, J. H.; Kelly, K.; Spiridonidis, H.; Sandler, A.; Albain, K. S.; Cella, D.; Wolf, M. K.; Averbuch, S. D.; Ochs, J. J. and Kay, A. C. *J. Am. Med. Assoc.* **2003**, *290*, 2149–2158. (e) Zahedifard, M.; Faraj, F. L.; Paydar, M.; Looi, C. Y.; Hajrezaei, M.; Hasanpourghadi, M.; Kamalidehghan, B.; Majid, N. A.; Ali, H. M. and Abdulla, M. A., *Sci. Rep.* **2015**, *5*, 11544.
8. (a) Zhang, J.; Zhu, D.; Yu, C.; Wan, C.; Wang, Z. *Org. Lett.* **2010**, *12*, 2841. (b) Olayinka, O. A.; Oluwatosin, Y. A.; Damilola, V. A.; Fisayo, E. O and Ayodele, O. O. *Am. J. Drug Discov. Dev.*, **2017**, *7*(1), 1-24. (c) Baghbanian, S.M.; Farhang, M. *RSC Adv.* **2014**, *4*, 11624-11633. (d) Derabli, C.; Boulcina, R.; Kirsch, G.; Carboni, B.; Debache, A. *Tetrahedron Lett.* **2014**, *55*, 200-204. (e) Yan, Y.; Xu, Y.; Niu, B.; Xie, H.; Liu, Y. *J. Org. Chem.* **2015**, *80*, 5581.
9. (a) Mengmeng, C.; Min, Z.; Biao, X.; Zhenda, T.; Wan, L. and Huanfeng, J. *J. org. Lett.* **2014**, *16*, 22, 6028–6031. (b) Bing, H.; Xiu, -L. Y.; Chao, W.; Yong, -W. B.; Tai, -C. P.; Xin, C. and Wei, Y. *J. Org. Chem.* **2012**, *77*, 1136–1142. (c) Yamaguchi, T.; Sakairi, K.; Yamaguchi, E.; Tada, N and Itoh, A. *RSC. Adv.* **2016**, *6*, 56892.
10. (a) Imtiaz, K.; Aliya, I.; Naeem, A.; Aamer, S. *Euro. J. Med. Chem.* **2014**, *76*, 193-244. (b) Imtiaz, K.; Sumera, Z.; Sadaf, B., Naeem, A.; Zaman, A.; Jamshed, I.; Aamer, S. *Bioorg. Med. Chem.* **2016**, *24*, 2361–2381. (c) Jinjin, C.; Dan, C.; Fuhong, X and Guo-Jun, D. *Green Chem.*, **2018**, *20*, 5459.
11. (a) Mishra, P.; Rajak, H.; Mehta, A. *J. Gen. Appl. Microbiol.* **2005**, *51*, 133. (b) Kashaw, S. K.; Gupta, V.; Kashaw, V.; Mishra, P.; Stables, J. P.; Jain, N. K. *Med. Chem. Res.* **2010**, *19*, 250. (c) Zheng, X.; Li, Z.; Wang, Y.; Chen, W.; Huang, Q.; Liu, C.; Song, G. *J. Fluorine Chem.* **2003**, *123*, 163–169. (d) Sonia, G.; K, R. T. *Med. Chem. Res.* **2013**, *22*, 3428. (e) Rai, K. M. L.; Linganna, N. *II Farmaco.* **2000**, *55*, 389. (f) Deshmukh, A. A.; Sattur, P. B.; Sheth, U. K. *Indian. J. Exp. Biol.* **1976**, *14*, 166–168. (g) Zarghi, A.; Tabatabai, S. A.; Faizi, M.; Ahadian, A.; Navabi, P.; Zanganeh, V.; Shafiee, A. *Bioorg. Med. Chem. Lett.* **2005**, *15*, 1863–1865. (h) Tamoto, N.; Adachi, C.; Nagai, K. *Chem. Mater.* **1997**, *9*, 1077–1085.
12. (a) Heravi, M. M.; Zadsirjan, V.; Bakhtiari, K & Bamoharram, F. F. *Synth. React. Inorg. Met. Org. Chem.* **2013**, *43* (3), 259–263. doi:10.1080/15533174.2012.740718. (b) Karolina, J.;

- Agnieszka, K.; Wojciech, Z and Nikodem, K *Arkivoc* **2017**, 87,106. (c) Zhang, G.; Yu, Y.; Zhao, Y.; Xie, X.; Ding, C. *Synlett*. **2017**, 28, 1373-1377. (d) Peng, G and Yunyang, W. *Heterocycl. Commun.* **2013**, 19 (2), 113–119. (e) Arvind, K. Y.; Lal, D. S. Y. *Tetrahedron Lett.* **2014**, 55, 2065–2069. (f) Cristian, D.; Codrut, C. P.; Ioana, D.; Mihaela, M.; Ion, B.; Lavinia, L. R. C. *Tetrahedron Lett.* **2009**, 50, 1886–1888. (g) Minoo, D.; Peyman, S.; Mostafa, B and Mahboobeh, B. *Tetrahedron Lett.*, **2006**, 47, 6983–6986. (h) Dabiri, M.; Salehi, P.; Baghbanzadeh, M.; Bahramnejad, M. *Tetrahedron Lett.* **2006**, 47, 6983. (i) Salassa, G. and Terenzi, A. *Int. J. Mol. Sci.* **2019**, 20 (14), 3483. <https://doi.org/10.3390/ijms20143483>. (j) Guin, S.; Ghosh, T.; Rout, S. K.; Banerjee, A.; Patel, B. K. *Org. Lett.* **2011**, 13, 5976-5979.
13. (a) Qiangqiang, J.; Xinghui, Q.; Chenyang, Z.; Xuan, J.; Jin, L and Renhua, L. *Org. Chem. Front.* **2018**, 5, 386–390. (b) Ganesh, M.; Saroj, K. R.; Srimanta, G.; Anupal, G and Bhisma, K. P. *RSC Adv.* **2014**, 4, 5357. (c) Wenquan, Y.; Gang, H.; Yueteng, Z.; Hongxu, L.; Lihong, D.; Xuejun, Y.; Yujiang, L and Junbiao, C. *J. Org. Chem.* **2013**, 78, 10337–10343. (d) Rao, V. S and Chandra, S. K. V. *G Synth. Commun.*, **2004** 34:12, 2153-2157. (e) Sakkani, N.; Divakar, K.; Banoth, P.; Dhurke, K. *New J. Chem.* 2017, **41**, 8993-9001.
14. (a) Tatiana, N. M.; Pascal, L. P.; Alberto, B.; Oldřich, P.; Filip, B.; Françoise, R. -L. G.; Sylvain, A.; Emiliya, V. N.; Galina, N. L and Valery, N. C *Eur. J. Org. Chem.* **2020**, 33, 5445-5454. (b) Wang, C.; Jung, G. Y.; Hua, Y.; Pearson, C. Bryce, M. R.; Petty, M. C.; Batsanov, A. S.; Goeta, A. E.; Howard, J. A. K. *Chem. Mater.* **2001**, 13, 1167. (c) Mitschke, U.; Bauerle, P. *J. Mater. Chem.* **2000**, 10, 1471. (d) Lee, C., Yang, W., Parr, R. G., *Phys. Rev. B.* **1988**, 37, 785–789.
15. (a) Berna, E.; Amarila, Malik.; Purwa, I. S. M.; Bianca, L. *Int. J. Pharmtech Res.* **2012**, 4 (4), 1667-1671. (b) Kimura, A.; Jin-Ha, L.; In-Su, L.; Hee-Seob, L.; Kwan-Hwa, P.; Seiya, C.; Doman, K. *Carbohydr. Res.* **2004**, 339 (6), 1035–1040. (c) Abbas, G.; Hassan, Z.; Al-Harrasi, A.; Muhammad, S. A.; Al-Quraini, A. J.; A-Maani, Z. K And Al-Adawai, A. M. *Turk. J. Chem.* **2018**, 42 (4), 14. DOI:10.3906/kim-1801-27. (d) Mohammed, B. H.; Esfandyari, R.; Tafesse, B. T.; Amini, M.; Faramarzi, A. M and Abdollahi, M. *Lett. Drug Des. Discov.* **2020**, 17(10), ISSN 1570-1808. DOI:10.2174/1570180817666200103130536.

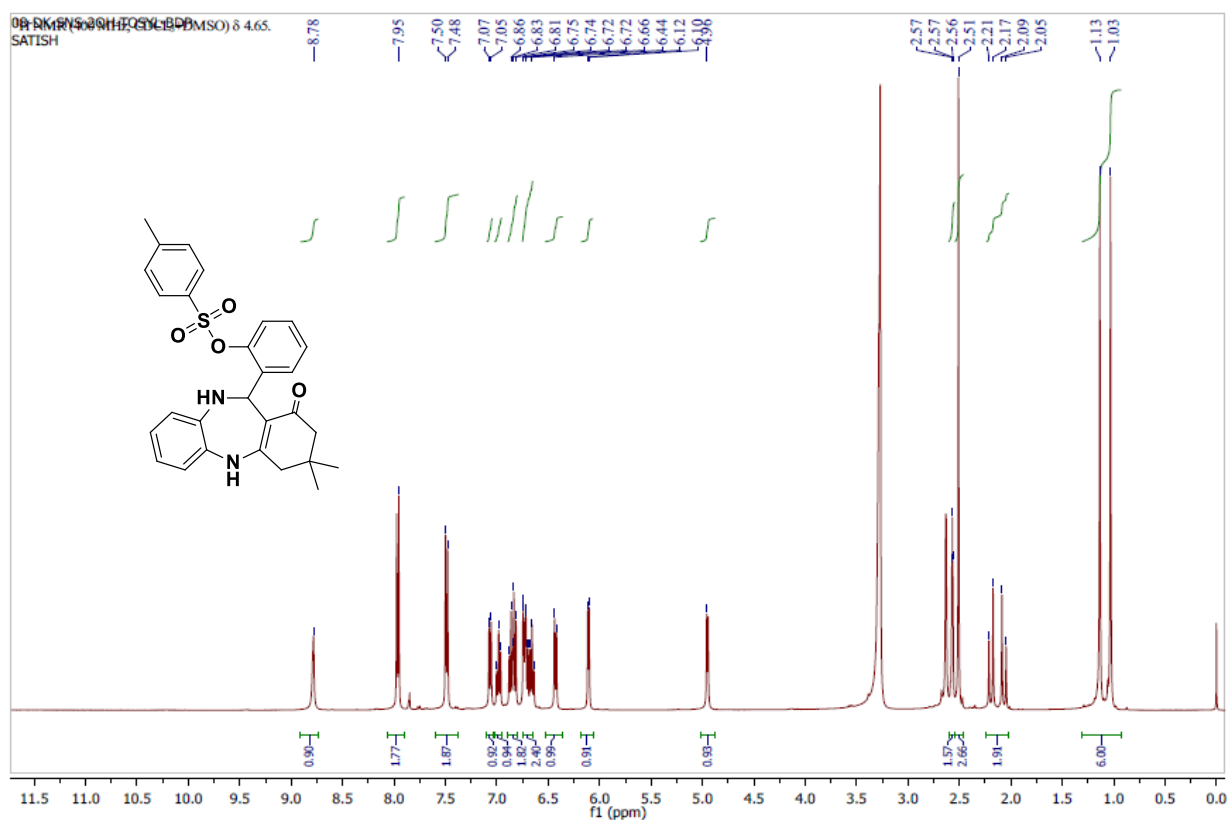
5.8 Selected Spectral data:

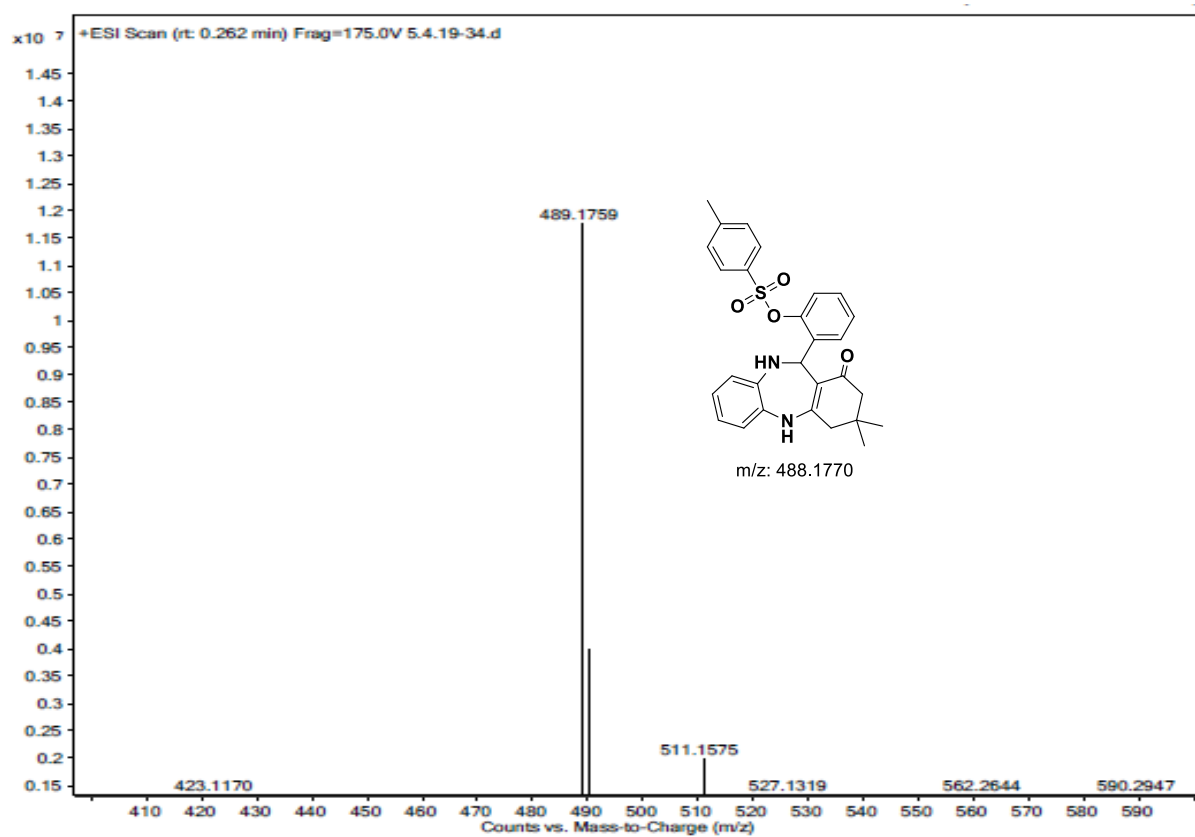
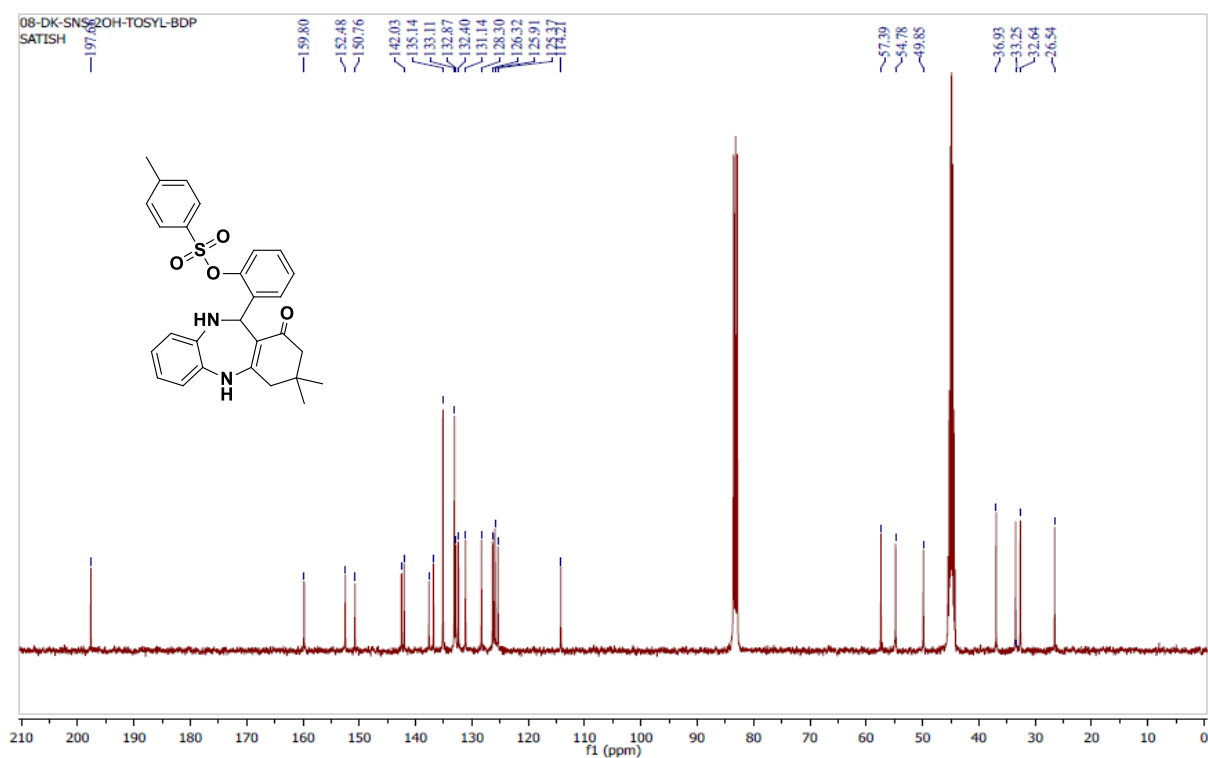
2-(2,4-Dioxo-2,3,4,5,6,11-hexahydro-1H-benzo[b]pyrimido[4,5-e][1,4]diazepin-5-yl)-6-methoxy phenyl benzenesulfonate (22a):





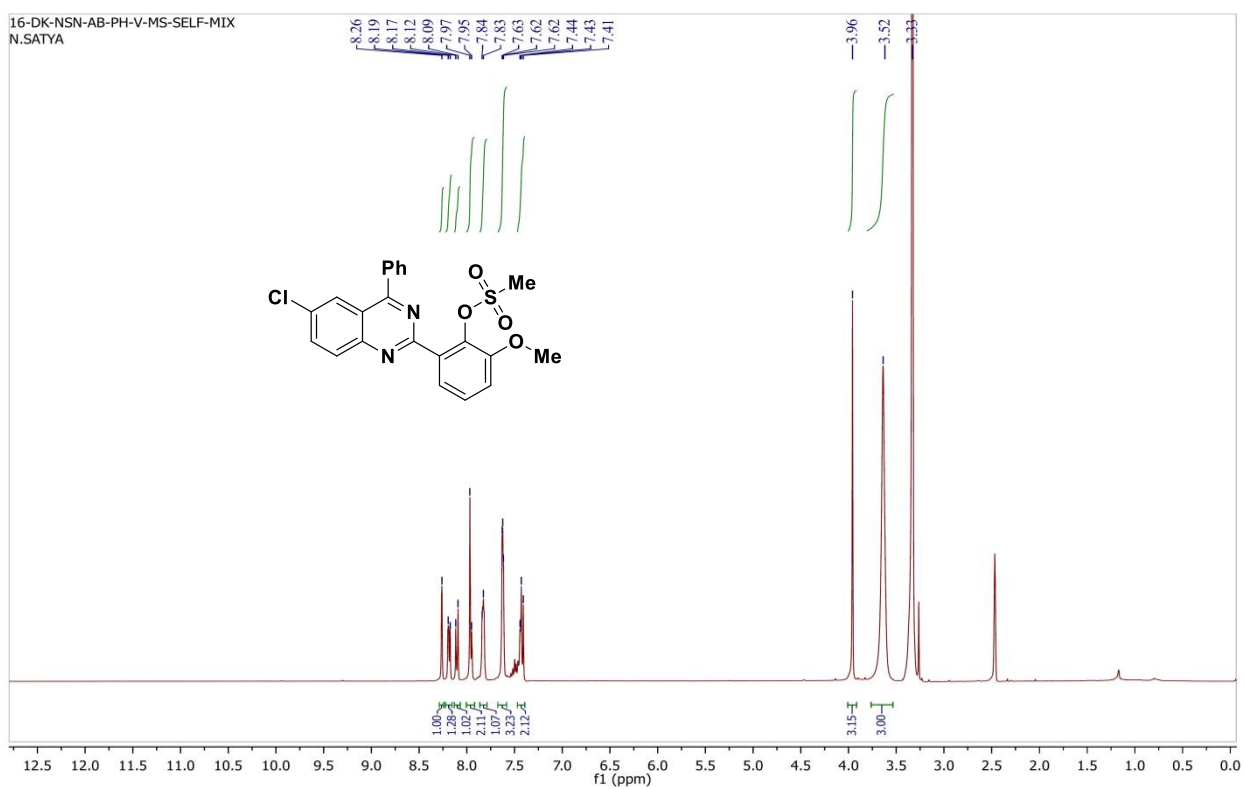
2-(3,3-Dimethyl-1-oxo-2,3,4,5,10,11-hexahydro-1H-dibenzo[b,e][1,4]diazepin-11-yl)phenyl 4-methylbenzenesulfonate (22b):



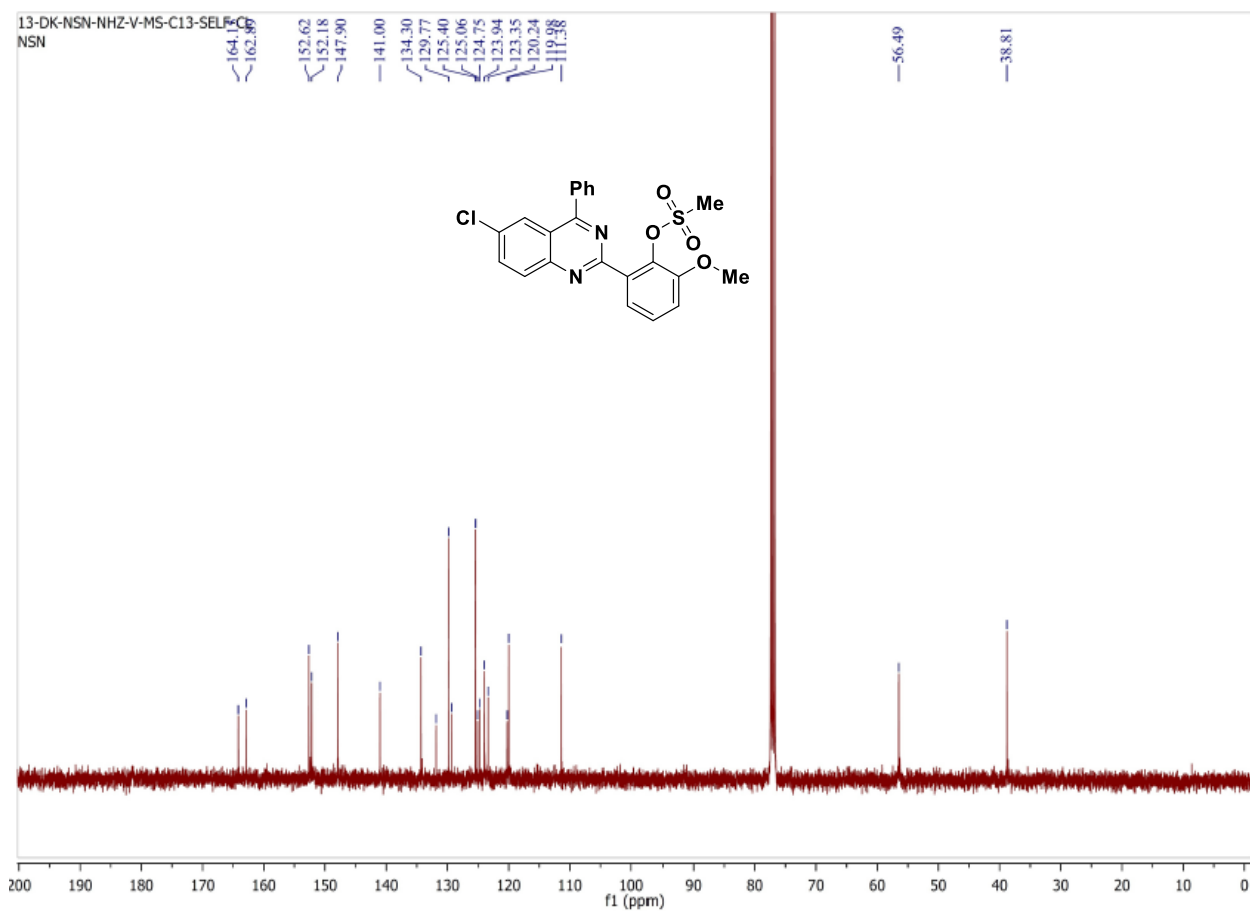


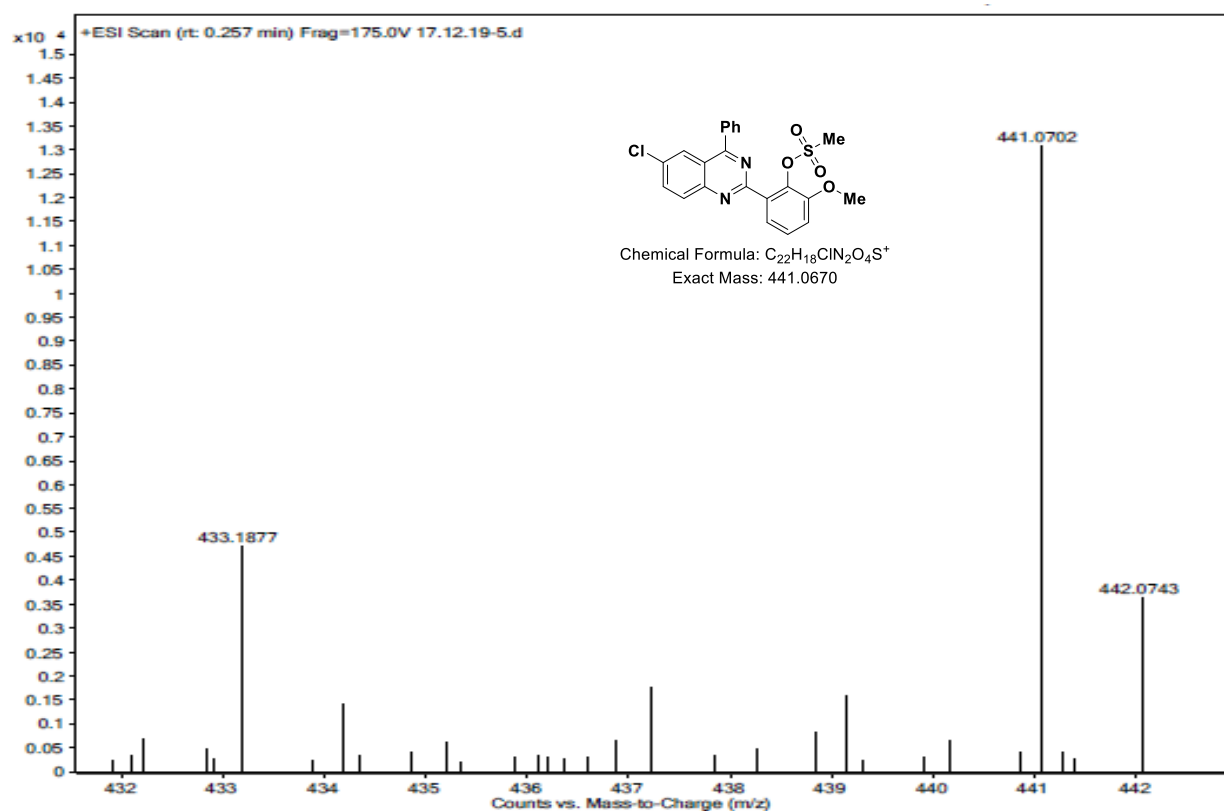
2-(6-Chloro-4-phenylquinazolin-2-yl)-6-methoxyphenyl methanesulfonate (24e):

16-DK-NSN-AB-PH-V-MS-SELF-MIX
N.SATYA

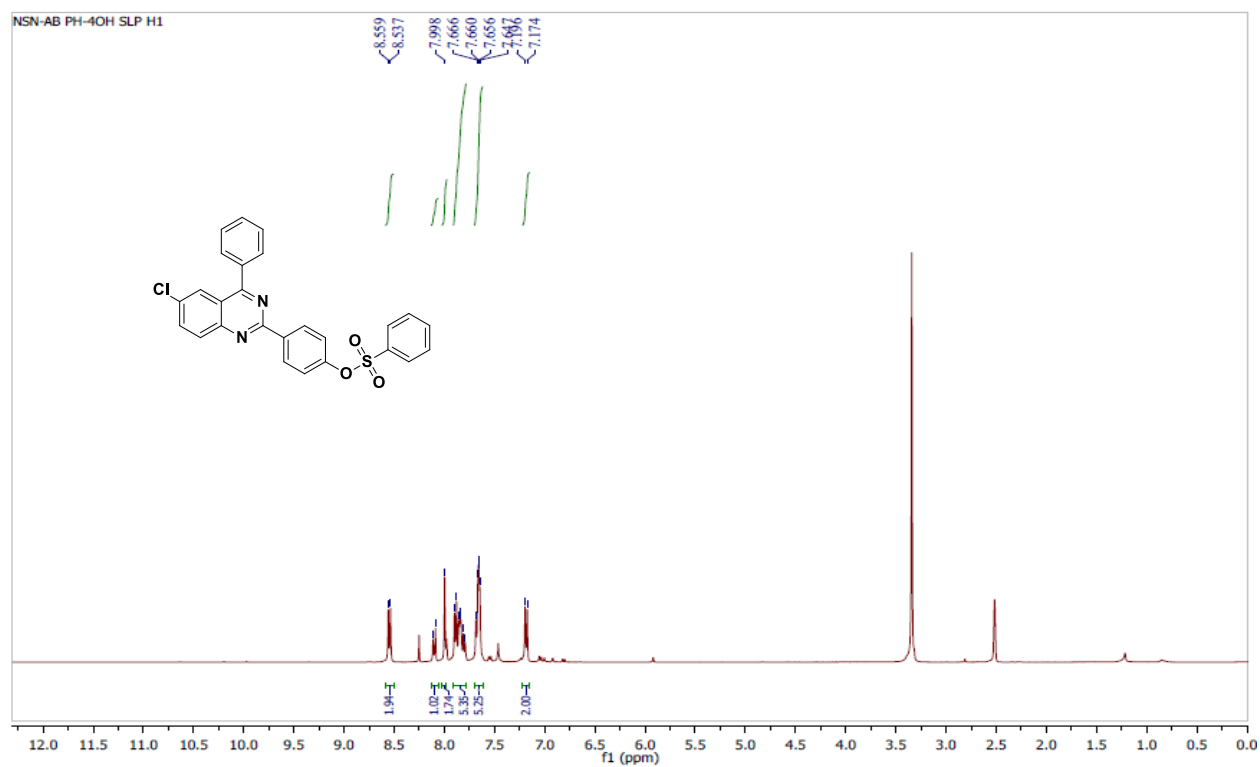


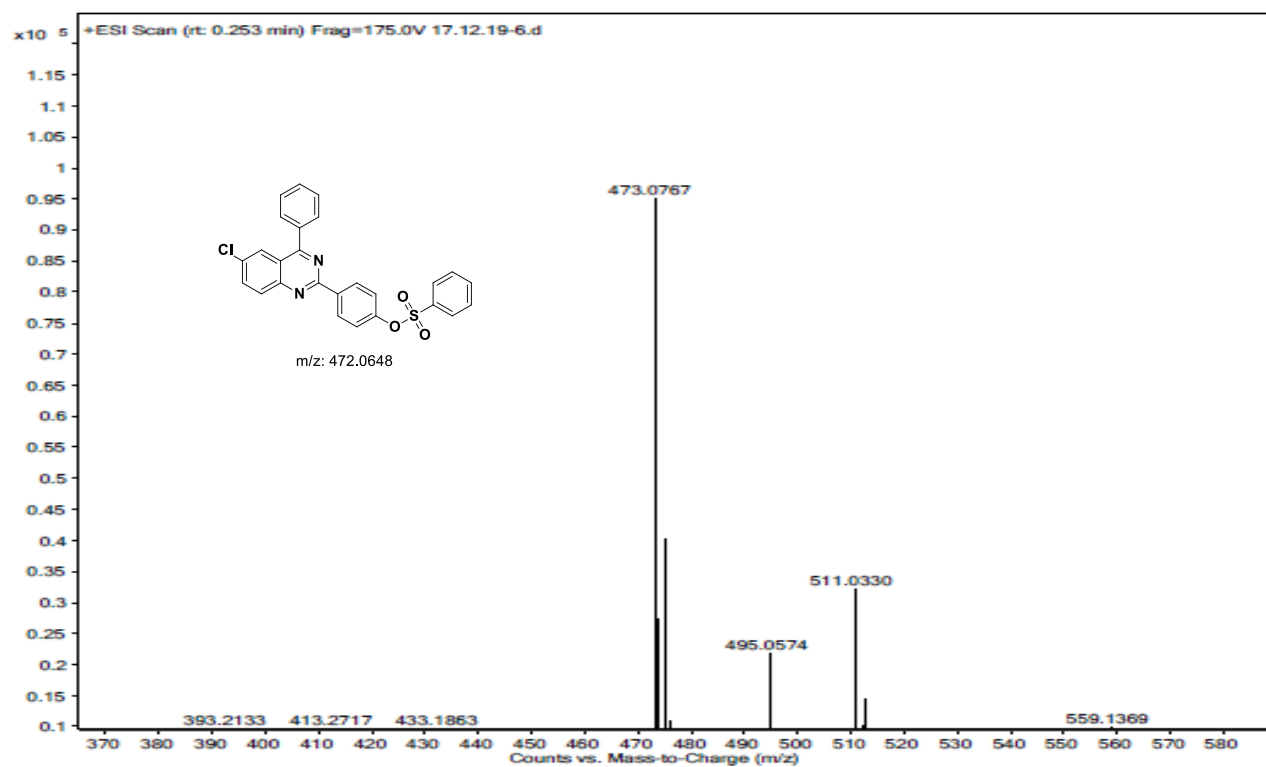
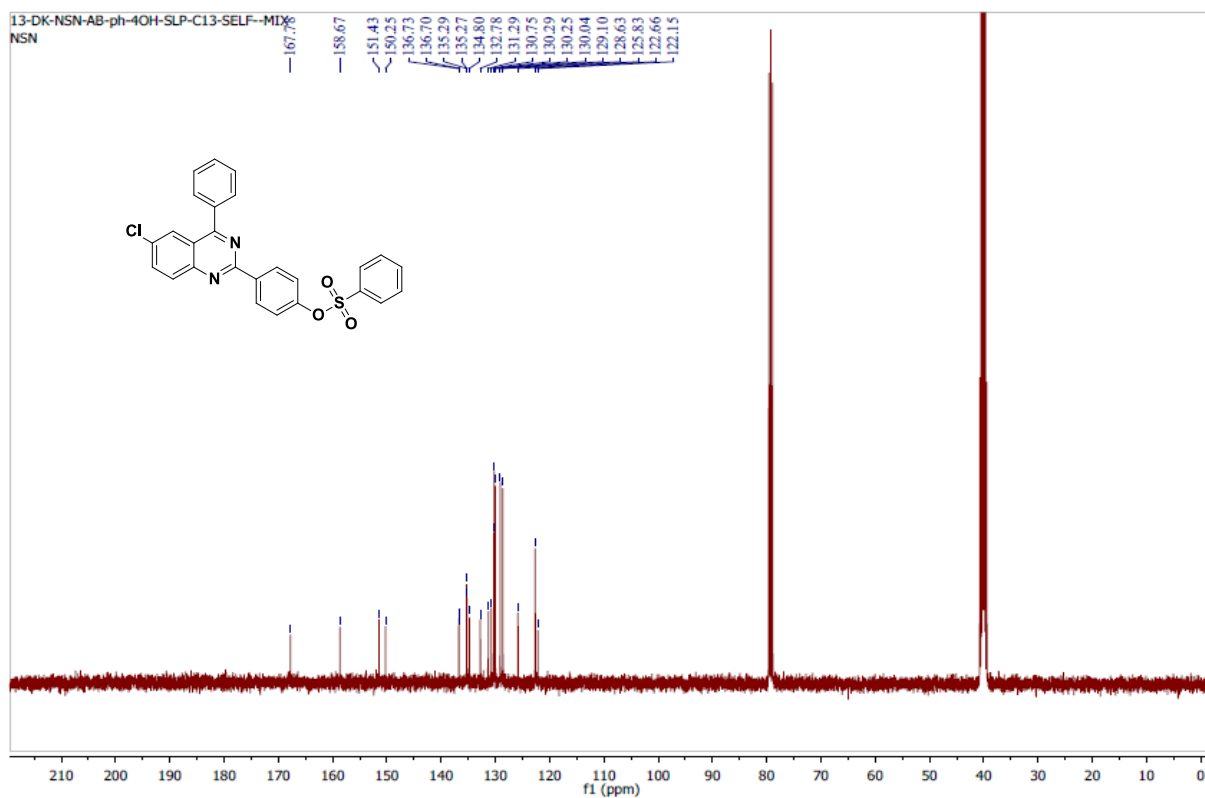
13-DK-NSN-NHZ-V-MS-C13-SELF-MIX
NSN



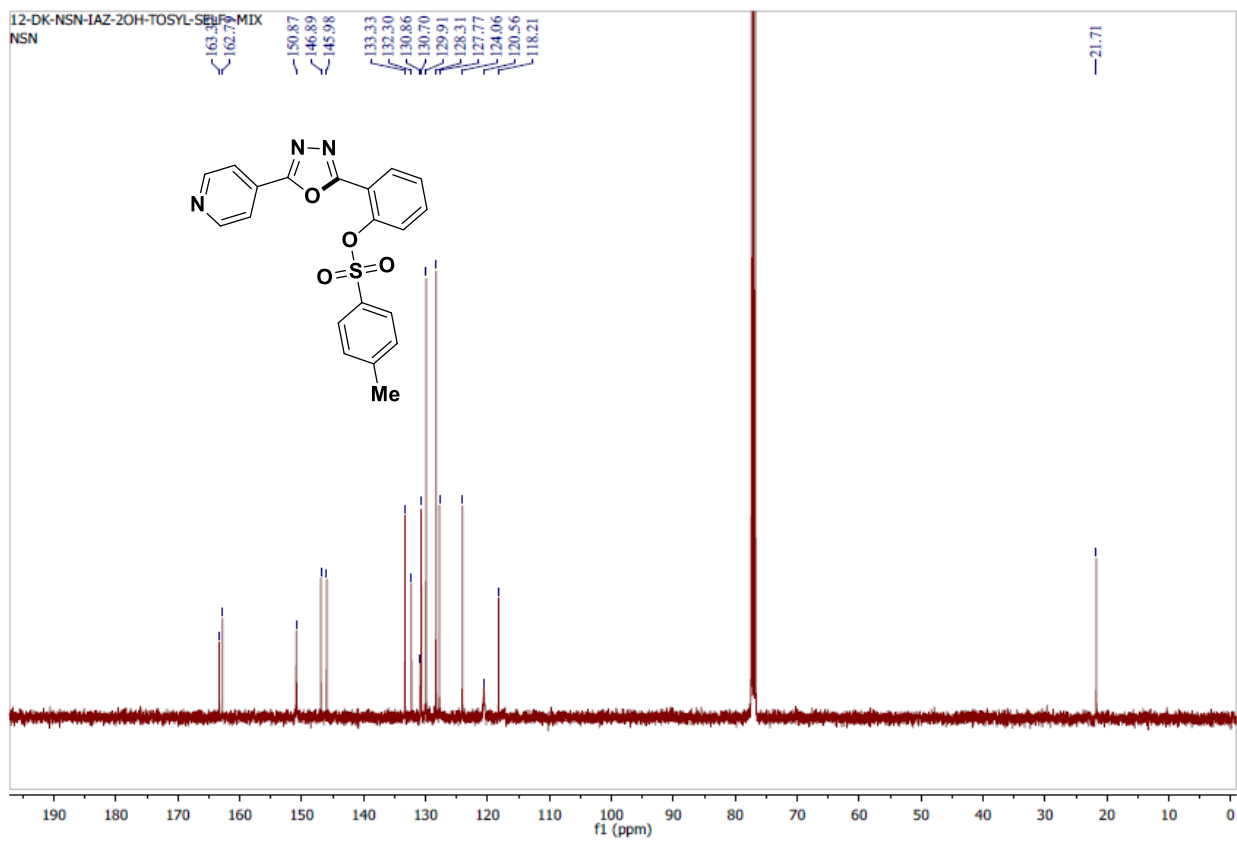
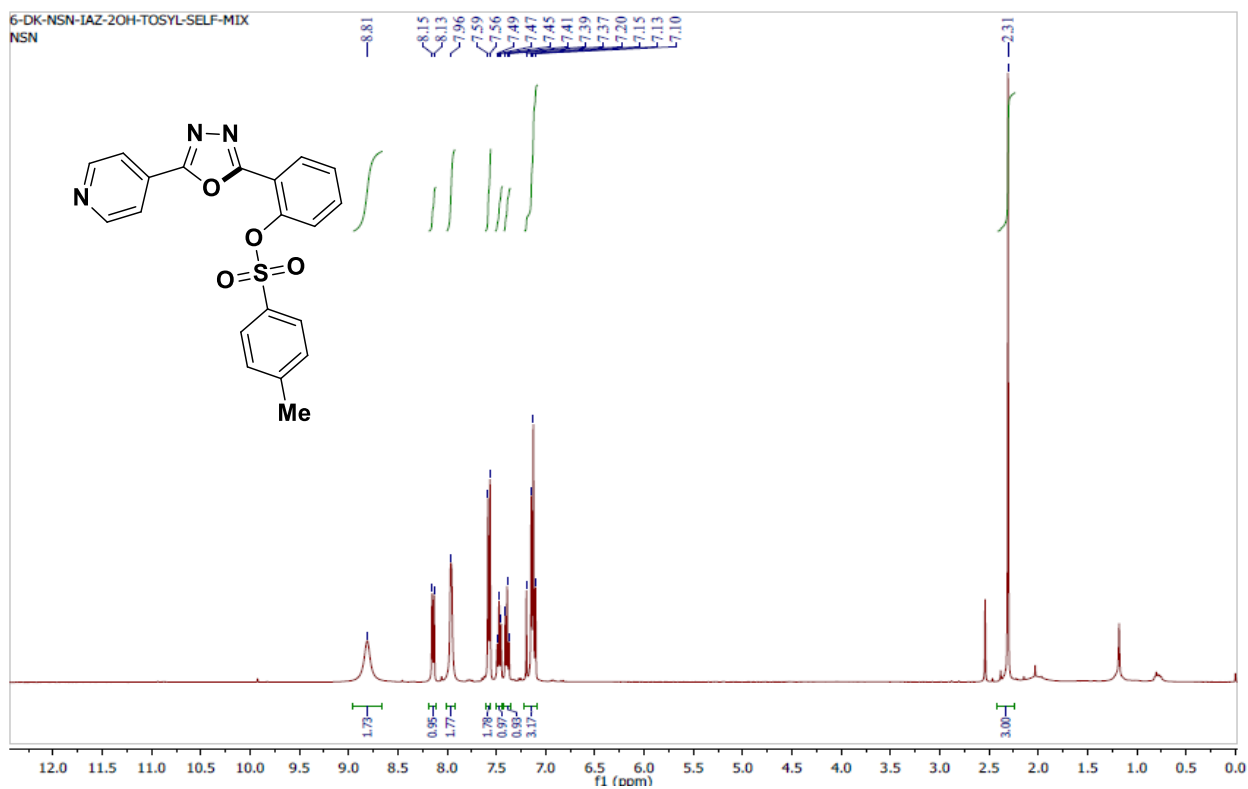


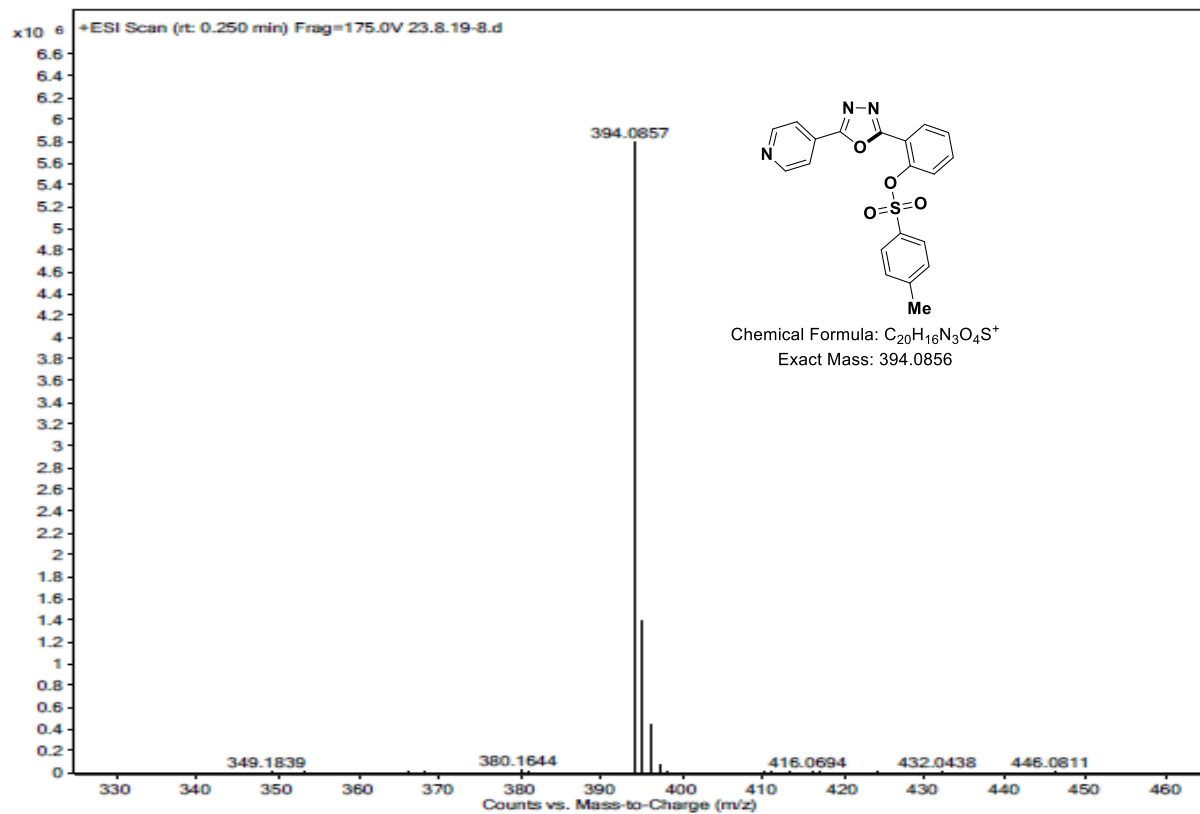
4-(6-Chloro-4-phenylquinazolin-2-yl)phenyl benzenesulfonate (24i):





2-(5-(Pyridin-4-yl)-1,3,4-oxadiazol-2-yl)phenyl 4-methylbenzenesulfonate (28b):





CHAPTER-6

Synthesis of quinazolinone-Schiff base, isoxazole-styrene and isoxazole-thiolane sulfonate ester conjugates

Abstract

Functionalized 2-arylquinazolineones exhibit many pharmacological properties and a vital role in medicinal chemistry. Isoxazole is another known molecule in biology. Sulfonate esters are key functional groups in the development of new therapeutic molecules. Considering the medicinal/biological importance of these compounds, the synthesis of 2-phenylquinazolinone based Schiff base sulfonates and styryl isoxazole-sulfonate conjugates is developed via one-pot (MCR) approach. The photophysical properties of the synthesized compounds were studied and found that the compound **8g** showed an emission band at **610** nm with the highest quantum yield (Φ) at **0.85** through intramolecular charge transfer (ICT). With stokes shift at **190** nm. The details are discussed in this chapter.

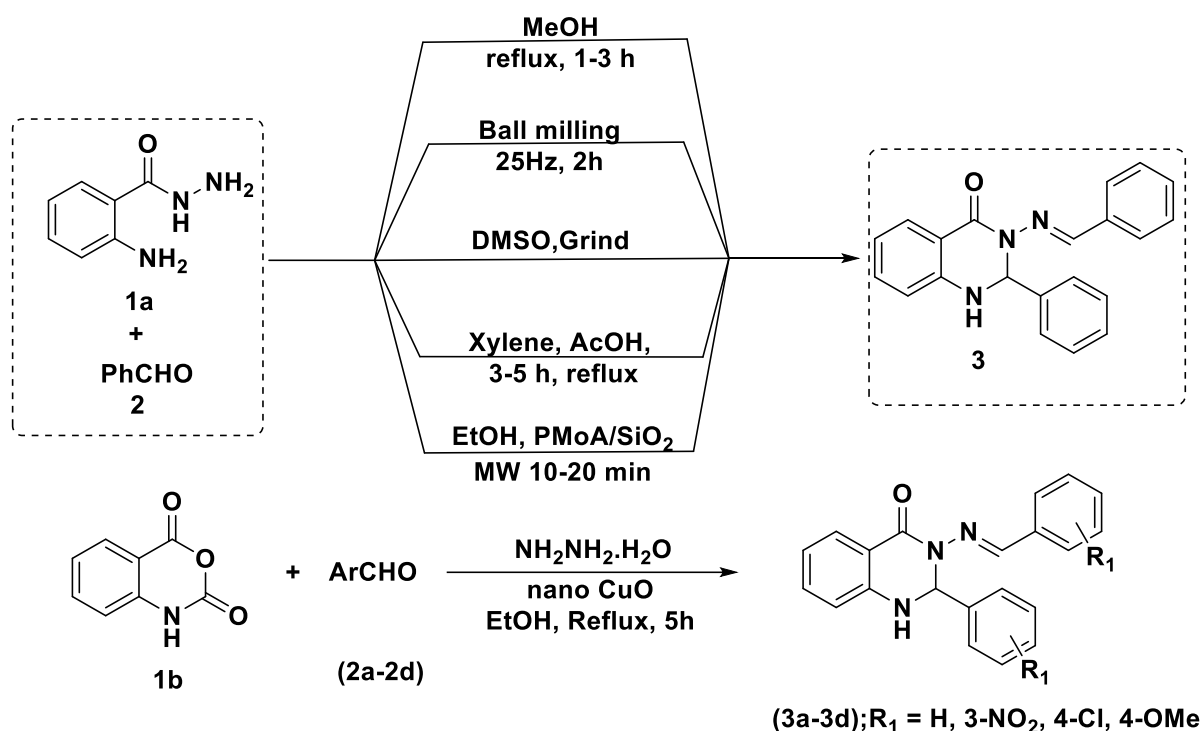
6.1 Introduction

Quinazolinones and their derivatives are an important class of heterocyclic compounds. They are found in many natural, synthetic molecules.^{1a} The quinazolinone based molecules have many pharmacological properties including anti-inflammatory,^{1b} anticancer,^{1c} anticonvulsant,^{1d} anti-TB,^{1e} anti-influenza^{1f} and anti-HIV,^{1g} chemotherapeutic agents^{2a} DNA intercalates,^{2b} and tubulin binders.³ The imidazolone fused quinazolinone molecules reported for the treatment of breast cancer (antileukemia against MCF-7, HL-60 cell lines),⁴ selective inhibition of EGFR tyrosine kinase,^{5a} cholecystokinin and angiotensin II receptors.^{5b} Recently, Zahedifard et al.^{5c} reported that the quinazolinone Schiff's base derivatives for the apoptotic activity towards MCF-7 cells through intrinsic and extrinsic apoptosis pathways. In addition, substituted quinazolinones are also used for linagliptin cancer cell lines for the prevention of type-2 diabetes.^{5d-5e}

Isoxazole derivatives are a significant class of heterocyclics. The structural units of isoxazole were found in many naturally occurring and biological compounds.⁶ They show the activity such as anti-inflammatory (Valdecocixib),⁷ anti-rheumatic (Leflunomide),⁸ antibiotic (sulfamethoxazole),⁹ herbicide (isoxafultole)¹⁰ etc.^{11a} The sulfonate esters can be used as isosteres and linking between the molecules. Some of the sulfonates show inhibitory activity towards aldose reductase,^{11b} and anti-hyperglycemic activity (PTP1B inhibitors).^{11c}

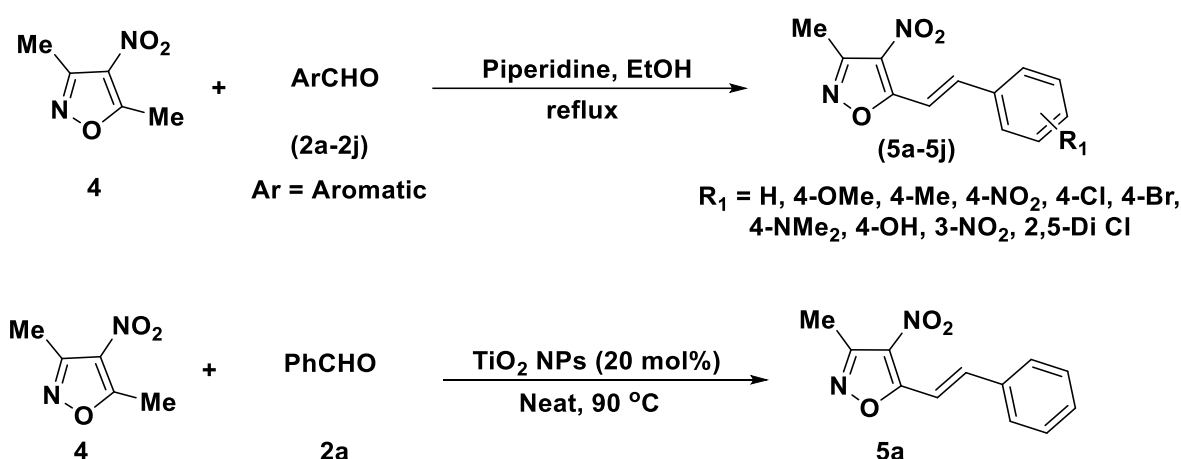
6.1.1 Synthetic methods for the preparation 2-phenylquinazolinones and isoxazole-styryl conjugates

From the above discussion, it is clear that the 2-phenyl quinazolinone hybrids are useful molecules in biology.^{12a-b} However, limited methods are available for the synthesis of 2-phenyl quinazoline hydrazides. The hydrazides of quinazoline are prepared by the reaction of 2-aminobenzohydride and aldehyde in presence of acids (catalytic amount) followed by intramolecular cyclization.^{5c} The synthesis of quinazolinone Schiff base (**3**) was reported from the coupling of 2-aminobenzohydrazide (**1a**) and benzaldehyde (**2**) under catalyst-free conditions in methanol,^{5c} AcOH,^{12c} PMoA/SiO₂^{12d} as catalysts, ball milling technique^{12e} as shown in **Scheme-1**. In addition, isotonic anhydride (**1b**), aromatic aldehydes, (**2a-2d**), and hydrazine hydrate were reacted in presence of CuO nanoparticles^{12f} to provide quinazolin-2-one Schiff bases (**3a-3d**) under reflux condition with moderate yields.



Scheme -1: Reported methods for quinazolinone Schiff base molecules.

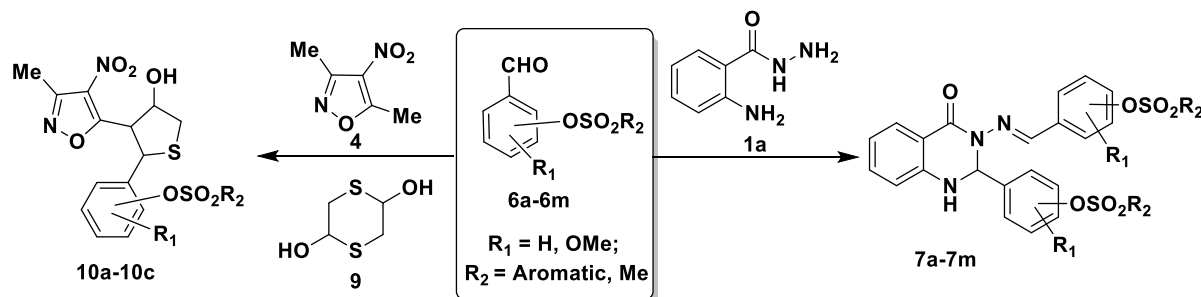
Along with others,^{13a-c} our group is actively engaged in the synthesis of isoxazole-styryl conjugates (**5a-5j**) from the reaction of 3,5-dimethyl-4-nitroisoxazole (**4**) with aromatic aldehydes (**2a-2j**)^{13d} via C-H functionalization of 3,5-dimethyl-4-nitroisoxazole (Knoevenagel condensation). Similarly, Raju et al.^{13e} described TiO₂ nanoparticles catalyzed synthesis of isoxazole-styryl scaffold (**5a**) under solvent-free conditions as shown in **Scheme-2**. However, there are no reports for these molecules based on sulfonates.



Scheme -2: Reported methods for synthesis of isoxazole-styryl conjugate scaffolds.

6.2 Present study

Considering the biological importance of quinazolinone Schiff-bases, sulfonate esters, and in continuation of our efforts in isoxazole-styryl chemistry, we envisaged a simple synthetic approach for this new class of quinazoline-Schiff base and styryl-isoxazole based molecules based on simple condensation and cyclization reactions as shown below.

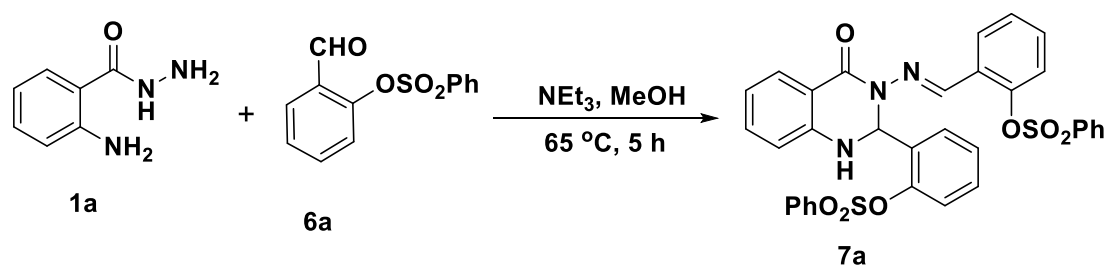


Scheme-3: Strategy for the synthesis of quinazolin-2-one Schiff base-sulfonate and isoxazole-tetrahydrothiophene sulfonate hybrids.

6.3 Results and Discussion

6.3.1 Synthesis of efficient sulfonate ester based substituted quinazolinones scaffolds

Considering the biological importance of the quinazolinone hybrids, towards the synthesis of 2-substituted quinazolin-2-one sulfonate-esters, the investigation started with the reaction of 2-aminobenzohydrazide (**1a**; 1.0 mmol) and 2-formyl phenyl benzene sulfonate (**6a**; 2.0 mmol) in NEt_3 , MeOH at 65 °C for 5 h, to provide the desired compound (**7a**) with less (40%) yield (**Scheme-4**).



Scheme-4. Initial attempt for the synthesis of compound (**7a**).

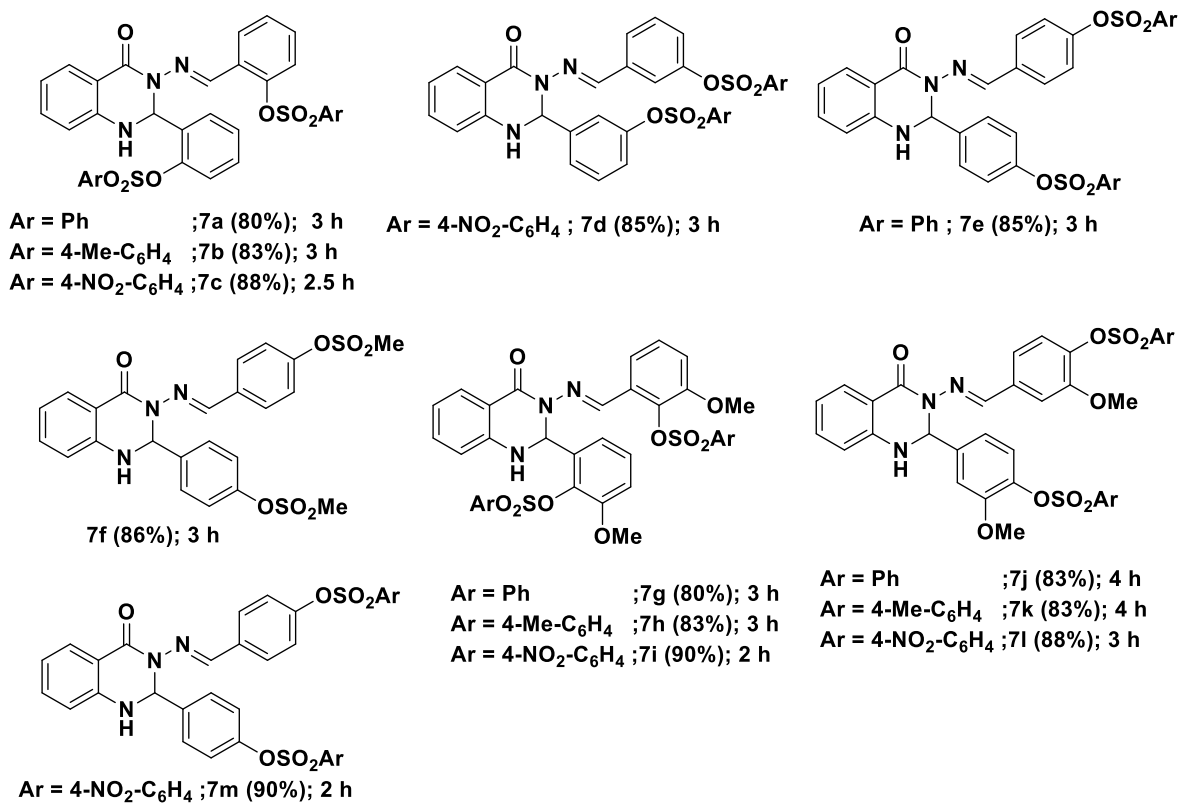
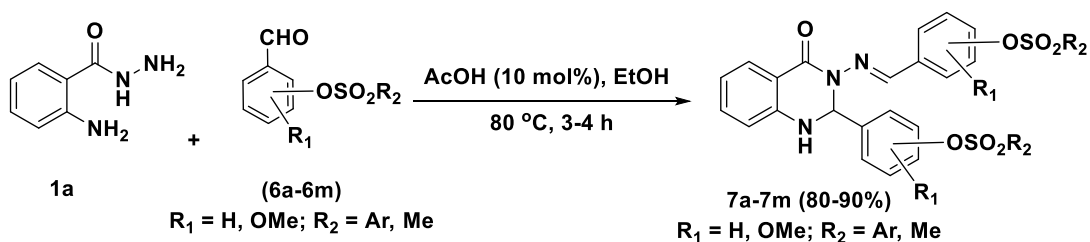
Further to improve the yield of the **7a**, optimization studies were performed in presence of organic bases (DABCO, DBU, NHET_2 , NEt_3 , and piperidine), inorganic bases (K_3CO_3 and Cs_2CO_3), organic and inorganic acids (AcOH, HCl and H_2SO_4) and catalyst free conditions in MeOH, EtOH, DCM, MeCN, water as reaction media (**Table-1**). Among the optimized conditions, it was found that a combination of 10 mol% of AcOH in EtOH at 80 °C (**Entry-8**; **Table-1**) was

a better suitable condition for the success of the reaction giving the desired product with 80% yield (**Entry-8; Table-1**). Having optimized reaction conditions, the next attention turned to exploring the substrate scope of the reaction. Thus, different sulfonate aldehydes were reacted with 2-amino-benzohydrazide (**1a**) (1.0 mmol) under optimized conditions to give the quinazolinone Schiff-base sulfonates (**7a-7m**) in good to excellent yields (**80-90%**) in 3-4 h (**Scheme-5**). It is noteworthy to mention that the substrates with withdrawing groups (-NO₂) provide better yields (up to 90%) in less reaction time (3 h) compare to electron donating groups. Based on the experimental observations, a plausible mechanism is shown in **Figure-1**.

Table-1: Optimization conditions^[a]

Entry	Catalyst (10 mol%)	Solvent	Temp (°C)	Time (h)	Yield ^[b] (%)
1	NEt ₃	MeOH	65	5	40
2	NEt ₃	EtOH	80	5	55
3	DABCO	EtOH	80	3	61
4	Piperidine	EtOH	80	3	50
5	DBU	EtOH	80	3	40
6	K ₂ CO ₃	MeCN	80	3	42
7	Cs ₂ CO ₃	DMF	80	3	40
8	AcOH	EtOH	80	3	80
9	AcOH	Water	100	3	62
10	HCl	EtOH	80	4	60
11	H ₂ SO ₄	EtOH	80	4	40
12	Catalyst free	EtOH	80	5	65
13	Catalyst free	MeOH	65	5	50
14	Catalyst free	MeCN	80	5	35
15	Catalyst free	Neat	80	6	trace

^[a]**Reaction conditions:** all reactions were conducted with **1a** (1.0 mmol.), **6a** (2.0 mmol.), catalyst: AcOH (10 mol %), 5 mL EtOH at 80 °C. ^[b]Yield: isolated yields of final products.



Scheme-5: Substrate scope of sulfonate ester based substituted quinazolinone-Schiff bases.

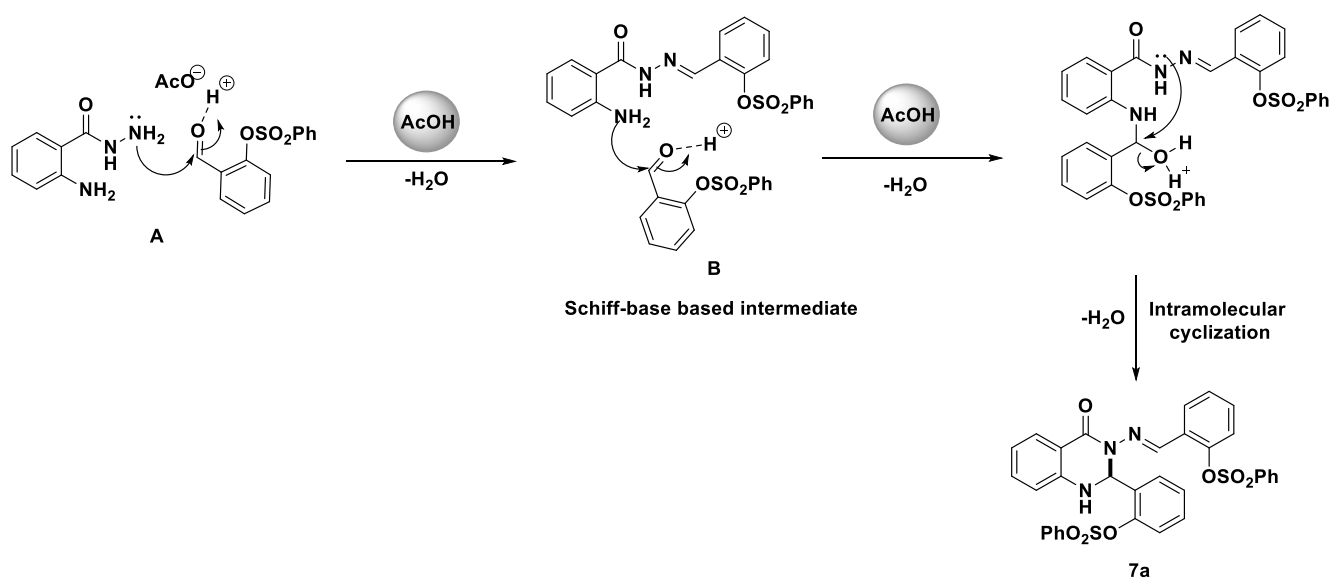
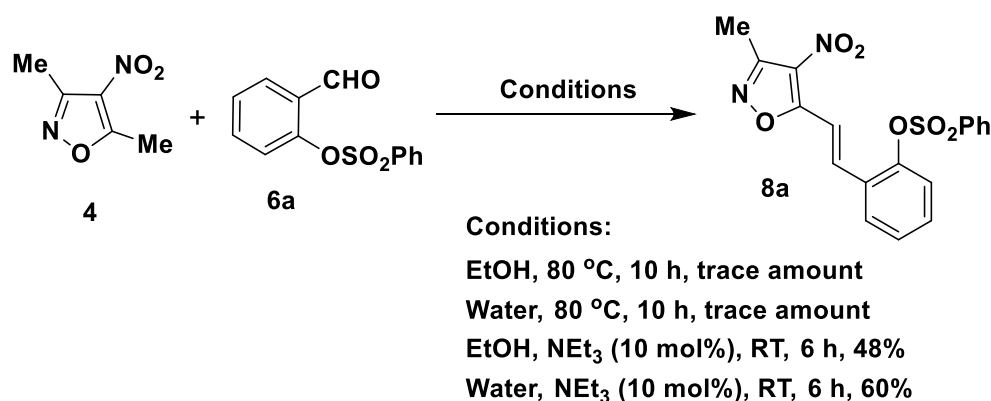


Figure-1: Plausible reaction mechanism of the compound (**7a**).

6.3.2 Synthesis of isoxazole-tetrahydrothiophene sulfonate esters

Based on the biological importance of the isoxazoles and tetrahydrothiophenes, our group is actively engaged in the synthesis of these molecules. As part of our study, we have reported a catalyst-free method for the synthesis of isoxazoles-thiolane hybrids.^{13(f-g)} With this background, we started the synthesis of isoxazole-thiolane sulfonate esters. Towards this, initially, the preparation of styryl-isoxazole (**8a**) was attempted in catalyst-free conditions using 3,5-dimethyl-4-nitro-isoxazole (**4**) (1.0 mmol) with 2-formyl phenylbenzene sulfonate ester (**6a**) (1.0 mmol) in EtOH and water (80°C). But, only trace amounts of the desired product were observed even at a longer reaction time (10 h). Later, the same reaction was performed using trimethylamine (10 mol%) at room temperature to get the desired product at 48% and 60% respectively (**Scheme-6**).



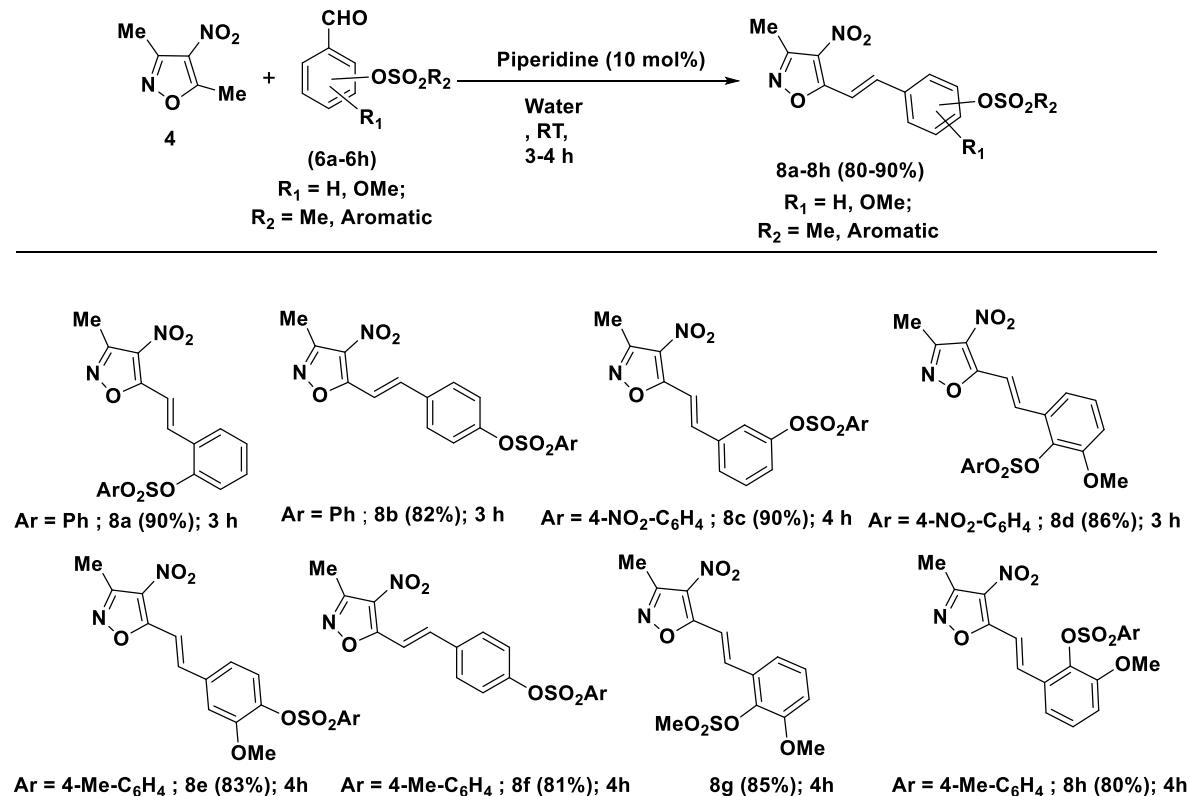
Scheme-6: Initial attempt of the isoxazole-styryl sulfonate (**8a**).

Encouraged by the above results, the reaction conditions were optimized by performing various experiments in different combinations of organic bases (piperidine, DIEPA, DBU, DABCO) and solvents (MeOH, EtOH, DCM, MeCN, DMSO, CHCl₃, water) as summarized in **Table-2**. Among the screened, a combination of piperidine (10 mol%) in water at RT was found to be the best condition giving the desired product (**8a**) in 90% yield in 3 h at room temperature (**Entry 6; Table-2**). Having optimized reaction conditions, the substrate scope was tested with 3,5-dimethyl-4-nitro-isoxazole (**4**) and functionalized sulfonate ester aldehydes (**6b-6h**) under optimized conditions to give isoxazole-styryl sulfonate-ester derivatives (**8a-8h**) with good to excellent yields (80-90%) (**Scheme-7**).

Table-2. Optimization conditions^[a]

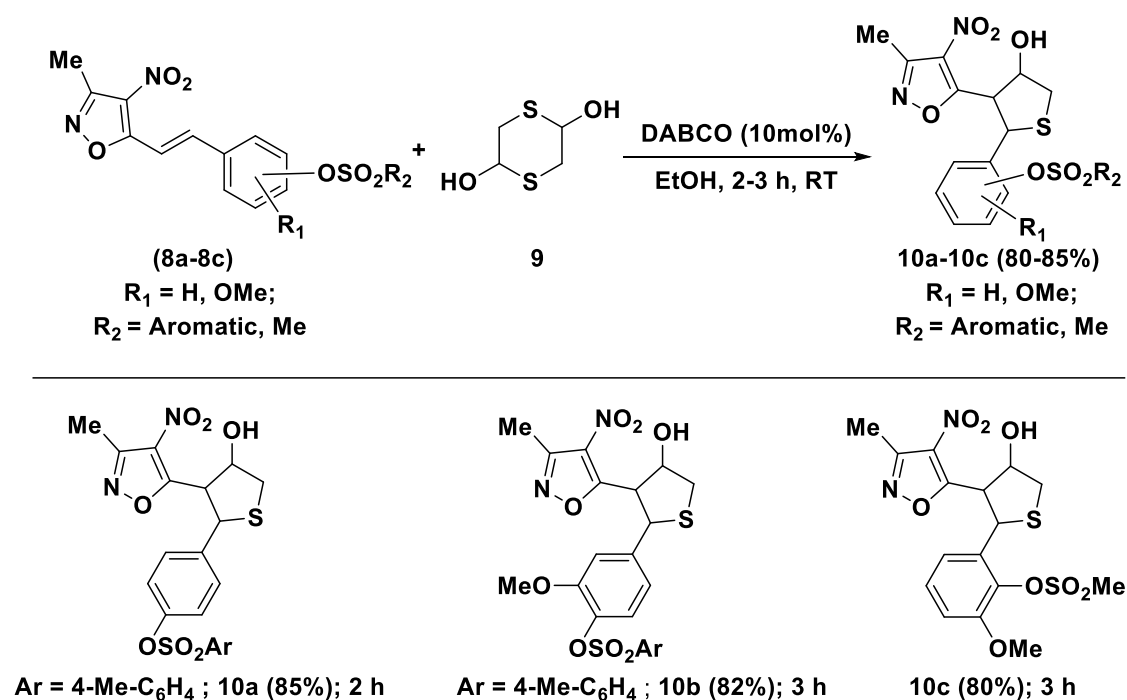
Entry	Catalyst (10 mol %)	Solvent	Temp (°C)	Time (h)	Yield ^[b] (%)
1	Catalyst free	EtOH	80	10	trace
2	Catalyst free	Water	80	10	trace
3	NEt ₃	EtOH	RT	6	48%
4	NEt ₃	Water	RT	6	60
5	Piperidine	EtOH	RT	3	85
6	Piperidine	Water	RT	3	90
7	Piperidine	DCM	RT	3	65
8	Piperidine	MeCN	RT	3	50
9	Piperidine	CHCl ₃	RT	3	62
10	Piperidine	DMSO	RT	3	47
11	DABCO	EtOH	RT	5	60
12	DBU	MeCN	RT	5	45
13	Pyridine	EtOH	RT	6	40
14	K ₂ CO ₃	MeOH	65	4	-
15	Cs ₂ CO ₃	EtOH	80	4	30

^[a] Reaction conditions: **4** (1.0 mmol), **6a** (1.0 mmol), Piperidine (10 mol%), EtOH (5mL), RT, 3 h. ^[b] Isolated yield.



Scheme-7: Derivatives of styryl isoxazole sulfonate esters (**8a-8h**).

After the synthesis of isoxazole-styryl sulfonate esters (**8a-8h**), the next task was to use them for the sulfa Michael-aldol reactions to generate the thiolane derivatives. Towards that, the unsaturated systems (**8a-8c**) were reacted with the 1,4-dithiane-2,5-diol (**9**; dimeric mercaptoacetaldehyde) in presence of DABCO (10 mol%) in EtOH, room temperature to give corresponding isoxazole-tetrahydrothiophene hybrids (**10a-10c**) in moderate yield (80-85%) as shown in **Scheme-8**. Based on our previous experience,^{14b} a Plausible mechanism for the formation of thiolane hybrids is given in **Figure-2**.



Scheme-8: Isoxazole-based sulfonate ester thiolane derivatives (**10a-10c**).

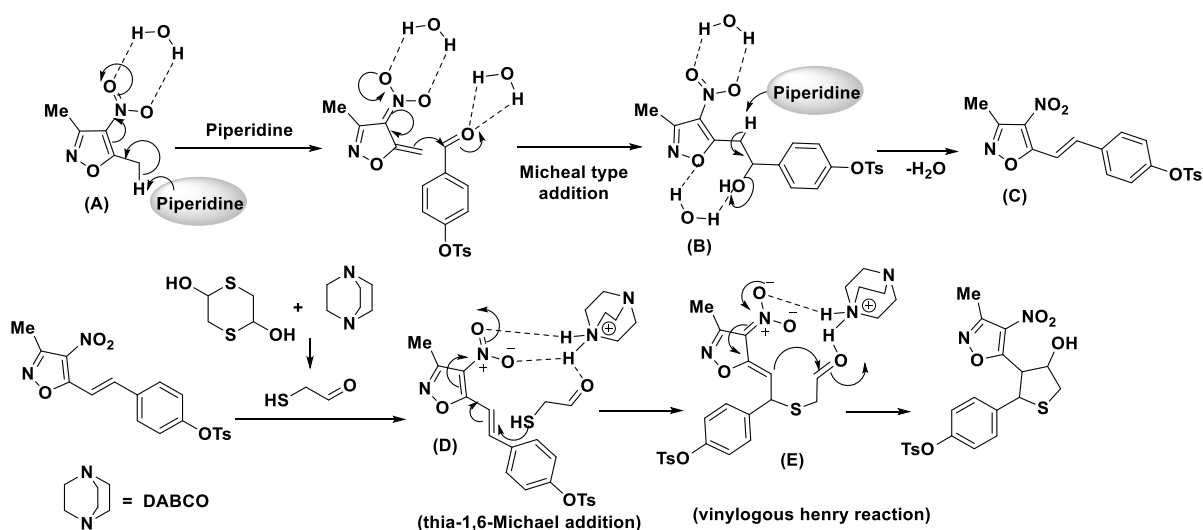


Figure-2: Plausible reaction mechanism of compounds **8a** and **10a**.

6.3.3 Photophysical properties of isoxazole-styryl sulfonate esters.

Organic molecules with chromophore, donor-accepter π -conjugation systems exhibit distinctive photophysical properties, which are having great use in biology. In this context, styryl-isoxazoles with donor-accepter moiety show hyperpolarizability.^{5d} Based on this, our next task was to study the photophysical properties of the isoxazole-styryl sulfonate esters (**8a-8h**). Thus, the absorption-emission spectra of compounds (**8a-8h**) were recorded in DMSO (100 μ M) at room temperature. The absorption band maxima of these compounds (**8a-8h**) were found in the range of **402-436 nm** (as shown in **Figure-3; A**), and their corresponding emission spectra shown in the range of **512-610 nm** (as shown in **Figure-3; B**) and all the photophysical properties data was tabulated in **Table-3**. Among all, compound (**8c**) has shown a maximum absorption wavelength at **436 nm**. Correspondingly, the emission band maxima are seen at **610 nm** for the compound (**8g**) which is having donor (methoxy and methylsulfonate) groups. These donating groups are responsible for intramolecular charge transfer (ICT).¹⁴ The compounds **8e** and **8f** show impressive emission wavelengths at **537 nm** and **570 nm** respectively. Also, quantum yield for the compound **8g** is seen at **0.84** (**Table-3**).^{15(a-b)}

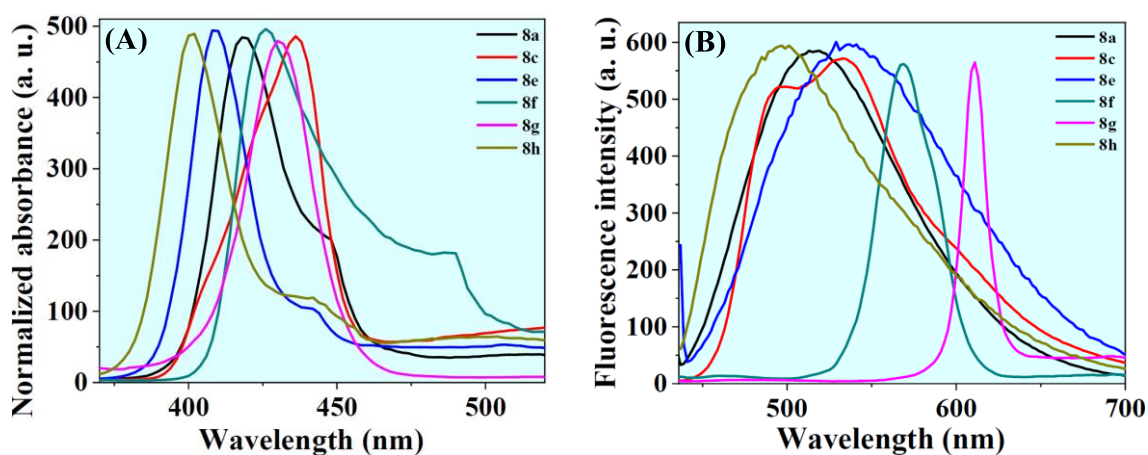


Figure-3: (A) Absorption (B) Emission spectra of the compounds **8a-8h**.

Table-3: Photo physical properties data of the resultant **8a-8h** in DMSO.

Compound no.	λ_{Abs} (nm)	λ_{Em} (nm)	Stokes shift ($\Delta\lambda$ nm)	Quantum yield (Φ)
8a	417	519	102	0.59
8c	436	532	96	0.58
8e	410	537	120	0.73
8f	425	570	128	0.77

8g	430	610	189	0.84
8h	402	512	97	0.63

6.4 Conclusions

In conclusion, a simple method for the synthesis of functionalized quinazolinone Schiff-base sulfonate ester derivatives, isoxazole-styryl sulfonate esters, and isoxazole-thiolane sulfonate esters are reported. Further, photophysical properties of compounds (**8a-8h**) were studied and observed that compound (**8c**) showed maximum absorption at **436** nm while compound (**8g**) showed emission band at **610** nm with highest stokes shift at **189** nm and quantum yield with **0.84**.

6.5 Supporting information

6.5.1 General: The starting materials were bought from SD-Fine, Sigma-Aldrich, and Spectrochem and used without further purification. The ¹H and ¹³C-NMR spectra were recorded on Bruker 400 MHz spectrometer using CDCl₃ or DMSO-d₆ solvents (reported in δ ppm). The mass spectra are recorded on Shimadzu LCMS-2020, the UV-Visible and Fluorescence spectra were recorded on FL 8500 Fluorescence Spectrophotometer and melting points are recorded using Stuart melting point apparatus.

General procedure for the synthesis of based quinazoline-one Schiff base sulfonate ester derivatives (7a-7m): To a solution of 2-aminobenzohydrazide (**1a**) (1.0 mmol) in EtOH (5 mL) was added various sulfonate ester aldehyde substrates (**6a-6m**) (2.0 mmol) and AcOH (cat). The mixture was heated at 80 °C for 3-4 h. After the completion of the reaction (monitored by TLC), the reaction mixture was cooled to room temperature and extracted with EtOAc (2X10mL). The combined organic layers were dried over sodium sulfate. Evaporation of the solvent gave the crude mixture which was purified by silica gel column chromatography. Elution of the column with hexane-EtOAc mixture gave the desired products (**7a-7m**) in good yields.

General procedure for the synthesis of isoxazole-styryl sulfonates ester derivative (8a-8h):

To a solution of 3,5-dimethyl-4-nitroisoxazole (**4**) (1.0 mmol) in EtOH (5 mL), were added various sulfonate ester aldehyde substrates (**6a-6h**) (1.0 mmol) followed by piperidine (10 mol %) and the mixture was stirred at room temperature for 3-4h. After, the complete conversion of starting materials (checked by TLC), the reaction mixture was extracted with EtOAc (2X10mL), washed with brine, and water, and dried over sodium sulfate. Evaporation of the solvent gave the

crude product which was purified by silica gel column chromatography. Elution of the column with EtOAc-hexanes gave the pure product (**8a-8h**) in good yields.

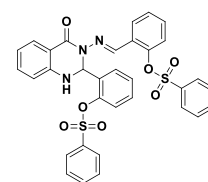
General procedure for the synthesis of nitro isoxazole-thiolane sulfonate derivatives (10a-10c):

To a solution of nitro isoxazole-styryl derivatives (**8a-8c**) (1.0 mmol) in EtOH (5 mL) was added 1,4-dithiane-2,5-diol (**9**) (1.0 mmol), DABCO (20 mol%). The mixture was stirred at RT for 2 h. After the completion of the reaction (on TLC), aq. NH₄Cl solution (5ml) was added and extracted with EtOAc (2X10ml). The combined organic layers were dried over sodium sulfate. Evaporation of the solvent gave the crude mixture which was purified by silica gel column chromatography. Elution of the column with hexane-EtOAc mixture gave the desired products (**10a-10c**) with good yields.

6.5.2 Spectral data of the synthesized compounds

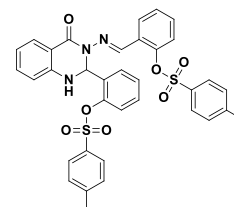
(E)-2-(((4-Oxo-2-(2-((phenylsulfonyl)oxy)phenyl)-1,2-dihydroquinazolin-3(4H)-yl)imino)

methyl)phenyl benzenesulfonate (7a): White powder, mp 149–150 °C, 80% yield. ¹H NMR (400 MHz, CDCl₃) δ 8.77 (s, 1H), 8.04–8.00 (m, 2H), 7.83–7.73(m, 4H), 7.63 (t, *J* = 7.2 Hz, 3H), 7.49 (t, *J* = 7.6 Hz, 2H), 7.31–7.28 (m, 2H), 7.18–7.12 (m, 4H), 6.8–6.82 (m, 2H), 6.63 (d, *J* = 8.0 Hz, 1H), 6.45 (s, 1H), 5.46 (s, 1H); ¹³C NMR (100 MHz, CDCl₃) δ 161.33, 148.34, 146.58, 144.77, 144.60, 135.26, 135.02, 134.85, 134.52, 134.37, 132.80, 131.12, 130.07, 129.69, 129.30, 129.02, 128.73, 128.62, 128.27, 127.88, 127.83, 127.22, 127.19, 123.10, 122.67, 119.51, 115.27, 114.85, 68.84. HRMS (ESI, *m/z*): calcd. For C₃₃H₂₅N₃O₇S₂H⁺ 640.1207, found 640.2263; IR (KBr thin film, cm⁻¹): ν_{max} 3275, 3085, 2983, 1659, 1502, 1355, 1185, 1069, 860.



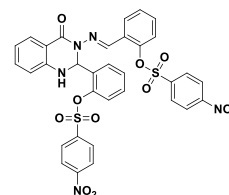
(E)-2-(((4-Oxo-2-(2-(tosyloxy) phenyl)-1,2-dihydroquinazolin-3(4H)-yl)imino) methyl) phenyl

4-methylbenzenesulfonate (7b): White solid, mp 153–154 °C, 83% yield. ¹H NMR (400 MHz, CDCl₃) δ 8.55 (s, 1H), 7.94 (d, *J* = 7.6 Hz, 1H), 7.84 (d, *J* = 7.6 Hz, 2H), 7.70 (d, *J* = 7.6 Hz, 1H), 7.62 (d, *J* = 8.0 Hz, 2H), 7.34 (d, *J* = 7.6 Hz, 2H), 7.22–7.03 (m, 9H), 6.81–6.74 (m, 2H), 6.55 (d, *J* = 8.0 Hz, 1H), 6.34 (s, 1H), 5.43 (s, 1H), 2.39 (s, 3H) 2.31(s, 3H); ¹³C NMR (100 MHz, CDCl₃) δ 161.23, 148.40, 146.65, 146.39, 145.86, 144.59, 144.21, 134.34, 132.62, 132.21, 131.82, 131.07, 130.29, 130.03, 129.93, 129.02, 128.72, 128.63, 128.23, 127.72, 127.19, 127.11, 123.25, 122.74, 119.47, 115.19, 114.80, 68.55, 21.82, 21.70; HRMS (ESI, *m/z*): calcd. For C₃₅H₂₉N₃O₇S₂H⁺ 668.1520, found 668.2596; IR (KBr thin film, cm⁻¹): ν_{max} 3285, 3072, 2978, 1662, 1506, 1354, 1194, 1078, 851.



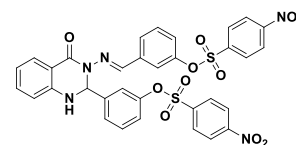
(E)-2-(3-((2-(((4-Nitrophenyl)sulfonyl)oxy)benzylidene)amino)-4-oxo-1,2,3,4-tetrahydro

quinazoline-2-yl)phenyl 4-nitrobenzenesulfonate (7c): Pale yellow solid, mp 229–230 °C, 88% yield. ¹H NMR (400 MHz, CDCl₃+DMSO-*d*₆) δ 9.10 (s, 1H), 8.43–8.37 (m, 4H), 8.26 (d, *J* = 8.8 Hz, 2H), 8.15 (d, *J* = 8.4 Hz, 2H), 7.72 (d, *J* = 7.6 Hz, 1H), 7.47–7.30 (m, 7H), 7.24 (d, *J* = 8.4 Hz, 1H), 7.17 (d, *J* = 8.4 Hz, 1H), 6.80–6.76 (m, 2H), 6.22 (s, 1H); ¹³C NMR (100 MHz, CDCl₃+DMSO-*d*₆) δ 166.80, 156.28, 156.06, 152.60, 151.86, 151.19, 145.29, 144.62, 139.39, 137.18, 137.01, 135.59, 135.27, 135.07, 133.59, 133.28, 133.09, 132.95, 132.77, 131.51, 130.15, 128.15, 127.61, 123.49, 121.55, 120.11, 119.35, 75.15; HRMS (ESI, *m/z*): calcd. For C₃₃H₂₃N₅O₁₁S₂H⁺ 730.0908, found 730.2032.



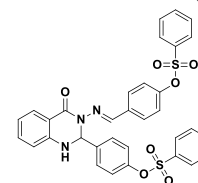
(E)-3-(3-((3-(((4-Nitrophenyl)sulfonyl)oxy)benzylidene)amino)-4-oxo-1,2,3,4-tetrahydro
quinazolin -2-yl)phenyl 4-nitrobenzenesulfonate (7d): Pale yellow

solid, mp 157–158 °C, 85% yield. ¹H NMR (400 MHz, CDCl₃+DMSO-*d*₆) δ 9.26–8.97 (m, 2H), 8.41 (d, *J* = 8.4 Hz, 1H), 8.24–8.20 (m, 1H), 8.10 (d, *J* = 8.4 Hz, 1H), 7.87–7.73 (m, 3H), 7.65–7.56 (m, 1H), 7.38–6.98 (m, 9H), 6.89–6.75 (m, 4H), 6.18 (s, 1H); ¹³C NMR (100 MHz, CDCl₃+DMSO-*d*₆) δ 161.66, 157.79, 150.99, 150.64, 149.26, 145.69, 145.64, 143.18, 140.63, 140.16, 137.41, 135.89, 134.34, 130.02, 129.75, 128.51, 127.00, 126.06, 124.63, 124.48, 123.53, 122.16, 120.15, 120.01, 119.47, 118.69, 118.11, 115.48, 73.63; HRMS (ESI, *m/z*): calcd. For C₃₃H₂₃N₅O₁₁S₂H⁺ 730.0908, found 730.3538 (M+1).



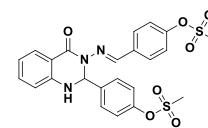
(E)-4-(((4-Oxo-2-(4-((phenylsulfonyl)oxy)phenyl)-1,2-dihydroquinazolin-3(4H)-yl)imino)

methyl)phenyl benzenesulfonate (7e): White solid, mp 149–150 °C, 85% yield. ¹H NMR (400 MHz, CDCl₃+DMSO-*d*₆) δ 9.03 (s, 1H), 7.84–7.70 (m, 12H), 7.52–7.51 (m, 2H), 7.40 (d, *J* = 8.4 Hz, 2H), 7.04–6.94 (m, 4H), 6.80–6.72 (m, 2H), 6.36 (s, 1H); ¹³C NMR (100 MHz, CDCl₃+DMSO-*d*₆) δ 161.56, 151.34, 150.76, 149.34, 146.54, 139.84, 135.23, 135.08, 135.06, 134.92, 134.48, 134.24, 131.87, 130.00, 129.87, 129.14, 128.68, 128.64, 128.47, 122.89, 122.43, 118.48, 115.32, 115.15, 73.10; HRMS (ESI, *m/z*): calcd. For C₃₃H₂₅N₃O₇S₂H⁺ 640.1207, found 640.2252.



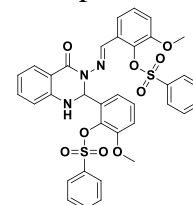
(E)-4-(3-((4-((Methylsulfonyl)oxy)benzylidene)amino)-4-oxo-1,2,3,4-tetrahydroquinazolin-2-yl)phenyl methanesulfonate (7f): White powder, mp 184–185 °C, 86% yield.

¹H NMR (400 MHz, CDCl₃+DMSO-*d*₆) δ 9.07 (s, 1H), 7.85–7.78 (d, 2H), 7.47–7.24 (m, 9H), 6.81–6.79 (m, 3H), 3.56 (s, 3H), 3.28 (s, 3H); ¹³C NMR (101 MHz, CDCl₃+DMSO) δ 161.71, 147.77, 145.97, 145.84, 145.11, 134.45, 132.43, 131.53, 130.34, 128.84, 128.09, 127.81, 127.73, 127.44, 123.13, 119.14, 115.03, 114.91, 68.81, 38.63, 37.80; HRMS (ESI, *m/z*): calcd. For C₂₃H₂₁N₃O₇S₂H⁺ 516.0894, found 516.1824; IR (KBr thin film, cm⁻¹): ν_{max} 3375, 3045, 2986, 1657, 1609, 1511, 1361, 1165, 1029, 880.



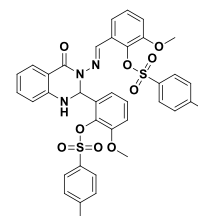
(E)-2-Methoxy-6-(((2-(3-methoxy-2-((phenylsulfonyl)oxy)phenyl)-4-oxo-1,2-dihydroquinazoline-3(4H)-yl)imino)methyl)phenyl benzenesulfonate (7g): White solid, mp 219–220 °C, 80% yield.

¹H NMR (400 MHz, CDCl₃+DMSO-*d*₆) δ 9.22 (s, 1H), 8.03 (d, *J* = 7.6 Hz, 2H), 7.86 (d, *J* = 7.6 Hz, 2H), 7.79–7.61 (m, 7H), 7.36–7.21 (m, 5H), 7.02–6.75 (m, 5H), 6.49 (s, 1H), 3.48 (s, 6H); ¹³C NMR (101 MHz, CDCl₃+DMSO-*d*₆) δ 161.61, 152.30, 152.11, 146.91, 145.57, 137.74, 136.61, 136.18, 136.12, 134.91, 134.48, 134.41, 134.27, 130.37, 129.13, 129.11, 128.54, 128.46, 128.38, 127.97, 127.76, 119.02, 118.67, 118.12, 115.11, 114.84, 114.11, 113.12, 69.50, 55.74, 55.61; HRMS (ESI, *m/z*): calcd. For C₃₅H₂₉N₃O₉S₂H⁺ 700.1418, found 700.1414; IR (KBr thin film, cm⁻¹): ν_{max} 3362, 3083, 2989, 1662, 1611, 1505, 1355, 1159, 1030, 875.

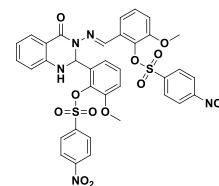


(E)-2-Methoxy-6-(((2-(3-methoxy-2-(tosyloxy)phenyl)-4-oxo-1,2-dihydroquinazolin-3(4H)-yl)imino)methyl)phenyl 4-methylbenzenesulfonate (7h): White crystalline solid, mp 189–190 °C, 83% yield.

¹H NMR (400 MHz, CDCl₃+DMSO-*d*₆) δ 9.01 (s, 1H), 7.75–7.66 (m, 4H), 7.57 (d, *J* = 8.0 Hz, 2H), 7.38 (d, *J* = 8.0 Hz, 2H), 7.29–7.13 (d, *J* = 6.8 Hz, 6H), 7.02 (d, *J* = 8.4 Hz, 1H), 6.91 (d, *J* = 8.0 Hz, 1H), 6.82–6.73 (m, 2H), 6.36 (s, 1H), 3.53 (s, 3H), 3.44 (s, 3H), 2.43 (s, 3H), 2.39 (s, 3H); ¹³C NMR (100 MHz, CDCl₃+DMSO-*d*₆) δ 161.55, 152.08, 151.81, 151.41, 146.74, 145.84, 145.66, 140.92, 139.59, 138.01, 135.27, 134.47, 132.83, 130.05, 129.92, 128.72, 128.55, 124.26, 123.65, 120.62, 119.28, 118.55, 115.31, 115.25, 112.12, 111.21, 73.33, 55.89, 40.21, 21.77, 21.73; HRMS (ESI, *m/z*): calcd. For C₃₇H₃₃N₃O₉S₂H⁺ 728.1731, found 728.1713; IR (KBr thin film, cm⁻¹): ν_{max} 3380, 3068, 2982, 1682, 1611, 1500, 1359, 1175, 1031, 870.

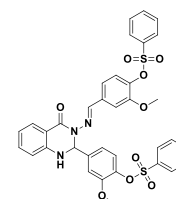


(E)-2-Methoxy-6-(((2-(3-methoxy-2-(((4-nitrophenyl)sulfonyl)oxy)phenyl)-4-oxo-1,2-dihydroquinazolin-3(4H)-yl)imino)methyl)phenyl 4-nitrobenzenesulfonate (7i): White solid, mp 205–206 °C, 90% yield. ¹H NMR (400 MHz, CDCl₃+DMSO-*d*₆) δ 9.25 (s, 1H), 8.46–8.41 (m, 4H), 8.27 (d, *J* = 9.2 Hz, 2H), 8.18 (d, *J* = 9.0 Hz, 2H), 7.69–7.67 (m, 1H), 7.30–7.22 (m, 5H), 7.08–7.04 (m, 2H), 6.97–6.94 (m, 1H), 6.82–6.73 (m, 2H), 6.44 (d, *J* = 2.0 Hz, 1H), 3.57 (s, 3H), 3.55 (s, 3H); ¹³C NMR (100 MHz, CDCl₃+DMSO-*d*₆) δ 166.67, 156.87, 156.76, 155.85, 155.59, 151.85, 150.96, 146.98, 146.42, 142.42, 142.37, 141.07, 139.39, 139.18, 134.93, 134.88, 134.66, 133.16, 133.06, 129.50, 129.37, 126.66, 124.22, 123.39, 122.61, 120.09, 119.49, 119.32, 118.52, 75.49, 60.73; HRMS (ESI, *m/z*): calcd. For C₃₅H₂₇N₅O₁₃S₂Na⁺ 812.0939, found 812.0932; IR (KBr thin film, cm⁻¹): ν_{max} 3378, 3106, 2944, 1665, 1610, 1527, 1352, 1196, 852.



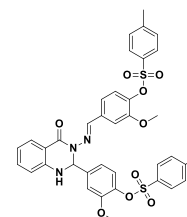
(E)-2-Methoxy-4-(((2-(3-methoxy-4-((phenylsulfonyl)oxy)phenyl)-4-oxo-1,2-dihydroquinazolin-3(4H)-yl)imino)methyl)phenyl benzenesulfonate (7j):

White solid, mp 133–134 °C, 83% yield. ¹H NMR (400 MHz, CDCl₃+DMSO-*d*₆) δ 9.08 (s, 1H), 7.81–7.42 (m, 12H), 7.30–6.69 (m, 7H), 6.82–6.75 (m, 2H), 6.29 (s, 1H), 3.50 (s, 3H), 3.42 (s, 3H); ¹³C NMR (100 MHz, CDCl₃) δ 166.46, 156.62, 156.36, 156.13, 151.23, 145.58, 144.22, 142.66, 140.48, 140.44, 139.94, 139.34, 139.20, 139.01, 133.93, 133.81, 133.30, 133.23, 133.08, 128.89, 128.27, 125.37, 124.02, 123.26, 120.00, 119.89, 116.53, 115.34, 78.56, 60.39; HRMS (ESI, *m/z*): calcd. For C₃₅H₂₉N₃O₉S₂H⁺ 700.1418, found 700.2501.

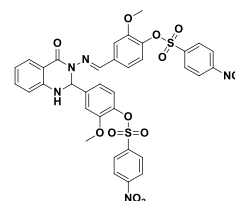


(E)-2-Methoxy-4-(((2-(3-methoxy-4-(tosyloxy)phenyl)-4-oxo-1,2-dihydroquinazolin-3(4H)-yl)imino)methyl)phenyl 4-methylbenzenesulfonate (7k): White solid, mp

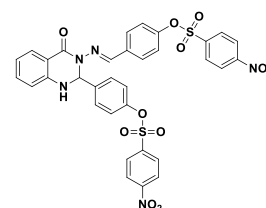
221–222 °C, 83% yield. ¹H NMR (400 MHz, CDCl₃+DMSO-*d*₆) δ 9.01 (s, 1H), 7.75–7.57 (m, 6H), 7.40–7.14 (m, 9H), 7.03 (d, *J* = 8.0 Hz, 1H), 6.92 (d, *J* = 8.4 Hz, 1H), 6.81–6.75 (m, 2H), 6.38 (s, 1H), 3.54 (s, 3H), 3.45 (s, 3H), 2.43 (s, 3H), 2.40 (s, 3H); ¹³C NMR (100 MHz, CDCl₃+DMSO) δ 161.35, 151.95, 151.67, 151.24, 146.62, 145.76, 145.58, 140.79, 139.42, 137.84, 135.13, 134.39, 132.67, 132.56, 129.97, 129.84, 128.59, 128.42, 124.15, 123.54, 120.46, 119.11, 118.41, 115.19, 115.08, 112.03, 111.18, 73.04, 55.79, 21.61. HRMS (ESI, *m/z*): calcd. For C₃₇H₃₃N₃O₉S₂H⁺ 728.1731, found 728.1549; IR (KBr thin film, cm⁻¹): ν_{max} 3332, 3036, 2973, 1680, 1505, 1372, 1170, 1089, 860.



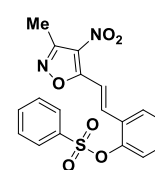
(E)-2-Methoxy-4-(((2-(3-methoxy-4-(((4-nitrophenyl)sulfonyl)oxy)phenyl)-4-oxo-1,2-dihydroquinazolin-3(4H)-yl)imino)methyl)phenyl 4-nitrobenzenesulfonate (7l): White solid, mp 196–197 °C, 88% yield. ¹H NMR (400 MHz, CDCl₃+DMSO-*d*₆) δ 9.22 (s, 1H), 8.43–8.37 (m, 4H), 8.25–8.13 (m, 4H), 7.67 (d, *J* = 7.6 Hz, 1H), 7.25–7.19 (m, 4H), 7.03–6.93 (m, 3H), 6.70–6.70 (m, 2H), 6.42 (s, 1H), 3.54 (s, 3H), 3.53 (s, 3H); ¹³C NMR (100 MHz, CDCl₃+DMSO-*d*₆) δ 166.65, 161.05, 157.11, 156.85, 155.81, 155.54, 150.80, 147.02, 146.45, 141.06, 139.17, 137.70, 136.79, 135.91, 134.87, 134.61, 133.12, 131.86, 130.33, 129.37, 129.25, 128.25, 126.33, 124.24, 123.47, 122.72, 120.52, 119.35, 75.35, 60.68; HRMS (ESI, *m/z*): calcd. For C₃₅H₂₇N₅O₁₃S₂Na⁺ 812.0939, found 812.0966; IR (KBr thin film, cm⁻¹): ν_{max} 3345, 3056, 2985, 1675, 1540, 1378, 1190, 1055, 875.



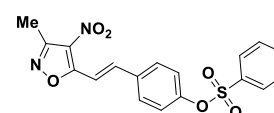
(E)-4-(3-(((4-(((4-Nitrophenyl)sulfonyl)oxy)benzylidene)amino)-4-oxo-1,2,3,4-tetrahydroquinazolin-2-yl)phenyl 4-nitrobenzenesulfonate (7m): Pale yellow solid, mp 201–202 °C, 90% yield. ¹H NMR (400 MHz, CDCl₃+DMSO-*d*₆) δ 9.05 (s, 1H), 8.42 (d, *J* = 8.4 Hz, 2H), 8.33 (d, *J* = 8.8 Hz, 2H), 8.12–8.02 (m, 4H), 7.73–7.64 (m, 4H), 7.40 (d, *J* = 8.4 Hz, 2H), 7.08–6.97 (m, 4H), 6.78–6.69 (m, 2H), 6.35 (s, 1H); ¹³C NMR (100 MHz, CDCl₃+DMSO-*d*₆) δ 161.69, 151.18, 151.14, 151.08, 150.27, 148.90, 146.13, 140.47, 140.36, 140.16, 134.53, 134.31, 130.18, 130.01, 129.06, 128.66, 128.55, 124.94, 124.83, 124.71, 122.54, 122.11, 118.51, 115.18, 73.49; HRMS (ESI, *m/z*): calcd. For C₃₃H₂₃N₅O₁₁S₂Na⁺ 752.0728, found 752.0729.



(E)-2-(2-(3-Methyl-4-nitroisoxazol-5-yl)vinyl)phenyl benzenesulfonate (8a): White solid, mp 119–120 °C, 90 % yield. ¹H NMR (400 MHz, CDCl₃) δ 7.83 (d, *J* = 7.2 Hz, 2H), 7.69 (d, *J* = 6.8 Hz, 1H), 7.58–7.33 (m, 8H), 2.60 (s, 3H); ¹³C NMR (100 MHz, CDCl₃+DMSO-*d*₆) δ 156.32, 153.64, 151.30, 139.15, 137.21, 133.89, 133.05, 131.75, 129.85, 127.15, 125.75, 121.30, 117.42, 115.40, 101.66, 11.44; HRMS (ESI, *m/z*): calcd. For C₁₈H₁₄N₂O₆S 386.0573, found 489.1759; IR (KBr thin film, cm⁻¹): ν_{max} 3010, 2986, 1644, 1535, 1380, 1275, 1184, 1066.

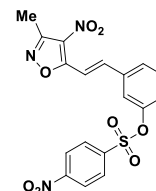


(E)-4-(2-(3-Methyl-4-nitroisoxazol-5-yl) vinyl)phenyl benzenesulfonate (8b): White solid, mp 183–184 °C, 82% yield. ¹H NMR (400 MHz, CDCl₃) δ 7.86 (d, *J* = 7.2 Hz, 2H), 7.72–7.56 (m, 7H), 7.08 (d, *J* = 8.0 Hz, 2H), 2.59 (s, 3H); ¹³C NMR (100 MHz, CDCl₃) δ 166.67, 156.20, 151.17, 141.13, 135.20,

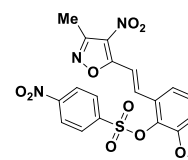


134.54, 133.41, 129.68, 129.33, 128.50, 123.27, 123.12, 111.90, 11.92; HRMS (ESI, m/z): calcd. For $C_{18}H_{14}N_2O_6SH^+$ 387.0645, found 387.0647; IR (KBr thin film, cm^{-1}): ν_{max} 3015, 2965, 1655, 1547, 1372, 1252, 1185, 1053.

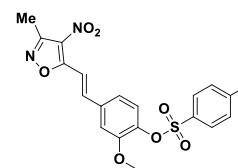
(E)-3-(2-(3-Methyl-4-nitroisoxazol-5-yl)vinyl)phenyl 4-nitrobenzenesulfonate (8c): White powder, mp 148–149 °C, 90% yield. 1H NMR (400 MHz, $CDCl_3$ +DMSO- d_6) δ 8.40 (d, J = 8.4 Hz, 1H), 8.25 (d, J = 8.4 Hz, 2H), 8.02 (d, J = 8.4 Hz, 2H), 7.70 (d, J = 7.2 Hz, 1H), 7.50–7.28 (m, 4H), 2.90 (s, 3H); ^{13}C NMR (100 MHz, $CDCl_3$ +DMSO- d_6) δ 159.27, 155.79, 152.45, 141.29, 136.23, 133.87, 132.15, 131.81, 130.46, 130.13, 129.05, 127.06, 121.35, 118.63, 101.33, 10.94; HRMS (ESI, m/z): calcd. For $C_{18}H_{13}N_3O_8SH^+$ 432.0496, found 489.2845.



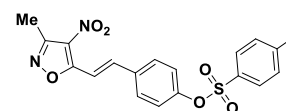
(E)-2-Methoxy-6-(2-(3-methyl-4-nitroisoxazol-5-yl)vinyl)phenyl 4-nitrobenzenesulfonate (8d): Pale yellow solid, mp 194–195 °C, 86% yield. 1H NMR (400 MHz, $CDCl_3$) δ 8.35 (d, J = 8.8 Hz, 2H), 8.16 (d, J = 8.4 Hz, 2H), 7.55 (d, J = 5.6 Hz, 2H), 7.36–7.35 (m, 2H), 7.06–7.04 (m, 1H), 3.76 (s, 3H), 2.57 (s, 3H); ^{13}C NMR (100 MHz, $CDCl_3$ +DMSO- d_6) δ 158.36, 155.52, 150.26, 149.33, 149.20, 141.43, 137.67, 129.70, 129.36, 128.77, 122.26, 120.69, 111.69, 110.60, 102.01, 55.95, 11.29; HRMS (ESI, m/z): calcd. For $C_{19}H_{15}N_3O_9SH^+$ 462.0602, found 484.0352; IR (KBr thin film, cm^{-1}): ν_{max} 3012, 2970, 1632, 1528, 1378, 1280, 1195, 1069.



(E)-2-Methoxy-4-(2-(3-methyl-4-nitroisoxazol-5-yl)vinyl)phenyl 4-methylbenzenesulfonate (8e): Light yellow solid, mp 146–147 °C, 83% yield. 1H NMR (400 MHz, $CDCl_3$) δ 7.81 (d, J = 8.0 Hz, 2H), 7.60 (d, J = 16.8 Hz, 1H), 7.48 (d, J = 16.8 Hz, 1H), 7.31–7.28 (m, 4H), 7.03 (d, J = 6.4 Hz, 1H), 3.77 (s, 3H), 2.59 (s, 3H), 2.36 (s, 3H); ^{13}C NMR (100 MHz, $CDCl_3$ +DMSO- d_6) δ 166.37, 155.86, 153.09, 145.64, 137.73, 135.97, 133.30, 129.88, 129.76, 128.31, 128.09, 118.42, 114.99, 112.85, 56.02, 21.59, 11.75; HRMS (ESI, m/z): calcd. For $C_{20}H_{18}N_2O_7SNa^+$ 453.0727, found 453.0651; IR (KBr thin film, cm^{-1}): ν_{max} 3093, 2935, 1627, 1578, 1514, 1359, 1286, 1071.

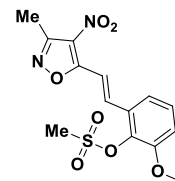


(E)-4-(2-(3-Methyl-4-nitroisoxazol-5-yl)vinyl)phenyl 4-methylbenzenesulfonate (8f): White solid, mp 175–176 °C, 81% yield. 1H NMR (400 MHz, $CDCl_3$) δ 7.74–7.69 (m, 3H), 7.60–7.56 (m, 3H), 7.34 (d, J = 8.0 Hz, 2H), 7.08 (d, J = 8.8 Hz, 2H), 2.60 (s, 3H), 2.47 (s, 3H); ^{13}C NMR (100 MHz, $CDCl_3$) δ

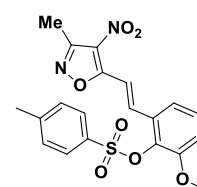


166.69, 156.19, 151.29, 145.76, 141.20, 133.30, 132.22, 129.93, 129.65, 128.52, 123.22, 111.82, 21.76, 11.82. HRMS (ESI, m/z): calcd. For $C_{19}H_{16}N_2O_6SNa^+$ 423.0621, found 423.0553; IR (KBr thin film, cm^{-1}): ν_{max} 3072, 2923, 1632, 1573, 1505, 1346, 1201, 1142.

(E)-2-Methoxy-6-(2-(3-methyl-4-nitroisoxazol-5-yl)vinyl)phenyl methanesulfonate (8g): Pale green solid, mp 173–174 °C, 85% yield. 1H NMR (400 MHz, $CDCl_3$) δ 8.07 (d, $J = 16.4$ Hz, 1H), 7.71–7.59 (m, 1H), 7.46–7.38 (m, 2H), 7.15 (d, $J = 6.8$ Hz, 1H), 3.95 (s, 3H), 3.41 (s, 3H), 2.59 (s, 3H); ^{13}C NMR (100 MHz, $CDCl_3 + DMSO-d_6$) δ 166.49, 155.99, 152.36, 137.63, 135.92, 130.45, 128.07, 118.69, 114.94, 113.60, 56.29, 39.74, 11.75; HRMS (ESI, m/z): calcd. For $C_{14}H_{14}N_2O_7SNa^+$ 377.0414, found 377.1244; IR (KBr thin film, cm^{-1}): ν_{max} 3102, 2978, 1630, 1583, 1439, 1377, 1143, 1045.

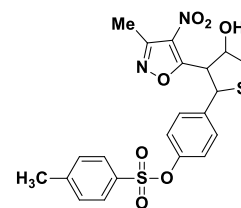


(E)-2-Methoxy-6-(2-(3-methyl-4-nitroisoxazol-5-yl)vinyl)phenyl 4-methylbenzenesulfonate (8h): White solid, mp 190–191 °C, 80% yield. 1H NMR (400 MHz, $CDCl_3$) δ 7.75–7.55 (m, 5H), 7.45–7.33 (m, 4H), 7.11 (s, 1H), 6.92 (d, $J = 8.0$ Hz, 1H), 6.78–6.68 (m, 1H), 3.65 (s, 3H), 2.47 (s, 3H), 2.43 (s, 3H). ^{13}C NMR (100 MHz, $CDCl_3 + DMSO-d_6$) δ 166.65, 156.06, 152.18, 145.56, 141.66, 140.07, 134.38, 132.70, 129.57, 128.49, 124.47, 121.15, 112.03, 111.79, 55.78, 21.67, 11.76; HRMS (ESI, m/z): calcd. For $C_{20}H_{18}N_2O_7SNa^+$ 453.0727, found 453.0650; IR (KBr thin film, cm^{-1}): ν_{max} 2978, 1633, 1508, 1355, 1188, 827.

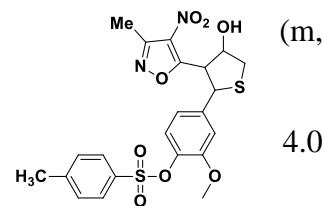


4-((2R,3R,4R)-4-Hydroxy-3-(3-methyl-4-nitroisoxazol-5-yl)tetrahydrothiophen-2-yl)phenyl 4-methylbenzenesulfonate (10a):

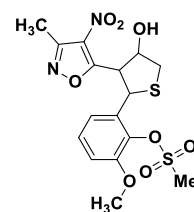
White solid, mp 190–191 °C, 85% yield. 1H NMR (400 MHz, $CDCl_3$) δ 7.67 (d, $J = 8.4$ Hz, 2H), 7.35 (dd, $J = 35.4, 8.4$ Hz, 4H), 6.89 (d, $J = 8.4$ Hz, 2H), 5.28 (d, $J = 11.2$ Hz, 1H), 5.04 (s, 1H), 4.24 (dd, $J = 11.4, 2.8$ Hz, 1H), 3.70 (dd, $J = 12.0, 3.6$ Hz, 1H), 3.11 (d, $J = 12.0$ Hz, 1H), 2.61–2.58 (m, 1H), 2.50 (s, 3H), 2.45 (s, 3H); ^{13}C NMR (100 MHz, $CDCl_3$) δ 170.42, 155.89, 149.15, 145.58, 137.33, 132.32, 129.86, 129.44, 128.50, 128.42, 122.72, 76.68, 56.67, 48.63, 40.67, 21.74, 11.61; HRMS (ESI, m/z): calcd. For $C_{21}H_{20}N_2O_7S_2H^+$ 477.0785, found 477.0780; IR (KBr thin film, cm^{-1}): ν_{max} 3380, 2985, 1620, 1536, 1363, 1175, 830.



4-(4-Hydroxy-3-(3-methyl-4-nitroisoxazol-5-yl)tetrahydrothiophen-2-yl)-2-methoxyphenyl 4-methylbenzenesulfonate (10b): White solid, mp 190–191 °C, 82% yield. ¹H NMR (400 MHz, CDCl₃) δ 7.77 (d, *J* = 8.0 Hz, 1H), 7.67 (d, *J* = 8.4 Hz, 1H), 7.24–7.22 (m, 2H), 7.15–7.06 (m, 2H), 6.63 (d, *J* = 9.6 Hz, 1H), 5.42 (d, *J* = 10.0 Hz, 1H), 5.08 (d, *J* = 10.4 Hz, 1H), 4.39–4.34 (m, 1H), 3.53 (dd, *J* = 11.8, 4.0 Hz, 1H), 3.35 (s, 3H), 3.19–3.14 (m, 1H), 2.98 (dd, *J* = 11.8, 2.0 Hz, 1H), 2.35 (s, 3H), 2.34 (s, 3H); ¹³C NMR (100 MHz, CDCl₃) δ 170.91, 155.83, 151.69, 145.01, 137.57, 137.05, 134.74, 134.68, 134.33, 134.12, 129.39, 128.28, 128.12, 120.62, 119.80, 111.86, 77.77, 54.77, 43.34, 40.50, 37.87, 21.70, 11.64; HRMS (ESI, *m/z*): calcd. For C₂₂H₂₂N₂O₈S₂H⁺ 507.0890, found 507.0885; IR (KBr thin film, cm⁻¹): ν_{max} 3405, 2985, 1620, 1540, 1370, 1162, 845.



2-(4-Hydroxy-3-(3-methyl-4-nitroisoxazol-5-yl)tetrahydrothiophen-2-yl)-6-methoxyphenyl methane sulfonate (10c): White sticky solid, mp 201–202 °C, 80% yield. ¹H NMR (400 MHz, CDCl₃) δ 7.19 (s, 1H), 7.15–7.14 (m, 2H), 5.58 (d, *J* = 10.4 Hz, 1H), 4.98 (s, 1H), 4.45 (dd, *J* = 10.2, 3.6 Hz, 1H), 3.78 (s, 3H), 3.62 (dd, *J* = 12.0, 4.4 Hz, 1H), 3.31 (s, 3H), 3.08 (dd, *J* = 11.8, 2.0 Hz, 1H), 2.43 (s, 3H). ¹³C NMR (100 MHz, CDCl₃) δ 170.48, 155.63, 151.89, 137.55, 134.50, 130.76, 128.07, 120.16, 112.13, 56.03, 54.49, 42.69, 40.50, 39.72, 29.68, 11.59; HRMS (ESI, *m/z*): calcd. For C₁₆H₁₈N₂O₈S₂H⁺ 431.0577, found 431.0570; IR (KBr thin film, cm⁻¹): ν_{max} 3390, 2956, 1650, 1545, 1381, 1154, 855.



6.6 References

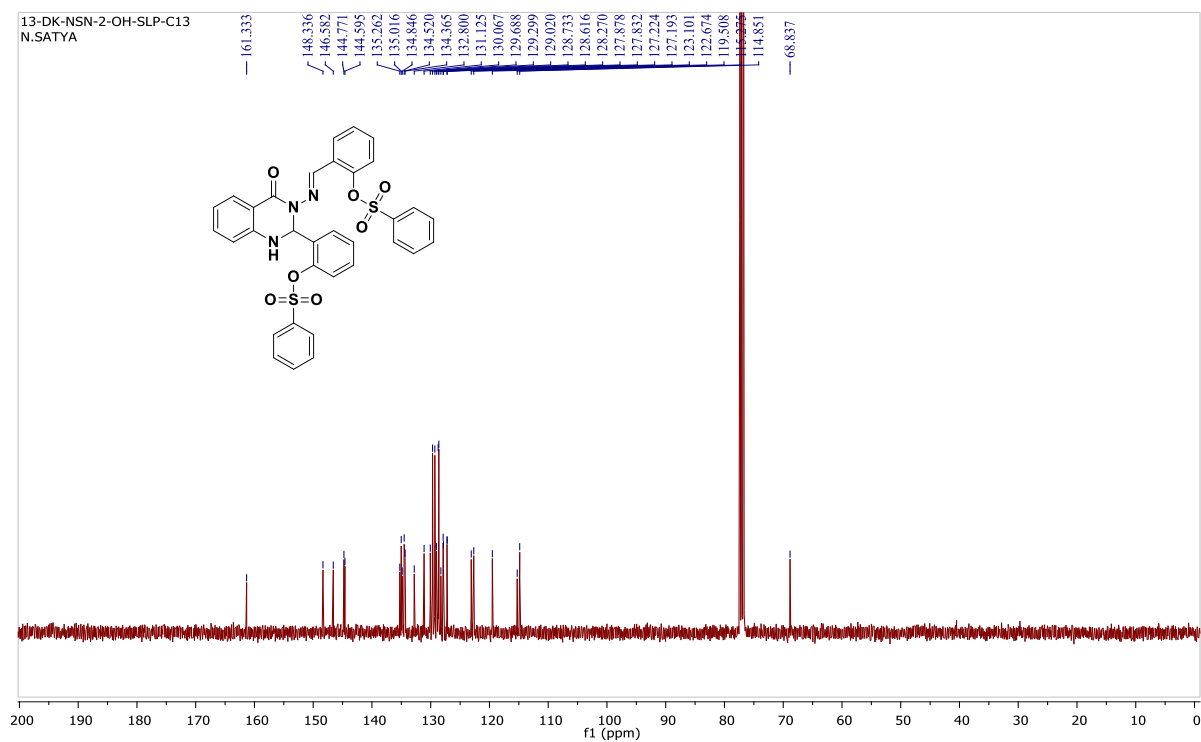
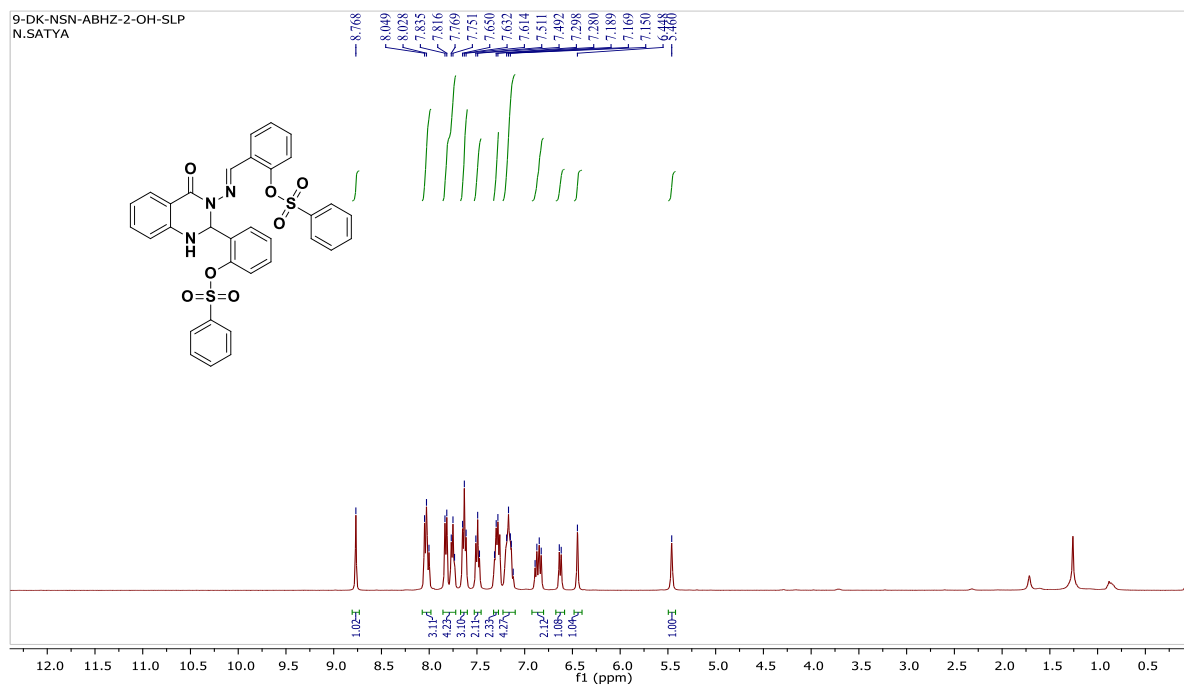
- (a) Saravanan, G.; Pannerselvam, P. & Prakash, C. R.; *Der Pharmacia Lett.* **2010**, 2, 216–226. (b) Shetha, A. & Wijdan, I. A. *J. Chem. Pharm. Res.* **2013**, 5, 42–45; (c) Zaranappa.; Vagdevi, H. M.; Lokesh, M. R.; Gowdarshivannanavar, B. C. *Int. J. Chem. Tech. Res.* **2012**, 4, 1527–1533. (e) Abid, O. H. & Ahmed, A.H. *Inter. J. Appl. Nat. Sci.* **2013**, 2, 11–20. (d) Fadhil, L. F.; Maryam, Z.; Mohammadjavah, P.; Chung, Y. L.; Nazia, A. M.; Hapipah, M. A.; Noraini, A.; Nura, S. G. and Mahmood, A. A. *Sci. World J.* **2014**, 15, 212096. (f) Imtiaz, K.; Sumera, Z.; Sadaf, B.; Naeem, A.; Zaman, A.; Jamshed, I.; Aamer, S. *Bioorg. Med. Chem.* **2016**, 24, 2361–2381. (g) Pati, B. & Banerjee, S. *J. Adv. Pharm. Edu. Res.* **2013**, 3, 136–151.
- (a) Sugden, R.; Kelly, R.; Davis, S. *Nature Microbiology.* **2016**, 1, 16187-16187; (b) Ventola. C. L. *Pharmacol. Ther.* **2015**, 40, 344-352.

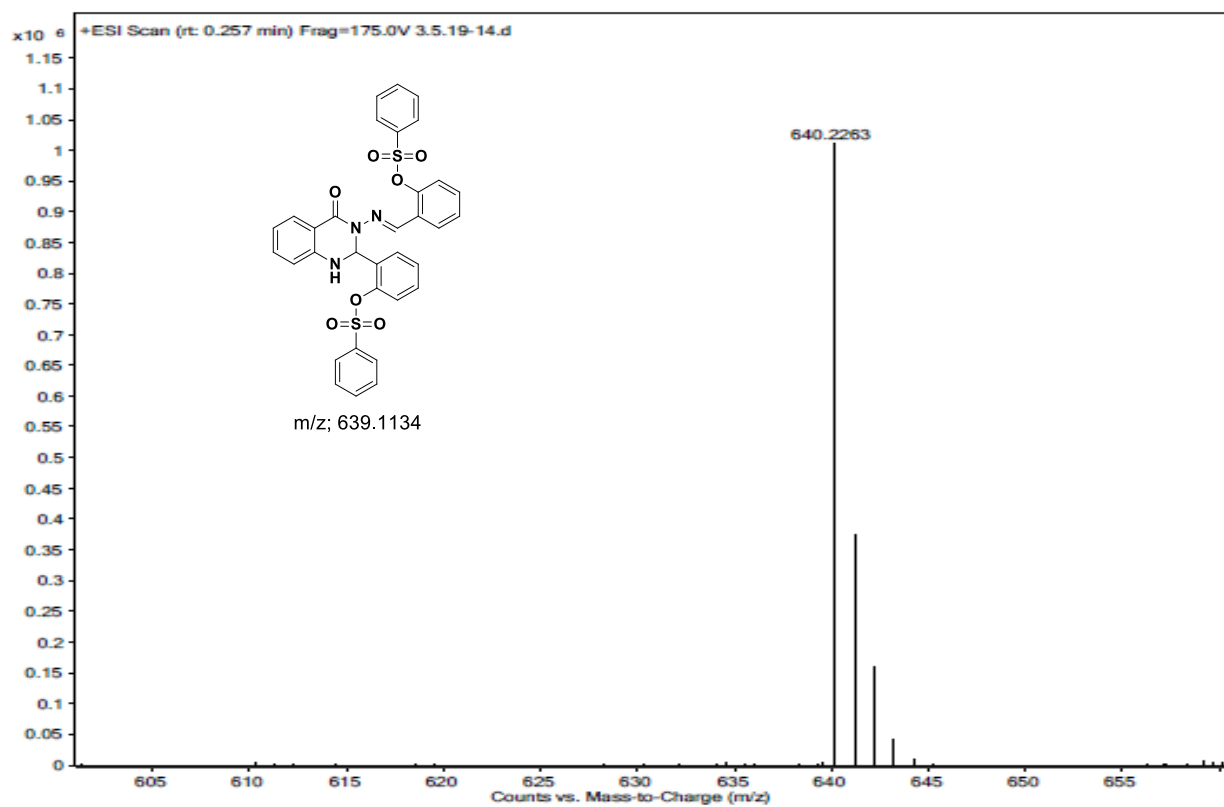
3. Wolfgang, D.; Fabrice, L. J.; Gregory, M.; Andrea, E. P.; Paul, A. F.; Pascoe, M.; Ernest, H.; Mark, P. T.; Philip, G. K.; Eric, F.; Michel, O. S.; Mathew, P. L. and Barry, V. L. Potter, *J. Med. Chem.* **2018**, *61*, 1031–1044; DOI: 10.1021/acs.jmedchem.7b01474.
4. Kumar, D.; Mariappan, G.; Husain, A.; Monga, J.; Kumar, S. *Arabian J. Chem.* **2017**, *10*, 344–350.
5. (a) Melvin, J. Y.; Jefferson, R. M.; Norman, R. M.; Jack, B. D. and Laurane, G. M. *Med. Chem.* **1992**, *35*, 14, 2534–2542. (b) Siamaki, A. R.; Black, D. A.; Arndtsen, B. A. *J. Org. Chem.* **2008**, *73*, 1135–1138. (c) Maryam, Z.; Fadhil, L. F.; Mohammad, Javad. P.; Chung, Y. L.; Maryam, H.; Mohadeseh, H.; Behnam, K.; Nazia, A. M.; Hapipah, M. A. and Mahmood, A. A. *Sci. Rep.*, **2015**, *5*, 11544; DOI: 10.1038/srep11544; (d) Katla, J.; Hazra, B.; Verma, M. S.; Palakollu, V.; Nagaraju, S.; Chandra, M and Kanvah. S. *Chemistry Select.* **2018**, *3*, 7416 – 7421. (e) Thiagarajan, V.; Selvaraju. C.; Malar, E. J. P., Ramamurthy. P., *Chem. Phys. Chem.* **2004**, *5*, 1200–1209.
6. (a) Katritzky, A. R.; Rees, C. W and Scriven, E. F. V. *Comprehensive Heterocyclic Chemistry II*, Pergamon, Oxford, UK, **1996**. (b) Katritzky, A. R., Ramsden, C. A.; Scriven, E. F. V and Taylor, R. J. K. *Comprehensive Heterocyclic Chemistry III*, Pergamon, Oxford, UK, **2008**.
7. (a) Kankala, S.; Kankala, R. K.; Gundepaka, P.; Thota, N.; Nerella, S.; Gangula, M. R.; Guguloth, H.; Kagga, M.; Vadde, R and Vasam, C. S. *Bioorg. Med. Chem. Lett.* **2013**, *23*, 1306–1309. (b) Frølund, B.; Jørgensen, A. T.; Tagmose, L.; Stensbøl, T. B., Vestergaard, H. T.; Engblom, C.; Kristiansen, U.; Sanchez, C.; Krosgaard, -L. P and Liljefors, T. *J. Med. Chem.* **2002**, *45*, 2454–2468.
8. Li, J. J. *Heterocyclic Chemistry in Drug Discovery*. John Wiley & Sons. **2013**, **720** ISBN: 978-1-118-14890-7.
9. Kakarla, R.; Liu, J.; Naduthambi, D.; Chang, W.; Mosley, R. T.; Bao, D.; Steuer, H. M. M.; Keilman, M.; Bansal, S.; Lam, A. M and Seibel, W. *J. Med. Chem.* **2014**, *57*, 2136–2160.
10. Kenneth, E. P.; Susan, M. C.; Julian, P. L.; Ponnann, V.; Amanda, J. C.; Ashley, E. S, *Pest Manag. Sci.* **2001**, *57*, 133-142.
11. (a) Jacobsen, N.; Pedersen, L.-E. K and Wengel. A. *Pestic. Sci.*, **1990**, *29*, 95–100. (b) Monge, D.; Jiang, H and Alvarez, -C. Y. *Chem.–Eur. J.* **2015**, *12*, 4494–4504. (c) Pisani, L.; Bareletta, M.; Soto-Otero, R.; Nicolotti, O.; Mendez, -A. E.; Catto, M.; Introcaso, A.; Stefanachi, A.; Cellamare, S.; Altomare, C and Carotti, A. *J. Med. Chem.* **2013**, *56*, 2651.
12. (a) Horton, D. A.; Bourne, G. T.; Smythe, M. L. *Chem. Rev.* **2003**, *103*, 893. (b) Liu, J. F.; Wilson, C. J.; Ye, P.; Sprague, K.; Sargent, K.; Si, Y.; Beletsky, G.; Yohannes, D.; Ng, S. C.

- Bioorg. Med. Chem. Lett.* **2006**, *16*, 686. (c) Sawant, V.A.; Yamgar, B.A.; Sawant, S.K.; Chavan, S. S. *Spectrochimica Acta Part A*, **2009**, *74*, 1100–1106. (d) Sahana, K.; Chinmay, B.; Manasa, K.; Subrahmanya, I. B. and Amit, K. *Chem. Select.* **2016**, *1*, 1723-1728. (e) Magyar. T.; Miklós, F.; Lázár, L and Fülöp, F. *Chem. Heterocycl. Compd.* **2015**, *50*, 10. (f) Jin, Z.; Pei, C.; Yangmin, M.; Jia; L.; Zhi, M.; Decheng. R., Chao. F., Ming. L., Le. L. *Tetrahedron Lett.* **2016**, *57*, 5271–5277.
13. (a) Jinlong, Z.; Xihong, L.; Xiaojuan, M. and Rui, W. *Chem. Commun.* **2013**, *49*, 9329. (b) Mauro, F. A. A.; Vivekananda, R. K.; Donato, D.; Piero, S. -F and Tomas. T. *Tetrahedron*. **2007**, *63*, 9741–9745. (c) Rajanarendar, E.; Nagi, R. M.; Rama, M. K; *Chinese Chemical Letters*. **2010**, *21*, 927–930. (d) Sakkani, N.; Neeli, S.; Banoth, P.; Anuji, K. V.; Sriram, K and Dhurke. K. *RSC Adv.* **2015**, *5*, 81768. (e) Kartikey, D. D.; Sameer, R. M.; Satish, K. N and Raju. L. C. *J. Chem. Sci.* **2018**, *130*, 129. (f) Sakkani, N.; Neeli, S.; Banoth, P., Anuji, V.; K., Sriram, K. and Dhurke, K., *RSC Adv.* **2015**, *5*, 81768-81773. (g) Sakkani, N.; Kota, S.; Banoth, P.; Dhurke, K. *Tetrahedron Lett.* **2017**, *58*, 2865–2871 2869.
14. Chen, C. Y.; Ho, J. H.; Wang. S. L. and Ho. T. I. *Photochem. Photobiol. Sci.* **2003**, *2*, 1232 1236.
15. (a) Alok, M.; Prabhas, B.; Anoop, K. P.; Rahul, Y.; Tasneem, P and Lokman, H. C. *New J. Chem.* **2020**, *44*, 4798. (b) Crosby, G. A and Demas, J. N. *J. Phys. Chem.* **1971**, *75*, 991.

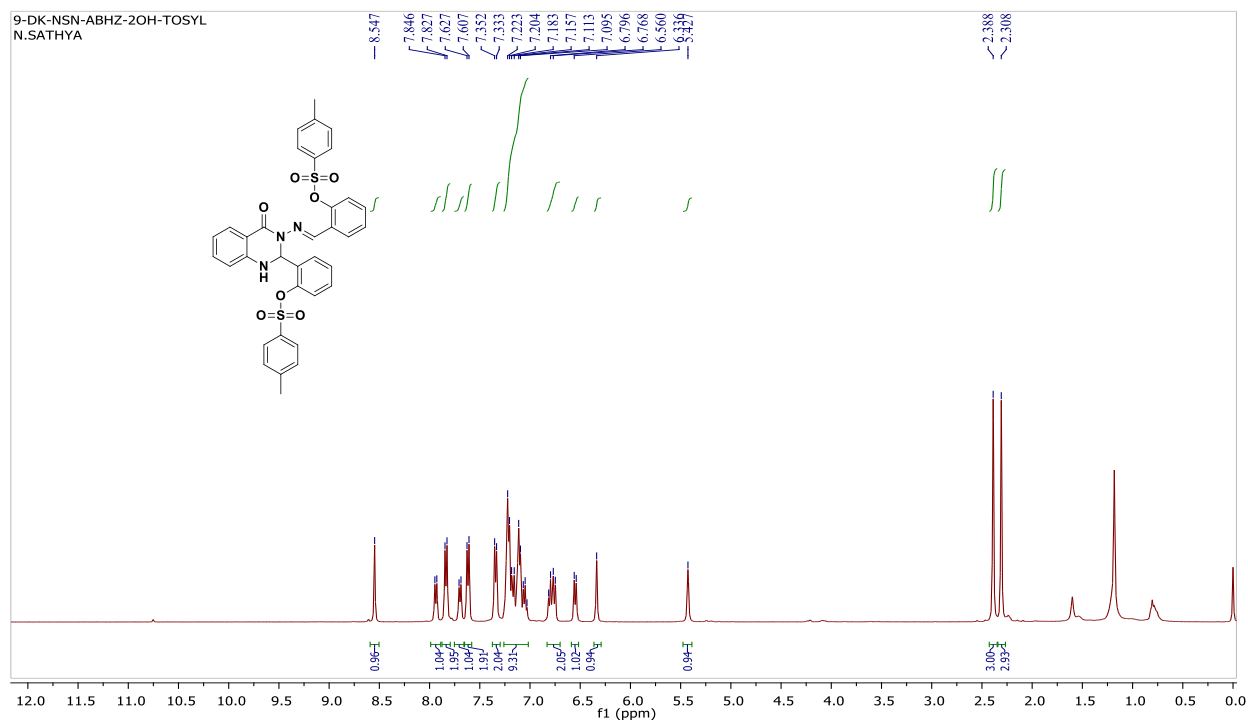
6.7 Selected spectra

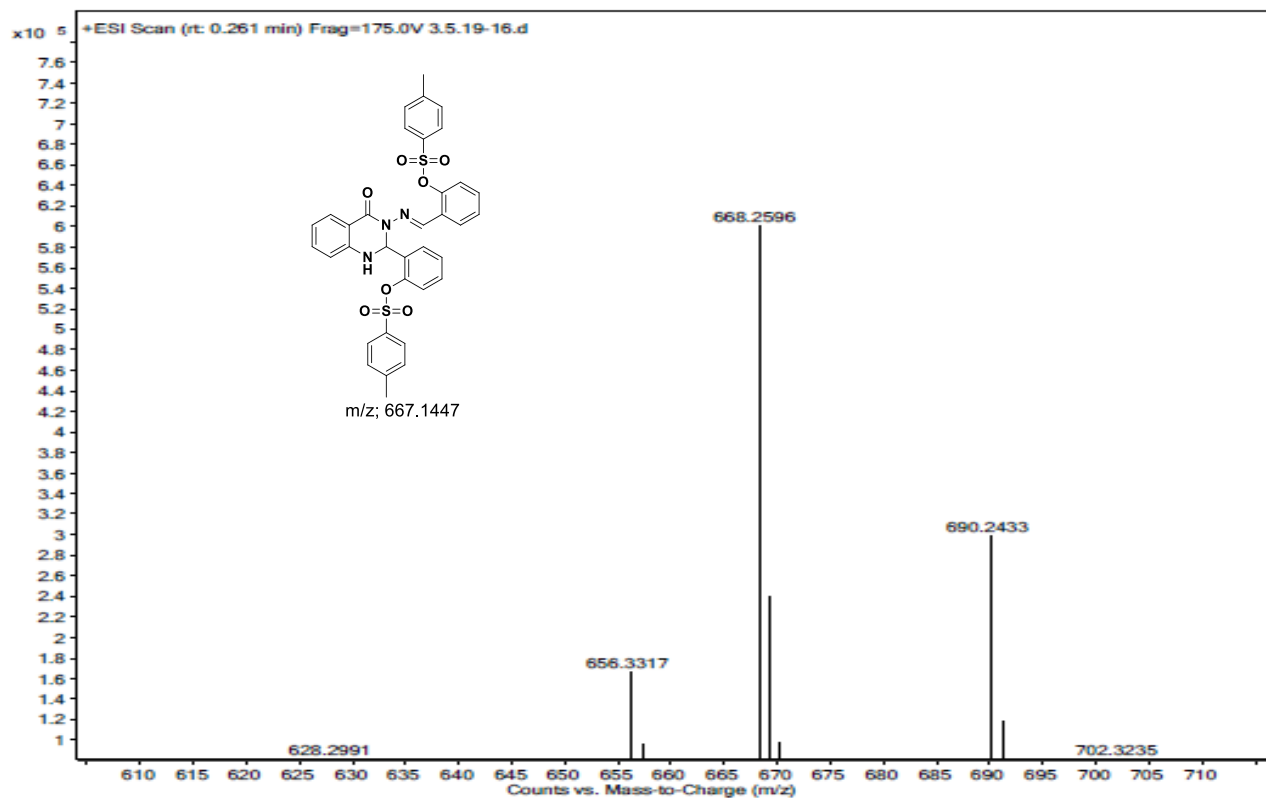
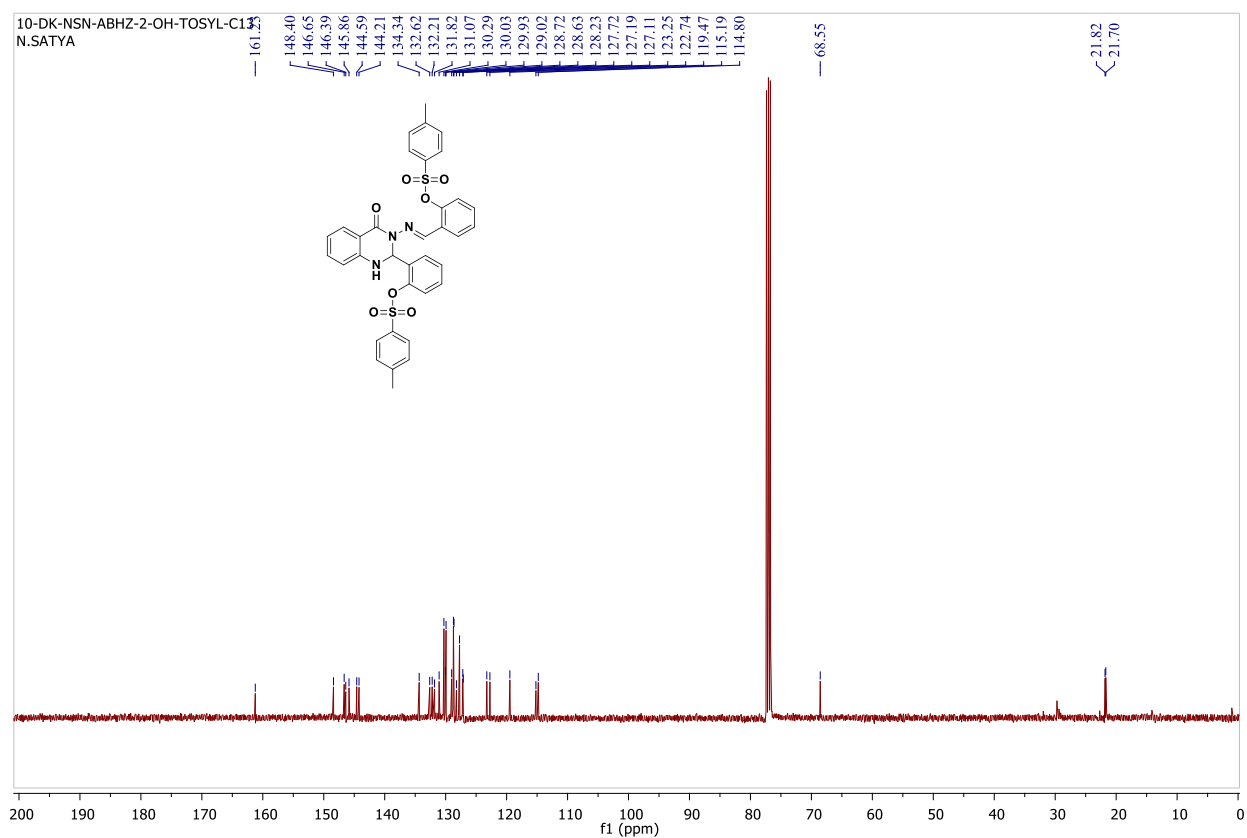
(E)-2-(((4-Oxo-2-(2-((phenylsulfonyl)oxy)phenyl)-1,2-dihydroquinazolin-3(4H)-yl)imino) methyl) phenyl benzenesulfonate (7a):



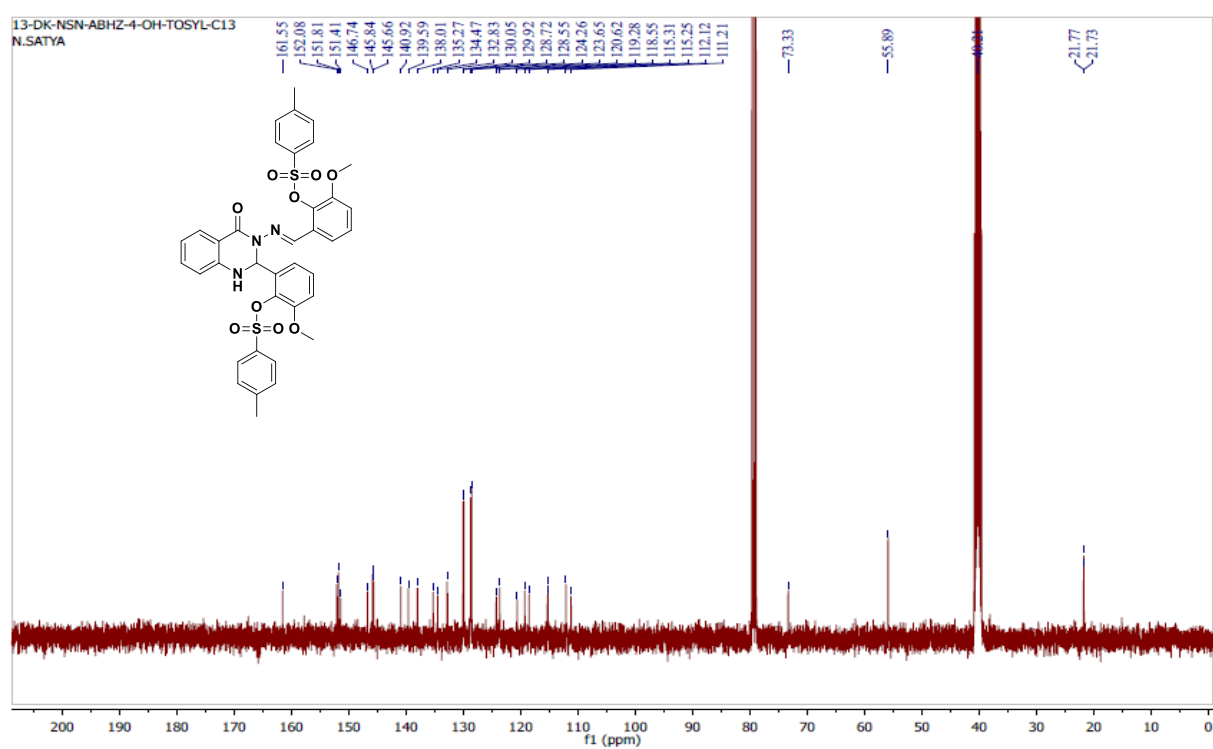
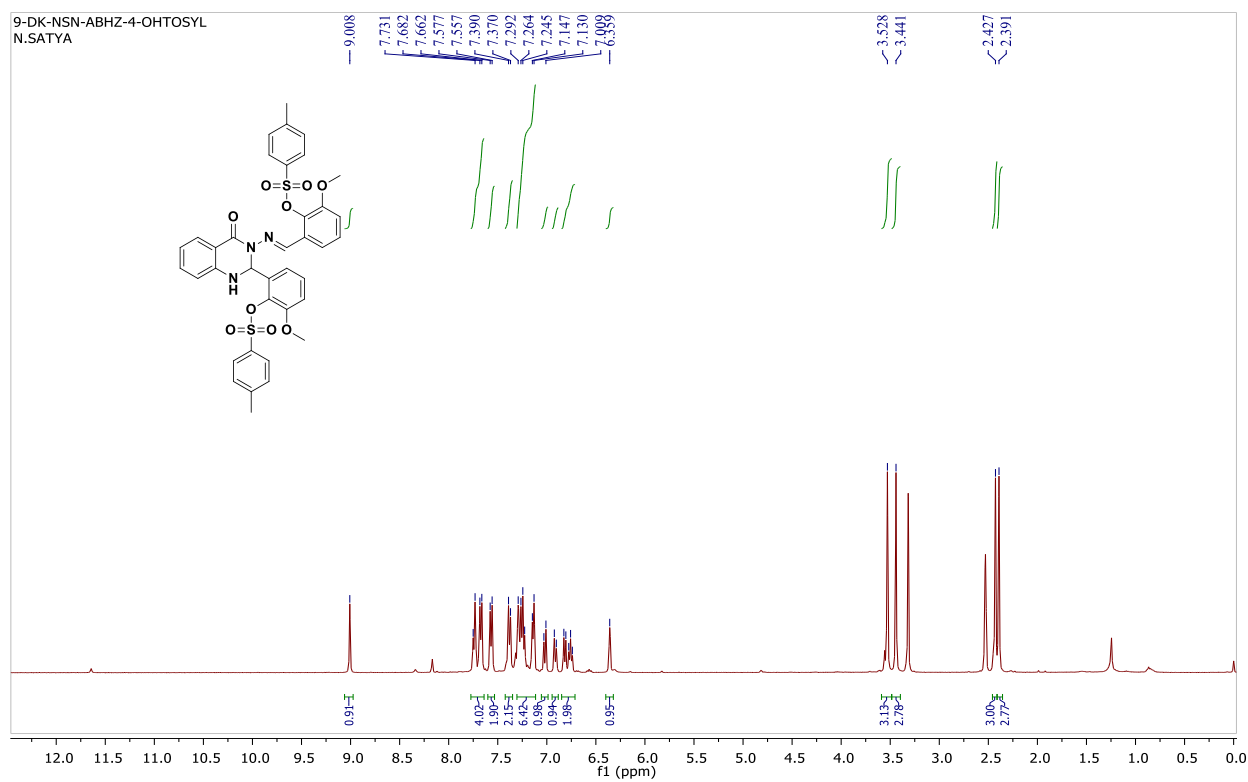


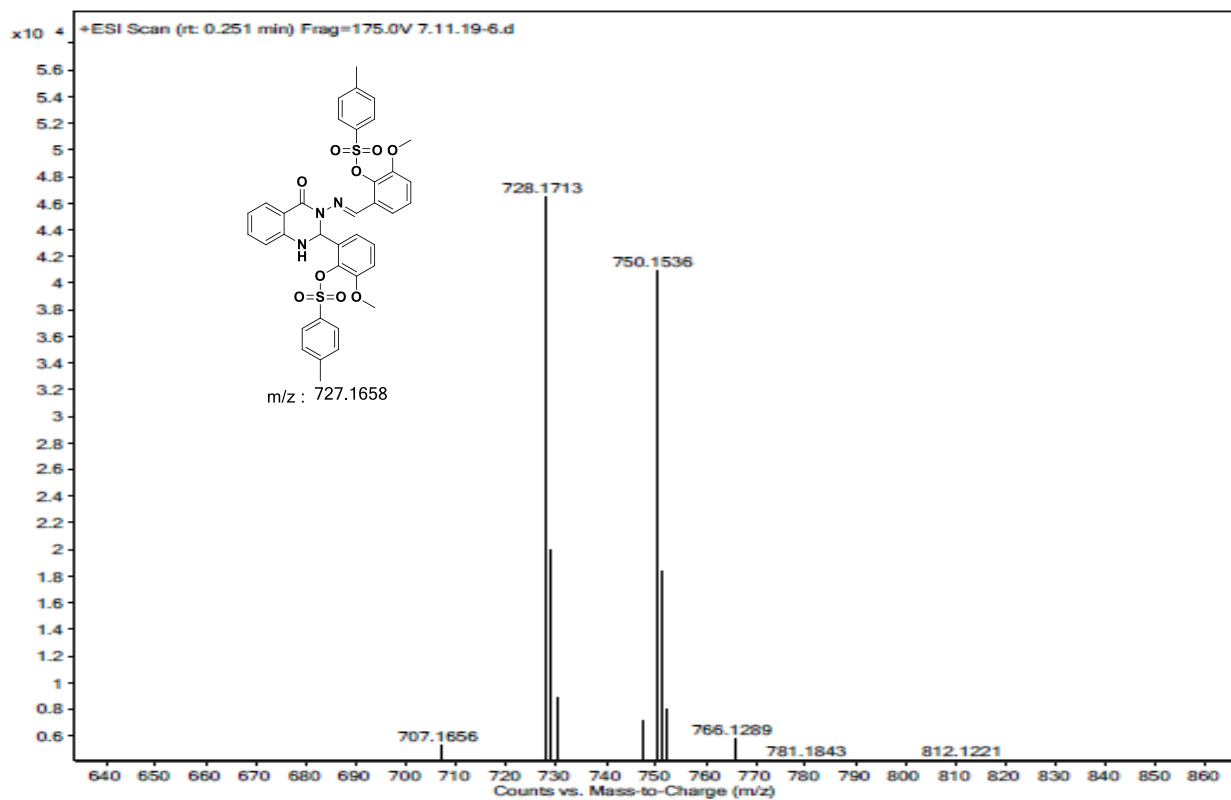
(E)-2-(((4-Oxo-2-(2-(tosyloxy)phenyl)-1,2-dihydroquinazolin-3(4H)-yl)imino)methyl)phenyl 4-methylbenzenesulfonate (7b):



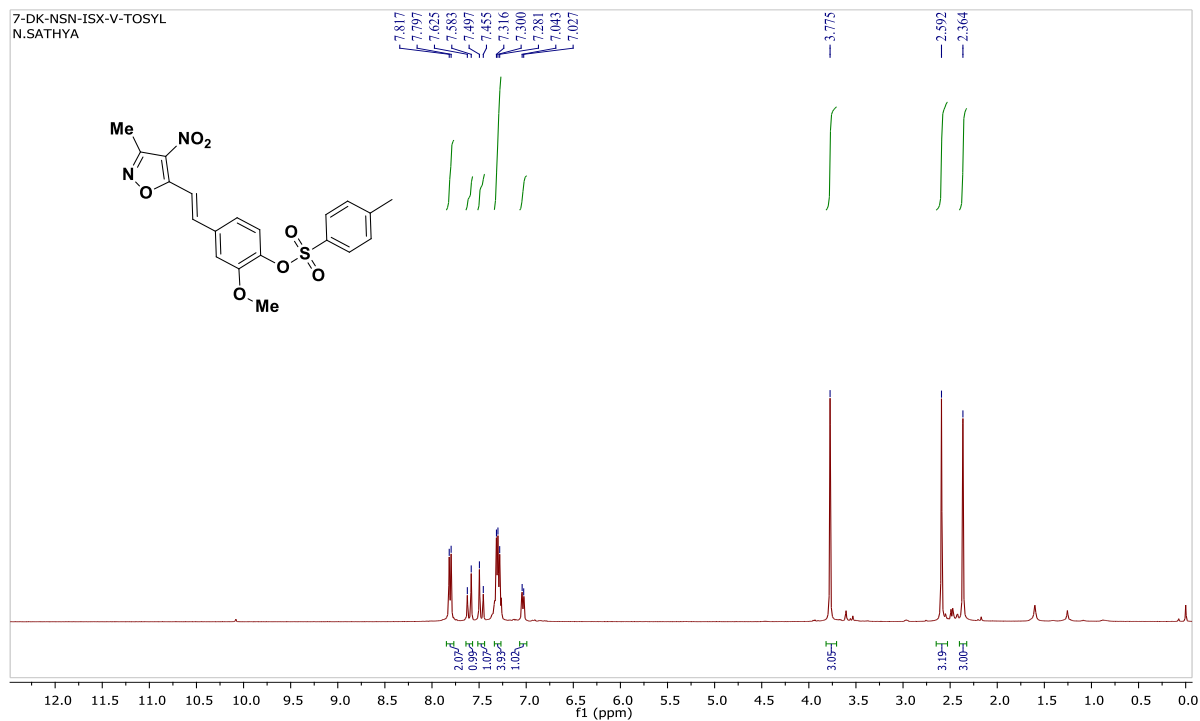


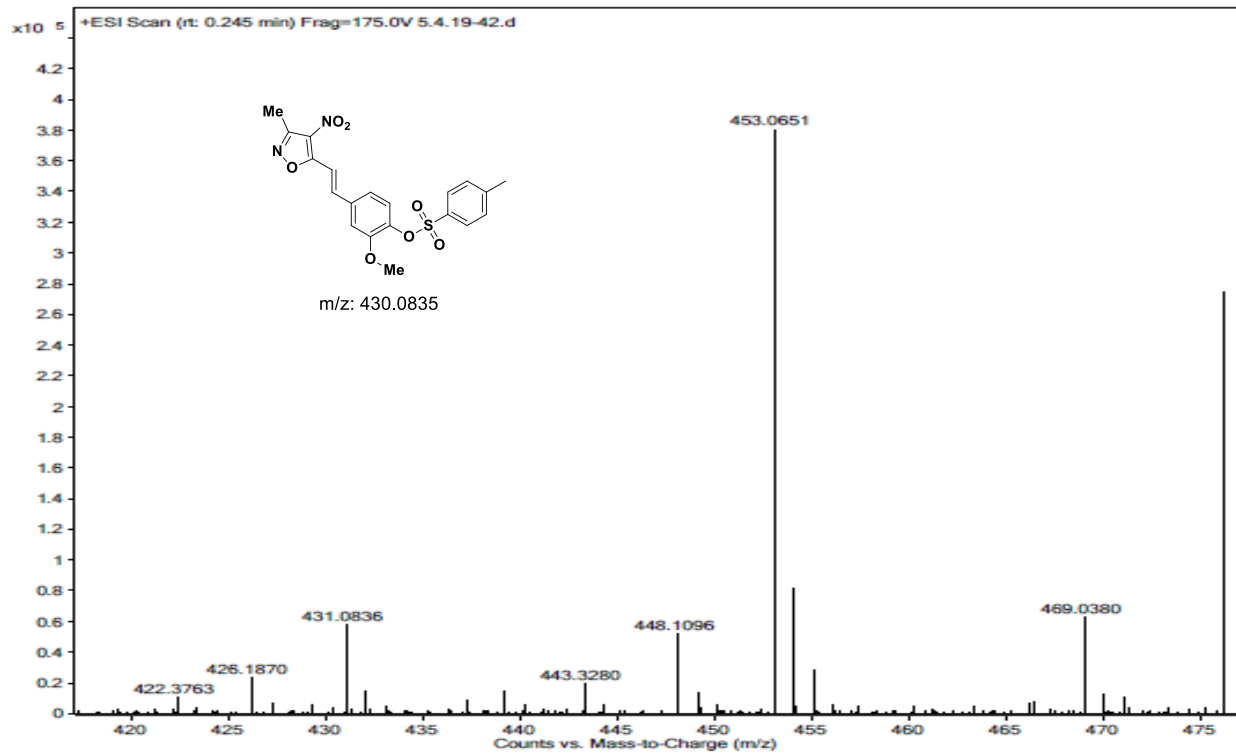
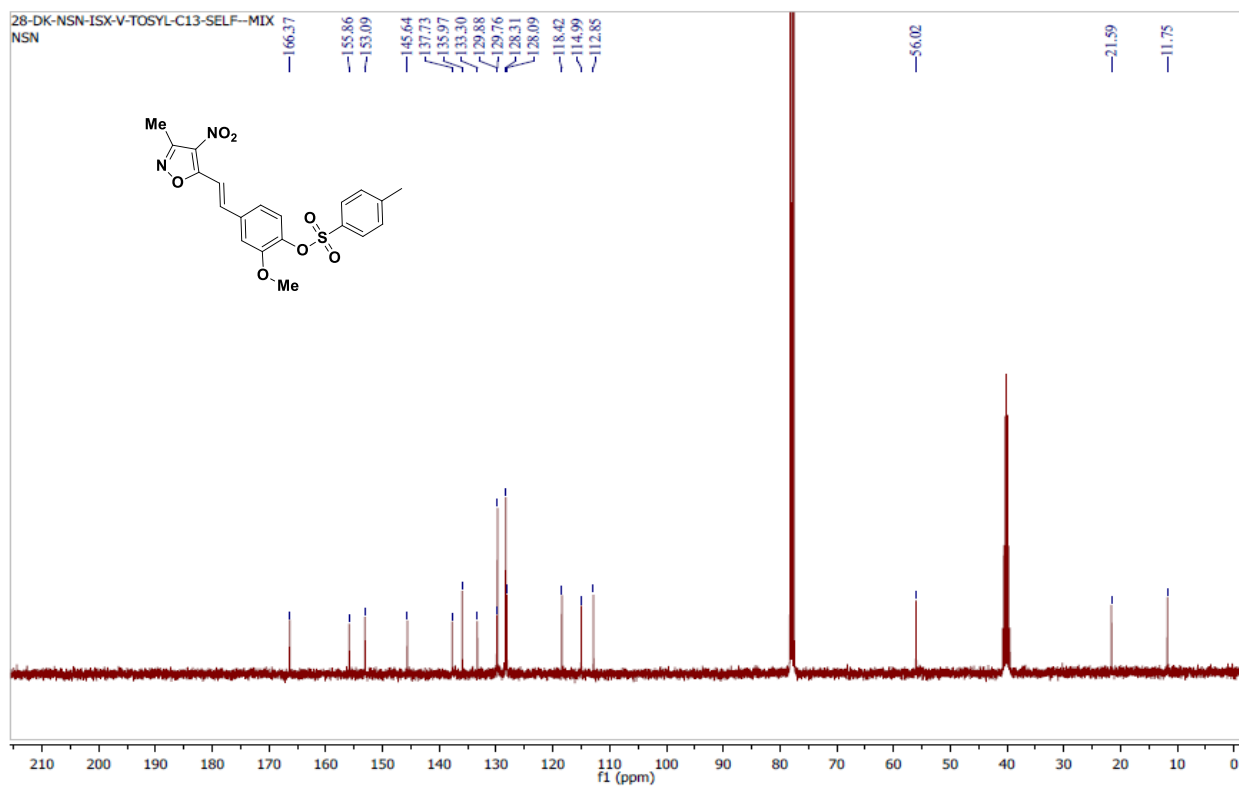
(E)-2-Methoxy-6-(((2-(3-methoxy-2-(tosyloxy)phenyl)-4-oxo-1,2-dihydroquinazolin-3(4H)-yl)imino)methyl)phenyl 4-methylbenzenesulfonate (7h):



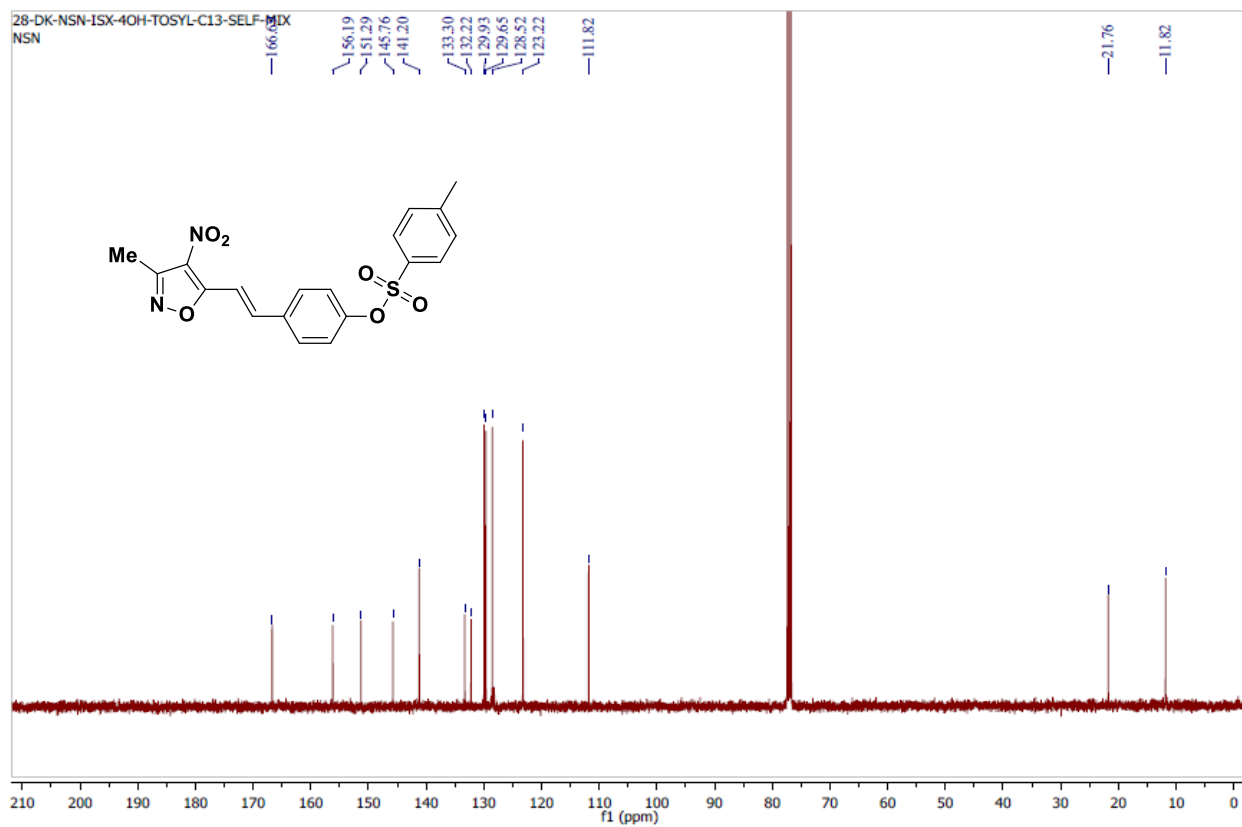
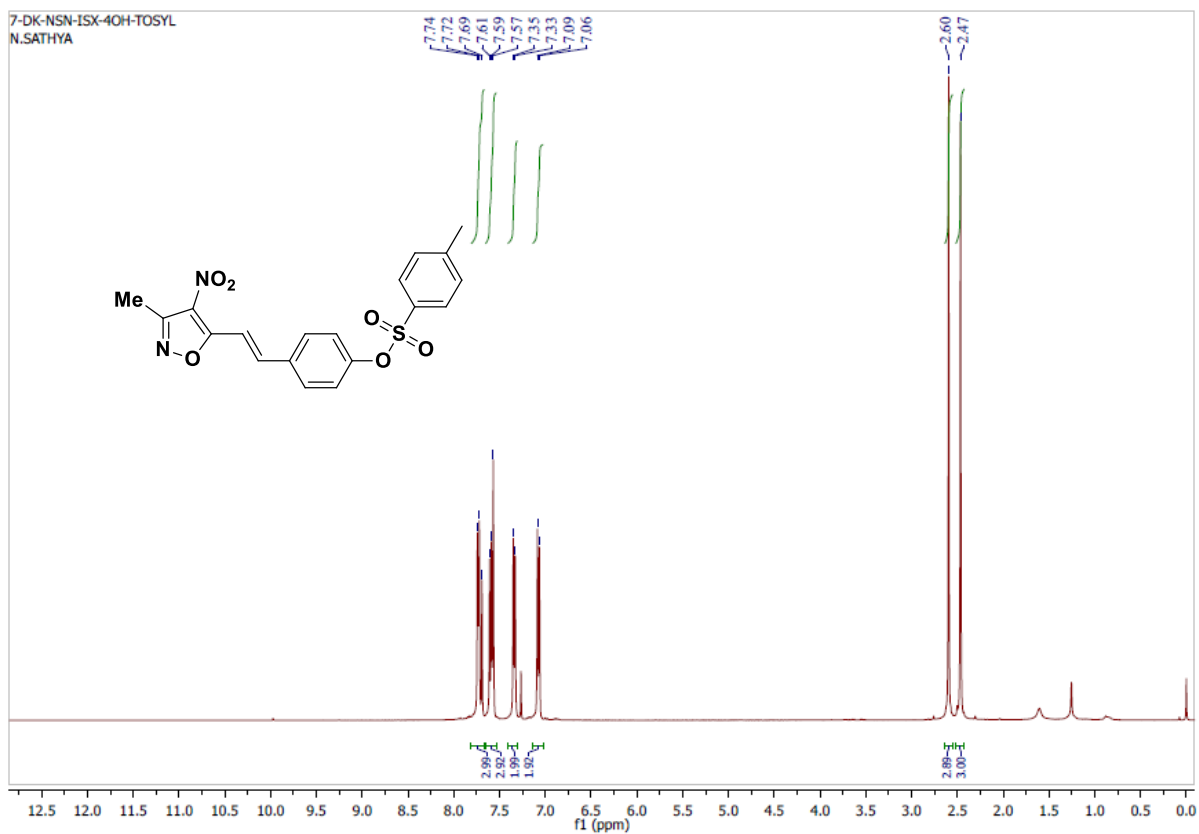


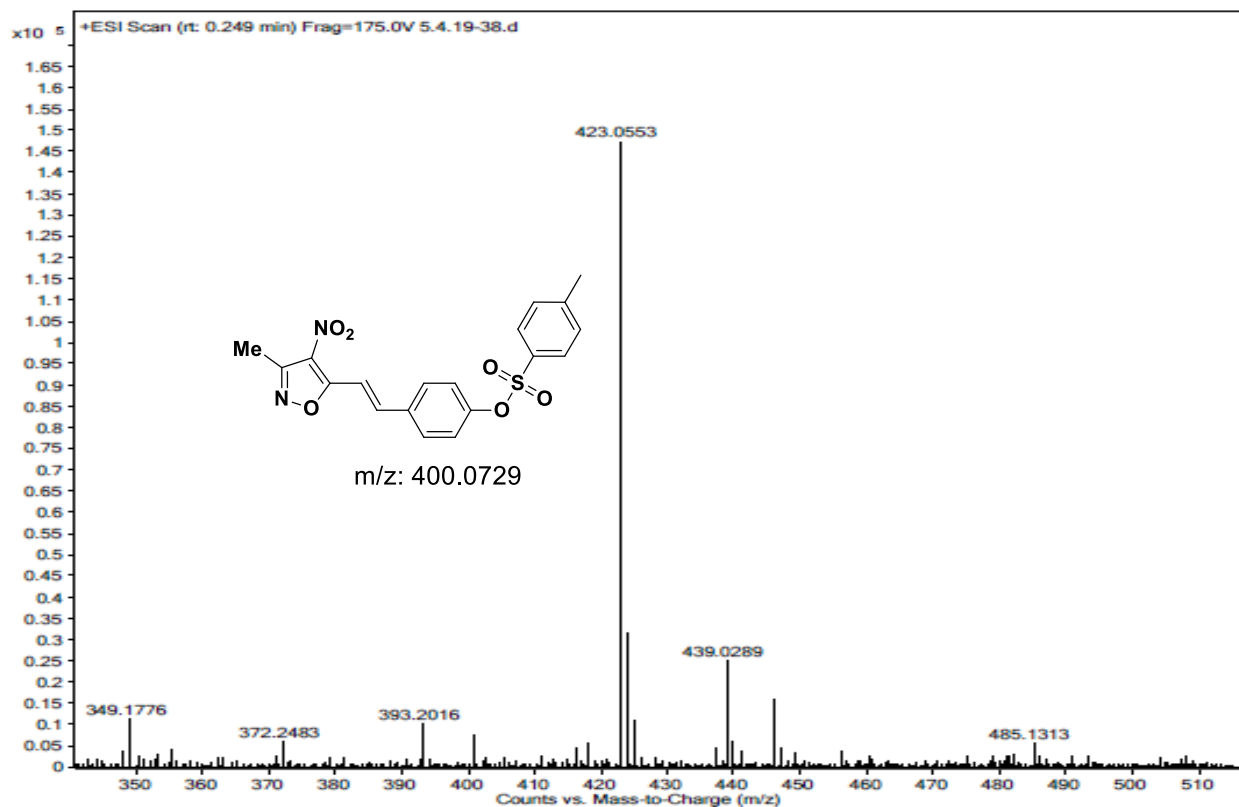
(E)-2-Methoxy-4-(2-(3-methyl-4-nitroisoxazol-5-yl)vinyl)phenyl 4-methylbenzenesulfonate (8e):





(E)-4-(2-(3-Methyl-4-nitroisoxazol-5-yl)vinyl)phenyl 4-methylbenzenesulfonate (8f):





Summary of the thesis

The thesis entitled “*Synthesis of sulfonate esters containing heterocyclic scaffolds via sp^3 C-H activation and their biological evaluation*” has been divided into **six chapters** with following titles. These titles have been decided based on the objectives set and results obtained in the present investigation. In correlation with the titles, a brief discussion on the biologically active molecules of respective chapters, the synthetic methods reported in the literature along with the detailed discussion on the results obtained along with the spectral, biological and photophysical data is discussed in the thesis.

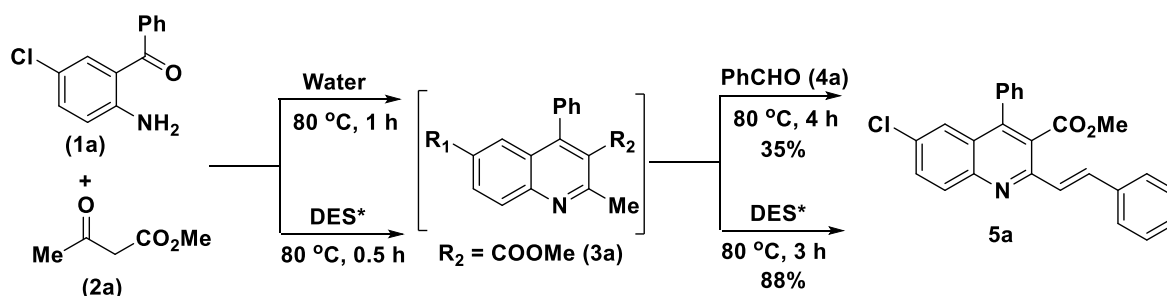
Chapter-1: Introduction of biologically active heterocyclic compounds

The heterocyclic compounds play vital role in the medicinal, synthetic organic and material chemistry. Heterocyclic compounds molecules like quinolines, quinoxalines, quinoxalines, benzodiazepines, rhodanines, thiolanes, 1,3,4-oxadiazoles can be seen in many synthetic/marketed drugs. Considering the biological importance of these scaffolds, the present thesis aims to synthesize new (hybrid) molecules based these skeletons using green condition. Thus, in the Chapter-1, a brief discussion on the biological activity of above molecules and the synthetic applications of green solvents like deep eutectic solvents, ionic liquids and water (catalyst-free reactions) is discussed. Also, a brief introduction on the literature covering the α -glucosidase inhibitors is discussed.

Chapter-2: Deep Eutectic Solvents (DES) mediated synthesis of styrylquinolines and styrylquinoline-sulfonates via Friedländer synthesis and sp^3 C-H activation, their biological evaluation as α -Glucosidase inhibitors and photophysical studies

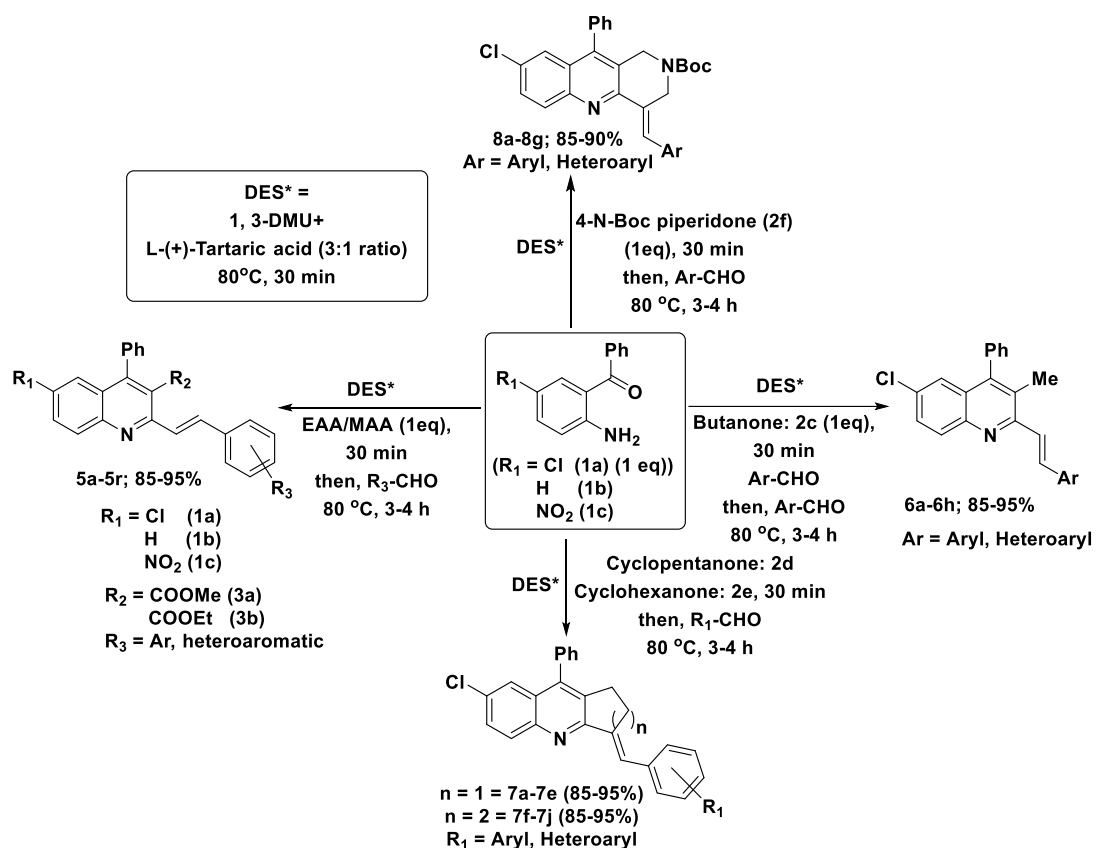
As mentioned above, the quinolones play important role in medicinal chemistry. There are many quinolone-based molecules in the market (as drugs). Also, the quinolone-based molecules are known to show excellent photophysical properties and used in developing fluorescent materials. In addition to this, the development of synthetic methods (sp^3 C-H activation) around 2-methyl quinolines is one of the attractive topic for the synthetic organic chemists in recent times. In this context, we envisaged the synthesis of 2-styryl-quinolines *via* Friedländer synthesis and sp^3 C-H activation of 2-methyl quinolones (a one-pot approach). Thus, with our background in the catalyst-free, one-pot and on-water reactions, the study started with the treatment of 5-chloro-2-aminobenzophenone (**1a**) with methyl acetoacetate (**2a**) in water (at 80 °C, 1 h) to give the 5-chloro-2-methylquinoline (**4a**) *in-situ*. To this, the addition of benzaldehyde (**3a**) to the same reaction pot

and heating at 80 °C for 4 h gave the 2-styrylquinoline (**5a**) in 35% yield (**Scheme-1**). Encouraged by these results, same reaction was performed in presence of ionic liquids (ILs) and deep eutectic solvents (DES). Among the screened, a combination of 1,3-dimethyl urea and L-tartaric acid (3:1) was found to be good reaction condition to give the desired product (**5a**) in 3.5 h with 88% yield. The product was confirmed by the spectral data. Later, a library of 2-styrylquinolines were synthesized under optimized conditions using 5-nitrobenzophenone, benzophenone, methylacetoacetate, ethylacetoacetate and substituted benzaldehydes as coupling partners to give 2-styrylquinolines (**5b-5r**) in 85-95% yields. Similarly, this strategy was extended to acyclic and cyclic diketones as shown in Scheme 2 to give functionalized styryl-quinolines in good to excellent yields (**Scheme-2**).

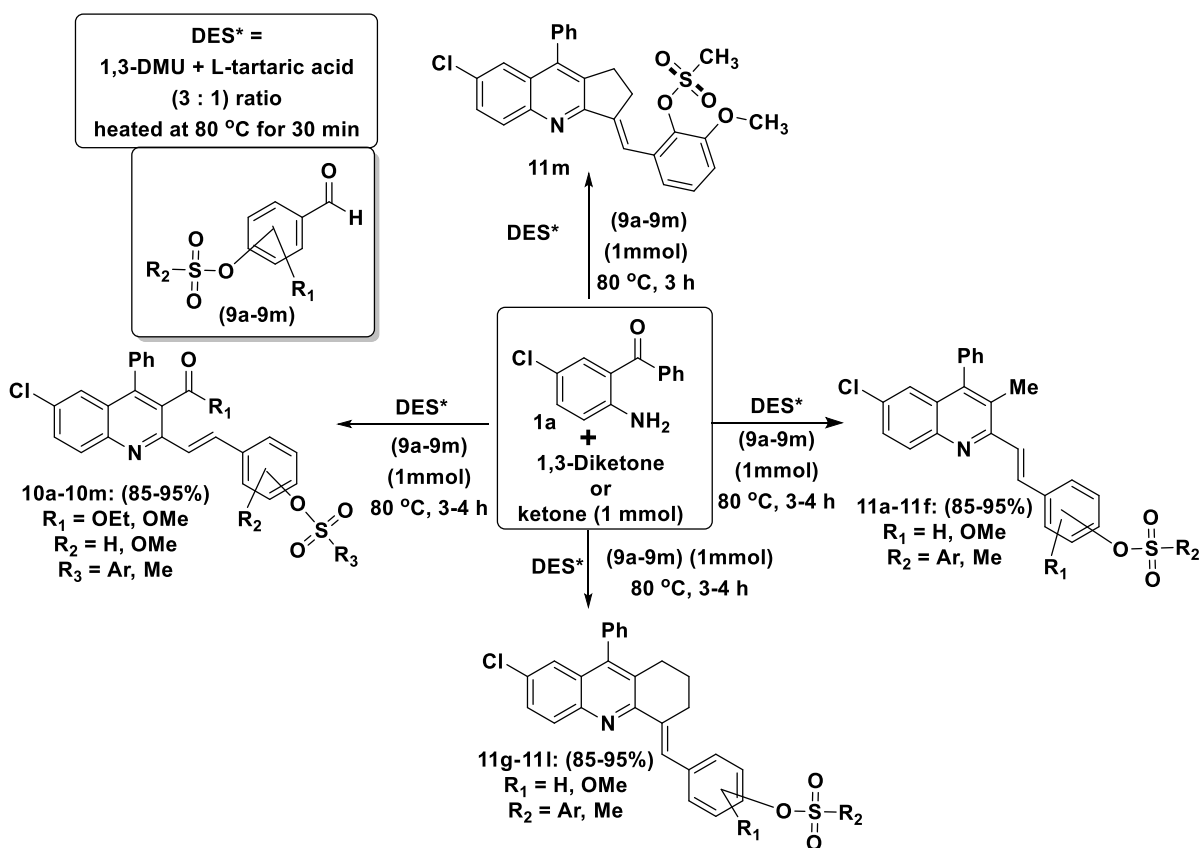


Scheme-1. Initial attempt for the synthesis of 2-styrylquinoline (**5a**).

Having successfully demonstrated of the styrylquinolines using simple aldehydes, the focus was shifted to increase the molecular complexity by introducing sulfonate moiety because sulfonates are importins for biological activity. Thus, the aldehydes containing sulfonate groups prepared by literature methods starting from corresponding hydroxyl benzene carbaldehydes and used for the Friedländer reaction followed by sp^3 C-H activation to give functionalized styrylquinolines with sulfonate moiety (**10a-10m** and **11a-11m**) in good to excellent yields (85-95%) (**Scheme-3**). All newly synthesized compounds were characterized by spectral data, i.e. ^1H -NMR, ^{13}C -NMR and HRMS.



Scheme-2. Synthesis of 2-styrylquinolines under optimized conditions.



Scheme-3: Synthesis of sulfonate ester based 2-styrylquinolines using acyclic and cyclic electrophiles.

1) Computational studies: To understand the role of the DES, Density functional theory (DFT) calculations were performed. For this, geometries of all the reactants, transition states, intermediates and products were fully optimized without any geometrical/symmetrical constraints using DFT based B3 exchange and Lee, Yong and Paar (LYP) correlation functional with inclusion empirical dispersion correction (D3) as suggested by Grimme's utilizing 6-31G* basis set. 1-3. The energetics of various reactions was calculated at 298.15 K temperature and 1 atm pressure in gaseous phase. All the calculations were performed using Gaussian 09 suite of program. These studies supported the experimental results and role of DES in the enolization of carbonyl compound (for Friedländer annulation) and formation of enamine, a key step in the sp^3 C-H activation.

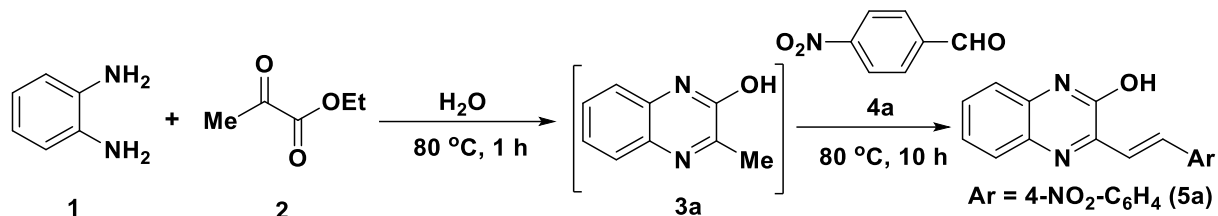
Applications of synthesized molecules:

After synthesis, the photophysical properties (absorption and emission spectra) of the resulting acyclic, cyclic styrylquinolines (**5**, **6**, **7** and **8** series) was recorded. It was found that the compound **7c** showed highest emission band maxima (**644 nm**) due to the intramolecular charge transfer. Also compounds **7b**, **8d** exhibited larger bathochromic shift at 551 nm and 558 nm respectively and compound **5o** showed highest Stokes shifts ($\Delta\lambda$ **182 nm**). Further the resultant 2-styrylquinoline-based sulfonates were evaluated for *in-vitro* α -glucosidase inhibition activity using acarbose as a standard drug (IC_{50} **32.15 \pm 2.04**) and found that the compounds **10b**, **11a** and **11l** showed best activity with IC_{50} **38.82 \pm 1.17** (for compound **11a**).

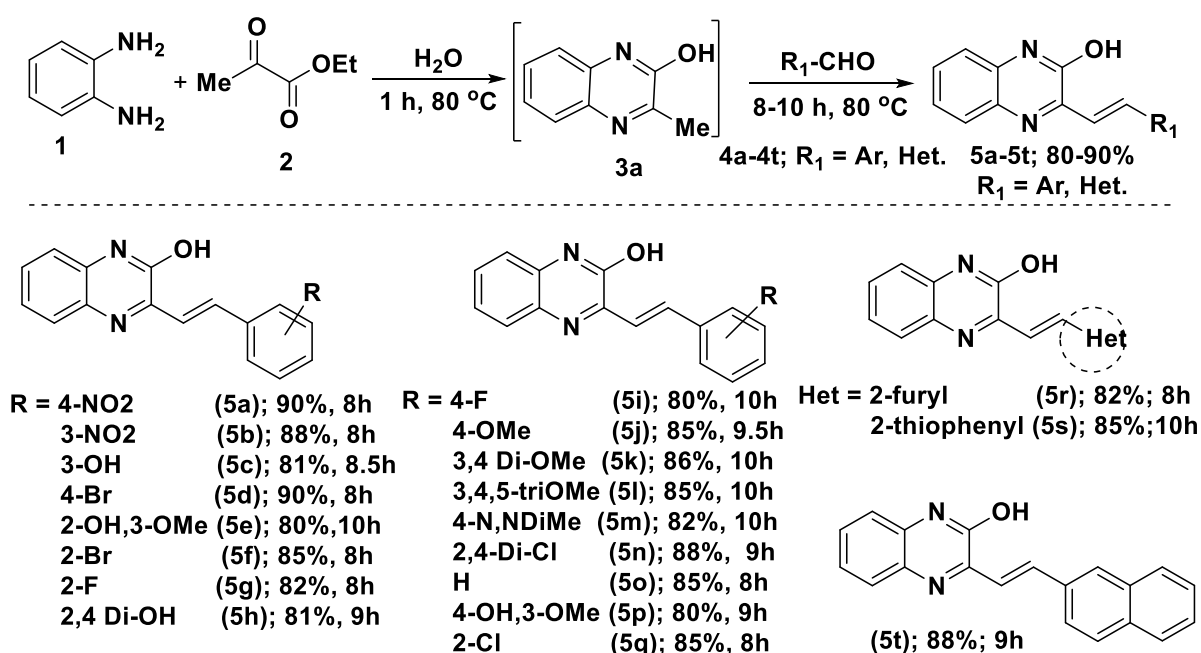
Chapter-3: Facile synthesis of quinoxaline, quinoxaline-2-one, quinazoline-based styrenes, sulfonate-styryls via sp^3 C-H activation and their evaluation as α -glucosidase inhibitors

Quinoxaline and Quinazoline are important scaffolds in medicinal chemistry. There are many reports for the synthesis and biological evaluation of the derivatives of these skeletons in different therapeutic areas. Specifically, the styryl derivative of these molecules known to show anticancer, antidiabetic and photophysical properties. Considering this, in this chapter, we describe facile synthesis of novel quinoxaline-2-one, phenyl-quinazoline, quinoxaline and bis-quinoxaline styryls and their sulfonate esters based styryls using aqueous and mild conditions. This work was initially started with the preparation of compound **5a** in a multicomponent approach under catalyst-free conditions. Thus, the quinoxaline-2-one (**3a**) was prepared *in-situ* from *ortho*-phenylenediamine (**1**) and ethyl pyruvate (**2**) and treated with 4-nitro-benzaldehyde (**4a**) to give the quinoxalinestyryl (**5a**) in 80% yield as shown in **Scheme-1**. After confirmation of the product, same

strategy was extended for other aromatic aldehydes with electron donating and withdrawing groups on them and heteroaromatic aldehydes to generate different styryl-quinoxalines (**5b-5t**) in moderate yields (80-90%). Though the reaction times are more, this method can be extended for the hierarchical activation on methyl group and the -OH group present in the molecule.

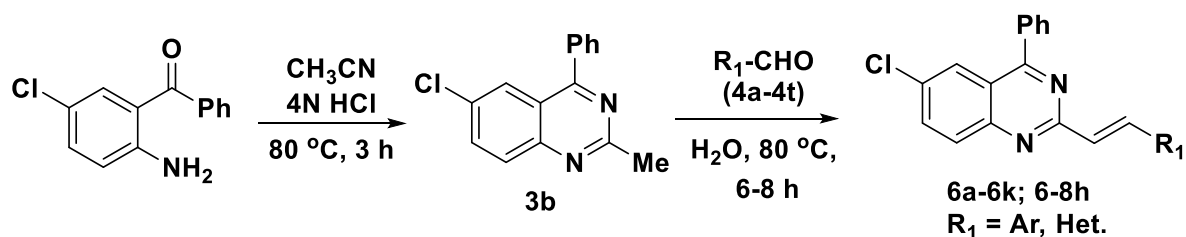


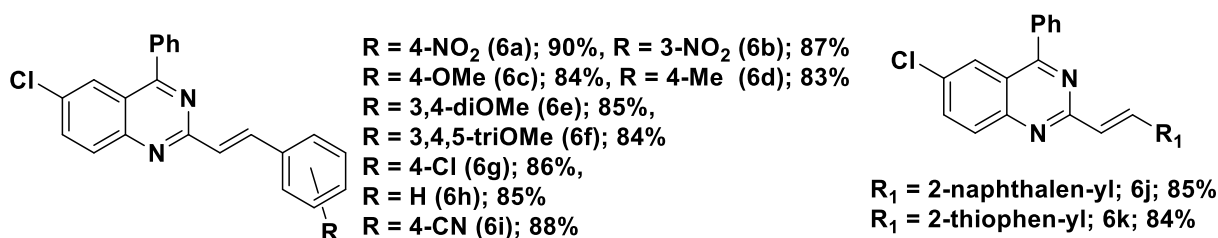
Scheme-1: Synthesis of quinoxaline-styryl hybrid (**4a**) *via* sp^3 C-H activation.



Scheme-2: Synthesis of quinoxaline-styryl hybrid (**5b-5t**) *via* sp^3 C-H activation.

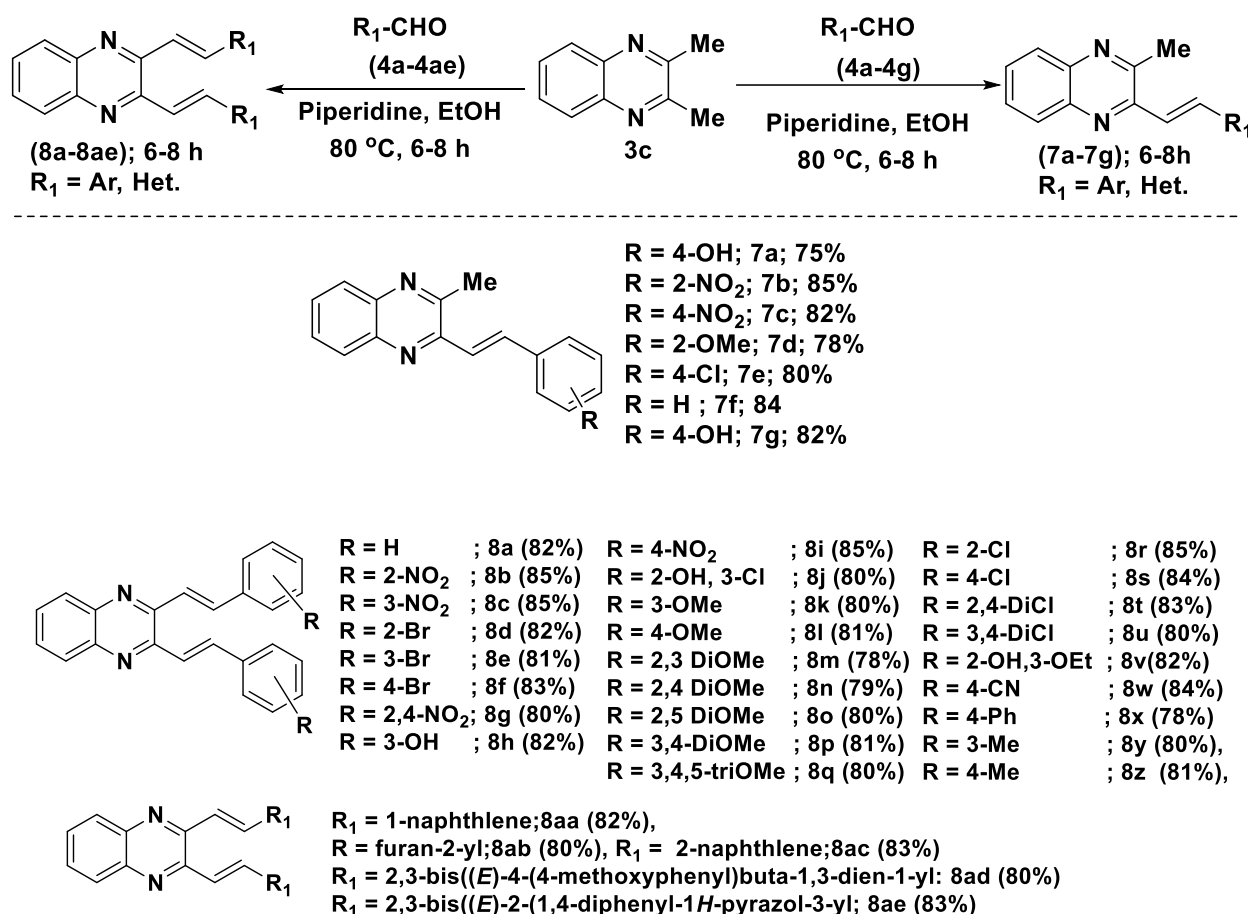
After successful synthesis of 3-styrylquinoxaline-2-ones **5a-5t**, further to check the reactivity the strategy extended for the preparation of quinoxaline derivatives. Thus, 5-chloro-2-methyl-4-phenylquinazoline (**3b**) was prepared and used for the sp^3 C-H activation under catalyst-free conditions to give unsaturated functionalized 2-styrylquinazoline derivatives (**6a-6k**) in good yields (**Scheme-3**).



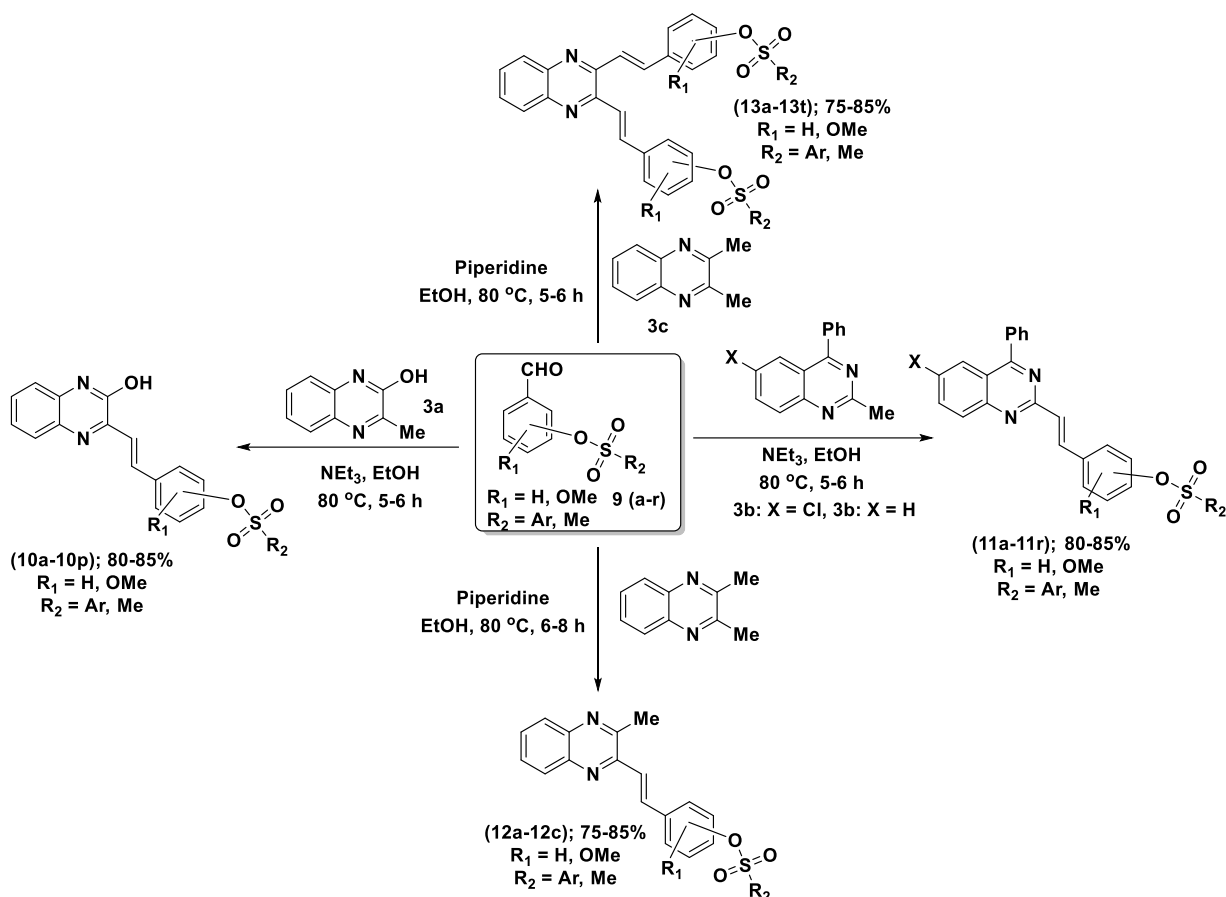


Scheme-3. Synthesis of (*E*)-6-chloro-4-phenyl-2-styrylquinazoline derivatives (**6a-6k**).

Similarly, the synthesis of (*E*)-2-methyl-3-styrylquinoxalines and 2,3-di(*E*)-styryl quinoxalines under basic conditions (piperidine; catalytic amount). Thus, the treatment of *ortho*-phenylene-diamine with 1,2-butanone in EtOH to give the 2,3-dimethylquinoxaline (**3c**) which was treated with aldehydes to give corresponding styrene derivatives. It is noteworthy to mention that the use of 1 equivalent of aldehyde gave mono activated products (**7a-7g**) and 2 equivalents of aldehydes delivered *bis*-styrylquinoxalines (**8a-8ae**) as shown in **Scheme-4**.



Scheme-3: Synthesis of styrylquinoxalines (**7a-7g** and **8a-8ae**).



Scheme-4: Synthesis of sulfonate ester based styryls *via* sp^3 C-H activation.

As mentioned in the introduction, the quinazoline and quinoxalines based compounds play important role in medicinal chemistry. Similarly, the sulfonates also contribute a lot for biological activity as bioisosteres. Moreover, there are not many reports for the quinazoline and quinoxaline-based sulfonate hybrids in the literature. Considering this, the present methodology was extended for the sulfonate-based aldehydes. Thus, the 3-methylquinoxalin-2-ol (**3a**), 6-chloro-2-methyl-4-phenylquinazoline (**3b**) and 2,3-dimethylquinoxaline (**3c**) were reacted with sulfonate aldehydes in presence of NEt_3 (catalytic amount) in EtOH at $80^\circ C$ for 5-8 h to give the corresponding quinazoline styryls (**10a-10r**), quinoxaline styryl (**11a-11p**), 3-methylquinoxaline styryl (**12a-12t**) and *bis*-quinoxaline sulfonate esters (**13a-13c**) with good to excellent yields.

Applications of synthesized molecules:

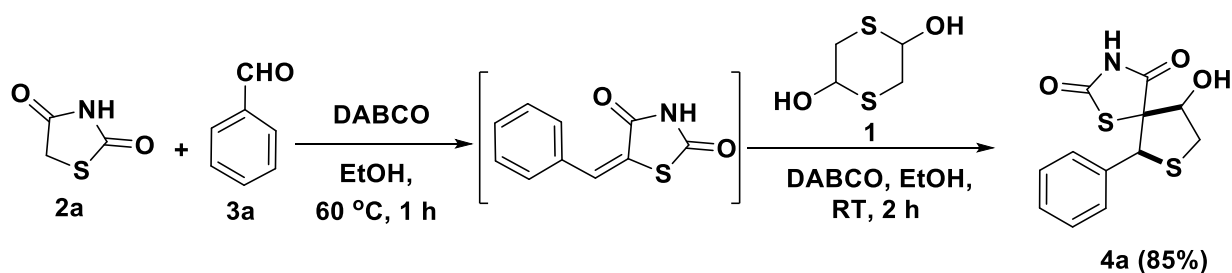
***In-vitro* α -glucosidase inhibition activity:** The synthesized quinazoline styryl (**10a-10r**) and quinoxaline styryl sulfonate esters (**11a-11p**) were tested for α -glucosidase inhibition activity (*in-vitro*) by taking acarbose as standard drug (IC_{50} **32.15 \pm 2.65**). It was found that the compounds **10o**, **11n** and **11o** showing best activity (IC_{50} **28.82 \pm 1.17** for compound-**10o** comparing with standard drug). In addition to the biological activity, the photophysical properties (absorbance and

emission spectra) of the resulting compounds (**10a-10r** and **11a-11p**) were studied in DCM (100 μ M concentration) at room temperature.

Chapter-4: Synthesis of spiro thiolane-thiazolidine-2,4-dione, thiolane-2-thioxothiazolidin-4-one and bicyclic thiolane-chromene derivatives via 1,4-Michael addition followed by intra molecular aldol reactions

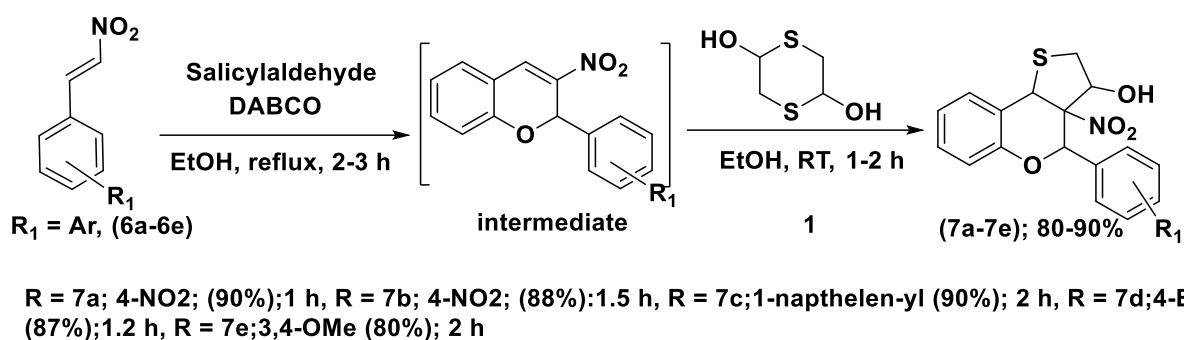
Thiolane (tetrahydrothiophene) found in natural products and synthetic molecules with biological activity. Thiozolidinone (2,4-thiozolidinone), rhodanine and chromenes moieties are also important scaffolds in medicinal chemistry. Considering the medicinal significance of these molecules, we planned the synthesis of spirocyclic thiozolidinone-thiolane and rhodanine-thiolane and bicyclic 3-nitro-[2H]-chromene-thiolanes using *via* Knoevenagel condensation, sulfa-1,4-Michael addition followed by intramolecular aldol reactions using 1,4-dithiane-2,5-diol (**1**) as key starting material.

In this context, 2,4-thiozolidinone (**2a**) was condensed with aldehyde (**3a**) using DABCO in ethanol at 60 °C, for 1h. This intermediate was treated in same reaction pot with 1,4-dithane-2,6-diol (**1**) at room temperature for 1 h to give the 2,4 thiozolidinone-thiolane hybrid **4a** in yield 85% (**Scheme-1**). After confirmation of the product, substrate scope was checked with different aldehydes (with electron donating and withdrawing groups), 2,4 thiozolidinone (**2a**)/2-imino-4-thiazolidinone (**2b**) and 1,4-dithane-2,6-diol (**1**) under optimized conditions (DABCO) to provide 2,4-thiozolidinone-thiolane derivatives (**4a-4m**) and 2-imino-4-thiazolidinone-thiolanes (**4o-4q**) as shown in **Scheme-2**. All the synthesized compounds were characterized by spectral data (¹H-NMR, ¹³C-NMR and mass spectra).



Scheme-1: One-pot synthesis of 2,4-thiozolidinone-based thiolane **4a**.

Rhodanines are known to show anticancer, antifungal, antidiabetic and antimalarial properties. Thus above strategy was applied for the generation of rhodanine-thiolane spiro cyclic molecules under optimized conditions. To achieve this, the reaction of rhodanine (**2c**) with aldehydes gave the unsaturated system in presence of DABCO. This was treated with 1,4-dithane-2,6-diol (**1**) to provide rhodanine-thiolane hybrids (**5a-5h**) with good yields (75-85%) in impressive reaction time 2-3h at room temperature (Scheme-3).

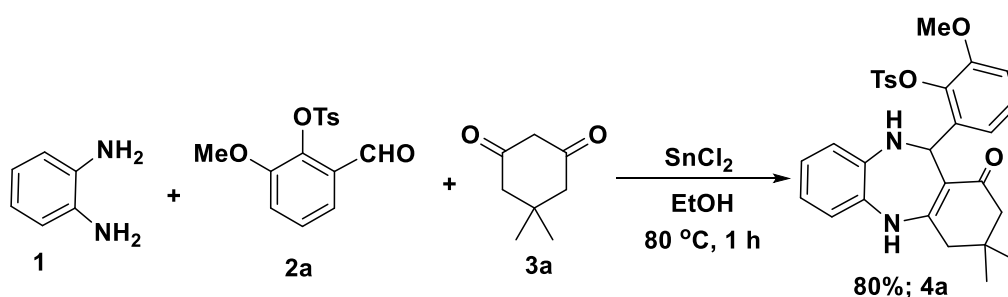


Scheme-4: Synthesis of 3-nitro-cromene-[2H]-thiolane hybrids (**7a-7e**) via 1,4-Micheal addition followed by intermolecular aldol reactions.

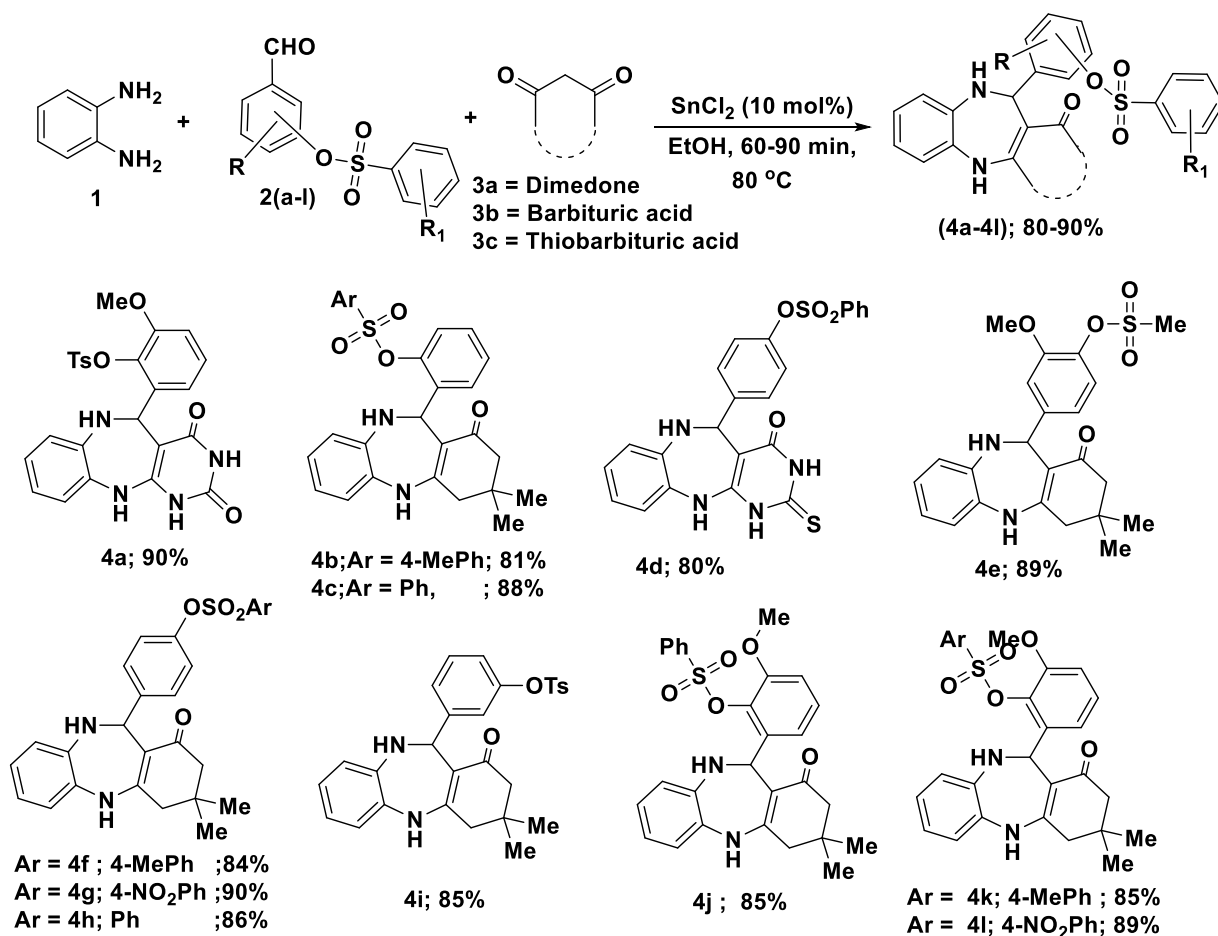
Chapter-5: *SnCl₂* catalyzed synthesis of dibenzo-[1, 4]-diazepin-1-one, phenyl quinazoline and 2,5-substituted 1,3,4 oxadiazoles based sulfonate esters and their evaluation as α -glucosidase inhibitors

Benziazepines, dibenzo-[1,4]-diazepin-1-ones, phenyl quinazolines, 1,3,4 oxadiazoles are considered as privileged molecules in medicinal chemistry. The synthetic derivatives of these molecules are known for many types of biological activities. Similarly, sulfonates also play important role in the medicinal chemistry in different therapeutic areas. With this background, in this chapter, the synthesis of dibenzo-[1,4]-diazepin-1-ones, phenyl quinazolines and 2,5-substituted 1,3,4 oxadiazoles-based sulfonate esters is described using SnCl_2 in ethanol under reflux conditions from OPDA and various active methylene compounds.

Towards this objective, initially *o*-phenyldiamine (OPDA) **1** and sulfonate ester aldehyde **2b** was treated with dimedone **3a** in presence of SnCl_2 in ethanol at 80 °C to provide sulfonate ester based dibenzo-[1,4]-diazepin-1-one **4a** in 85% yield in 60 min (**Scheme-1**). After confirmation of the desire product, attempts were made to optimize the reaction conditions using different Lewis acids. Among the screened, SnCl_2 was found good for success of the reaction. Later, to generalize the methodology, various benzene sulfonate aldehydes (**2a-2l**) were reacted with OPDA and active methylene groups (dimedone **3a**, barburaric acid **3b** and thio-barbutaric acid **3c**) under optimized conditions *via* to provide functionalized dibenzo-[1,4]-diazepin-one derivatives (**4a-4l**) with good yields (80-90%) (**Scheme-2**).

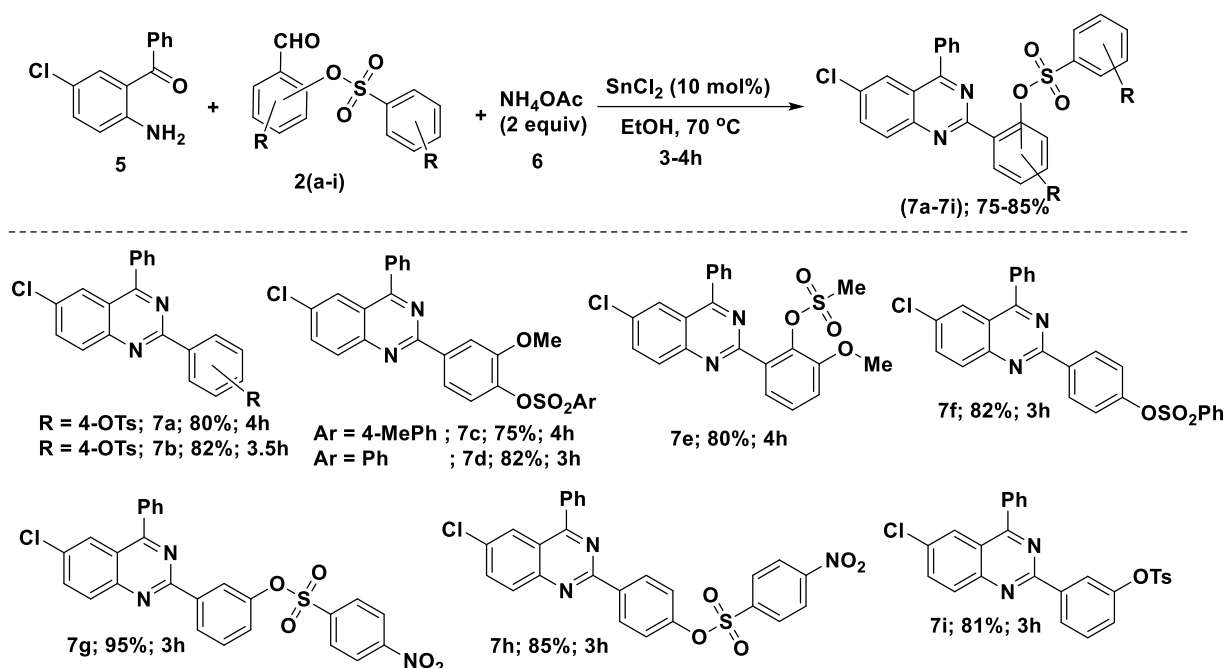


Scheme-1: Synthesis of sulfonate ester based dibenzo-[1,4]-diazepin-1-one derivative (**4a**).

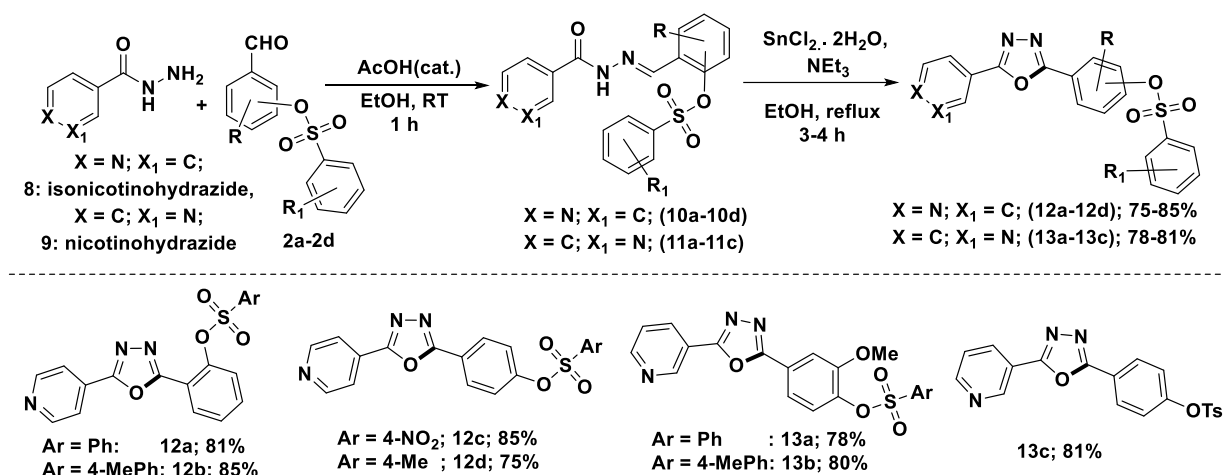


Scheme-2: Synthesis of sulfonate ester based dibenzo-[1,4]-diazepin-1-ones (**4a-4l**).

Correspondingly, believing the importance medicinal properties of substituted 2-phenylquinazolines, efforts made to design the simple method for the synthesis of sulfonate ester based phenylquinazolines using above conditions and MCR approach. Thus, 5-chloro, 2-amino benzophenone **5**, ammonium acetate **6** were reacted with benzenesulfonate aldehydes (**2a-2i**) to afford functionalized phenylquinazolines (**7a-7i**) with good yields (75%-85%) in 3-4 h as shown in **Scheme-3**. This methodology was also extended for sulfonate ester schiff-bases (**10a-10d** and **11a-11c**) for oxidative cyclization to generate a verity of sulfonate ester based 2,5-disubstituted 1,3,4-oxadizole derivatives **12a-12d** and **13a-13c** under optimized conditions with moderate to good yields 75-85% (**Scheme-4**).



Scheme-3: One-pot synthesis of sulfonate ester based phenylquinazoline derivatives.



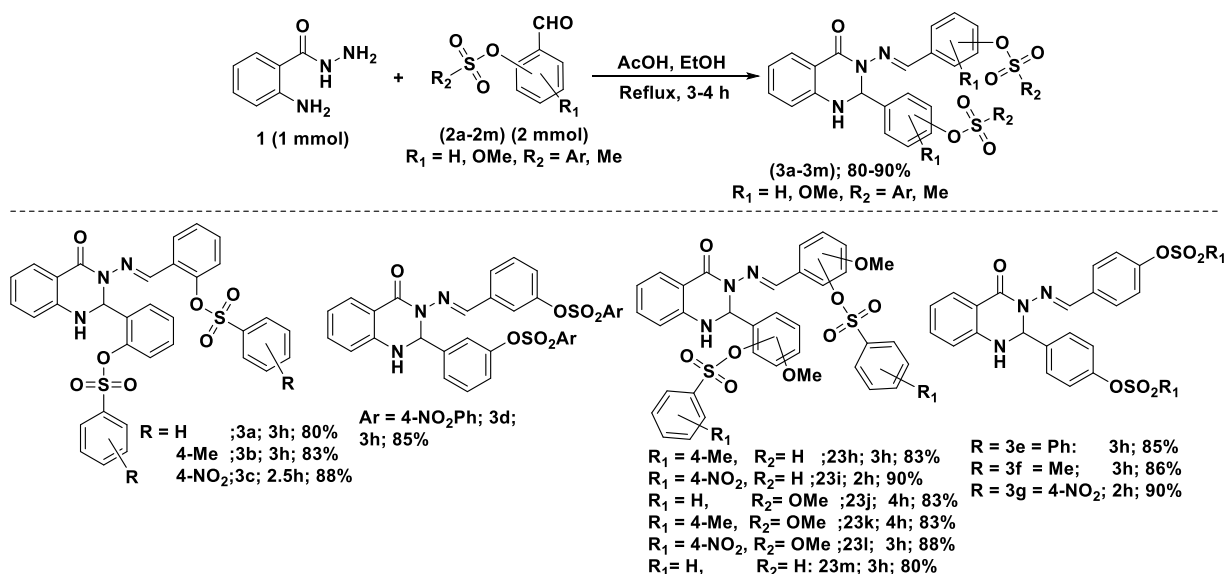
Scheme-4: Synthesis of sulfonate ester based substituted 1,3,4-oxadiazoles.

1) *In-vitro* α -glucosidase activity: The resulting compounds were evaluated for α -glucosidase inhibition (*in-vitro*) against acarbose as a standard drug (IC₅₀ **32.15 \pm 2.04**) and found that the compounds **4b**, **4g** and **7h** showed good activity with IC₅₀ values (best IC₅₀ **33.58 \pm 1.51** for compound-**4g**).

Chapter-6: Synthesis of quinazolinone Schiff base, isoxazole-styrene and isoxazole-thilane sulfonate ester conjugates

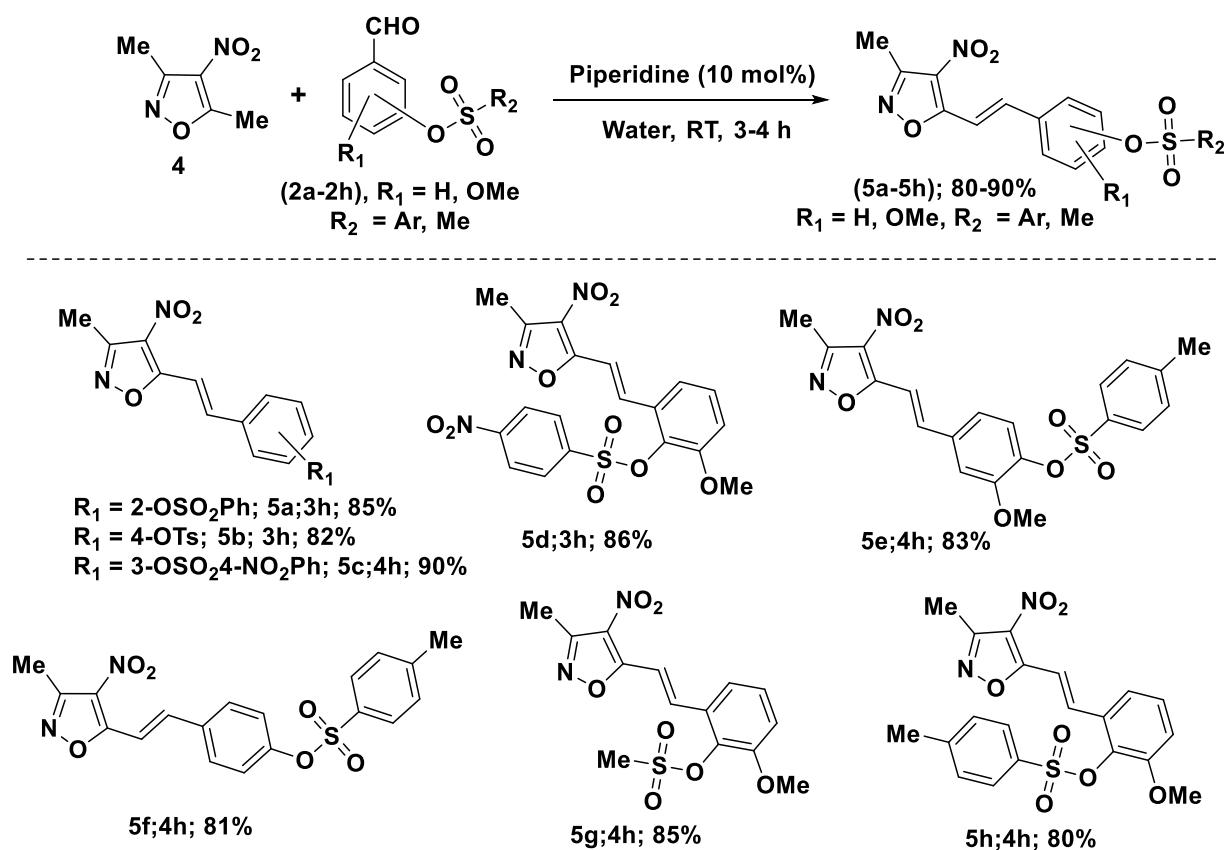
Schiff bases play important pharmacophore in medicinal chemistry. In addition, the Schiff bases are used in complex formation with different metals to study the properties of the complexes.

There are many examples of the Schiff bases used as therapeutic molecules. The quinazolinones and isoxazoles are also important molecules as discussed in above chapters. With this background, we describe here the synthesis of quinazolinone-Schiff base sulfonate esters and styryl-isoxazole sulfonate esters using AcOH in ethanol 70 °C. Towards this, 2-aminobenzohydrazide **1** and sulfonate ester aldehyde **3a** were reacted in AcOH and ethanol, at 70 °C for 3h to give the quinazolinone-Schiff base sulfonate esters (**3a-3m**) with moderate in 80-90% yields as shown in **Scheme-1**.

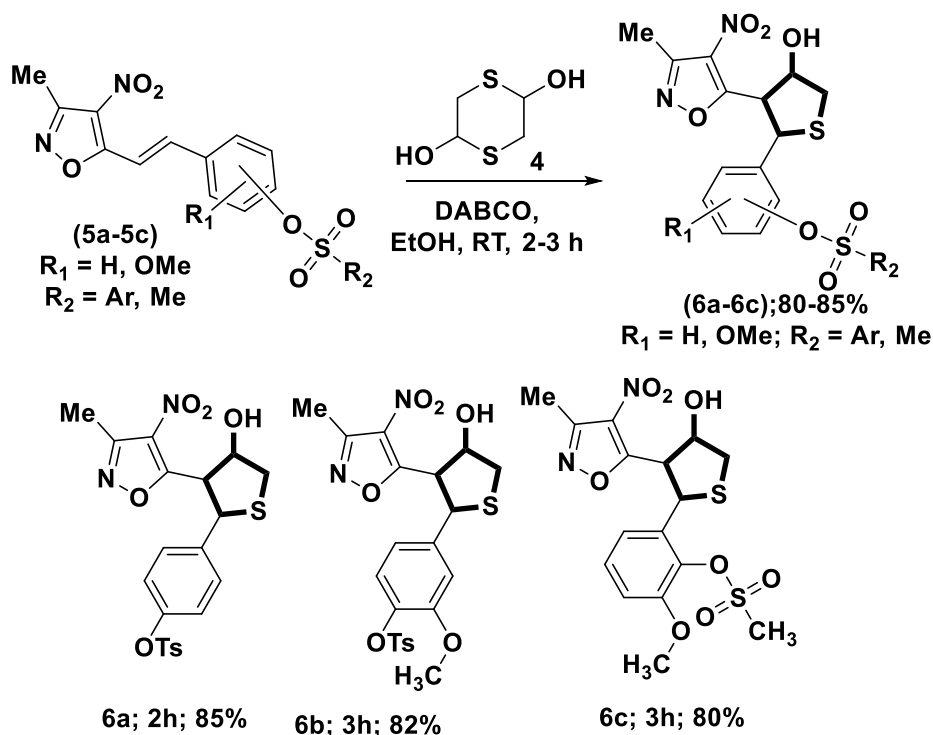


Scheme-1: Quinazolinone Schiff base sulfonate esters (**3a-3m**).

In a similar approach, 4-nitro-isoxazolestyryl sulfonate esters (**5a-5h**) was achieved *via* Knoevenagel condensation of 3,5-dimethyl-4-nitroisoxazole (**4**) with corresponding aldehyde with sulfonate moiety (**2a-2h**) in presence of piperidine (catalytic amount) in water (**Scheme-2**). All the products obtained were characterized by spectral data. Further, to show the application of the resulting products, the compounds **5a-5c** were treated with 1,4-dithiane-2,5-diol **4** in presence of DABCO (0.1eq) at RT for 2-3h [1.4-thiaMichael addition followed by intramolecular aldol condensation] to give functionalized tetrahydrothiophenes (**6a-6c**) with moderate to good yields (80-85%) as shown in **scheme-3**.



Scheme-2: Substrate scope of isoxazolestyryl based sulfonate ester scaffolds.



Scheme-3: Preparation of tetrahydrothiophene-sulfonate ester hybrids **6a-6c** via Michael addition and aldol reactions.

1) Photophysical properties: Further, the photophysical properties (absorption and emission spectra) of resulting products (isoxazolestyryl based sulfonate esters **5a-5h**) were studied in methanol (100 μ M) at room temperature. The emission band maxima of these molecules were seen in the range of 471-610 nm with highest bathochromic shift (λ_{em} 610 nm) for the sulfonate ester **5g**.

List of publications

1. **Neeli Satyanarayana**, Kota Sathish, Sakkani Nagaraju, Ravinder Pawar, Mohmmad Faizan, Murgan Arumugavel, Thangellapally Shirisha, Dhurke Kashinath. “*Metal-free, one-pot synthesis of styrylquinolines via Friedländer annulation and sp^3 C-H activation using 1,3-dimethylurea and L-tartaric acid (3:1) as deep eutectic solvent*” *New. J. Chem.*, 2022, 46, 1637.
2. **Neeli Satyanarayana**, Sakkani Neeli Satyanarayana, Boddu Ramya Sree, Kota Sathish, Sakkani Nagaraju, Kalivarathan Divakar, Ravinder Pawar, Thangellapally Shirisha, and Dhurke Kashinath. “*Synthesis of 2-styryl-quinazoline and 3-styryl-quinoxaline based sulfonate esters via sp^3 CH activation and their evaluation for α -glucosidase inhibition*” *New J. Chem.*, 2022, **46**, 5162-5170
3. Sakkani Nagaraju, **Neeli Satyanarayana**, Banoth Paplal, Anuji K. Vasu, Sriram Kana and Dhurke Kashinath. “*Synthesis of functionalized isoxazole–oxindole hybrids via on water, catalyst free vinylogous Henry and 1,6-Michael addition reactions.*” *RSC Adv.*, 2015, 5, 81768
4. Sakkani Nagaraju, **Neeli Satyanarayana**, Banoth Paplal, Anuji K. Vasu, Sriram Kanvah, Balasubramanian Sridhar, Prabhakar Sripadid and Dhurke Kashinath, “*One-pot synthesis of functionalized isoxazole-thiolane hybrids via Knoevenagel condensation and domino sulfa-1,6-Michael / intramolecular vinylogous Henry reactions*” *RSC Adv.*, 2015, 5, 94474
5. S Nagaraju, K Sathish, B Paplal, **N Satyanarayana**, D Kashinath, “*3-Hydroxy-3-((3-methyl-4-nitroisoxazol-5-yl) methyl) indolin-2-one as a versatile intermediate for retro-Henry and Friedel–Crafts alkylation reactions in aqueous medium.*” *N. J. Chem.*, 2019, 43 (35), 14045-14050
6. Sakkani Nagaraju, Kota Sathish, **Neeli Satyanarayana**, Banoth Paplal, Dhurke Kashinath “*Regioselective synthesis of spiro isoxazole-oxindole tetrahydrothiophene hybrids via cascade reactions under catalyst-free conditions*” *J. Heterocyclic Chem.* 2019;1–8.
7. **Neeli Satyanarayana**, Sakkani Nagaraju, Ravinder Pawar, K Divakar, and Dhurke Kashinath. “*Deep Eutectic Solvents (DES) mediated synthesis of styrylquinoline-sulfonates via Friedländer synthesis and sp^3 C-H activation, their biological evaluation as α -Glucosidase inhibitors and photophysical studies*” (To be submitted)
8. **N. Satyanarayana**, B. Ramya Sree, S. Nagaraju, K. Divakar, R. Pawar, and D. Kashinath, “*Facile synthesis of fluorescent probe of 3-styrylquinoxaline-2-ol, 2-styryls quinazoline and*

- 3-methyl-2-styrylquinoxaline, scaffolds via sp^3 C-H activation and their evaluation as α -glucosidase inhibitors.” (To be submitted to New. J. Chem)
9. **N. Satyanarayana**, B. Ramya Sree, S. Nagaraju, K. Divakar, R. Pawar, and D. Kashinath, “Facile synthesis of bis-styrylquinoxaline, bis-styrylquinoxaline based sulfonate ester conjugates via sp^3 C-H activation and their evaluation as α -glucosidase inhibitors.” (To be submitted)
 10. **Satyanarayana, N.**; Nagaraju, S.; Paplal, B.; Kashinath. “*Synthesis of spiro and bicyclic thiolane derivatives via 1,4-Michael addition followed by intra molecular aldol reactions*” (Manuscript to be submitted)
 11. **Satyanarayana, N.**; Nagaraju, S.; Paplal, B.; Kashinath. D. (Under communication) “*SnCl₂-catalyzed synthesis of dibenzo-[1,4]-diazepin-1-one, phenyl quinazoline and 2,5-substituted 1,3,4-oxadiazoles based sulfonate esters and their evaluation as α -glucosidase inhibitors*” (To be submitted to RSC journal)
 12. **Satyanarayana, N.**; Nagaraju, S.; Paplal, B.; Kashinath. “*Synthesis of quinazolinone Schiff base, isoxazole-styrene and isoxazole-thiolane sulfonate ester conjugates*” (Under communication)

The author Mr. Neeli Satyanarayana was born in Boddavaram village, Tuni via, East Godavari District, Andhrapradesh, India. He received B.Sc. degree from Andhra University, Vishakhapatnam 2010 and M.Sc. degree from Andhra University, Vishakhapatnam in 2012. After completing his M.Sc., he joined in the Ph.D. programme under the guidance of Dr. D. Kashinath, Associate Professor in the Department of Chemistry, National Institute of Technology Warangal in December 2014. Presently, he is continuing as Senior Research Fellow in the Department of Chemistry, National Institute of Technology-Warangal. His research interests are development of synthetic methods and synthesis of biologically active compounds.